AD-A068 679 ARMY MISSILE RESEARCH AND DEVELOPMENT COMMAND REDSTO--ETC F/G 20/5
COMPILATION OF DATA RELEVANT TO NUCLEAR PUMPED LASERS. VOLUME I--ETC(U)
DEC 78 E W MCDANIEL, M R FLANNERY, E W THOMAS

UNCLASSIFIED DRDMI-H-78-1-VOL-3 NL

1 OF 5
AD A068679

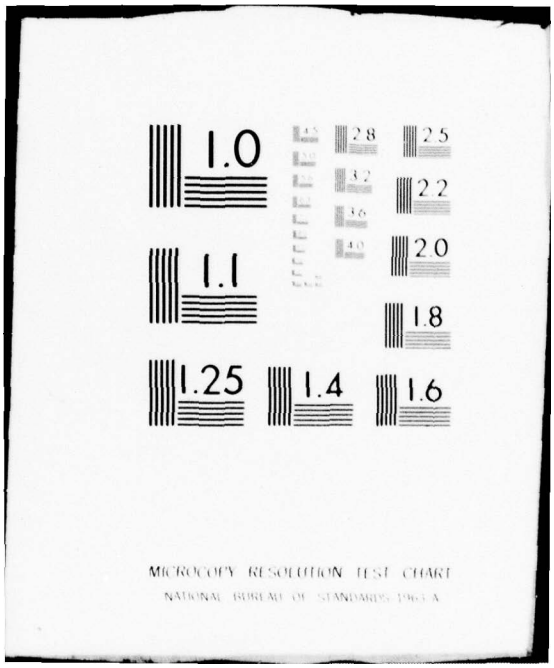
1.0
1.1
1.25
1.4
1.6
2.8
3.2
3.6
4.0
2.5
2.2
2.0
1.8
MICROCOPY RESOLUTION TEST CHART
NATIONAL BUREAU OF STANDARDS 1963-A

AD A068679

LEVEL II
A053828

U.S. ARMY MISSILE RESEARCH AND DEVELOPMENT COMMAND

DDC FILE COPY

Redstone Arsenal, Alabama 35809

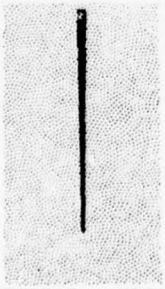

DMI FORM 1000, 1 APR 77

TECHNICAL REPORT H-78-1

COMPILATION OF DATA RELEVANT TO NUCLEAR PUMPED LASERS

VOLUME III

E. W. McDaniel, M. R. Flannery, E. W. Thomas, H. W. Ellis, and K. J. McCann
School of Physics
Georgia Institute of Technology
Atlanta, Georgia 30332

S. T. Manson
Physics Department
Georgia State University
Atlanta, Georgia 30303

J. W. Gallagher, J. R. Rumble, and E. C. Beaty
Joint Institute for Laboratory Astrophysics
University of Colorado
Boulder, Colorado 80302

and

T. G. Roberts
High Energy Laser Laboratory

DDC
DECEMBER
MAY 16 1979
C

December 1978

Approved for public release; distribution unlimited

PREPARED FOR:
High Energy Laser Laboratory
US Army Missile Research and Development Command
Redstone Arsenal, Alabama 35809

79 05 14 055

DISPOSITION INSTRUCTIONS

DESTROY THIS REPORT WHEN IT IS NO LONGER NEEDED. DO NOT RETURN IT TO THE ORIGINATOR.

DISCLAIMER

THE FINDINGS IN THIS REPORT ARE NOT TO BE CONSTRUED AS AN *OFFICIAL DEPARTMENT* OF THE ARMY POSITION UNLESS SO DESIGNATED BY OTHER AUTHORIZED DOCUMENTS.

TRADE NAMES

USE OF TRADE NAMES OR MANUFACTURERS IN THIS REPORT DOES NOT CONSTITUTE AN OFFICIAL INDORSEMENT OR APPROVAL OF THE USE OF SUCH COMMERCIAL HARDWARE OR SOFTWARE.

UNCLASSIFIED

SECURITY CLASSIFICATION OF THIS PAGE (When Data Entered)

REPORT DOCUMENTATION PAGE

READ INSTRUCTIONS BEFORE COMPLETING FORM

1. REPORT NUMBER: H-78-1

2. GOVT ACCESSION NO.

3. RECIPIENT'S CATALOG NUMBER: (9)

4. TITLE (and Subtitle): (6) COMPILATION OF DATA RELEVANT TO NUCLEAR PUMPED LASERS, Volume III.

5. TYPE OF REPORT & PERIOD COVERED: Technical Data Rept.

6. PERFORMING ORG. REPORT NUMBER

7. AUTHOR(s): (10) E. W. McDaniel, M. R. Flannery, E. W. Thomas, H. W. Ellis,* and K. J. McCann, S. T. Manson, J. W. Gallagher, J. R. Rumble, E. C. Beaty, and T. G. Roberts

8. CONTRACT OR GRANT NUMBER(s)

9. PERFORMING ORGANIZATION NAME AND ADDRESS
Commander
US Army Missile Research and Development Command
Attn: DRDMI-H
Redstone Arsenal, Alabama 35809

10. PROGRAM ELEMENT, PROJECT, TASK AREA & WORK UNIT NUMBERS: (11)

11. CONTROLLING OFFICE NAME AND ADDRESS
Commander
US Army Missile Research and Development Command
Attn: DRDMI-TI
Redstone Arsenal, Alabama 35809

12. REPORT DATE: December 1978

13. NUMBER OF PAGES: (12) 462p.

14. MONITORING AGENCY NAME & ADDRESS (if different from Controlling Office): (14) DRDMI-H-78-1-Vol-3

15. SECURITY CLASS. (of this report): Unclassified

15a. DECLASSIFICATION/DOWNGRADING SCHEDULE

16. DISTRIBUTION STATEMENT (of this Report)

Approved for public release; distribution unlimited

17. DISTRIBUTION STATEMENT (of the abstract entered in Block 20, if different from Report)

18. SUPPLEMENTARY NOTES

*Present Address: Eckerd College, St. Petersburg, FL 33733

**Volume I contains pages 1 through 427;
Volume II contains pages 429 through 892;
Volume III contains pages 893 through 1348.

19. KEY WORDS (Continue on reverse side if necessary and identify by block number)

Excitation
Ionization
Laser pumping mechanisms
Heavy nuclides
Light nuclides
High energy electron beams
High energy ion beams

20. ABSTRACT (Continue on reverse side if necessary and identify by block number)

This volume, and the succeeding Volumes No. IV and V, contain a compilation of data relevant to nuclear pumped lasers and are part of a series on atomic and molecular data for gas laser research and development. The first two volumes, published as MIRADCOM Technical Report H-78-1 in December 1977, contained "Compilation of Data Relevant to Rare Gas-Rare Gas and Rare Gas-Monohalide Excimer Lasers" by E. W. McDaniel, M. R. Flannery, H. W. Ellis, F. L. Eisele, W. Pope, and T. G. Roberts.

ABSTRACT (CONTINUED)

next page

DD FORM 1 JAN 73 1473 EDITION OF 1 NOV 65 IS OBSOLETE

UNCLASSIFIED

SECURITY CLASSIFICATION OF THIS PAGE (When Data Entered)

410 127 LB

ABSTRACT (CONCLUDED)

Volumes III, IV, and V contain data on many different species of atoms, molecules, and ions: a large fraction of them are already of direct interest in laser media; many more may become important in the future. These volumes cover all of the subjects treated in Vols. I and II; one difference is that now secondary electron energy spectra are discussed in a separate chapter. A chapter on nuclear data has also been added.

A species index for all five volumes will be published separately.

PREFACE

This volume, and the succeeding Volumes No. IV and V, contain a compilation of data relevant to nuclear pumped lasers and are part of a series on atomic and molecular data for gas laser research and development. The first two volumes, published as MIRADCOM Technical Report H-78-1 in December 1977, contained "Compilation of Data Relevant to Rare Gas-Rare Gas and Rare Gas-Monohalide Excimer Laser" by E. W. McDaniel, M. R. Flannery, H. W. Ellis, F. L. Eisele, W. Pope, and T. G. Roberts. These first two volumes are referred to herein as "Vol. I" and "Vol. II," usually without further designation.

In Vols. I and II, heavy emphasis was placed on the rare gases and halogens (atoms, molecules, and ions), and on the rare gas-halides, although a significant amount of material on other species was included. Vol. I deals with structural properties and with heavy particle-heavy particle collisions. Vol. II treats the collisions of electrons and photons with heavy particles; transport properties of electrons, ions, and neutrals; interactions of heavy particles with electric and magnetic fields; particle penetration in gases; and particle and photon interactions with solids.

Vols. I and II were prepared in the context of the two most-used techniques for gas laser pumping: electrical discharges and high intensity, high energy electron and ion beams. Vols. III, IV, and V contain much information relevant to electrical discharges and high intensity, high energy electron and ion beams, but are oriented toward a third pumping technique: nuclear pumping. This mechanism involves direct nuclear excitation of the laser gas in which, for example, a pulsed nuclear reactor generates a high intensity pulse of neutrons of duration between 0.1 and 10 msec. These neutrons produce fission in reactions with heavy nuclides within the laser or interact with light nuclides in (n,p) or (n,α) reactions. The high energy charged particles thus produced then deposit their energy in excitation and ionization of the laser gas in reactions similar to those taking place when a high energy electron beam traverses the laser. Nuclear pumping has been achieved with He, Ne, Ar, Kr, Xe, C, N, O, Hg, CO, mixtures of the rare gases, and possibly with CO_2, KrF, and XeF. These nuclear reactions may also become interesting in some form of a hybrid laser where the excitation and ionization produced might be used to supply electrons for an electrical discharge laser or an initiator for a pulsed chemical laser, or as an initiator and sustainer for a continuous wave (CW) chemical laser. Therefore, some data relevant to those systems have also been included.

The laser pumping mechanisms, when viewed on the molecular level, are frequently extremely complex. Some inkling of this situation is provided by consideration of the bizarre combinations of gases often

used in lasers to produce and/or pump the atomic or molecular species of interest. Some of these combinations are as unexpected, felicitous, and efficacious as that of lox, bagels, and cream cheese. In these volumes, data on many different species of atoms, molecules, and ions are provided: a large fraction of them are already of direct interest in laser media; many more may become important in the future. This volume and the succeeding volumes cover all of the subjects treated in Vols. I and II; one difference is that now secondary electron energy spectra are discussed in a separate chapter. A chapter on nuclear data has also been added.

A species index for all five volumes will be published separately.

ACKNOWLEDGMENTS FOR VOLUME III (CHAPTER A)

The generous contribution made to this volume by Professors Stanley Bashkin and John O. Stoner of the University of Arizona who supplied the 228 atomic energy level and Grotrian diagrams used in Section A-1 is acknowledged. They also supplied most of the references that appear in Section A-2.

Special thanks are due to Dr. Nick Winter of the Lawrence Livermore Laboratories and to Dr. W. R. Wadt and Dr. P. Jeffrey Hay of the Los Alamos Scientific Laboratory for providing material for Chapter A in advance of its publication.

Drs. J. T. Moseley, D. Heustis, R. E. Olson, R. Saxon, and P. Jullienne provided much useful information on the subject of interaction potentials.

Professor W. Carl Lineberger gave expert advice on electron affinities that was much appreciated. Dr. R. D. Cowan kindly supplied information on the spectrum of the uranium atom.

Finally, we wish to thank Dr. Edward L. Wilkinson, Mr. John E. Hagefstration, and Dr. J. R. Fisher of the Ballistic Missile Advanced Technology Center for their support and encouragement during the preparation of this report.

A. STRUCTURAL PROPERTIES OF ATOMS, MOLECULES, AND IONS

CONTENTS

		Page
A-1.	Periodic Table. Energy Level and Grotrian Diagrams of Atoms and Singly-Charged Positive Ions	895
A-2.	References on Atomic Energy Levels, Spectral Lines, Lifetimes, Oscillator Strengths, and Transition Probabilities.	1131
A-3.	Polarizabilities and Multipole Moments	1155
A-4.	Electron Affinities of Atoms and Molecules	1159
A-5.	General References on Potential Energy Curves, Electronic Energies, Spectroscopic Constants, and Absorption and Emission Spectra of Excimer Systems	1163
A-6.	Potential Energy Curves, Electronic Energies, and Spectroscopic Constants for Xe_2^+ and Xe_2^*. Interactions Between Like and Unlike Pairs of Rare-Gas Atoms.	1167
A-7.	Potential Energy Curves, Electronic Energies, Spectroscopic Constants, and Absorption Spectra for Ne_2^+, Ar_2^+, Kr_2^+, Xe_2^+, and $ArKr^+$.	1183
A-8.	Potential Energy Curves, Vibrational Levels, Transition Moments, Fluorescence and Einstein Transition Probabilities for NeF, ArF, ArCℓ, KrF, and KrCℓ. Wavenumbers, Franck-Condon Factors, and R^n-Centroids for XeF.	1211
A-9.	Potential Energy Curves, Electronic Energies, Spectroscopic Constants, and Transition Moments for Ar_2F and Kr_2F. . . .	1247
A-10.	Potential Energy Curves, Spectroscopic Constants, and Emission Data for HgCℓ and HgBr.	1269
A-11.	Potential Energy Curves, Electronic Energies, Spectroscopic Constants, and Dipole and Transition Moments for the Rare Gas Oxides	1282

Page

A-12. Potential Energy Curves, Electronic Energies, Spectroscopic Constants, Transition Moments, and Emission and Absorption Data for GaKr, InKr, and TℓKr. 1300

A-13. Potential Energy Curves and Spectroscopic Constants for AuH, AuCℓ, $HgC\ell_2$, and HgH. 1317

A-14. Potential Energy Curves, Electronic Energies, and Spectroscopic Constants for Valence States of O_2 1337

A-1. PERIODIC TABLE. ENERGY LEVEL AND GROTRIAN DIAGRAMS OF ATOMS AND SINGLY-CHARGED POSITIVE IONS

CONTENTS

		Page
A-1.1.	Table of Chemical-Scale Atomic Weights	897
A-1.2.	Periodic Table of the Elements	898
Notes on Use of Energy Level and Grotrian Diagrams		899
A-1.3. — A-1.5.	Diagrams for H (Z = 1)	902
A-1.6. — A-1.9.	Diagrams for He (Z = 2)	905
A-1.10. — A-1.11.	Diagrams for He^+ (Z = 2)	909
A-1.12. — A-1.13.	Diagrams for B (Z = 5)	911
A-1.14. — A-1.17.	Diagrams for B^+ (Z = 5).	913
A-1.18. — A-1.28.	Diagrams for C (Z = 6)	917
A-1.29. — A-1.33.	Diagrams for C^+ (Z = 6).	928
A-1.34. — A-1.43.	Diagrams for N (Z = 7)	933
A-1.44. — A-1.55.	Diagrams for N^+ (Z = 7).	943
A-1.56. — A-1.63.	Diagrams for O (Z = 8).	955
A-1.64. — A-1.70.	Diagrams for O^+ (Z = 8).	963
A-1.71. — A-1.76.	Diagrams for F (Z = 9)	970
A-1.77. — A-1.91.	Diagrams for F^+ (Z = 9).	976
A-1.92. — A-1.102.	Diagrams for Ne (Z = 10)	991
A-1.103. — A-1.109.	Diagrams for Ne^+ (Z = 10).	1002
A-1.110. — A-1.112.	Diagrams for Al (Z = 13)	1009
A-1.113. — A-1.119.	Diagrams for Al^+ (Z = 13).	1012
A-1.120. — A-1.128.	Diagrams for S (Z = 16).	1019

Page

A-1.129. — A-1.132. Diagrams for S^+ (Z = 16) 1028

A-1.133. — A-1.156. Diagrams for Cl (Z = 17) 1032

A-1.157. — A-1.181. Diagrams for Cl^+ (Z = 17). 1056

A-1.182. — A-1.204. Diagrams for Ar (Z = 18) 1081

A-1.205. — A-1.230. Diagrams for Ar^+ (Z = 18). 1104

Tabular Data. A-1.1. Table of the chemical-scale atomic weights.

Element	Symbol	Atomic number	Atomic weight†	Element	Symbol	Atomic number	Atomic weight
Actinium	Ac	89	227	Mendelevium	Md	101	[256]
Aluminum	Al	13	26.98	Mercury	Hg	80	200.61
Americium	Am	95	[243]‡	Molybdenum	Mo	42	95.95
Antimony	Sb	51	121.76	Neodymium	Nd	60	144.27
Argon	A	18	39.944	Neptunium	Np	93	[237]
Arsenic	As	33	74.91	Neon	Ne	10	20.183
Astatine	At	85	[210]	Nickel	Ni	28	58.69
Barium	Ba	56	137.36	Niobium (Columbium)	Nb	41	92.91
Berkelium	Bk	97	[247]	Nitrogen	N	7	14.008
Beryllium	Be	4	9.013	Nobelium	No	102	[256]
Bismith	Bi	83	209.00	Osmium	Os	76	190.2
Boron	B	5	10.82	Oxygen	O	8	16
Bromine	Br	35	79.916	Palladium	Pd	46	106.7
Cadmium	Cd	48	112.41	Phosphorus	P	15	30.975
Calcium	Ca	20	40.08	Platinum	Pt	78	195.23
Californium	Cf	98	[249]	Plutonium	Pu	94	[242]
Carbon	C	6	12.011	Polonium	Po	84	210
Cerium	Ce	58	140.13	Potassium	K	19	39.100
Cesium	Cs	55	132.91	Praseodymium	Pr	59	140.92
Chlorine	Cl	17	35.457	Promethium	Pm	61	[145]
Chromium	Cr	24	52.01	Protactinium	Pa	91	231
Cobalt	Co	27	58.94	Radium	Ra	88	226.05
Columbium (see Niobium)				Radon	Rn	86	222
Copper	Cu	29	63.54	Rhenium	Re	75	186.31
Curium	Cm	96	[247]	Rhodium	Rh	45	102.91
Dysprosium	Dy	66	162.46	Rubidium	Rb	37	85.48
Einsteinium	Es	99	[254]	Ruthenium	Ru	44	101.1
Erbium	Er	68	167.2	Samarium	Sm	62	150.43
Europium	Eu	63	152.0	Scandium	Sc	21	44.96
Fermium	Fm	100	[253]	Selenium	Se	34	78.96
Fluorine	F	9	19.00	Silicon	Si	14	28.09
Francium	Fr	87	[223]	Silver	Ag	47	107.880
Gadolinium	Gd	64	156.9	Sodium	Na	11	22.991
Gallium	Ga	31	69.72	Strontium	Sr	38	87.63
Germanium	Ge	32	72.60	Sulfur	S	16	32.066
Gold	Au	79	197.0	Tantalum	Ta	73	180.95
Hafnium	Hf	72	178.6	Technetium	Tc	43	[99]
Helium	He	2	4.003	Tellurium	Te	52	127.61
Holmium	Ho	67	164.94	Terbium	Tb	65	158.93
Hydrogen	H	1	1.0080	Thallium	Tl	81	204.39
Indium	In	49	114.76	Thorium	Th	90	232.05
Iodine	I	53	126.91	Thulium	Tm	69	168.94
Iridium	Ir	77	192.2	Tin	Sn	50	118.70
Iron	Fe	26	55.85	Titanium	Ti	22	47.90
Krypton	Kr	36	83.80	Tungsten	W	74	183.92
Lanthanum	La	57	138.92	Uranium	U	92	238.07
Lawrencium	Lr	103	[257]	Vanadium	V	23	50.95
Lead	Pb	82	207.21	Xenon	Xe	54	131.3
Lithium	Li	3	6.940	Ytterbium	Yb	70	173.04
Lutetium	Lu	71	174.99	Yttrium	Y	39	88.92
Magnesium	Mg	12	24.32	Zinc	Zn	30	65.38
Manganese	Mn	25	54.94	Zirconium	Zr	40	91.22

† Atomic weights are from the Committee on Atomic Weights of the American Chemical Society, *J. Am. Chem. Soc.*, **76**: 2033 (1954).

‡ Atomic weights in brackets represent the isotope of longest known half-period.

Tabular Data. A-1.2. Periodic table of elements.

1a	2a	3b	4b	5b	6b	7b	8	1b	2b	3a	4a	5a	6a	7a	0	Orbit
1 +1 −1 **H** 1.00797 1		Atomic Number → **50** +2 +4 Symbol → **Sn** Atomic Weight → 118.69 ← Electron Configuration: −18−18−4 ← Oxidation States KEY TO CHART													**2** 0 **He** 4.0026 2	K
3 +1 **Li** 6.939 2−1	**4** +2 **Be** 9.0122 2−2									**5** +3 **B** 10.811 2−3	**6** +2 +4 −4 **C** 12.01115 2−4	**7** +1 +2 +3 +4 +5 −1 **N** 14.0067 −2 −3 2−5	**8** −2 **O** 15.9994 2−6	**9** −1 **F** 18.9984 2−7	**10** 0 **Ne** 20.183 2−8	K-L
11 +1 **Na** 22.9898 2−8−1	**12** +2 **Mg** 24.312 2−8−2	Transition Elements						Transition Elements		**13** +3 **Al** 26.9815 2−8−3	**14** +2 +4 −4 **Si** 28.086 2−8−4	**15** +3 +5 −3 **P** 30.9738 2−8−5	**16** +4 +6 −2 **S** 32.064 2−8−6	**17** +1 +5 +7 −1 **Cl** 35.453 2−8−7	**18** 0 **Ar** 39.948 2−8−8	K-L-M
19 +1 **K** 39.102 −8−8−1	**20** +2 **Ca** 40.08 −8−8−2	**21** +3 **Sc** 44.956 −8−9−2	**22** +2 +3 +4 **Ti** 47.90 −8−10−2	**23** +2 +3 +4 +5 **V** 50.942 −8−11−2	**24** +2 +3 +6 **Cr** 51.996 −8−13−1	**25** +2 +3 +4 +7 **Mn** 54.9380 −8−13−2	**26** +2 +3 **Fe** 55.847 −8−14−2	**27** +2 +3 **Co** 58.9332 −8−15−2	**28** +2 +3 **Ni** 58.71 −8−16−2	**29** +1 +2 **Cu** 63.54 −8−18−1	**30** +2 **Zn** 65.37 −8−18−2	**31** +3 **Ga** 69.72 −8−18−3	**32** +2 +4 **Ge** 72.59 −8−18−4	**33** +3 +5 −3 **As** 74.9216 −8−18−5	**34** +4 +6 −2 **Se** 78.96 −8−18−6	**35** +1 +5 −1 **Br** 79.909 −8−18−7	**36** 0 **Kr** 83.80 −8−18−8	-L-M-N
37 +1 **Rb** 85.47 −18−8−1	**38** +2 **Sr** 87.62 −18−8−2	**39** +3 **Y** 88.905 −18−9−2	**40** +4 **Zr** 91.22 −18−10−2	**41** +3 +5 **Nb** 92.906 −18−12−1	**42** +3 +6 **Mo** 95.94 −18−13−1	**43** +4 +6 +7 **Tc** (99) −18−13−2	**44** +3 **Ru** 101.07 −18−15−1	**45** +3 **Rh** 102.905 −18−16−1	**46** +2 +4 **Pd** 106.4 −18−18−0	**47** +1 **Ag** 107.870 −18−18−1	**48** +2 **Cd** 112.40 −18−18−2	**49** +3 **In** 114.82 −18−18−3	**50** +2 +4 **Sn** 118.69 −18−18−4	**51** +3 +5 −3 **Sb** 121.75 −18−18−5	**52** +4 +6 −2 **Te** 127.60 −18−18−6	**53** +1 +5 +7 −1 **I** 126.9044 −18−18−7	**54** 0 **Xe** 131.30 −18−18−8	-M-N-O
55 +1 **Cs** 132.905 −18−8−1	**56** +2 **Ba** 137.34 −18−8−2	**57*** +3 **La** 138.91 −18−9−2	**72** +4 **Hf** 178.49 −32−10−2	**73** +5 **Ta** 180.948 −32−11−2	**74** +6 **W** 183.85 −32−12−2	**75** +4 +6 +7 **Re** 186.2 −32−13−2	**76** +3 +4 **Os** 190.2 −32−14−2	**77** +3 +4 **Ir** 192.2 −32−15−2	**78** +2 +4 **Pt** 195.09 −32−16−2	**79** +1 +3 **Au** 196.967 −32−18−1	**80** +1 +2 **Hg** 200.59 −32−18−2	**81** +1 +3 **Tl** 204.37 −32−18−3	**82** +2 +4 **Pb** 207.19 −32−18−4	**83** +3 +5 **Bi** 208.980 −32−18−5	**84** +2 +4 **Po** (210) −32−18−6	**85** **At** (210) −32−18−7	**86** 0 **Rn** (222) −32−18−8	-N-O-P
87 +1 **Fr** (223) −18−8−1	**88** +2 **Ra** (226) −18−8−2	**89**** +3 **Ac** (227) −18−9−2														-O-P-Q

*Lanthanides	**58** +3 +4 **Ce** 140.12 −19−9−2	**59** +3 **Pr** 140.907 −20−9−2	**60** +3 **Nd** 144.24 −22−8−2	**61** +3 **Pm** (145) −23−8−2	**62** +2 +3 **Sm** 150.35 −24−8−2	**63** +2 +3 **Eu** 151.96 −25−8−2	**64** +3 **Gd** 157.25 −25−9−2	**65** +3 **Tb** 158.924 −26−9−2	**66** +3 **Dy** 162.50 −28−8−2	**67** +3 **Ho** 164.930 −29−8−2	**68** +3 **Er** 167.26 −30−8−2	**69** +3 **Tm** 168.934 −31−8−2	**70** +2 +3 **Yb** 173.04 −32−8−2	**71** +3 **Lu** 174.97 −32−9−2	-N-O-P
**Actinides	**90** +4 **Th** 232.038 −19−9−2	**91** +5 +4 **Pa** (231) −20−9−2	**92** +3 +4 +5 +6 **U** 238.03 −21−9−2	**93** +3 +4 +5 +6 **Np** (237) −22−9−2	**94** +3 +4 +5 +6 **Pu** (242) −23−9−2	**95** +3 +4 +5 +6 **Am** (243) −24−9−2	**96** +3 **Cm** (247) −25−9−2	**97** +3 +4 **Bk** (249) −26−9−2	**98** +3 **Cf** (251) −28−8−2	**99** **Es** (254) −29−8−2	**100** **Fm** (252) −30−8−2	**101** **Md** (256) −31−8−2	**102** (254) −32−8−2	**103** **Lw**	-O-P-Q

Numbers in parentheses are mass numbers of most stable isotope of that element.

Notes on the Use of Energy Level and Grotrian Diagrams

(Based on book by Bashkin and Stoner)

Two types of diagrams have been indispensable since their first appearance in the literature of atomic structure: energy-level diagrams and electronic transition (Grotrian) diagrams.

Energy-Level Diagrams

The general format of these diagrams is quite standard — a level is represented by a short, horizontal line which is located by two coordinates. The ordinate is the level's energy, always given in inverse centimeters [cm^{-1}], and the abscissa indicates a combination of orbital and spin angular momenta quantum numbers. The notation adhered to is primarily that of Kelly's[1] with the adoption of the "primed" convention consistent with Moore[2].

To clarify the diagrams, each system is exhibited in a format best suited for it. For example, when energy-level densities are inconveniently high, the topmost levels are indicated together with all lower levels having a reasonable density.

The full precision of the latest experimental energy-level values has been retained and is exhibited on the diagram. In general, theoretically calculated values are shown with less precision than is given in the original sources.

The primary data on which the diagrams are based were taken primarily from Kelly's[1] exhaustive tabulations and several other references[2-5]. In addition to these general references, several other references are cited for many of the systems.

Several instances occur in which ions possessing various core configurations result in many different final configurations. When this occurs, each core is given a separate diagram — specifically differentiated from the others in the title and corner labels.

Each energy-level diagram contains (1) a key which defines various symbols, (2) the ionization level (from Kelly and Palumbo[3]), and (3) the ground configurations of the ion and the next higher ion. The j-ℓ and j-j intermediate coupling schemes are respectively represented by [ ] and { }. All energy-levels and j-values are listed in order of increasing excitation. When intermediate coupling occurs, the intermediate-coupling angular momenta are shown in a vertical array in order of

increasing excitation, from bottom to top. In cases where a single energy occurs for two or more j-values, the following notation has been adopted.

For example: 797270 ———— 3d ([5/2, 3/2], 1/2),
797060

which means that the lower level is common to the first two j-values and the upper level belongs to j = 1/2.

The ionization level is shown as a horizontal dashed line. The ionization level is simply the energy difference between the ground term and the bottom of the continuum for the terms having the ground-term core.

Grotrian Diagrams

Diagrams showing transitions from one spectroscopic term to another are called "Grotrian Diagrams." Most of the transitions have been extracted from the listing of Kelly and Palumbo[3] and Striganov and Sventitskii[4]. A few others were taken from later publications. When line densities became too great for clarity, the line of shortest wavelengths together with as many of the other lines as could be conveniently drawn, were included. Lines that were omitted were selected arbitrarily. In some cases, the diagram was divided into two or more diagrams. In most cases, the same energy scales were used for both the Grotrian and energy-level diagrams.

The full precision with which wavelengths have been measured has not been incorporated into the diagrams. Usually, the precisions illustrated on the diagrams is one significant figure less than that occurring in the literature. When two lines occur in a multiplet, two numbers are given, separated by a comma. When more than two lines occur, the extreme wavelengths are given, separated by a dash. Wavelengths are in vacuum for values shorter than 2000 $\mathring{A}$ and in air for longer values.

Hyperfine effects, radio-frequency spectroscopy, and inner-shell transitions have been, for the most part, neglected.

Acknowledgments

The up-to-date enery-level and Grotrian diagrams contained herein have been provided by Stanely Bashkin[6] and John O. Stoner, Jr., who are directing an extensive compilation project at the University of Arizona. Complete information on all neutral atoms and positive ions through Titanium XXII is presently available in three of their publications[7,8,9]

References

1. R. L. Kelly, Tabulation of Energy Levels for Atoms and Ions (unpublished).

2. C. E. Moore, Atomic Energy Levels, Circular 467, National Bureau of Standards, 1 (1949), Reprinted as NSRDS-NBS 35, Vol. 1.

3. R. L. Kelly and L. J. Palumbo, Atomic and Ionic Emission Lines Below 2000 Angstroms, Hydrogen Through Krypton, U.S. Government Printing Office, Washington, D.C., Stock No. 0851-00061 (1973).

4. A. R. Striganov and N. S. Sventitskii, Tables of Spectral Lines of Neutral and Ionized Atoms, IFI/Plenum, New York (1968).

5. C. E. Moore and P. W. Merrill, Partial Grotrian Diagrams of Astrophysical Interest, Appendix A of Lines of the Chemical Elements in Astronomical Spectra, Carnegie Institute of Washington Publication 610 (1958). Reprinted as NSRDS-NBS-23.

6. Stanley Bashkin (private communication).

7. Stanley Bashkin and John O. Stoner, Jr., Atomic Energy Levels and Grotrian Diagrams, Vol. I, Hydrogen I - Phosphorus XV, North Holland, New York (1975).

8. Stanley Bashkin and John O. Stoner, Jr., Atomic Energy Levels and Grotrian Diagrams, Vol. II, Sulfur I - Titanium XXII, North Holland, New York (1978).

9. Stanley Bashkin and John O. Stoner, Jr., Atomic Energy Levels and Grotrian Diagrams, Vol. I, Addenda, North Holland, New York (1978).

Tabular Data. A-1.3. Diagram for H (Z = 1).

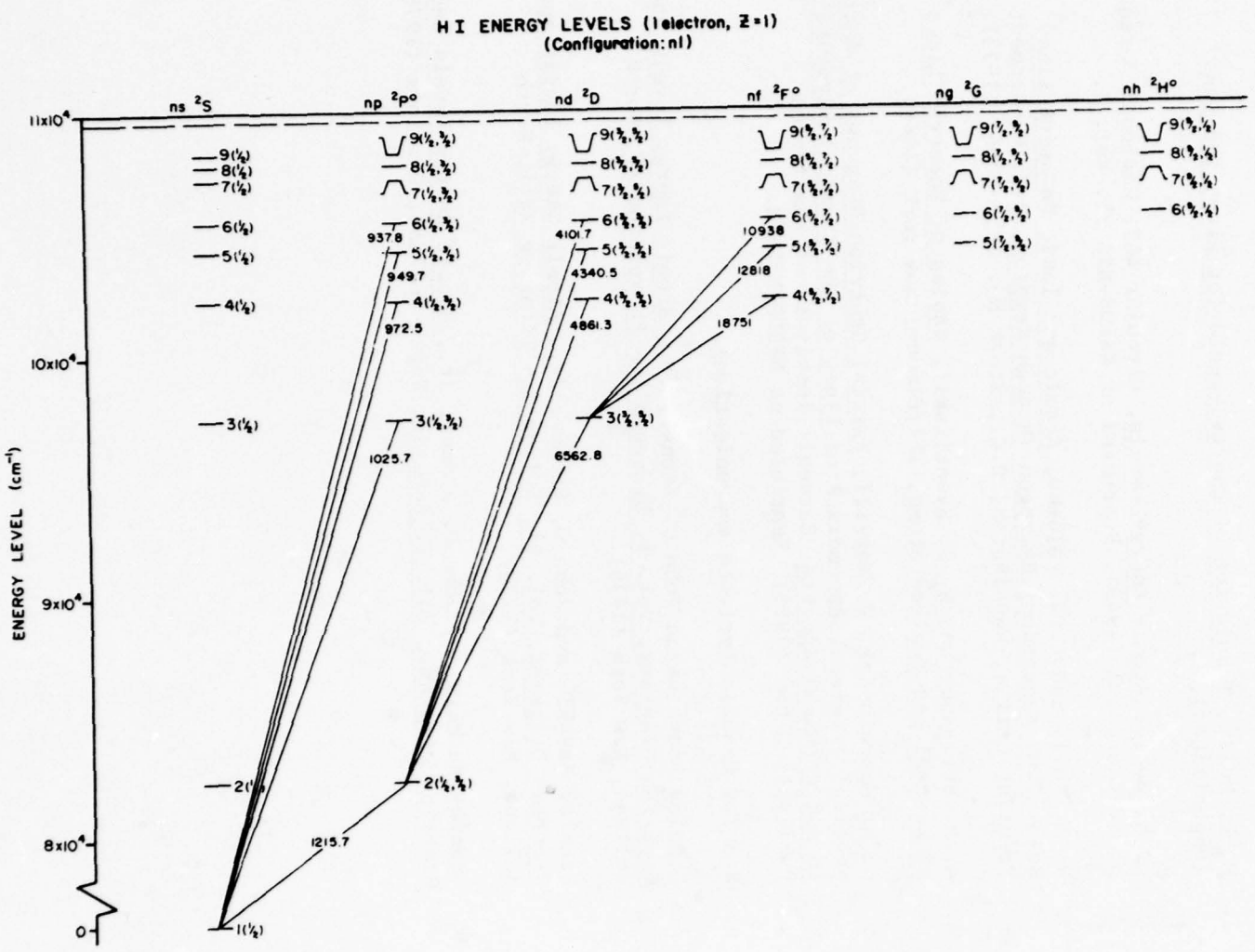

Tabular Data. A-1.4. Diagram for H (Z = 1).

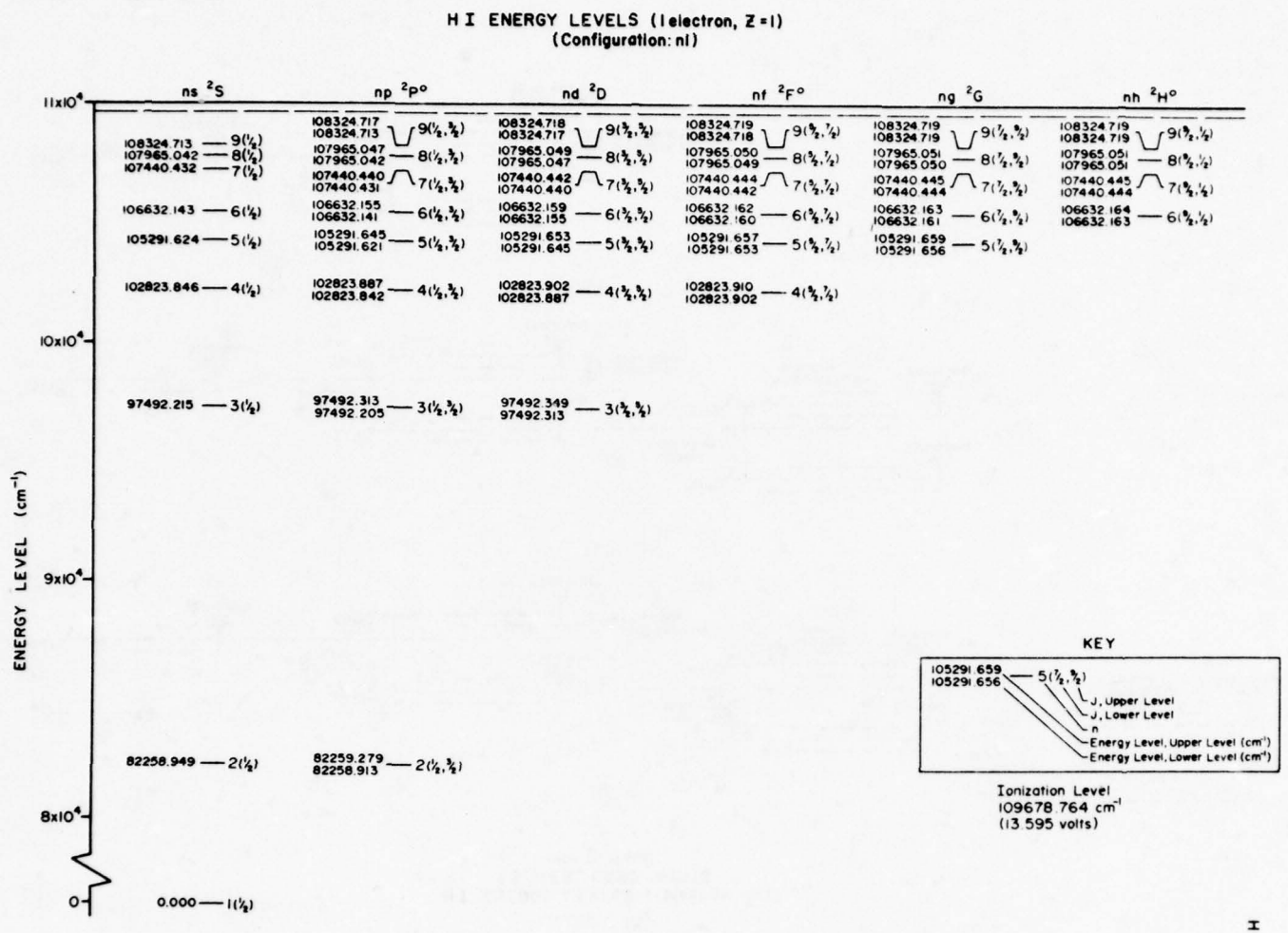

Tabular Data. A-1.5. Diagram for H (Z = 1).

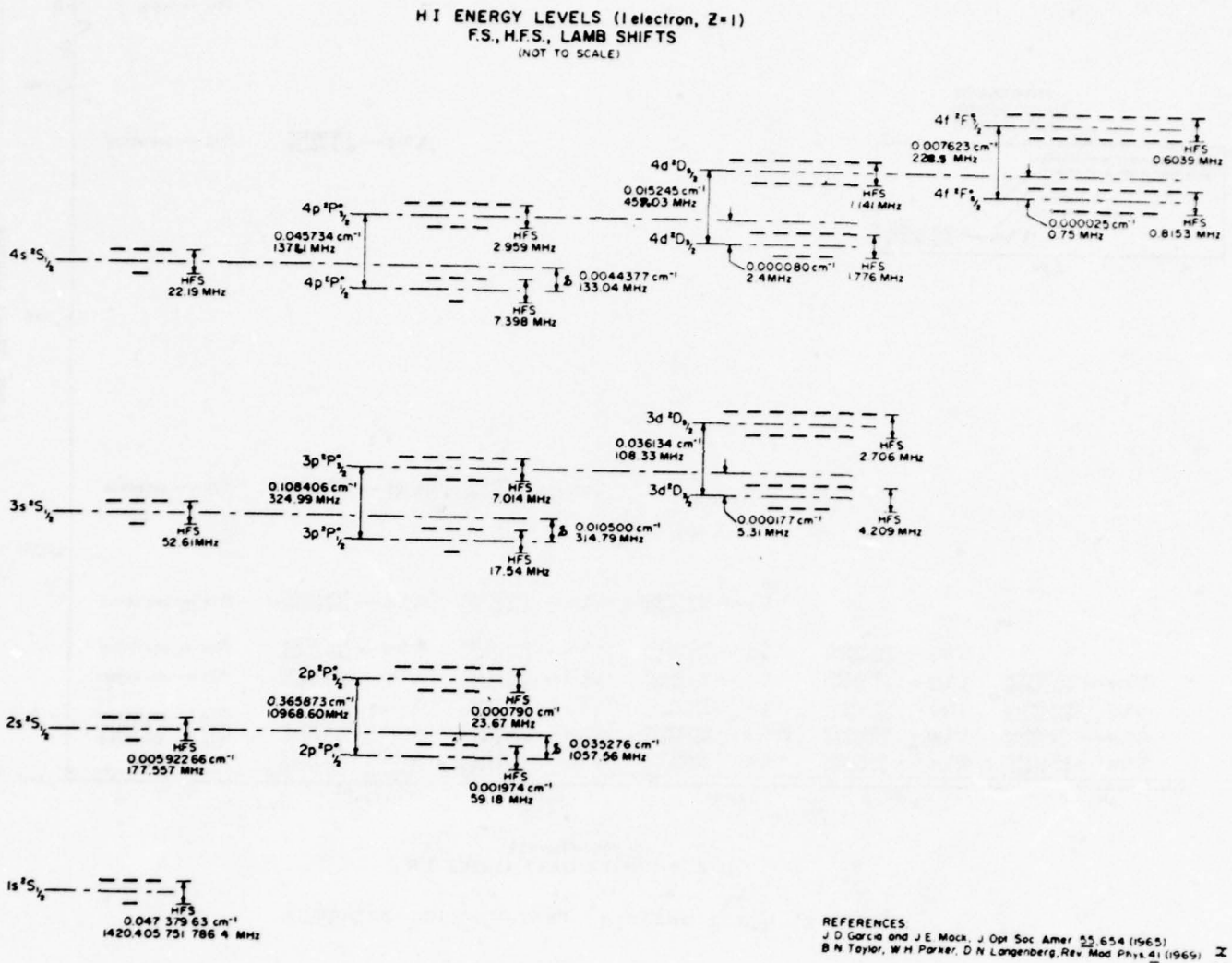

REFERENCES
J. D. Garcia and J. E. Mack, J. Opt. Soc. Amer. 55, 654 (1965)
B. N. Taylor, W. H. Parker, D. N. Langenberg, Rev. Mod. Phys. 41 (1969)

Tabular Data. A-1.6. Diagram for He (Z = 2).

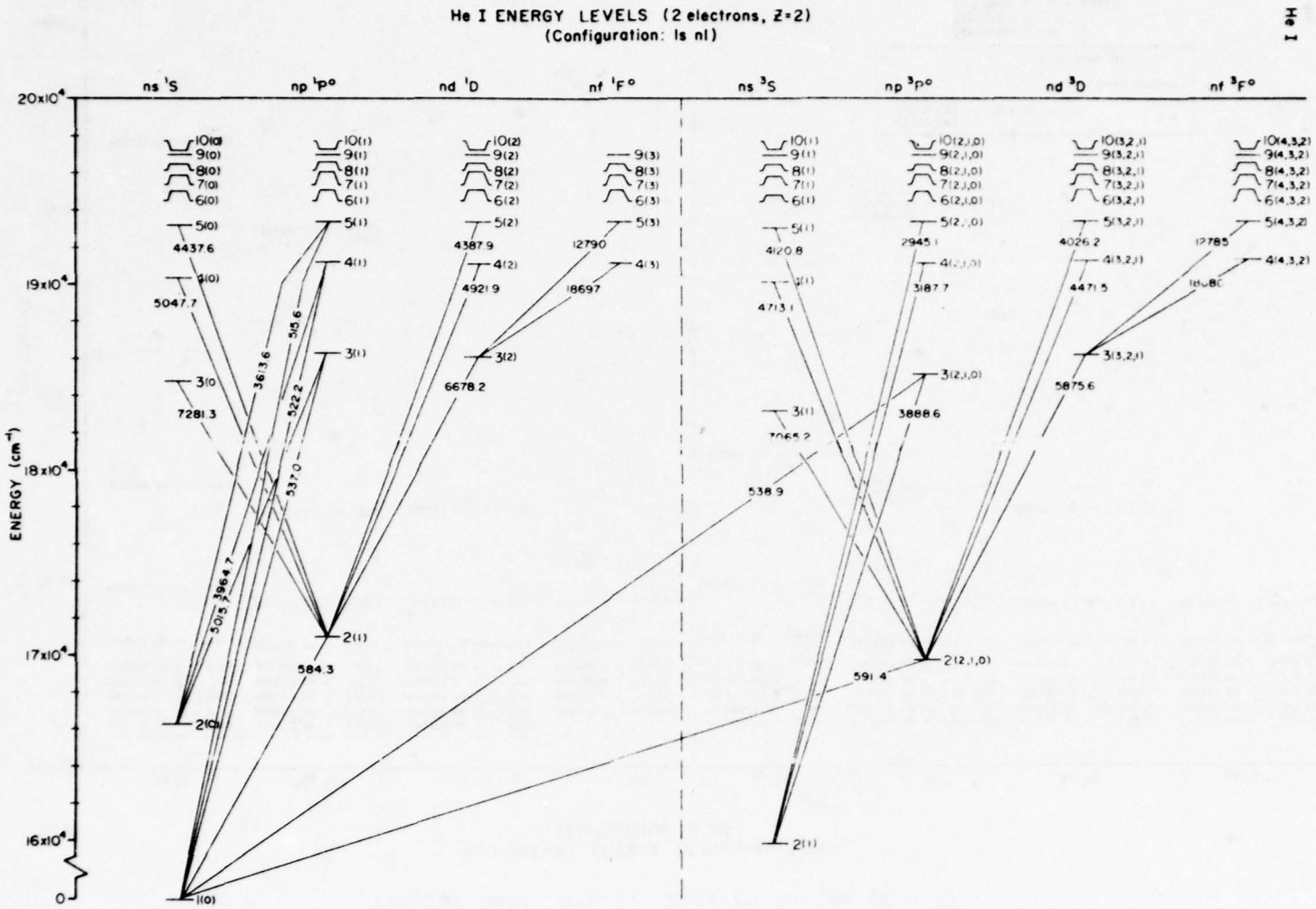

Tabular Data. A-1.7. Diagram for He (Z = 2).

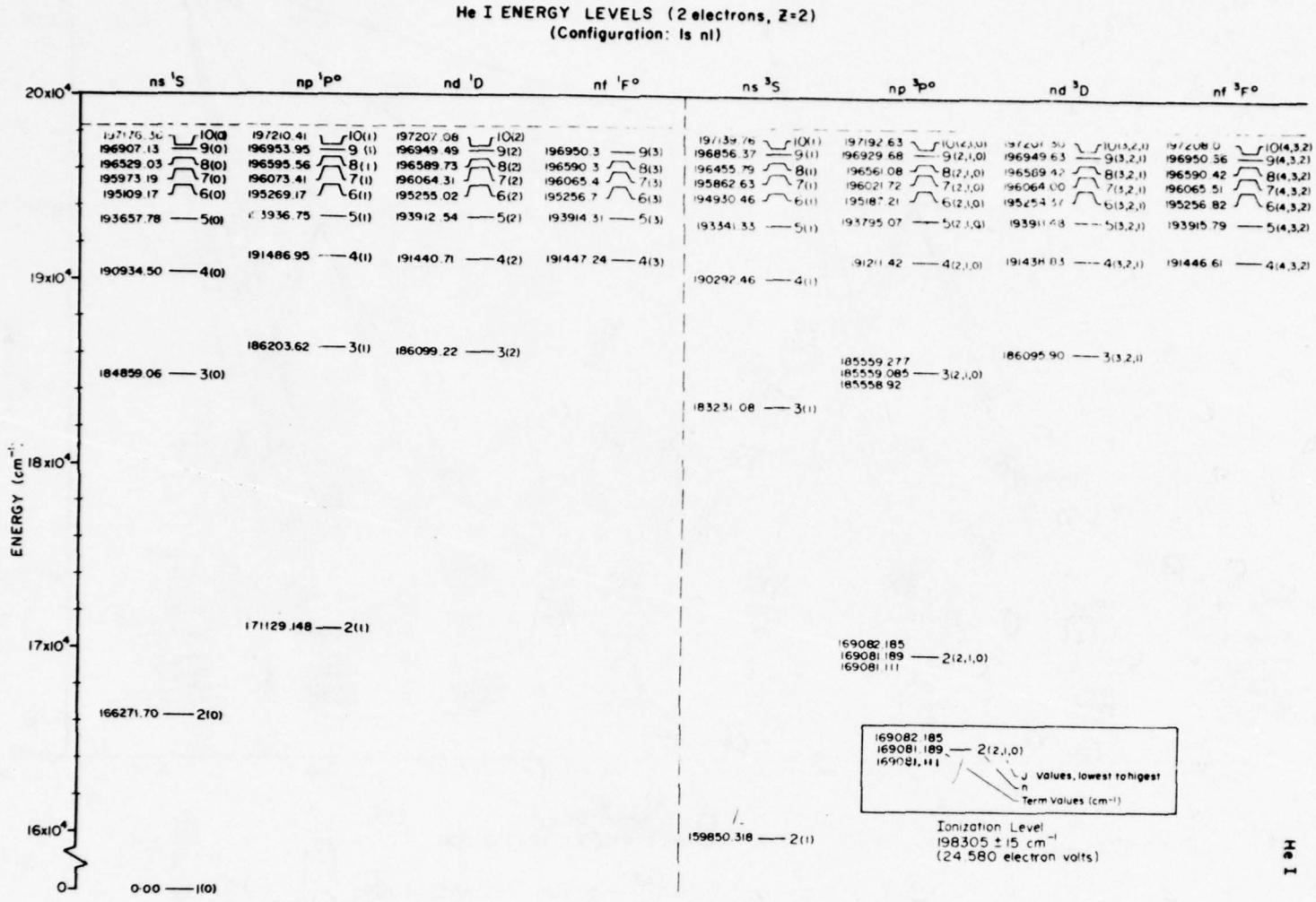

Tabular Data. A-1.8. Diagram for He (Z = 2).

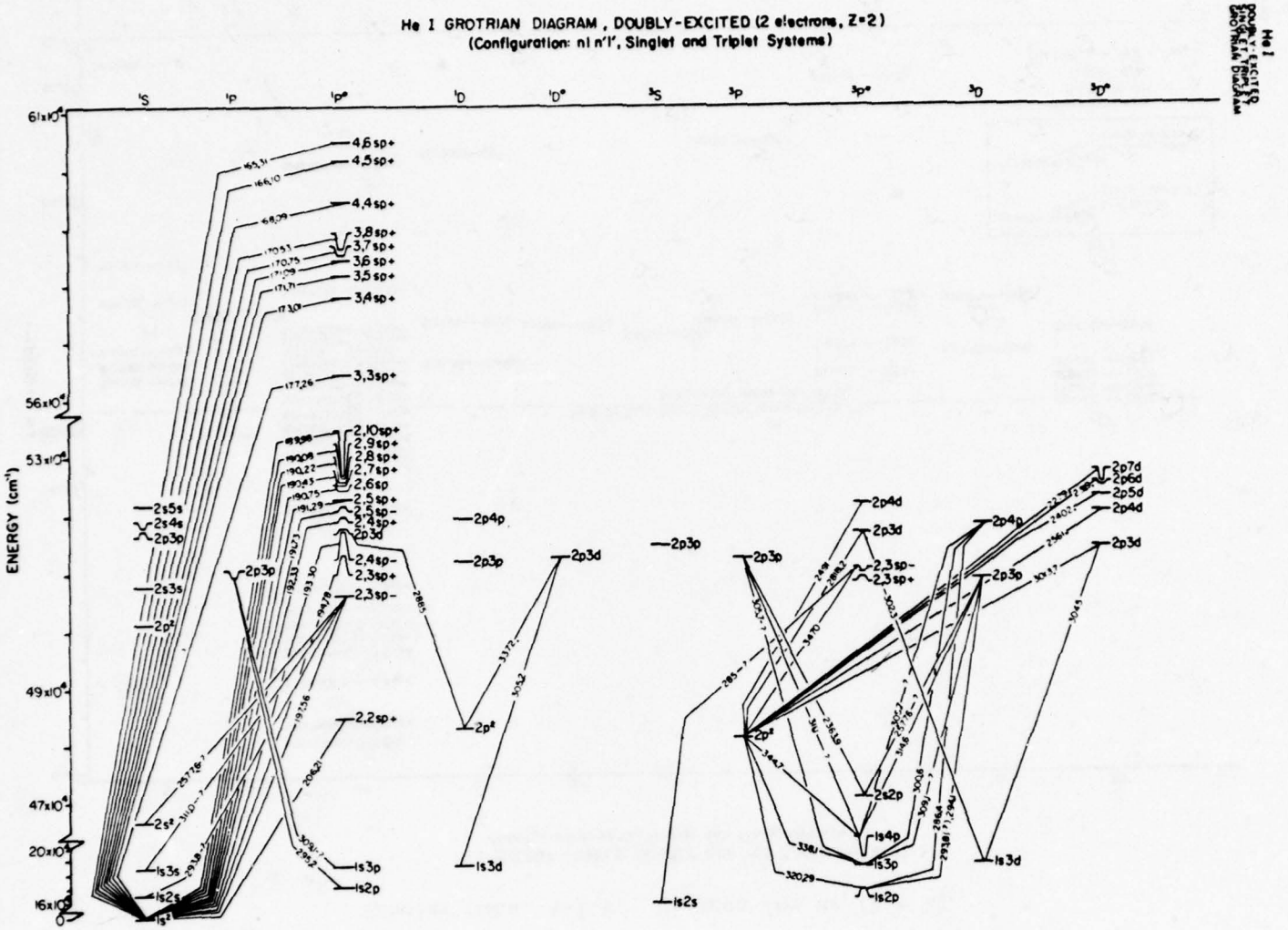

Tabular Data. A-1.9. Diagram for He (Z = 2).

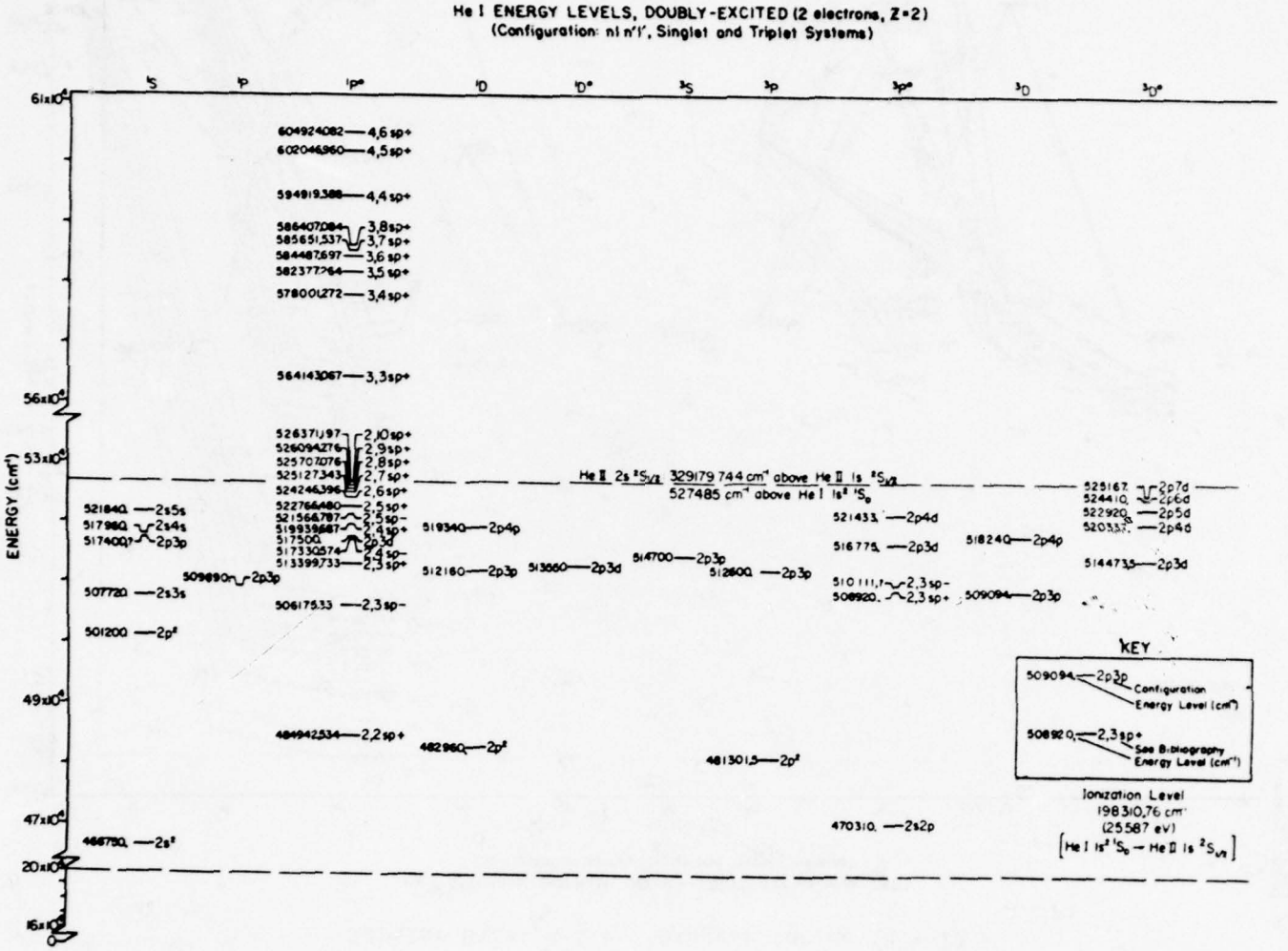

Tabular Data. A-1.10. Diagram for He^+ (Z = 2).

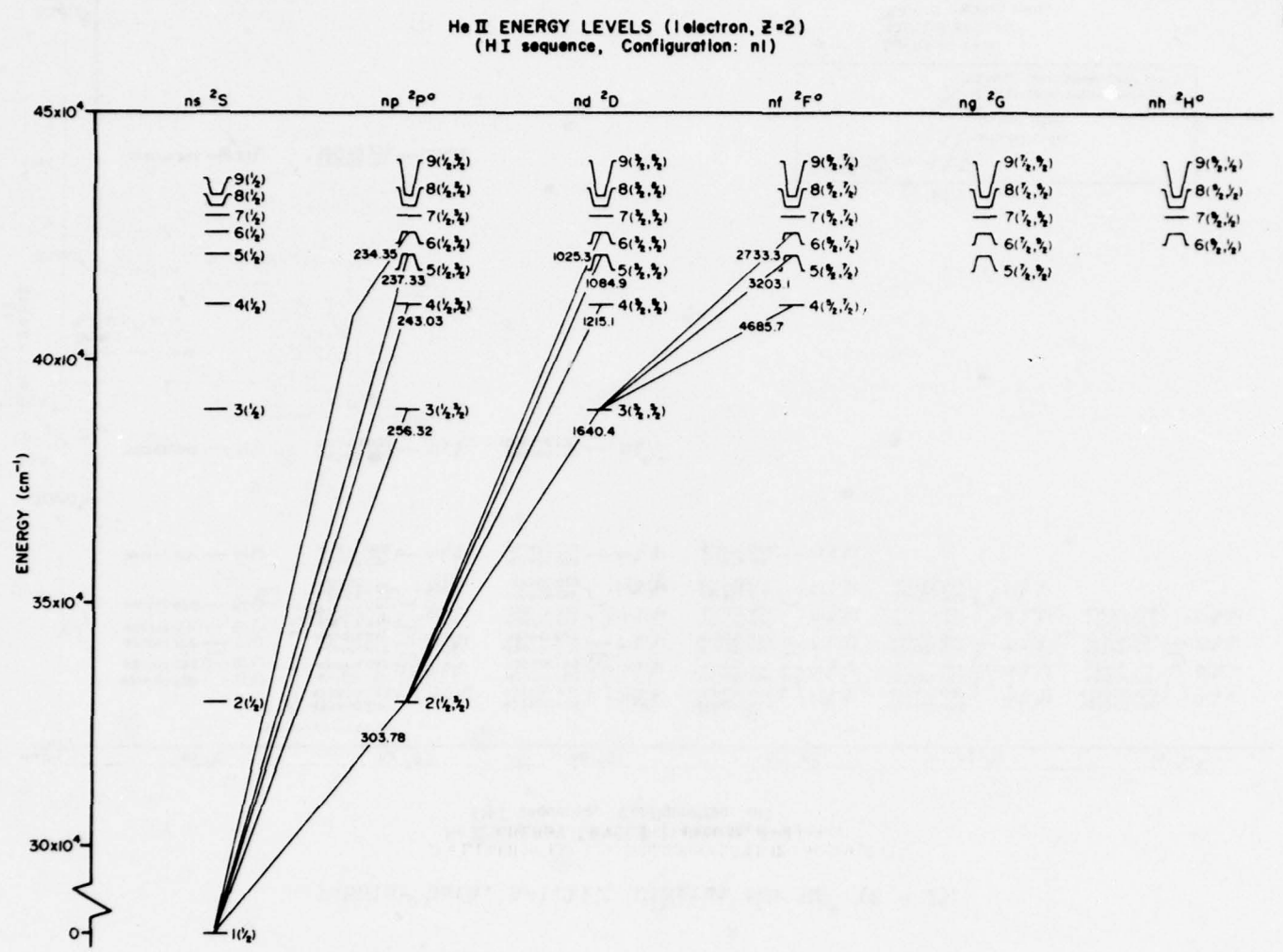

Tabular Data. A-1.11. Diagram for He^{+} (Z = 2).

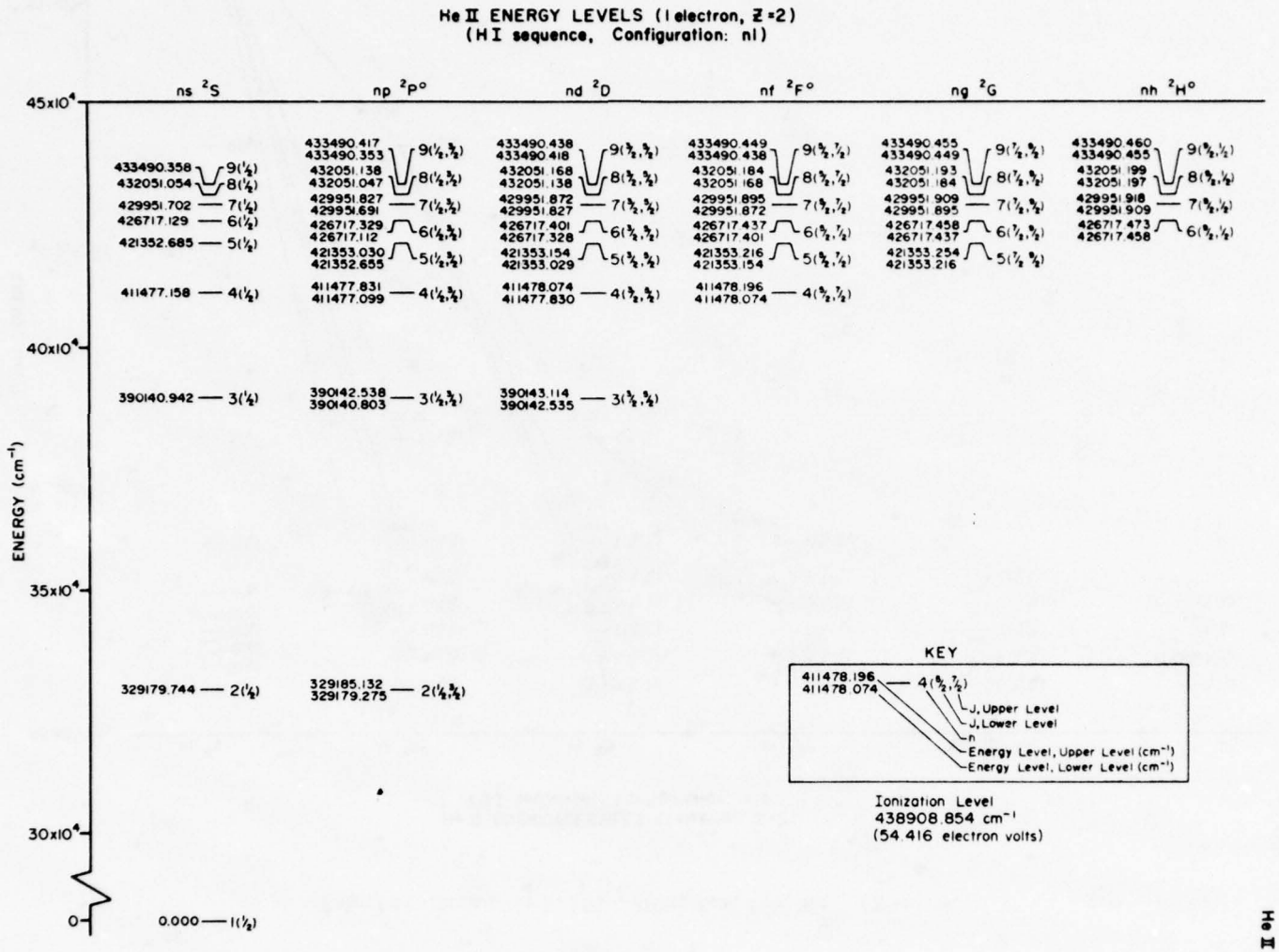

Tabular Data. A-1.12. Diagram for B (Z = 5).

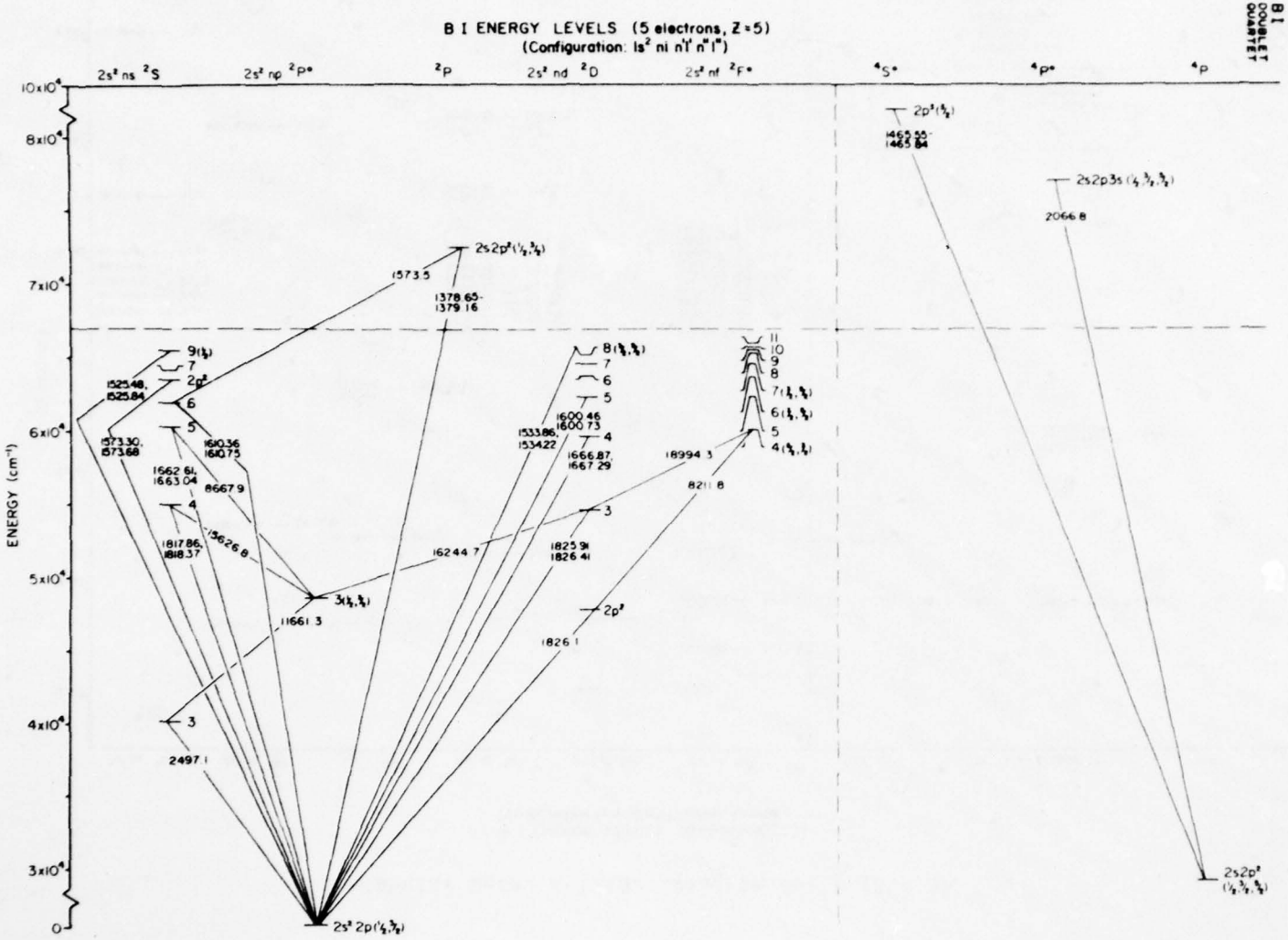

Tabular Data. A-1.13. Diagram for B (Z = 5).

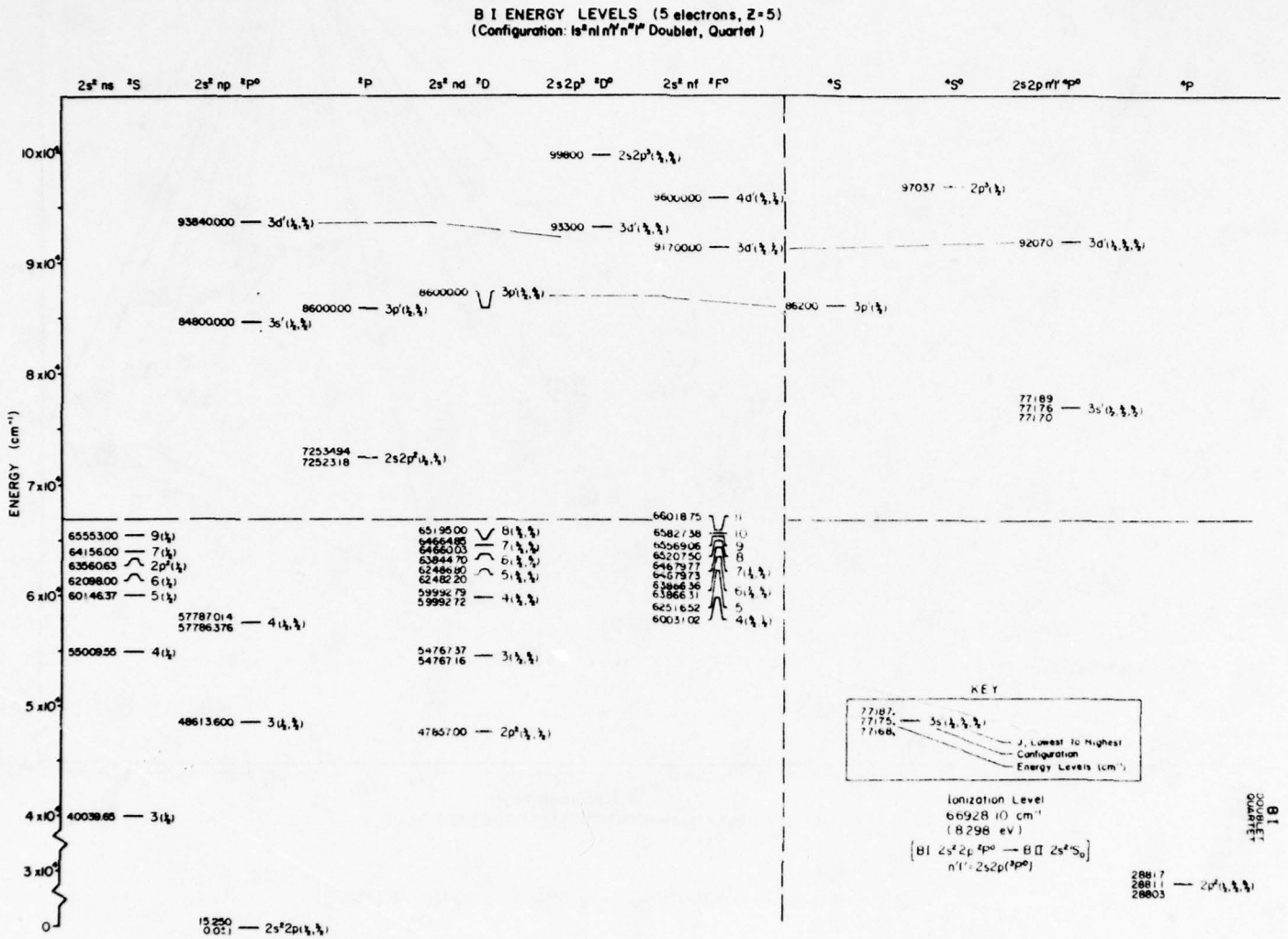

Tabular Data. A-1.14. Diagram for B^+ (Z = 5).

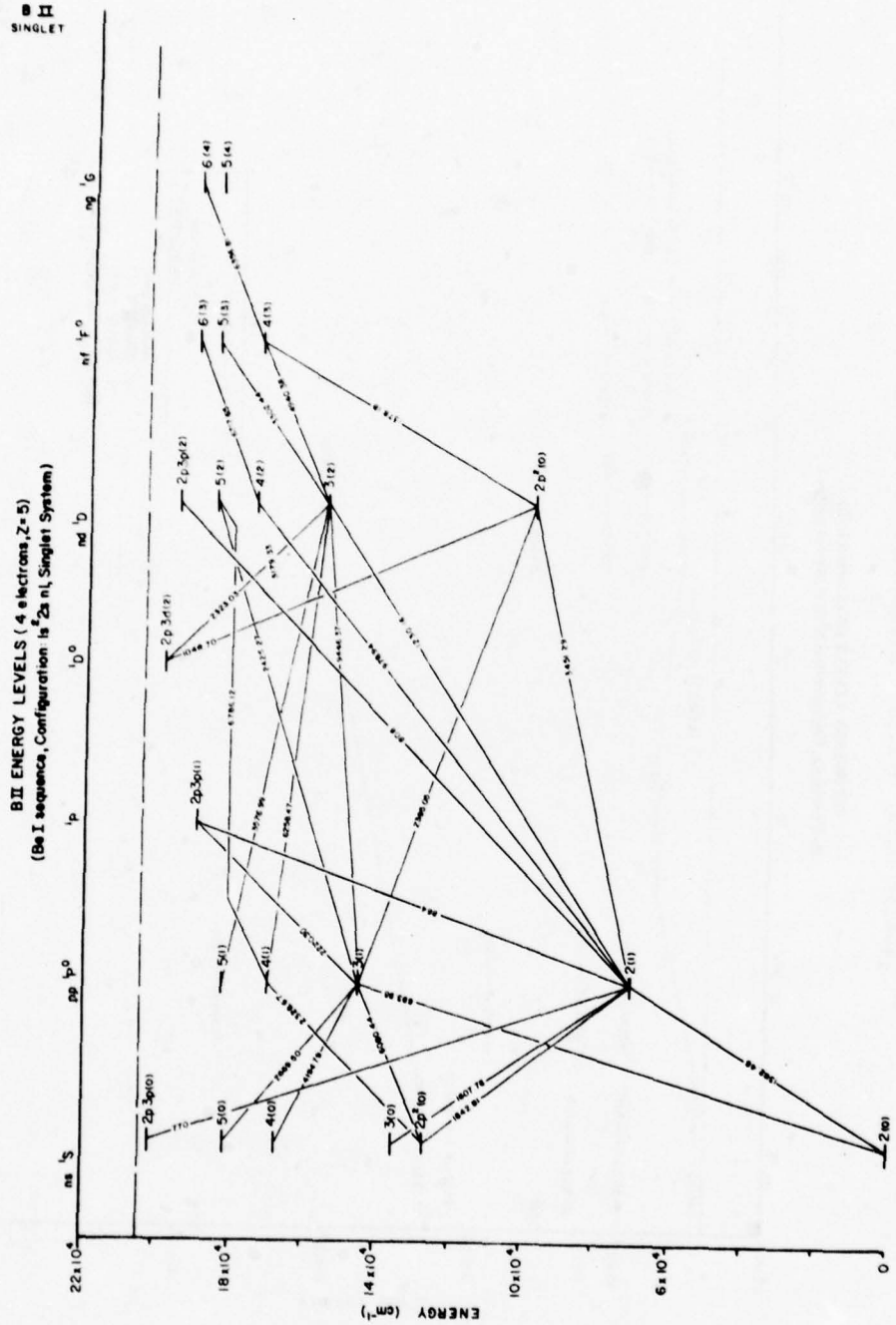

Tabular Data. A-1.15. Diagram for B^{+} (Z = 5).

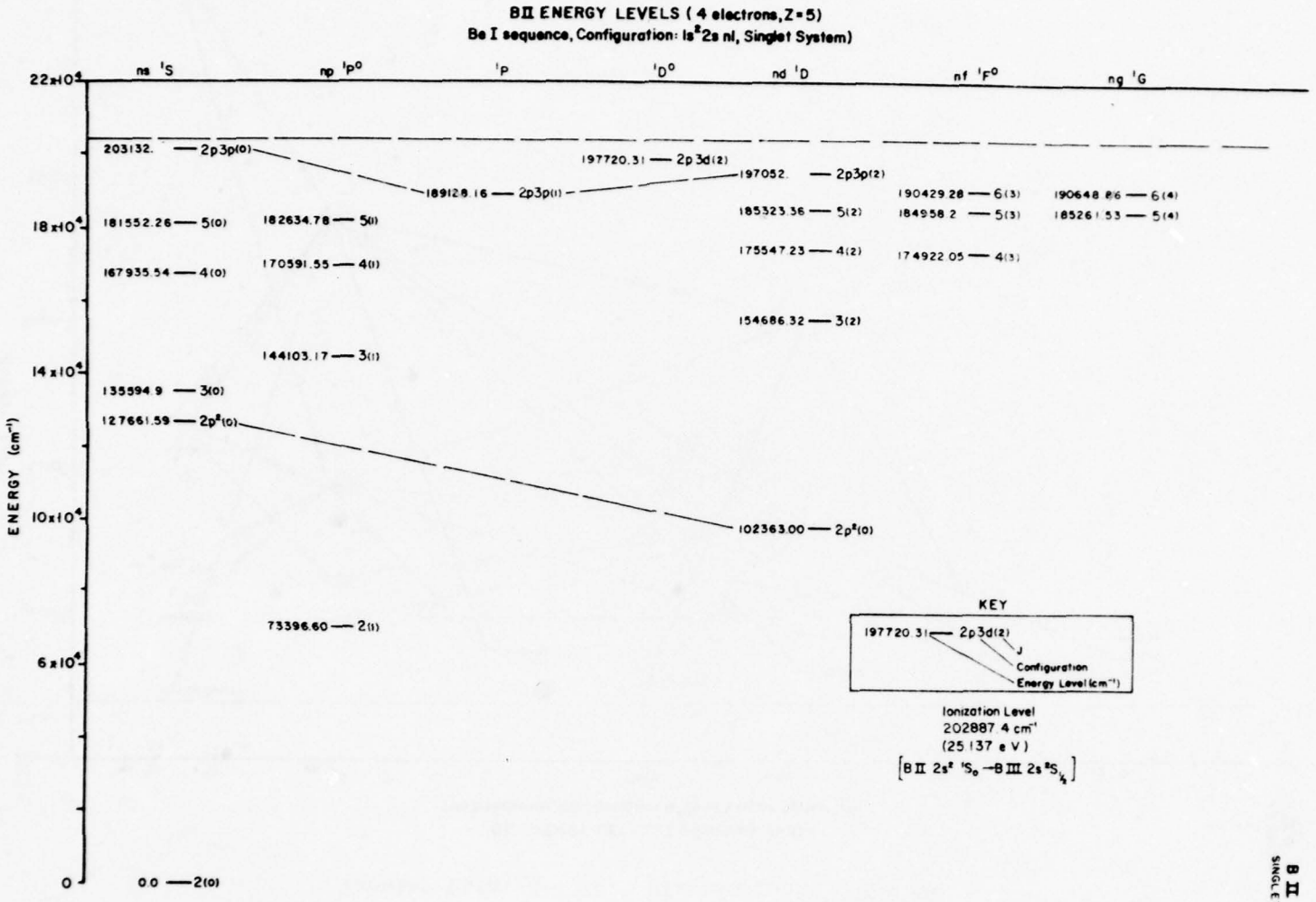

Tabular Data. A-1.16. Diagram for B^+ (Z = 5).

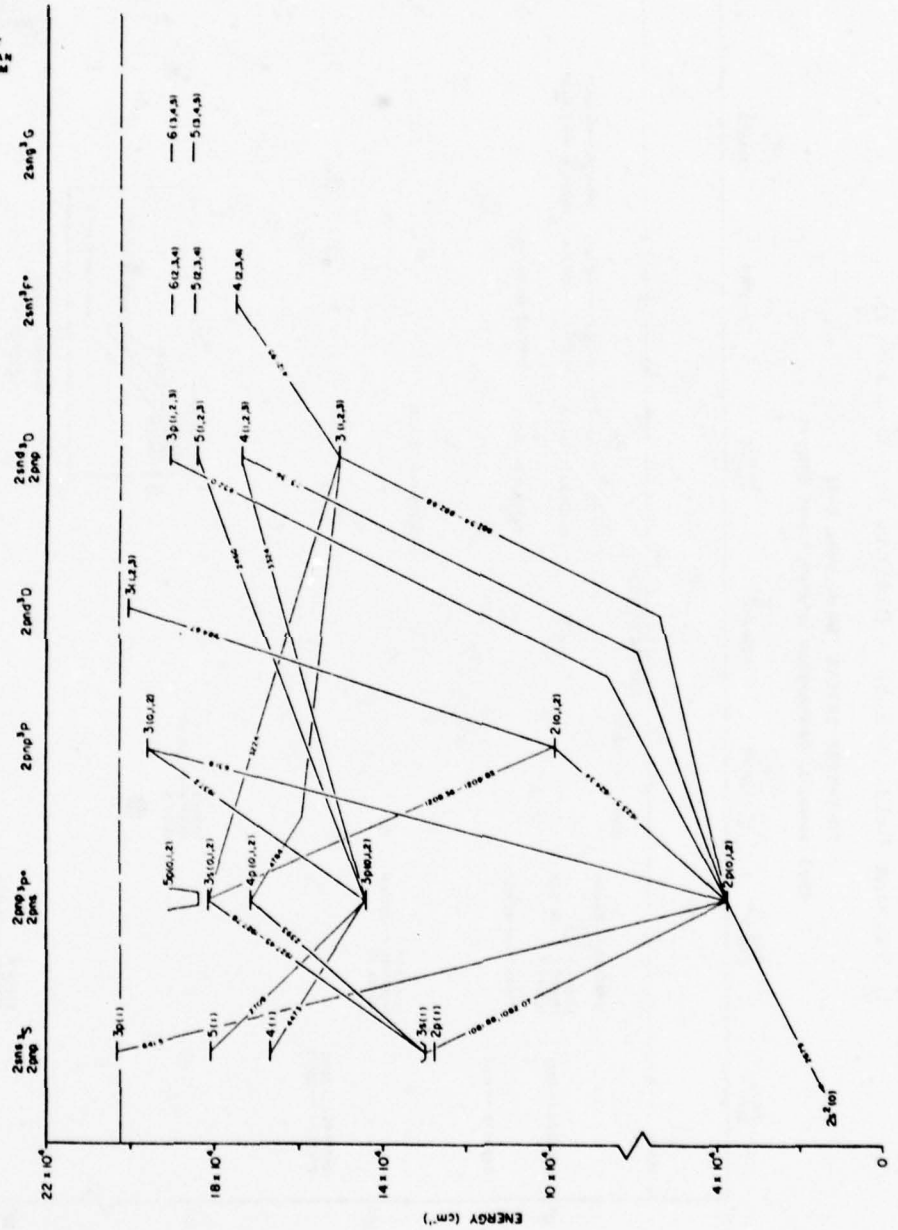

Tabular Data. A-1.17. Diagram for B^{+} (Z = 5).

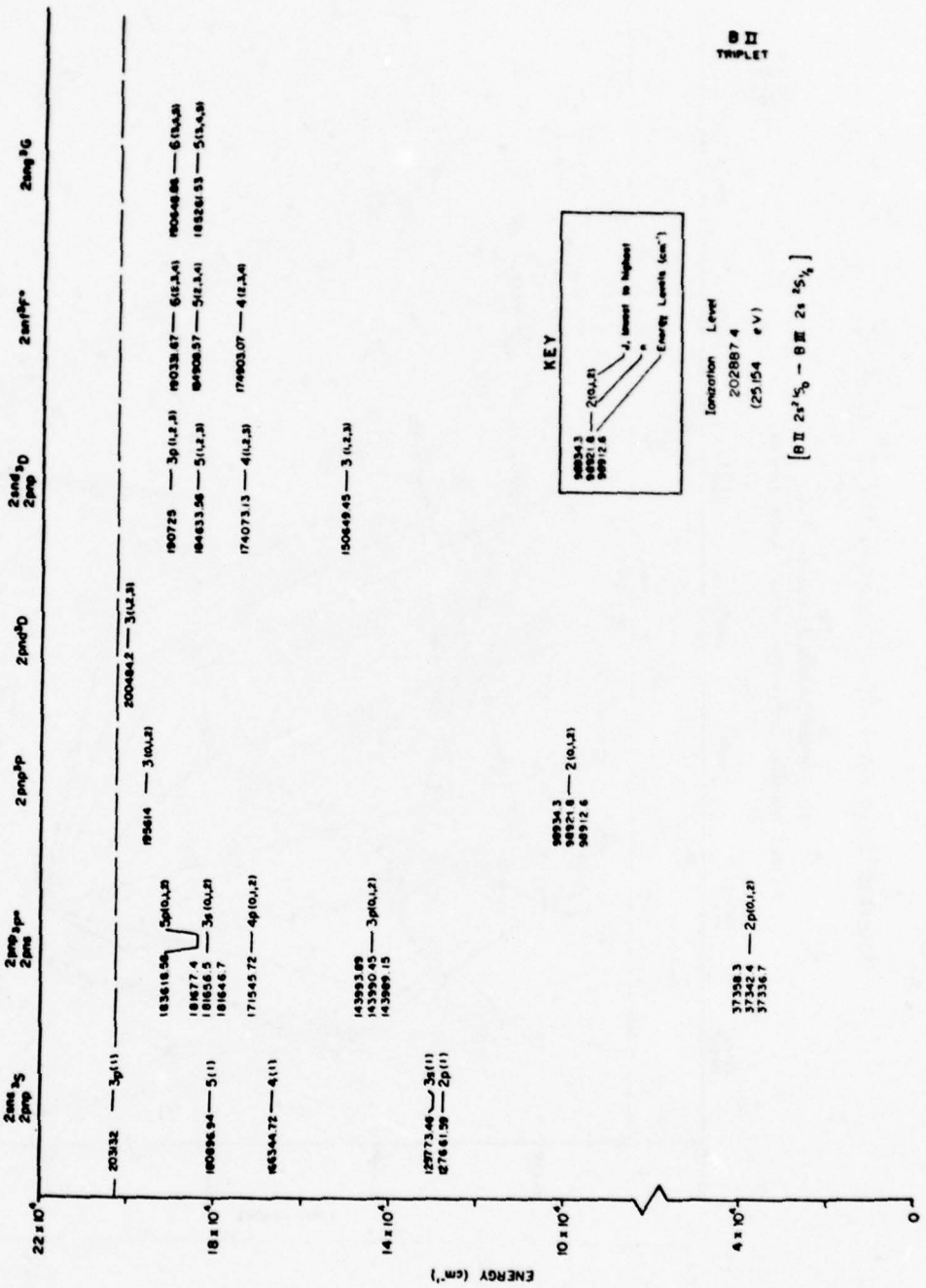

Tabular Data. A-1.18. Diagram for C (Z = 6).

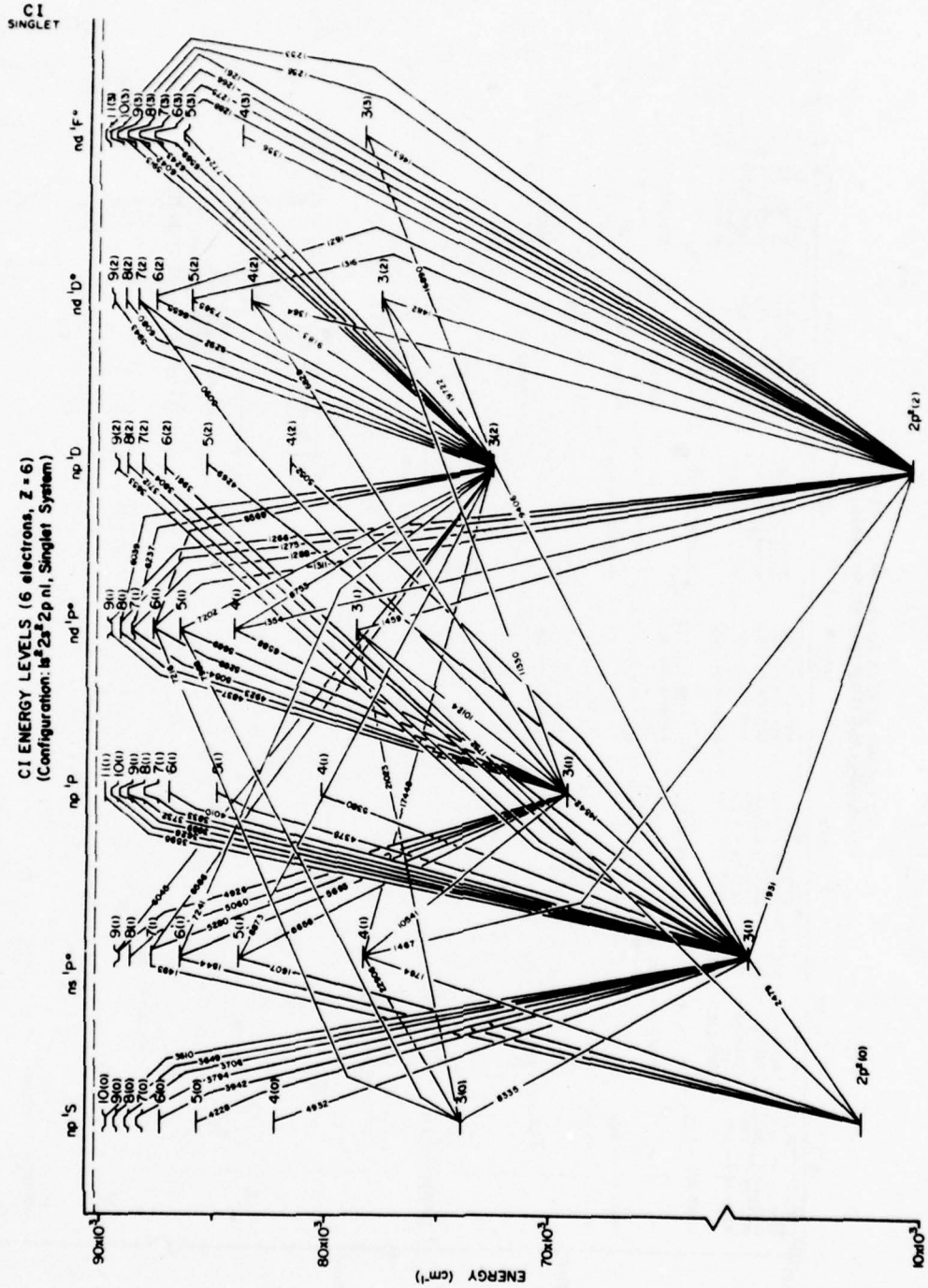

Tabular Data. A-1.19. Diagram for C (Z = 6).

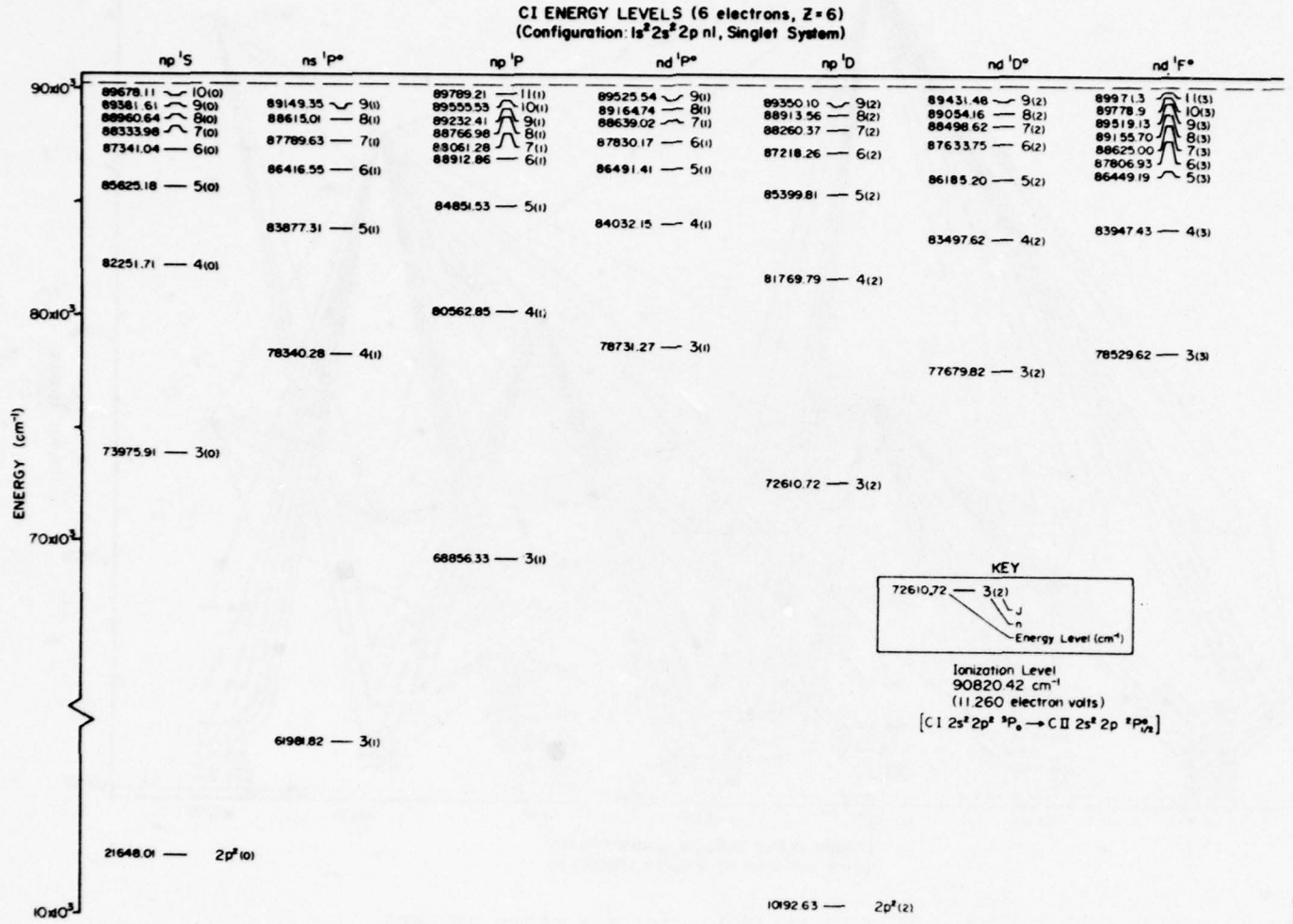

Tabular Data. A-1.20. Diagram for C (Z = 6).

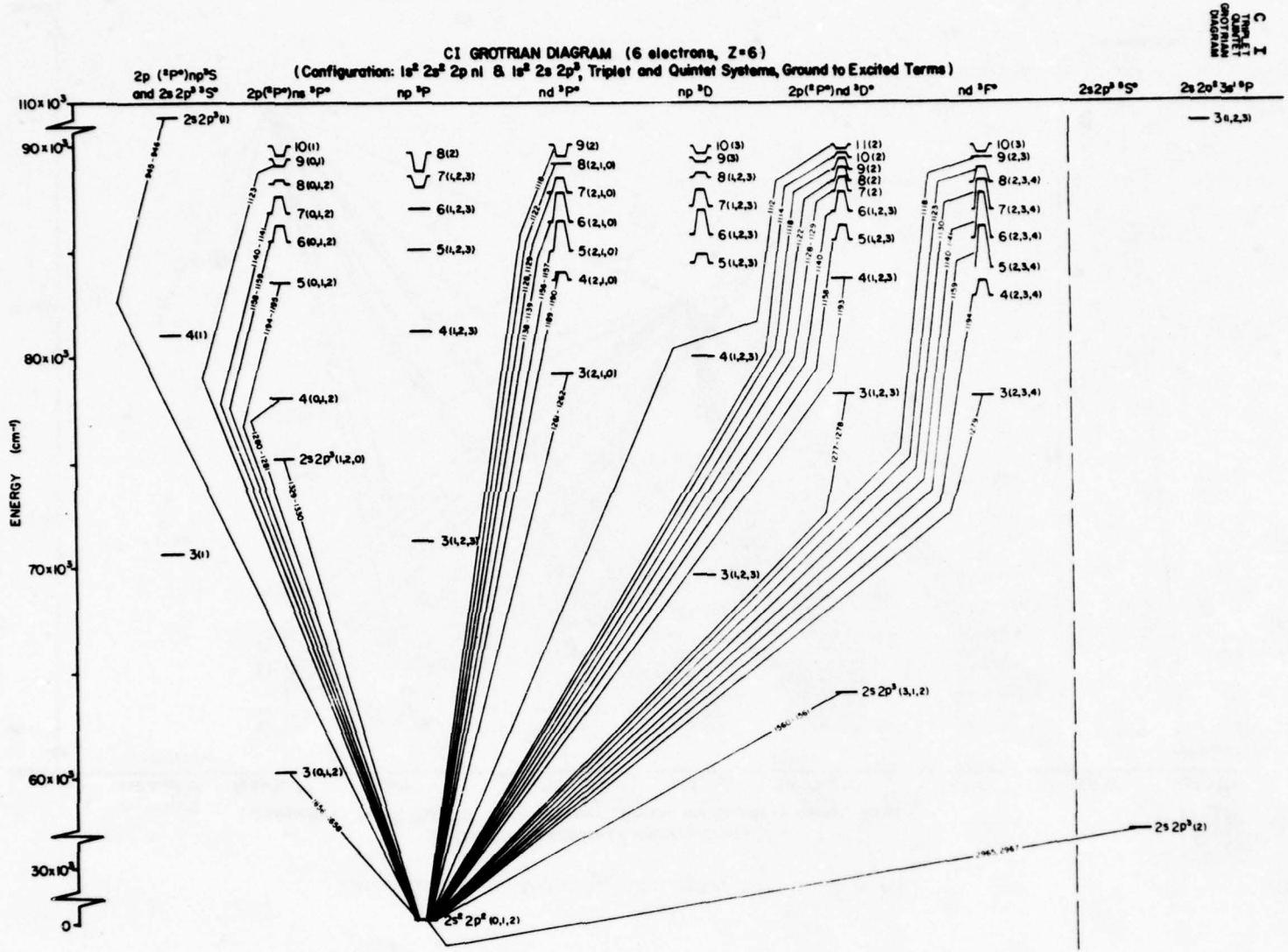

Tabular Data. A-1.21. Diagram for C (Z = 6).

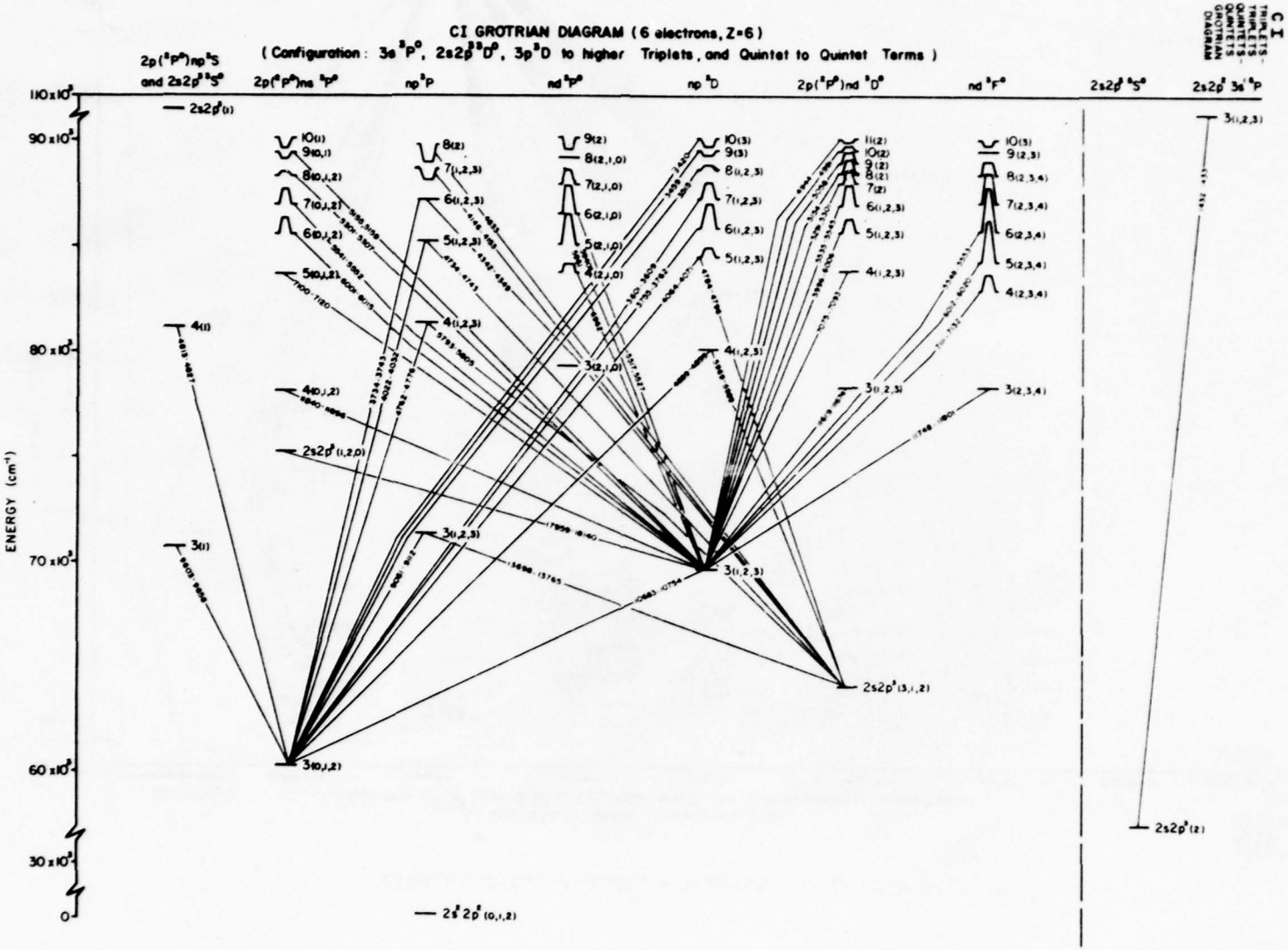

Tabular Data. A-1.22. Diagram for C (Z = 6).

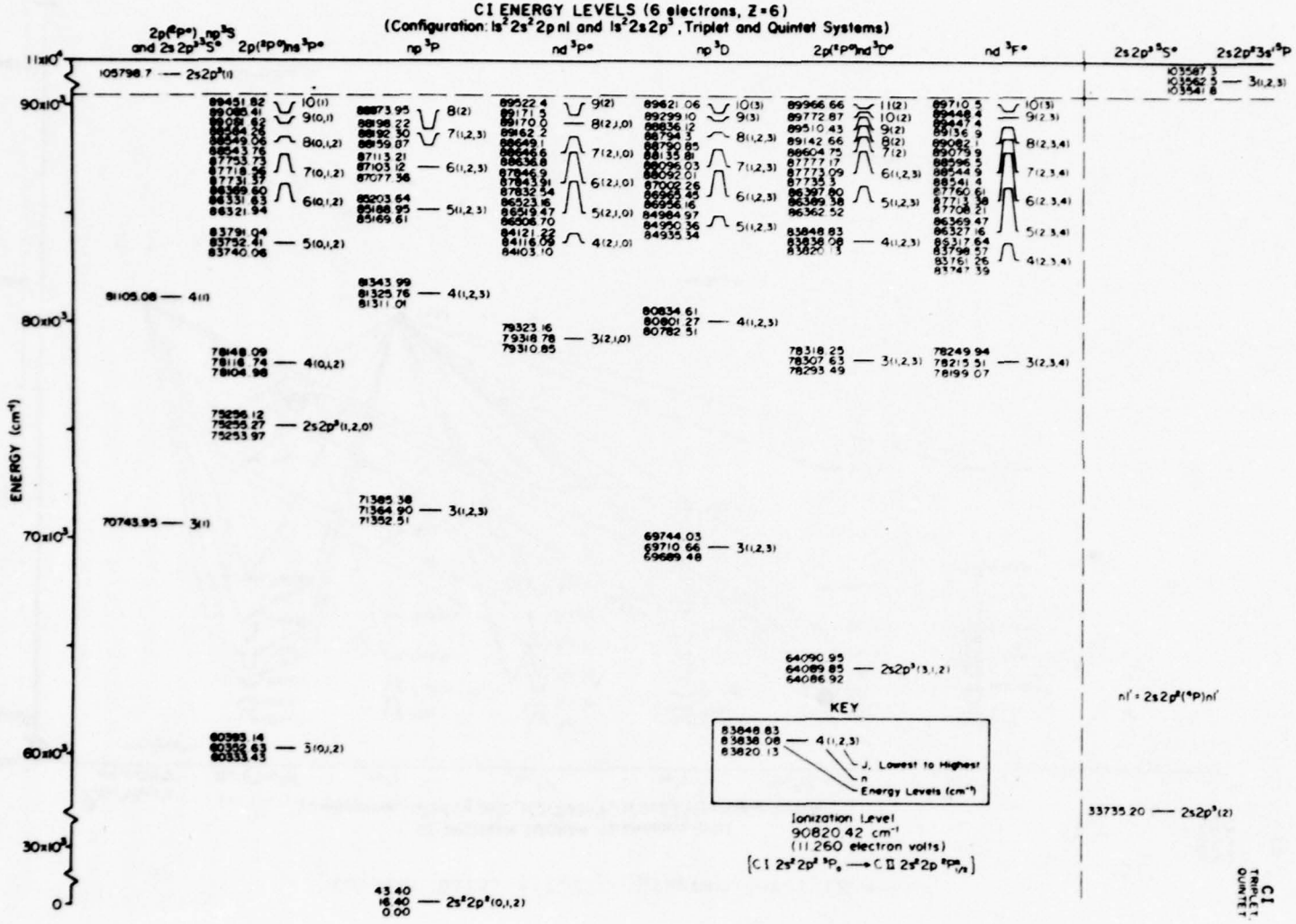

Tabular Data. A-1.23. Diagram for C (Z = 6).

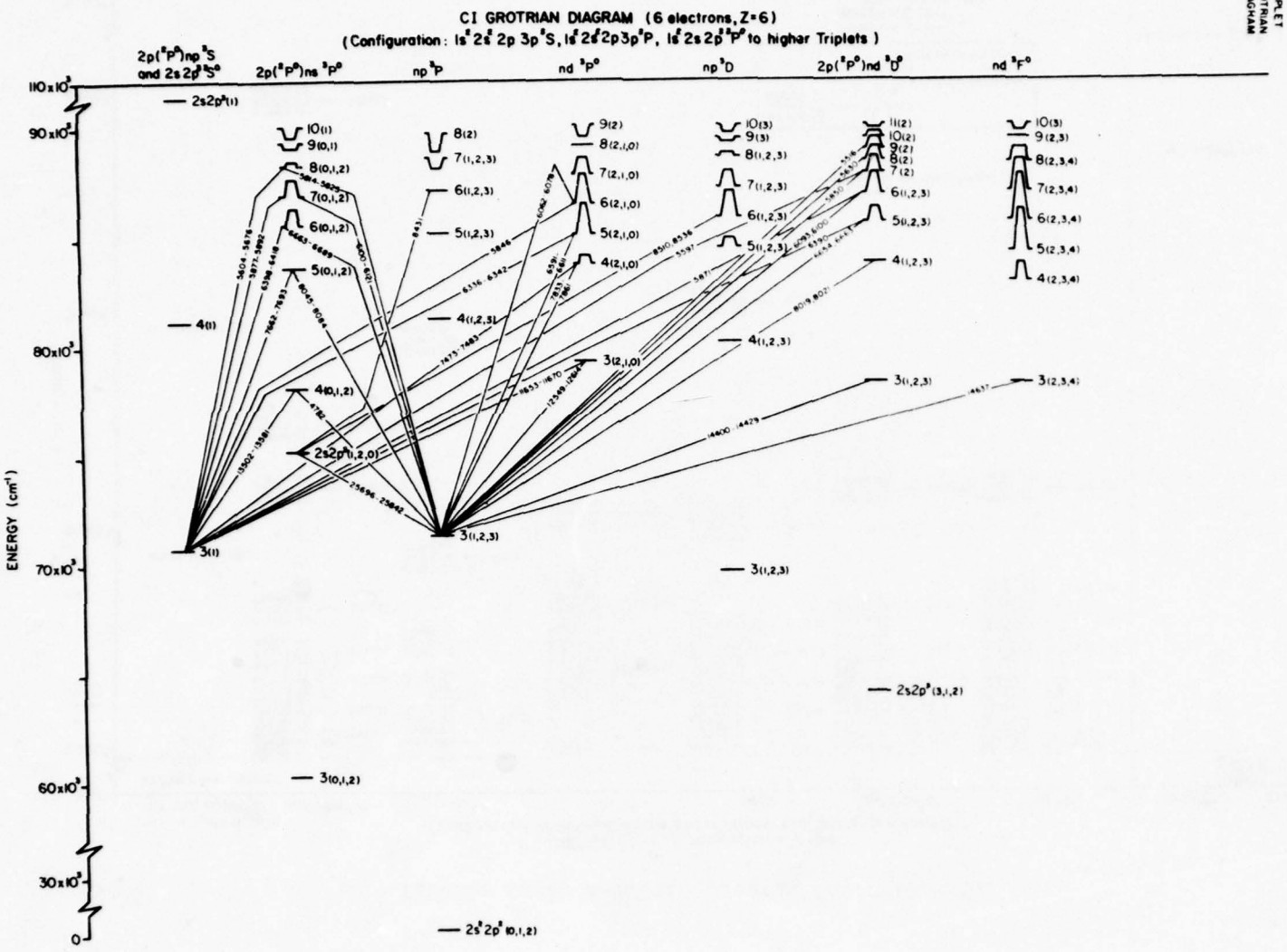

Tabular Data. A-1.24. Diagram for C (Z = 6).

C I ENERGY LEVELS (6 electrons, Z=6)

(Configurations: $1s^2\,2s^2\,2p\,(^3P^o)nf\,L_j(J)$ and $1s^2\,2s2p^2\,(^4P)\,3s\,{}^5P$)

Intermediate Coupling and Autoionizing Terms

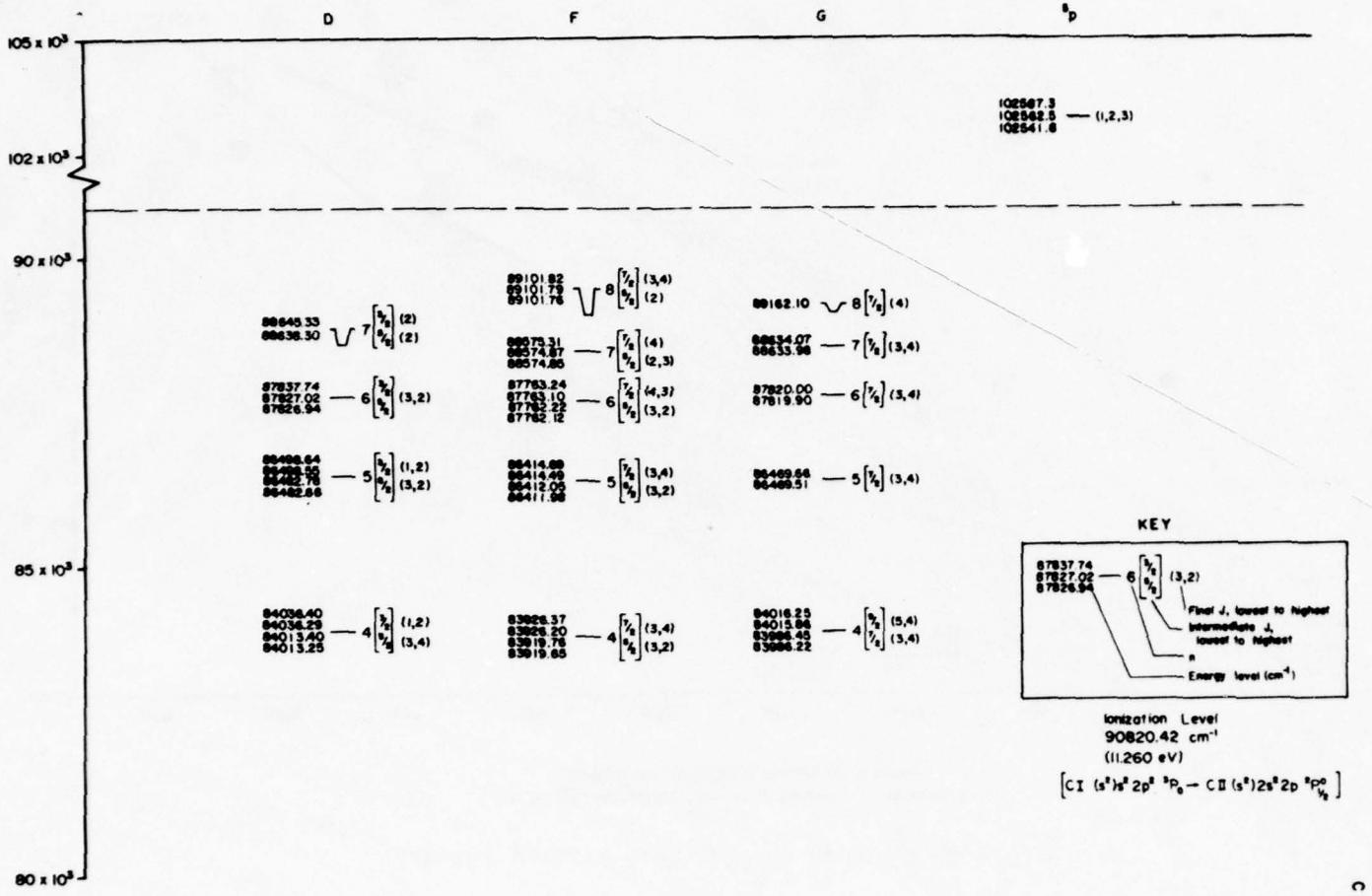

Ionization Level
90820.42 cm^{-1}
(11.260 eV)

[C I $(s^2)s^2\,2p^2\,{}^3P_0$ — C II $(s^2)2s^2\,2p\,{}^2P^o_{1/2}$]

Tabular Data. A-1.25. Diagram for C (Z = 6).

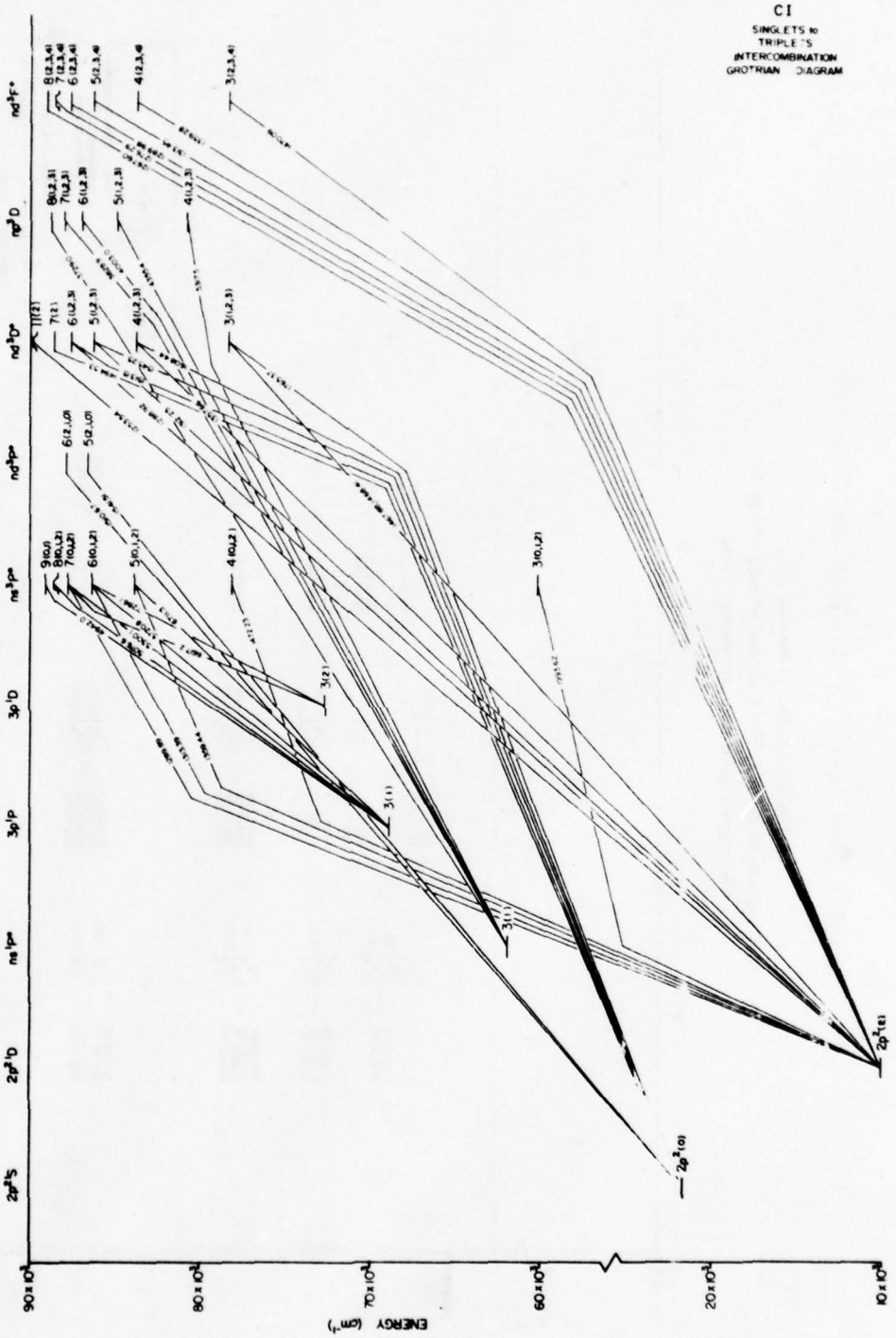

Tabular Data. A-1.26. Diagram for C (Z = 6).

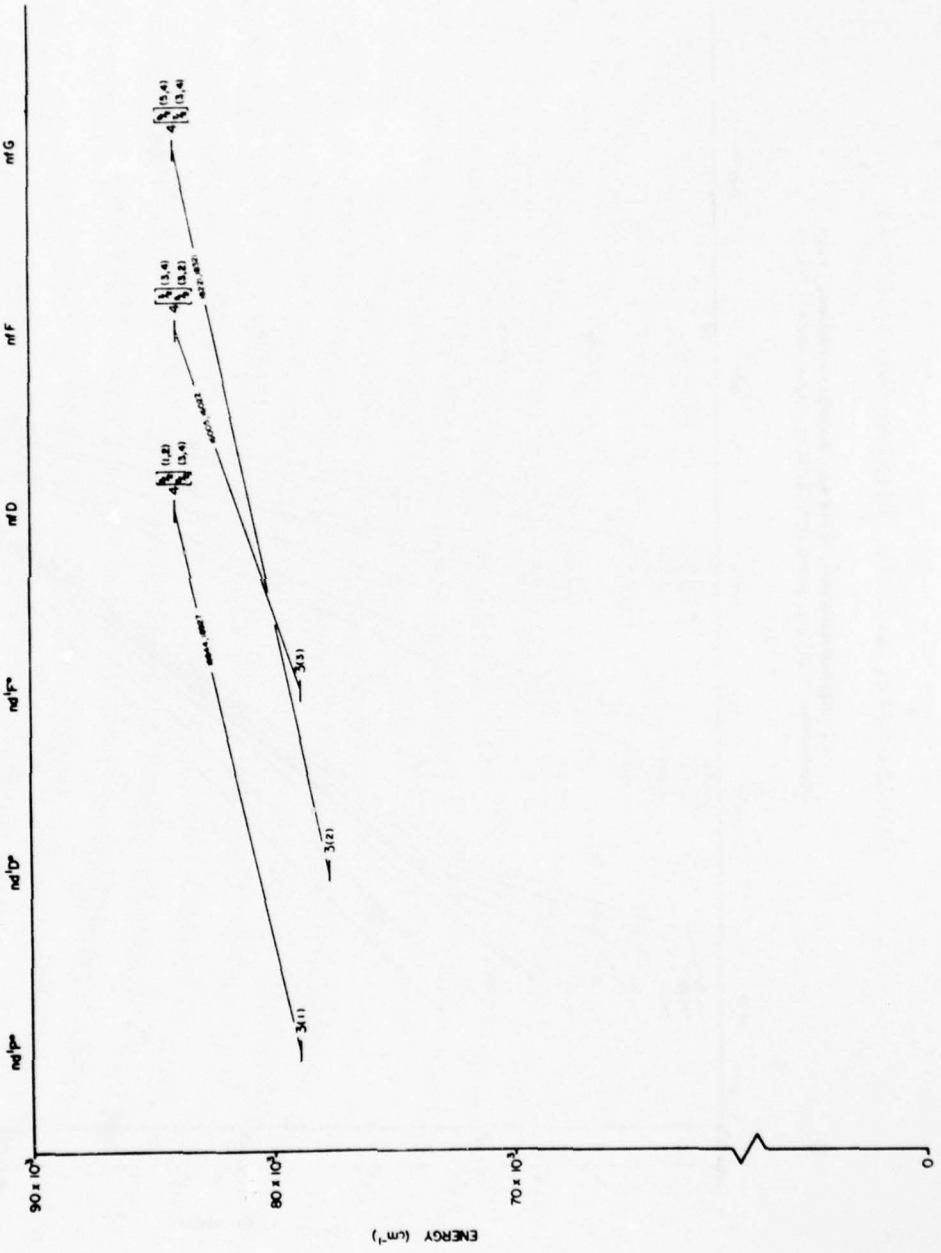

Tabular Data. A-1.27. Diagram for C (Z = 6).

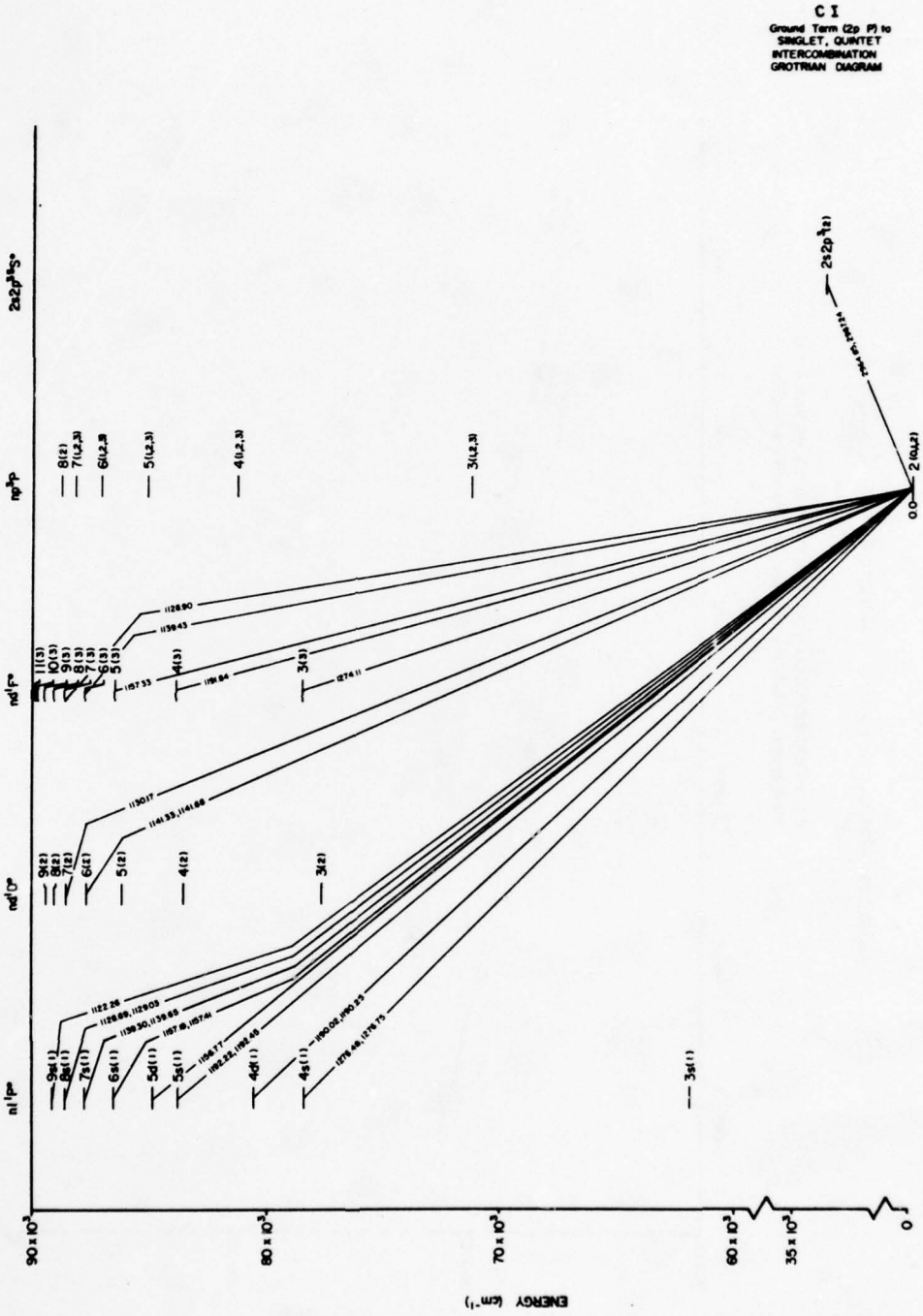

Tabular Data. A-1.28. Diagram for C (Z = 6).

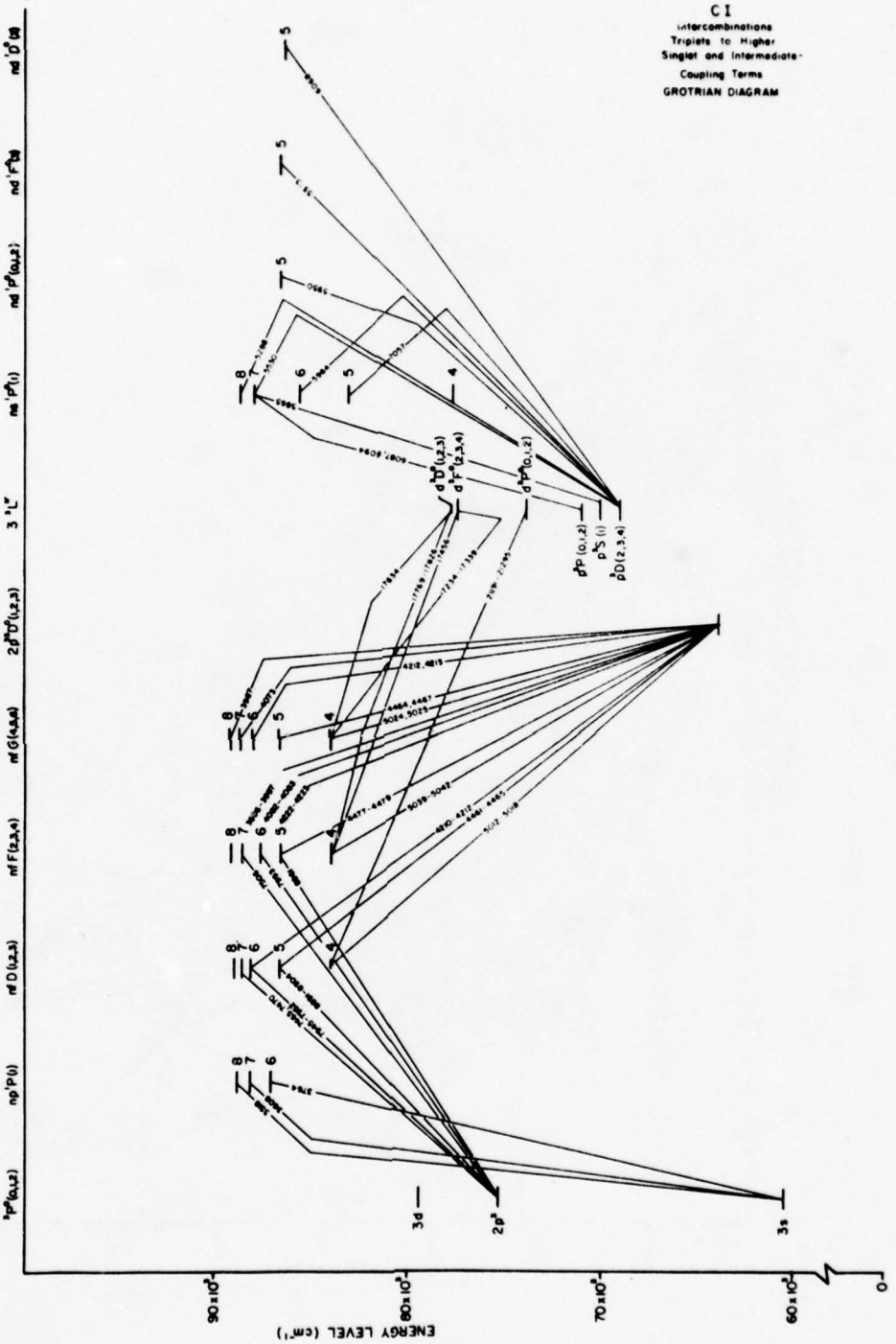

Tabular Data. A-1.29. Diagram for C^+ (Z = 6).

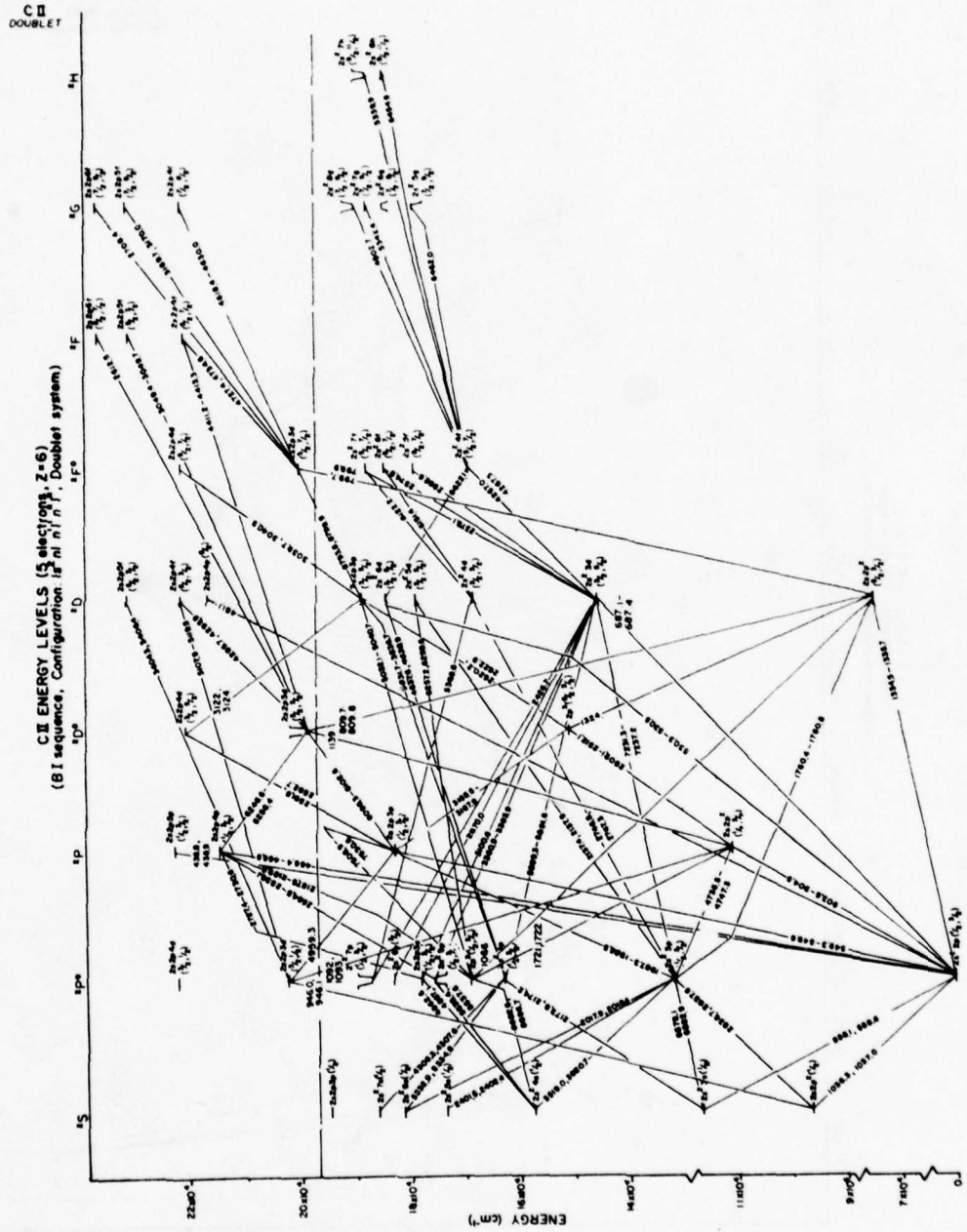

Tabular Data. A-1.30. Diagram for C^+ ($Z = 6$).

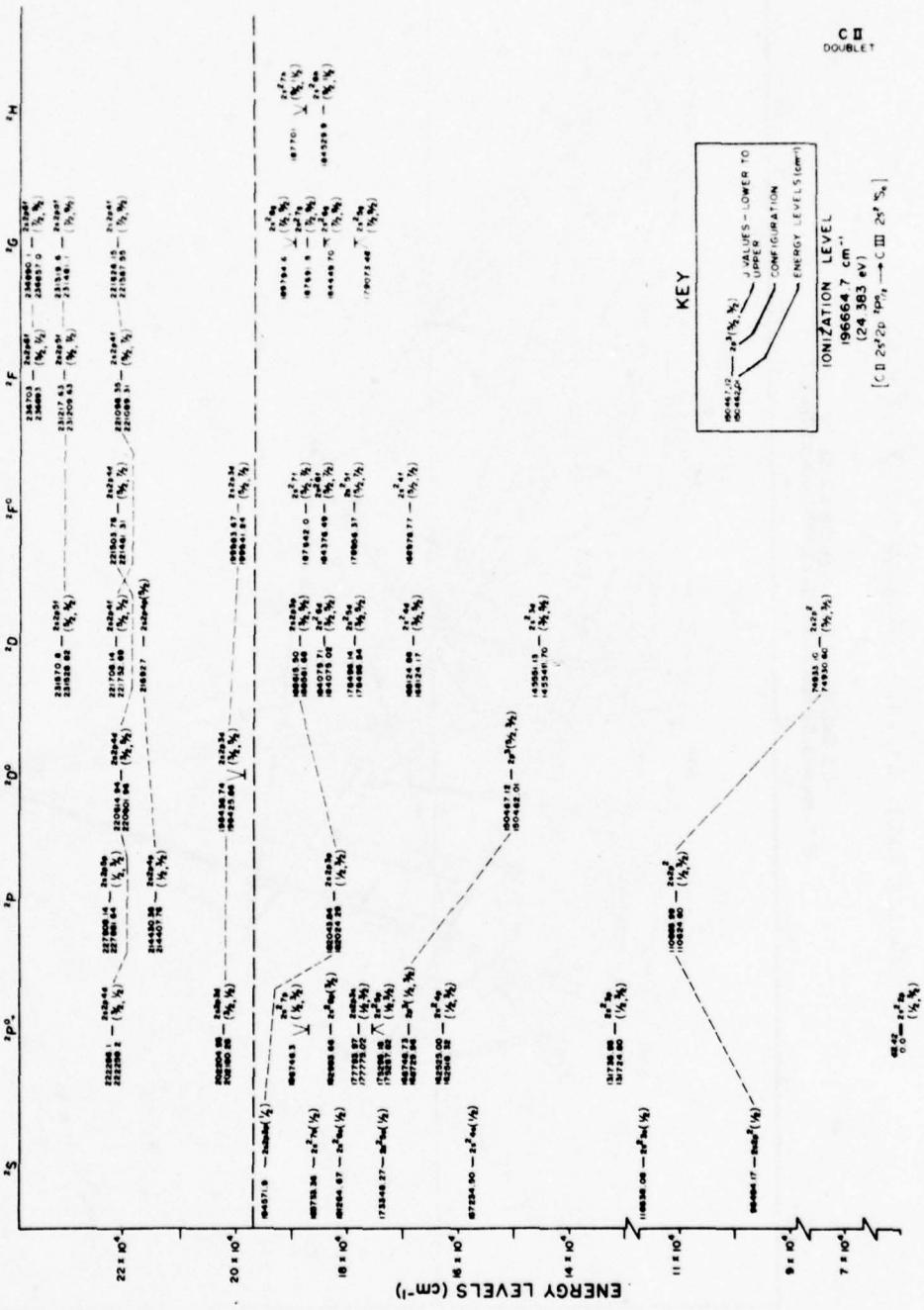

Tabular Data. A-1.31. Diagram for C^+ (Z = 6).

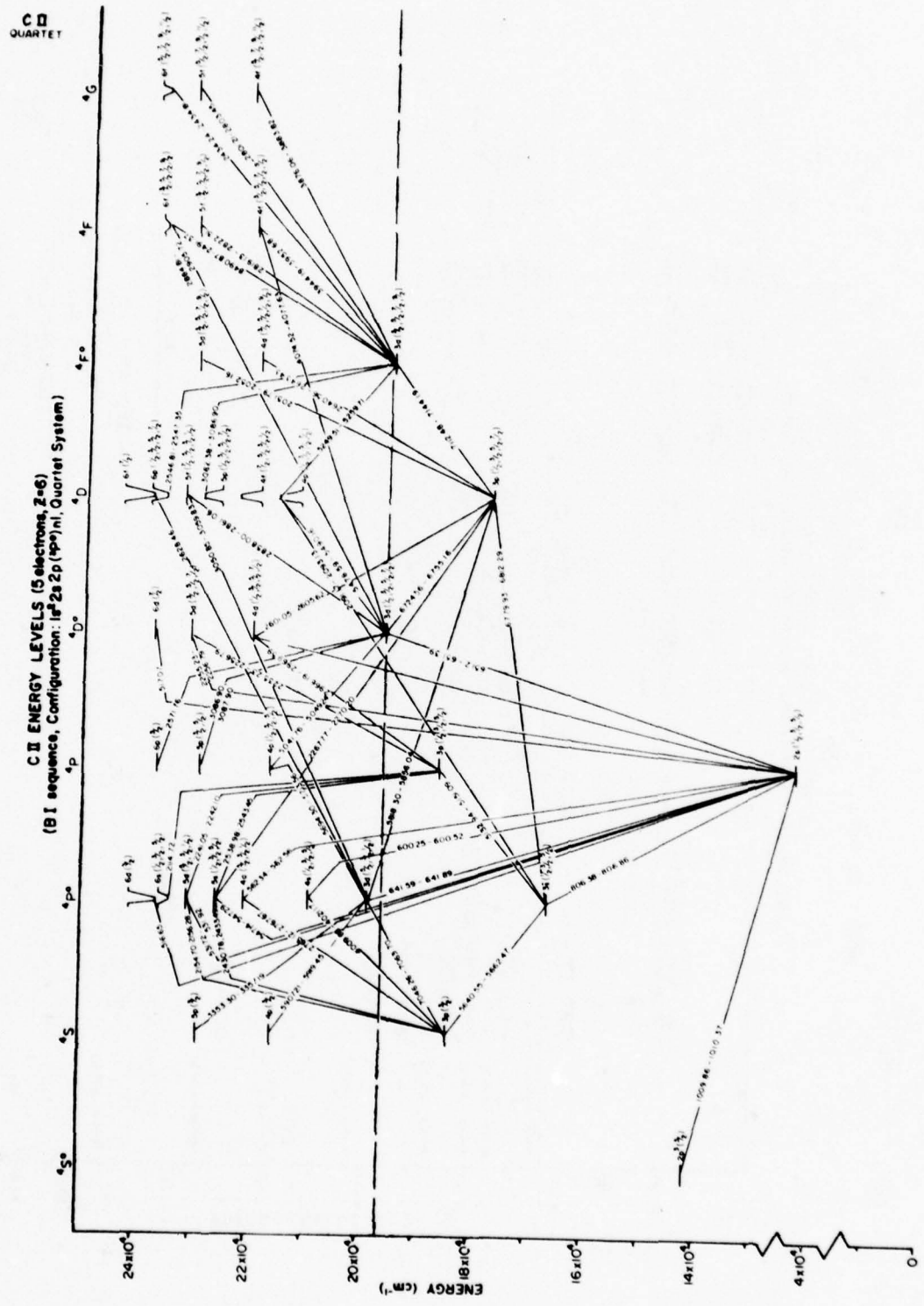

Tabular Data. A-1.32. Diagram for C^+ (Z = 6).

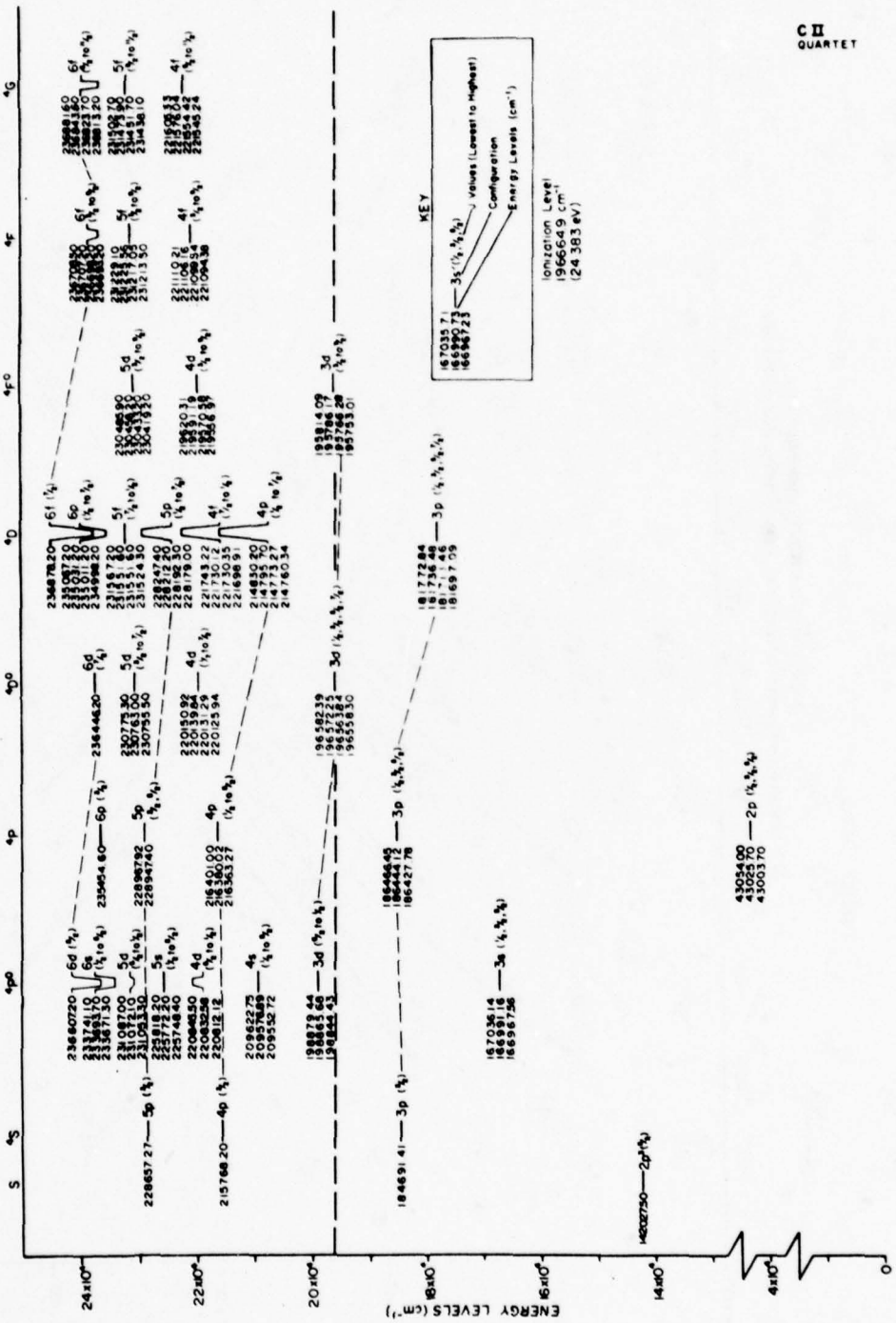

Tabular Data. A-1.33. Diagram for C^{+} (Z = 6).

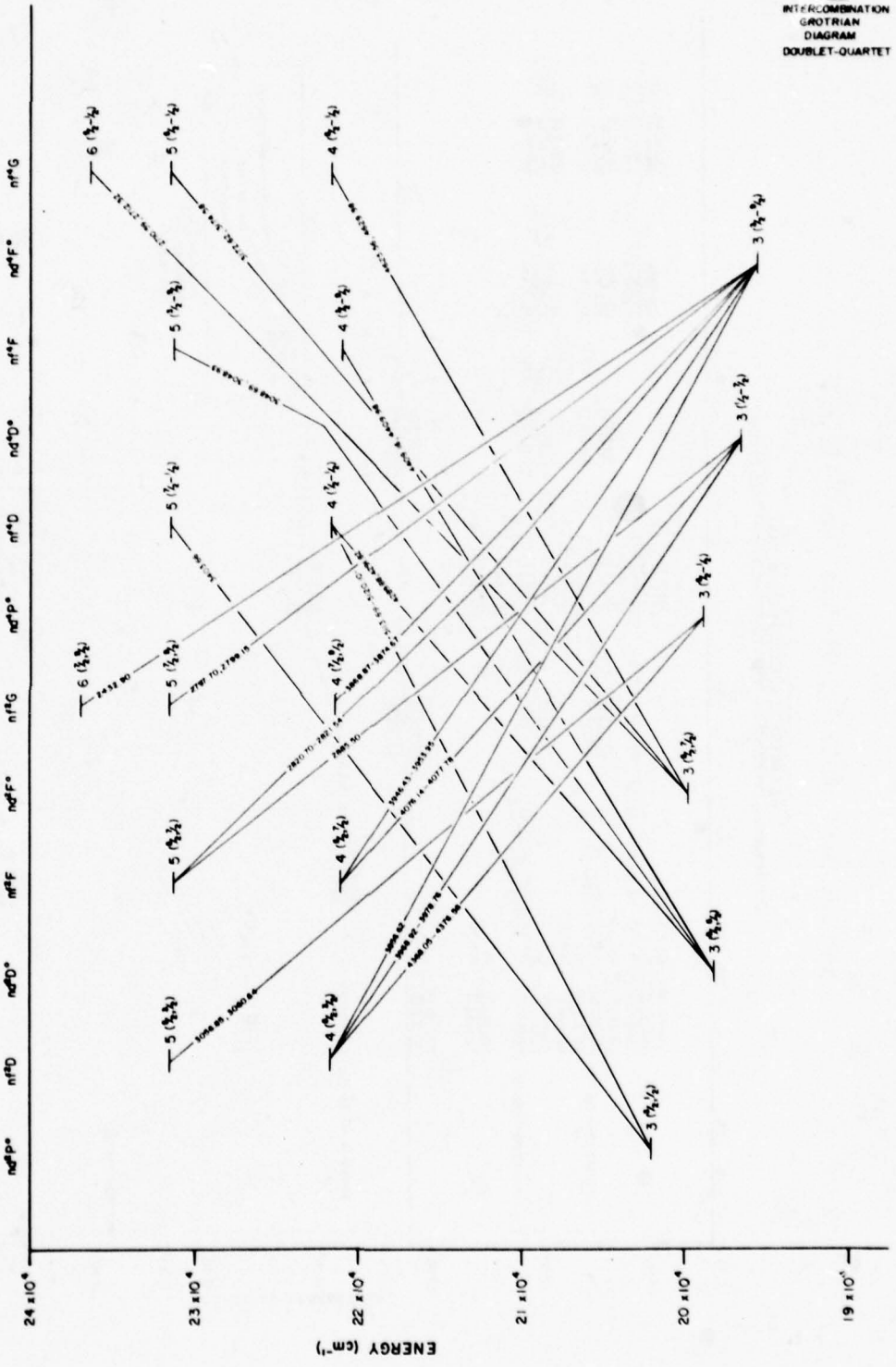

Tabular Data. A-1.34. Diagram for N (Z = 7).

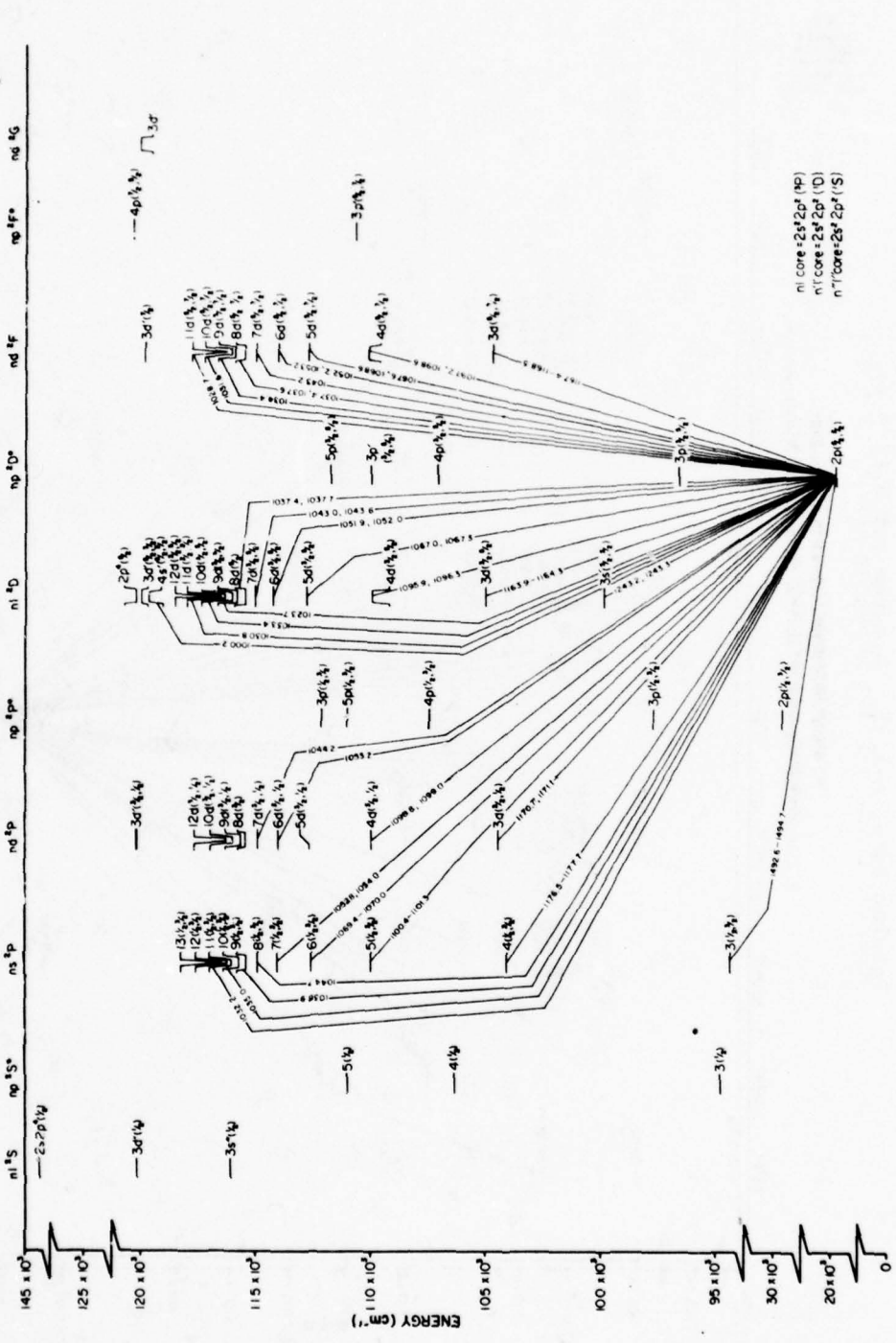

Tabular Data. A-1.35. Diagram for N (Z = 7).

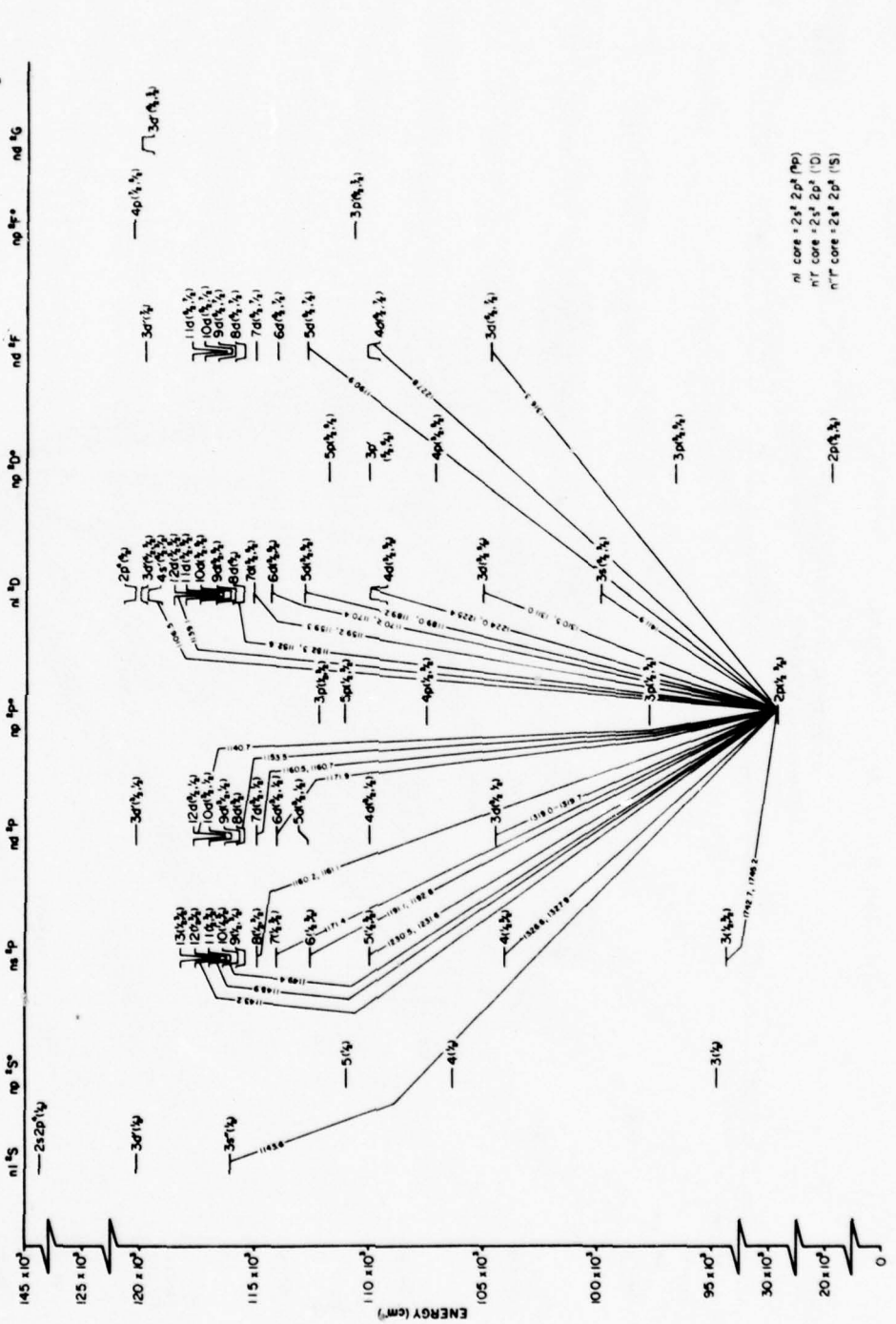

Tabular Data. A-1.36. Diagram for N (Z = 7).

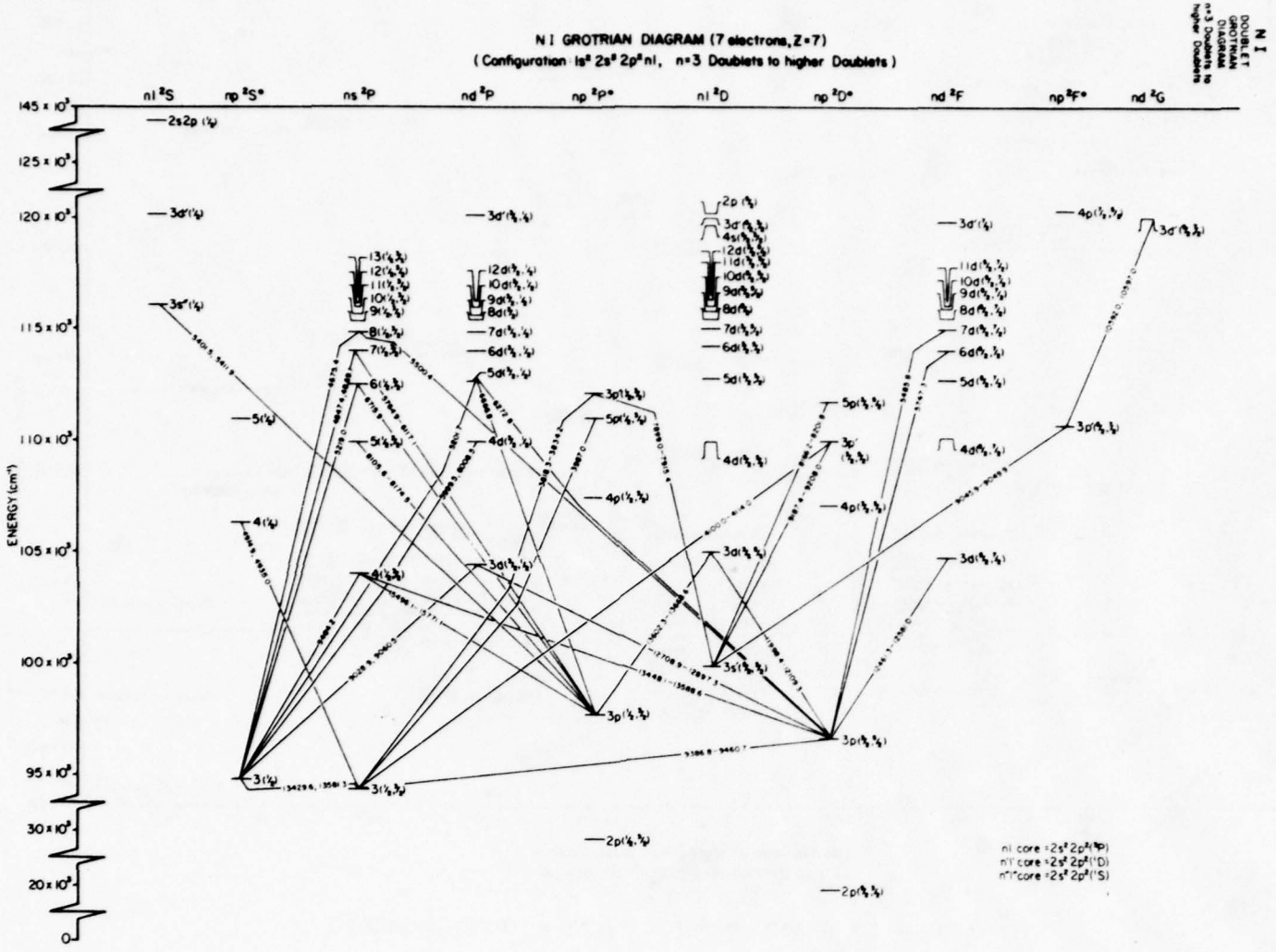

Tabular Data. A-1.37. Diagram for N (Z = 7).

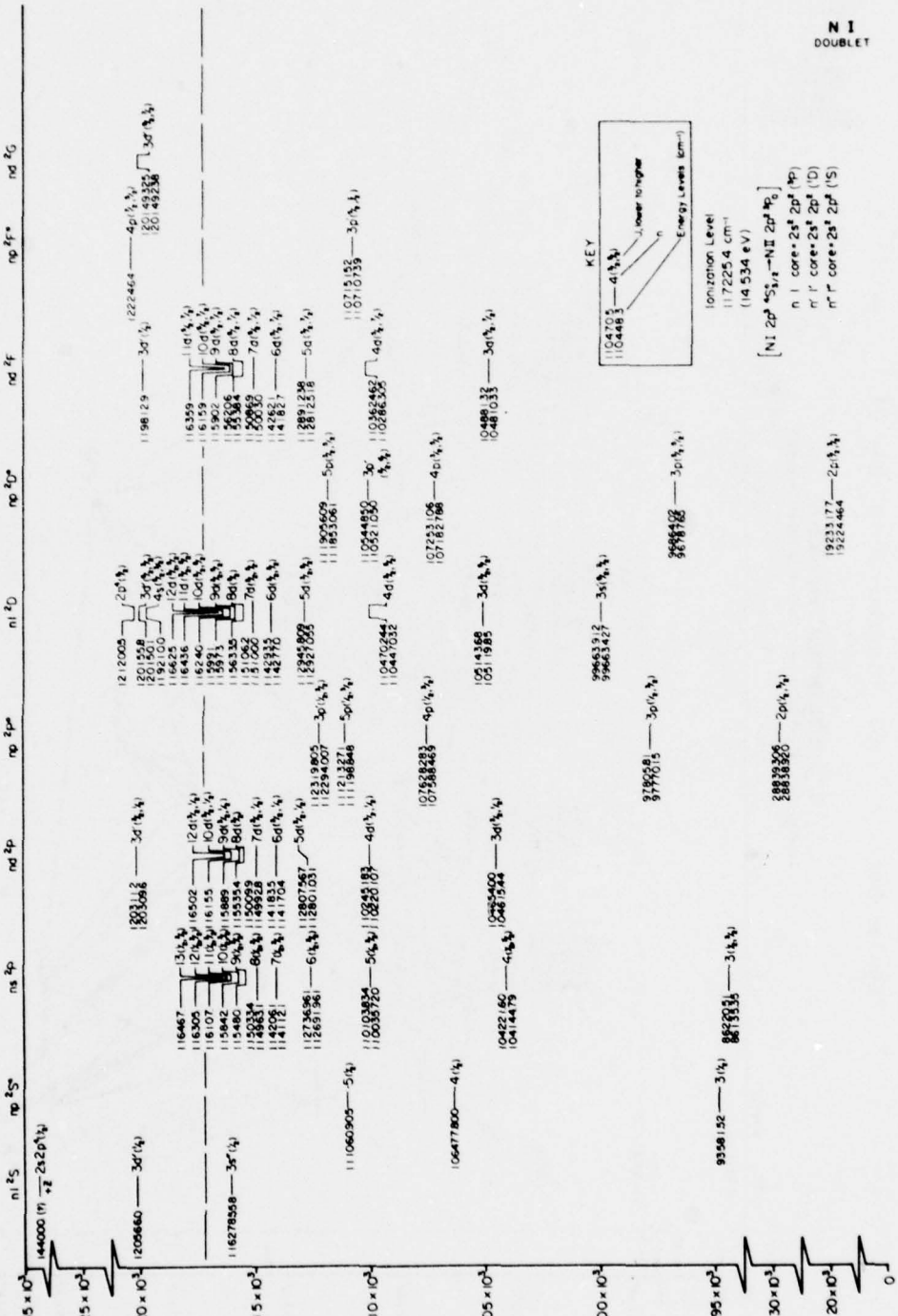

Tabular Data. A-1.38. Diagram for N (Z = 7).

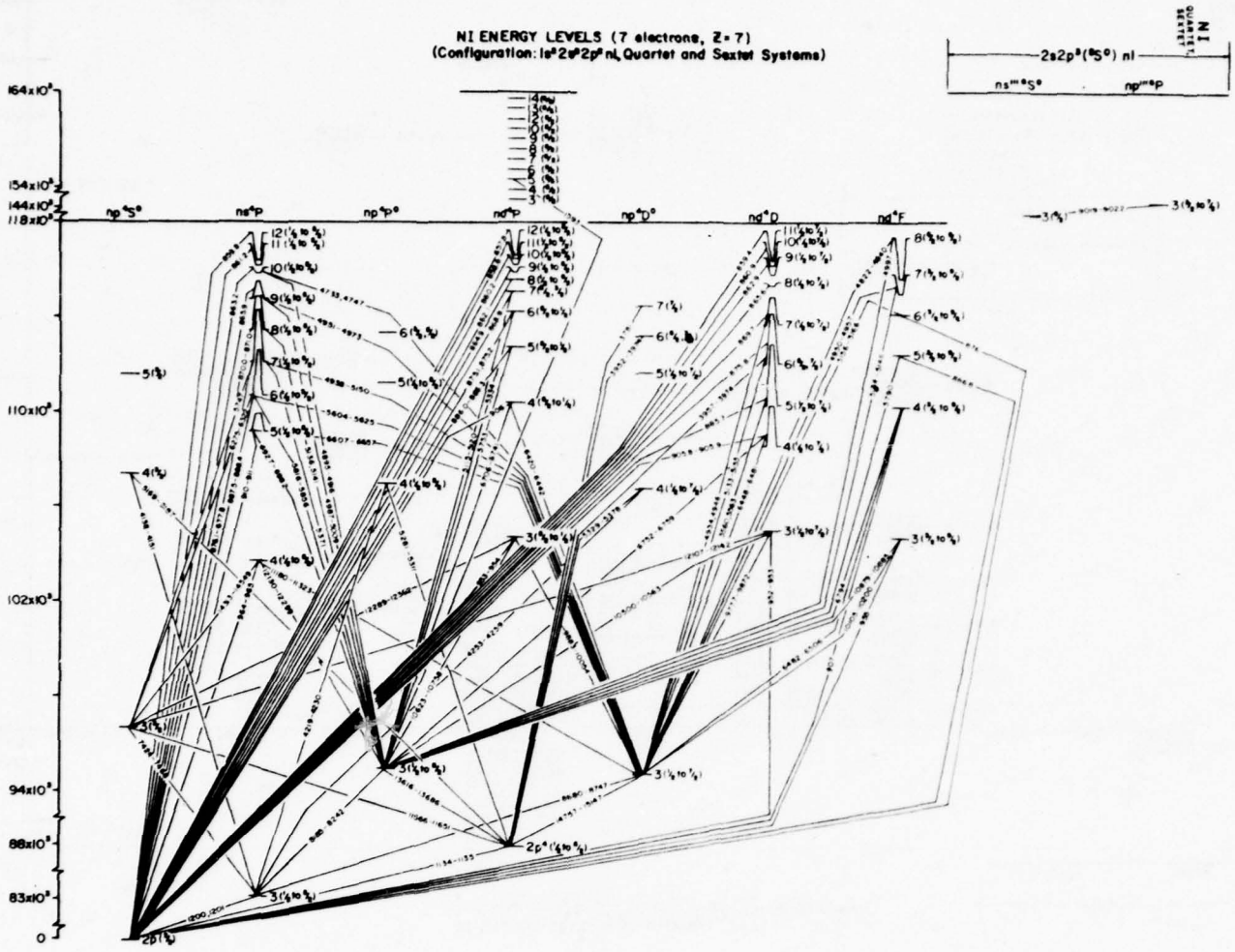

Tabular Data. A-1.39. Diagram for N (Z = 7).

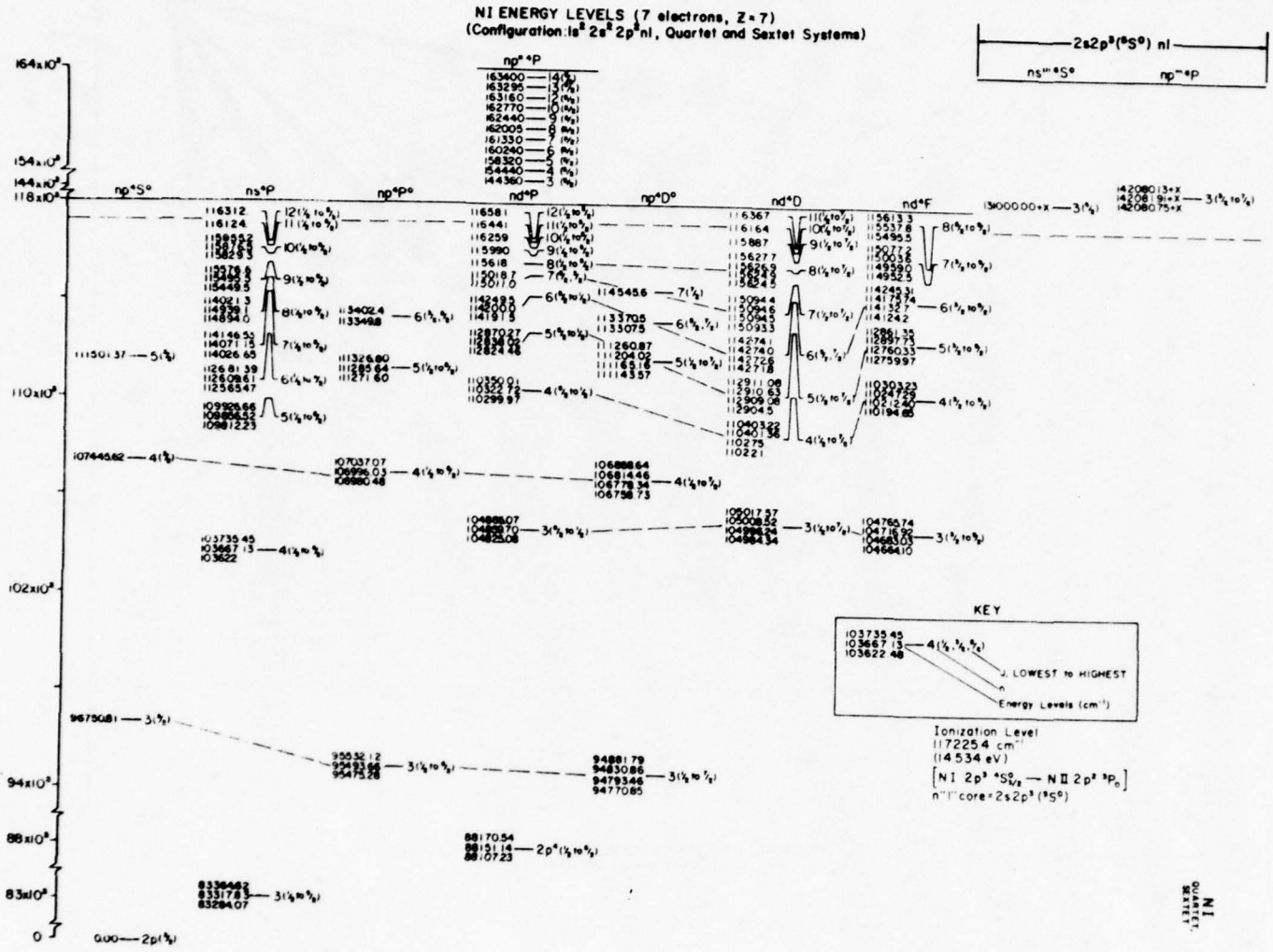

Tabular Data. A-1.40. Diagram for N (Z = 7).

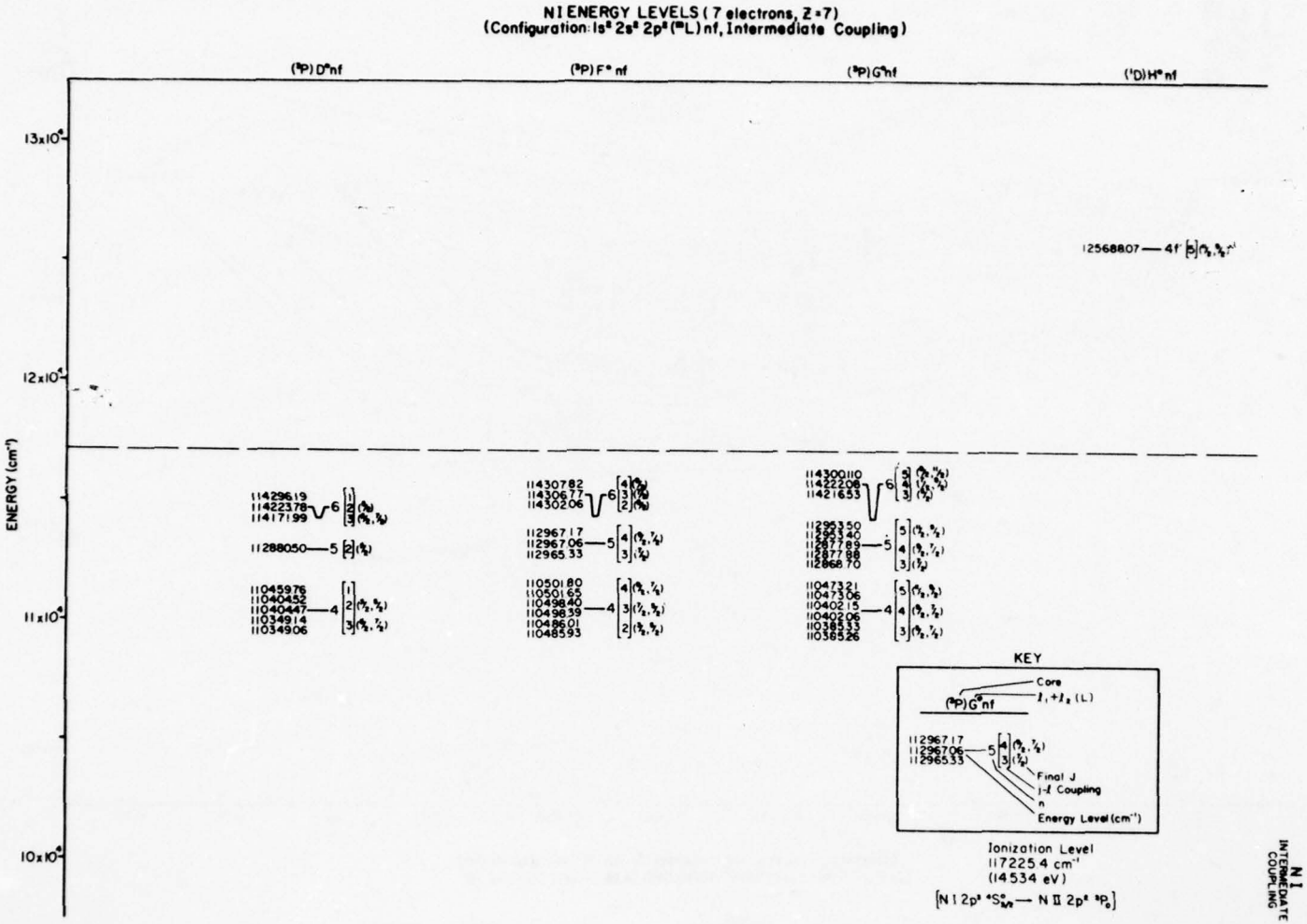

Tabular Data. A-1.41. Diagram for N (Z = 7).

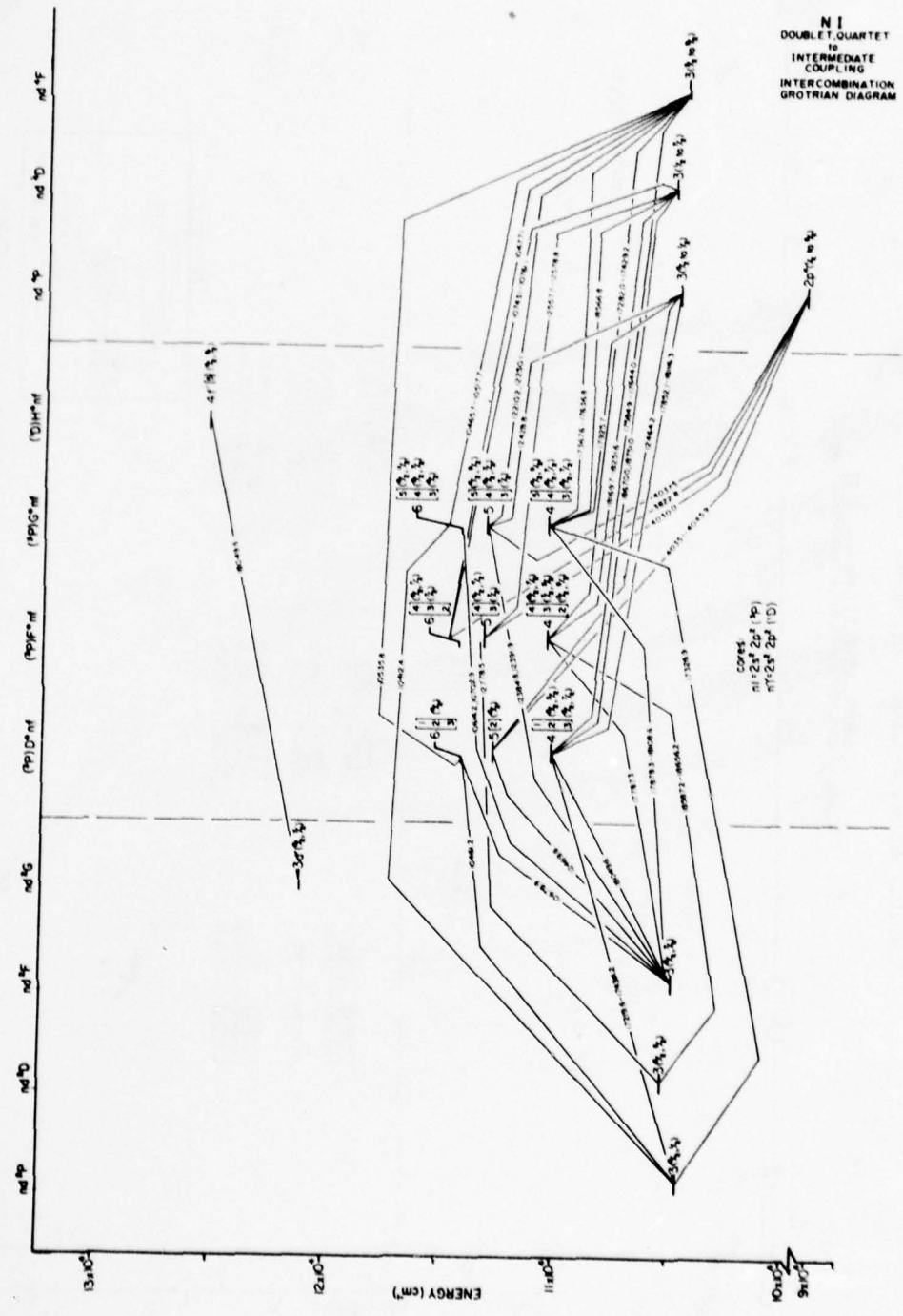

Tabular Data. A-1.42. Diagram for N (Z = 7).

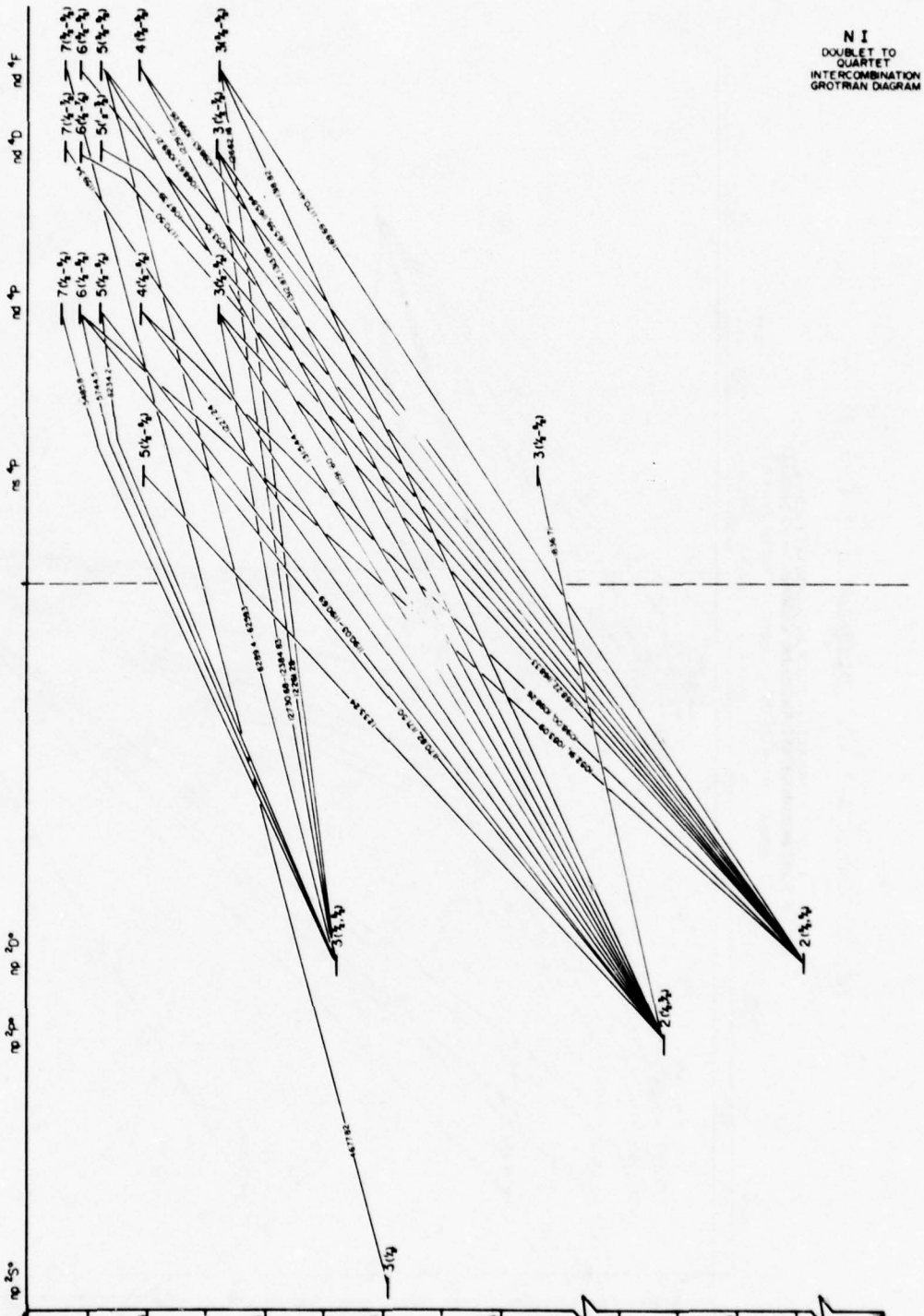

Tabular Data. A-1.43. Diagram for N (Z = 7).

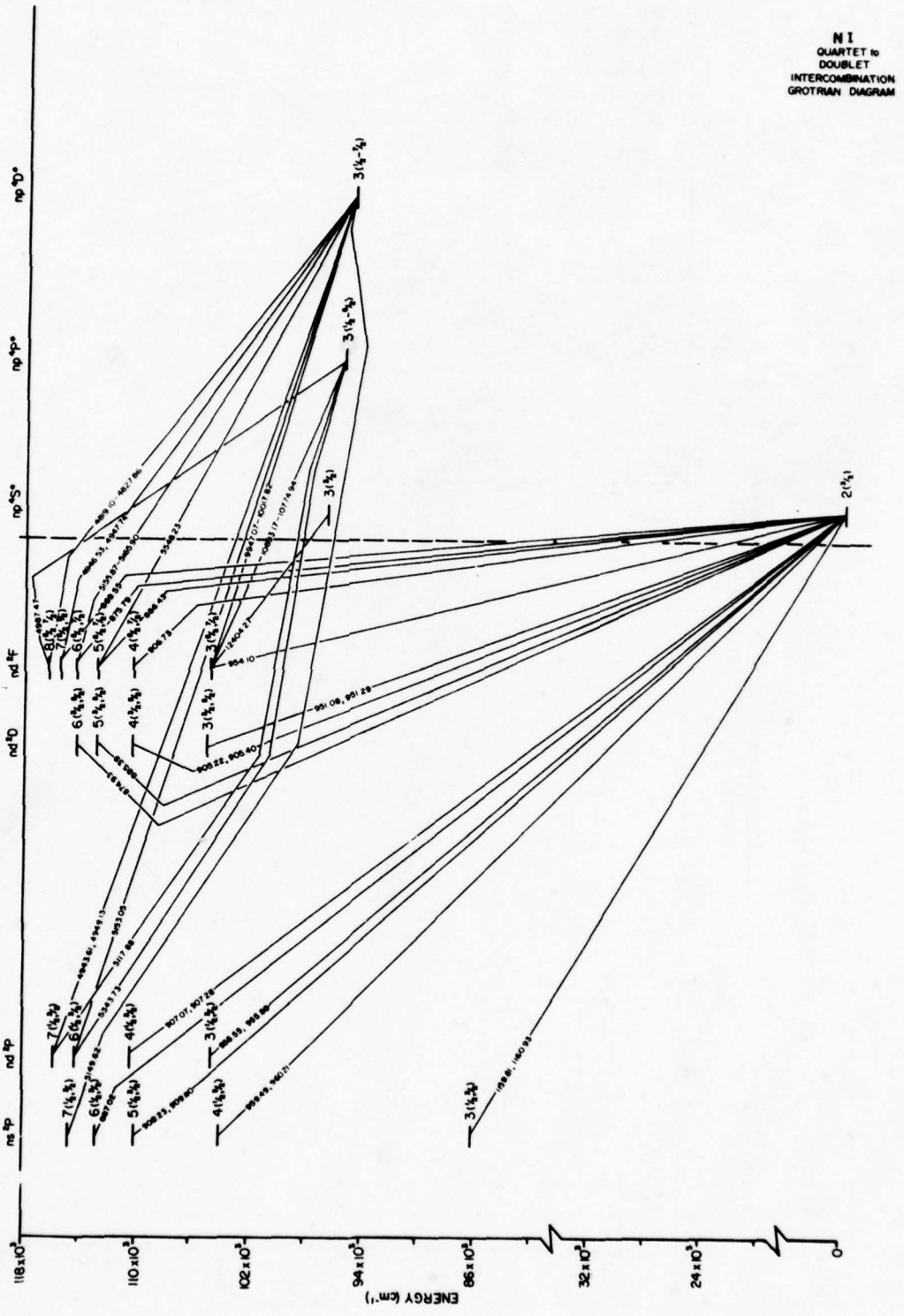

Tabular Data. A-1.44. Diagram for N^+ (Z = 7).

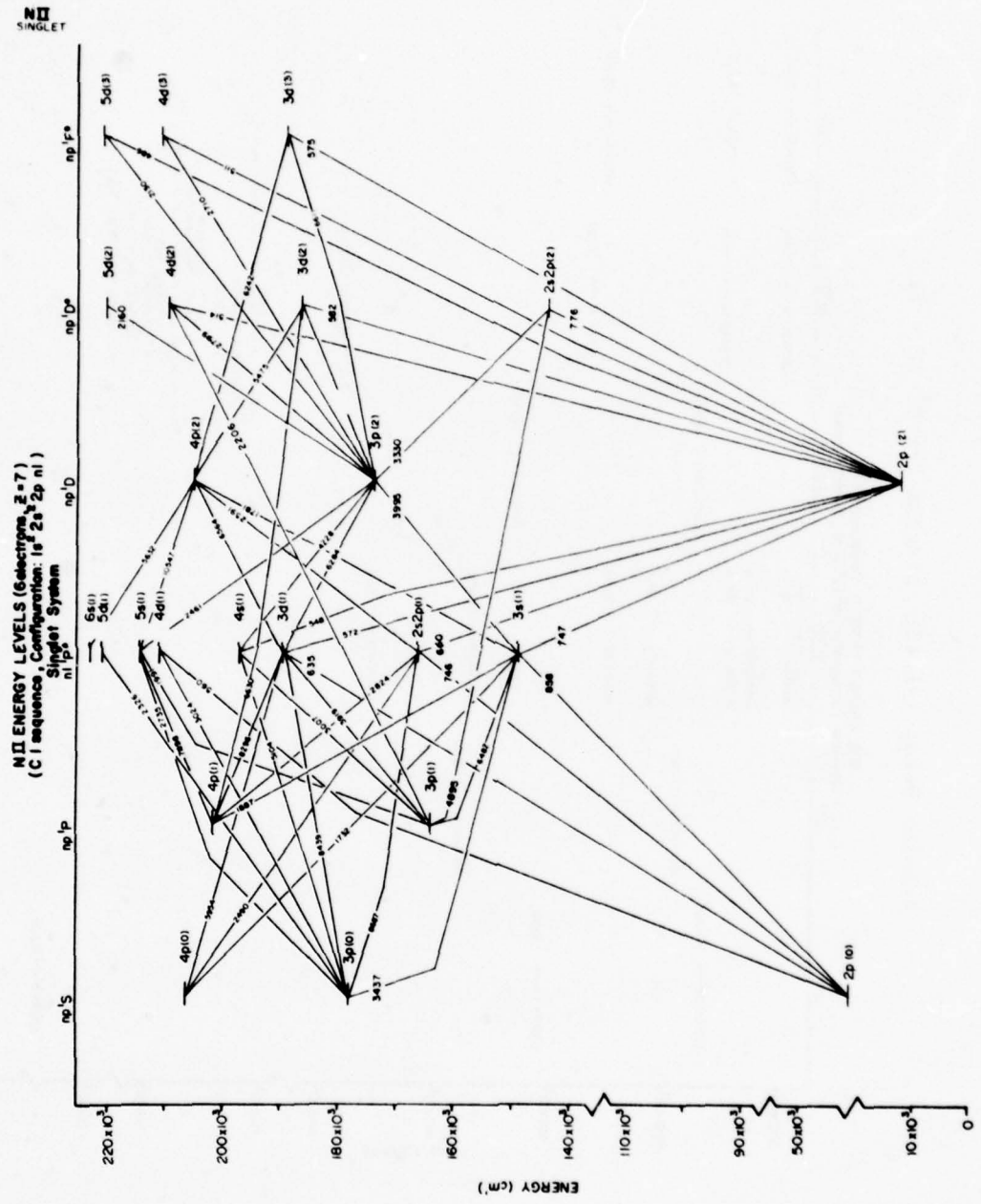

Tabular Data. A-1.45. Diagram for N^+ (Z = 7).

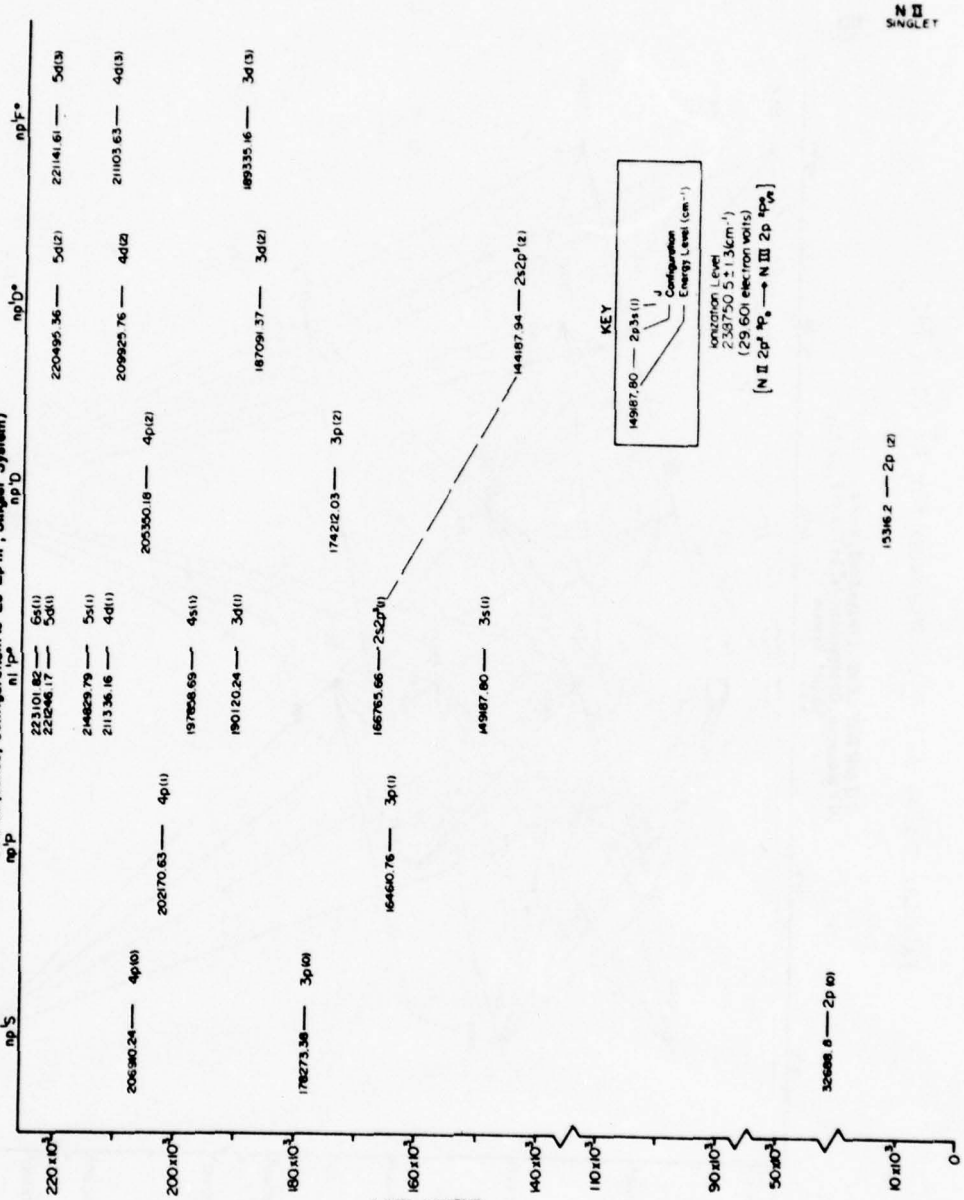

Tabular Data. A-1.46. Diagram for N^+ (Z = 7).

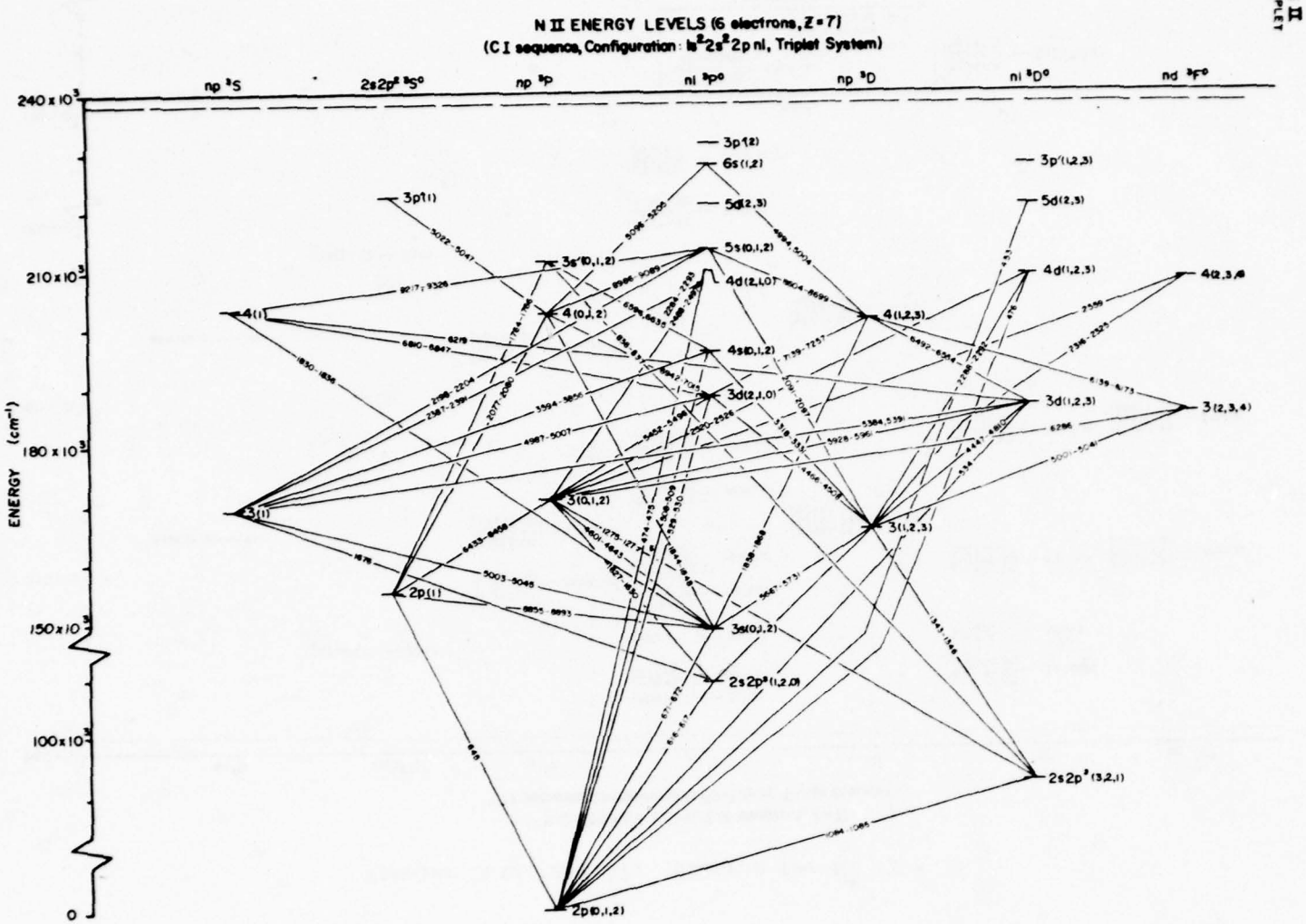

Tabular Data. A-1.47. Diagram for N^+ (Z = 7).

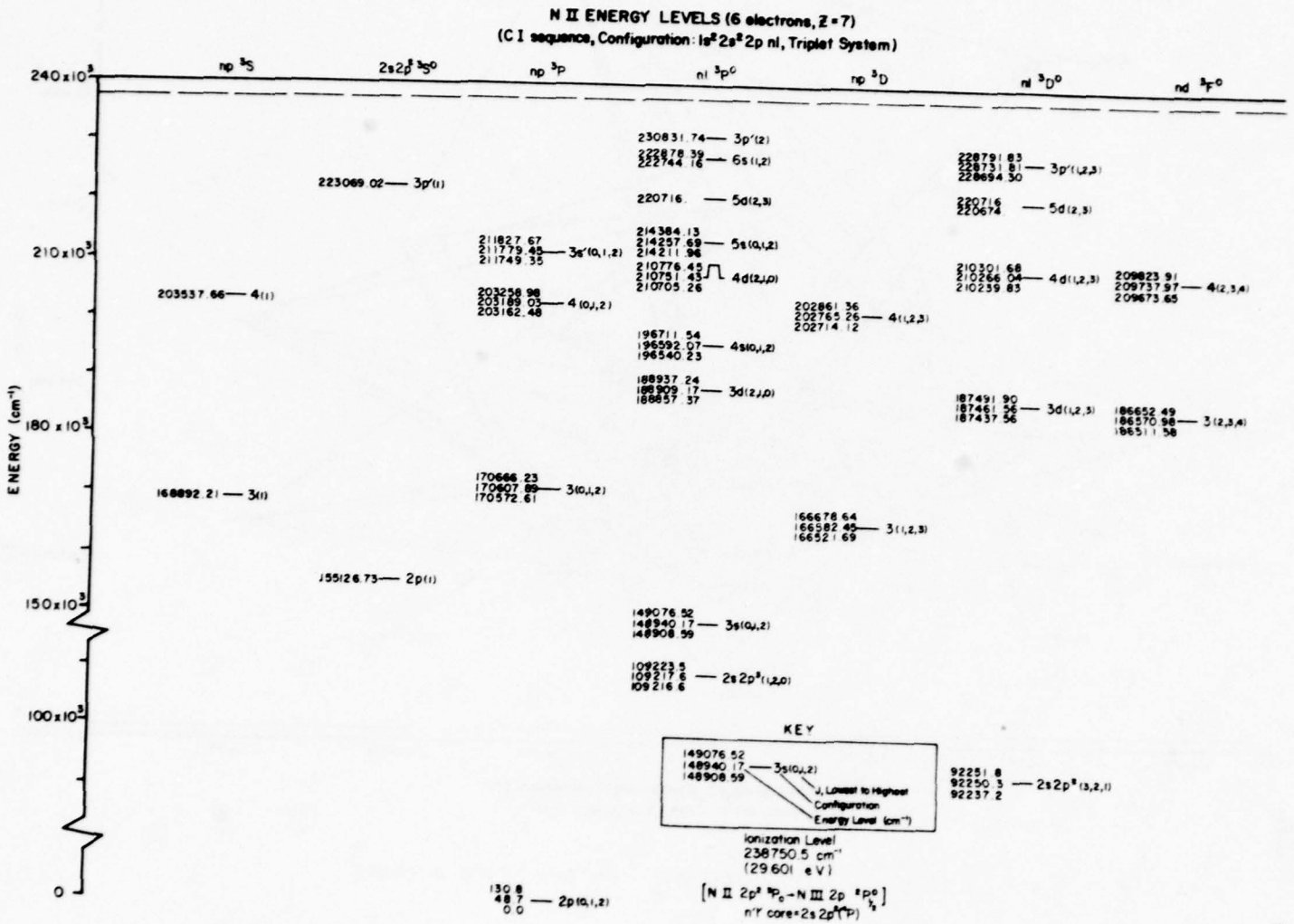

Tabular Data. A-1.48. Diagram for N^+ (Z = 7).

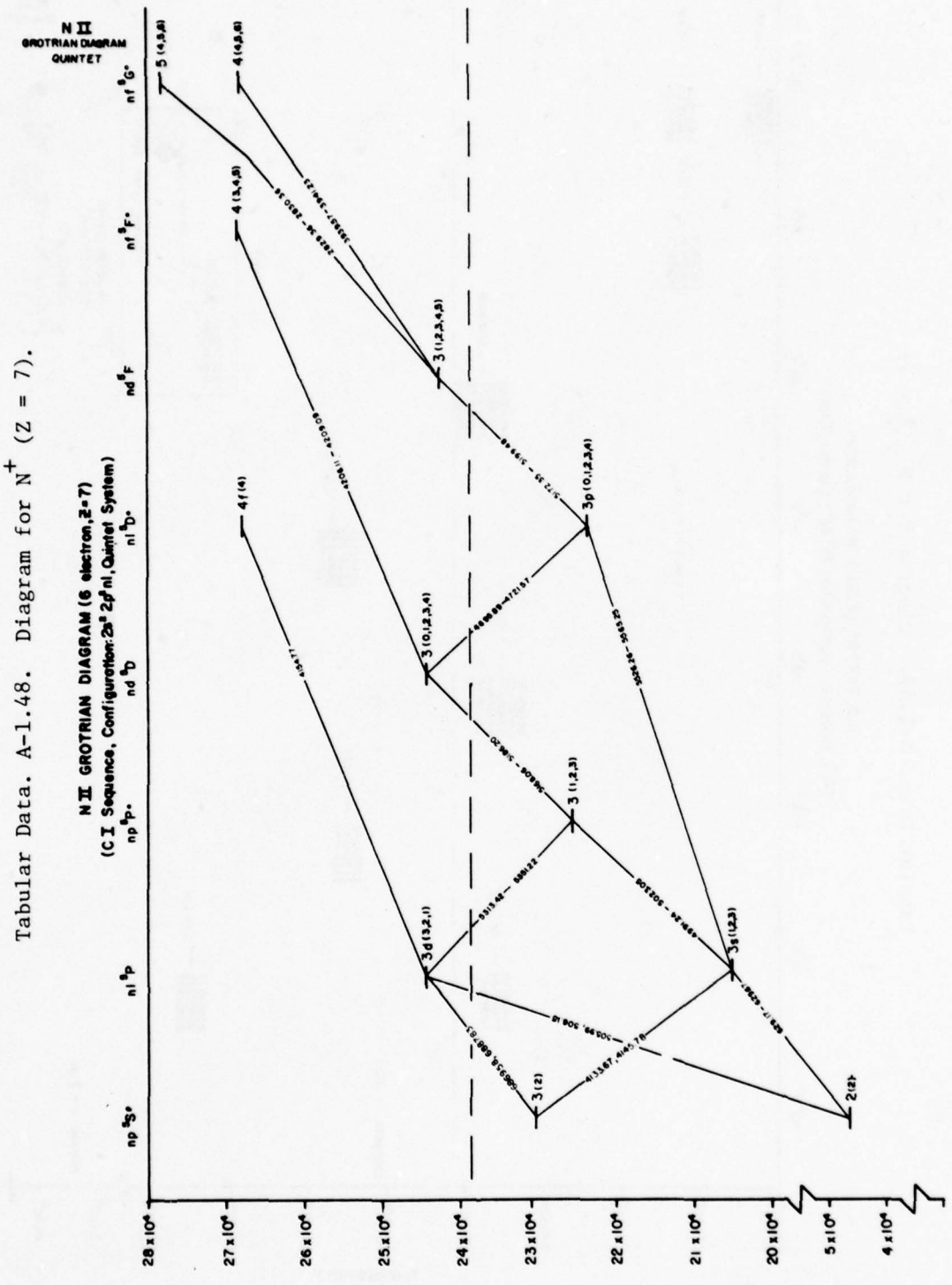

Tabular Data. A-1.49. Diagram for N^+ (Z = 7).

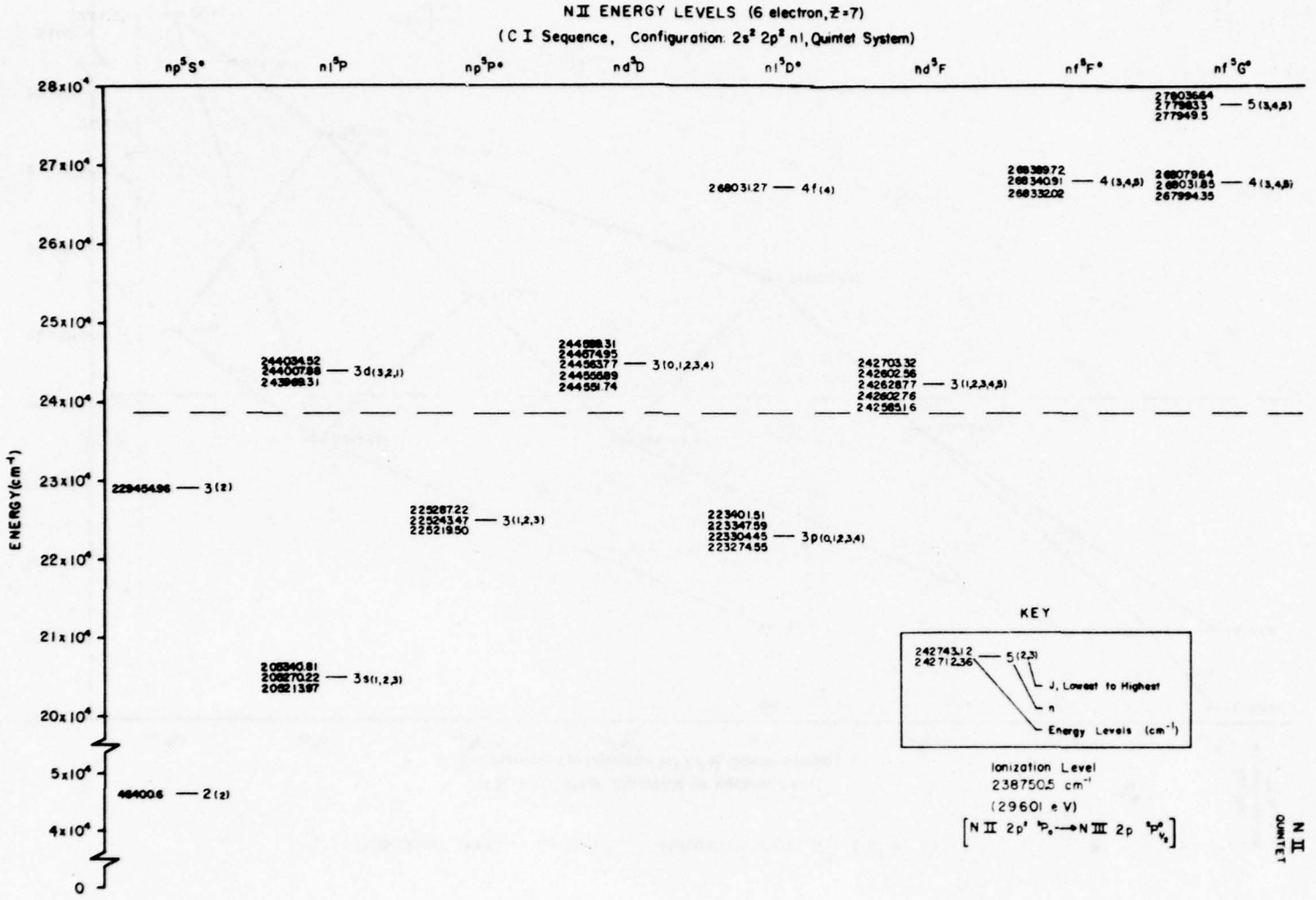

Tabular Data. A-1.50. Diagram for N^{+} (Z = 7).

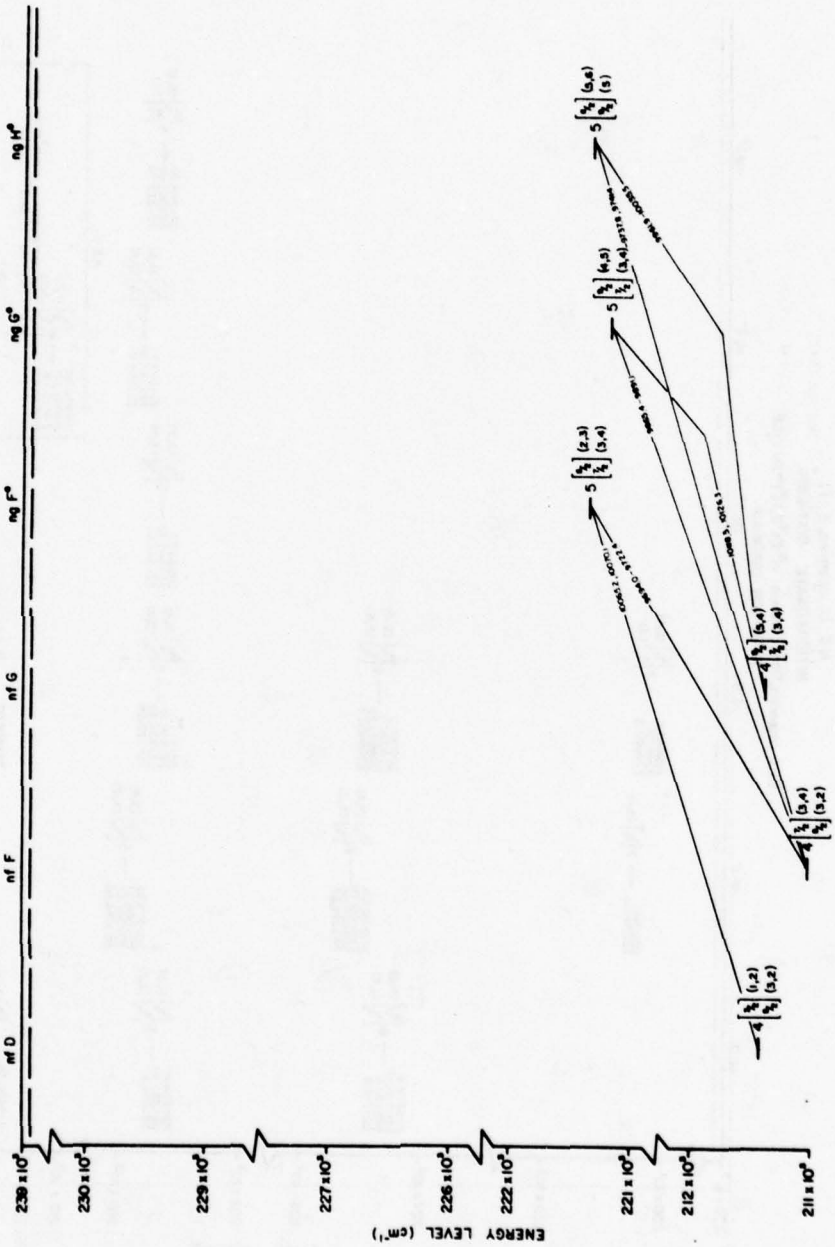

Tabular Data. A-1.51. Diagram for N^+ (Z = 7).

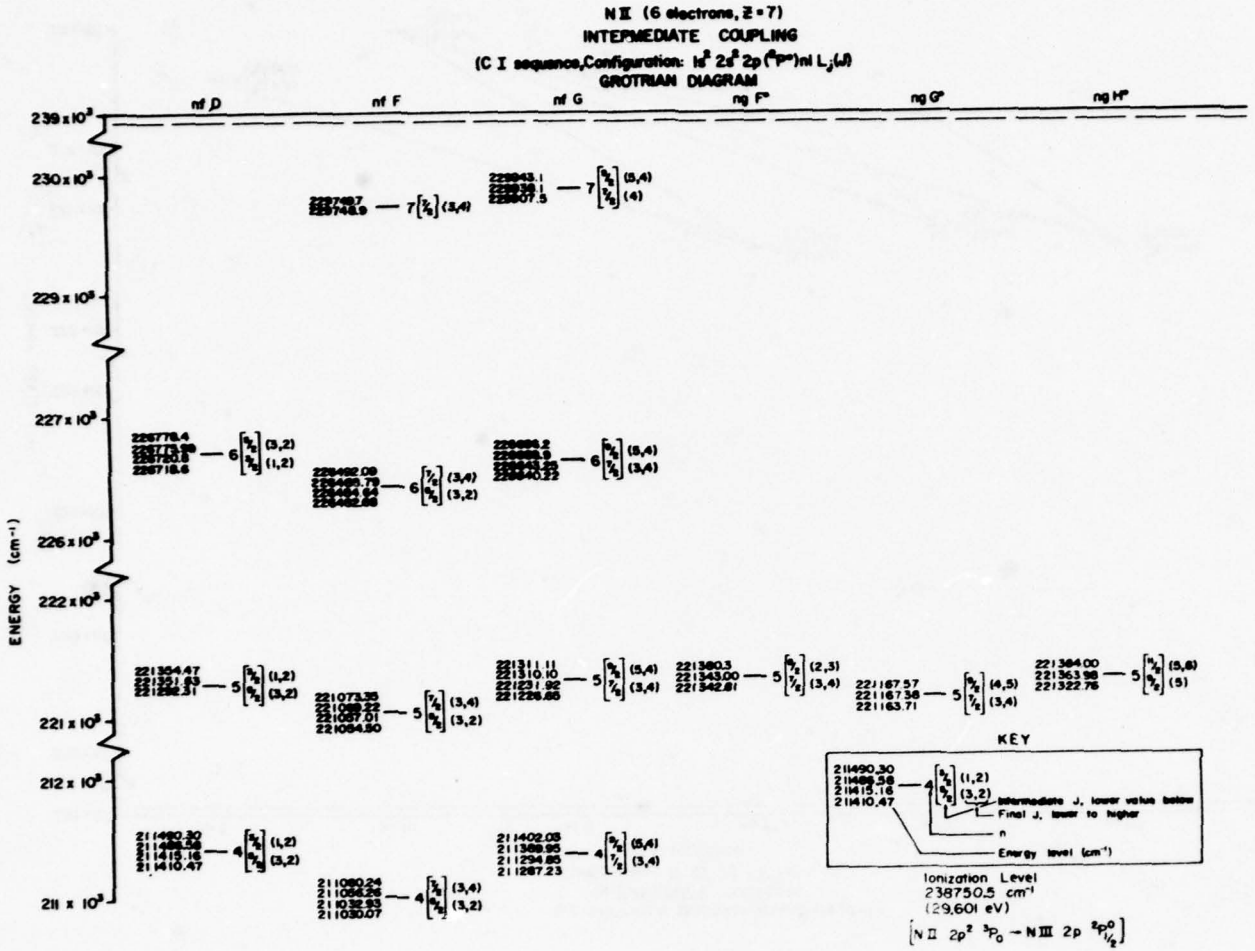

N II
INTERMEDIATE COUPLING
GROTRIAN DIAGRAM

Tabular Data. A-1.52. Diagram for N^{+} (Z = 7).

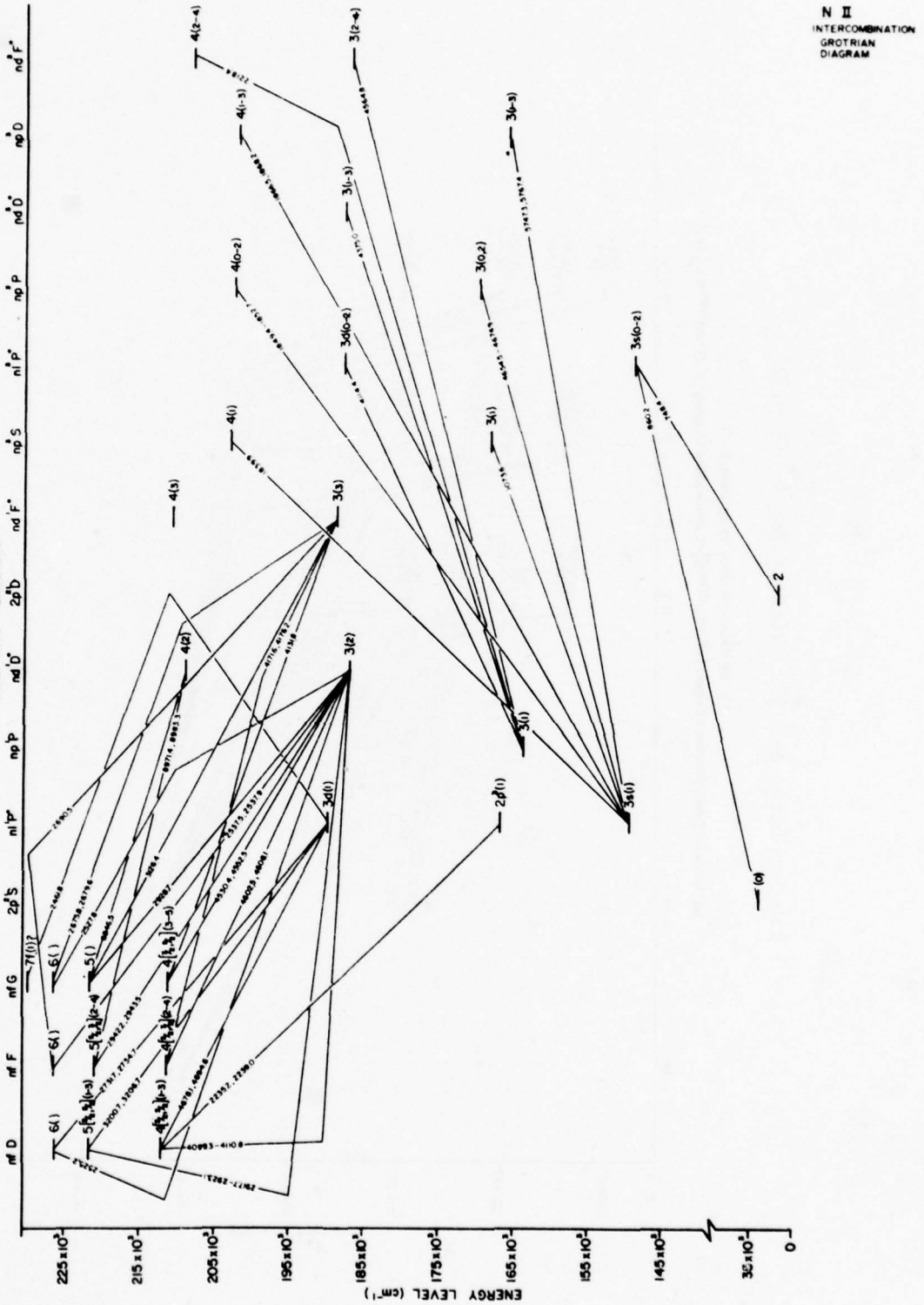

Tabular Data. A-1.53. Diagram for N^{+} (Z = 7).

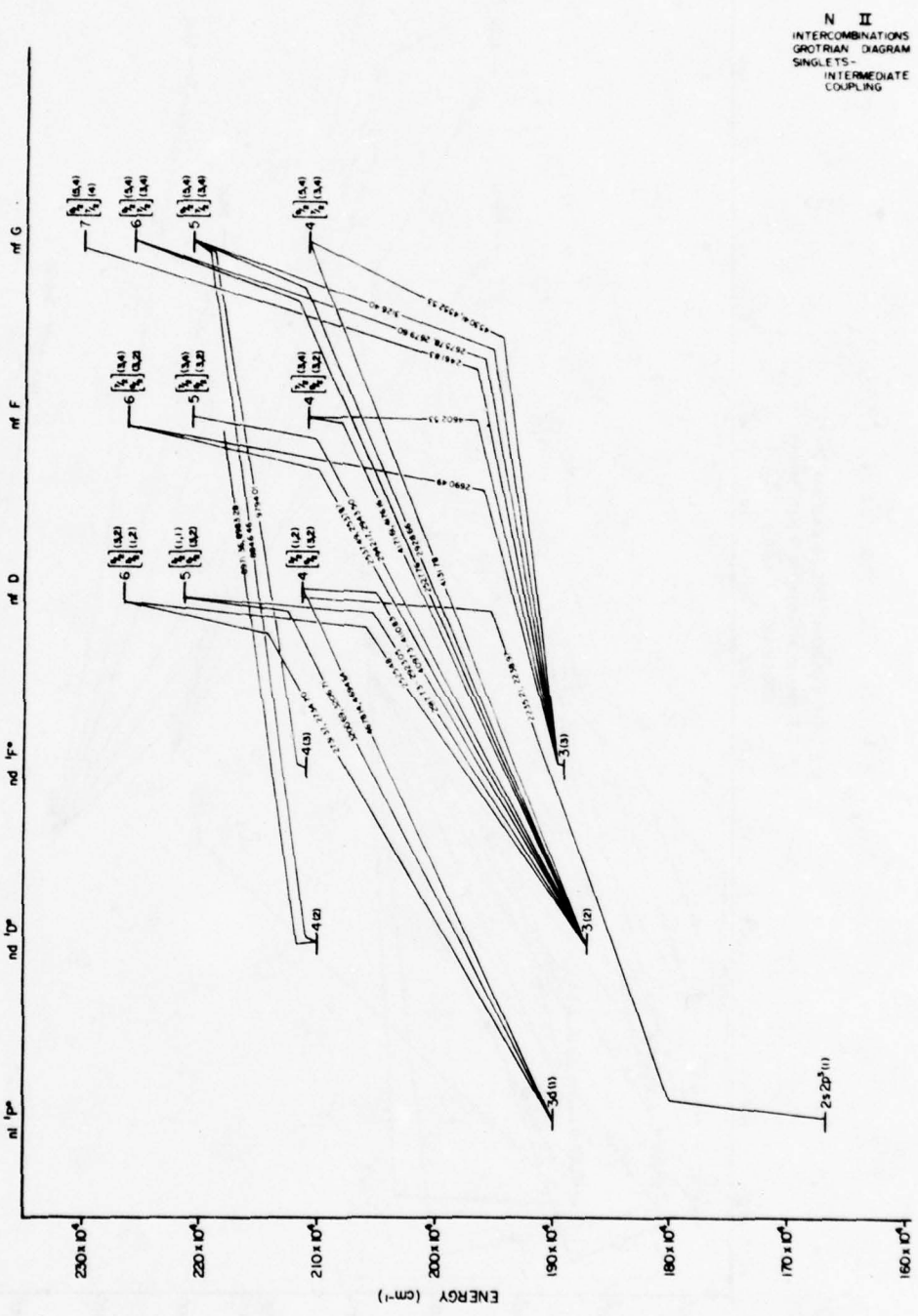

Tabular Data. A-1.54. Diagram for N^+ ($Z = 7$).

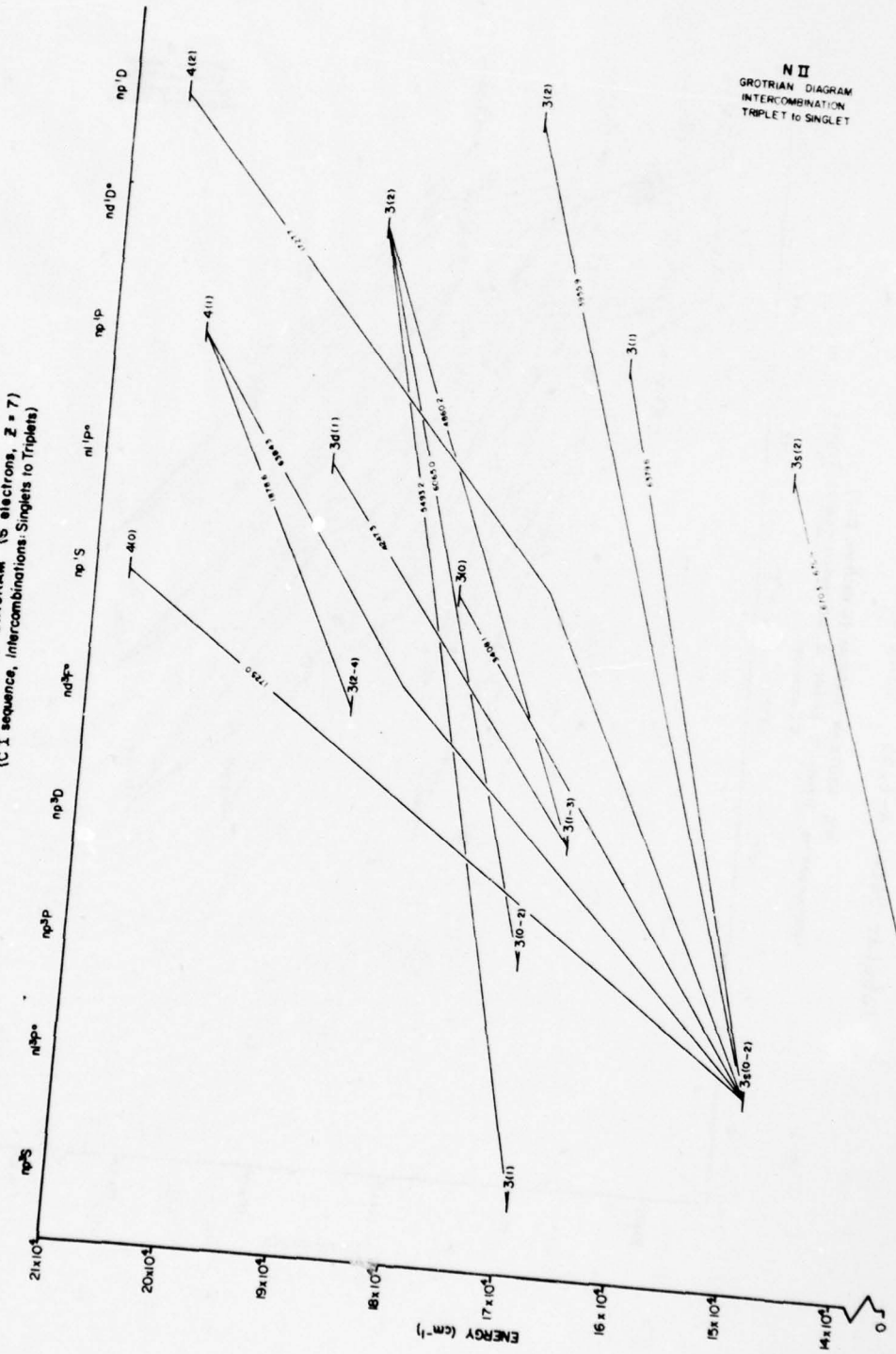

Tabular Data. A-1.55. Diagram for N^{+} ($Z = 7$).

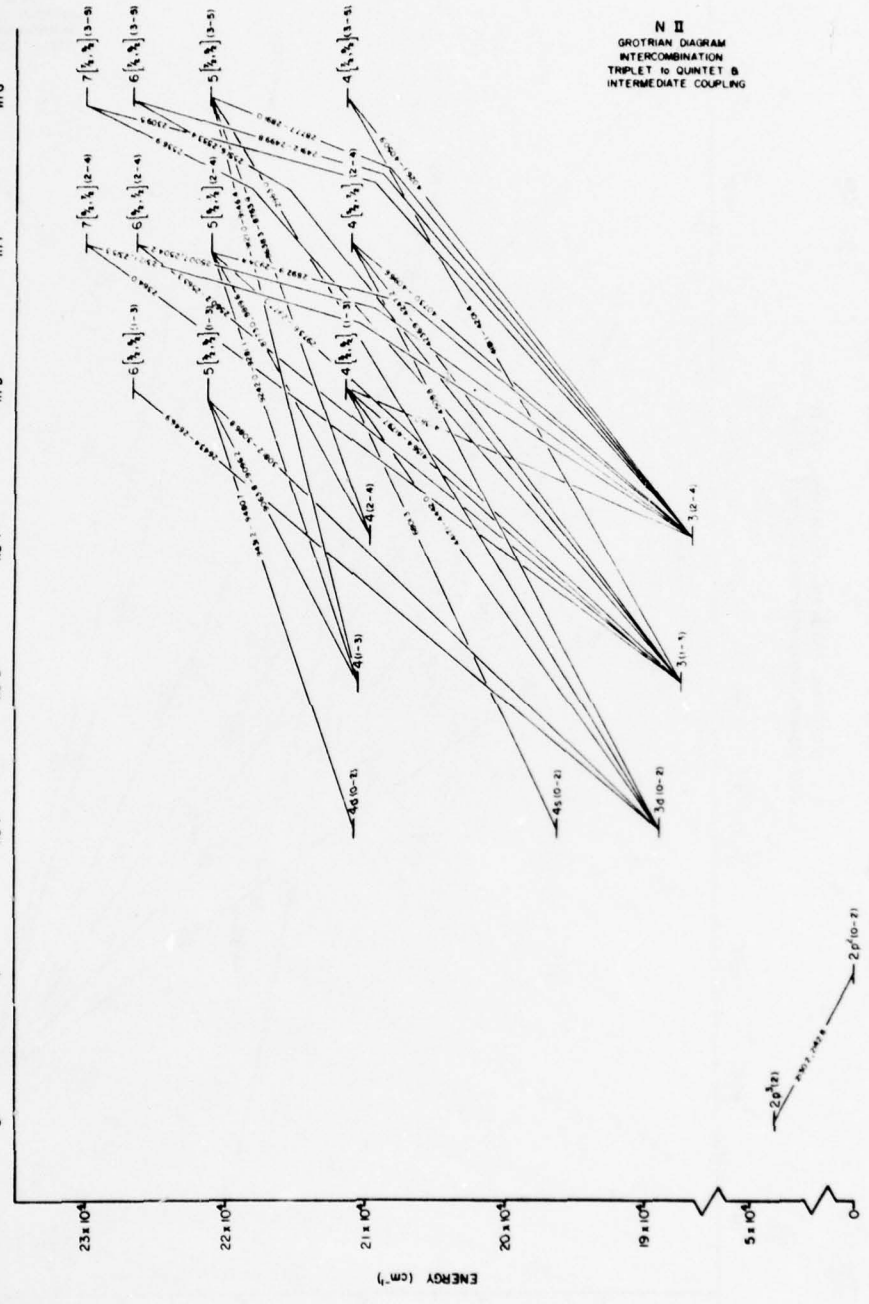

Tabular Data. A-1.56. Diagram for O (Z = 8).

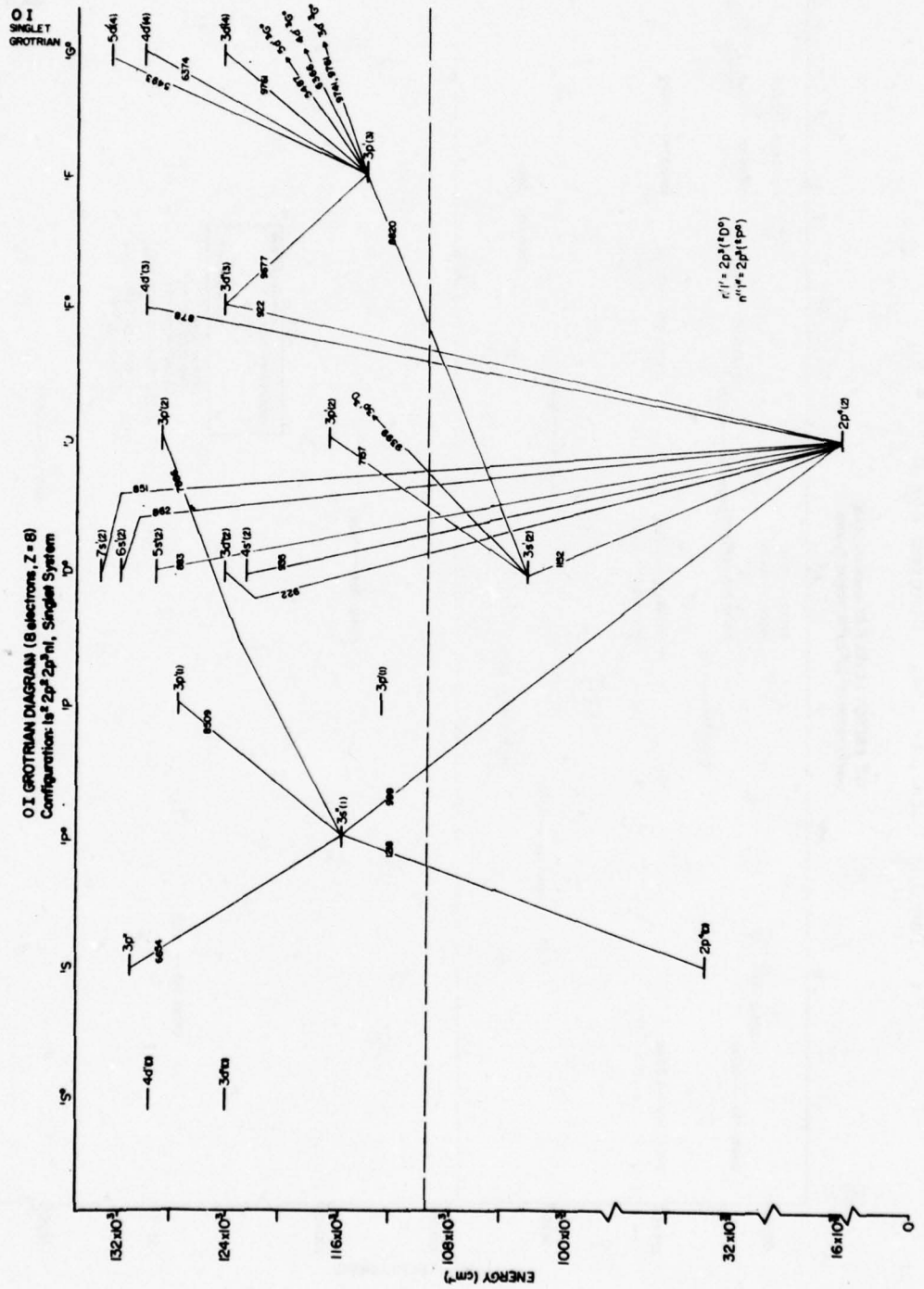

Tabular Data. A-1.57. Diagram for O (Z = 8).

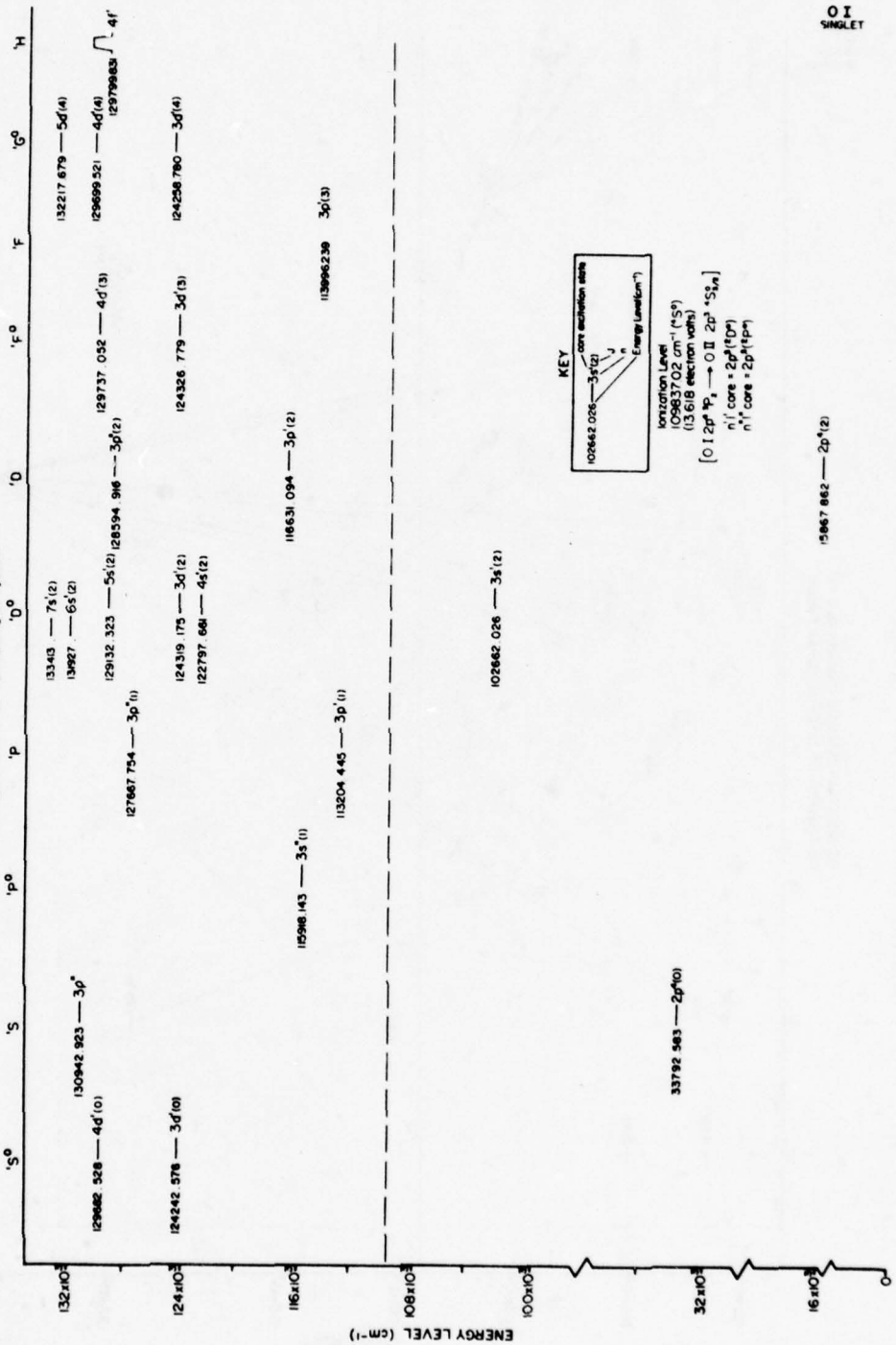

Tabular Data. A-1.58. Diagram for O (Z = 8).

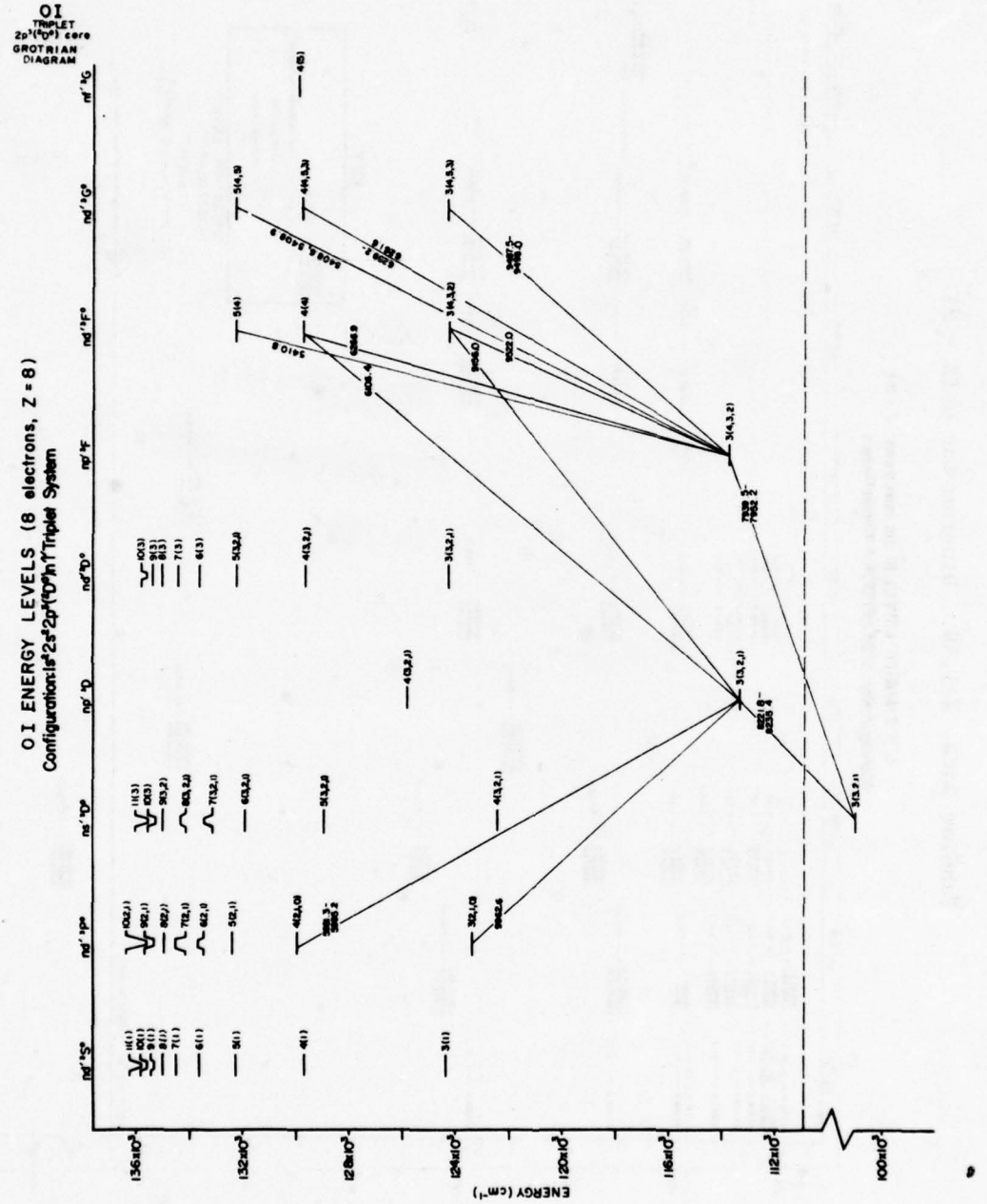

Tabular Data. A-1.59. Diagram for O (Z = 8).

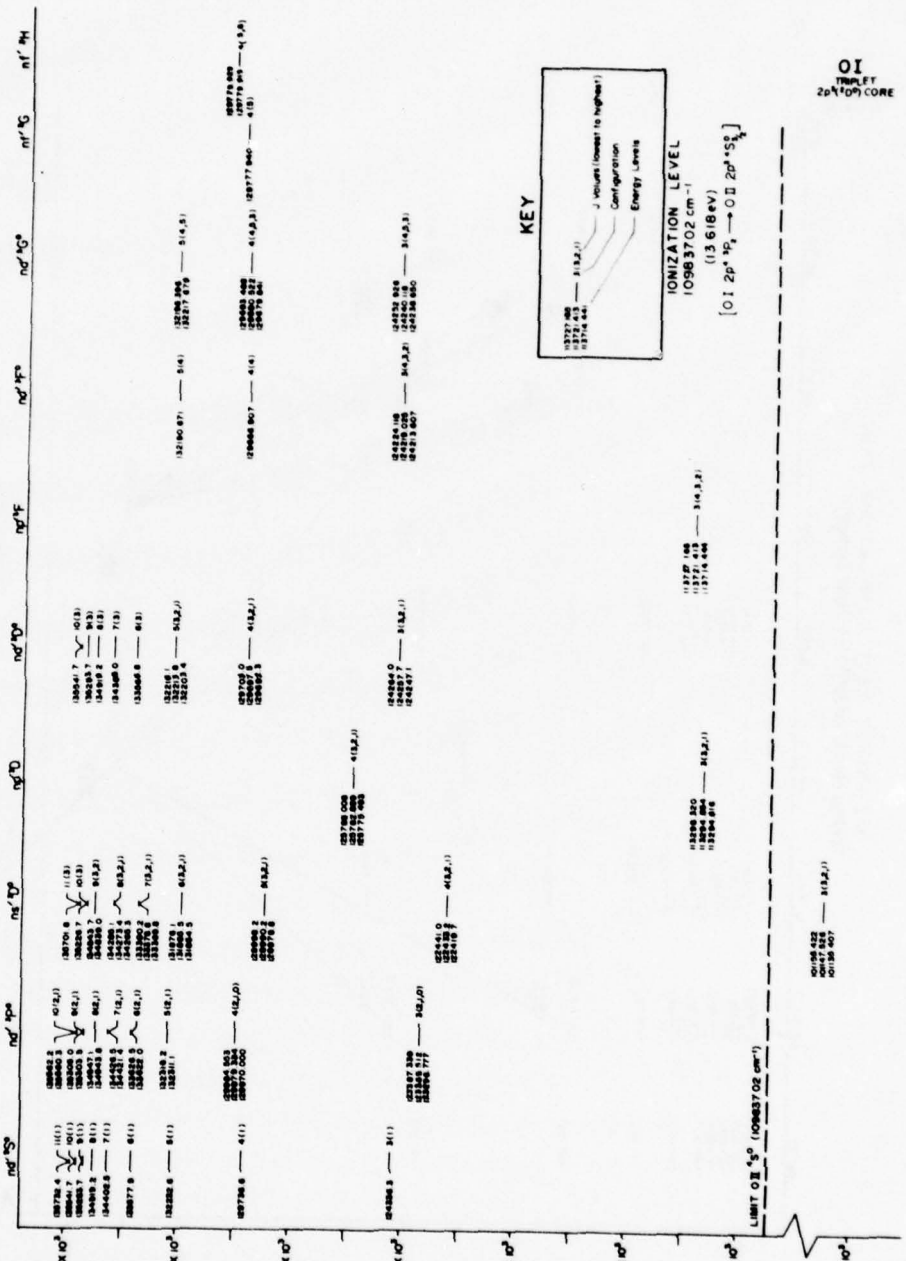

Tabular Data. A-1.60. Diagram for O (Z = 8).

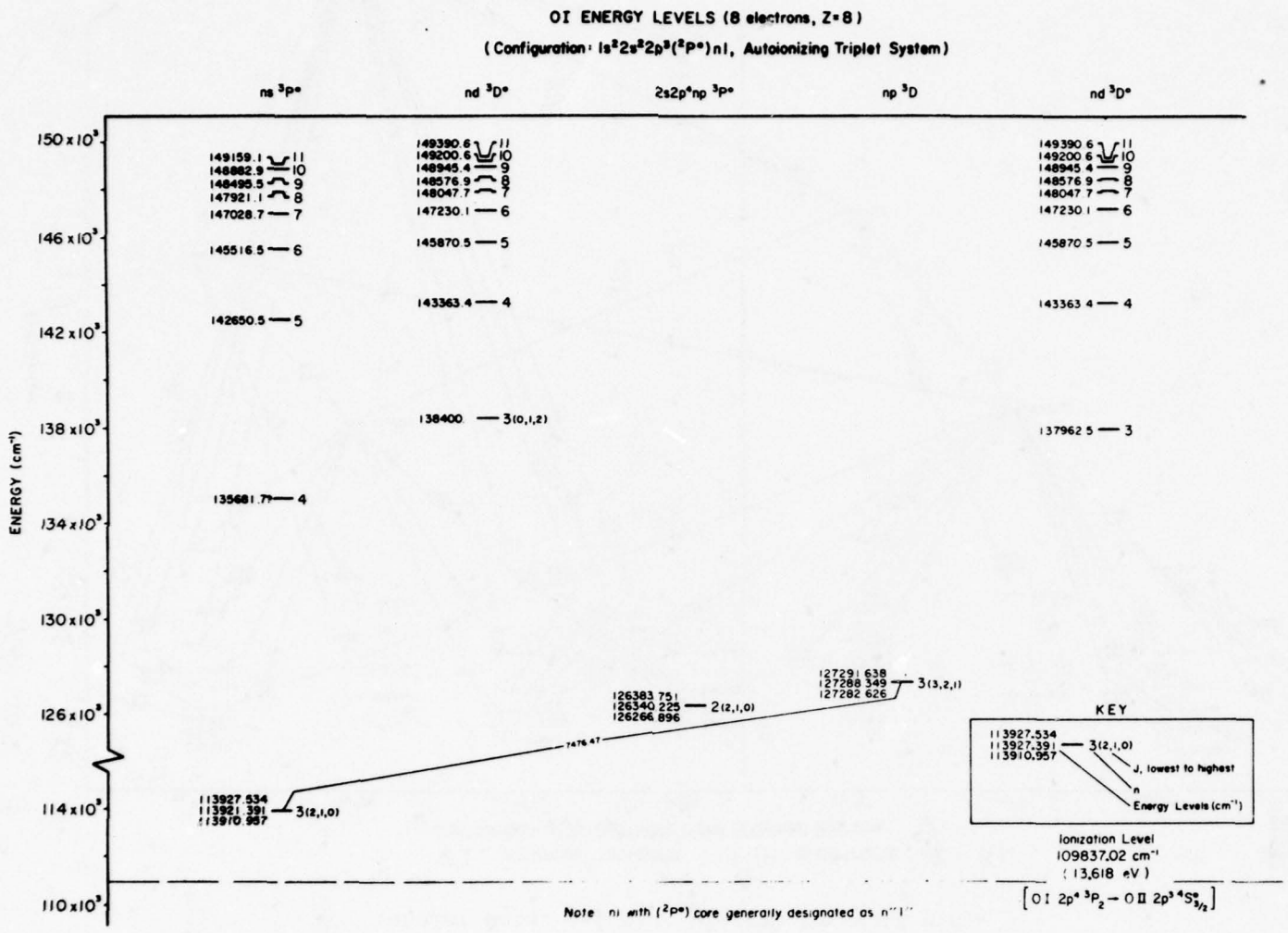

Tabular Data. A-1.61. Diagram for O (Z = 8).

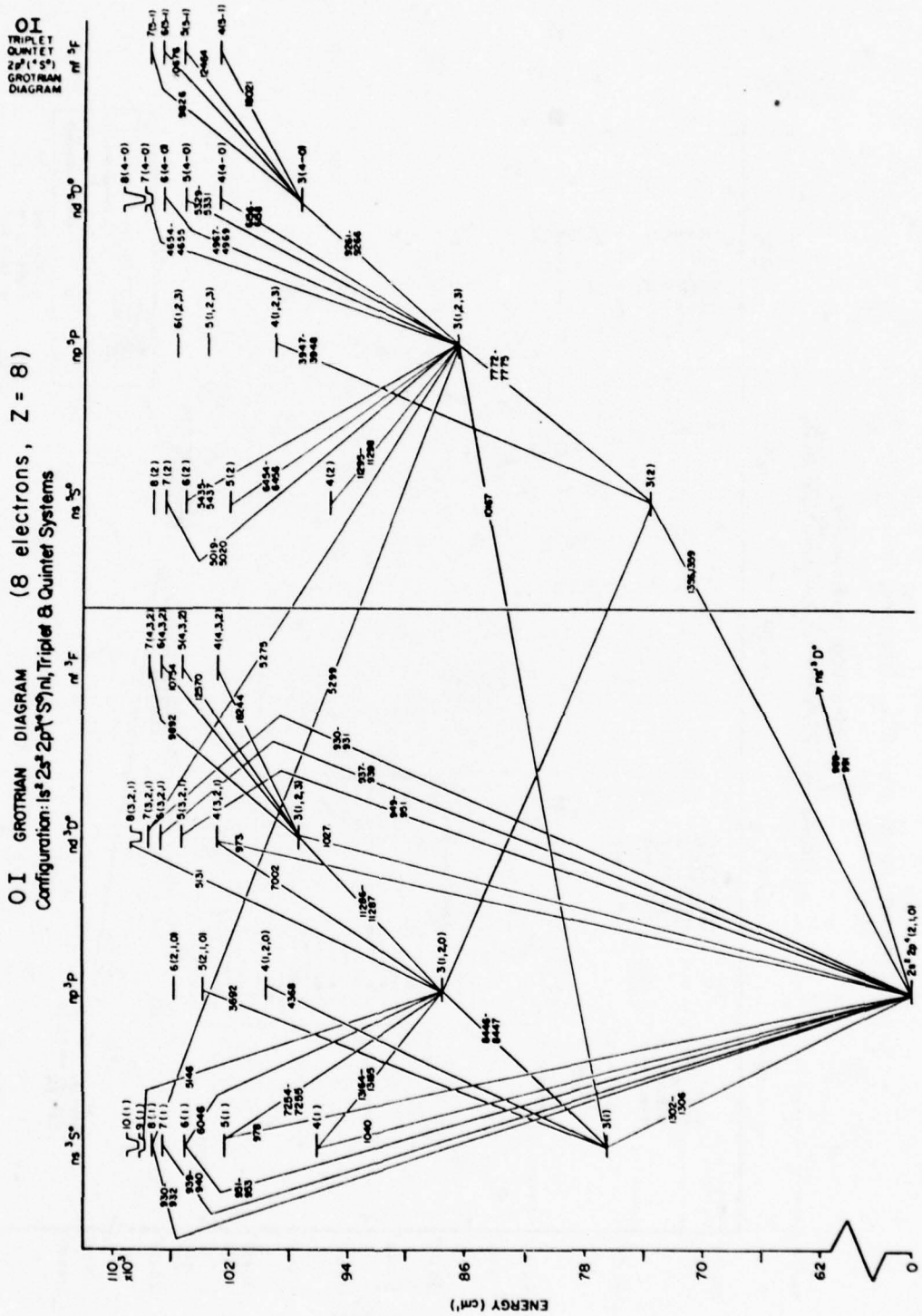

Tabular Data. A-1.62. Diagram for O (Z = 8).

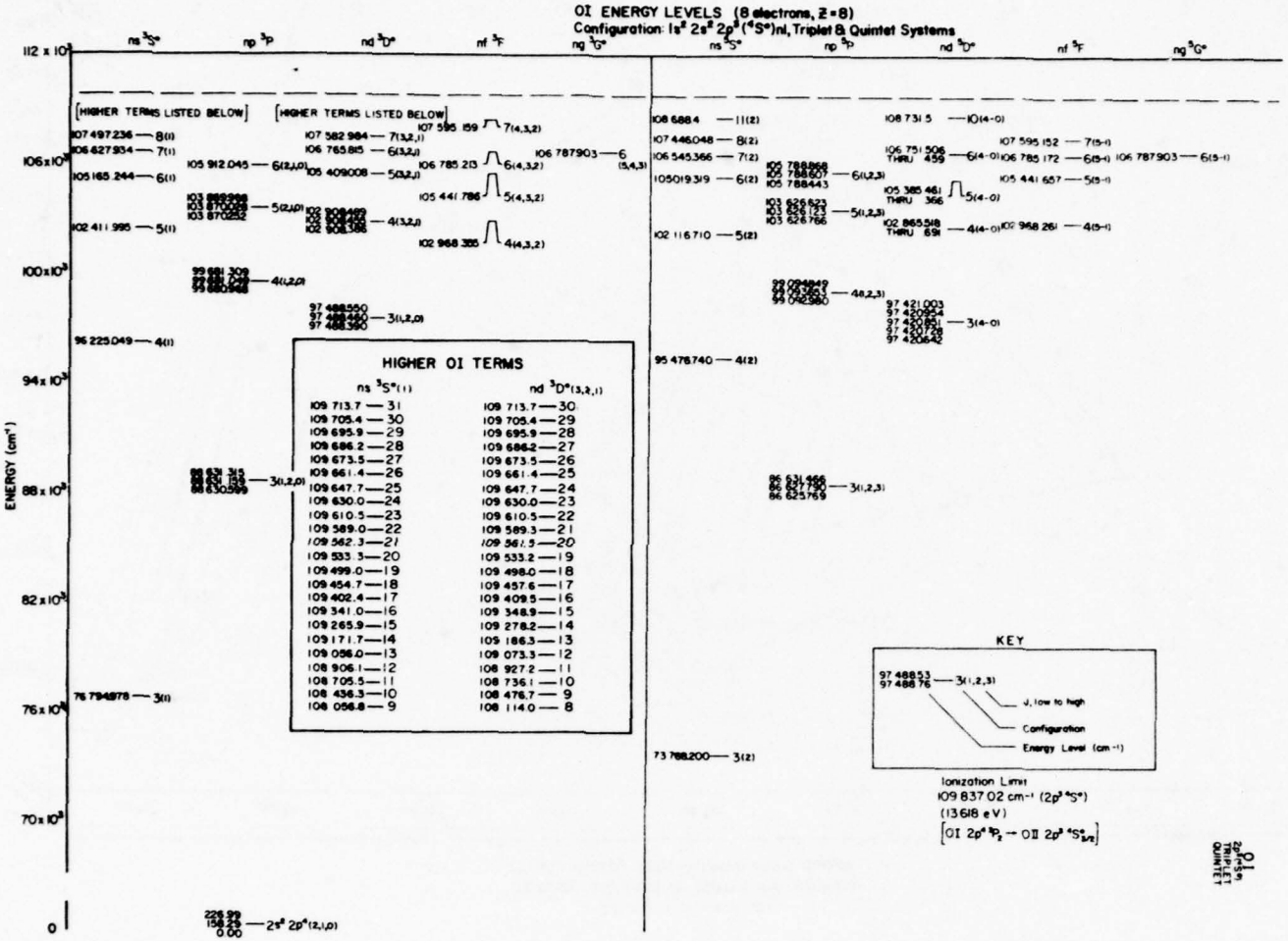

Tabular Data. A-1.63. Diagram for O (Z = 8).

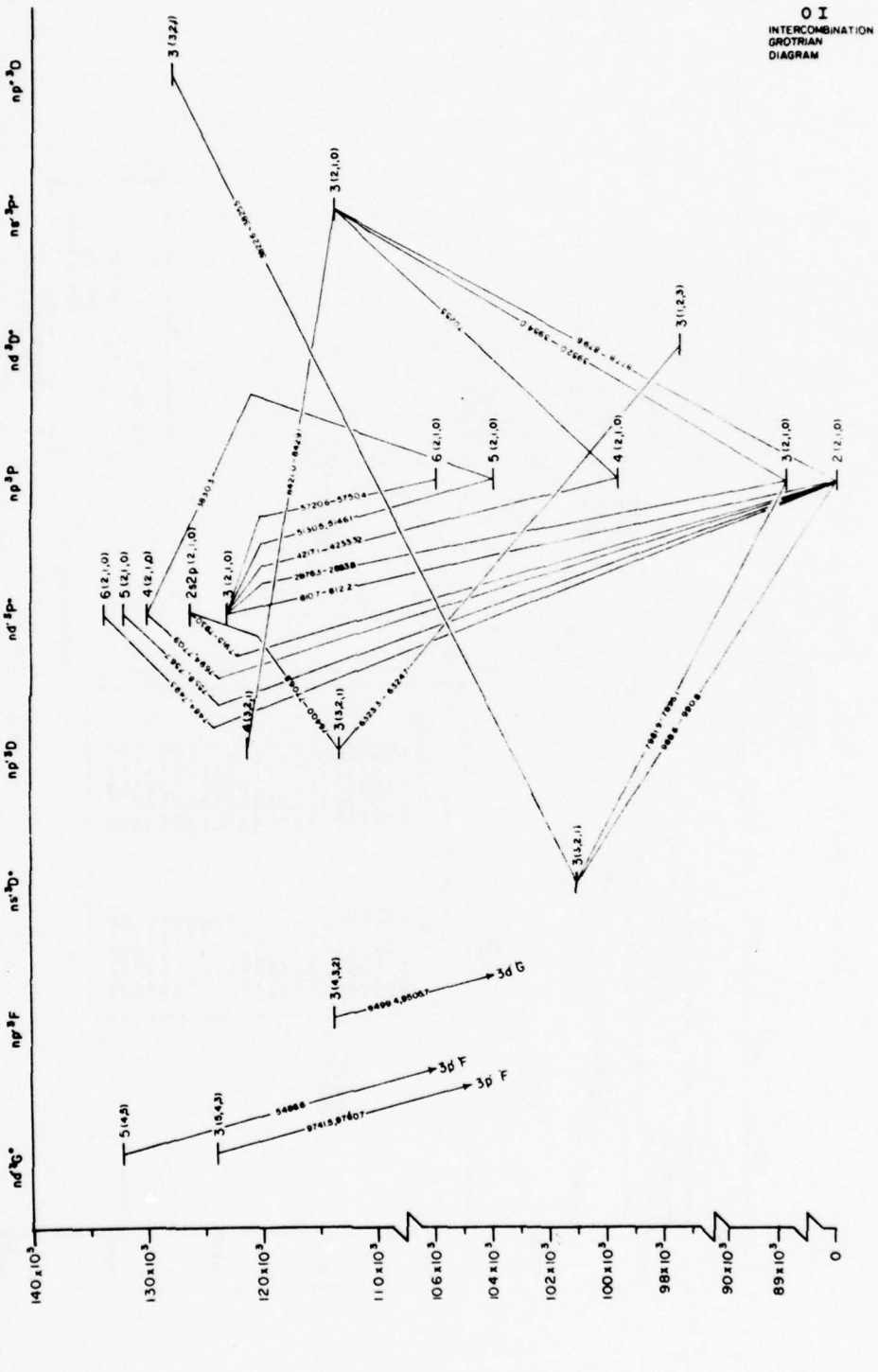

Tabular Data. A-1.64. Diagram for O^{+} (Z = 8).

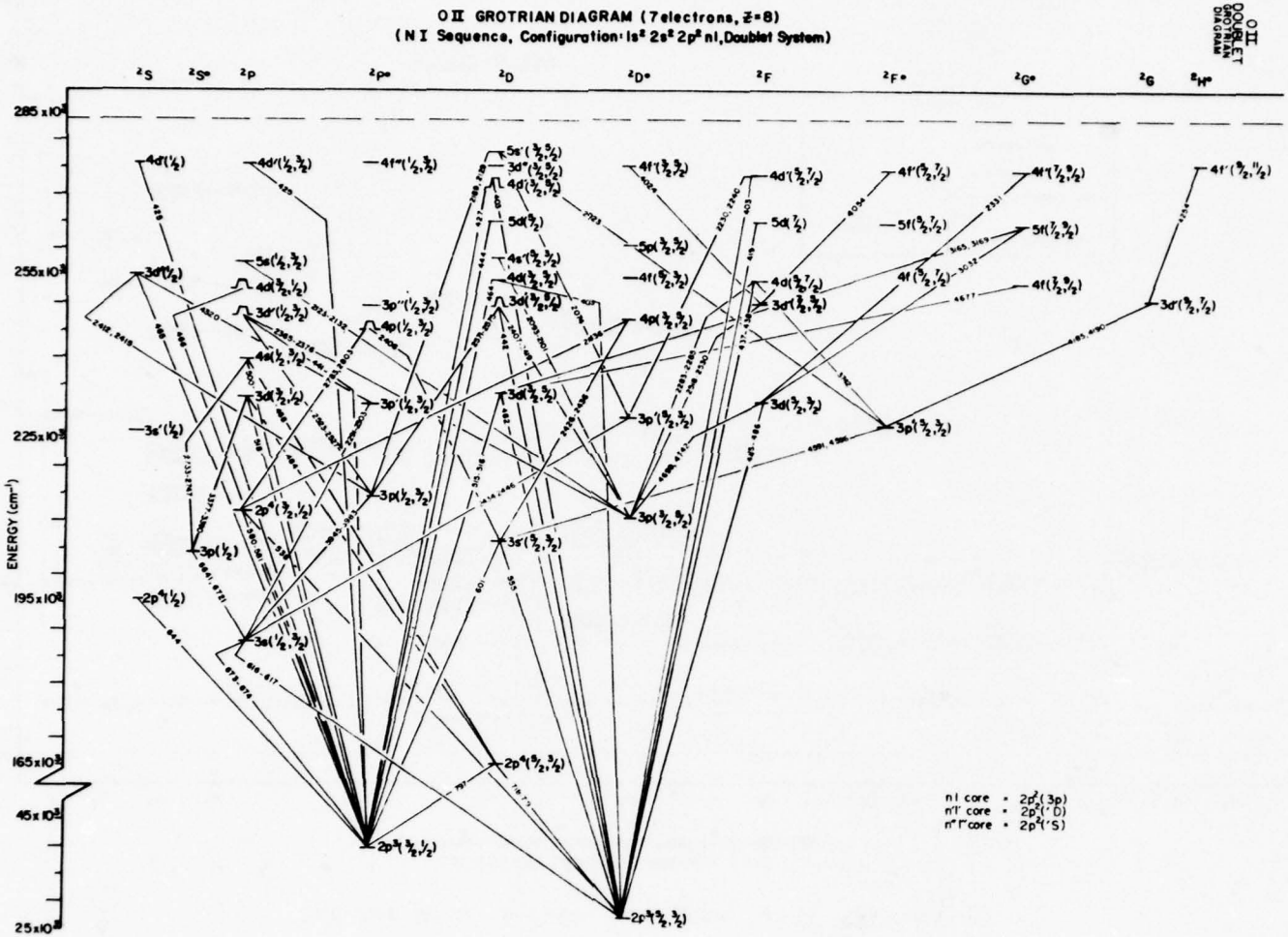

Tabular Data. A-1.65. Diagram for O^+ (Z = 8).

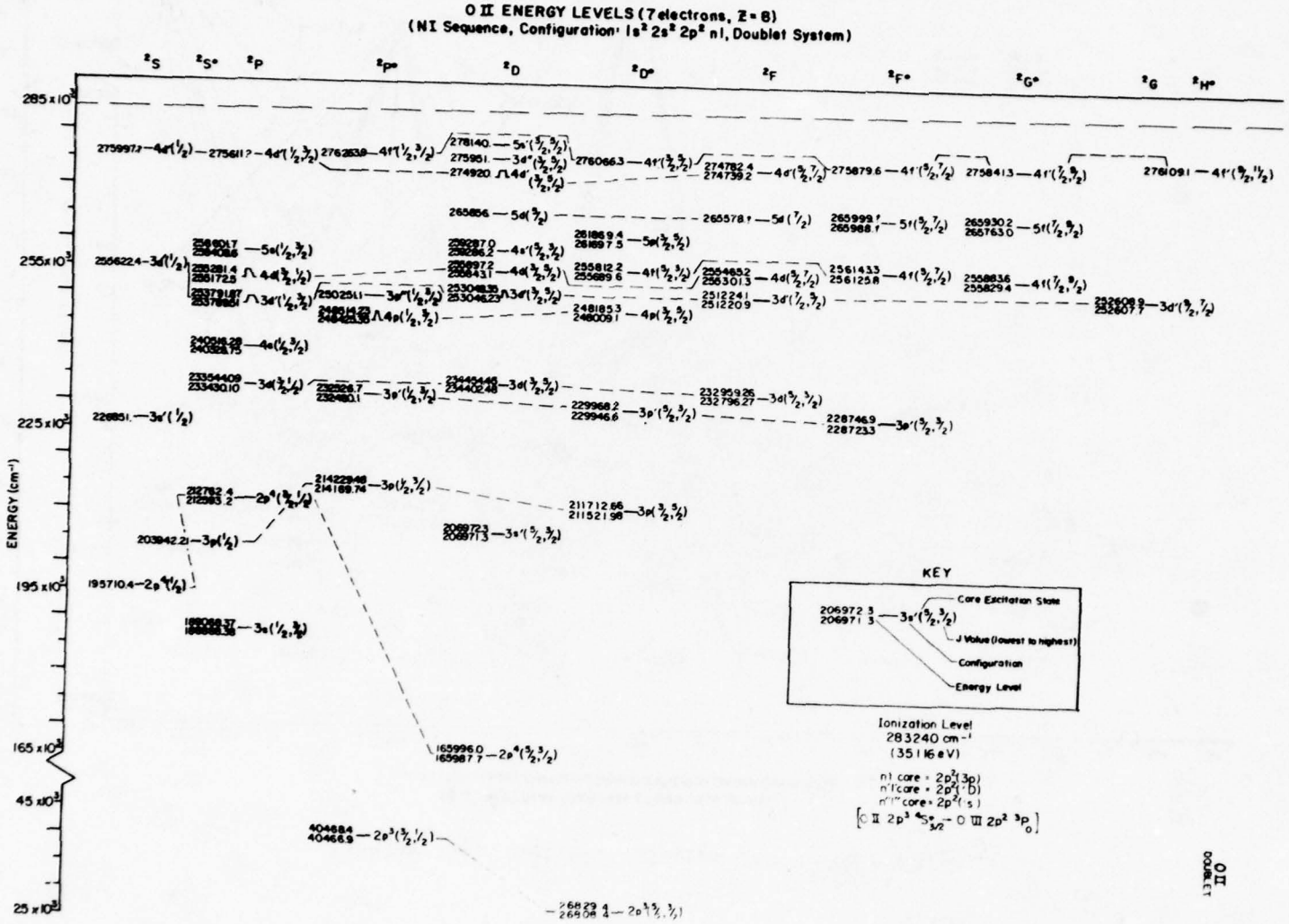

Tabular Data. A-1.66. Diagram for O^{+} (Z = 8).

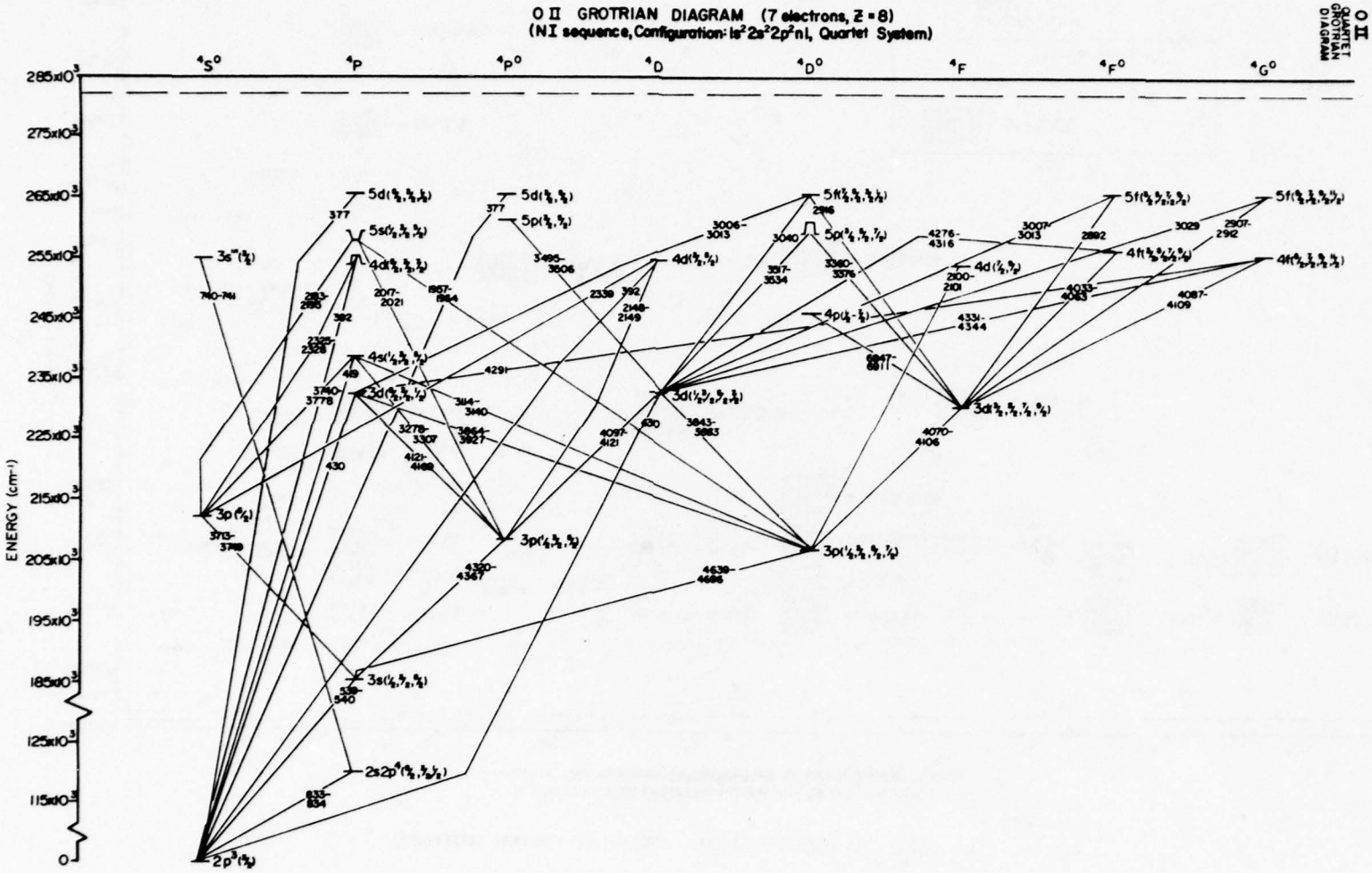

Tabular Data. A-1.67. Diagram for O^{+} (Z = 8).

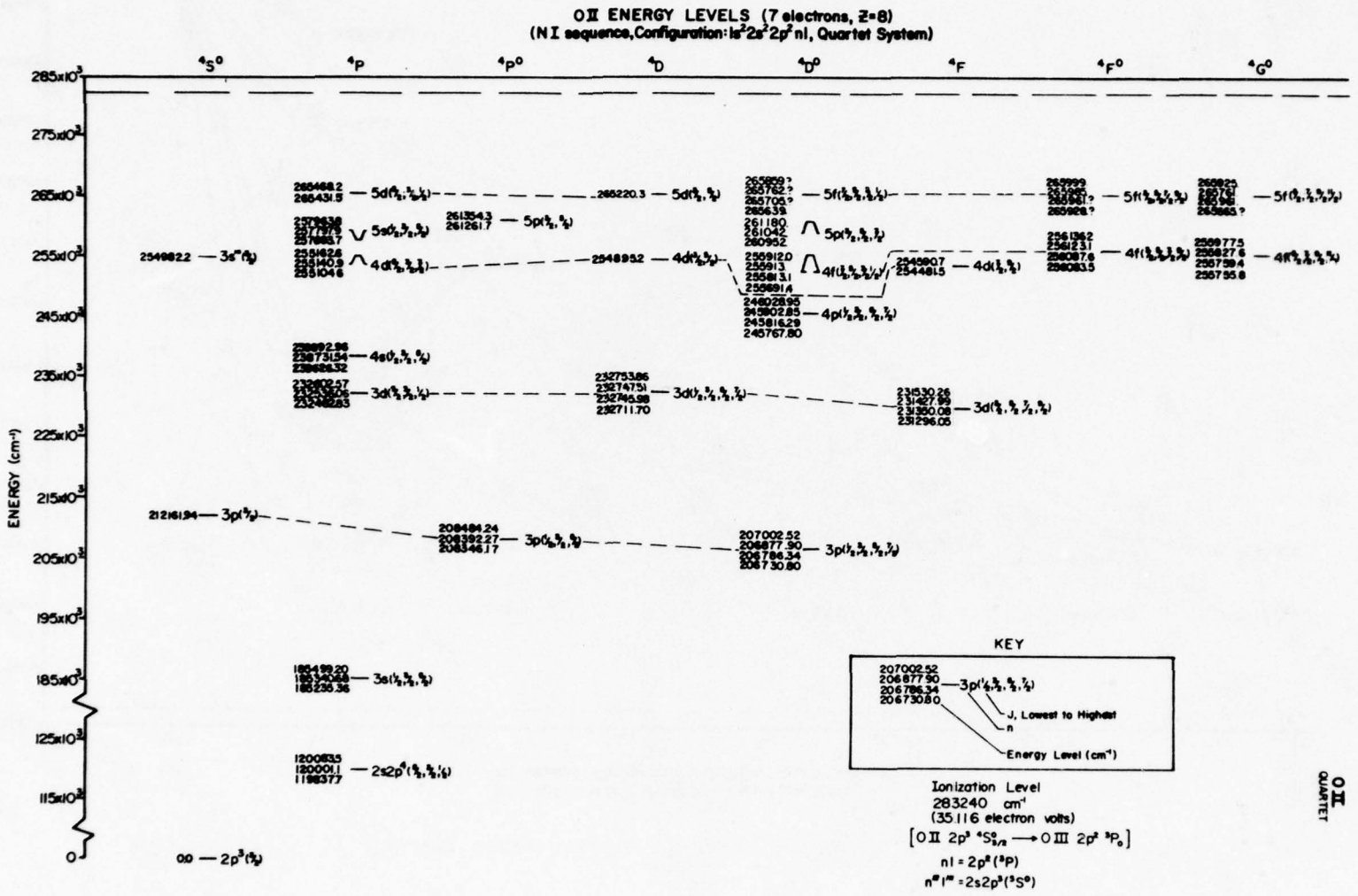

Tabular Data. A-1.68. Diagram for O^+ (Z = 8).

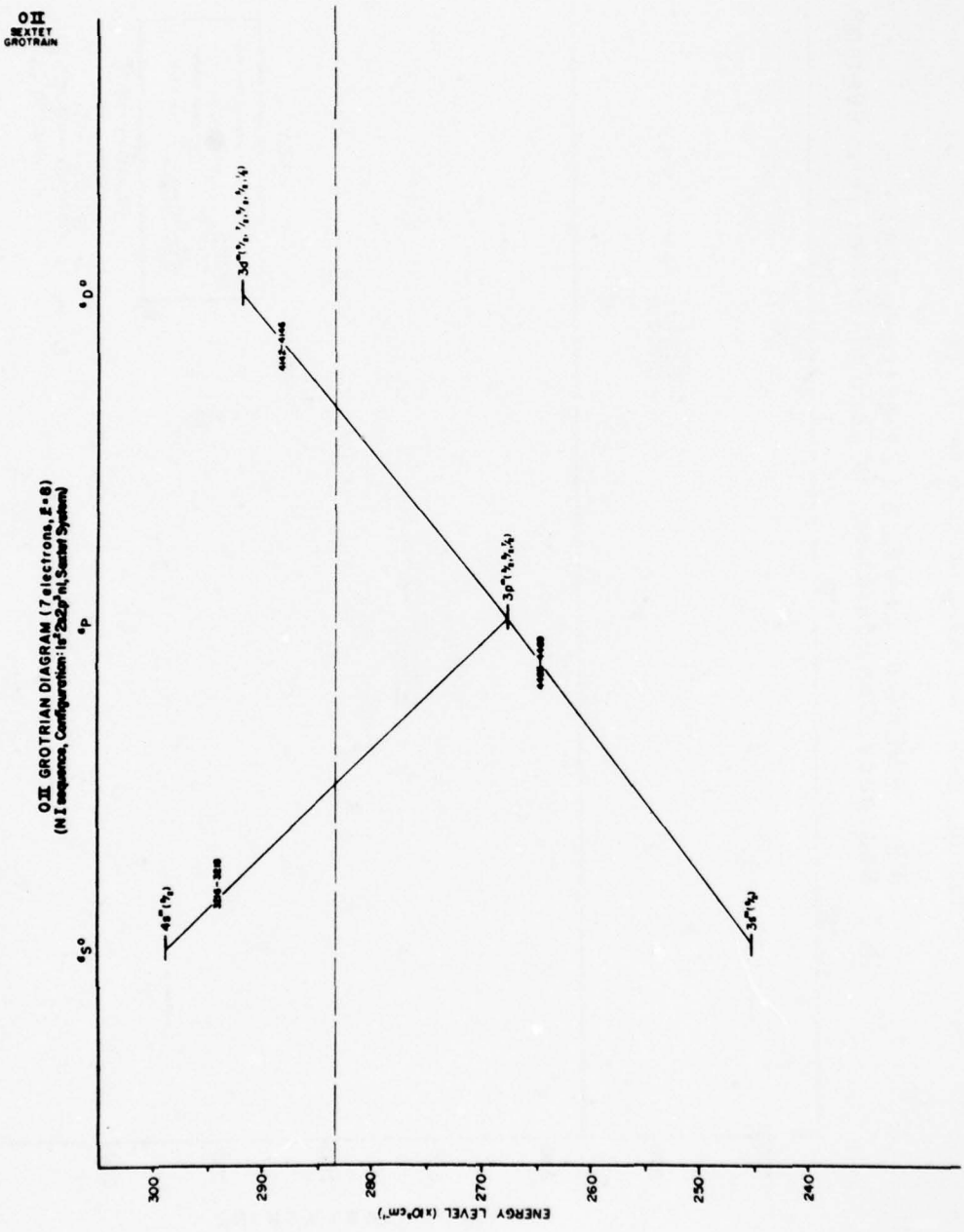

Tabular Data. A-1.69. Diagram for O^+ (Z = 8).

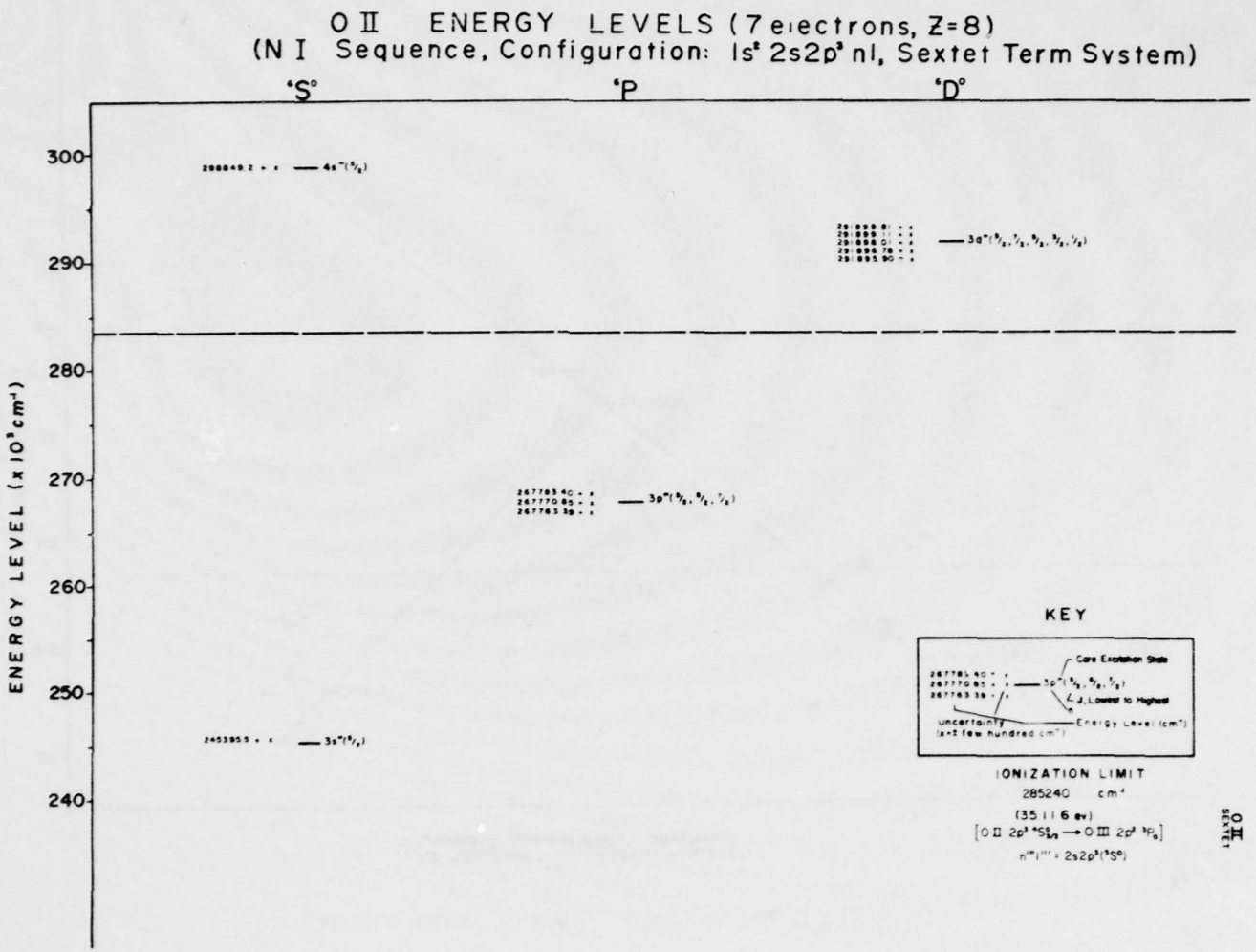

Tabular Data. A-1.70. Diagram for O^{+} (Z = 8).

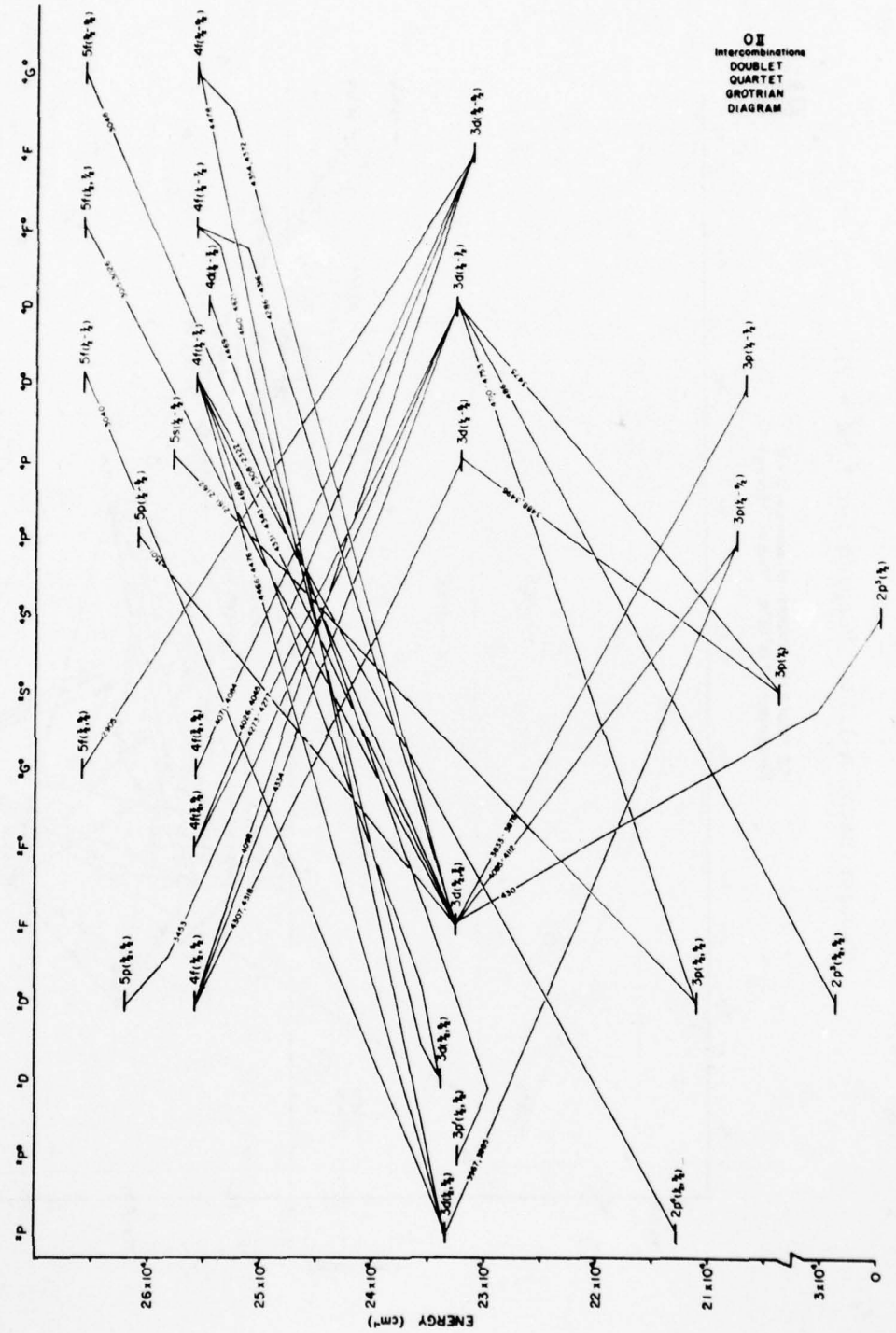

Tabular Data. A-1.71. Diagram for F (Z = 9).

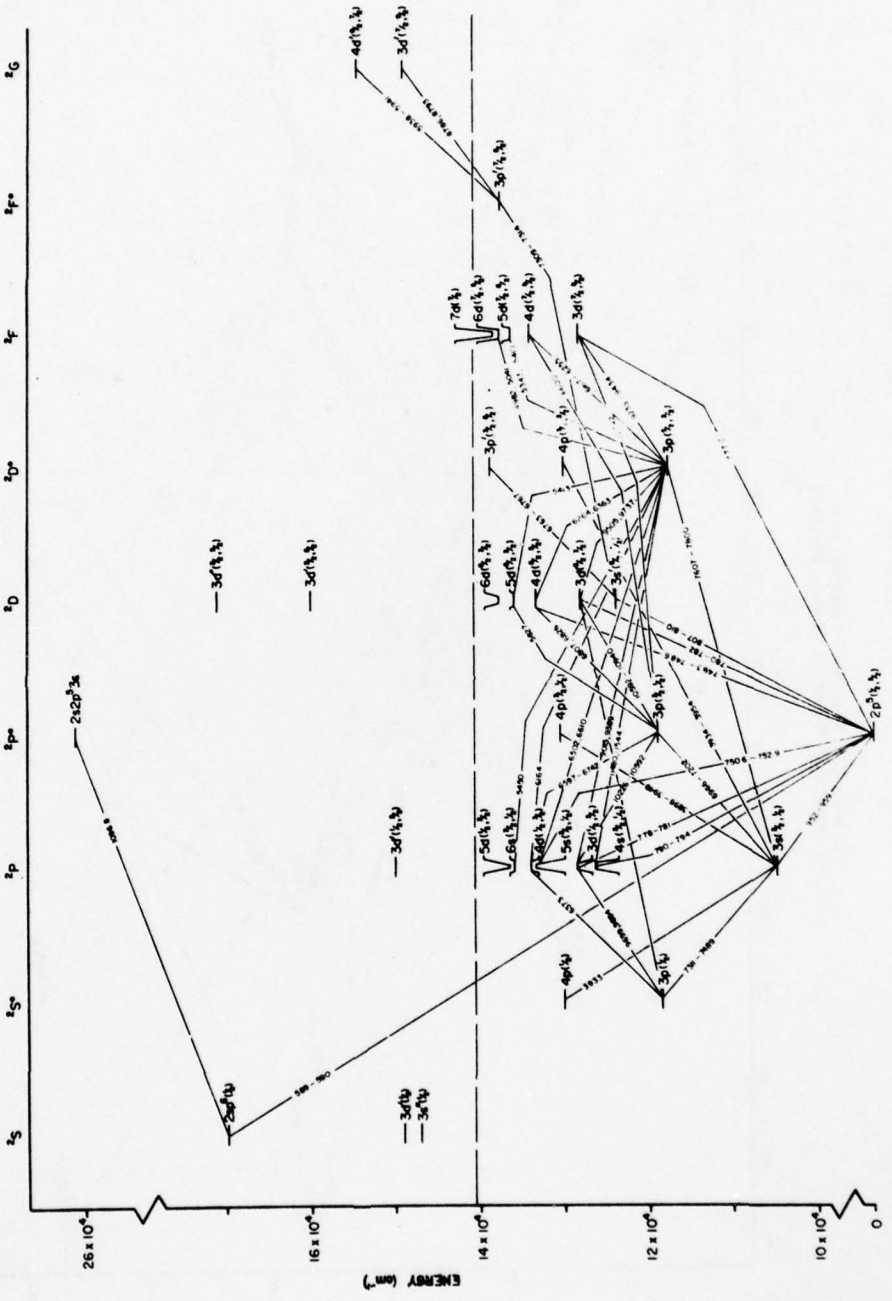

Tabular Data. A-1.72. Diagram for F (Z = 9).

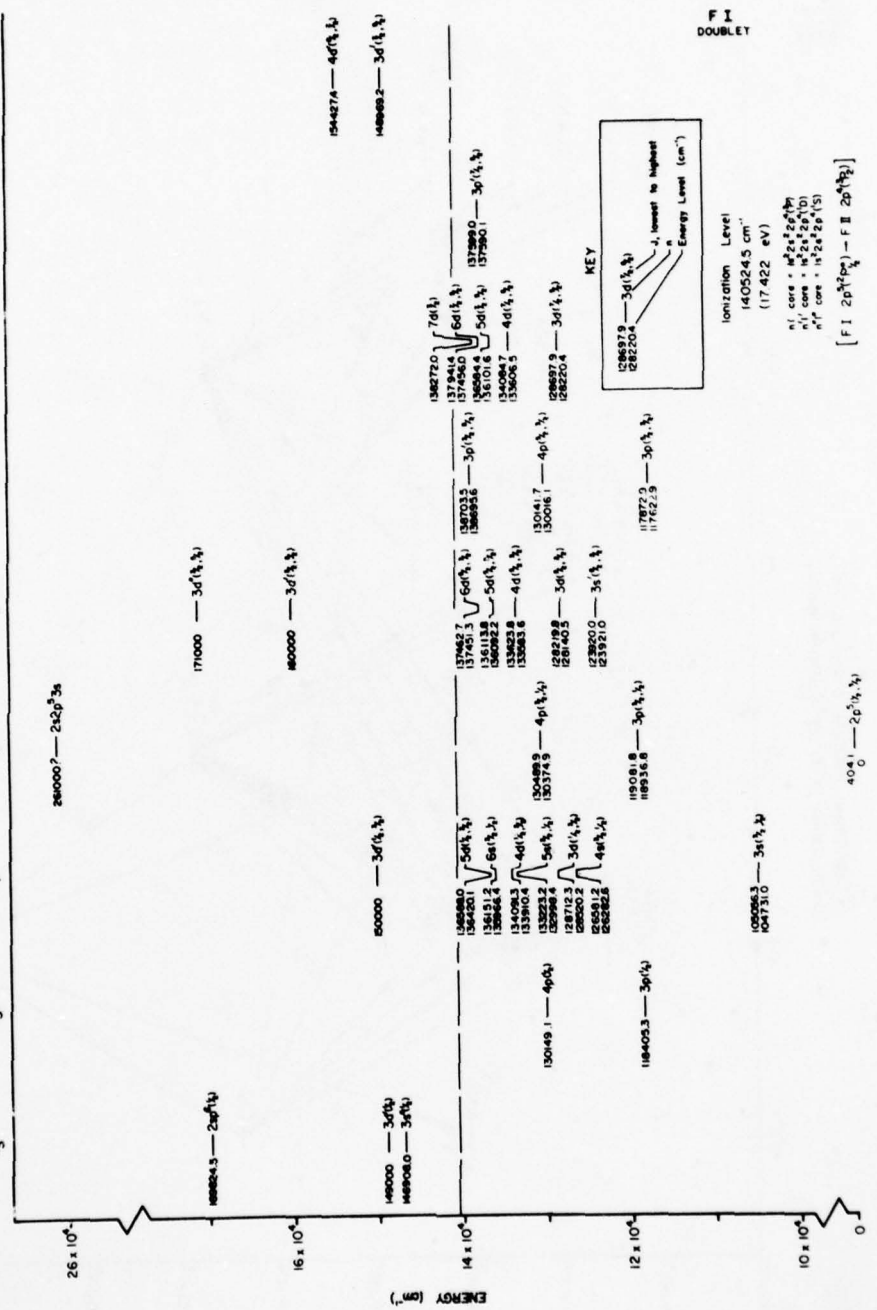

Tabular Data. A-1.73. Diagram for F (Z = 9).

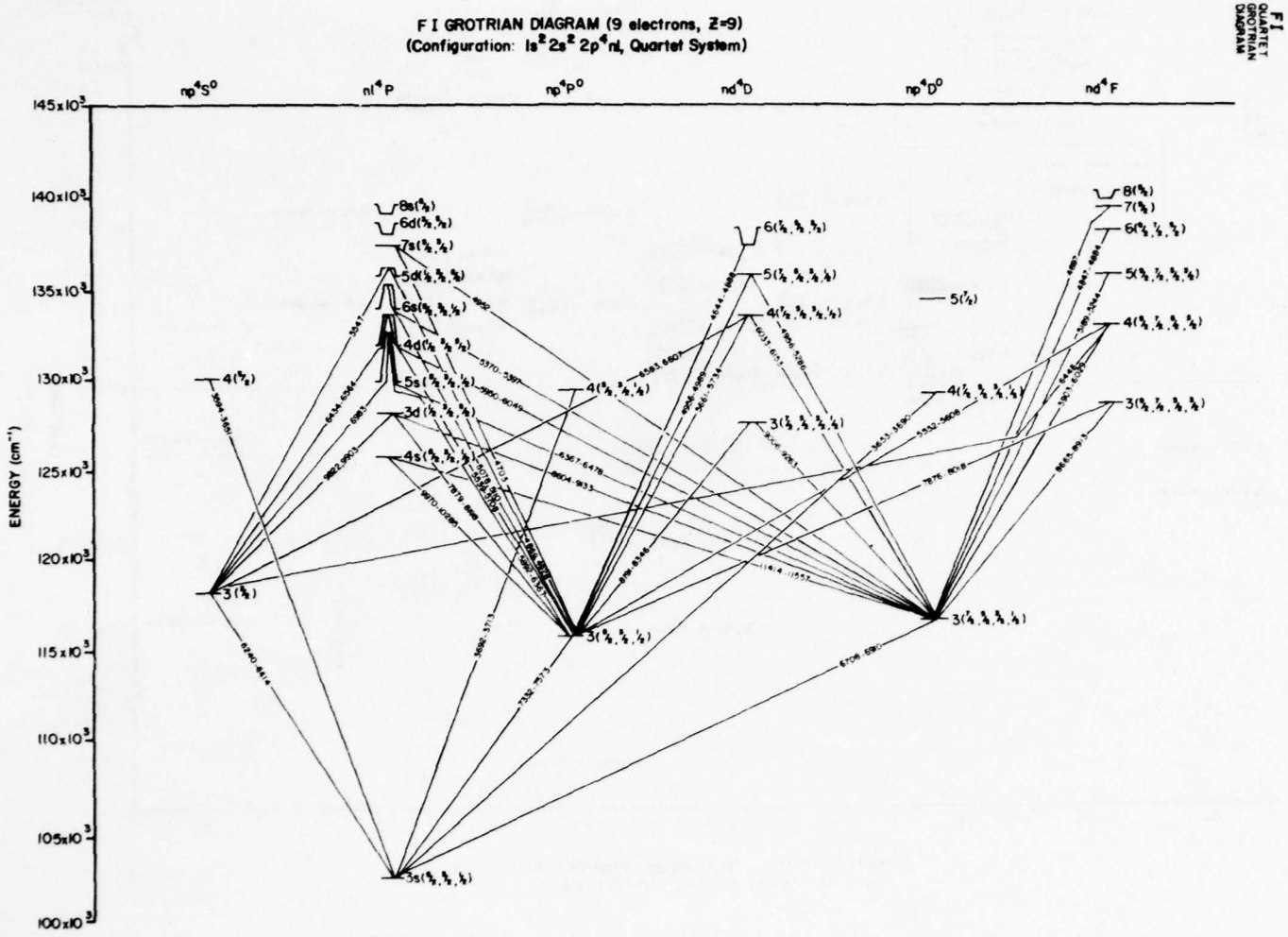

Tabular Data. A-1.74. Diagram for F (Z = 9).

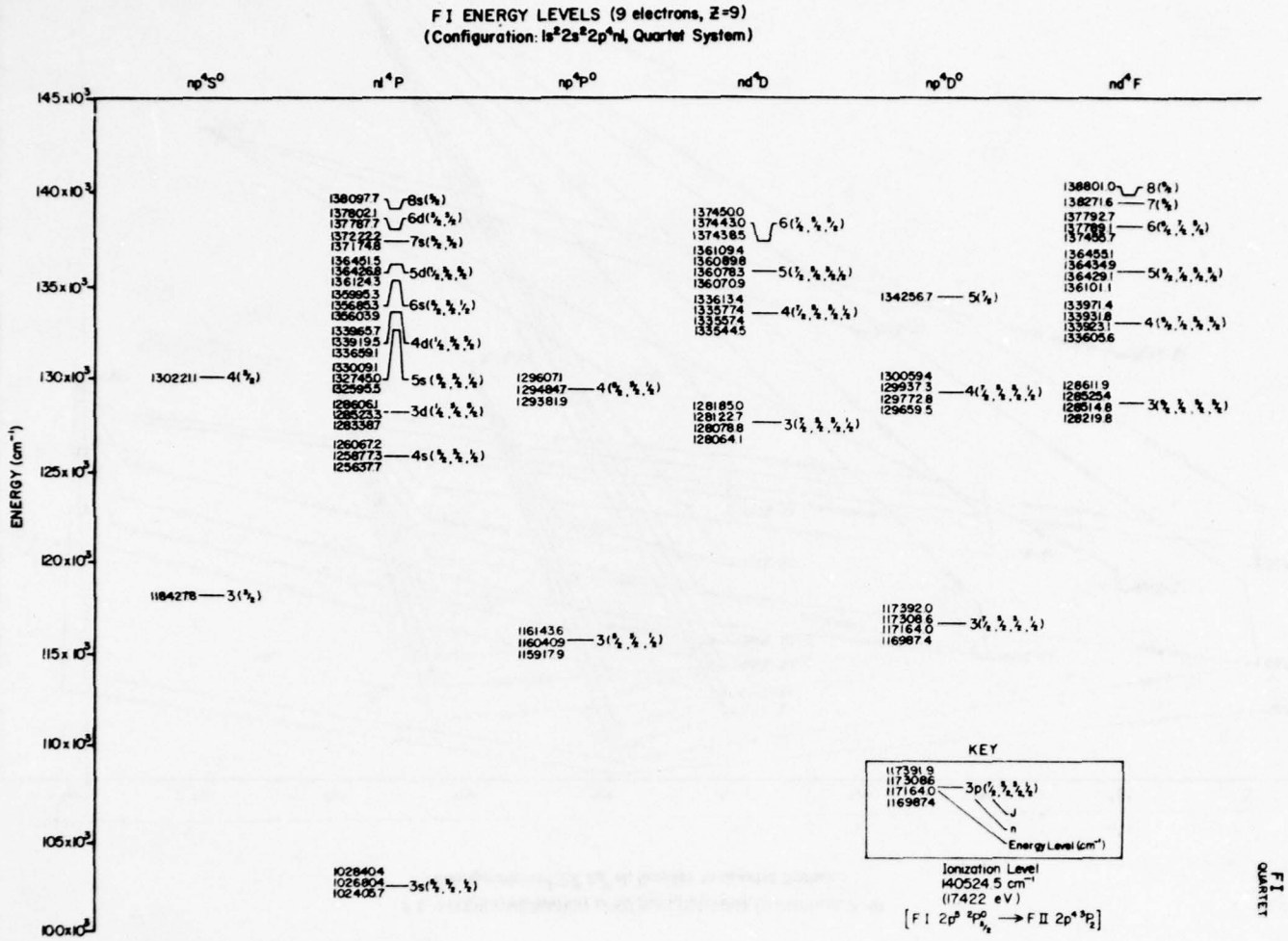

Tabular Data. A-1.75. Diagram for F (Z = 9).

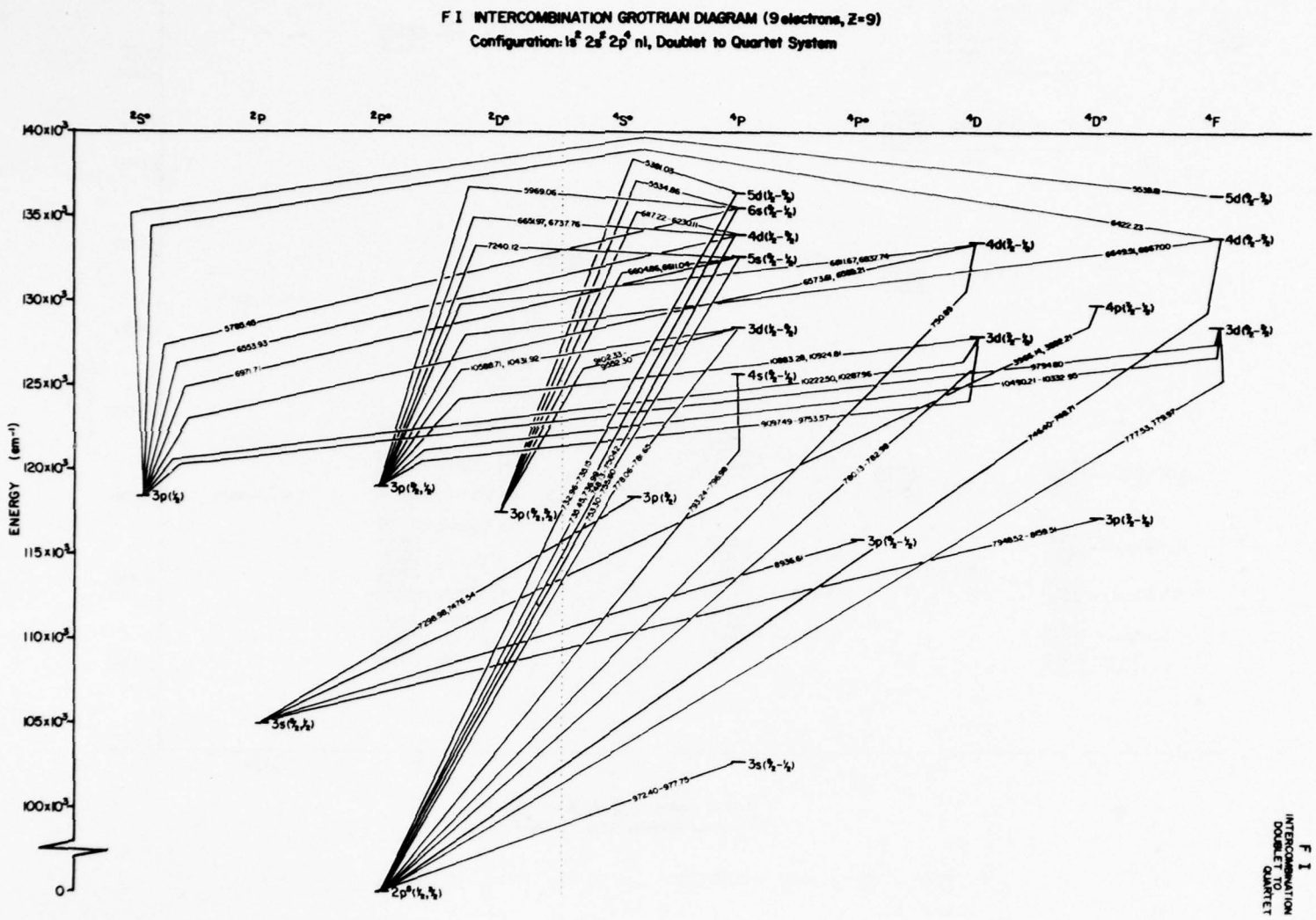

Tabular Data. A-1.76. Diagram for F (Z = 9).

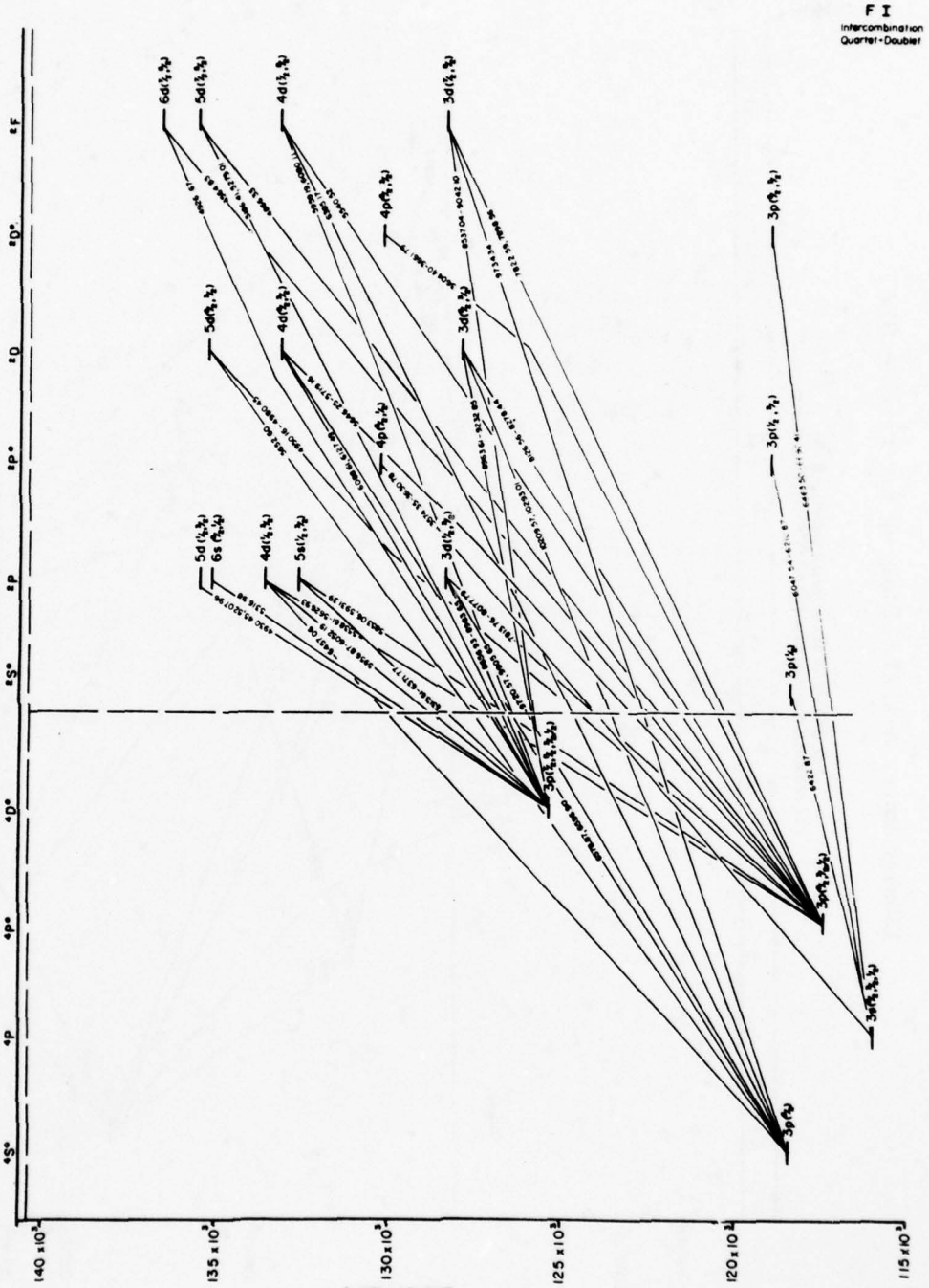

Tabular Data. A-1.77. Diagram for F^{+} (Z = 9).

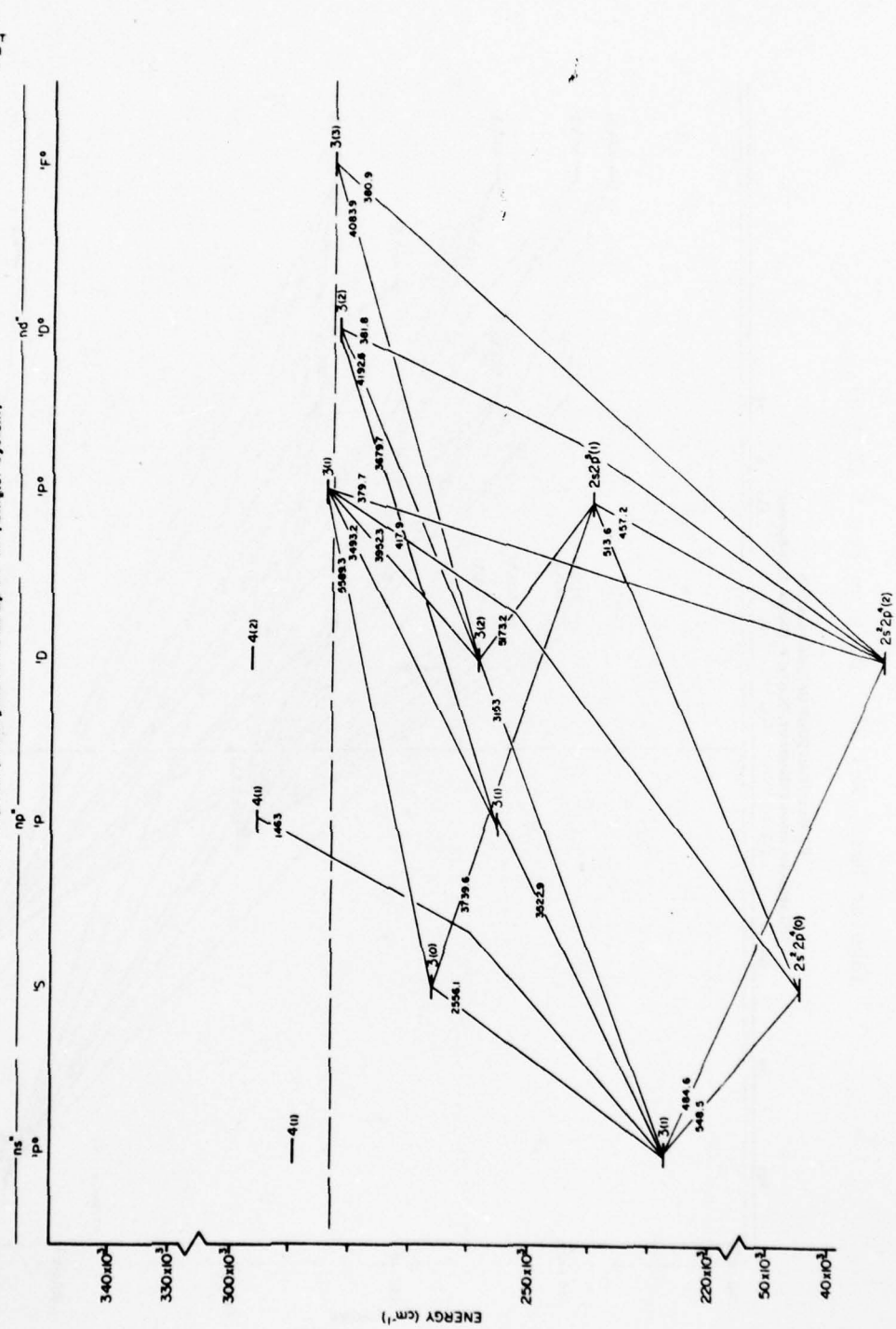

Tabular Data. A-1.78. Diagram for F^+ (Z = 9).

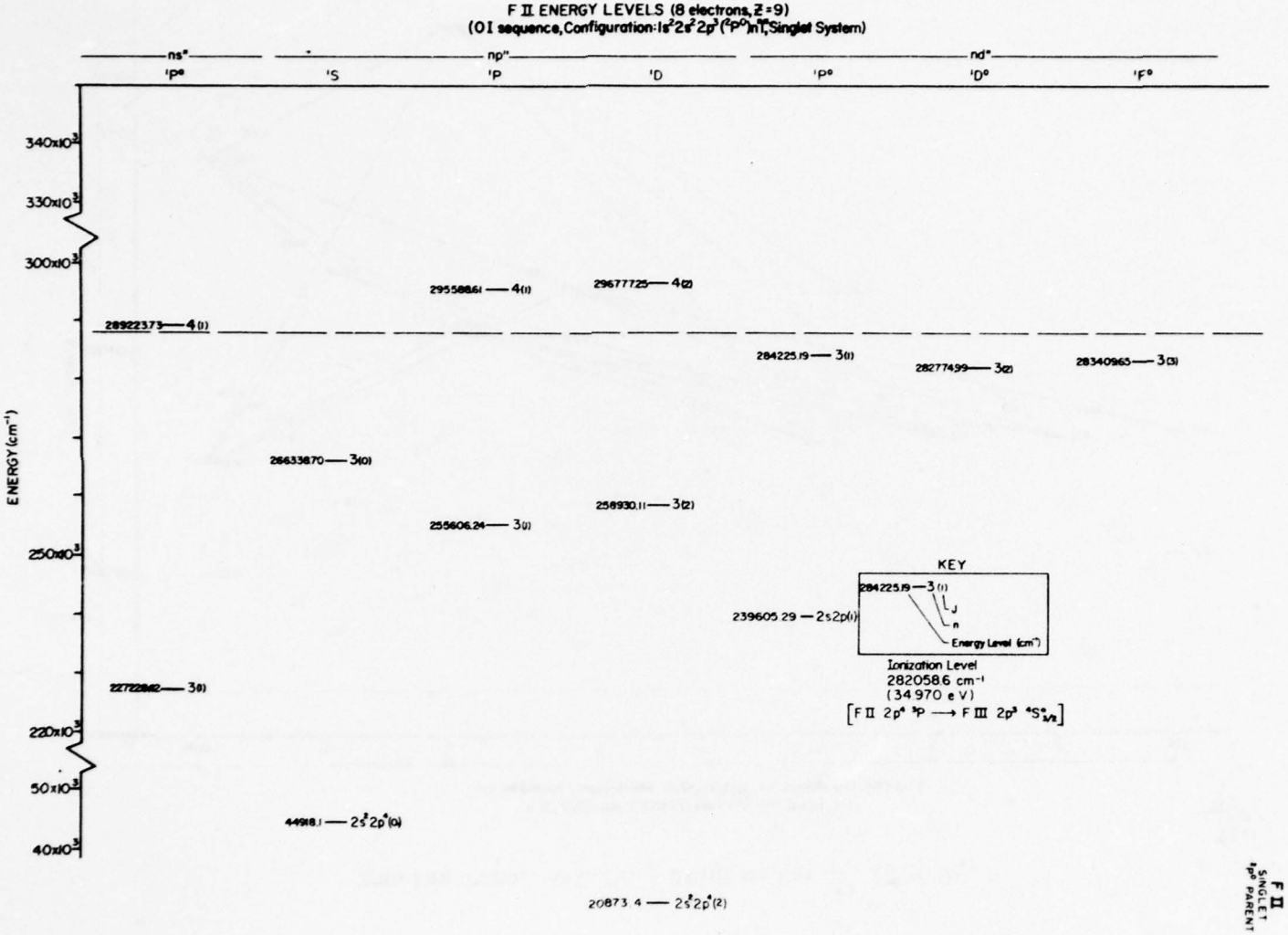

Tabular Data. A-1.79. Diagram for F^{+} (Z = 9).

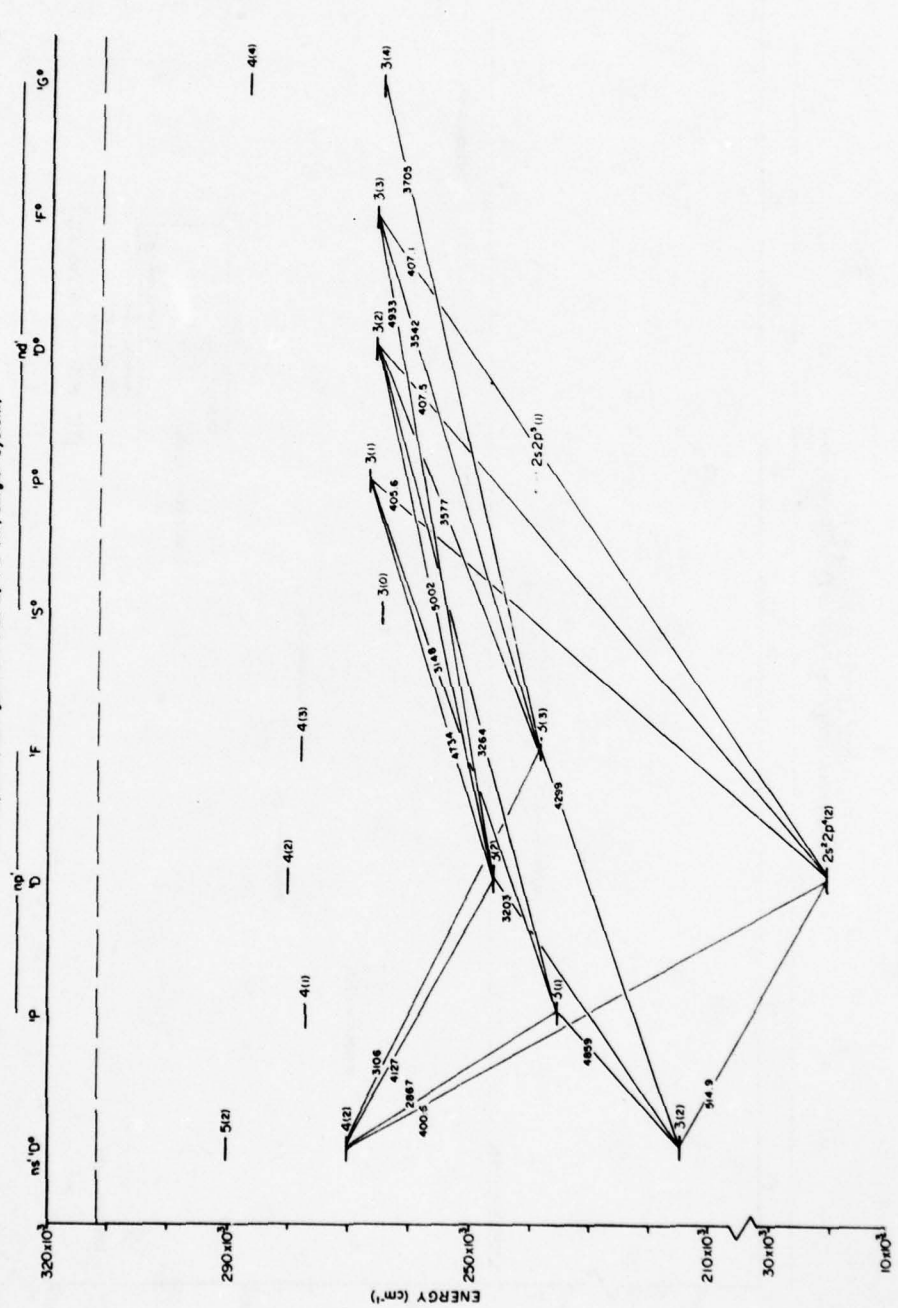

Tabular Data. A-1.80. Diagram for F^{+} (Z = 9).

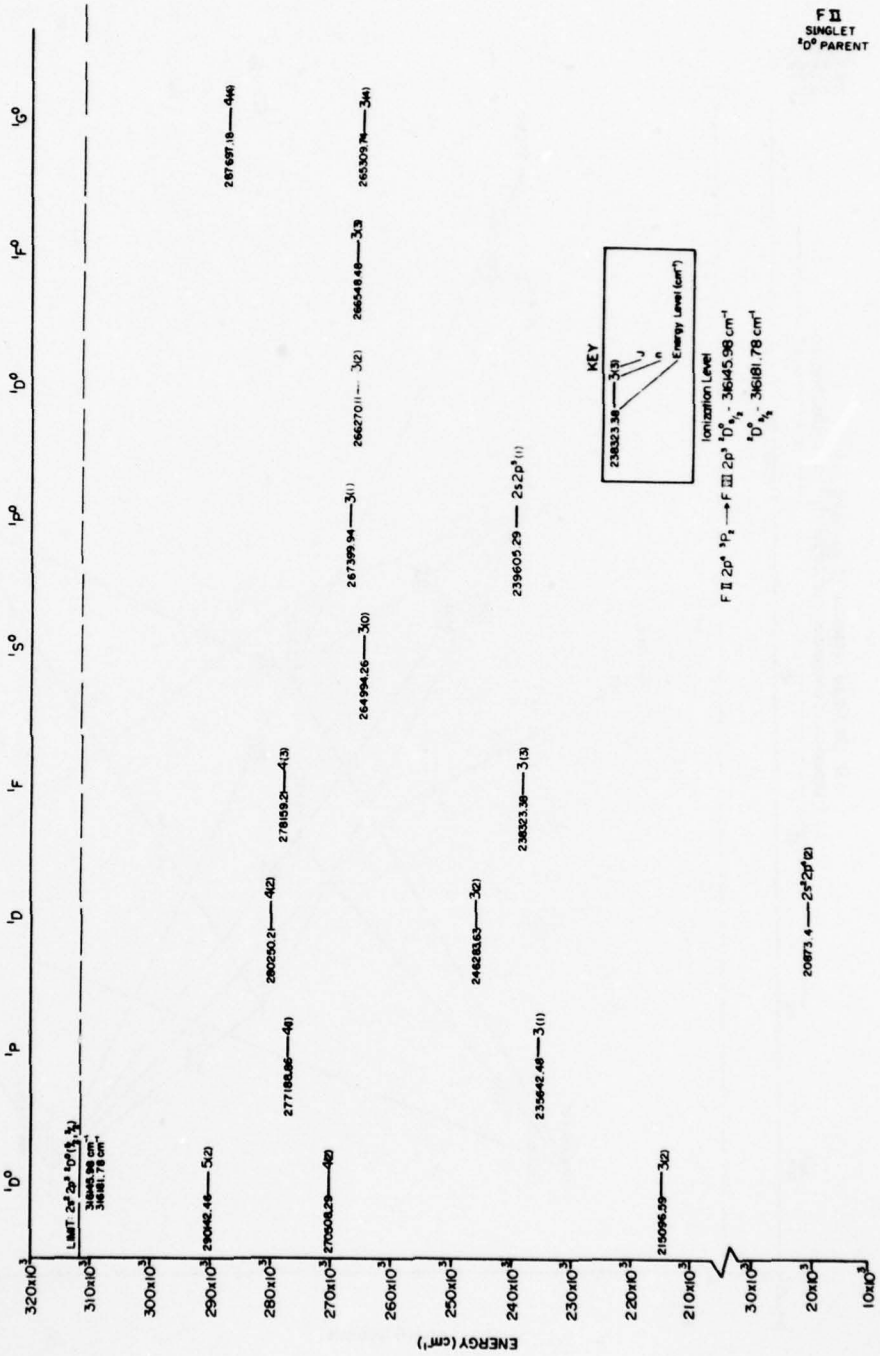

Tabular Data. A-1.81. Diagram for F^{+} (Z = 9).

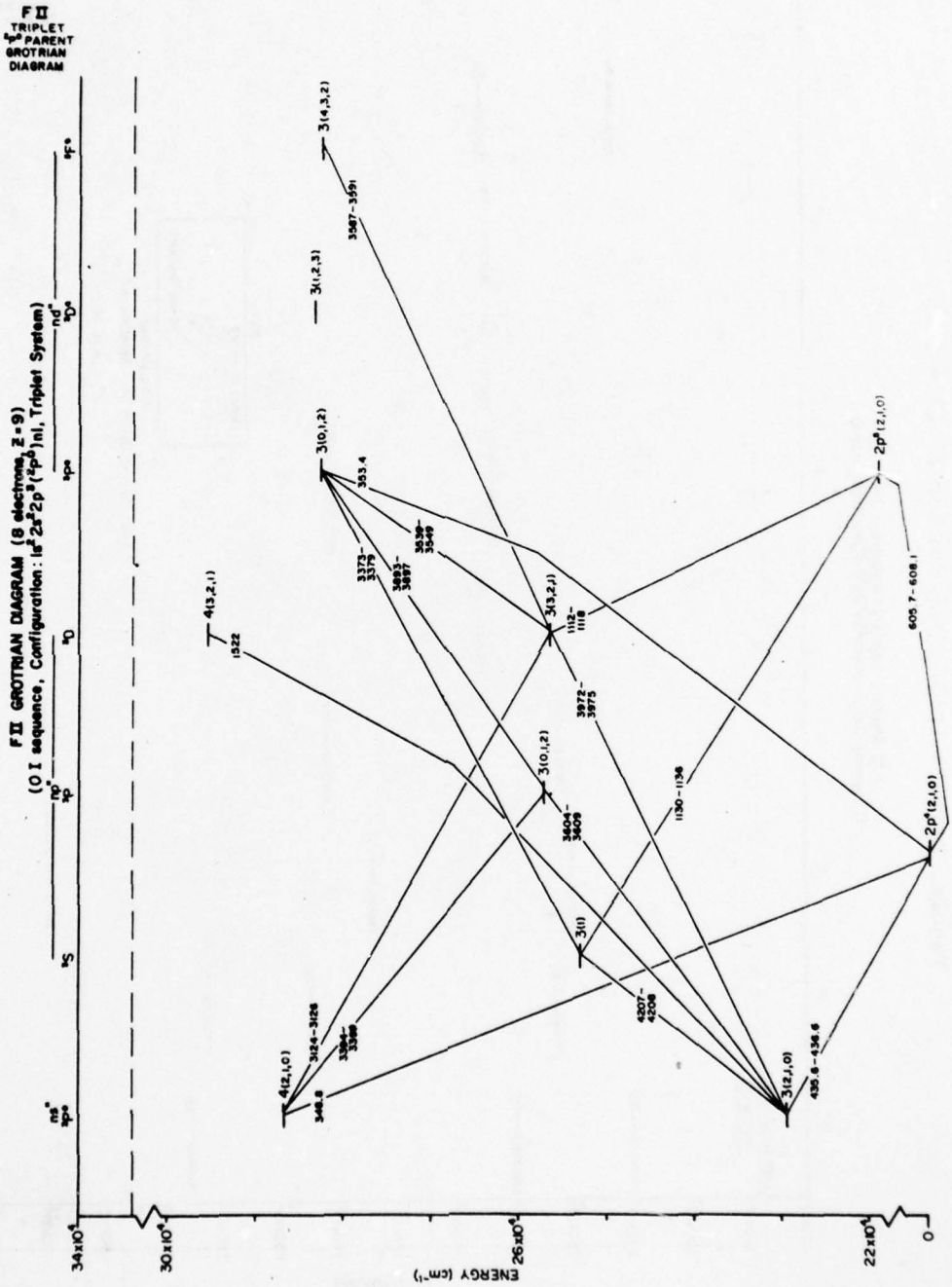

Tabular Data. A-1.82. Diagram for F^+ (Z = 9).

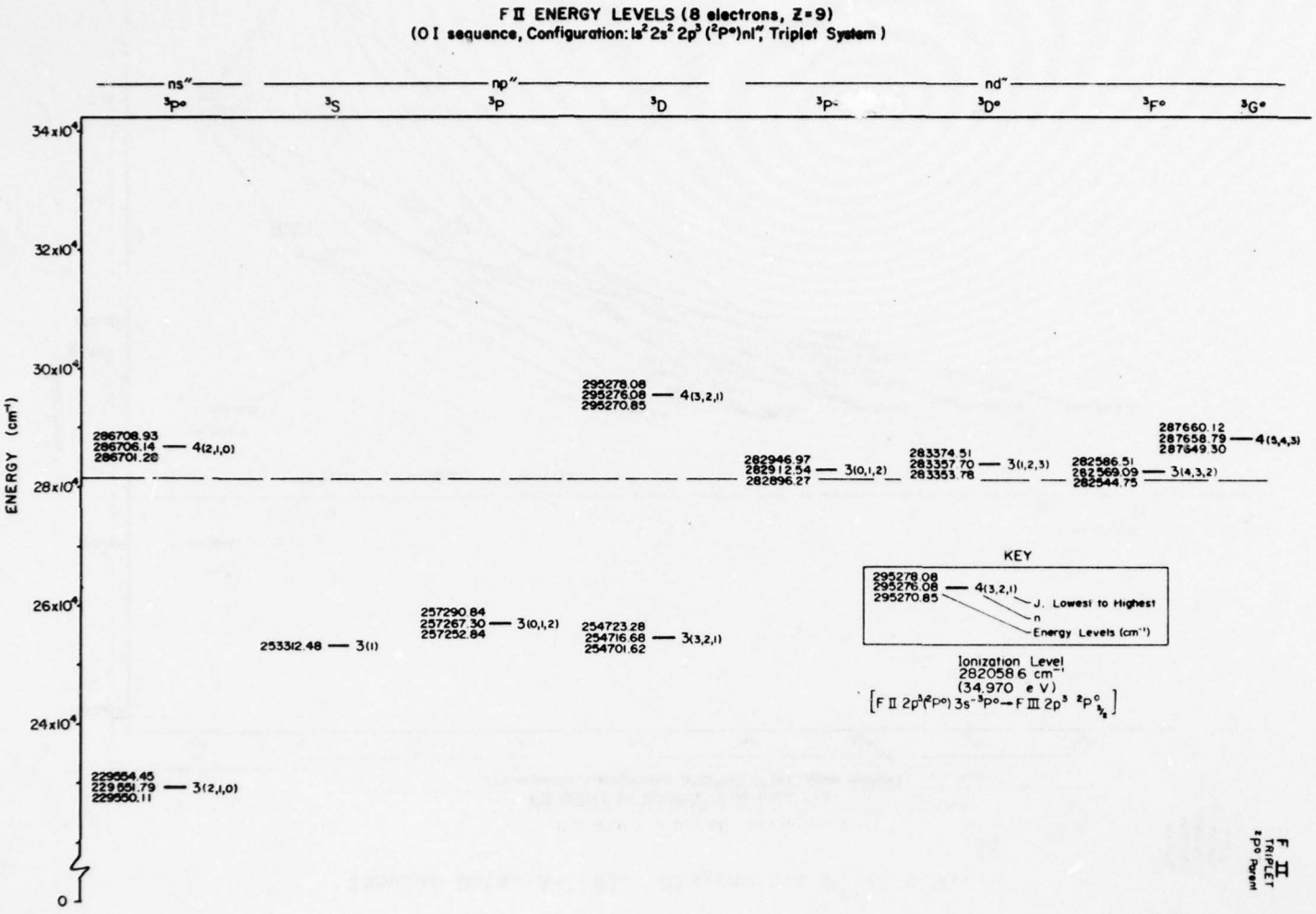

AD-A068 679 ARMY MISSILE RESEARCH AND DEVELOPMENT COMMAND REDSTO--ETC F/G 20/5
COMPILATION OF DATA RELEVANT TO NUCLEAR PUMPED LASERS. VOLUME I--ETC(U)
DEC 78 E W MCDANIEL, M R FLANNERY, E W THOMAS

UNCLASSIFIED DRDMI-H-78-1-VOL-3 NL

2 OF 5

AD A068679

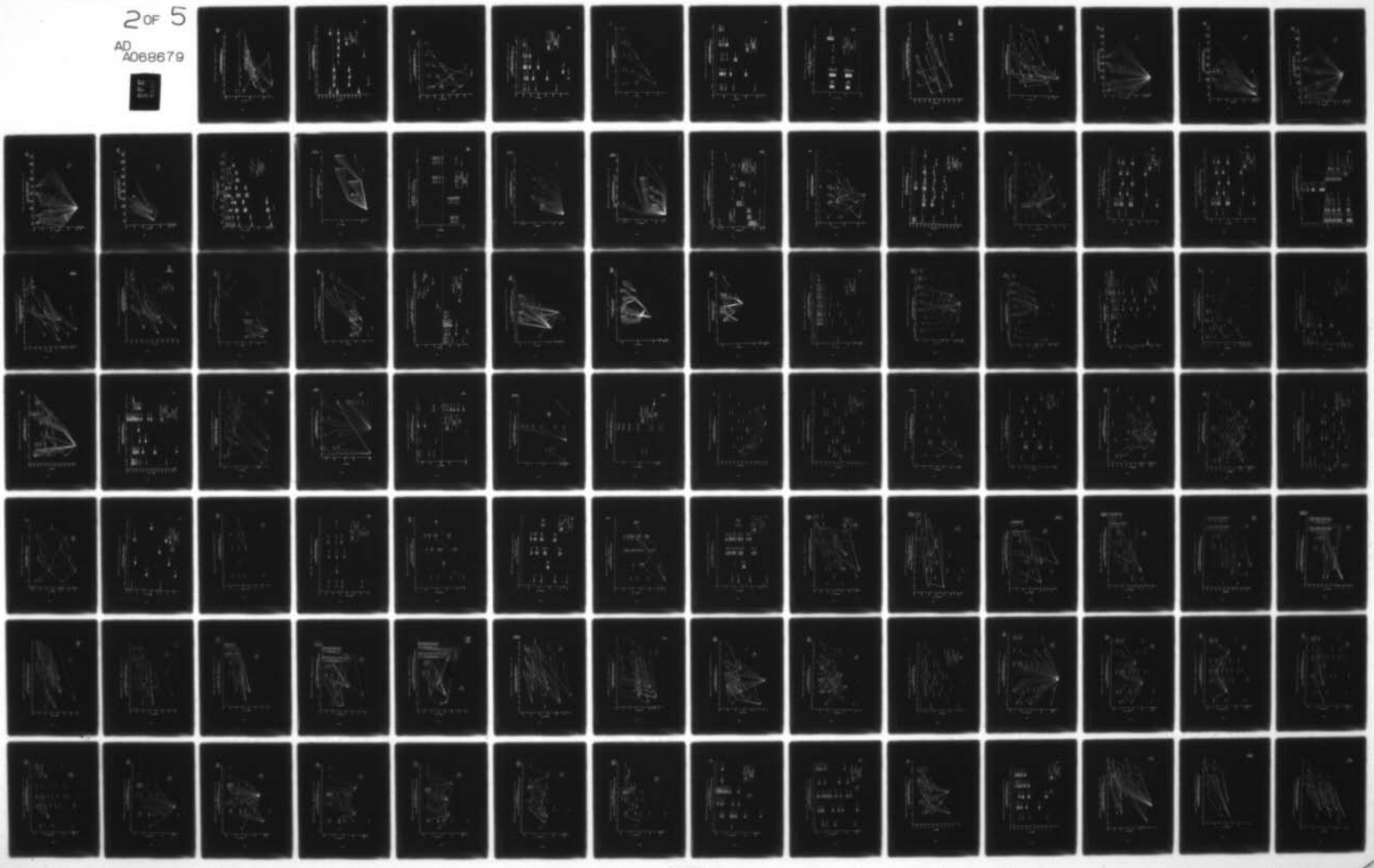

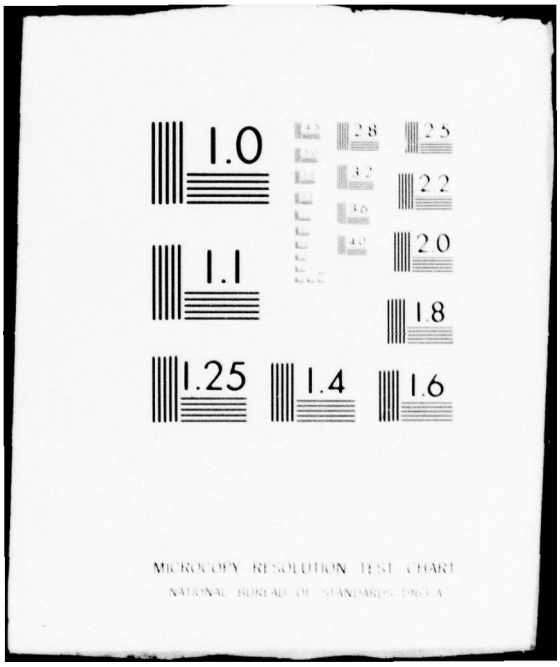
1.0
1.1
1.25
1.4
1.6
2.8
2.5
2.2
2.0
1.8
MICROCOPY RESOLUTION TEST CHART
NATIONAL BUREAU OF STANDARDS 1963 A

Tabular Data. A-1.83. Diagram for F^{+} (Z = 9).

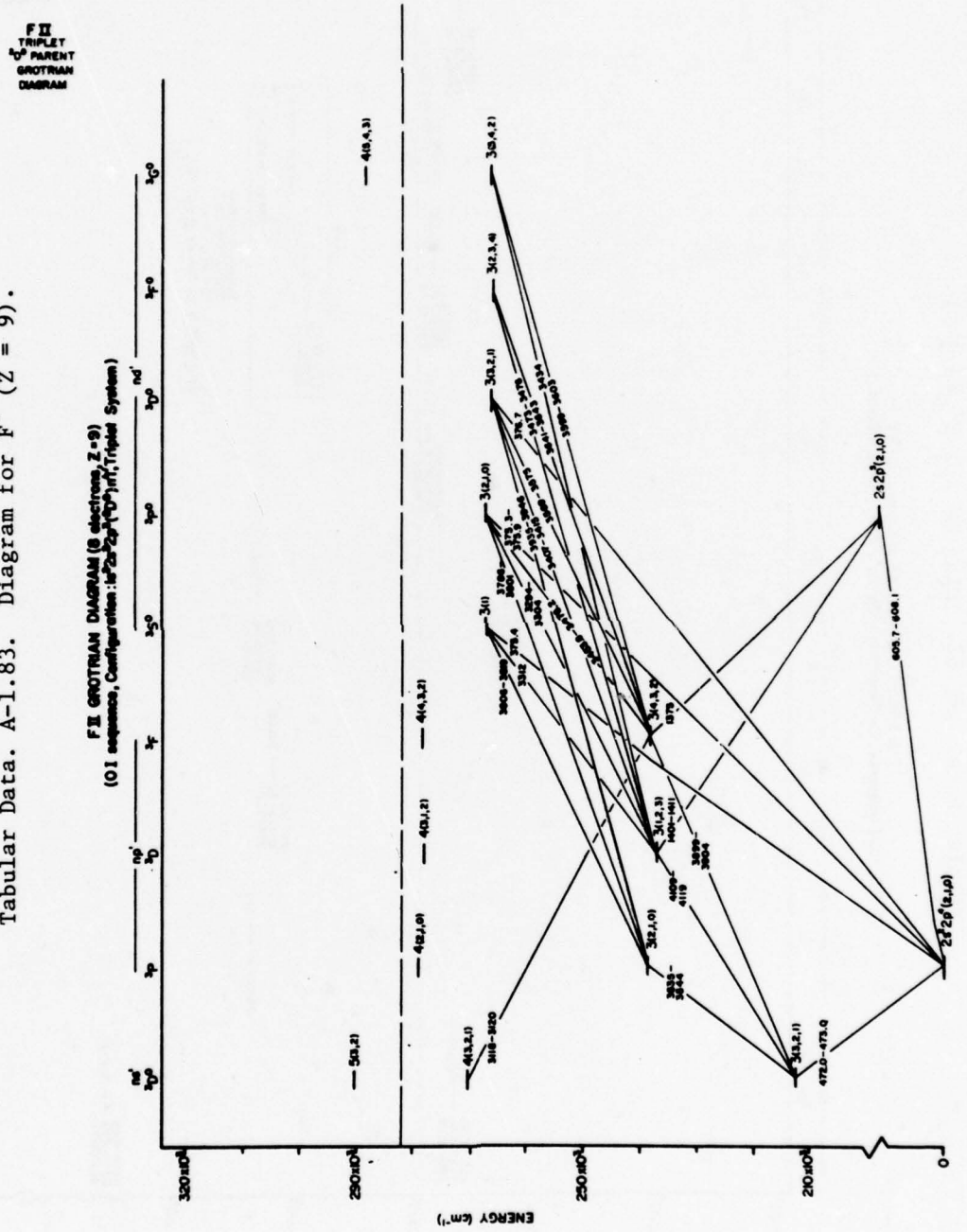

Tabular Data. A-1.84. Diagram for F^+ (Z = 9).

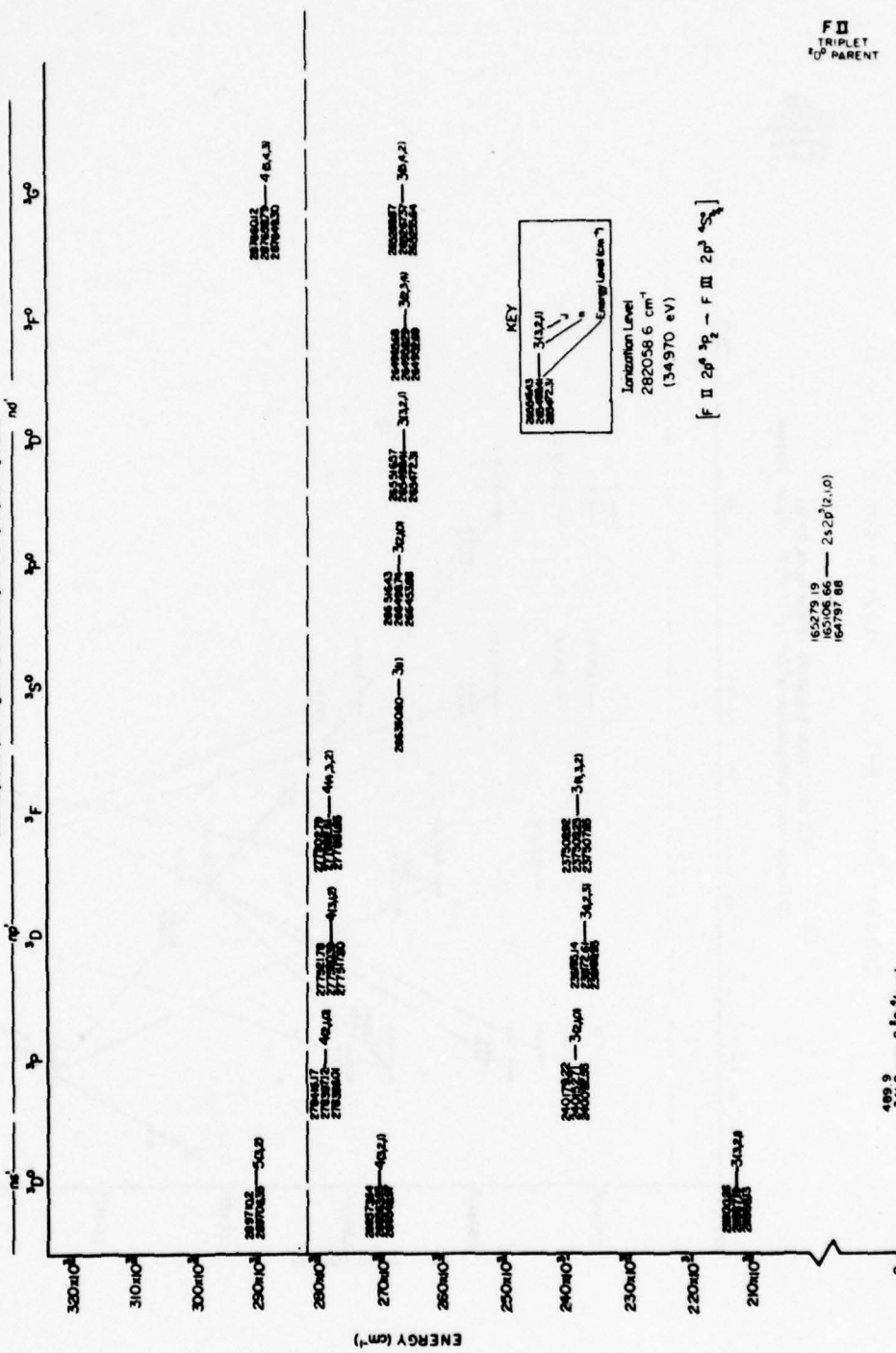

Tabular Data. A-1.85. Diagram for F^{+} ($Z = 9$).

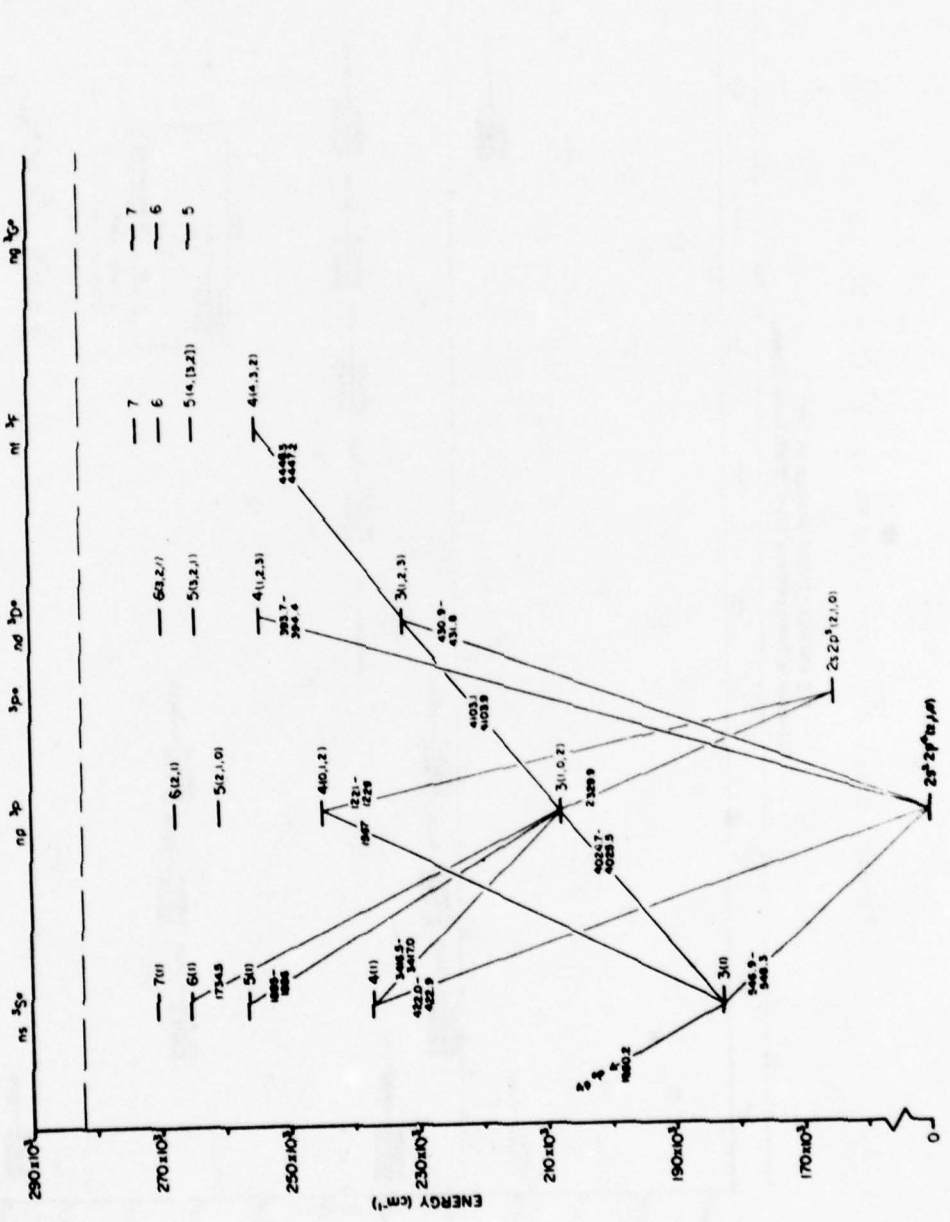

Tabular Data. A-1.86. Diagram for F^{+} (Z = 9).

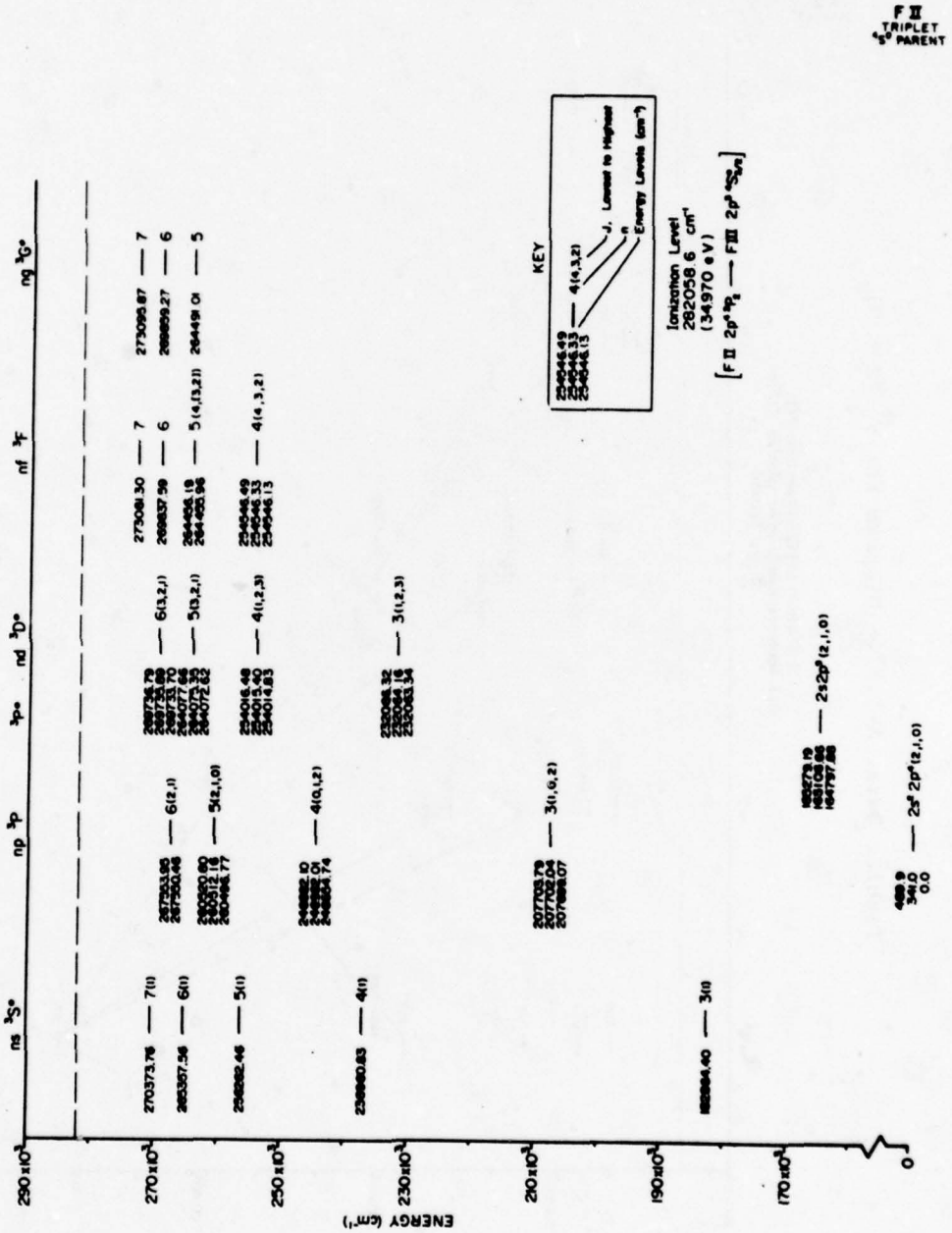

Tabular Data. A-1.87. Diagram for F^{+} (Z = 9).

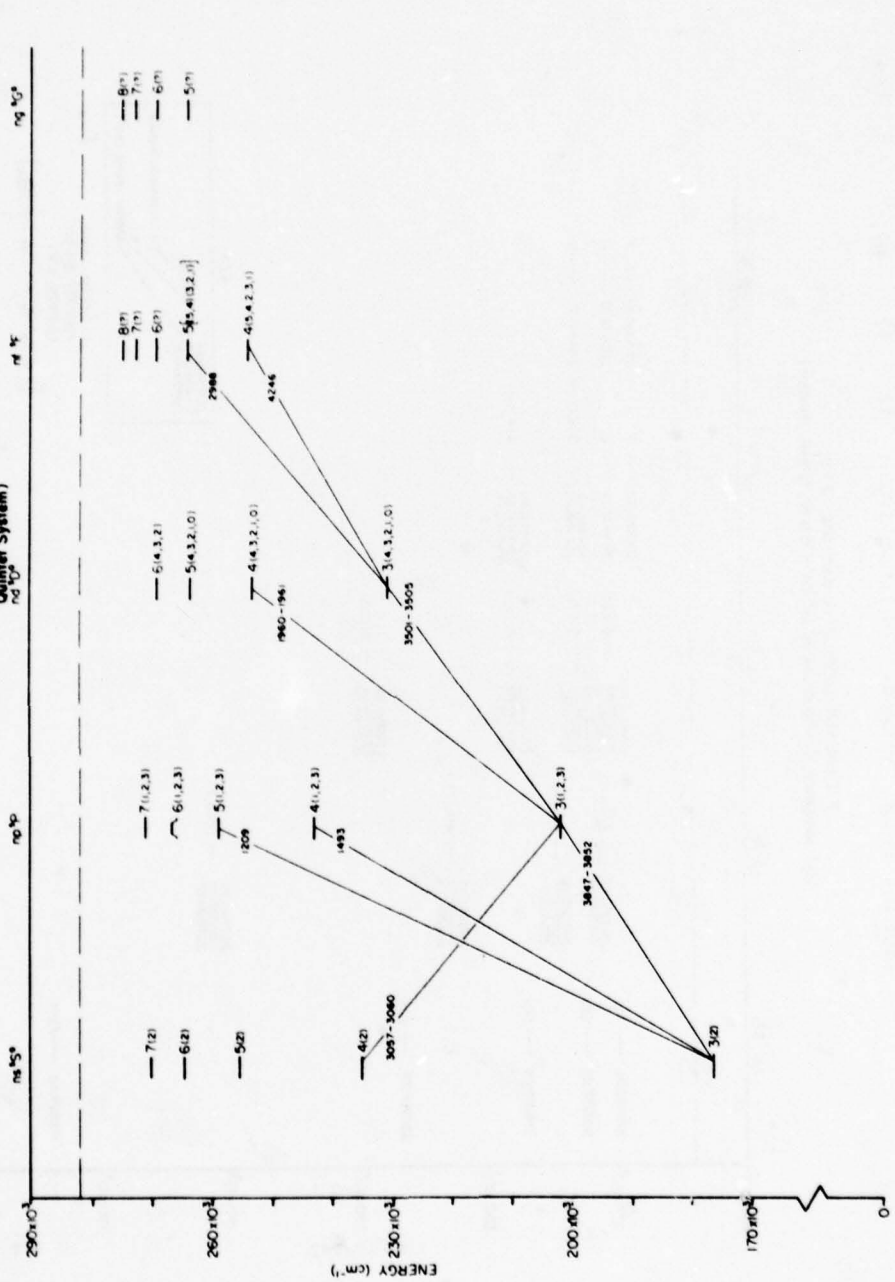

Tabular Data. A-1.88. Diagram for F^{+} ($Z = 9$).

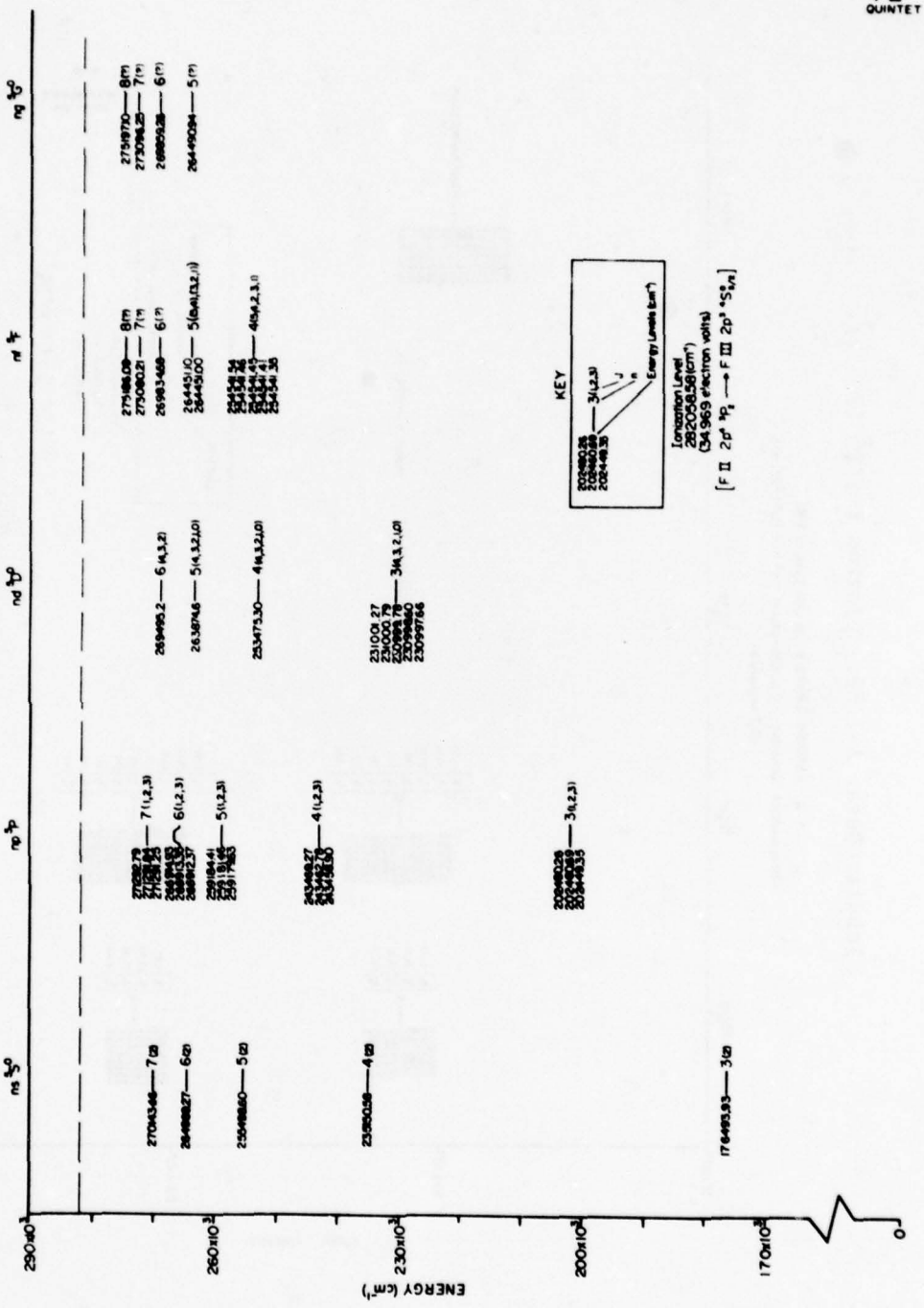

Tabular Data. A-1.89. Diagram for F^+ (Z = 9).

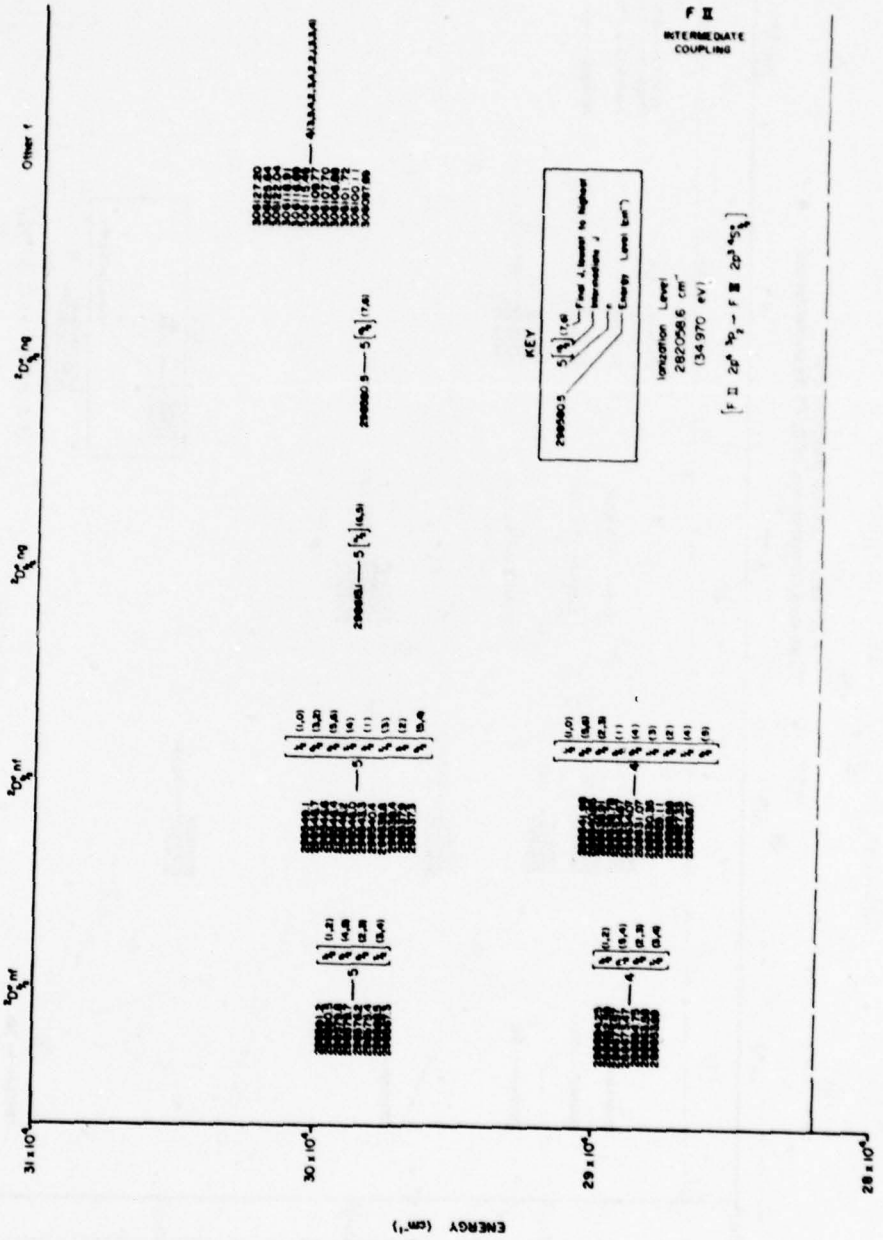

Tabular Data. A-1.90. Diagram for F^+ (Z = 9).

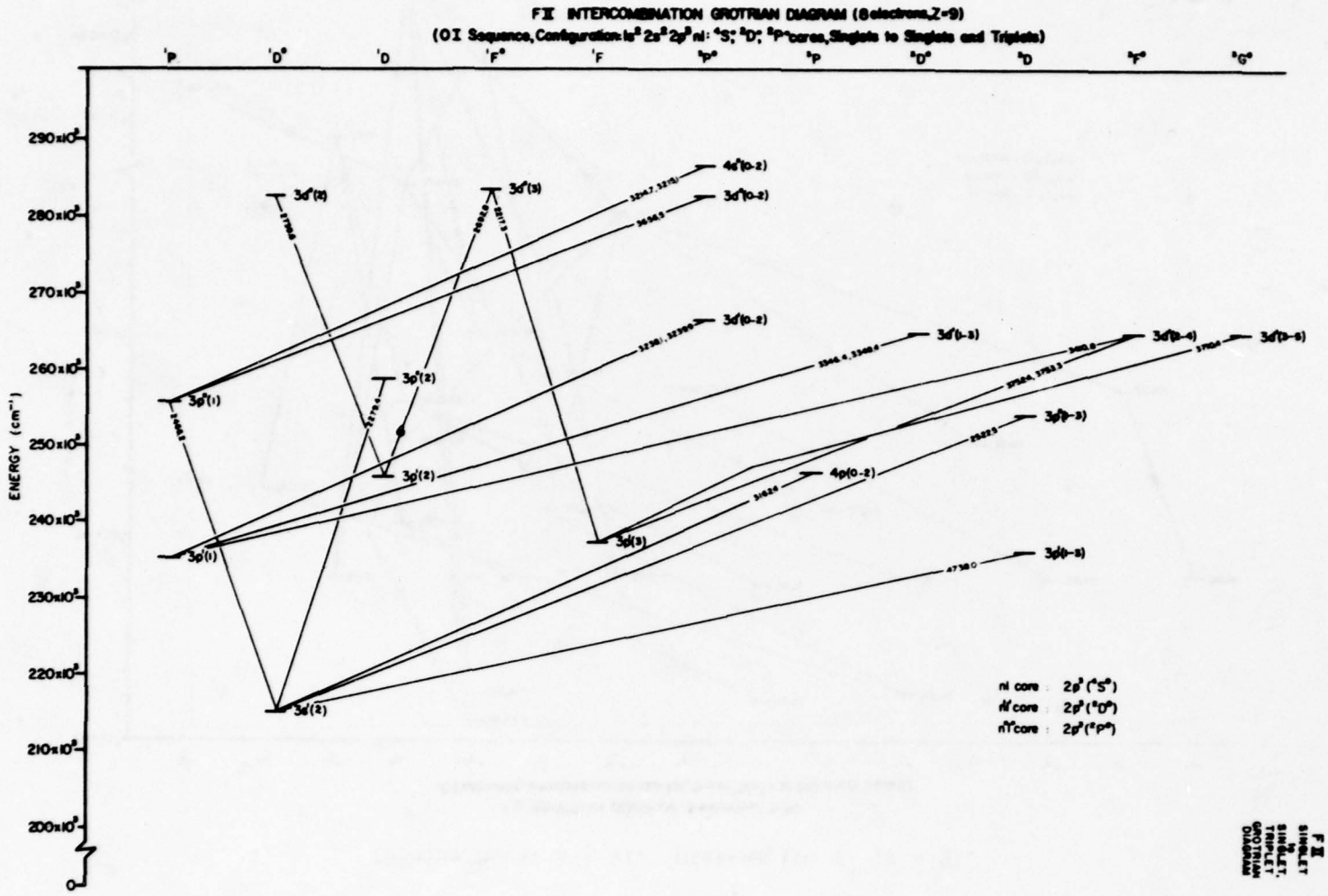

FII SINGLET TO SINGLET, TRIPLET GROTRIAN DIAGRAM

Tabular Data. A-1.91. Diagram for F^{+} ($Z = 9$).

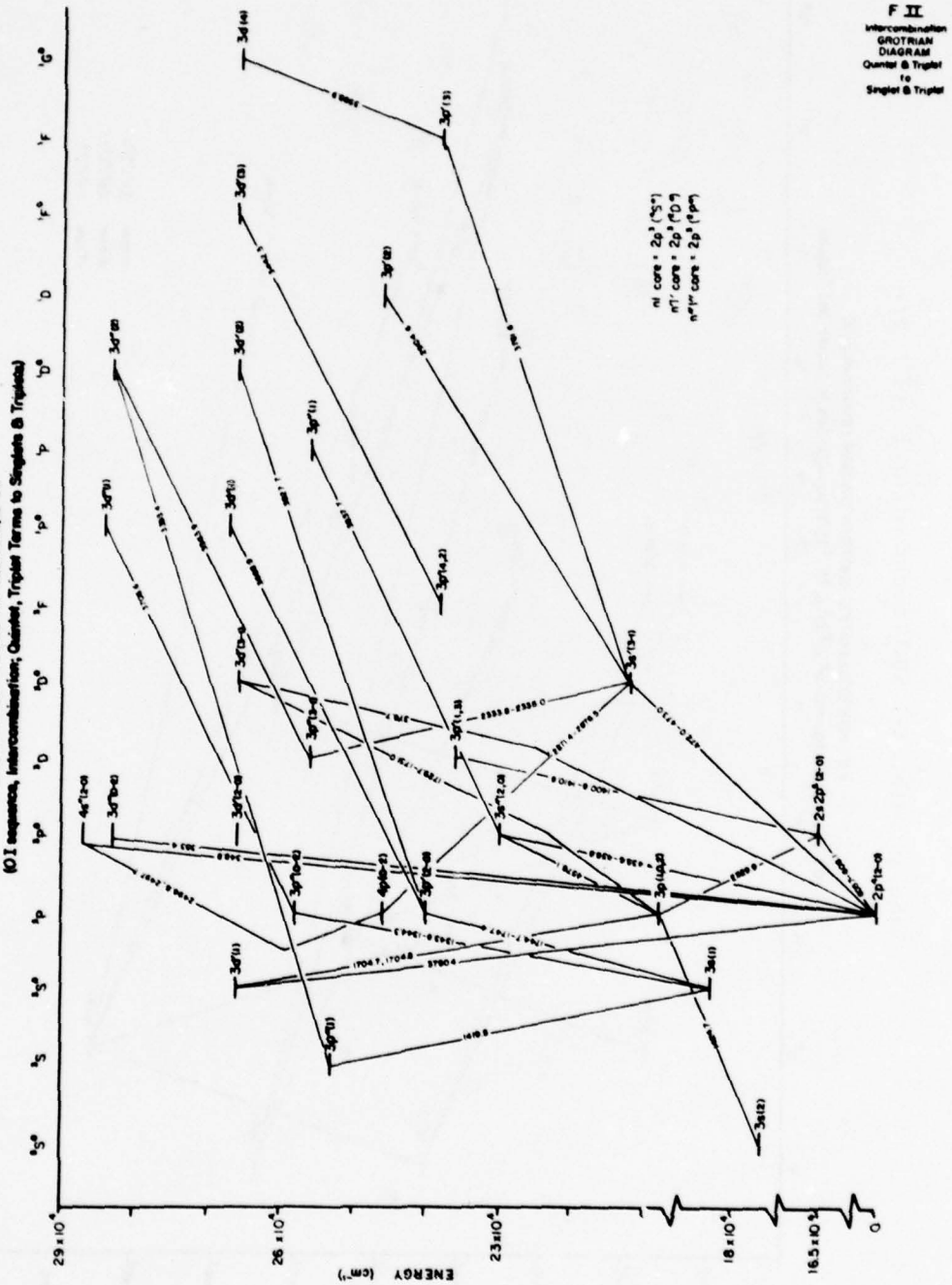

Tabular Data. A-1.92. Diagram for Ne (Z = 10).

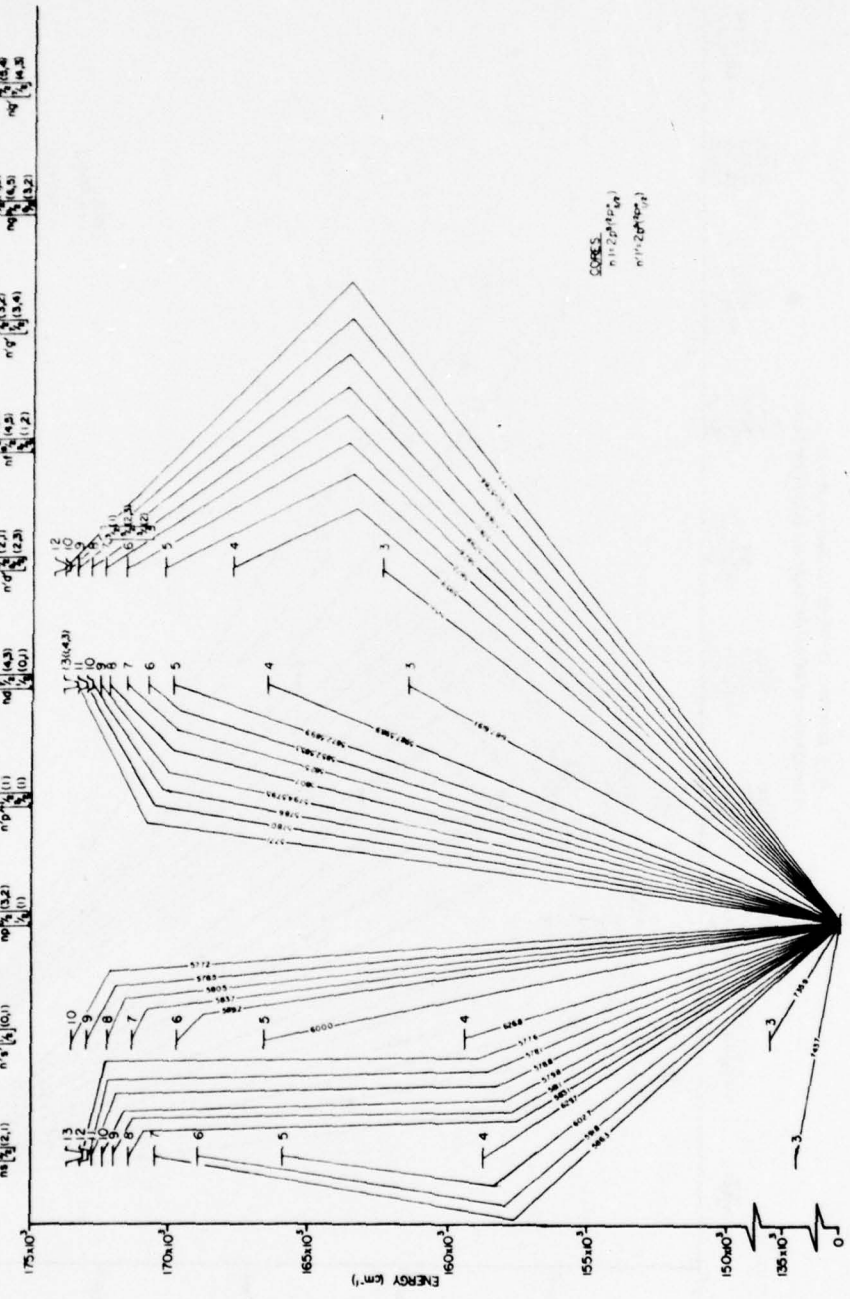

Tabular Data. A-1.93. Diagram for Ne (Z = 10).

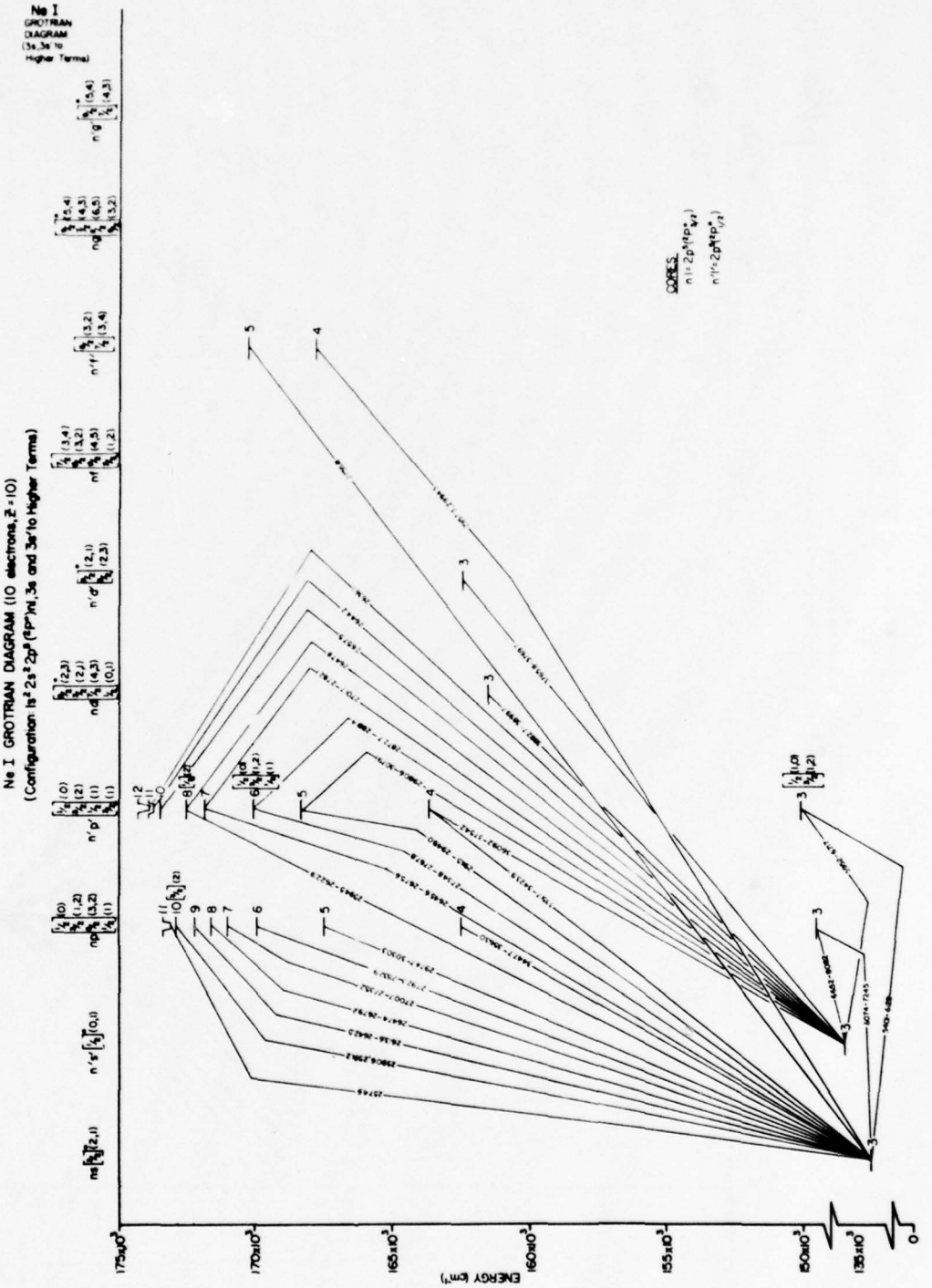

Tabular Data. A-1.94. Diagram for Ne (Z = 10).

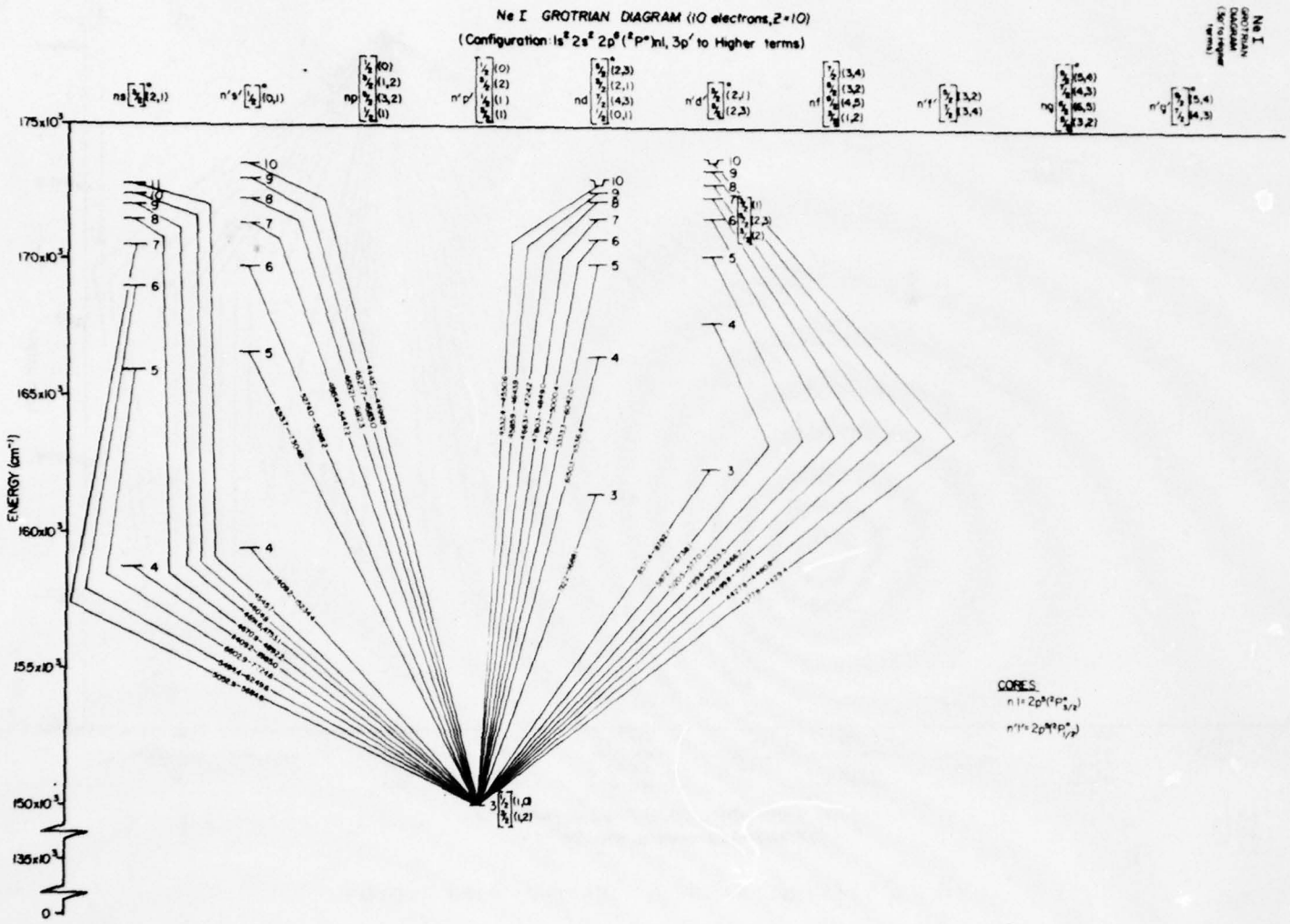

Tabular Data. A-1.95. Diagram for Ne (Z = 10).

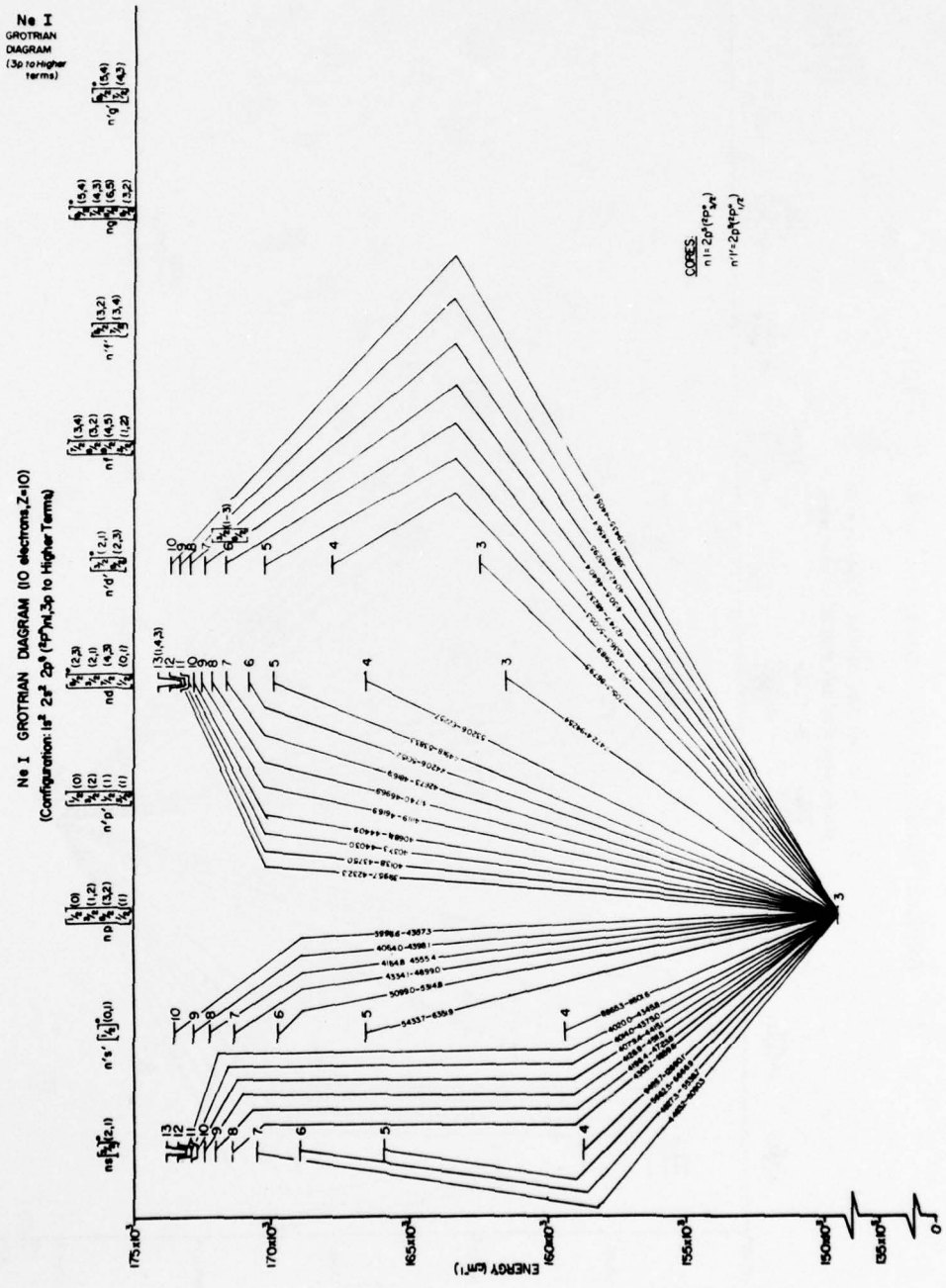

Tabular Data. A-1.96. Diagram for Ne (Z = 10).

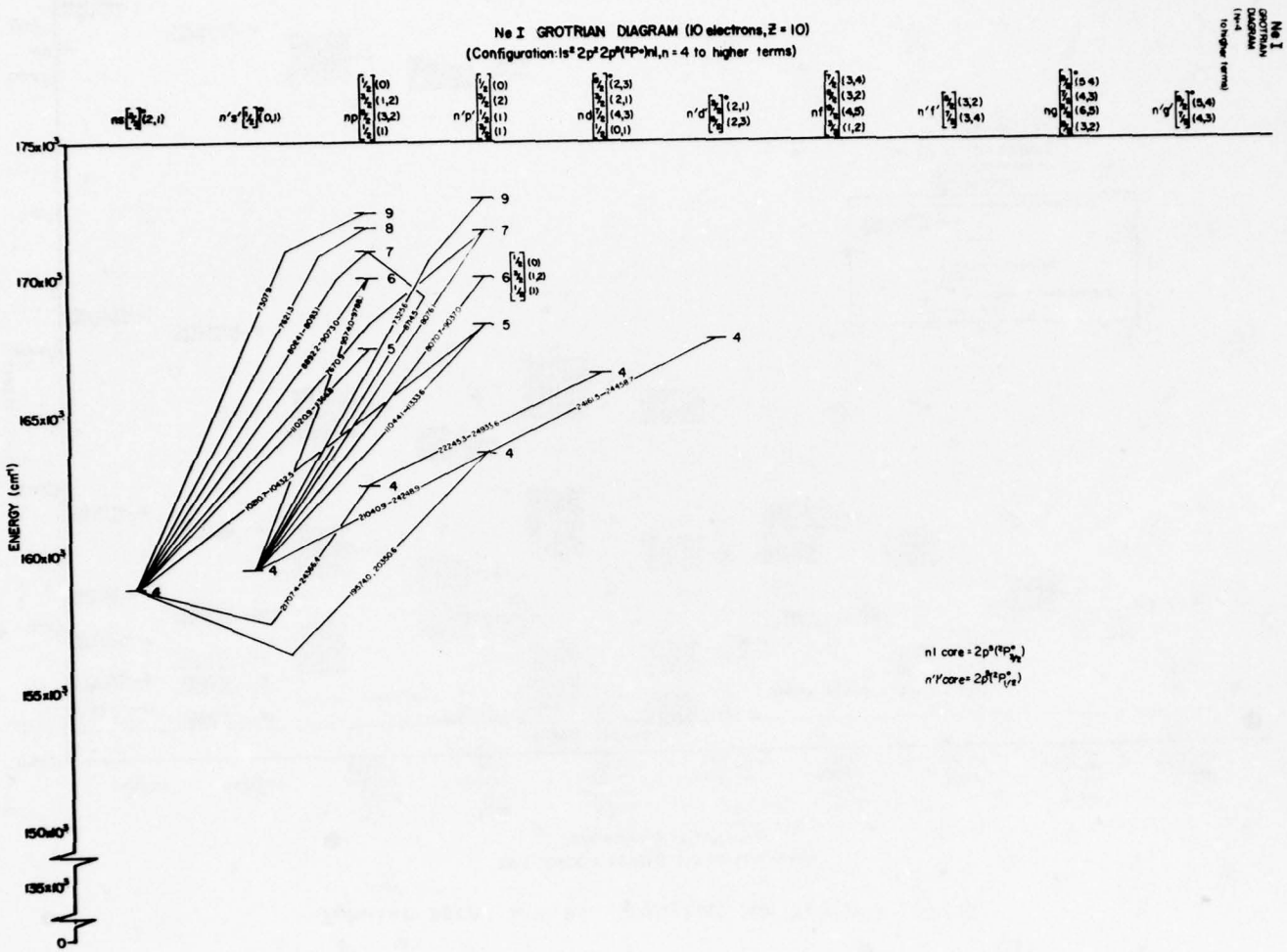

Tabular Data. A-1.97. Diagram for Ne (Z = 10).

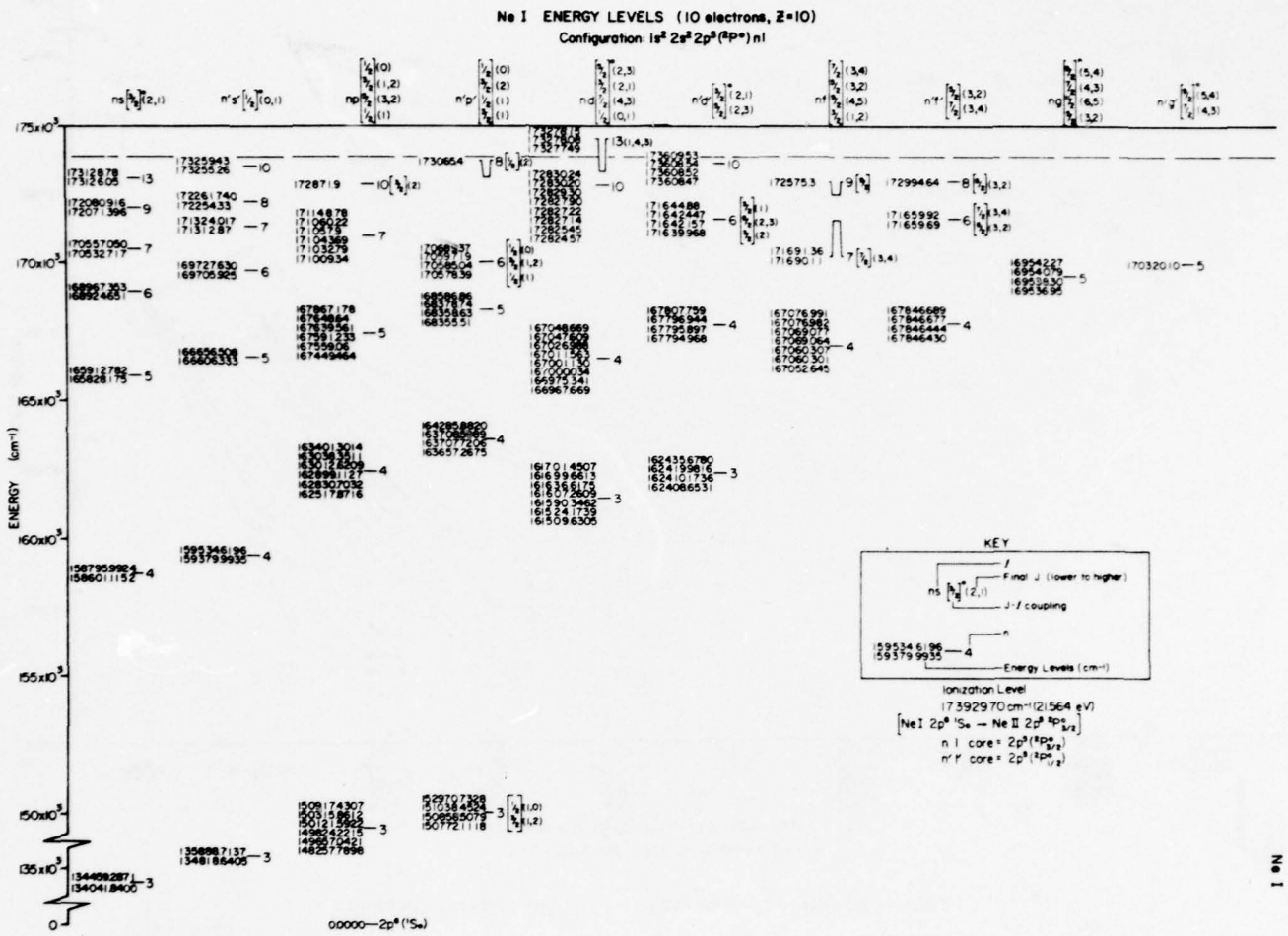

Tabular Data, A-1.98. Diagram for Ne (Z = 10).

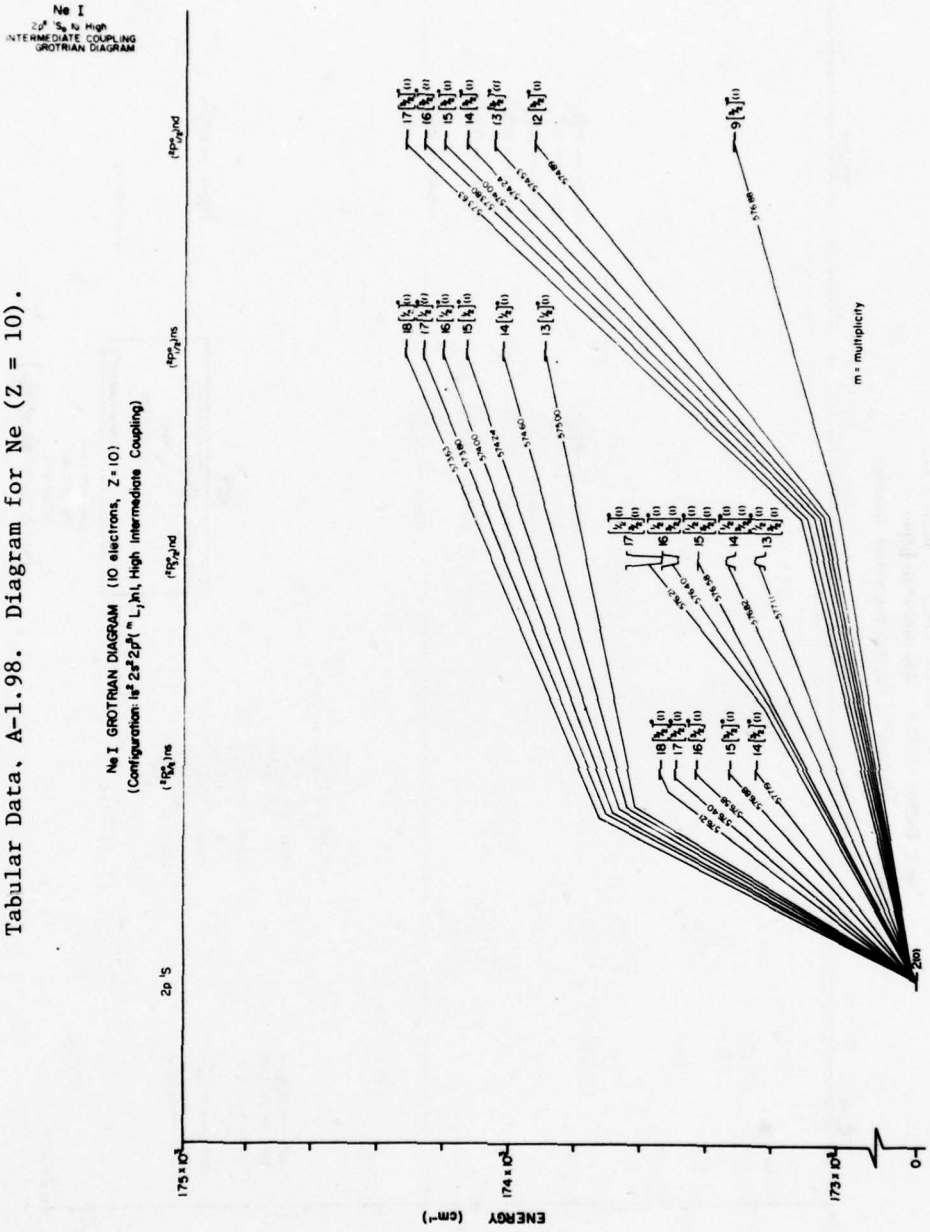

Tabular Data. A-1.99. Diagram for Ne (Z = 10).

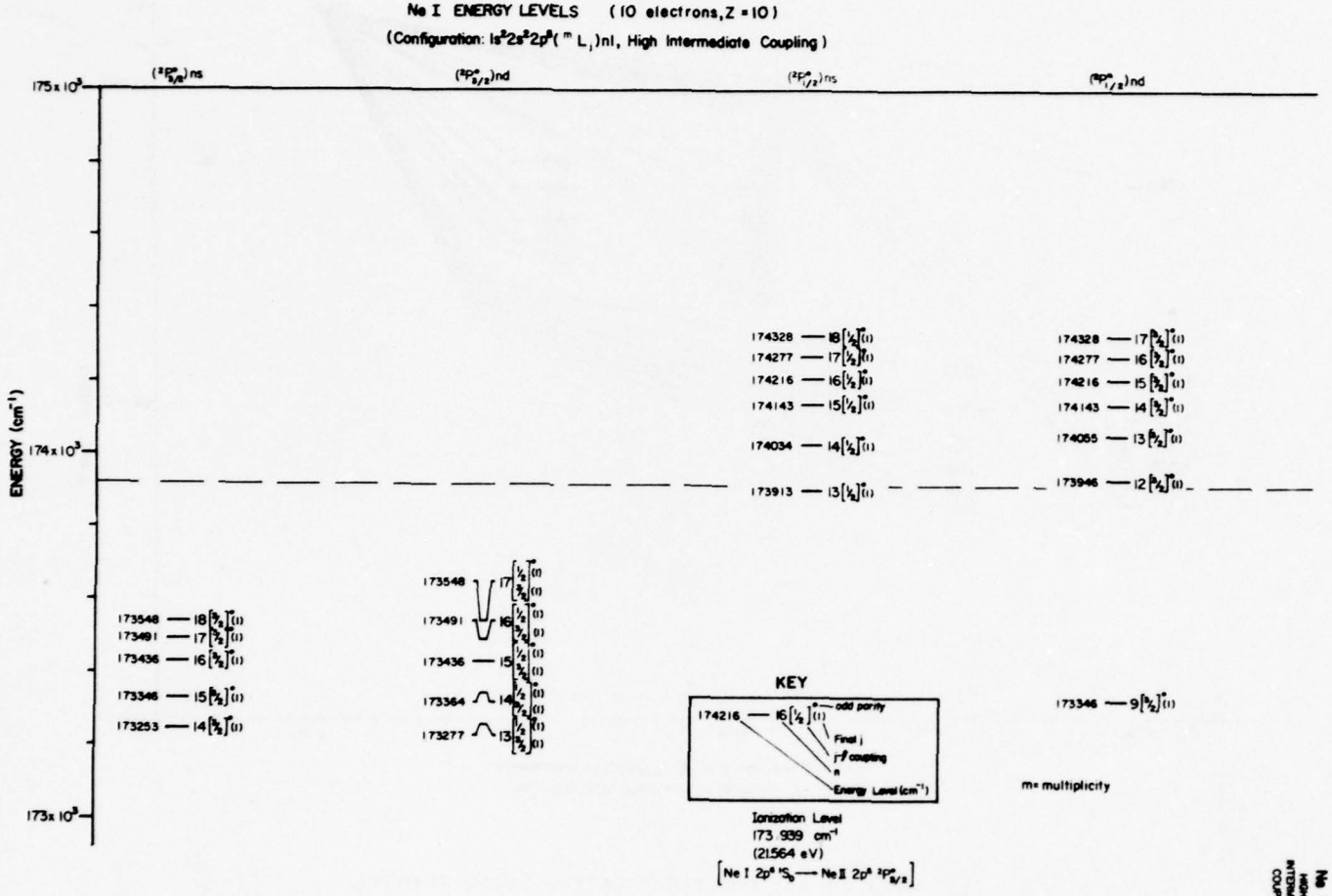

Tabular Data. A-1.100. Diagram for Ne (Z = 10).

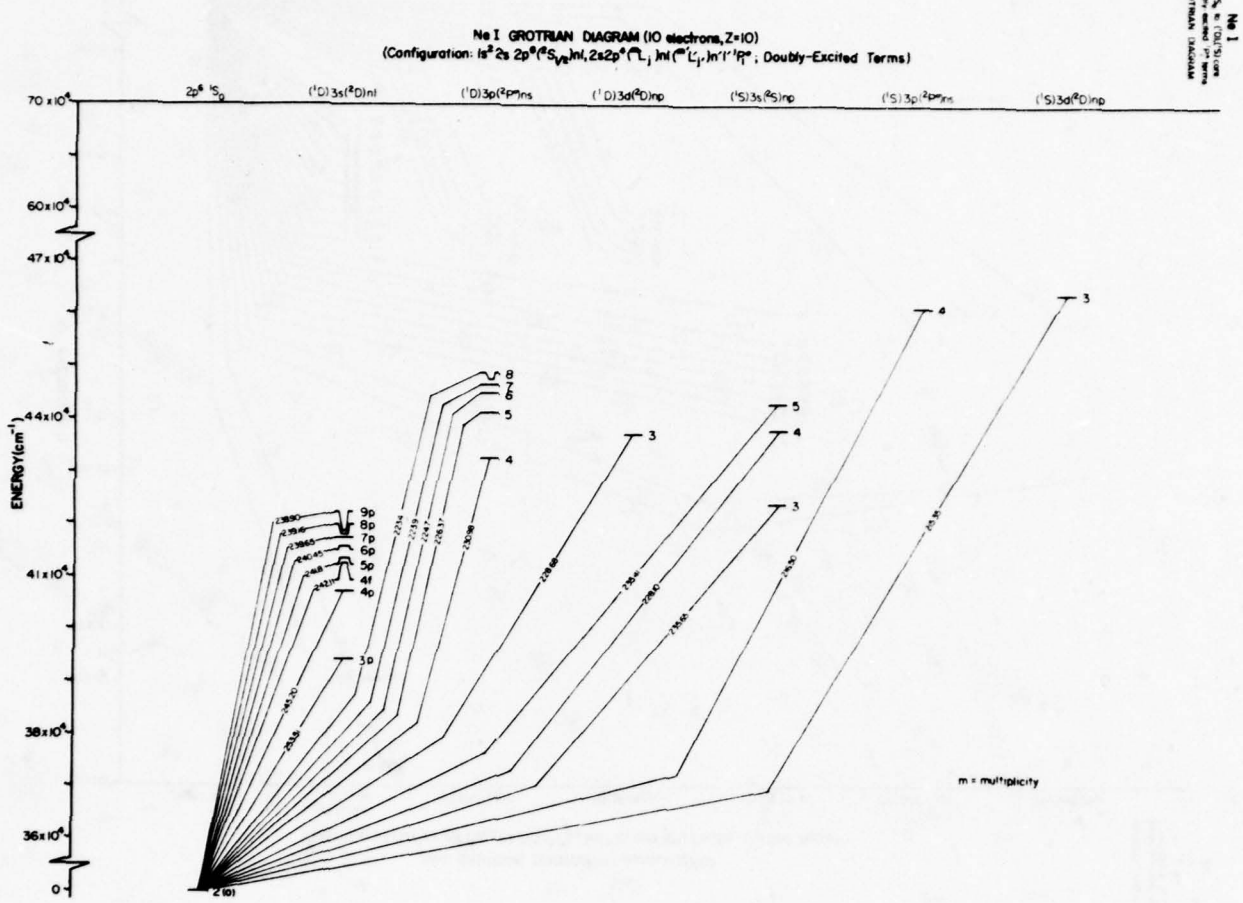

Tabular Data. A-1.101. Diagram for Ne (Z = 10).

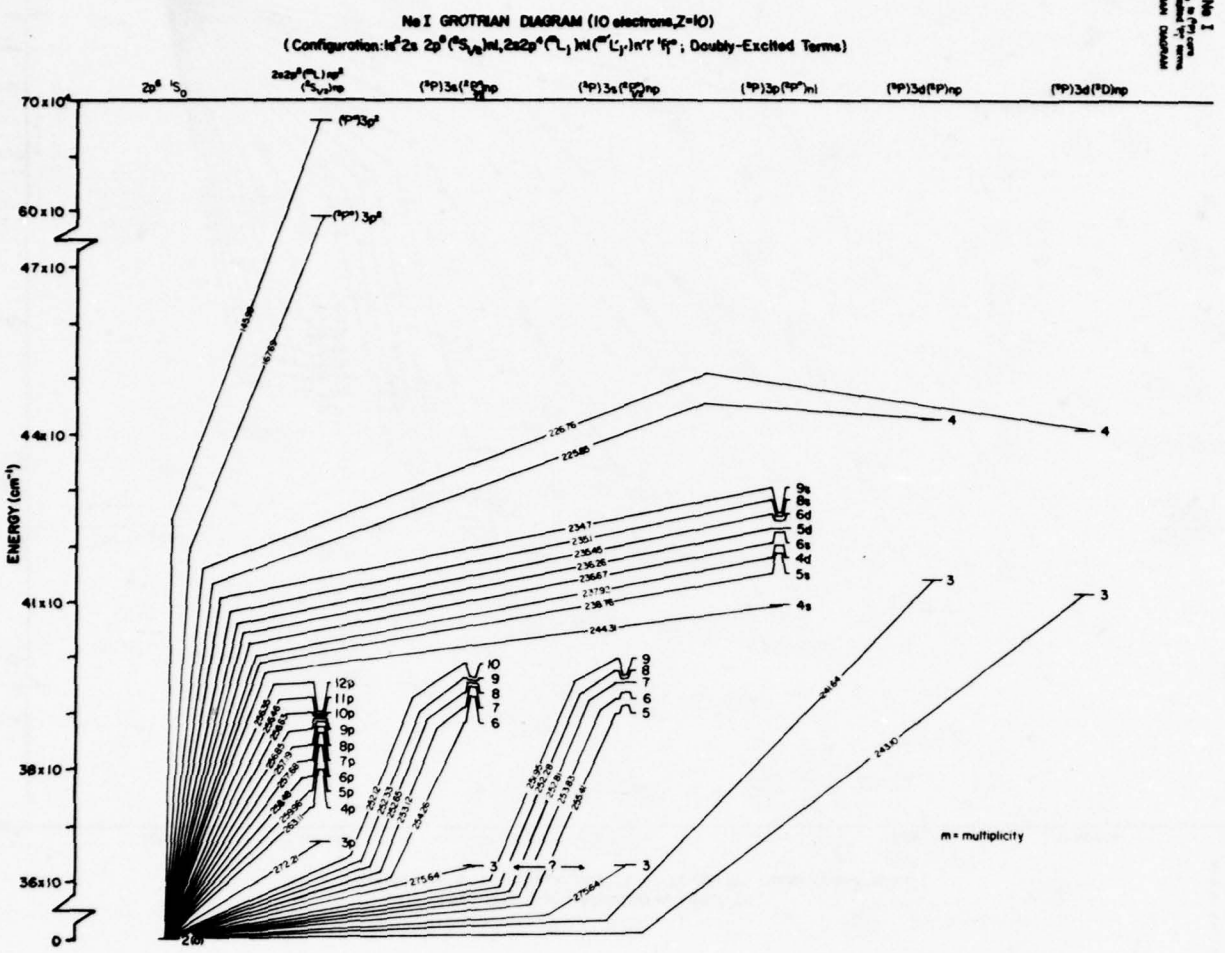

Tabular Data. A-1.102. Diagram for Ne (Z = 10).

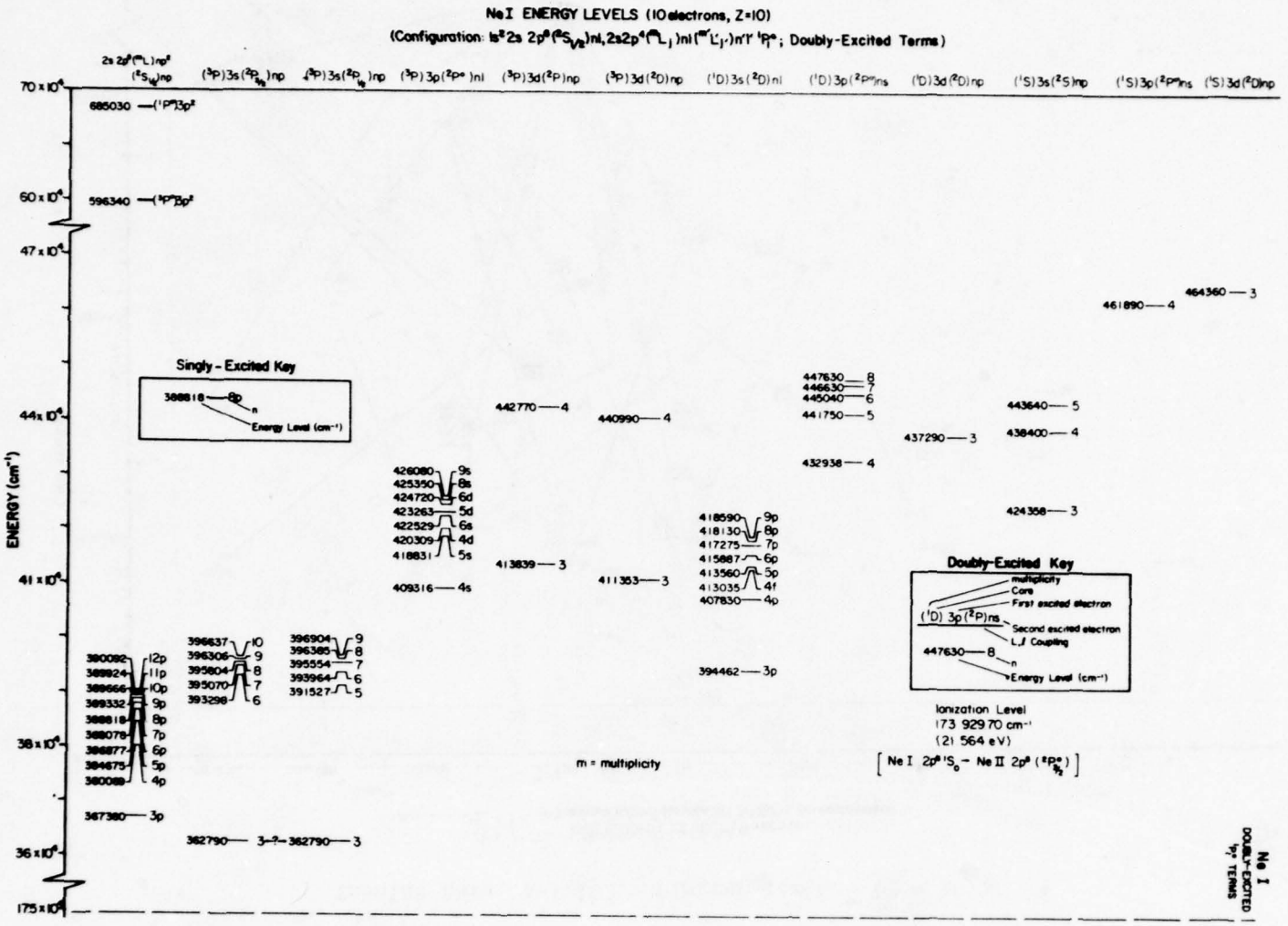

Tabular Data. A-1.103. Diagram for Ne^{+} ($Z = 10$).

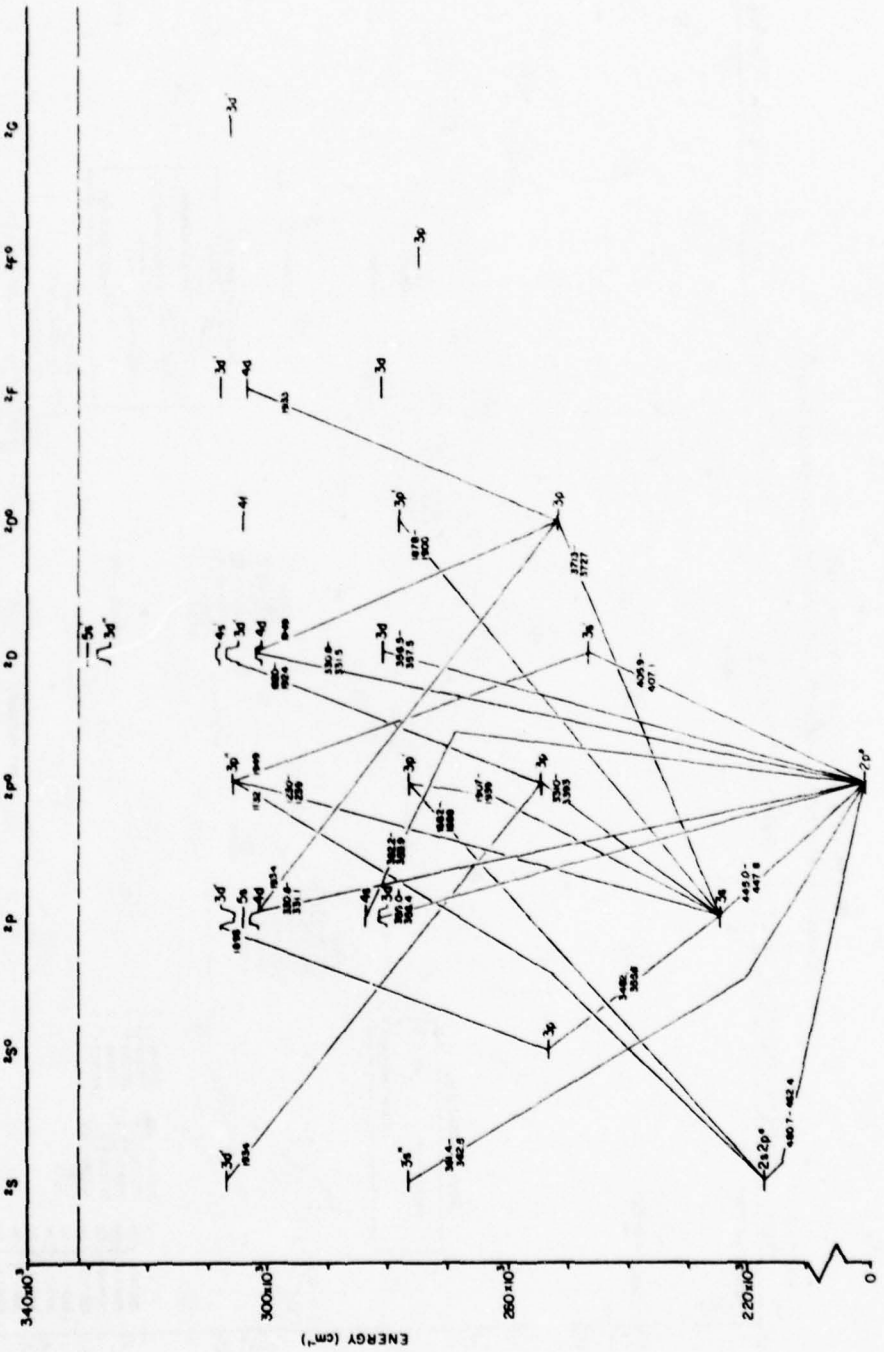

Tabular Data. A-1.104. Diagram for Ne^{+} (Z = 10).

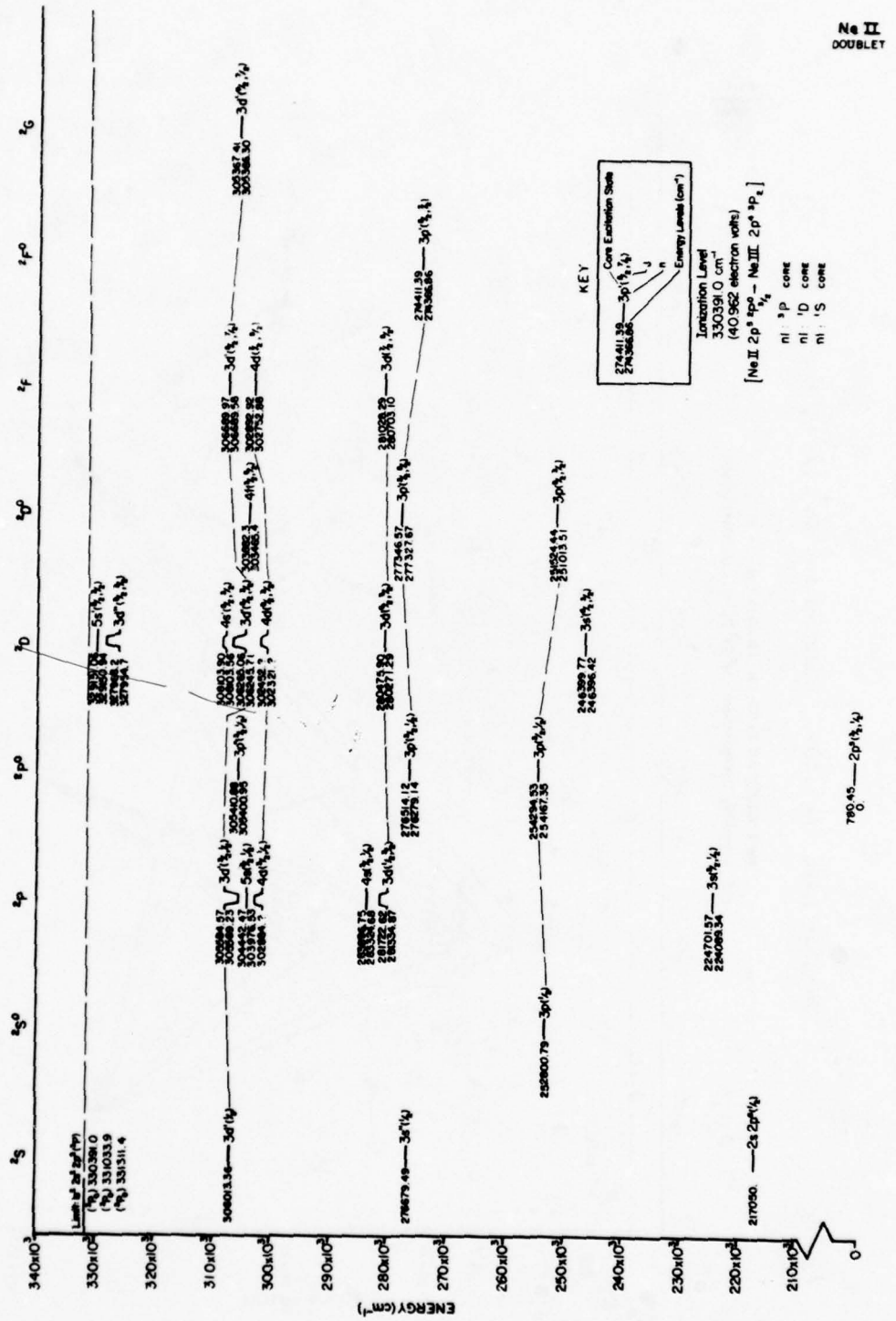

Tabular Data. A-1.105. Diagram for Ne^{+} (Z = 10).

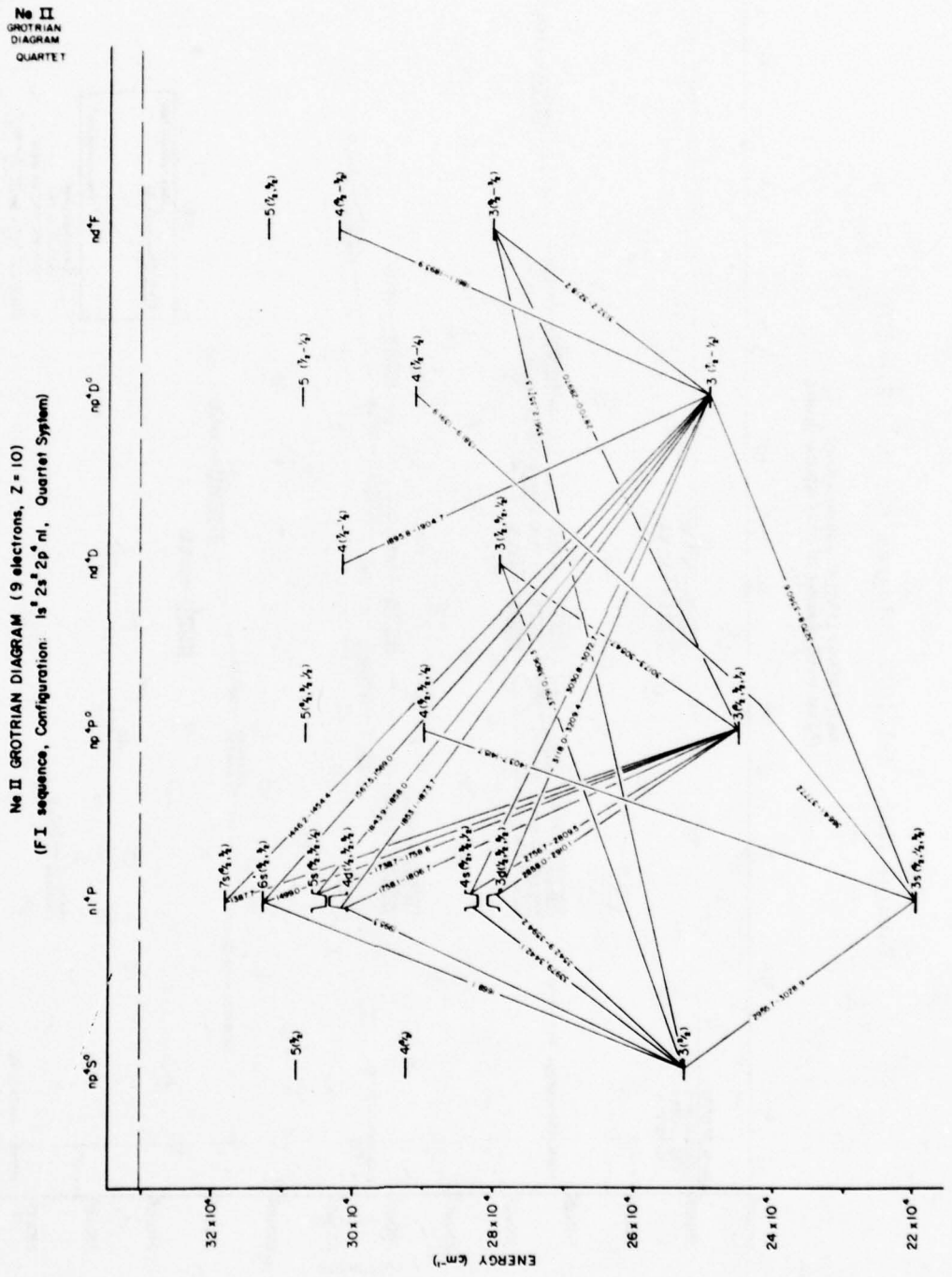

Tabular Data. A-1.106. Diagram for Ne^{+} (Z = 10).

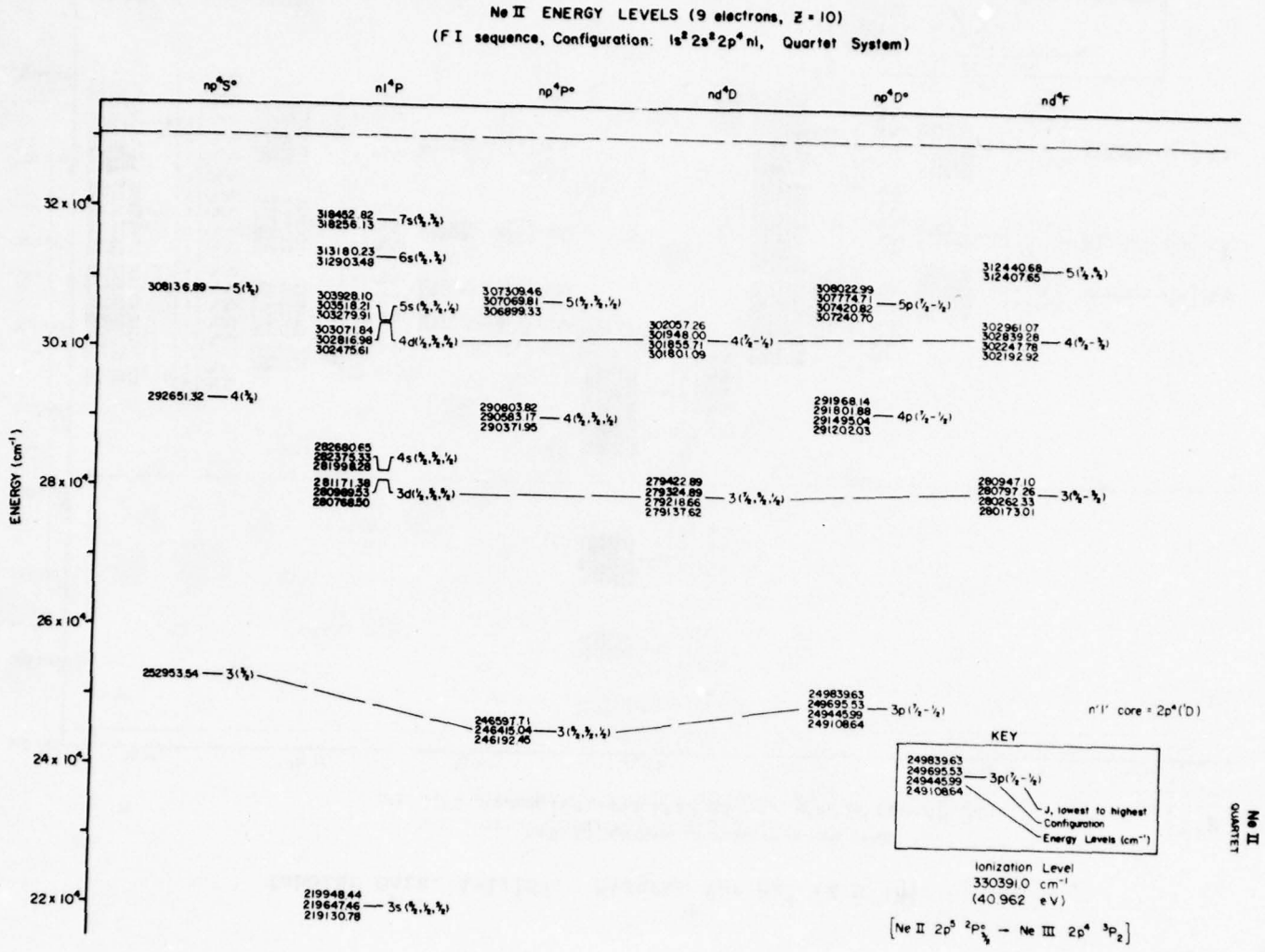

Tabular Data. A-1.106. Diagram for Ne^{+} (Z = 10).

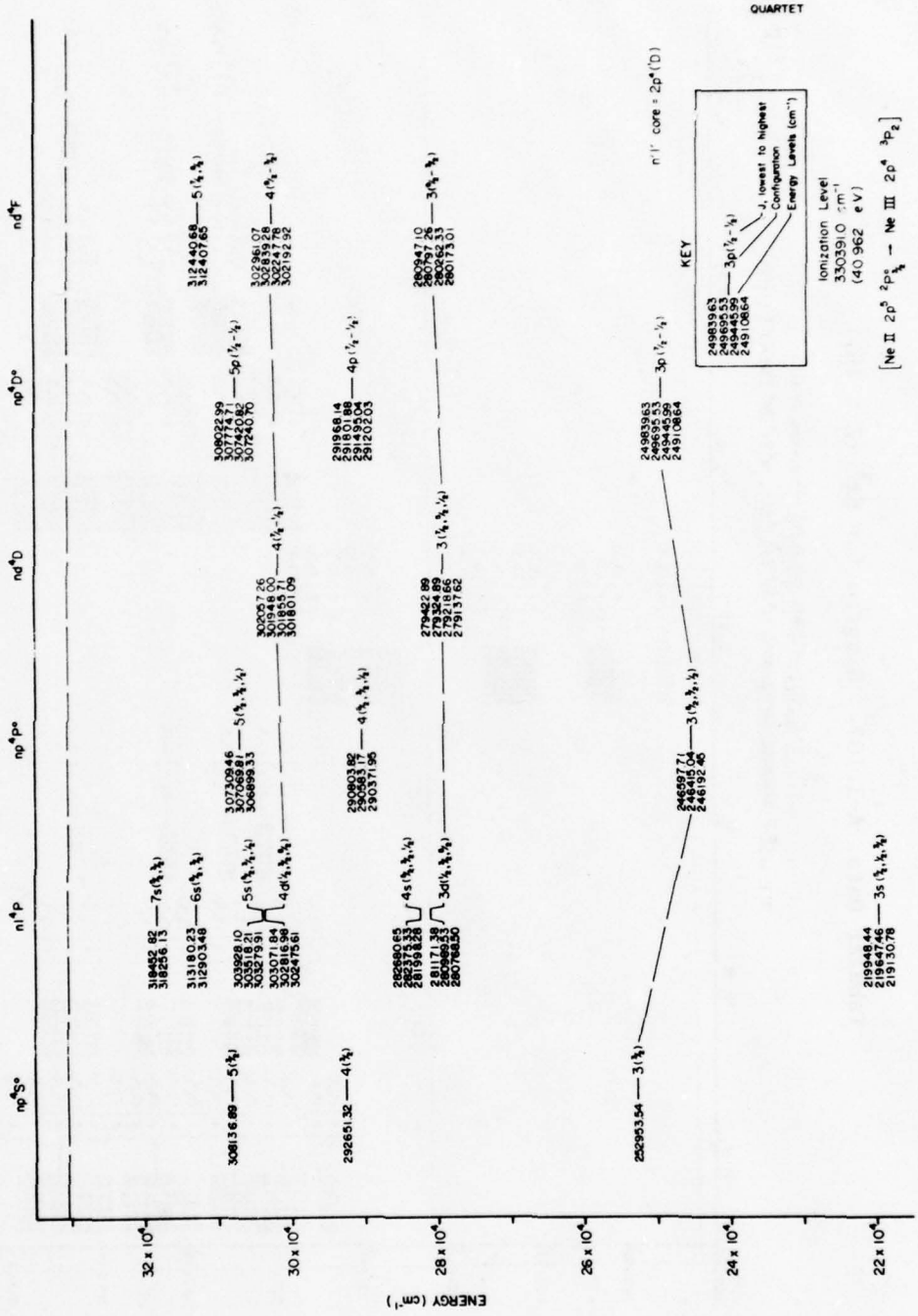

Tabular Data. A-1.107. Diagram for Ne^{+} (Z = 10).

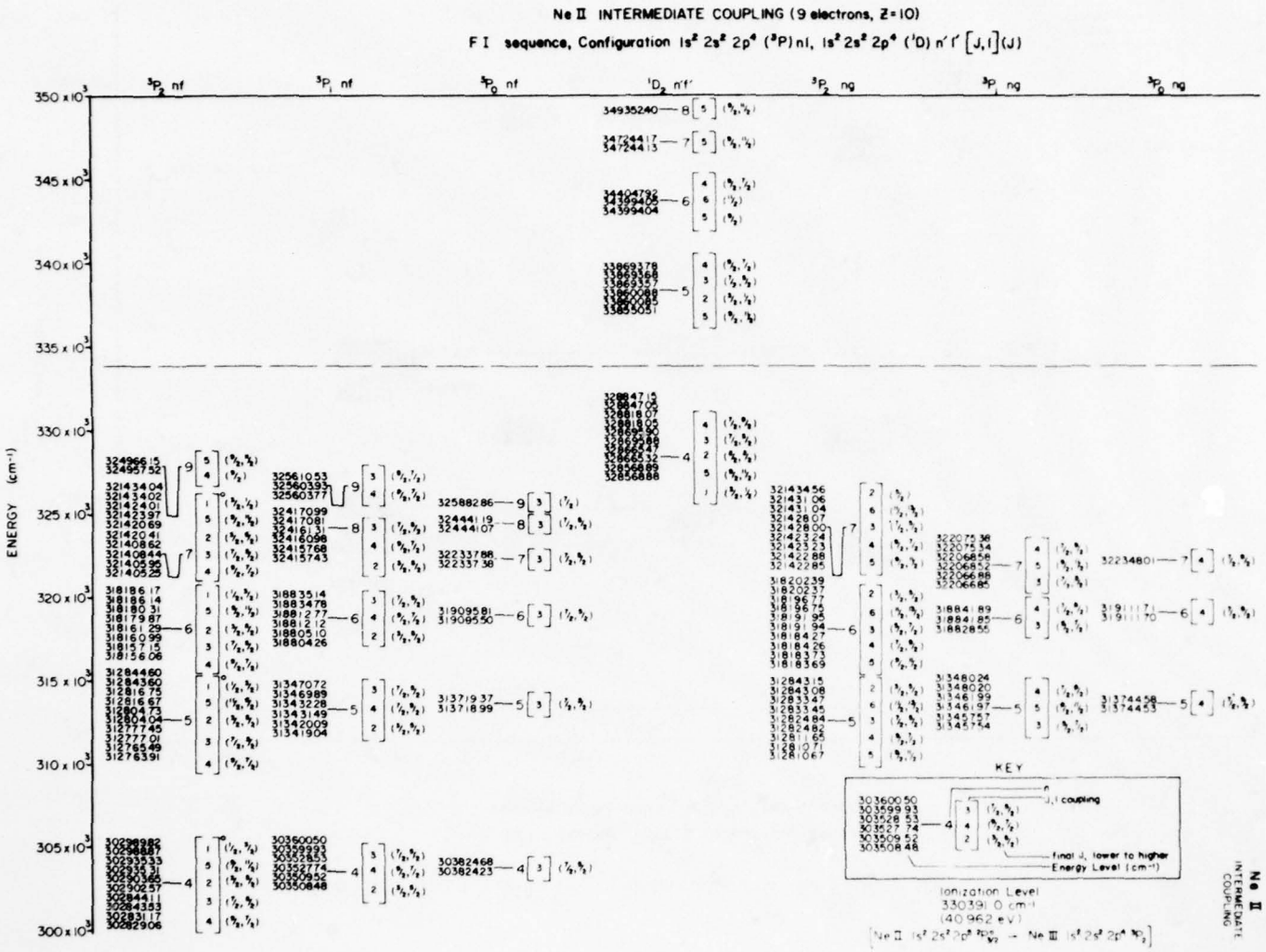

Tabular Data. A-1.108. Diagram for Ne^{+} (Z = 10).

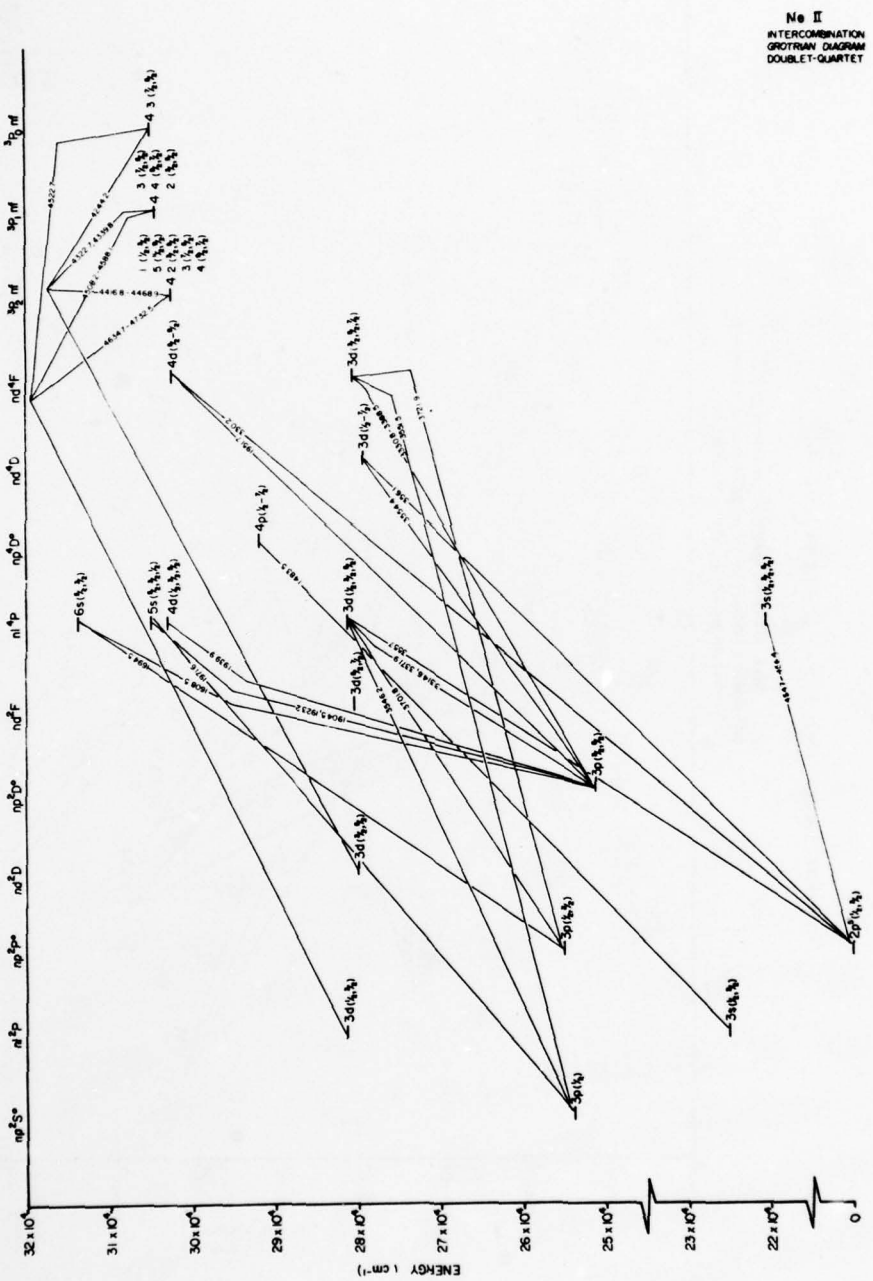

Tabular Data. A-1.109. Diagram for Ne^{+} (Z = 10).

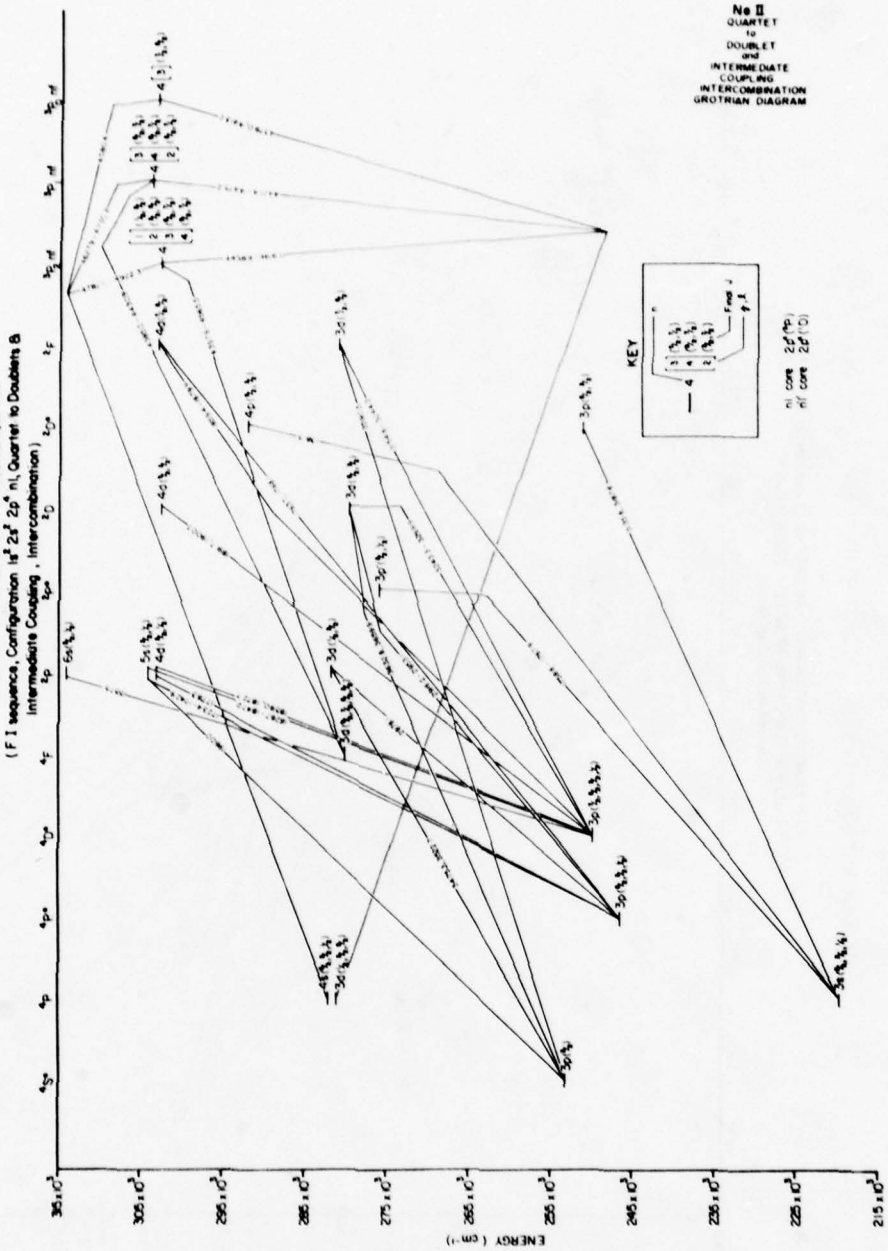

Tabular Data. A-1.110. Diagram for Al (Z = 13).

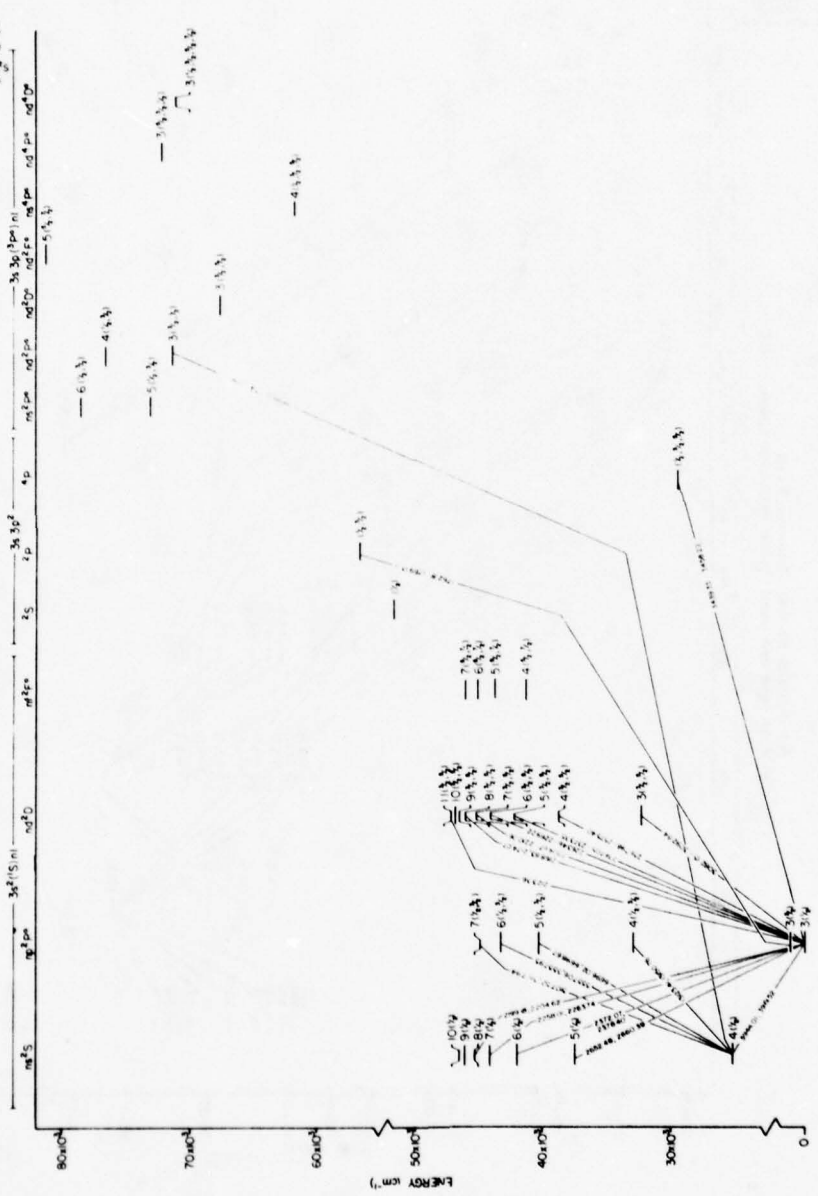

Tabular Data. A-1.111. Diagram for Al (Z = 13).

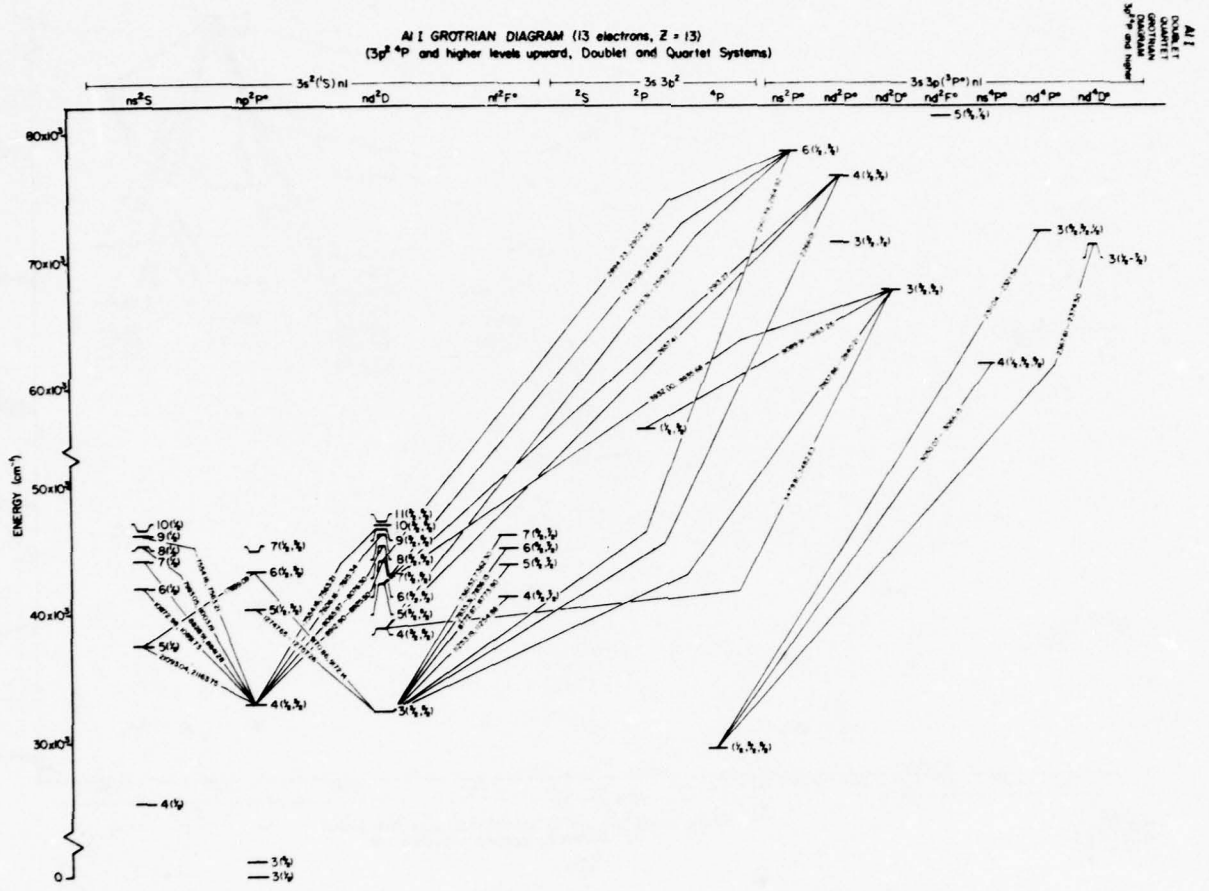

Tabular Data. A-1.112. Diagram for Al (Z = 13).

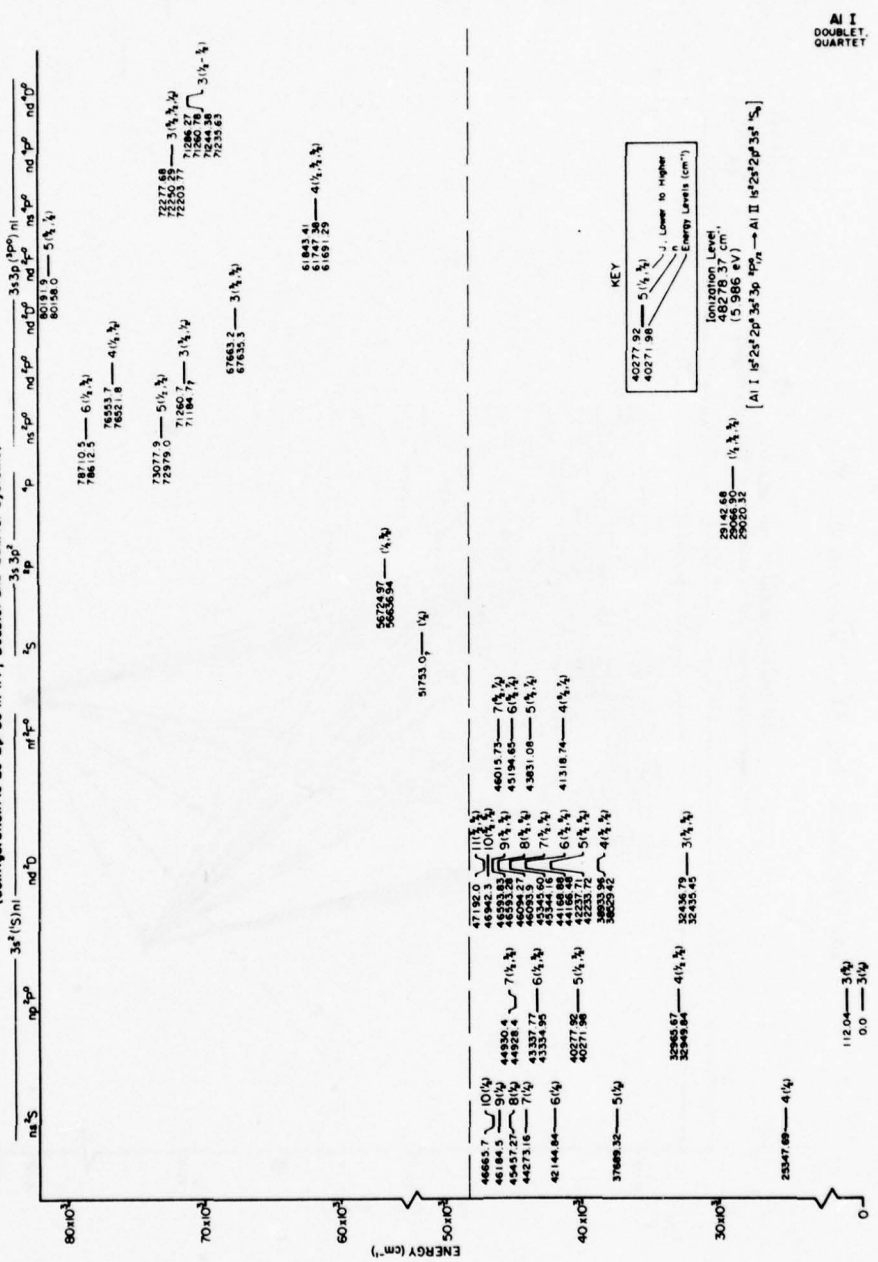

Tabular Data. A-1.113. Diagram for Al^{+} (Z = 13).

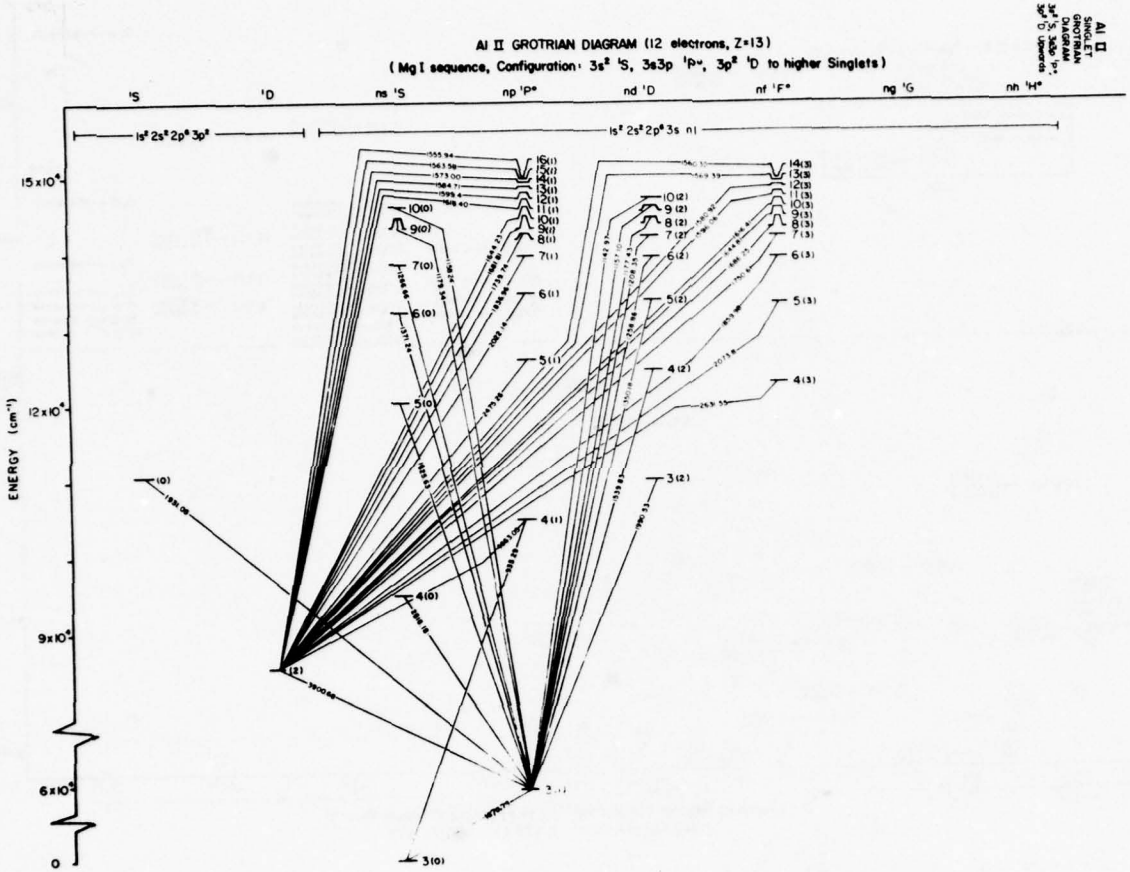

Tabular Data. A-1.114. Diagram for Al^+ (Z = 13).

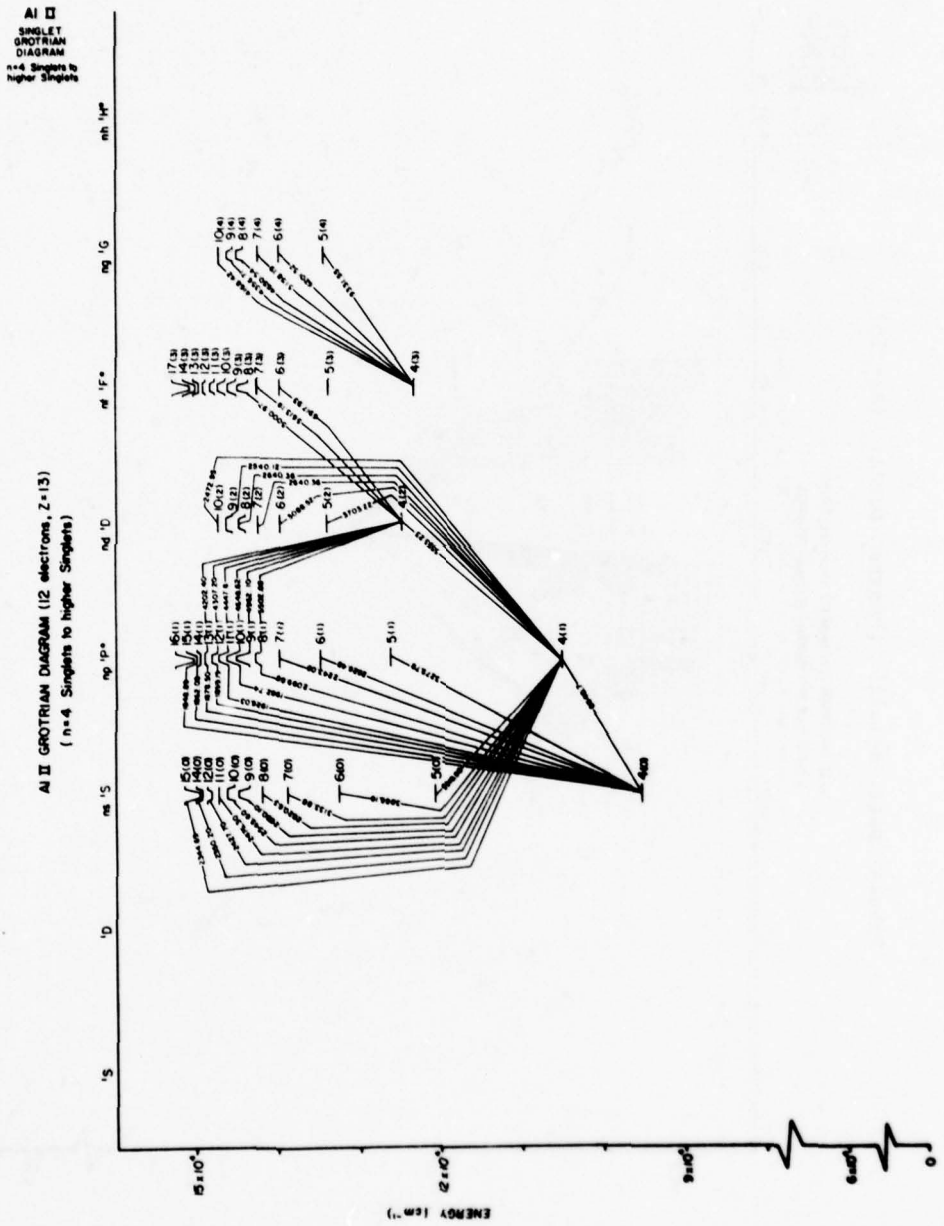

Tabular Data. A-1.115. Diagram for Al^{+} (Z = 13).

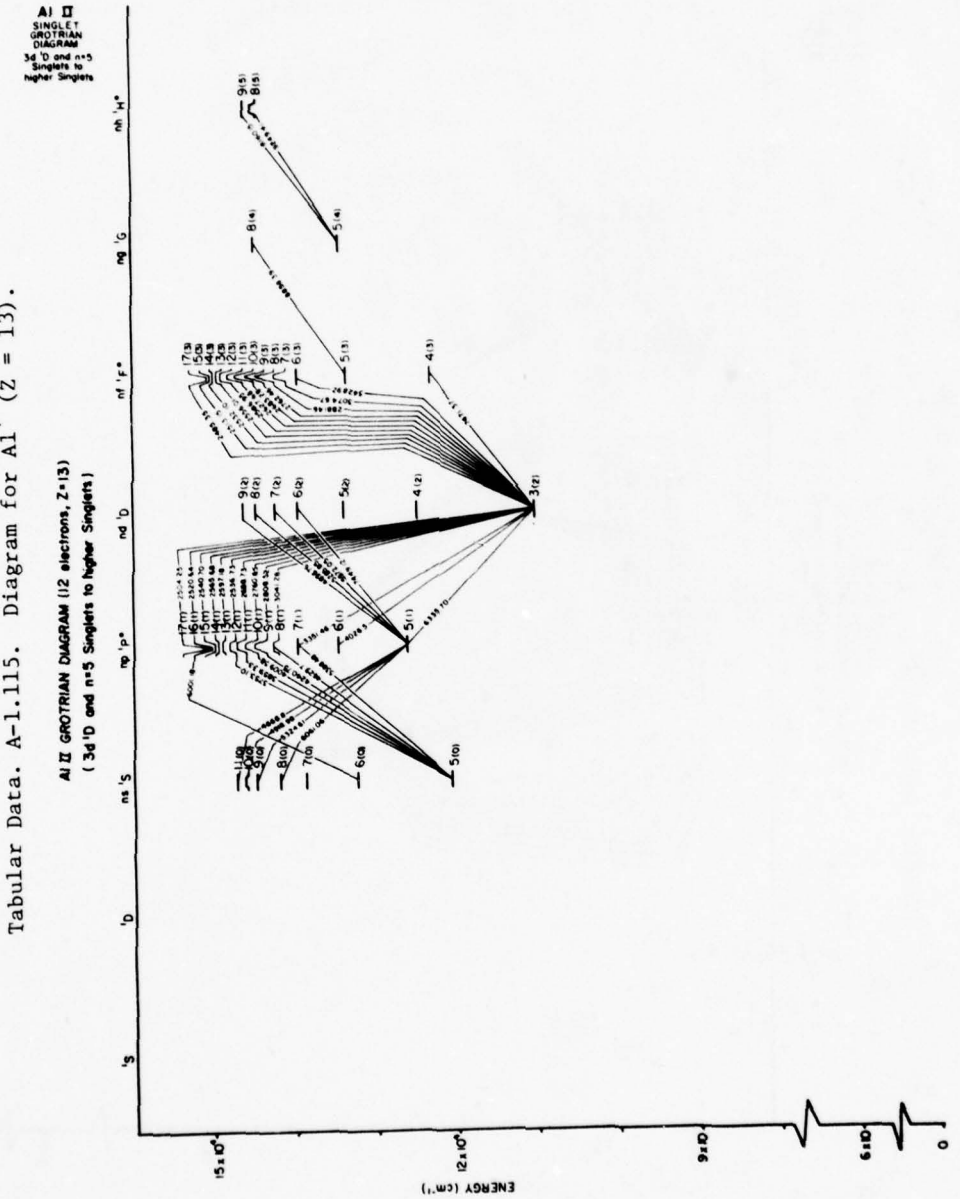

Tabular Data. A-1.116. Diagram for Al^{+} (Z = 13).

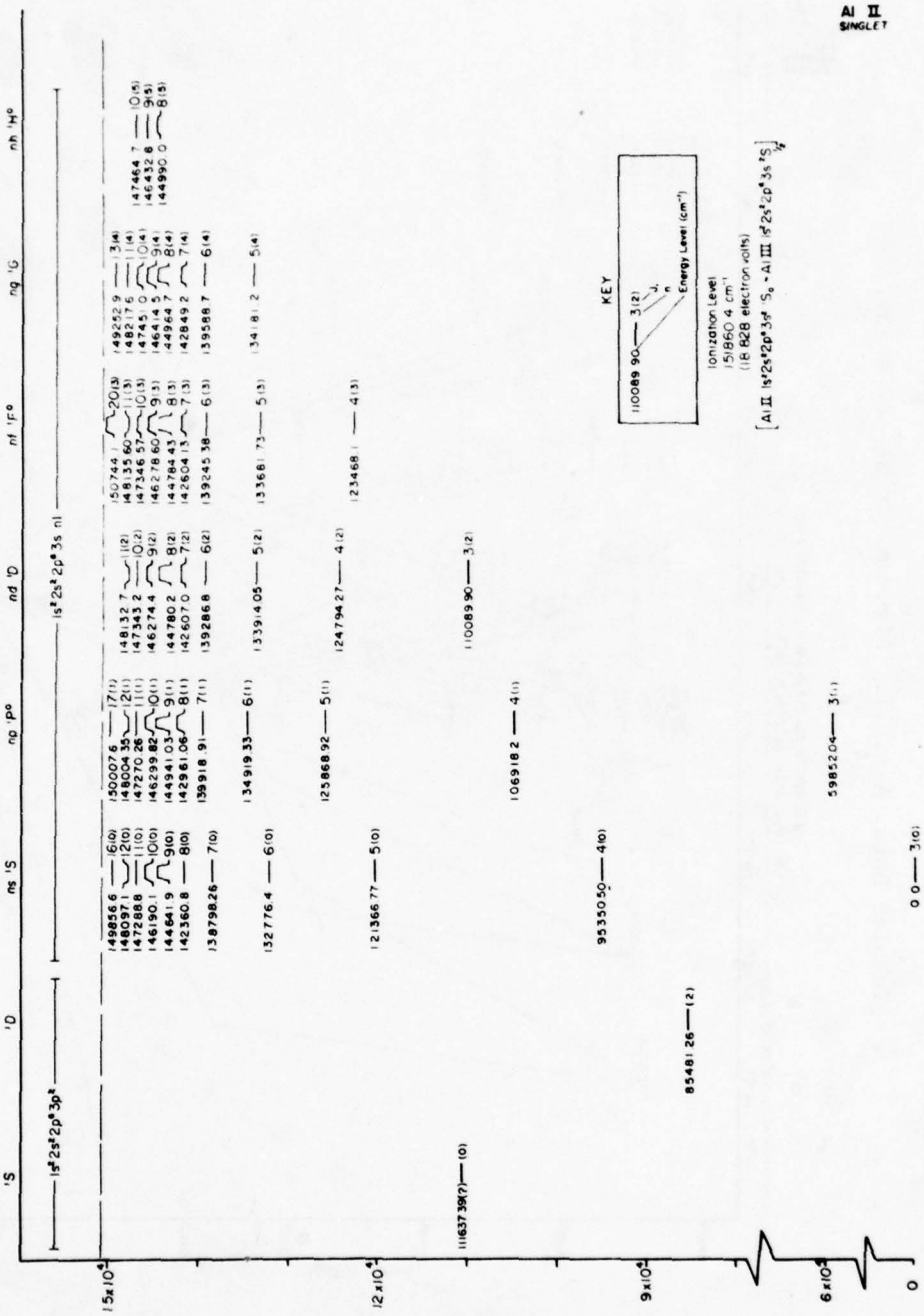

Tabular Data. A-1.117. Diagram for Al^{+} (Z = 13).

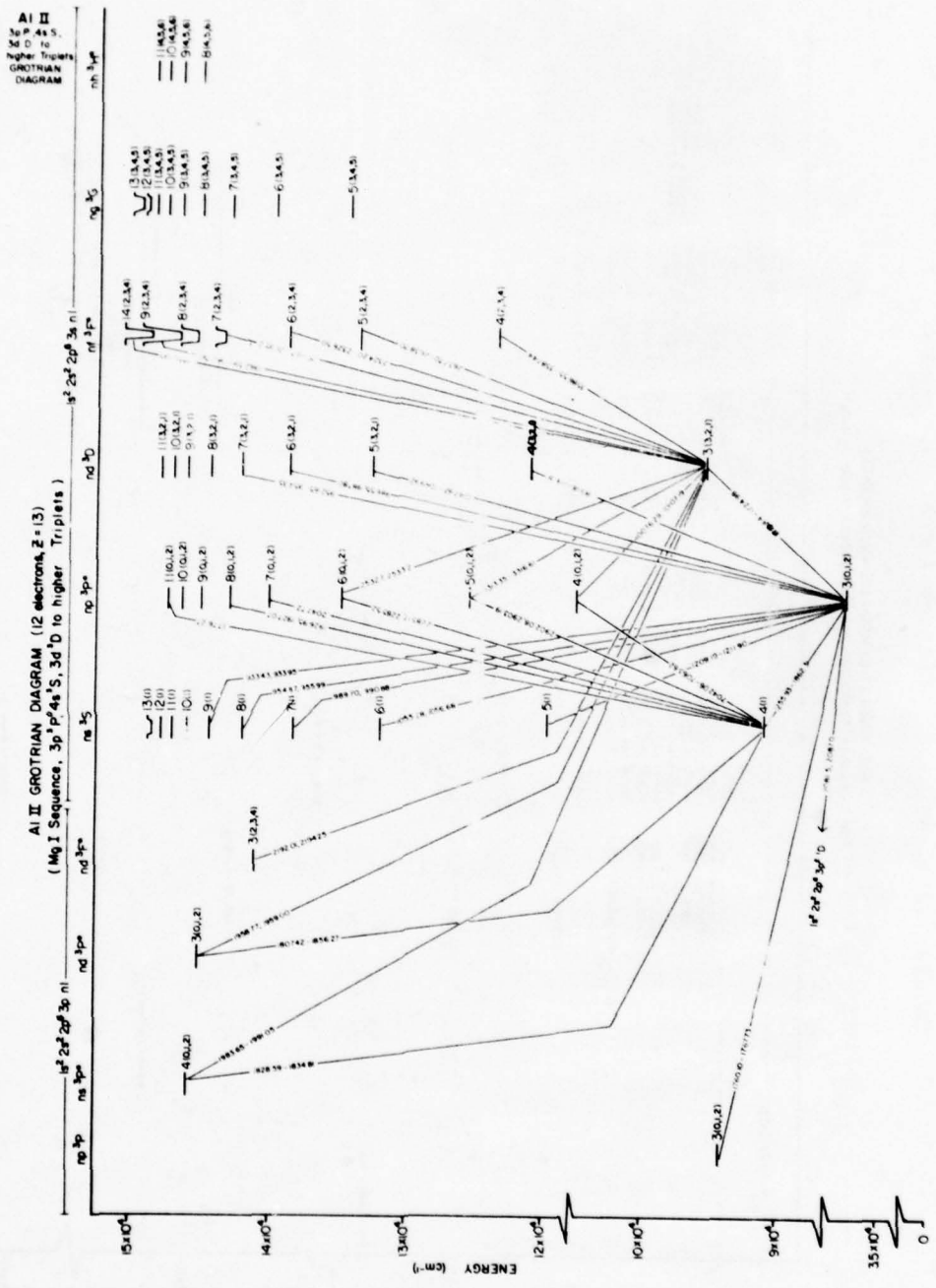

Tabular Data. A-1.118. Diagram for Al^{+} (Z = 13).

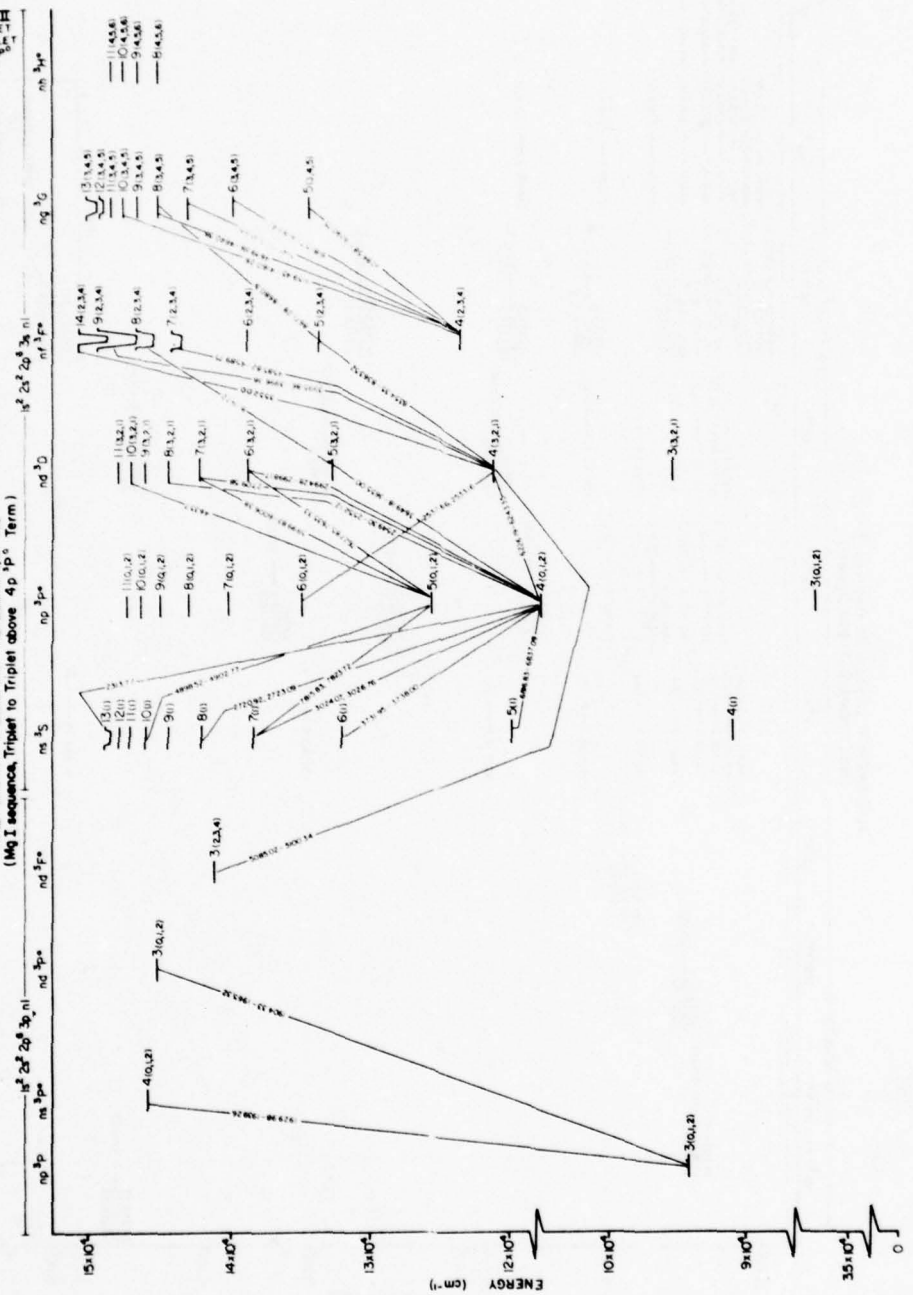

Tabular Data. A-1.119. Diagram for Al^{+} (Z = 13).

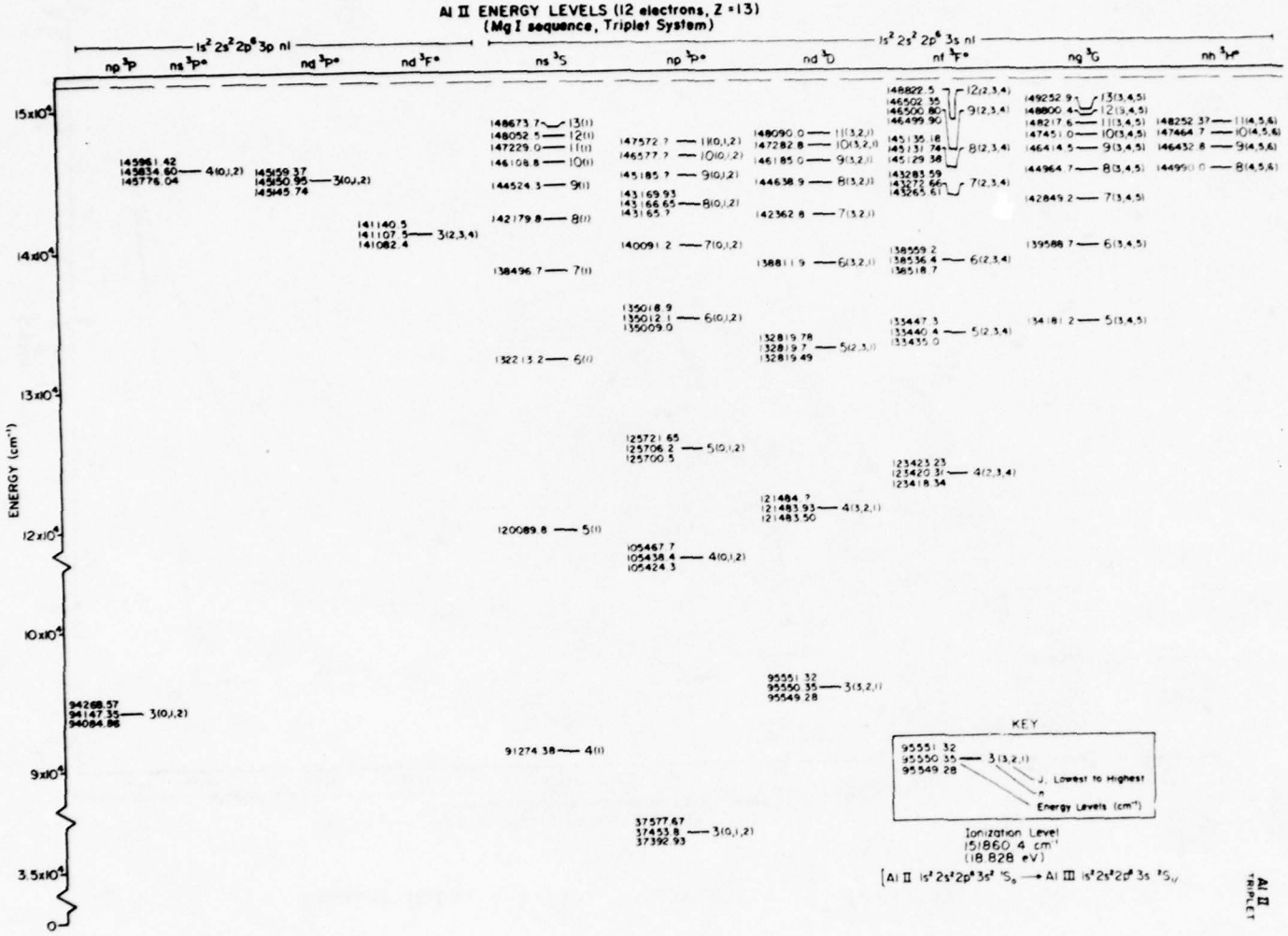

Tabular Data. A-1.120. Diagram for S (Z = 16).

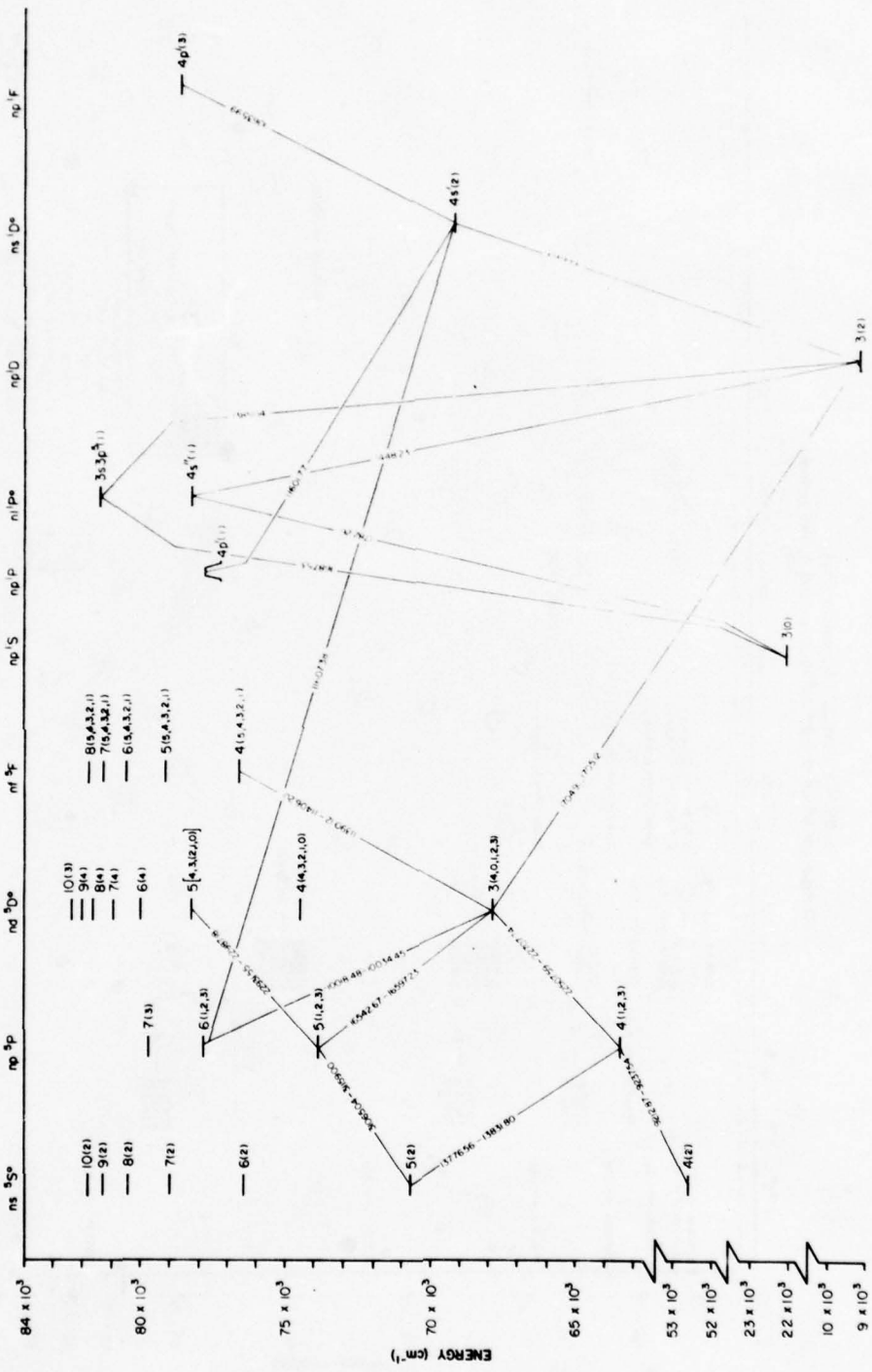

Tabular Data. A-1.121. Diagram for S (Z = 16).

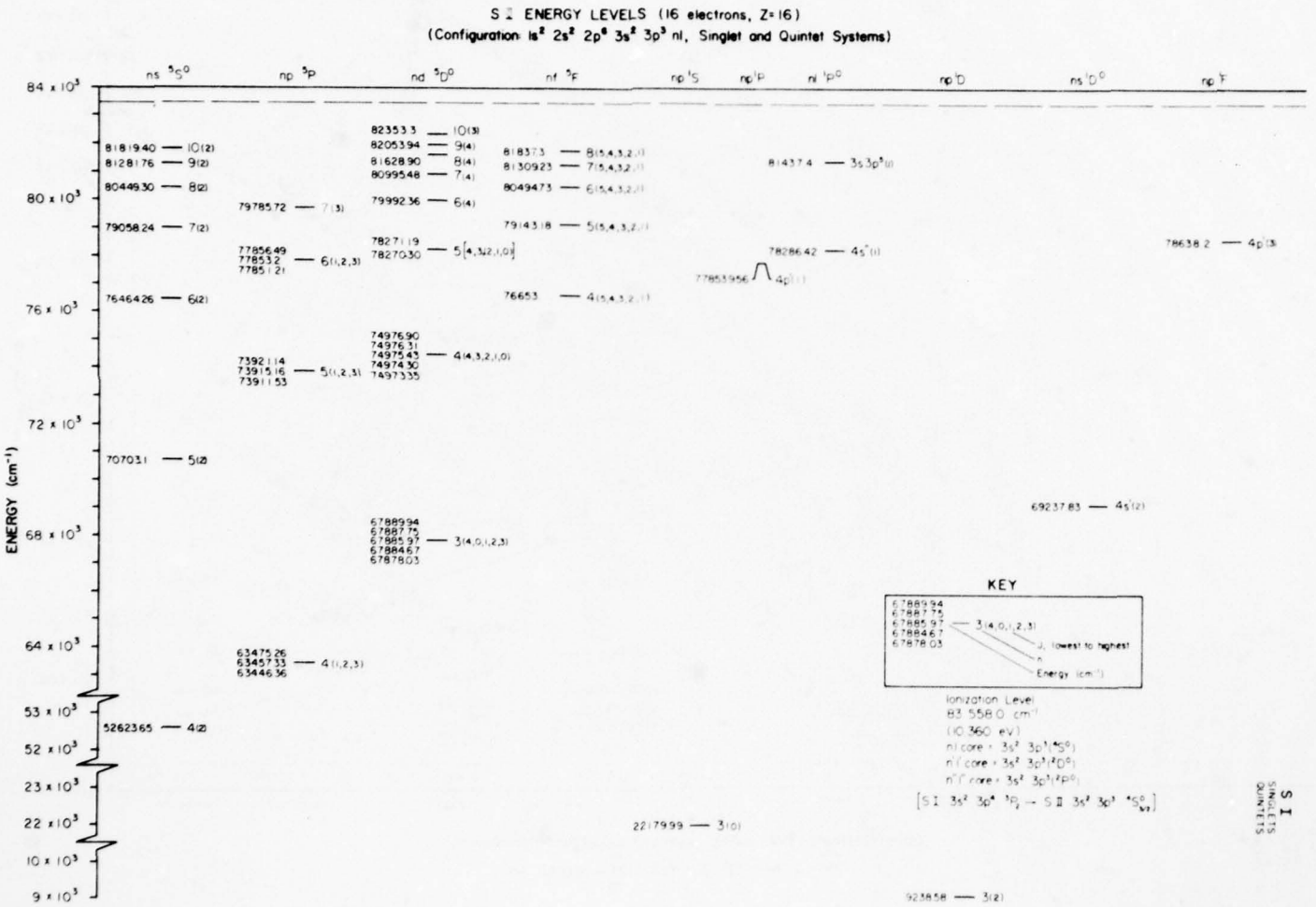

Tabular Data. A-1.122. Diagram for S (Z = 16).

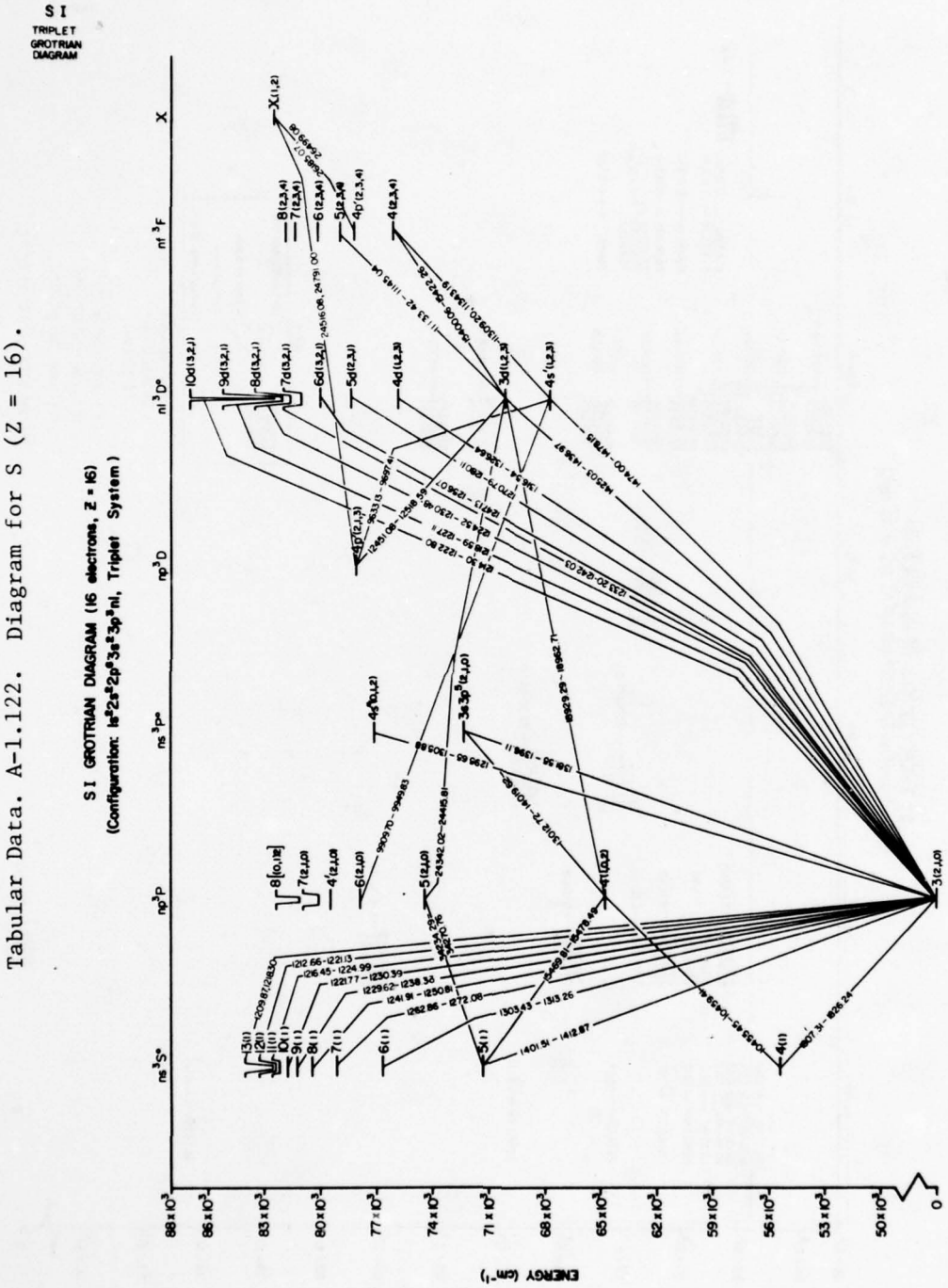

Tabular Data. A-1.123. Diagram for S (Z = 16).

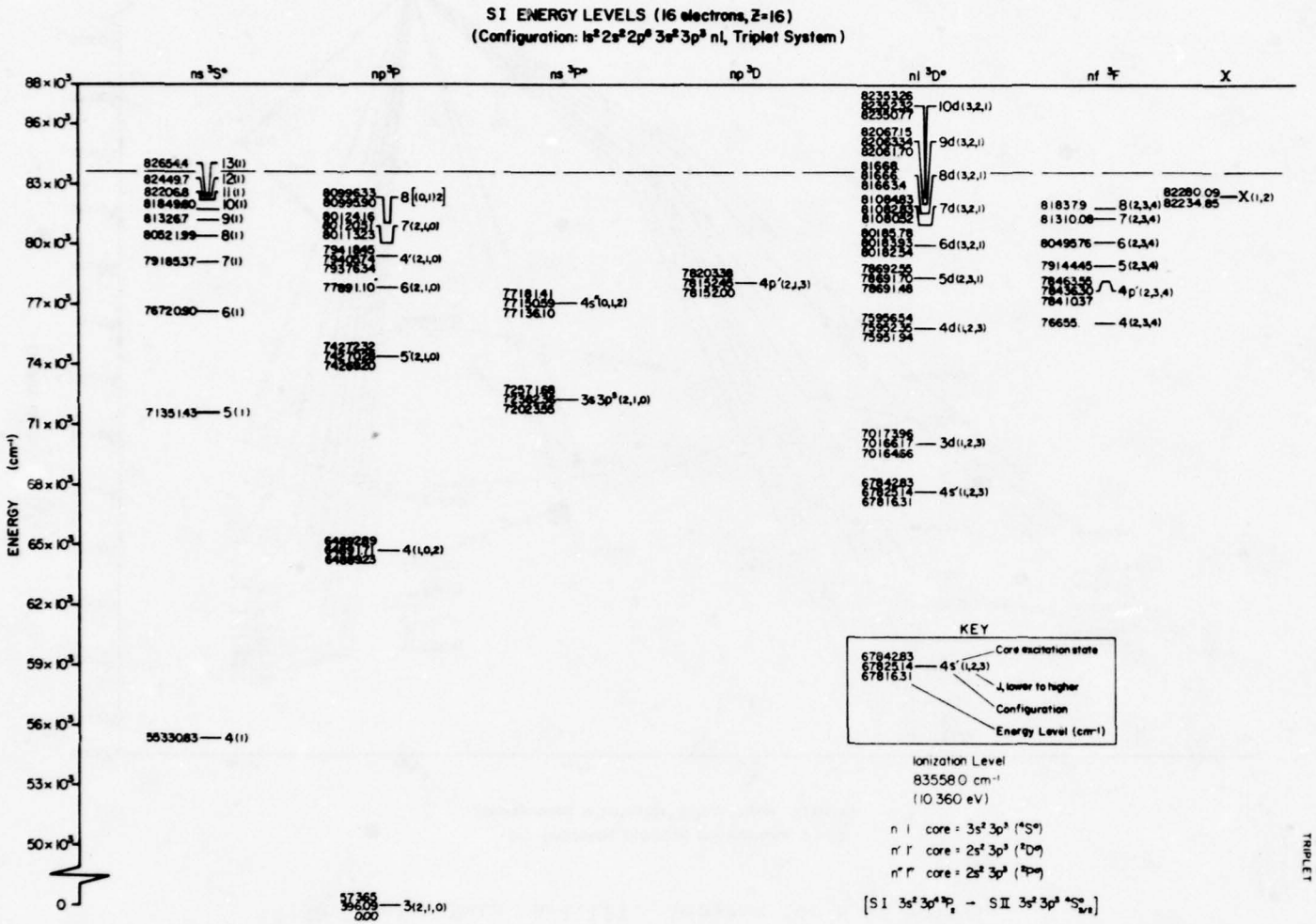

Tabular Data. A-1.124. Diagram for S (Z = 16).

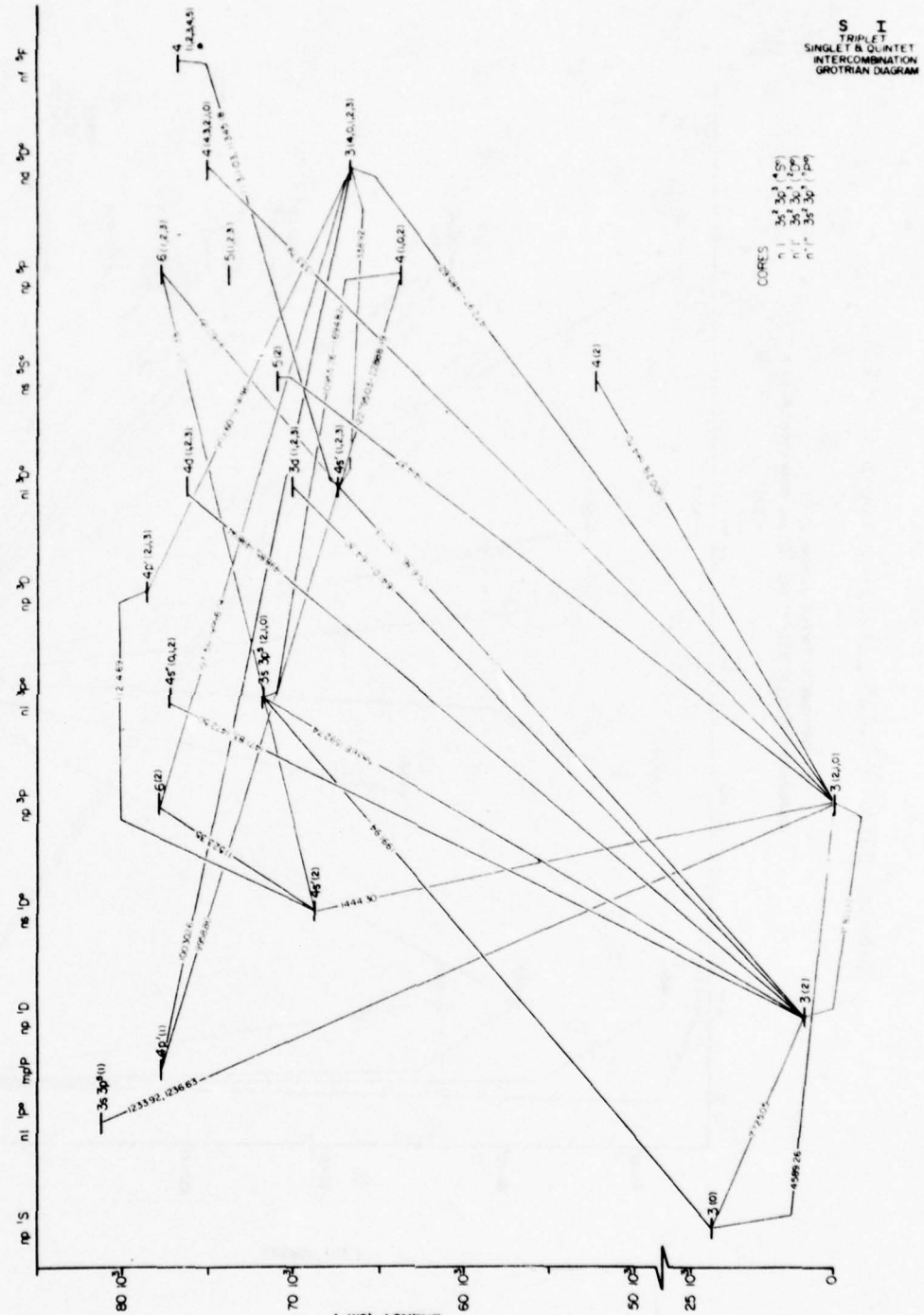

Tabular Data. A-1.125. Diagram for S (Z = 16).

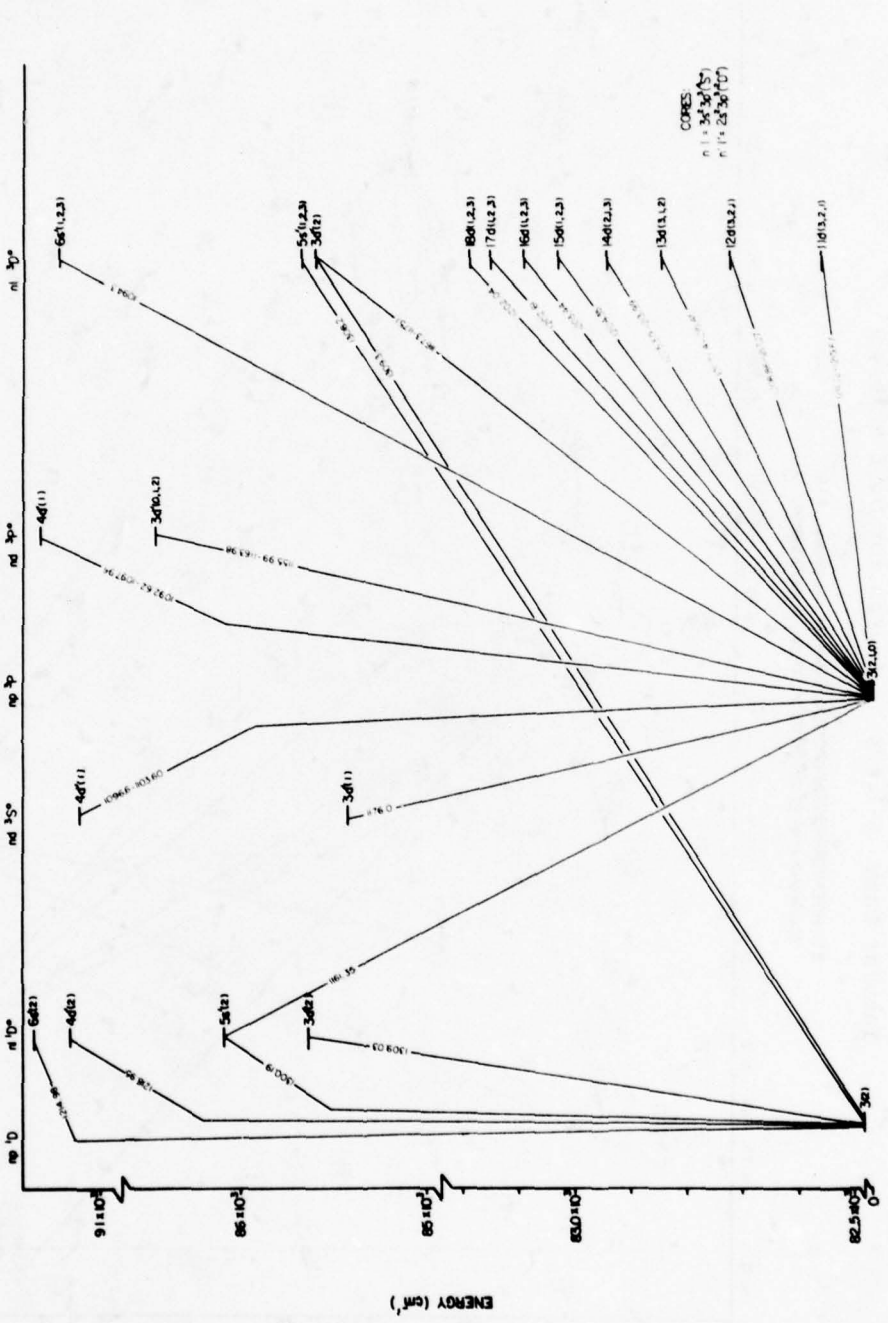

Tabular Data. A-1.126. Diagram for S (Z = 16).

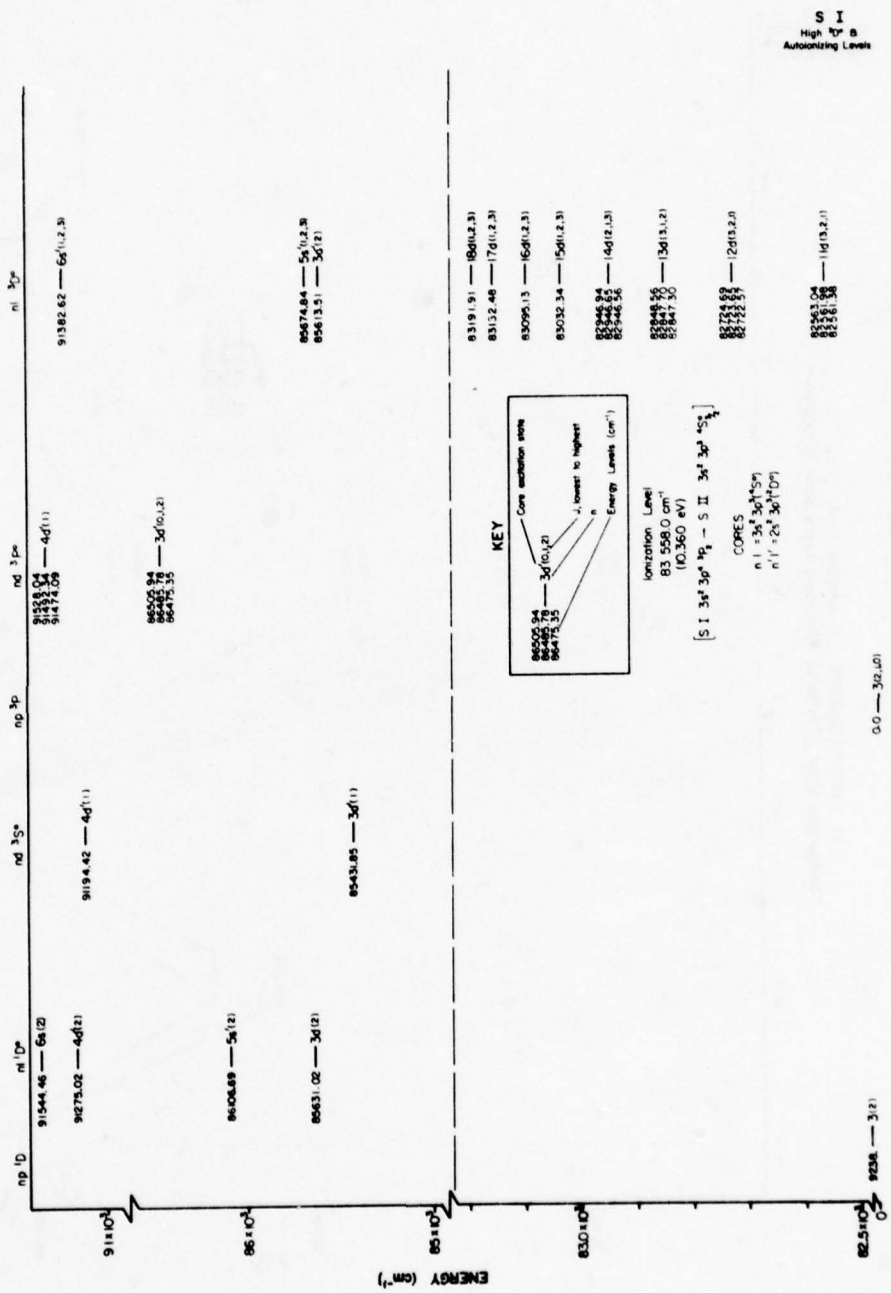

Tabular Data. A-1.127. Diagram for S (Z = 16).

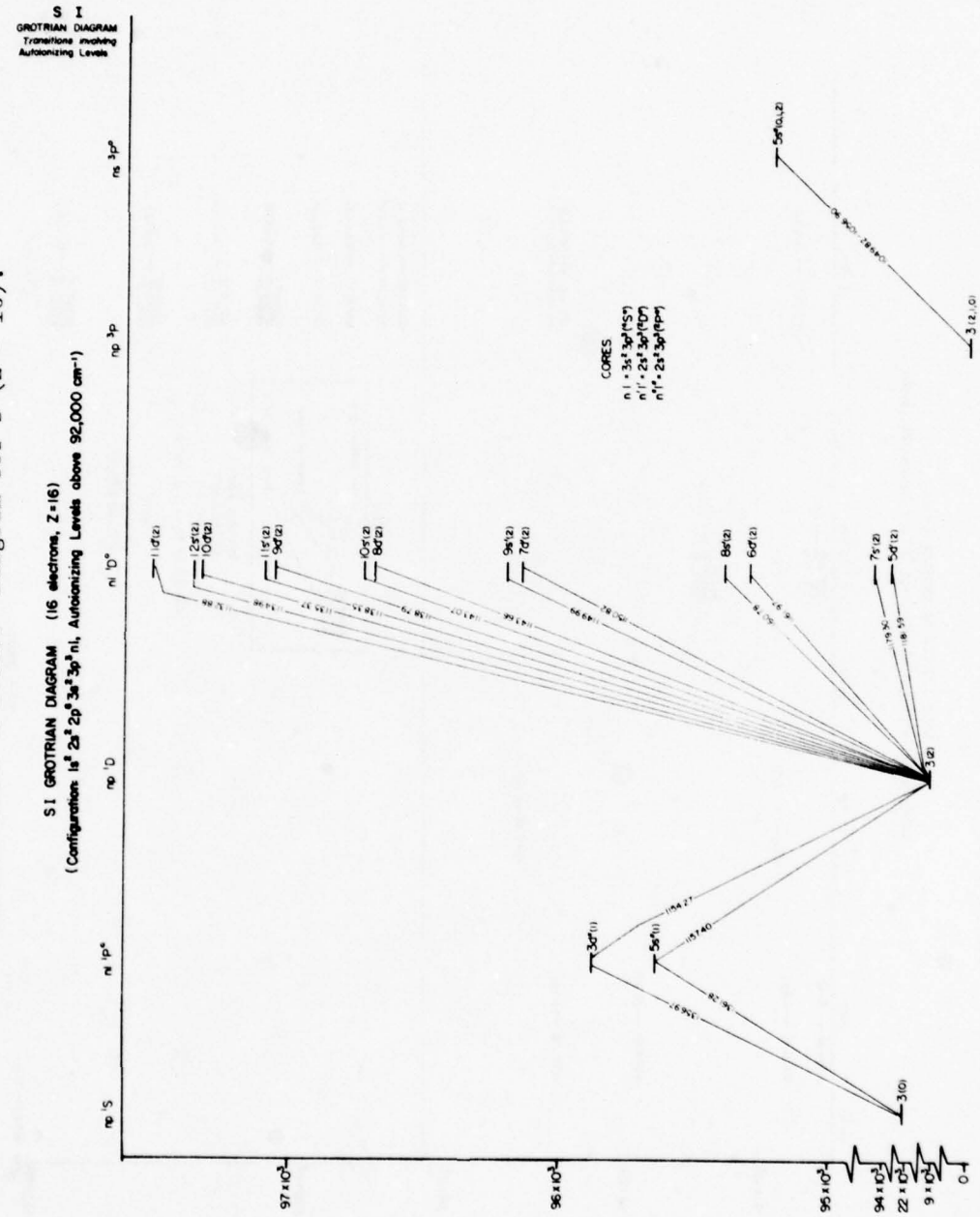

Tabular Data. A-1.128. Diagram for S (Z = 16).

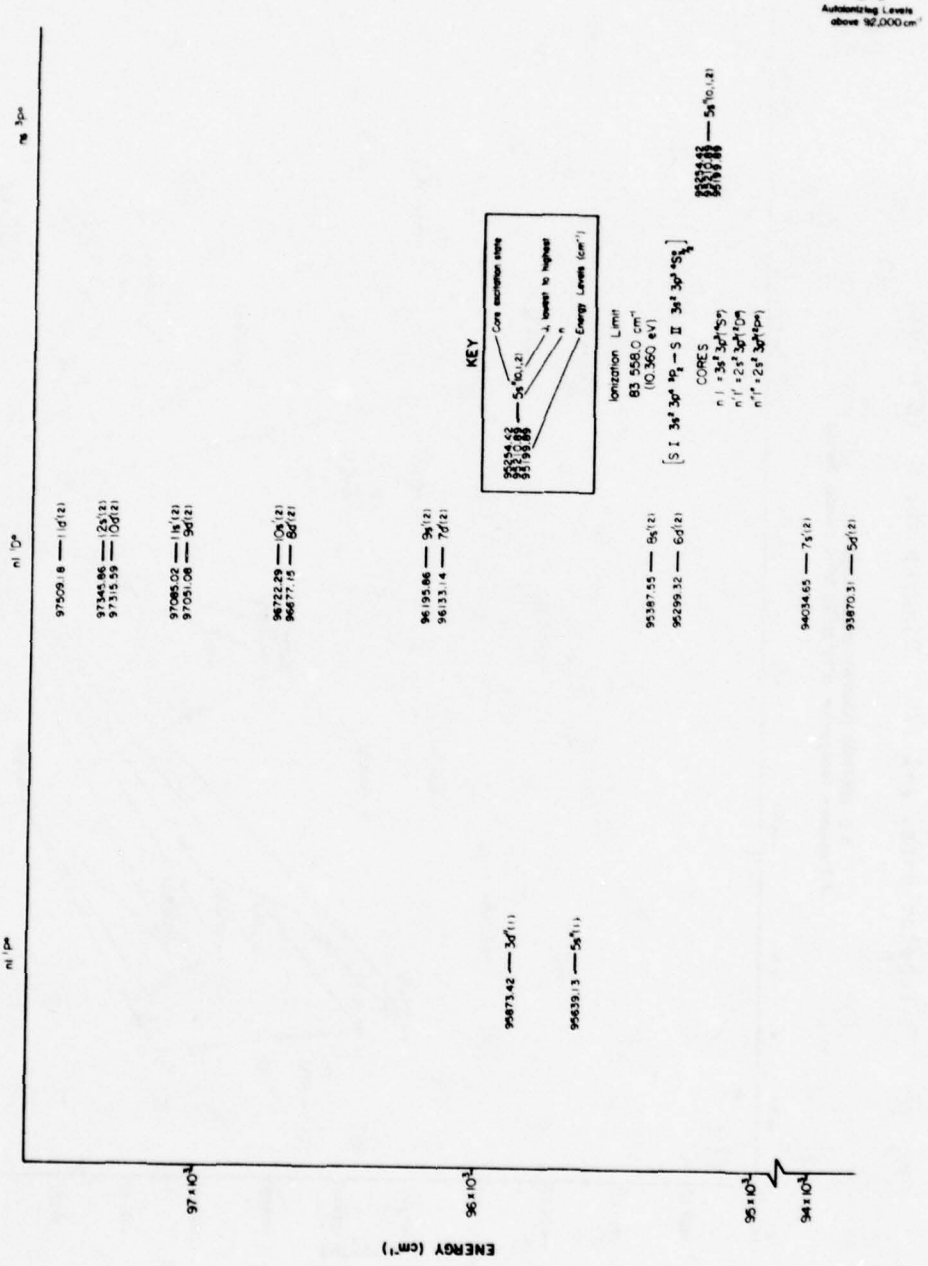

Tabular Data. A-1.129. Diagram for S^{+} (Z = 16).

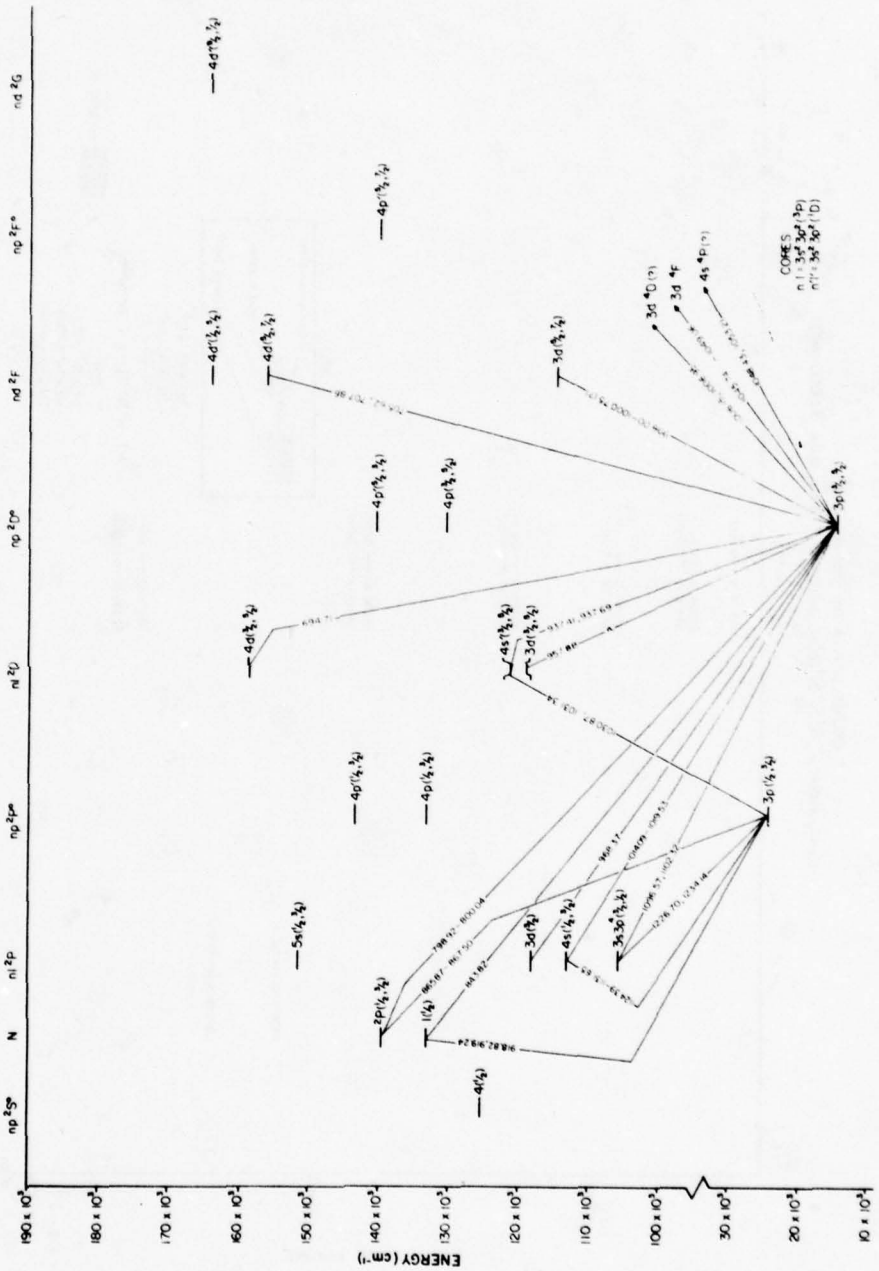

Tabular Data. A-1.130. Diagram for S^{+} (Z = 16).

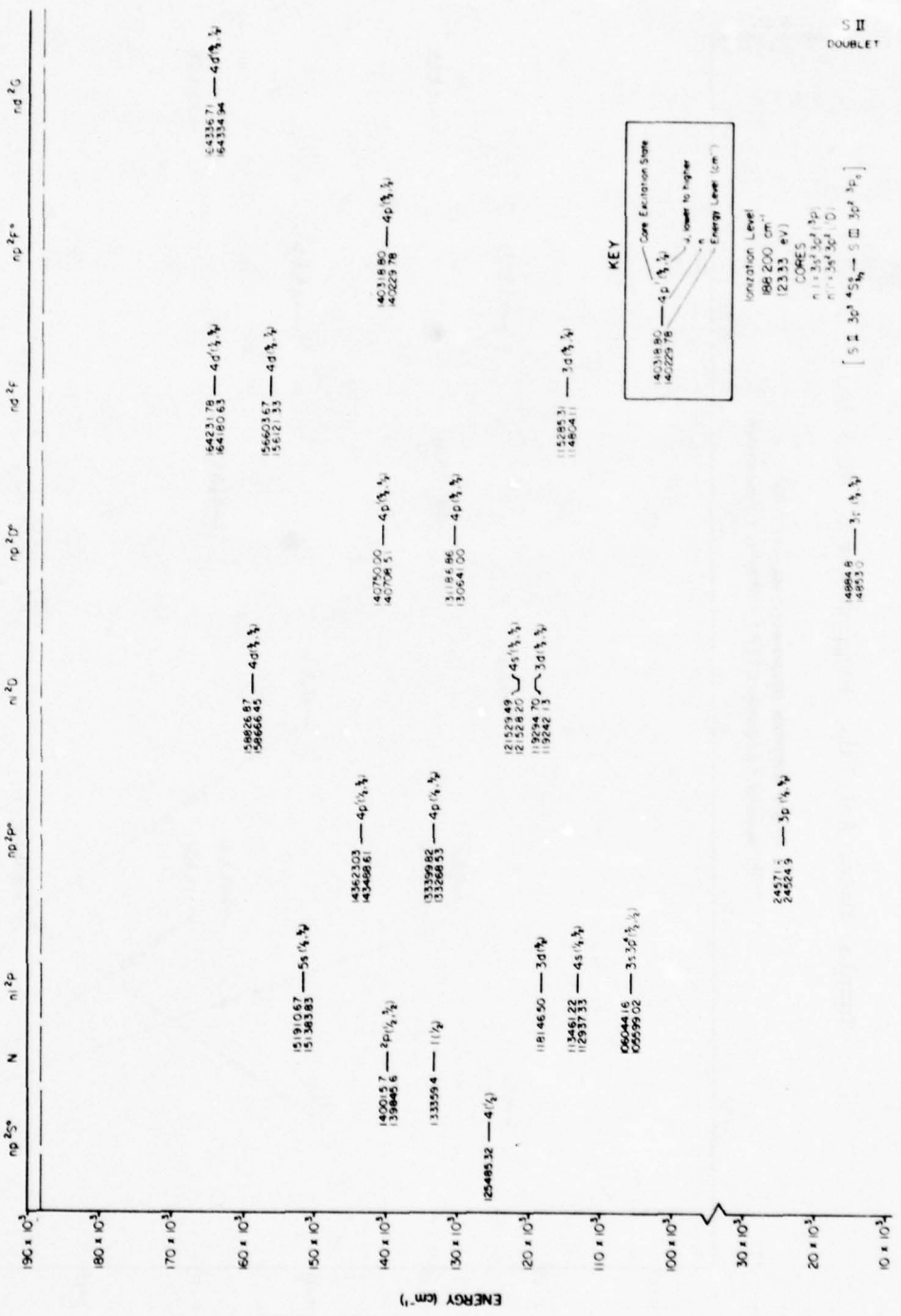

Tabular Data. A-1.131. Diagram for S^{+} (Z = 16).

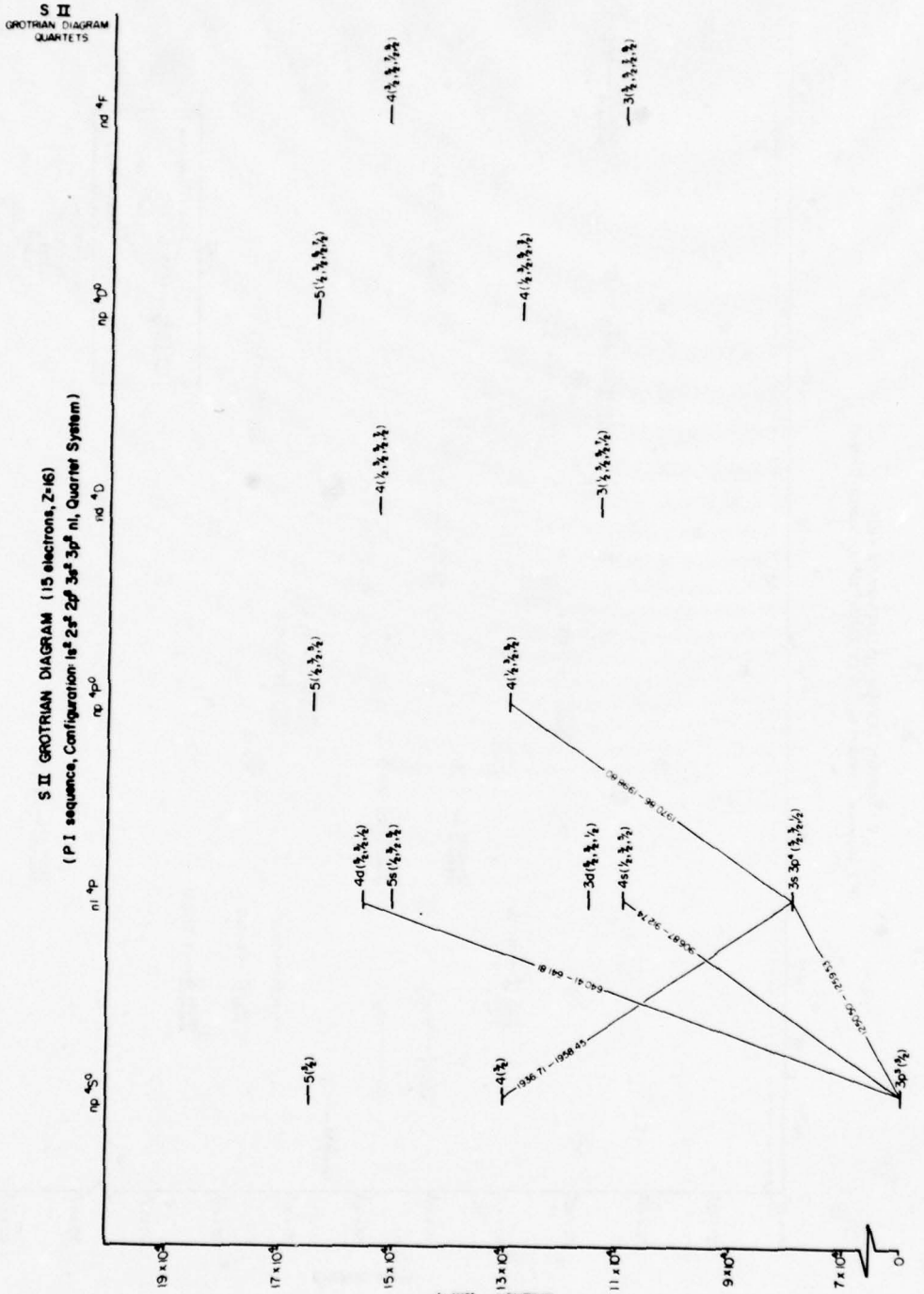

Tabular Data. A-1.132. Diagram for S^+ (Z = 16).

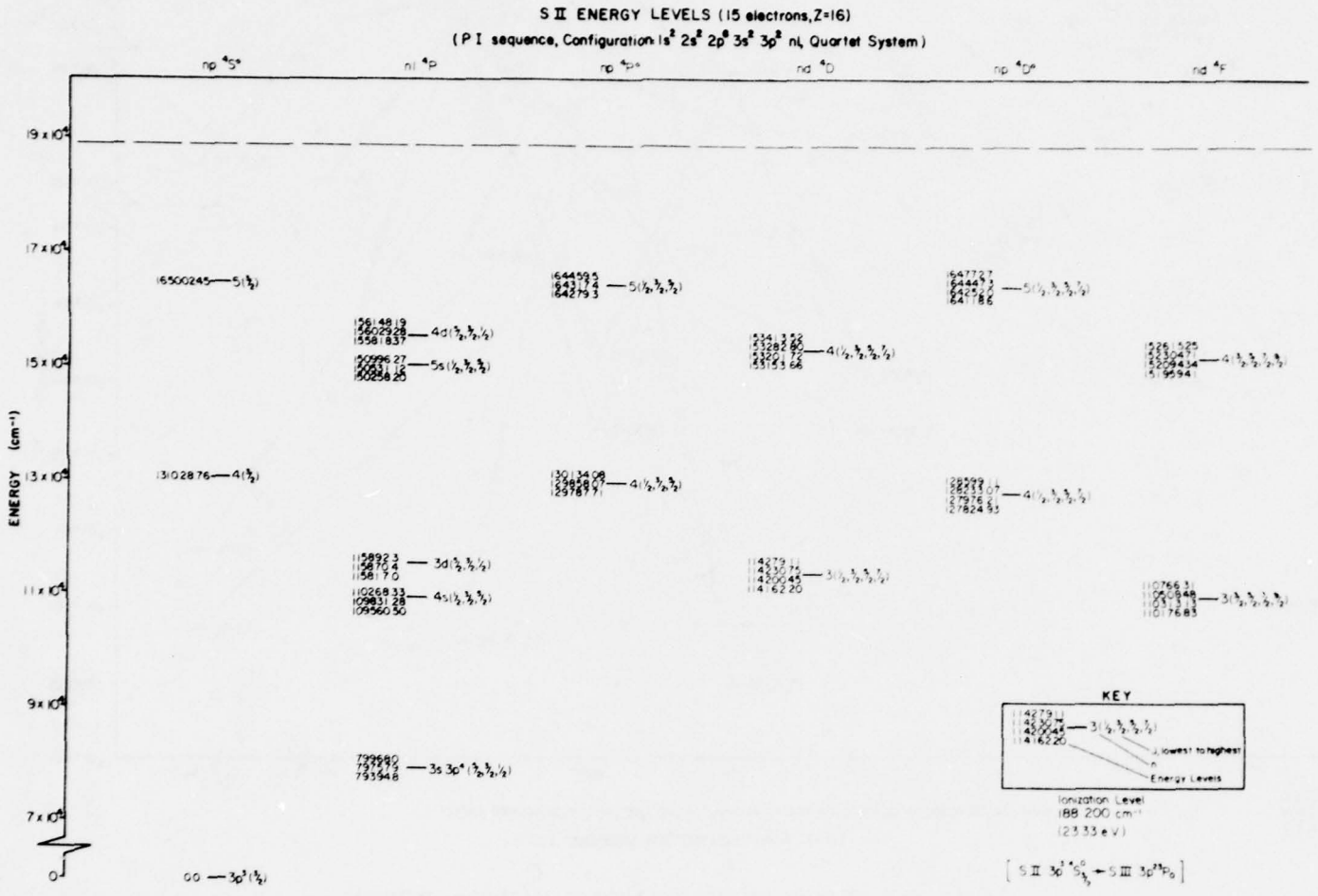

Tabular Data. A-1.133. Diagram for Cl (Z = 17).

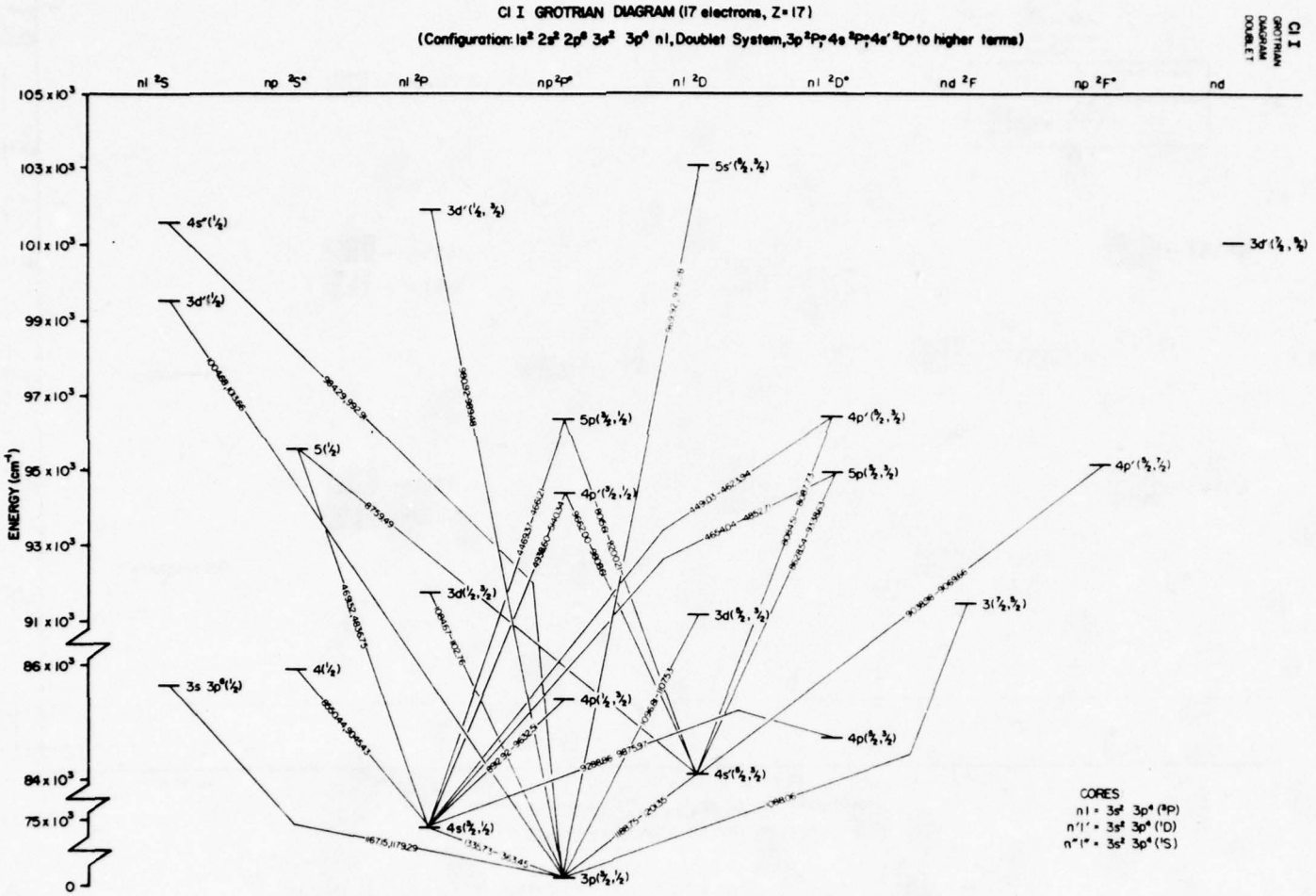

Tabular Data. A-1.134. Diagram for Cl (Z = 17).

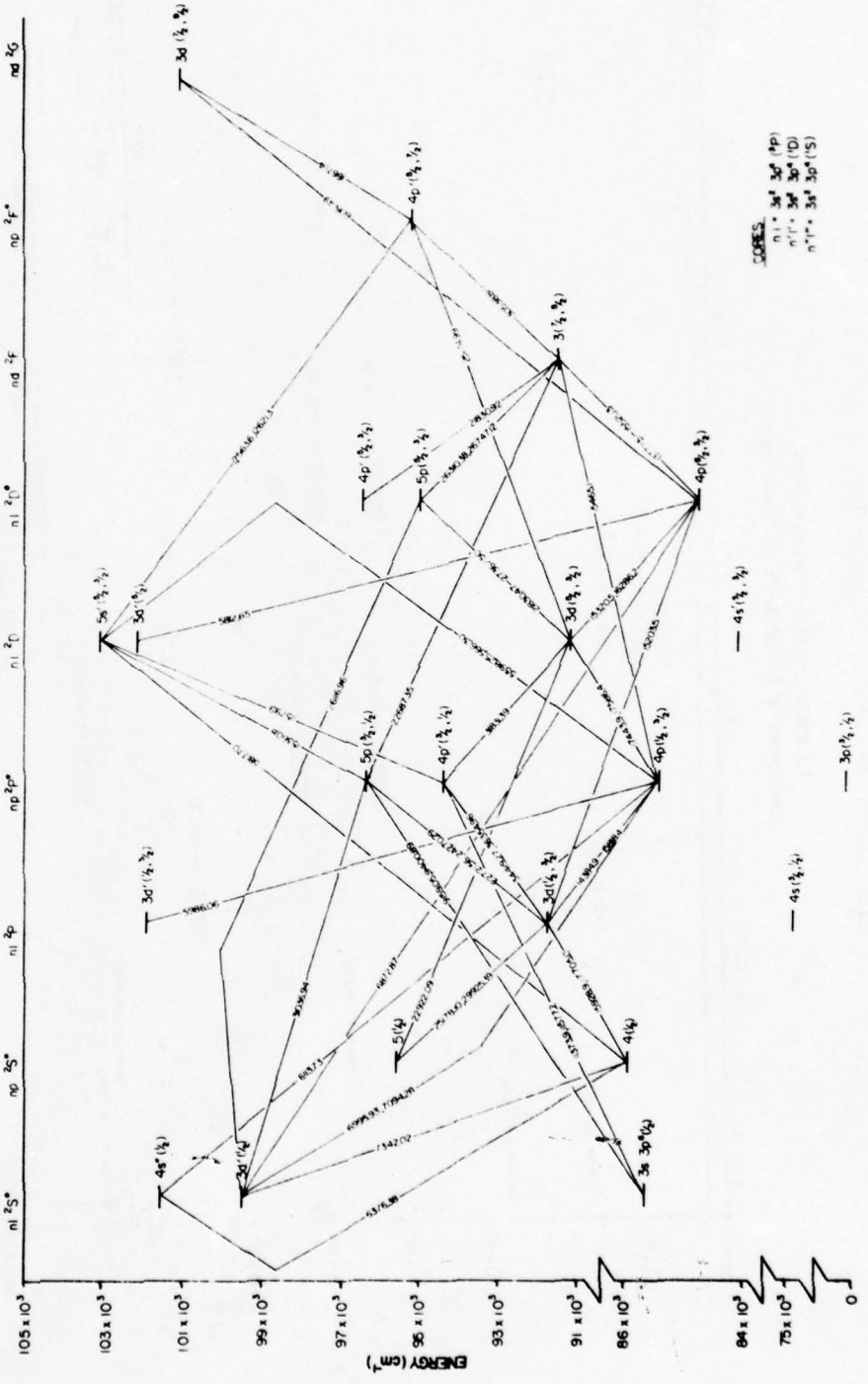

Tabular Data. A-1.135. Diagram for Cl (Z = 17).

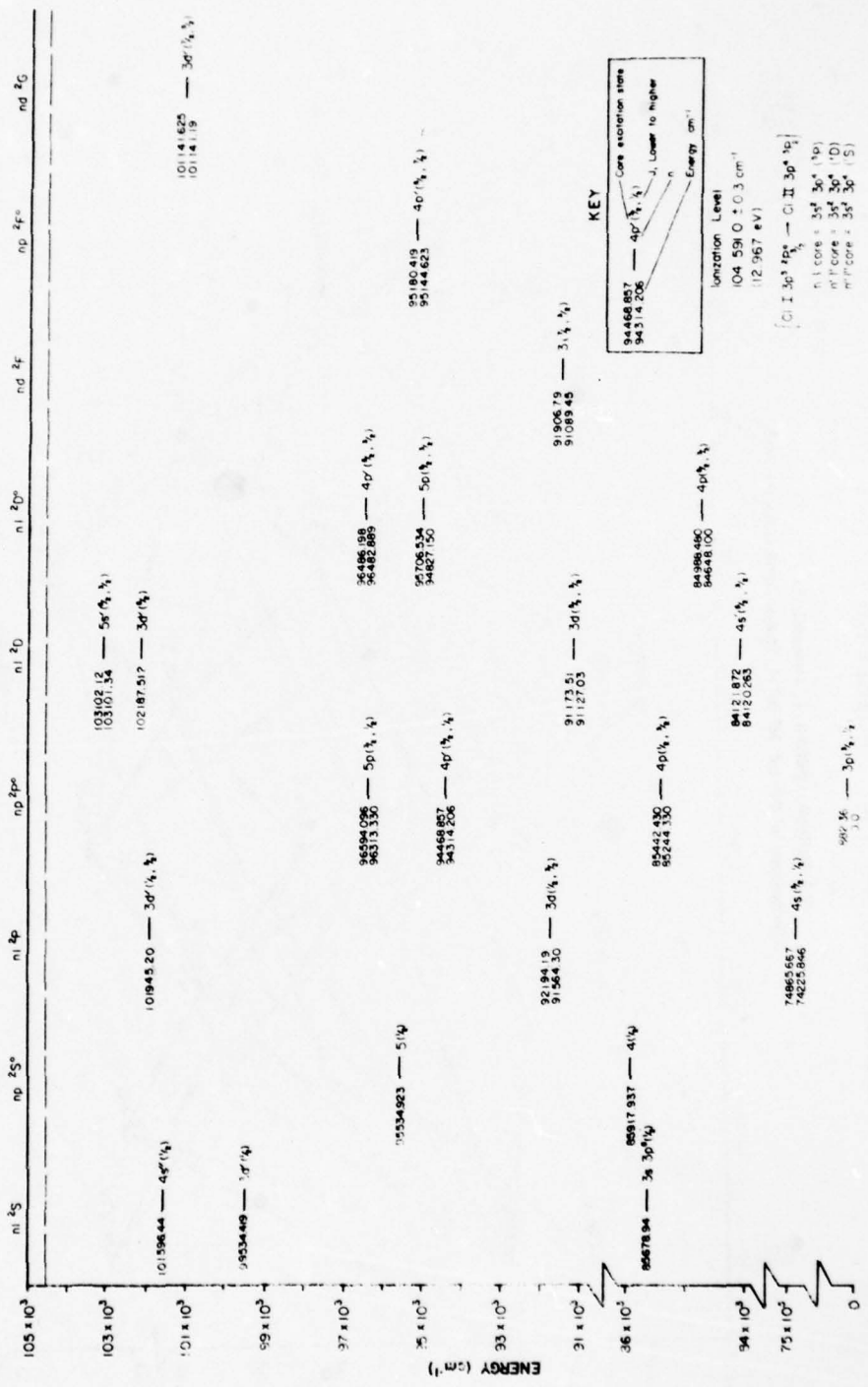

Tabular Data. A-1.136. Diagram for Cl (Z = 17).

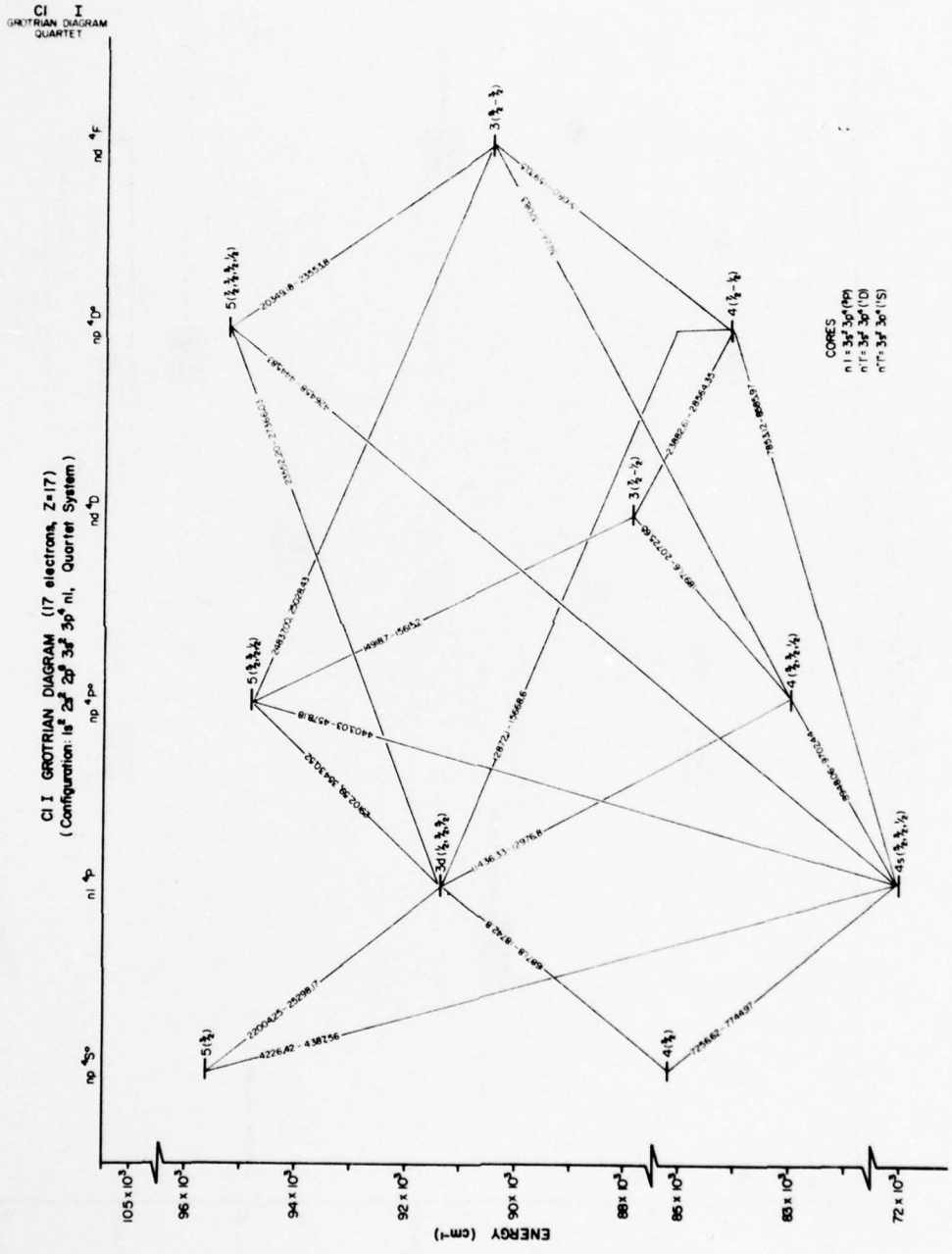

Tabular Data. A-1.137. Diagram for Cl (Z = 17).

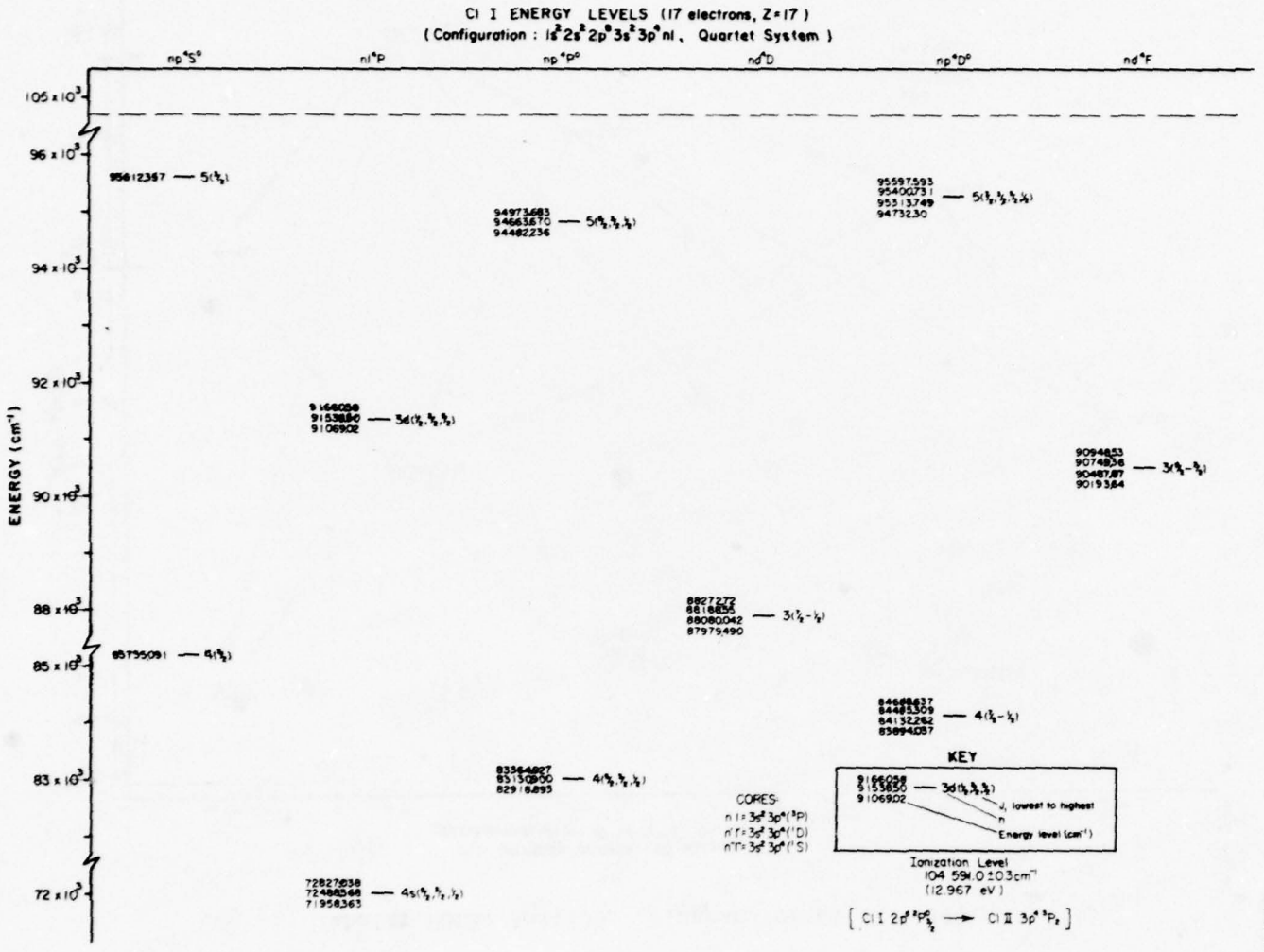

Tabular Data. A-1.138. Diagram for Cl (Z = 17).

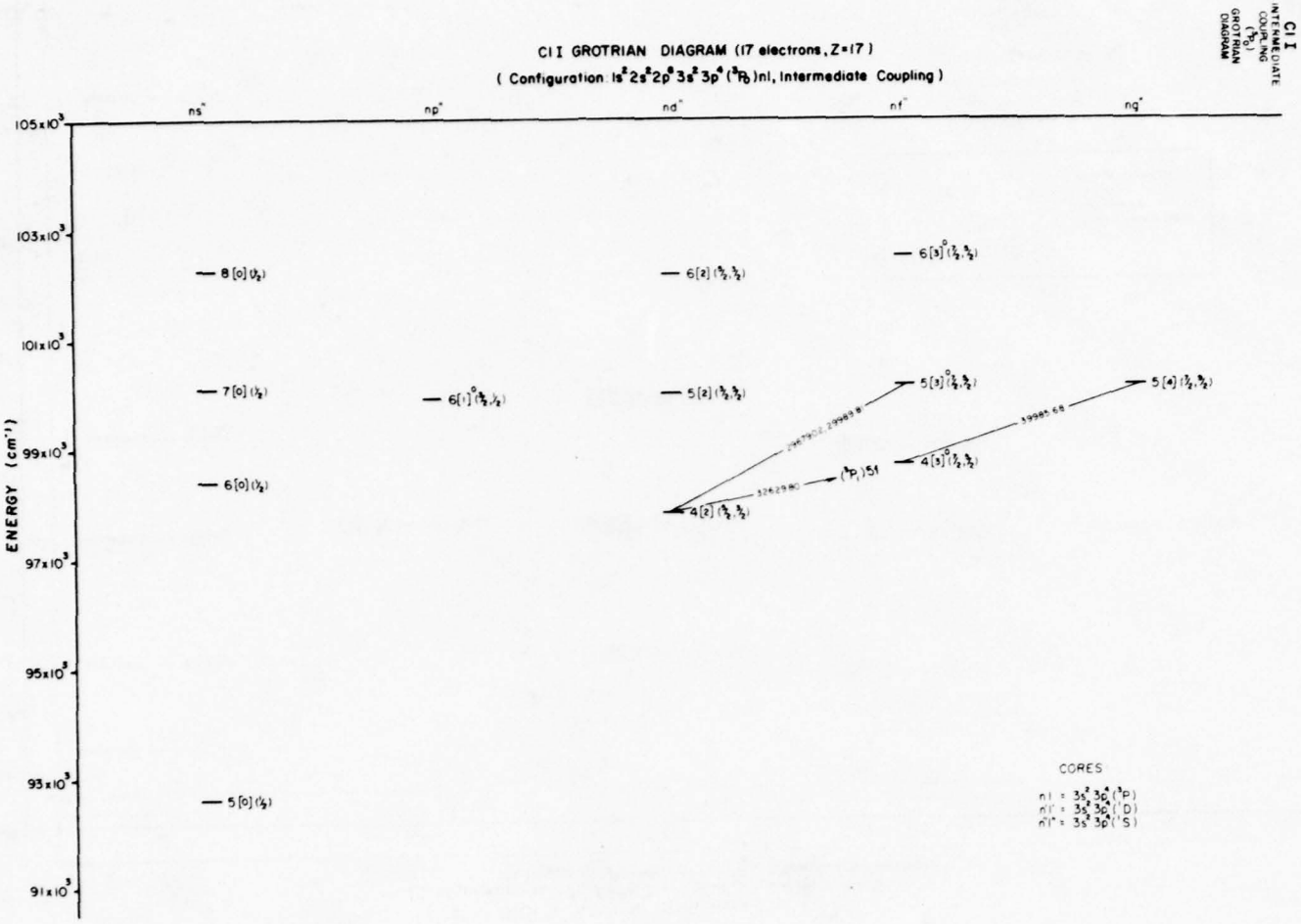

Tabular Data. A-1.139. Diagram for Cl (Z = 17).

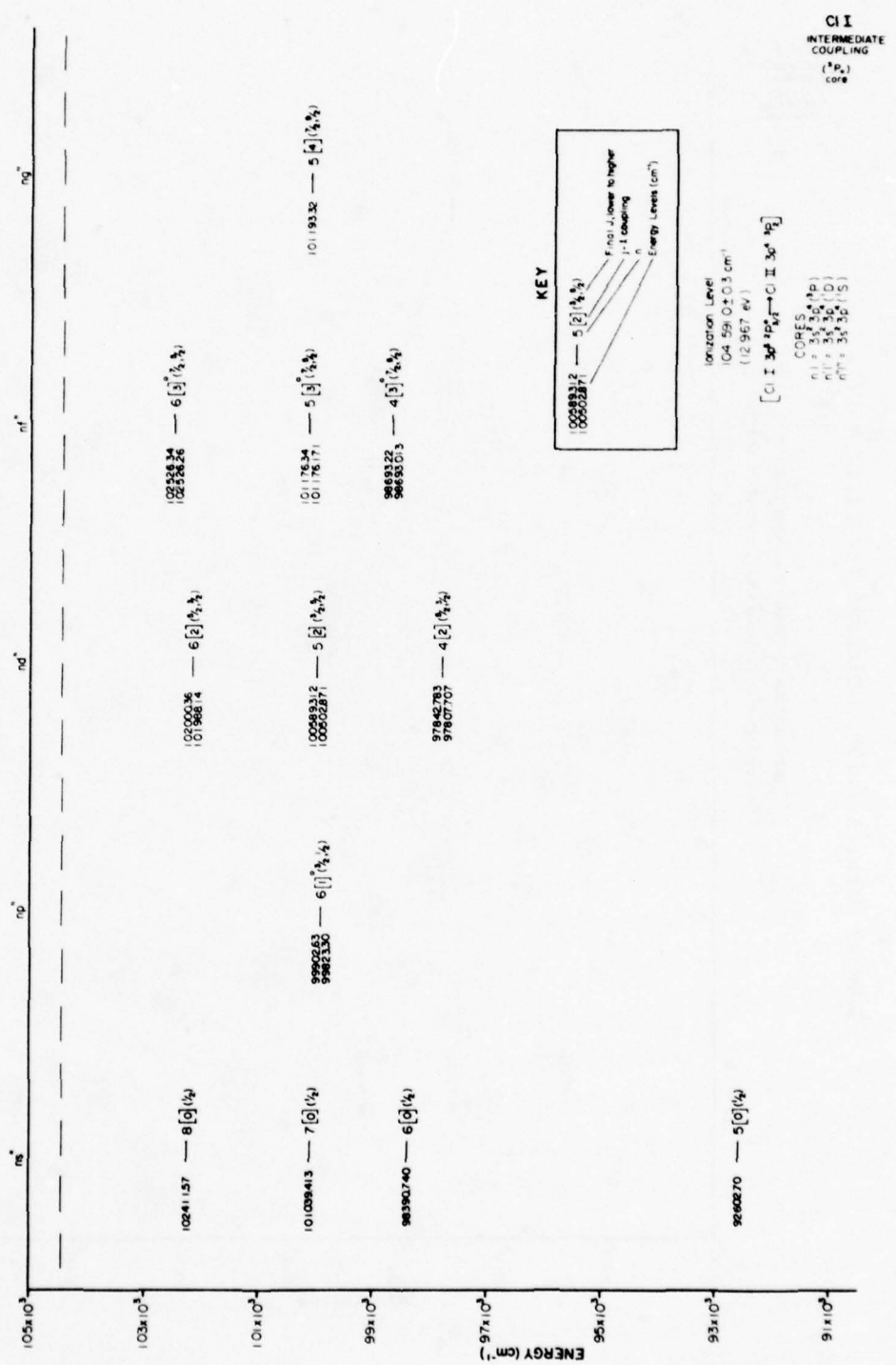

Tabular Data. A-1.140. Diagram for Cl (Z = 17).

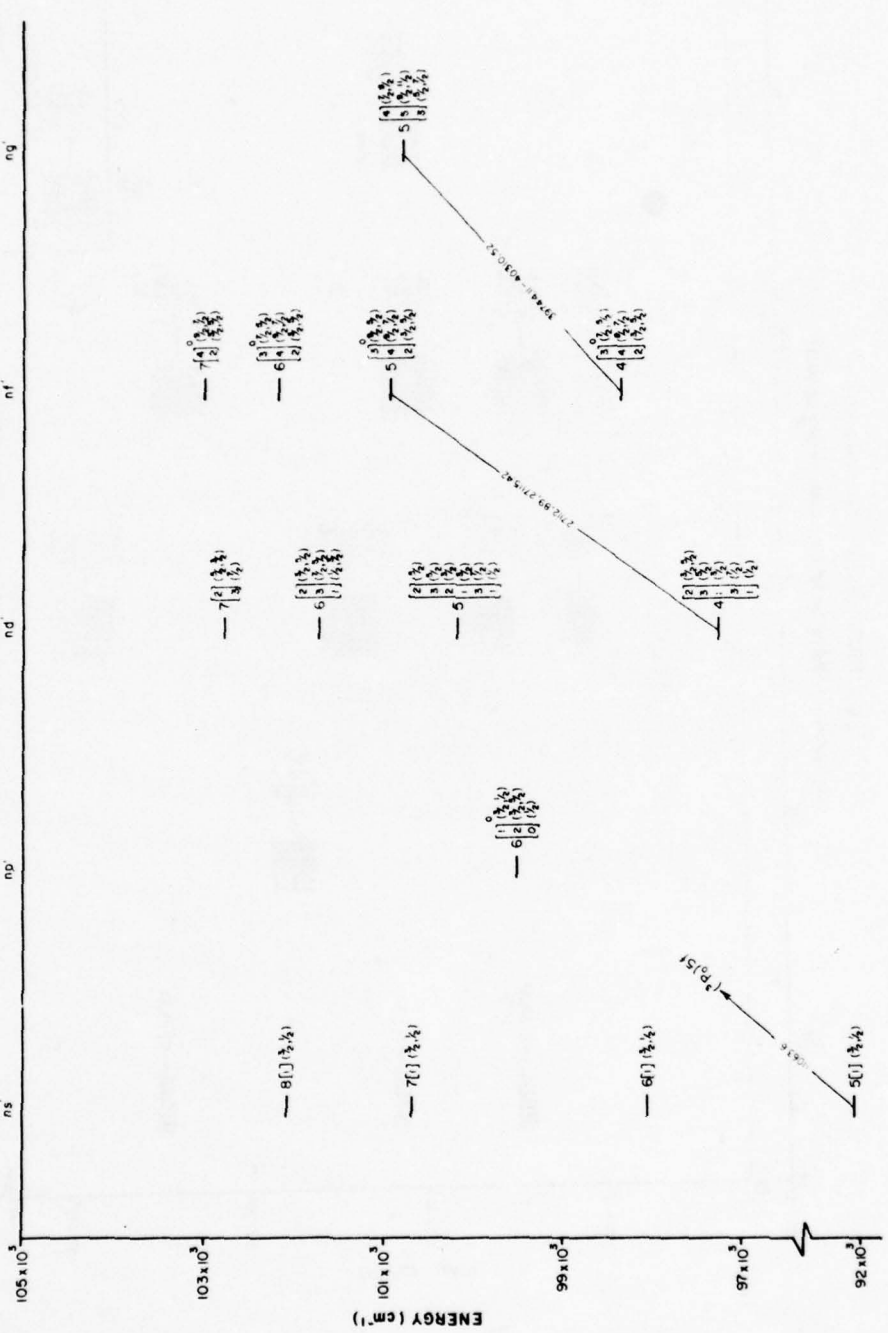

Tabular Data. A-1.141. Diagram for Cl (Z = 17).

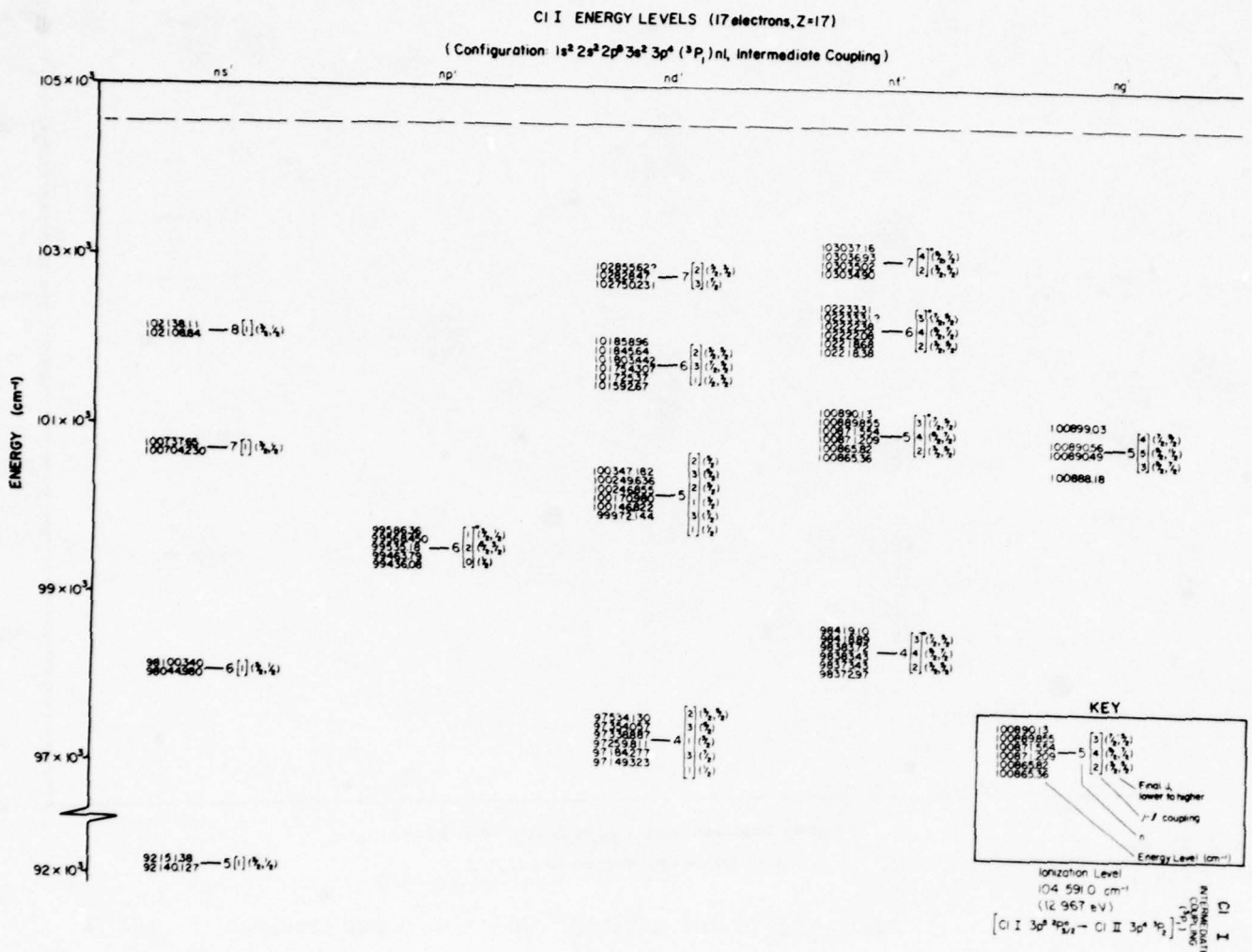

Tabular Data. A-1.142. Diagram for Cl (Z = 17).

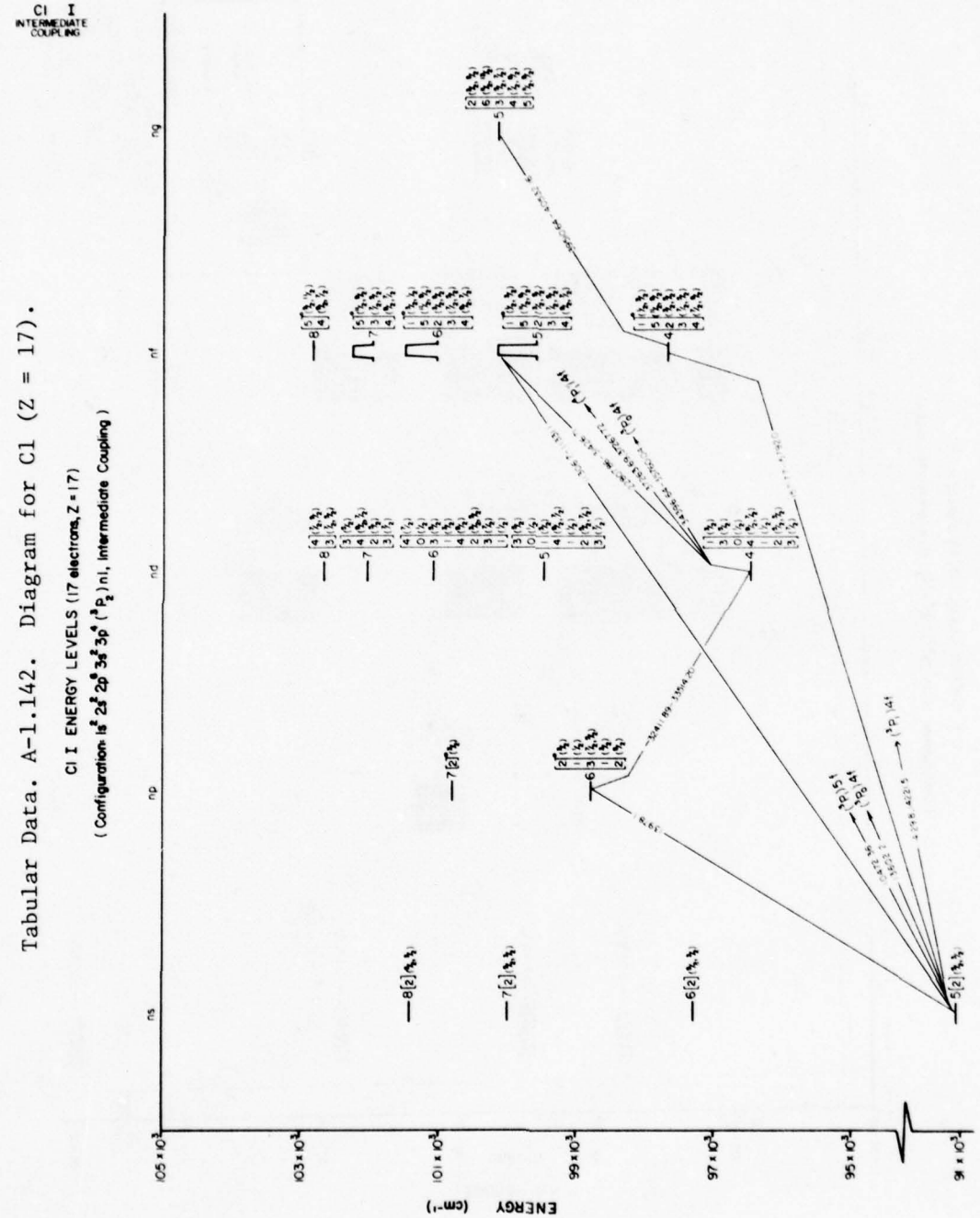

Tabular Data. A-1.143. Diagram for Cl (Z = 17).

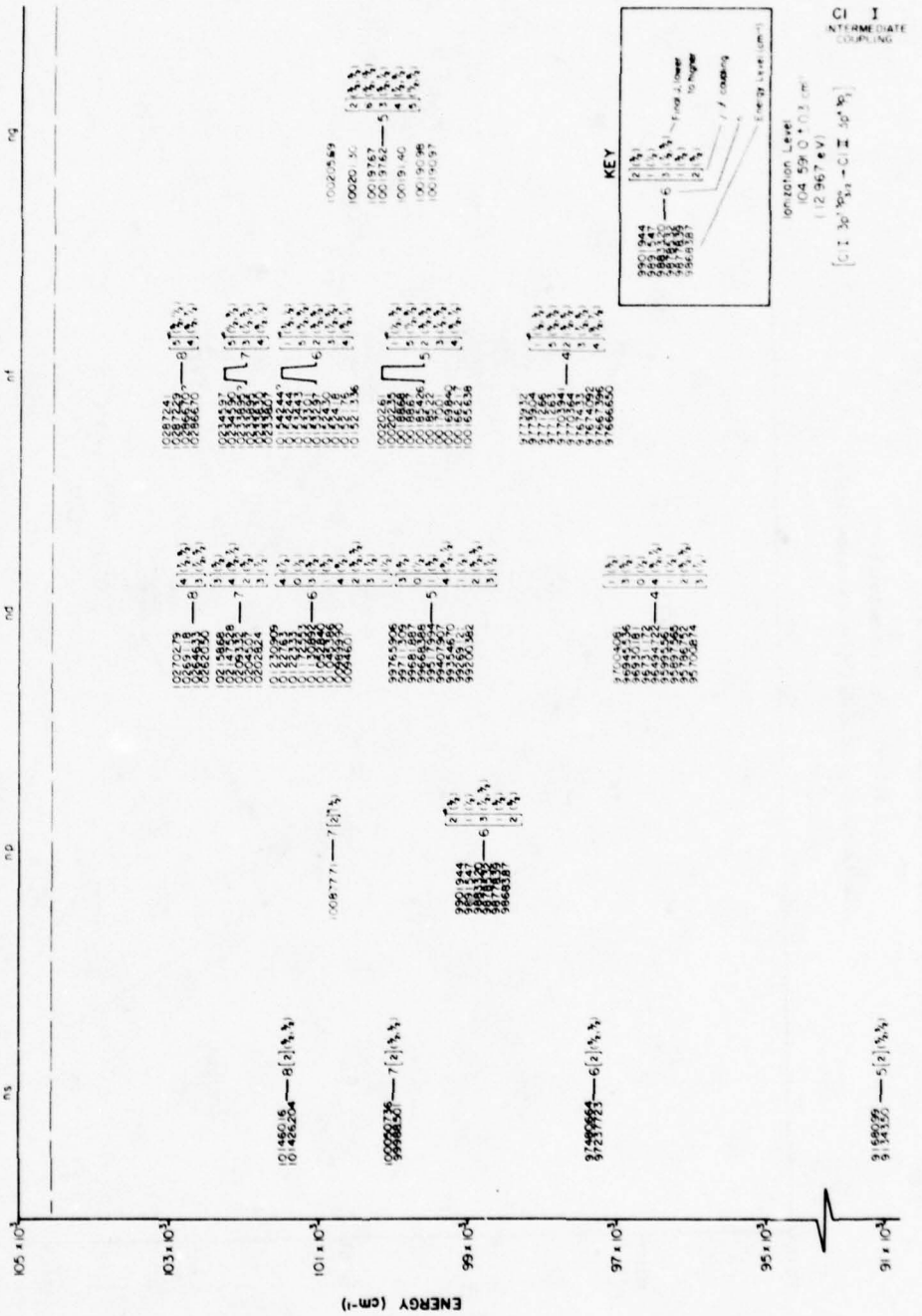

Tabular Data. A-1.144. Diagram for Cl (Z = 17).

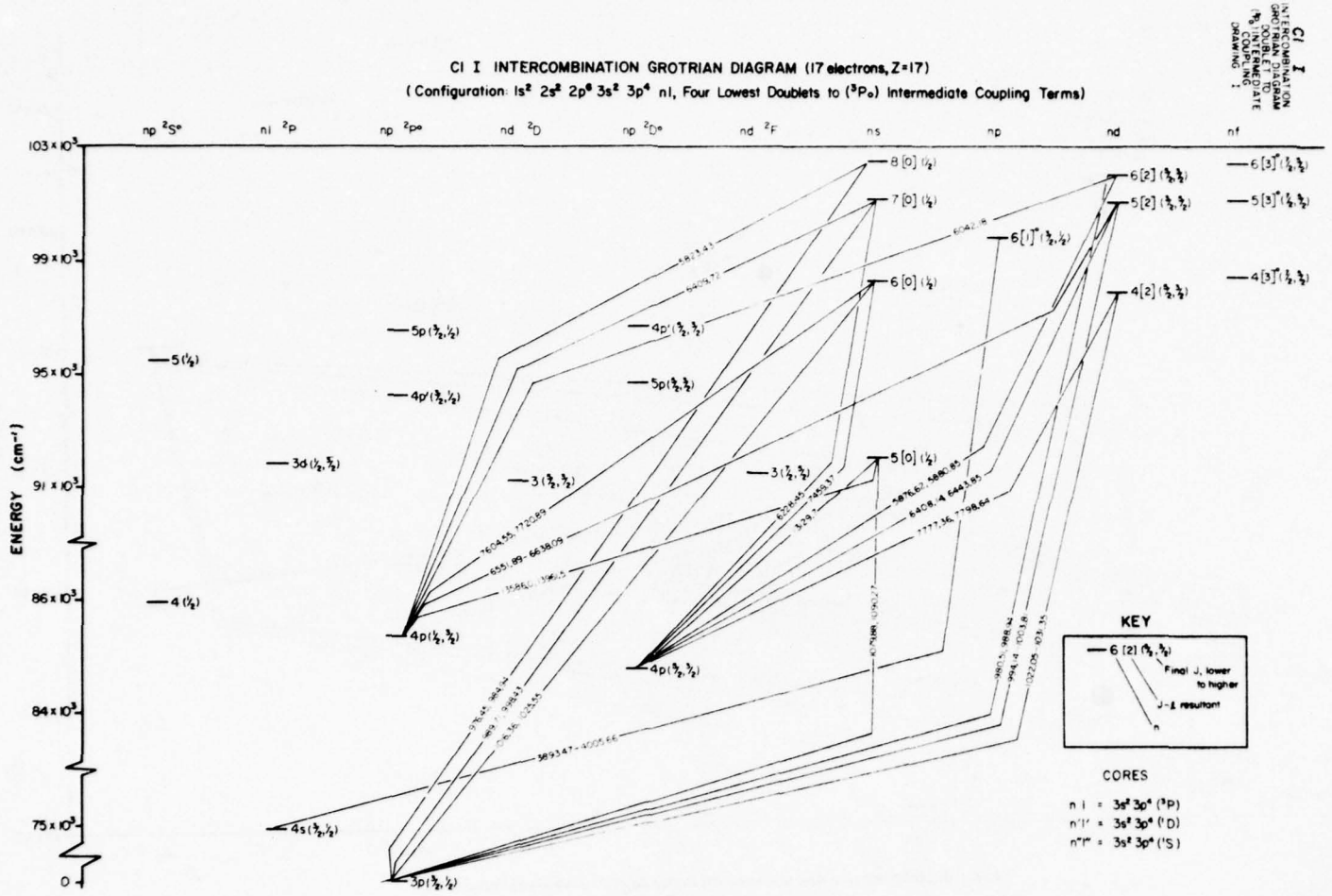

Tabular Data. A-1.145. Diagram for Cl (Z = 17).

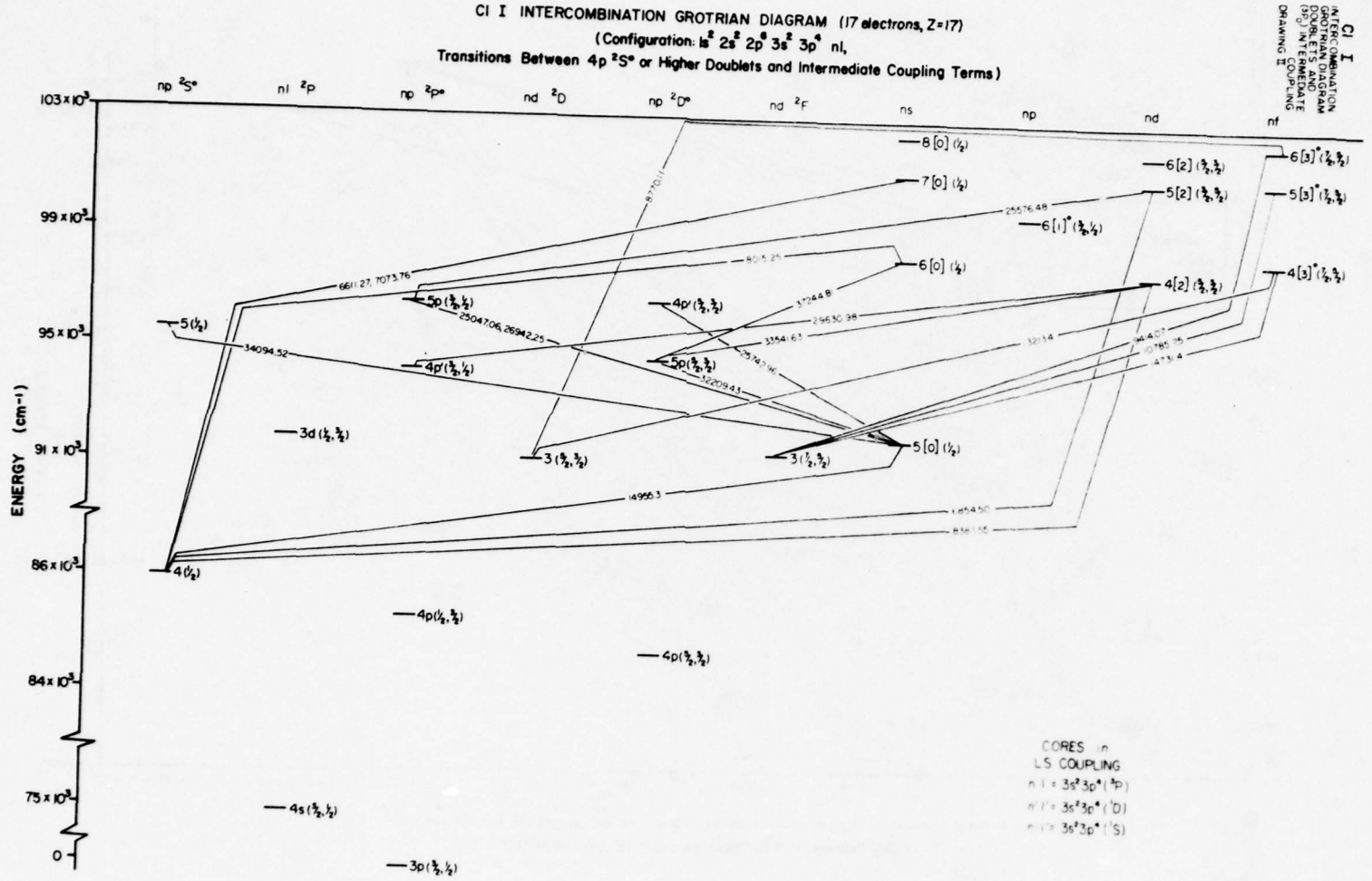

Tabular Data. A-146. Diagram for Cl (Z = 17).

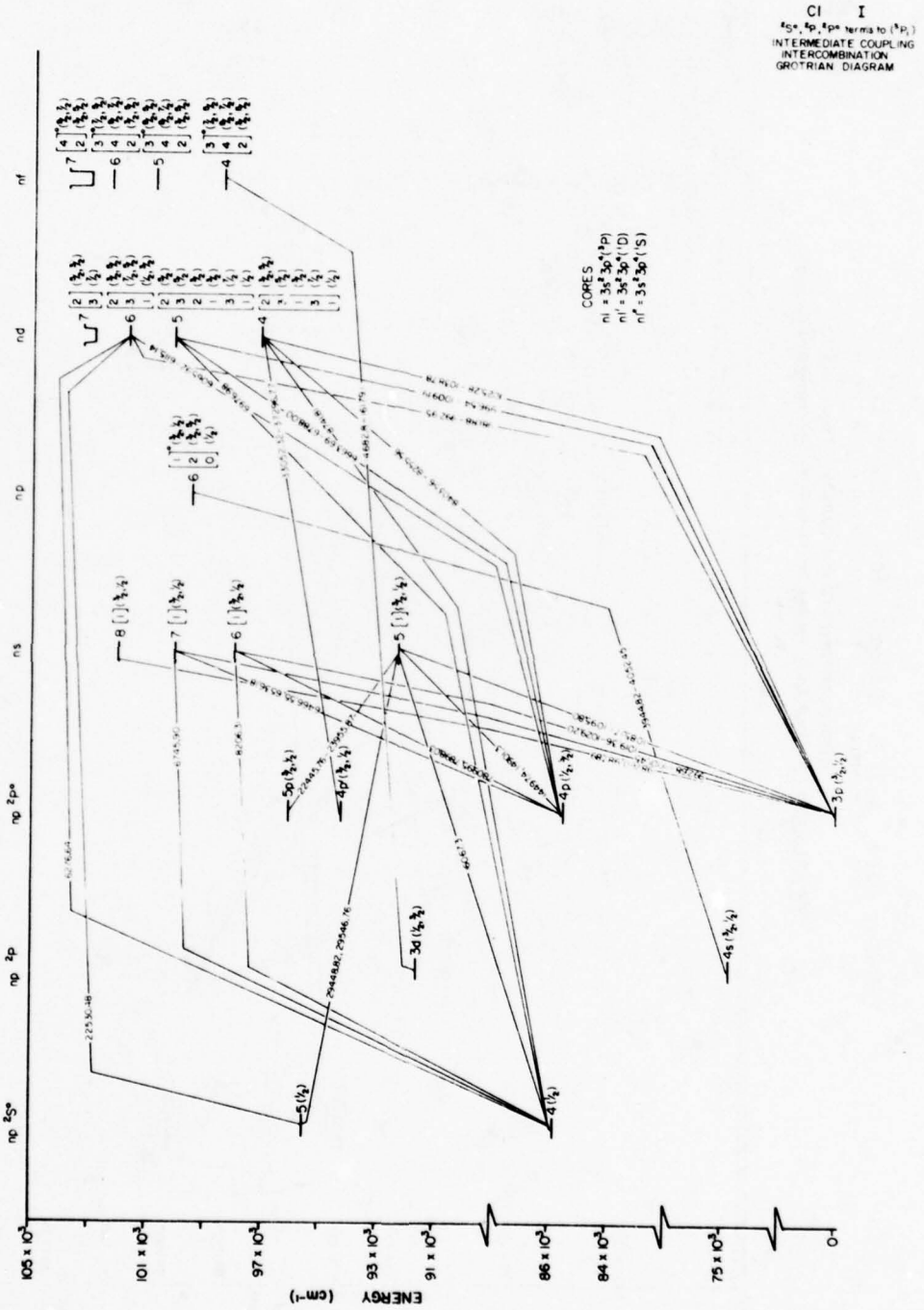

Tabular Data. A-147. Diagram for Cl (Z = 17).

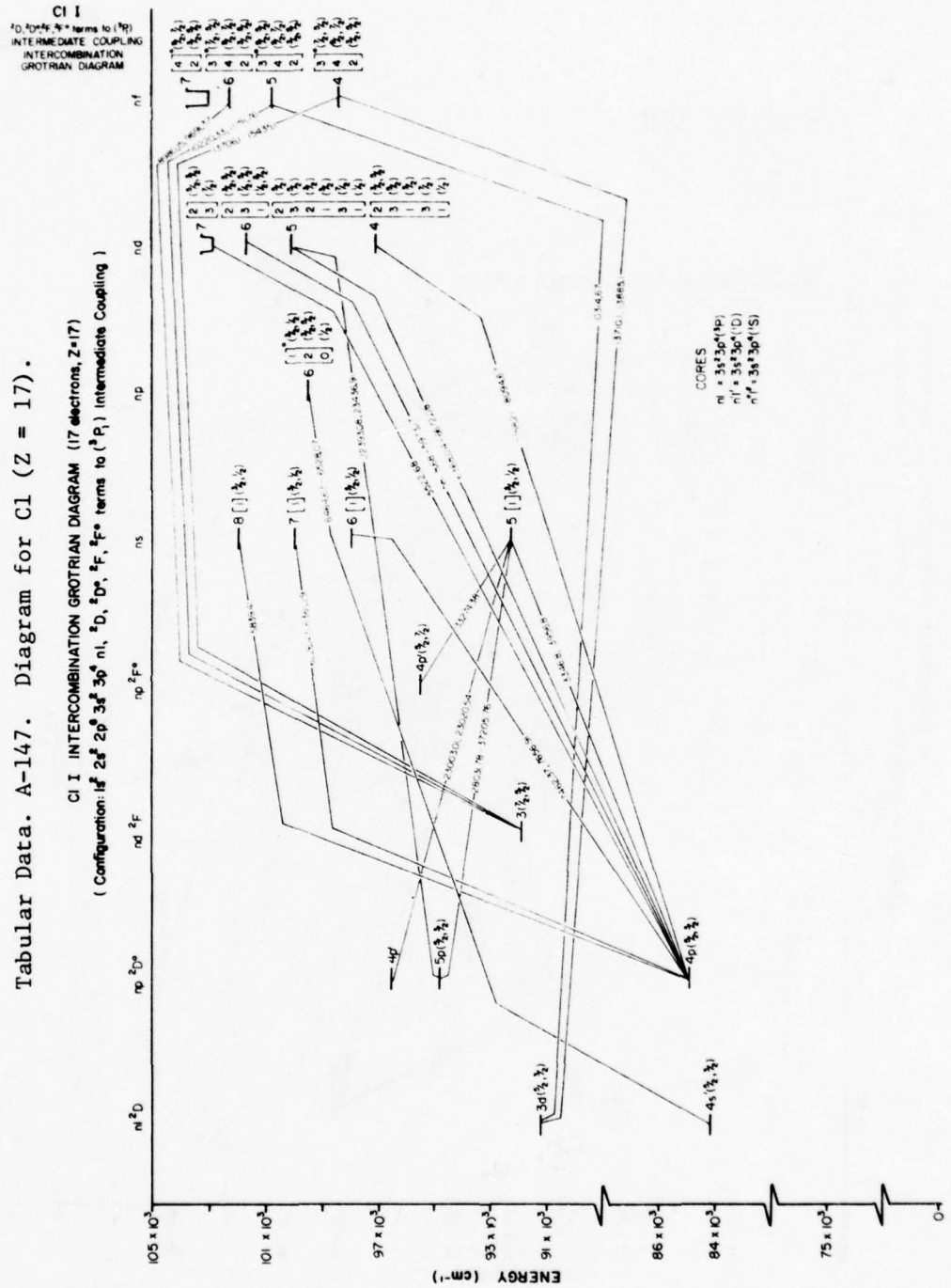

Tabular Data. A-1.148. Diagram for Cl (Z = 17).

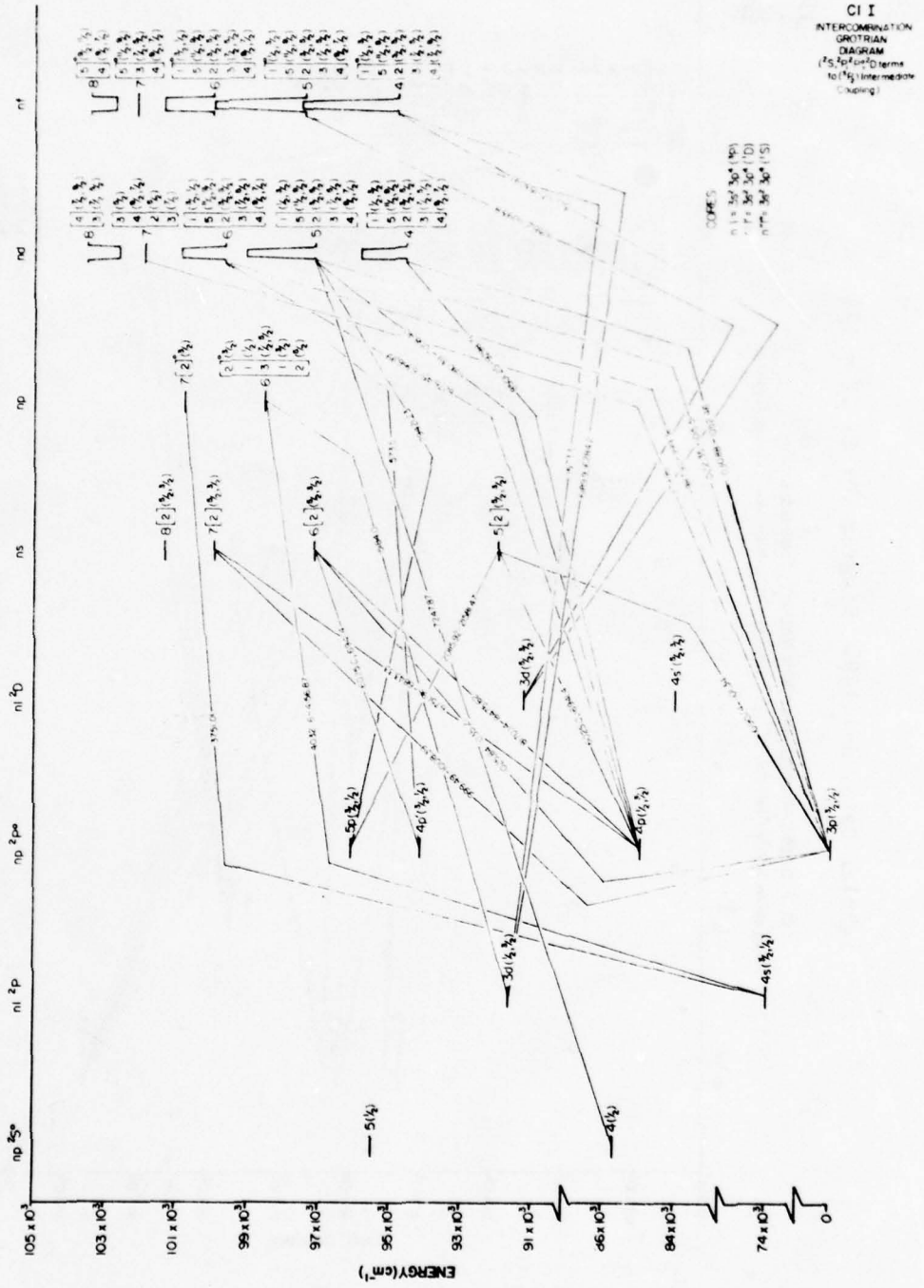

Tabular Data. A-1.149. Diagram for Cl (Z = 17).

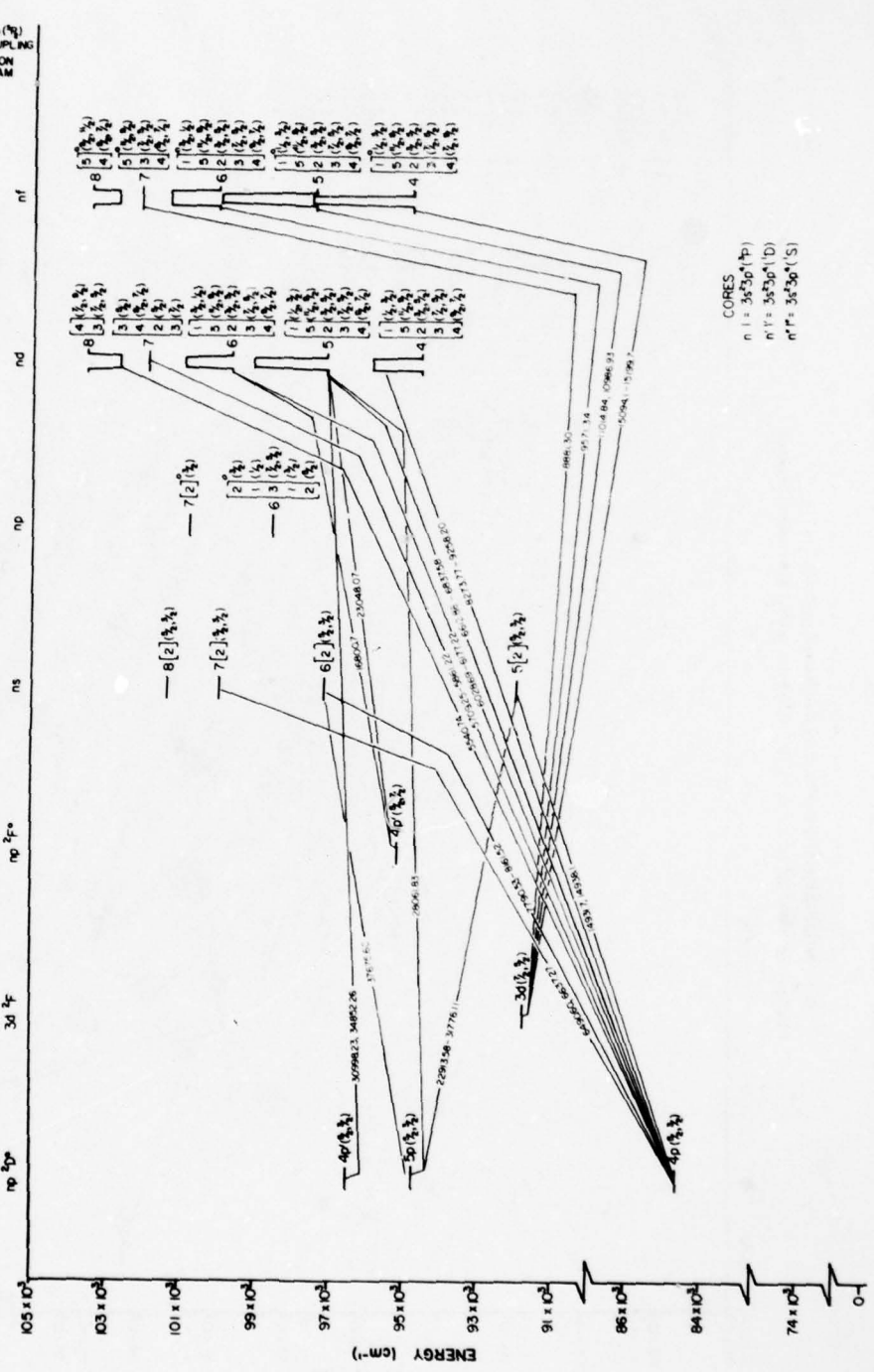

Tabular Data. A-1.150. Diagram for Cl (Z = 17).

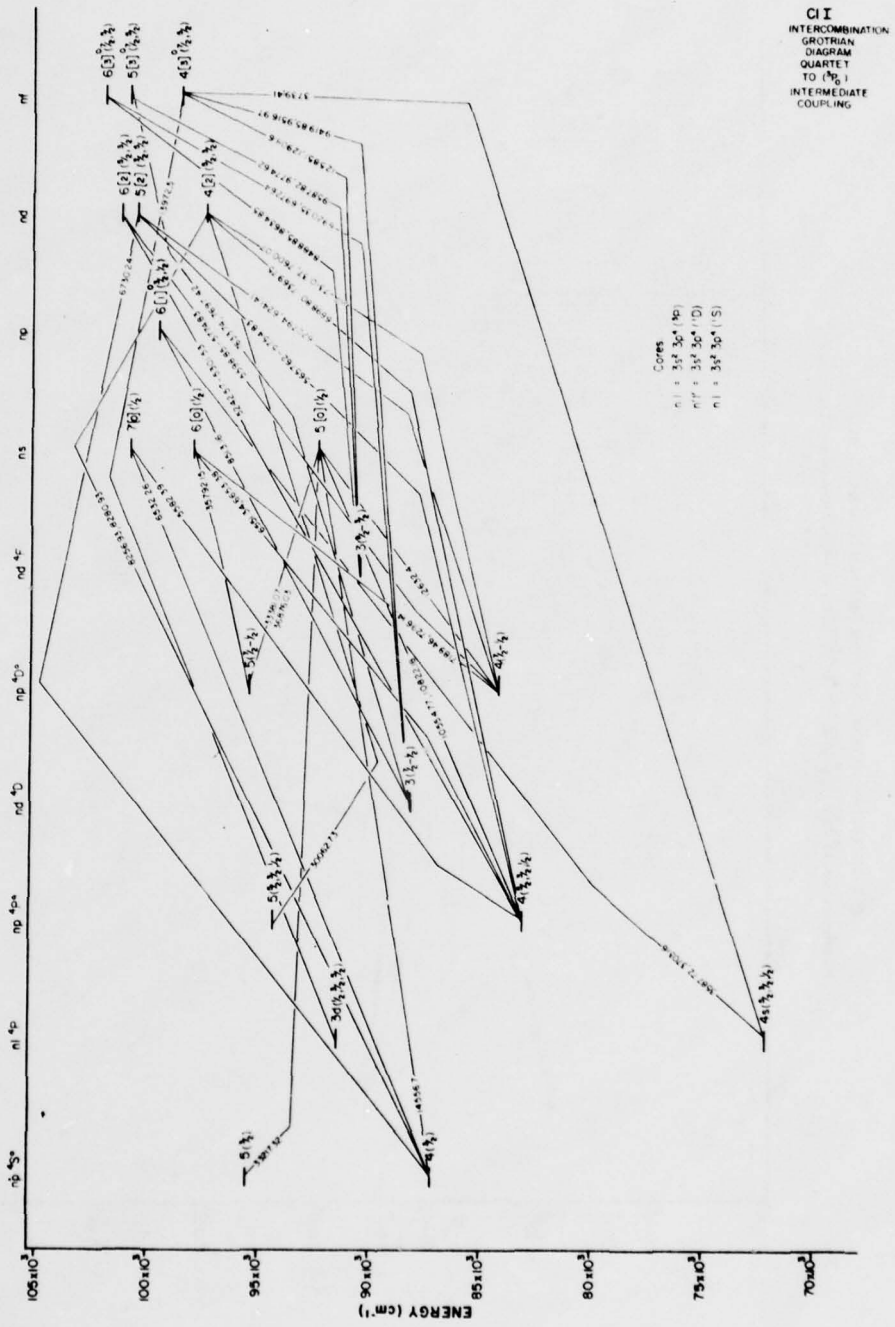

Tabular Data. A-1.151. Diagram for Cl (Z = 17).

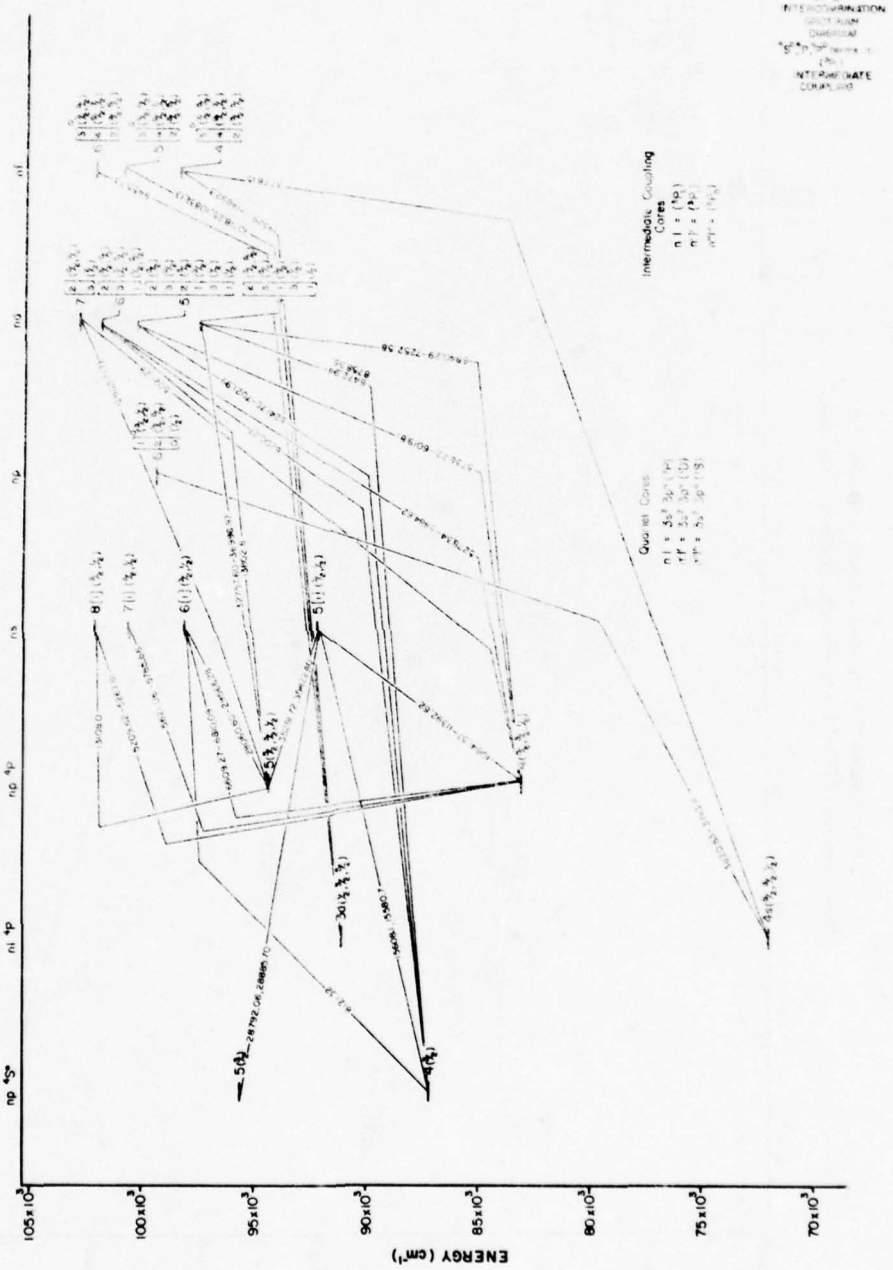

Tabular Data. A-1.152. Diagram for Cl (Z = 17).

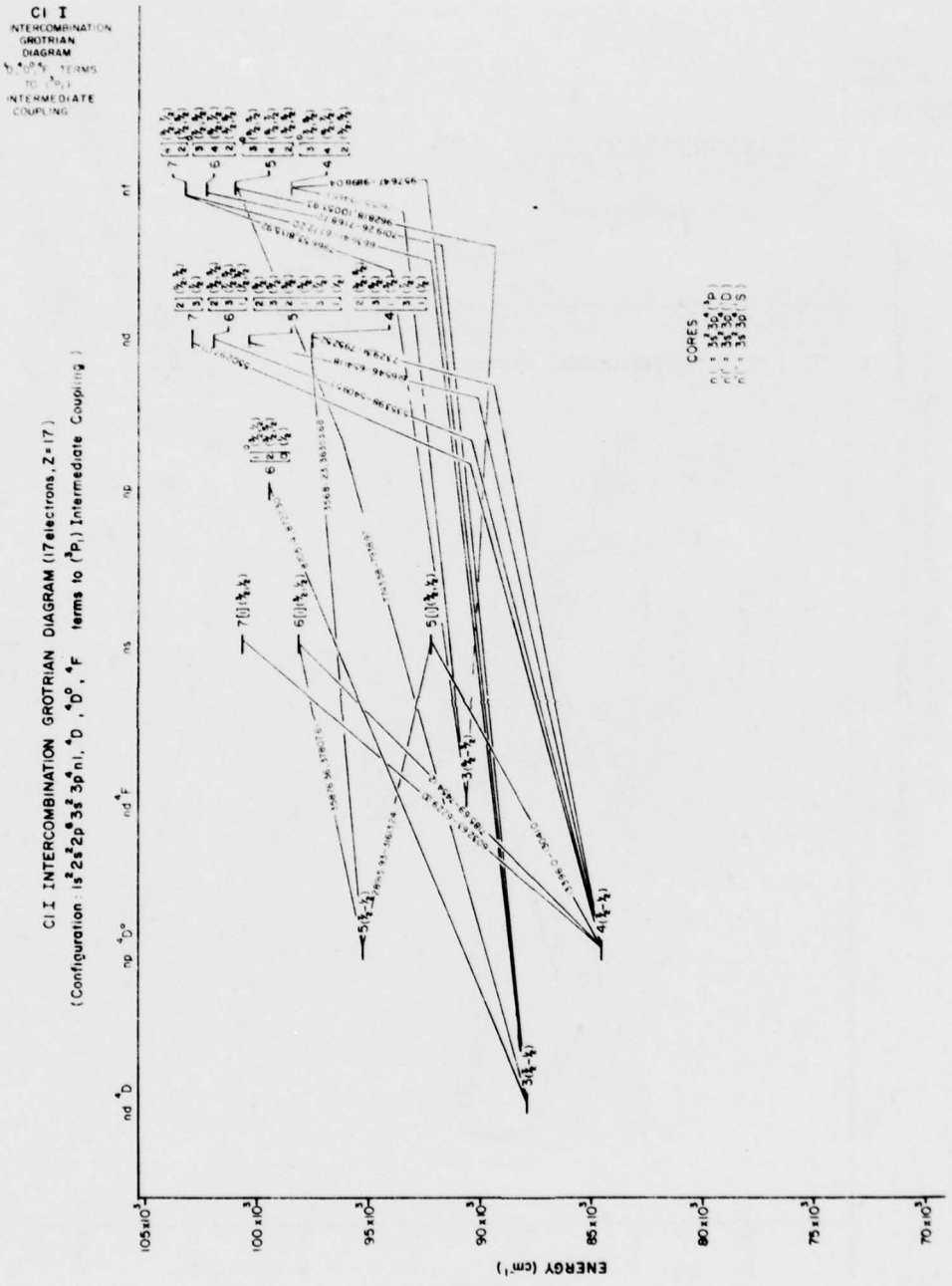

Tabular Data. A-1.153. Diagram for Cl (Z = 17).

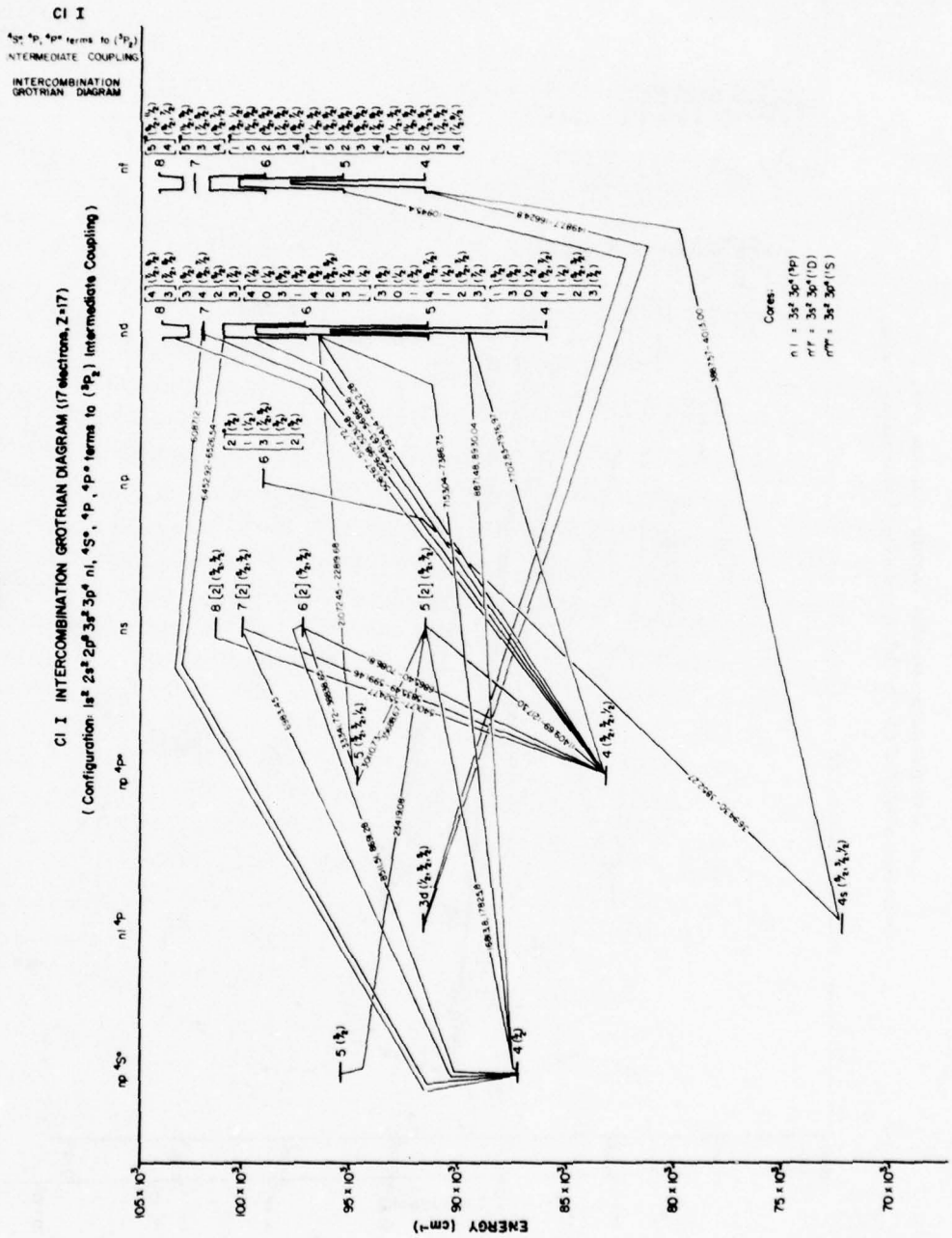

Tabular Data. A-1.154. Diagram for Cl (Z = 17).

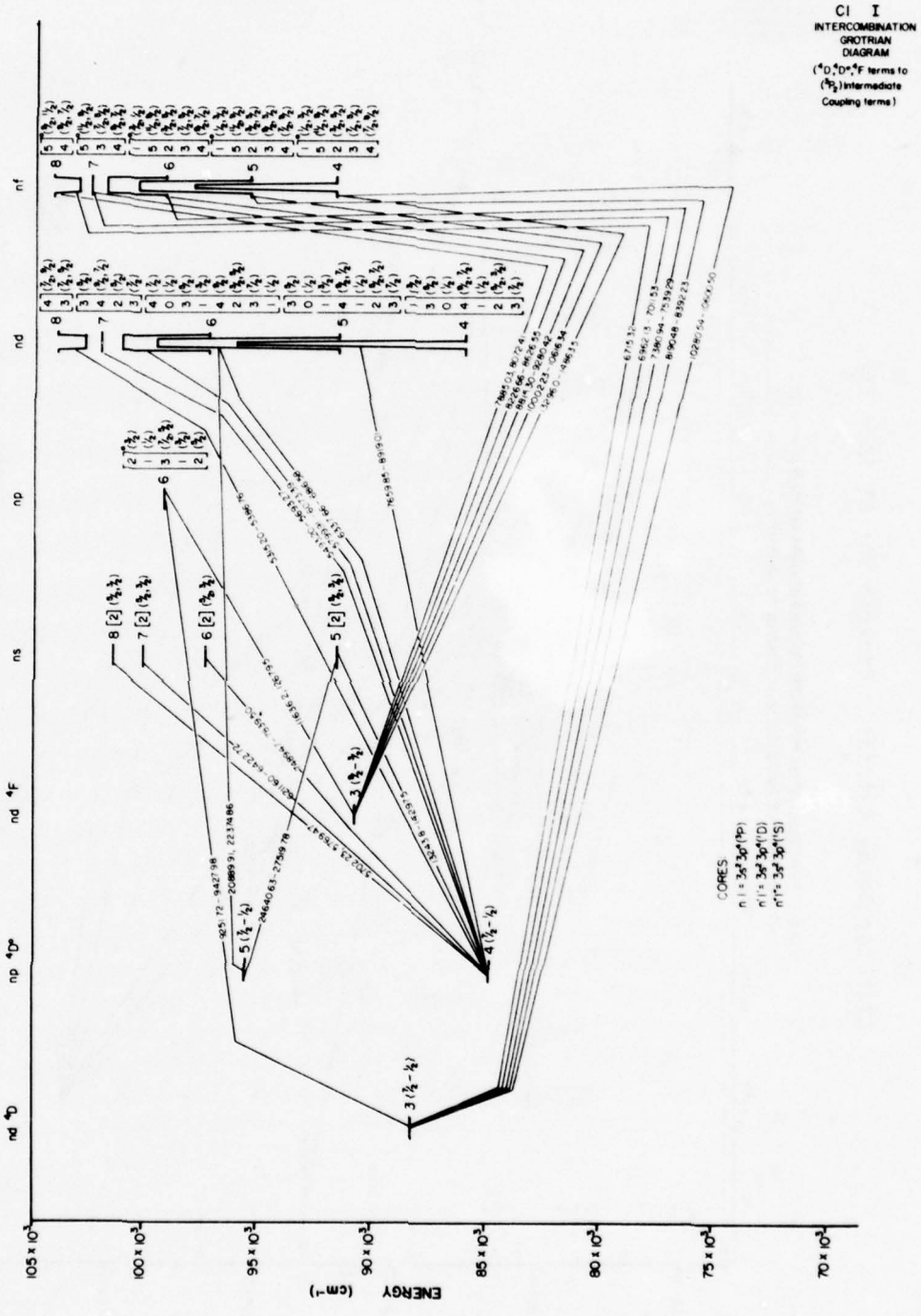

Tabular Data. A-1.155. Diagram for Cl (Z = 17).

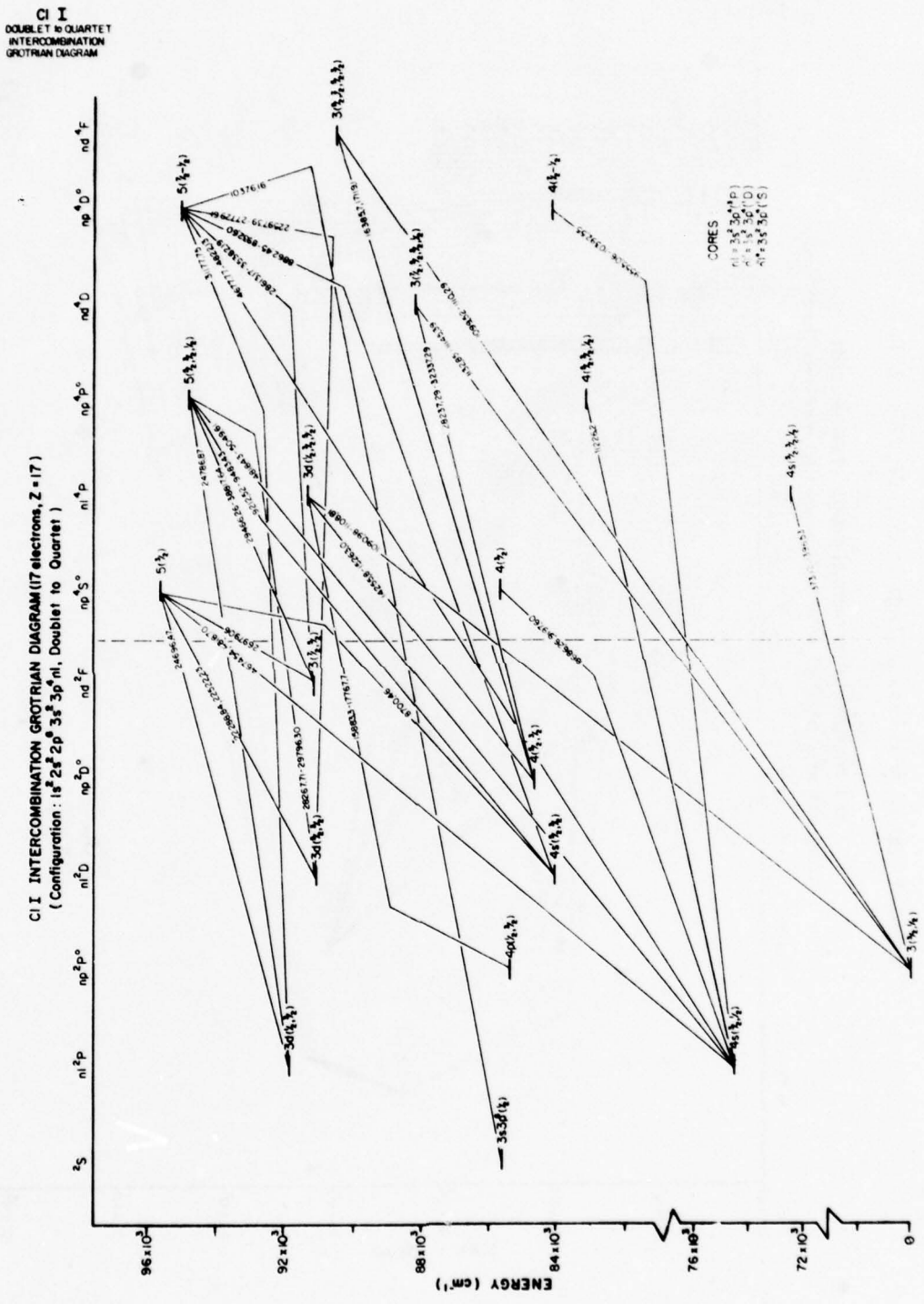

Tabular Data. A-1.156. Diagram for Cl (Z = 17).

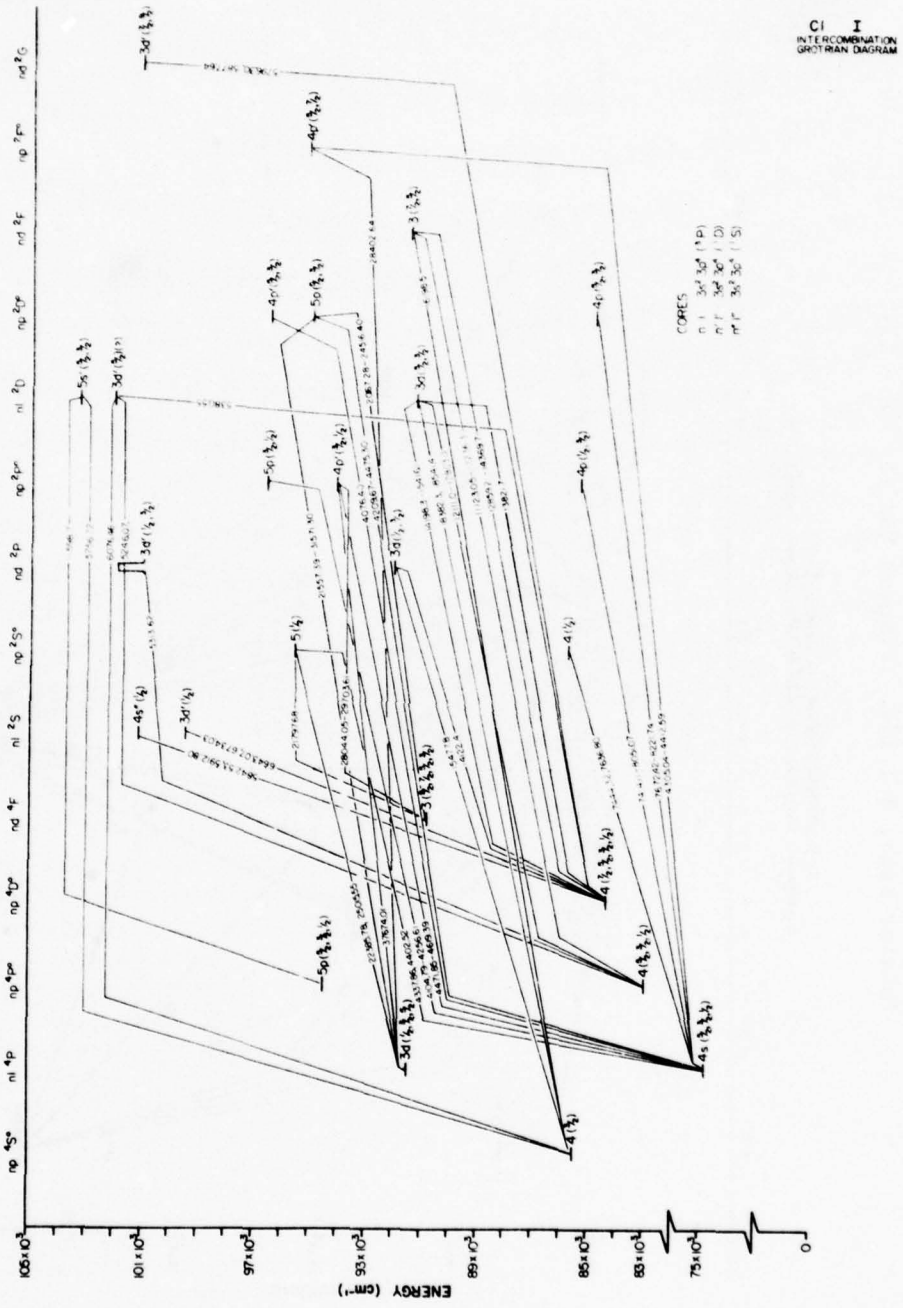

Tabular Data. A-1.157. Diagram for Cl^{+} (Z = 17).

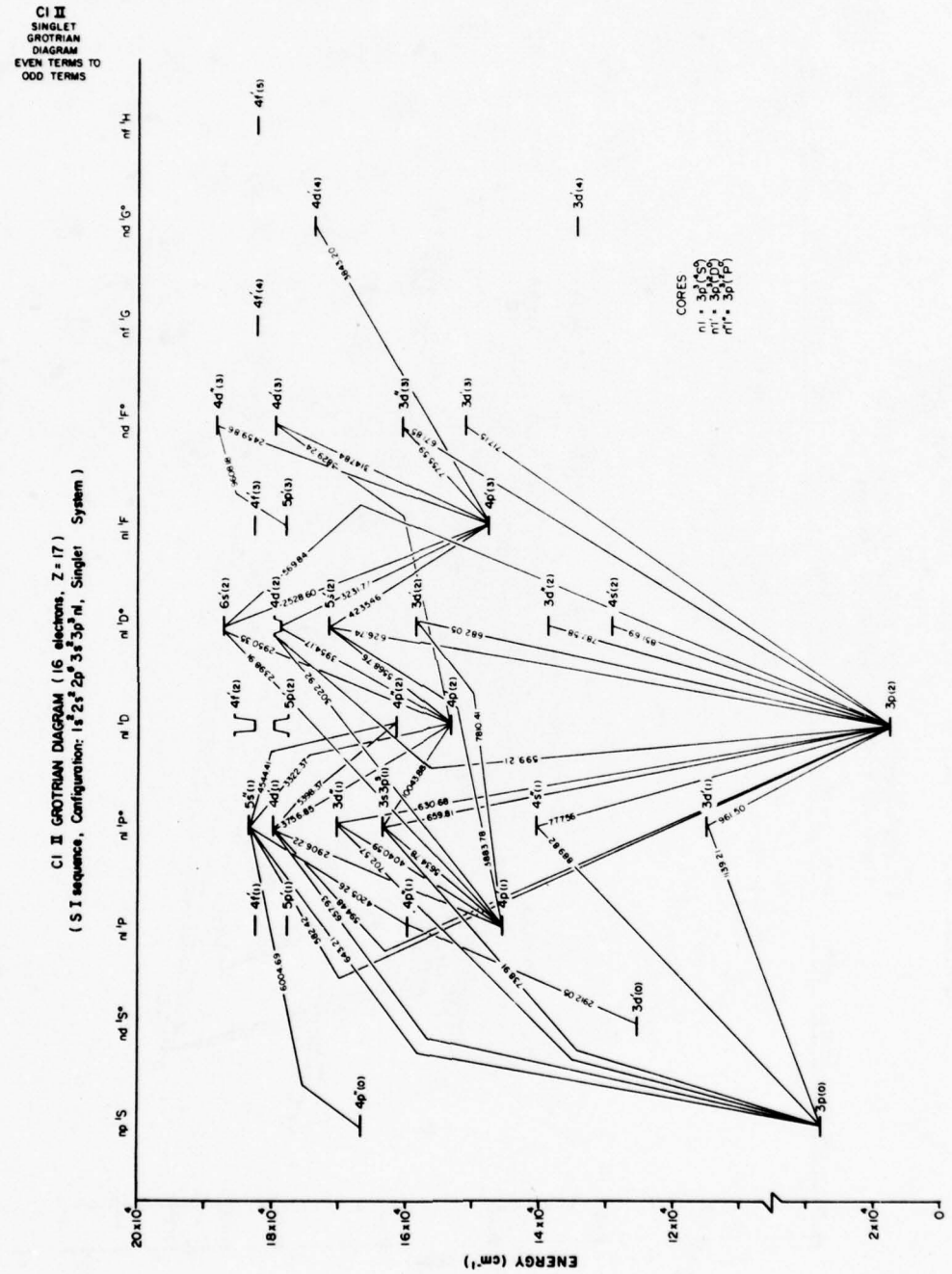

Tabular Data. A-1.158. Diagram for Cl^+ (Z = 17).

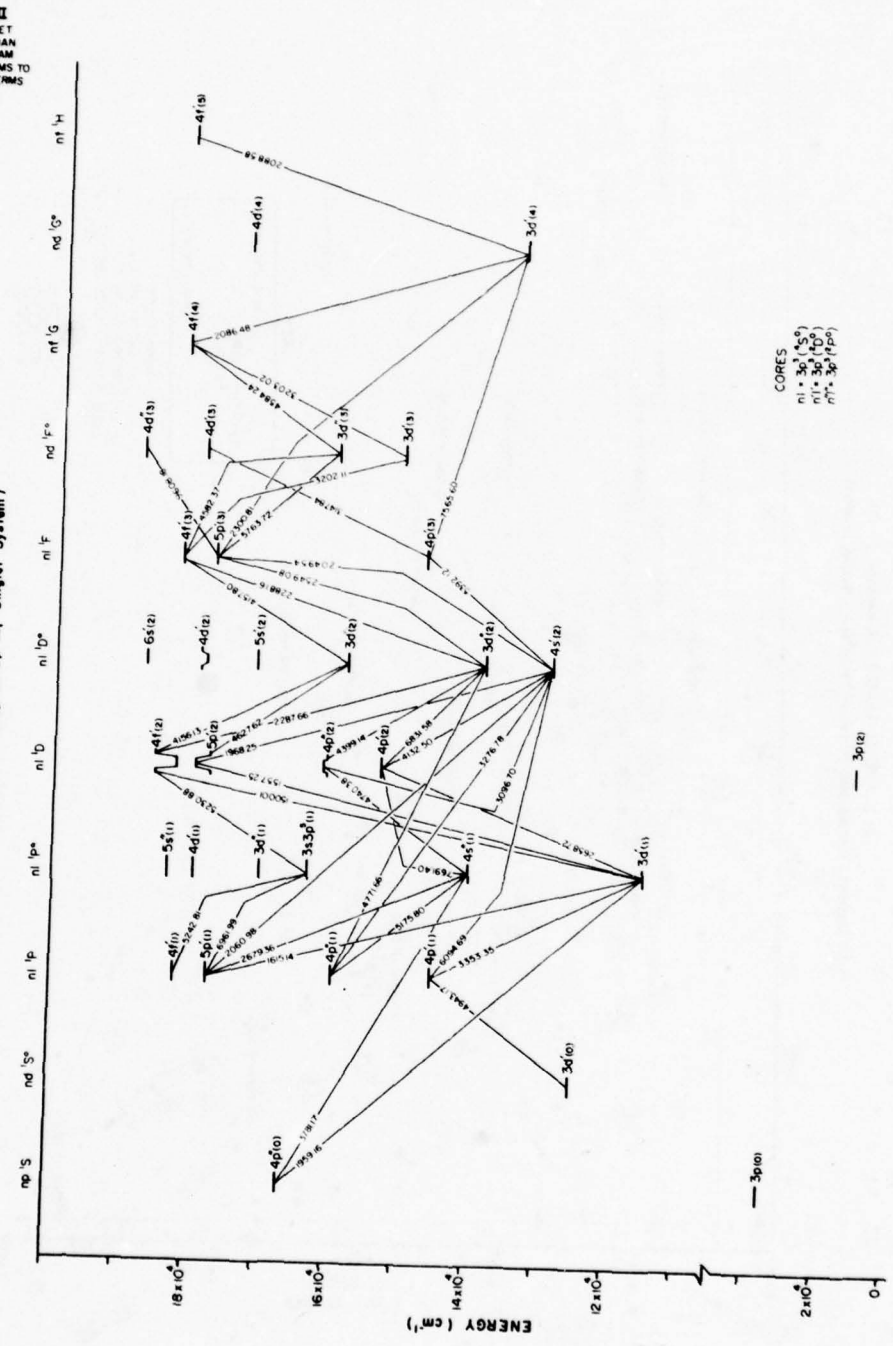

Tabular Data. A-1.159. Diagram for Cl^{+} ($Z_i = 17$).

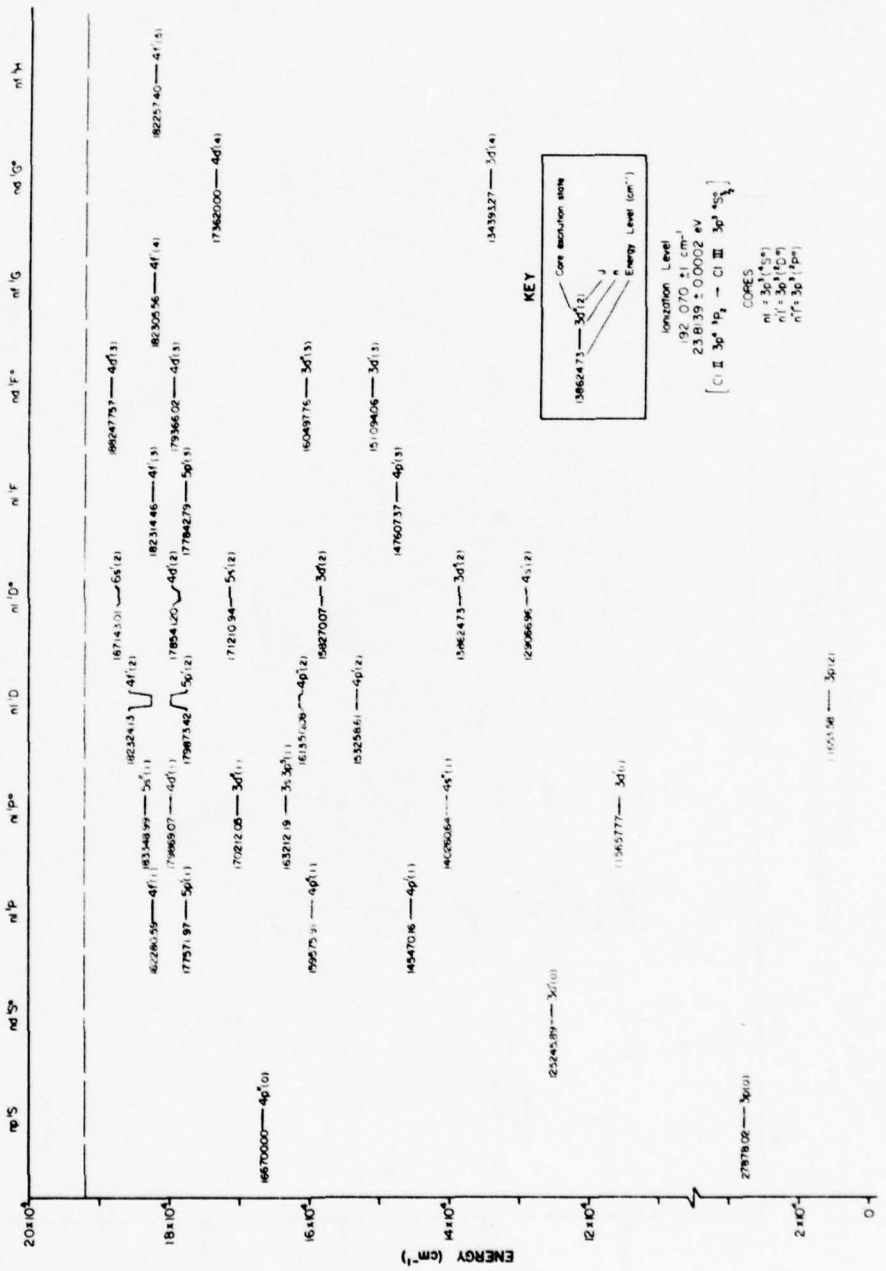

Tabular Data. A-1.160. Diagram for Cl^{+} (Z = 17).

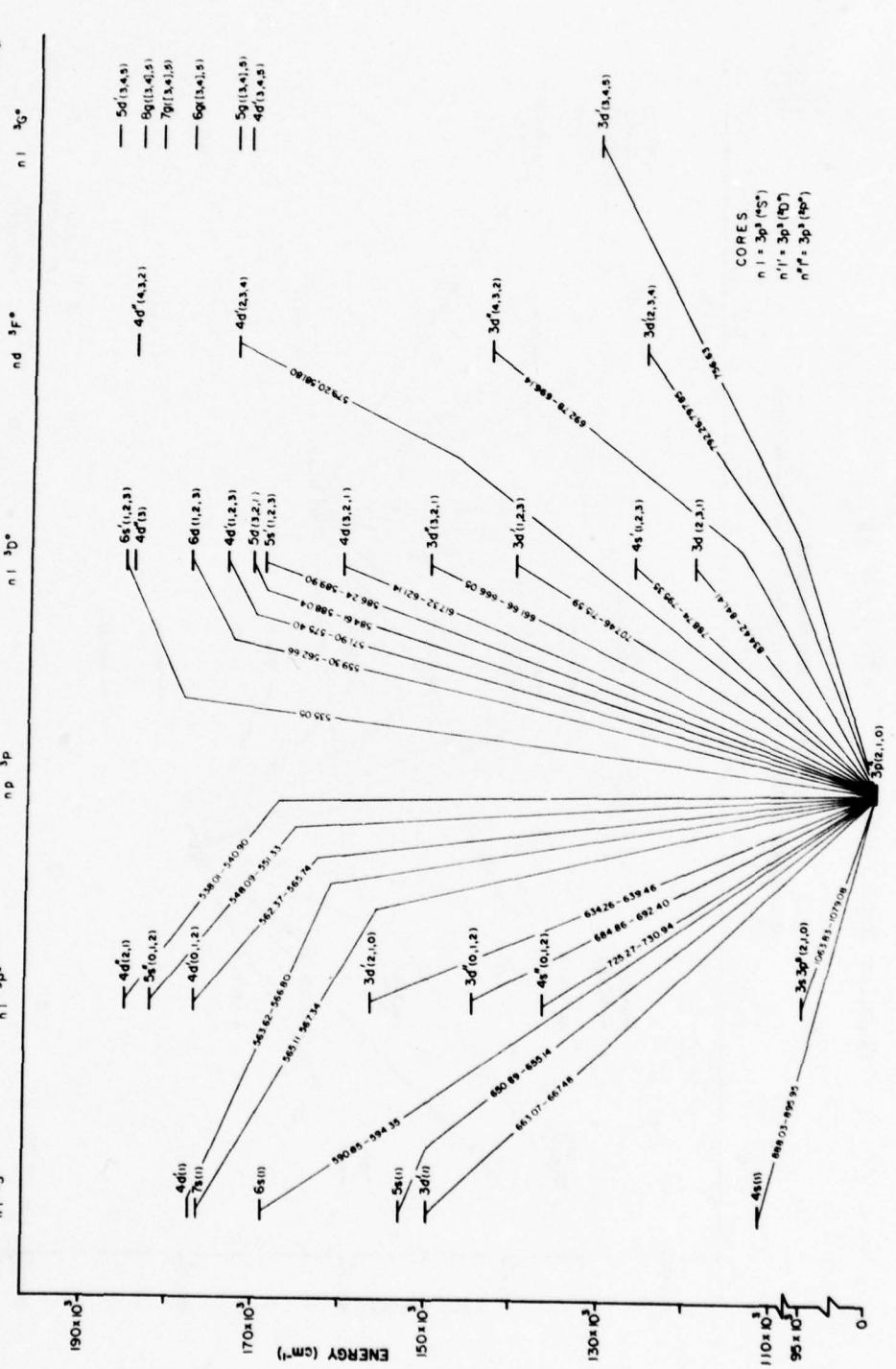

Tabular Data. A-1.161. Diagram for Cl^{+} (Z = 17).

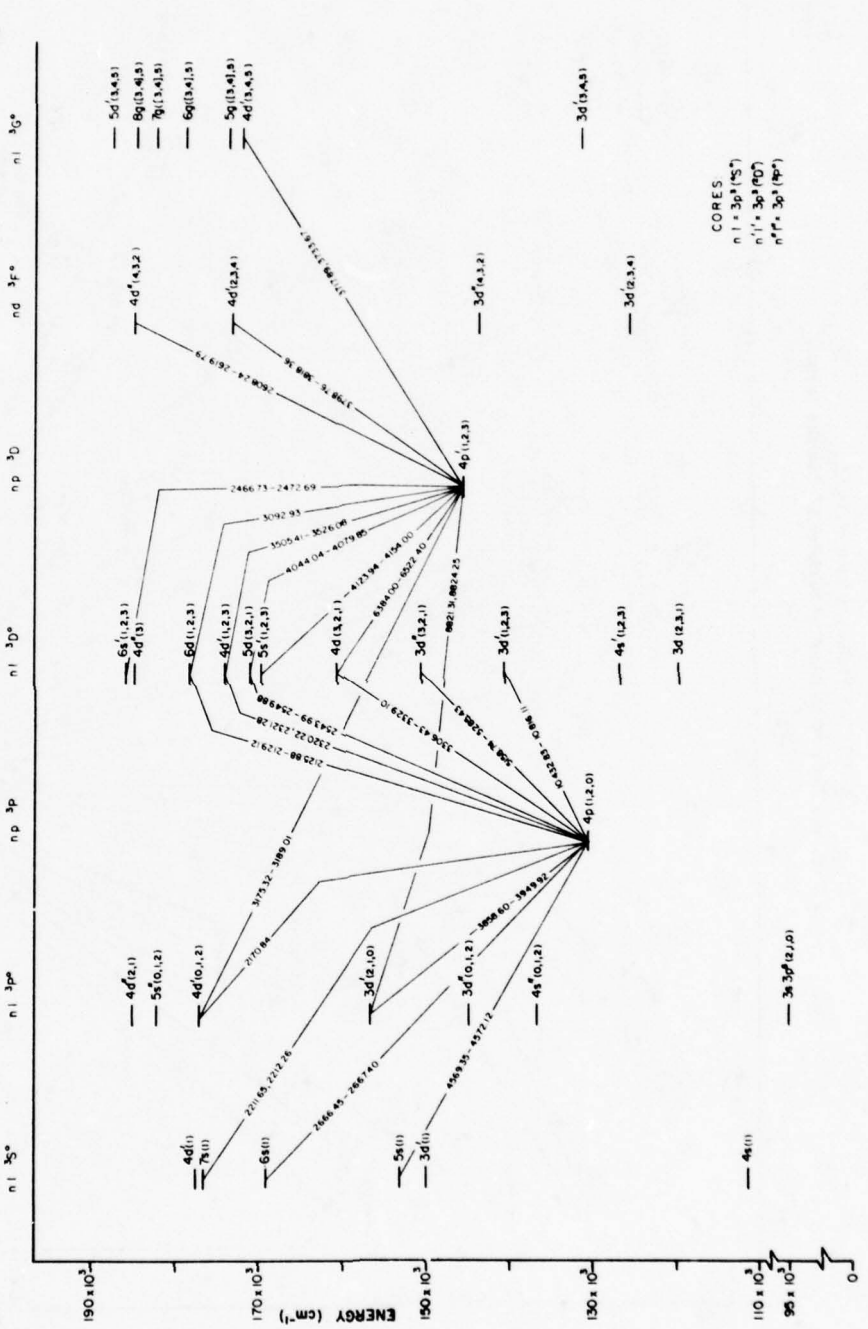

Tabular Data. A-1.162. Diagram for Cl^{+} (Z = 17).

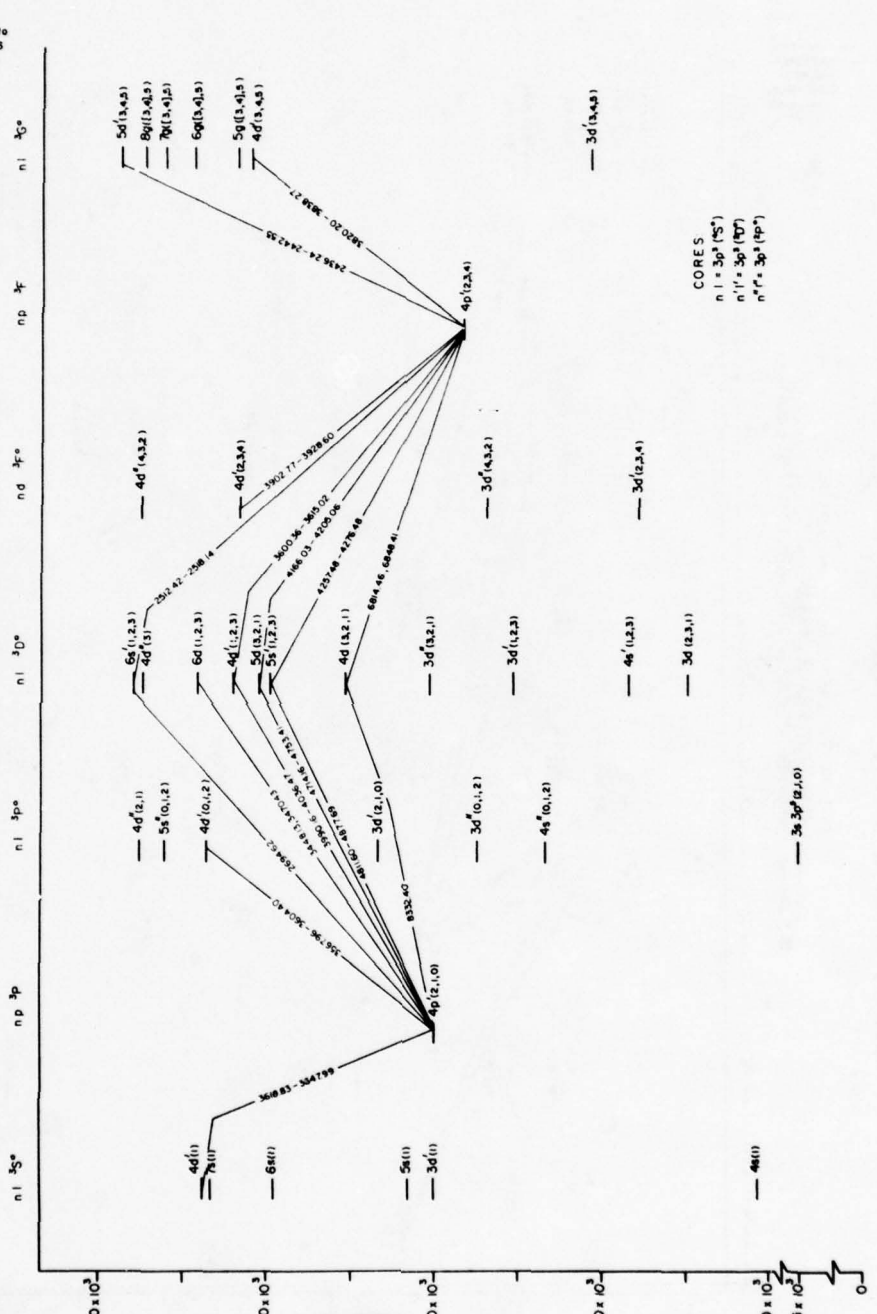

Tabular Data. A-1.163. Diagram for Cl^{+} (Z = 17).

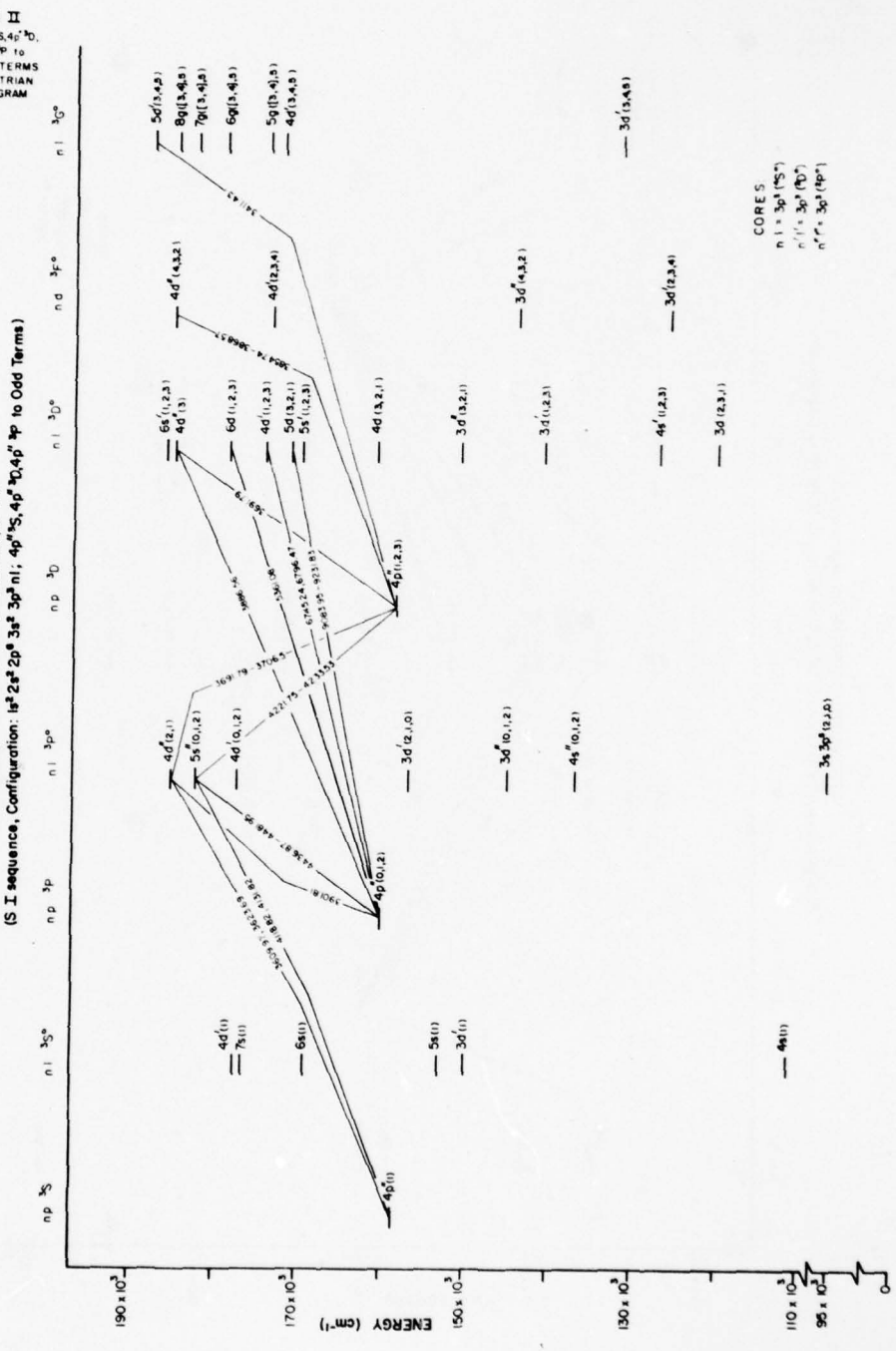

Tabular Data. A-1.164. Diagram for Cl^{+} (Z = 17).

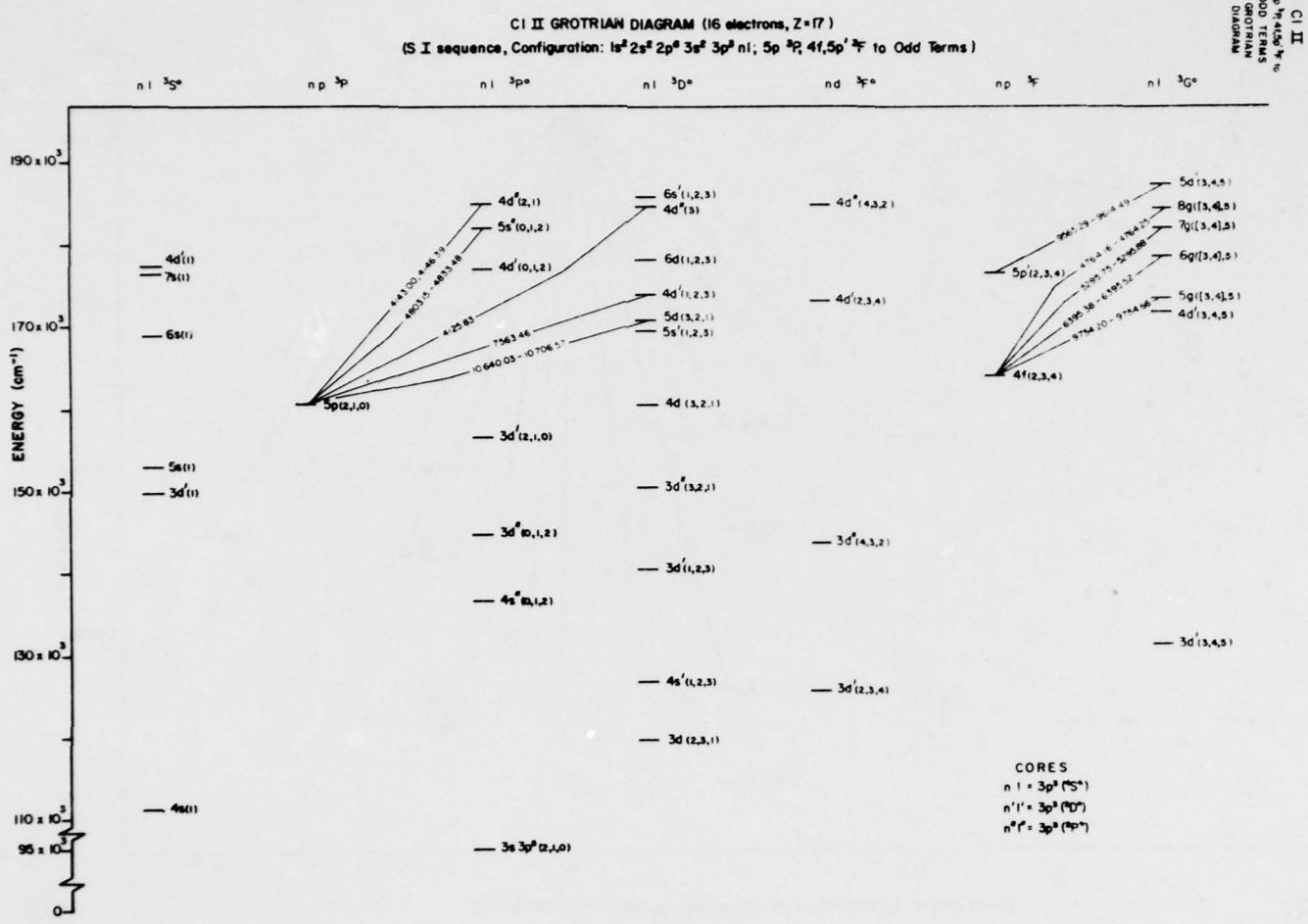

Tabular Data. A-1.165. Diagram for Cl^+ (Z = 17).

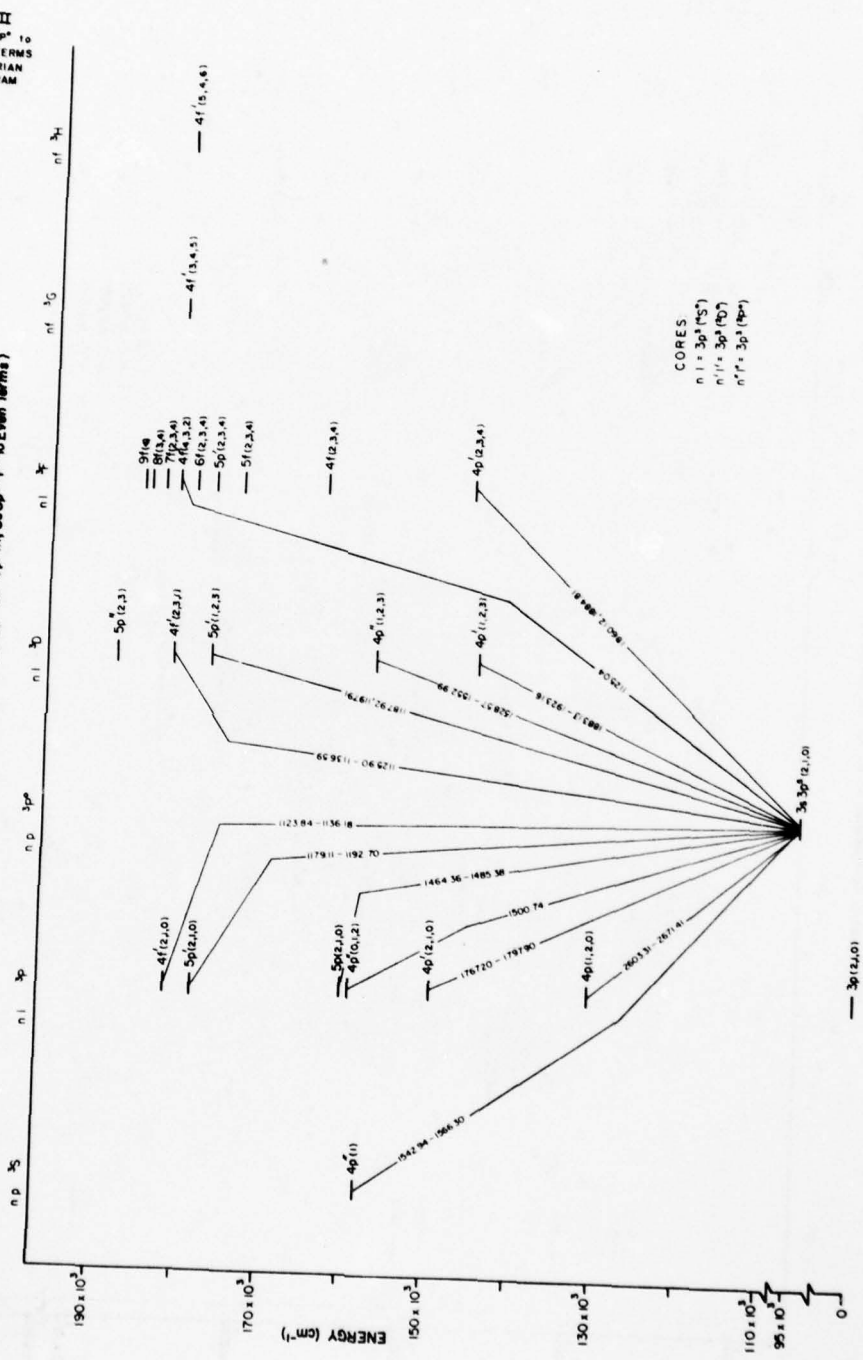

Tabular Data. A-1.166. Diagram for Cl^{+} (Z = 17).

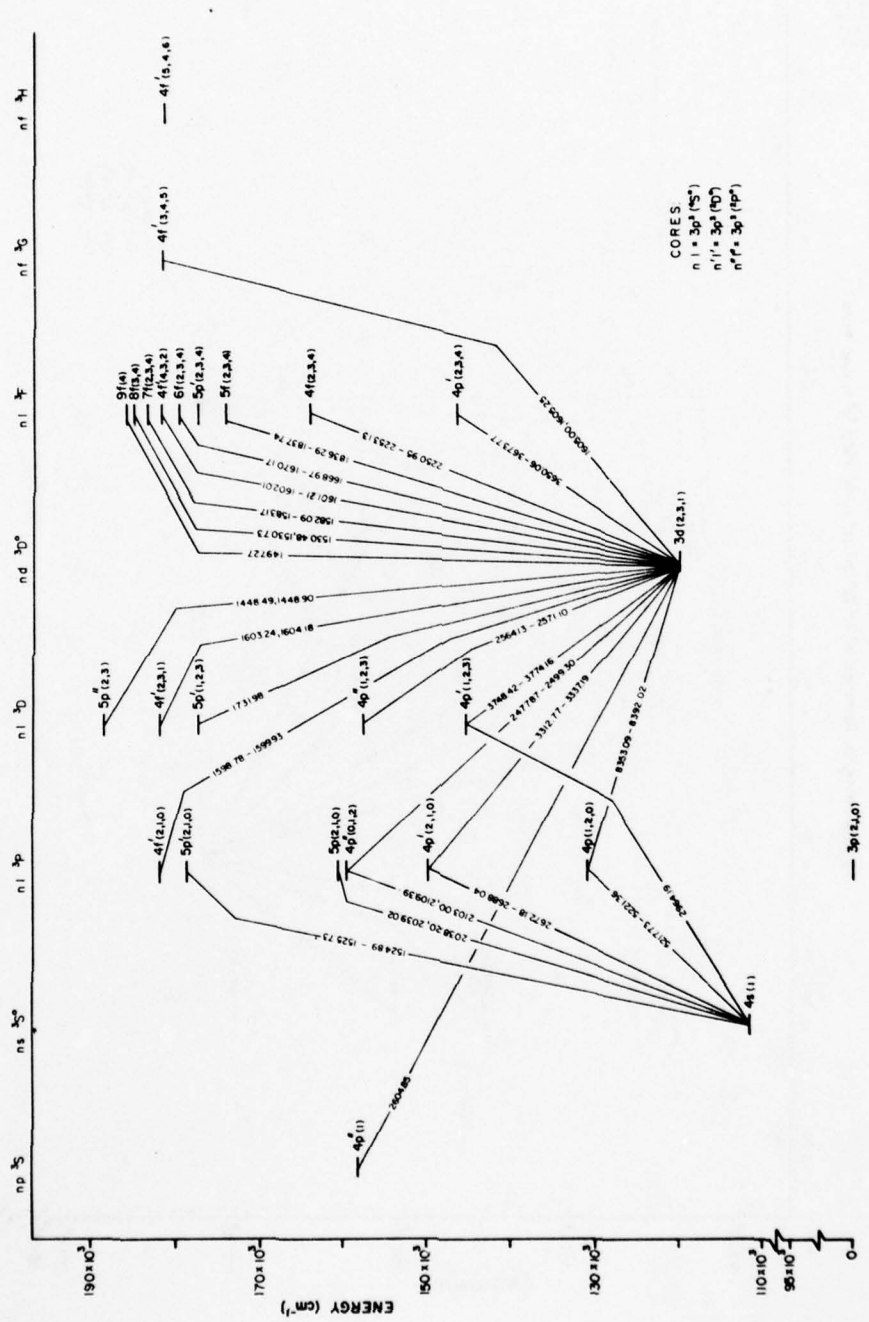

Tabular Data. A-1.167. Diagram for Cl^+ (Z = 17).

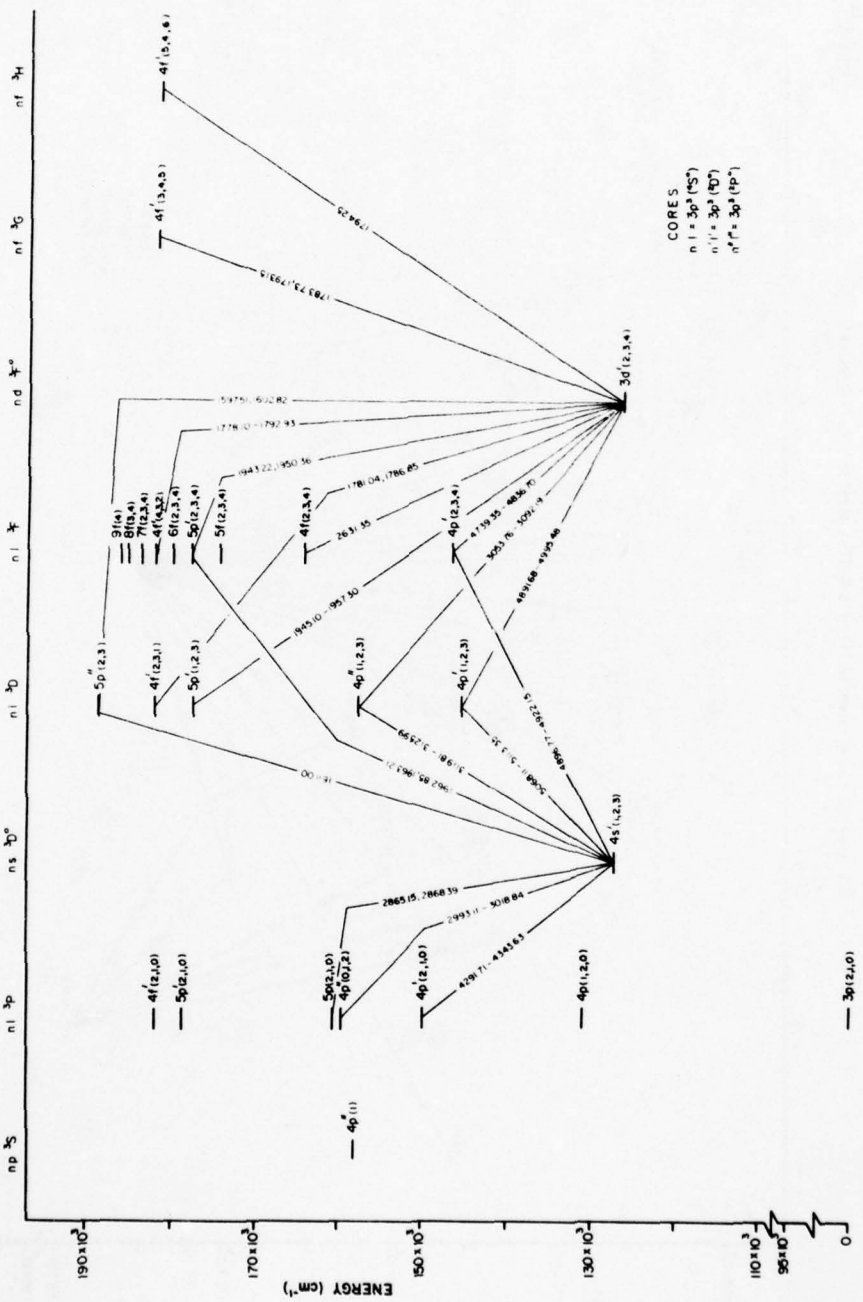

Tabular Data. A-1.168. Diagram for Cl^{+} (Z = 17).

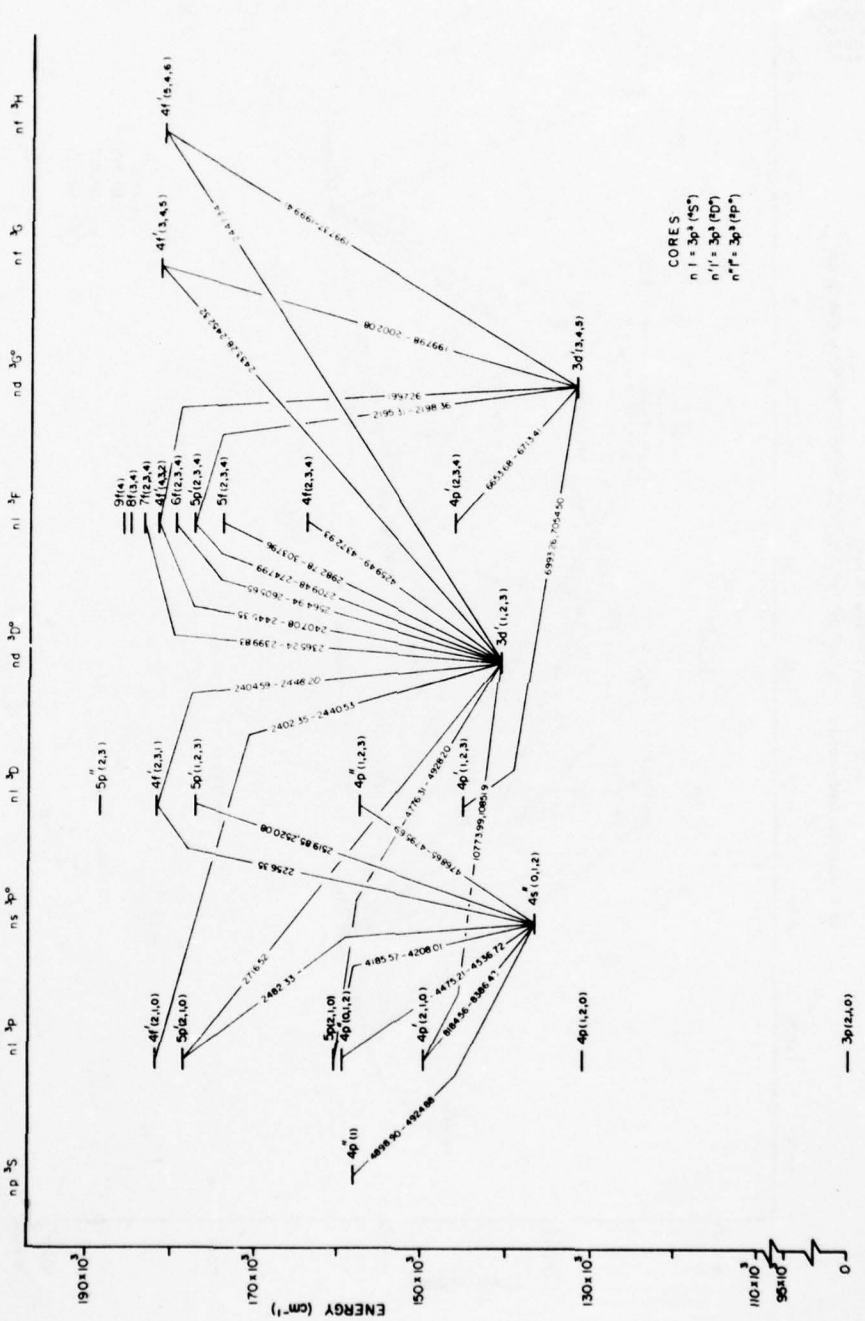

Tabular Data. A-1.169. Diagram for Cl^{+} (Z = 17).

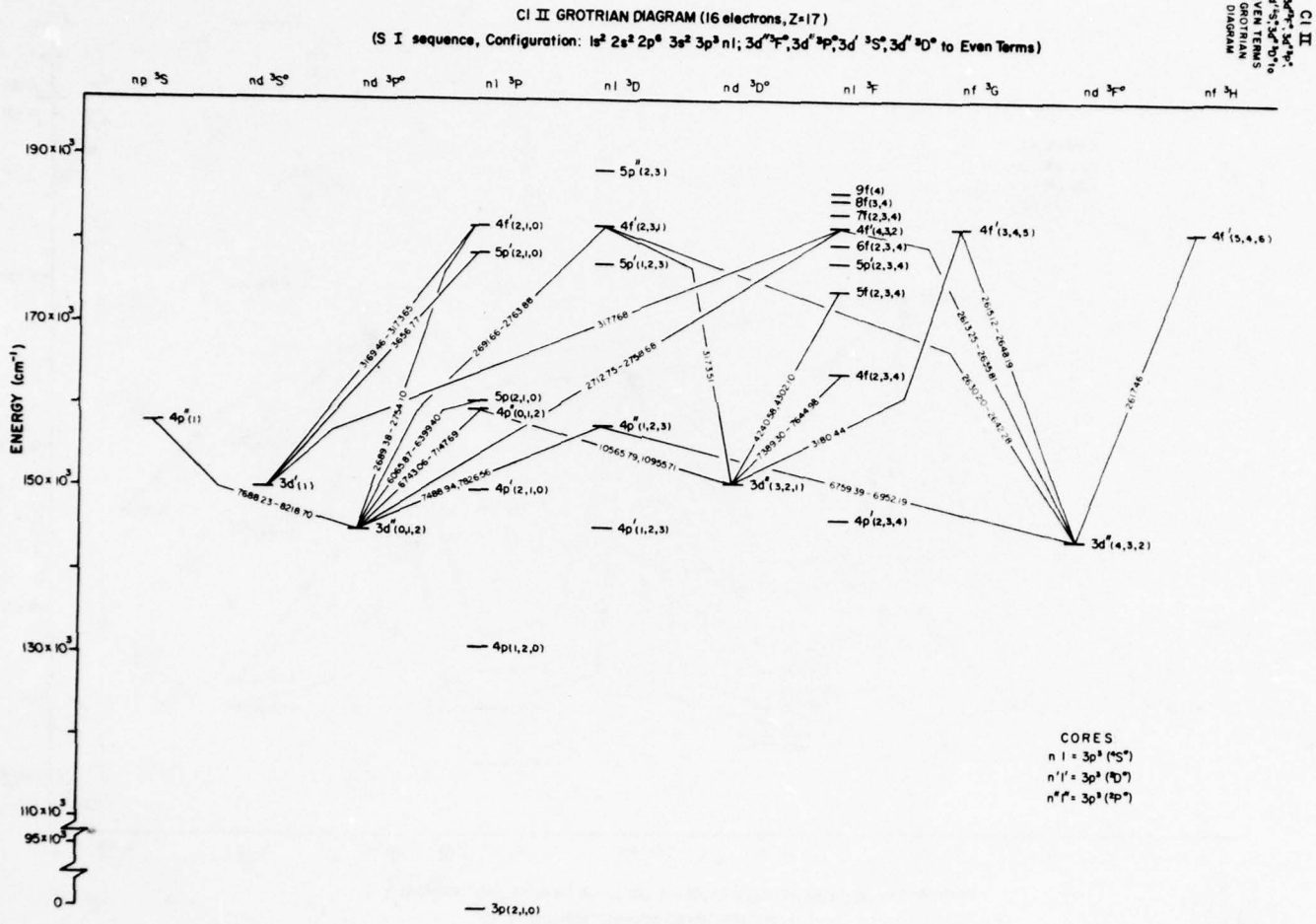

Tabular Data. A-1.170. Diagram for Cl^{+} (Z = 17).

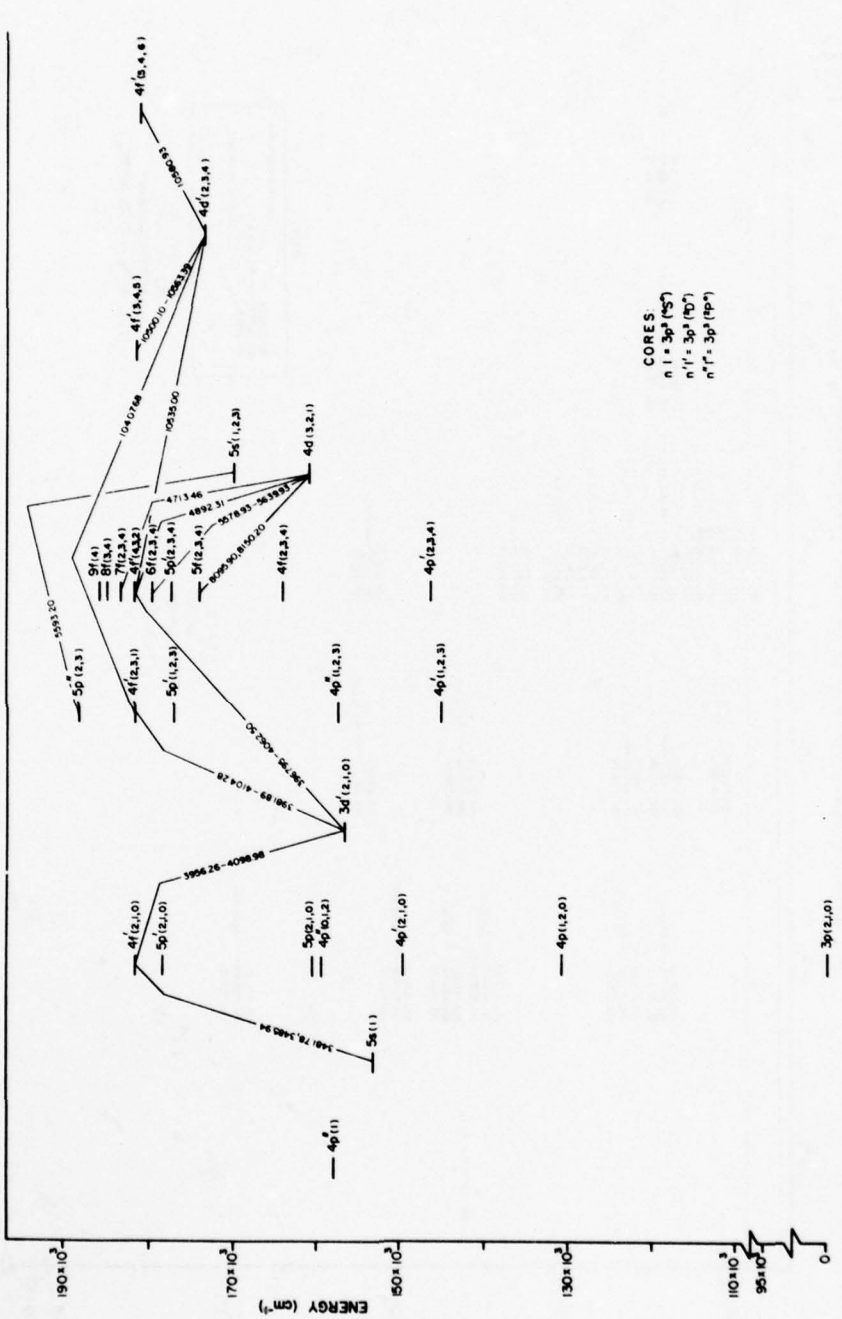

Tabular Data. A-1.171. Diagram for Cl^{+} (Z = 17).

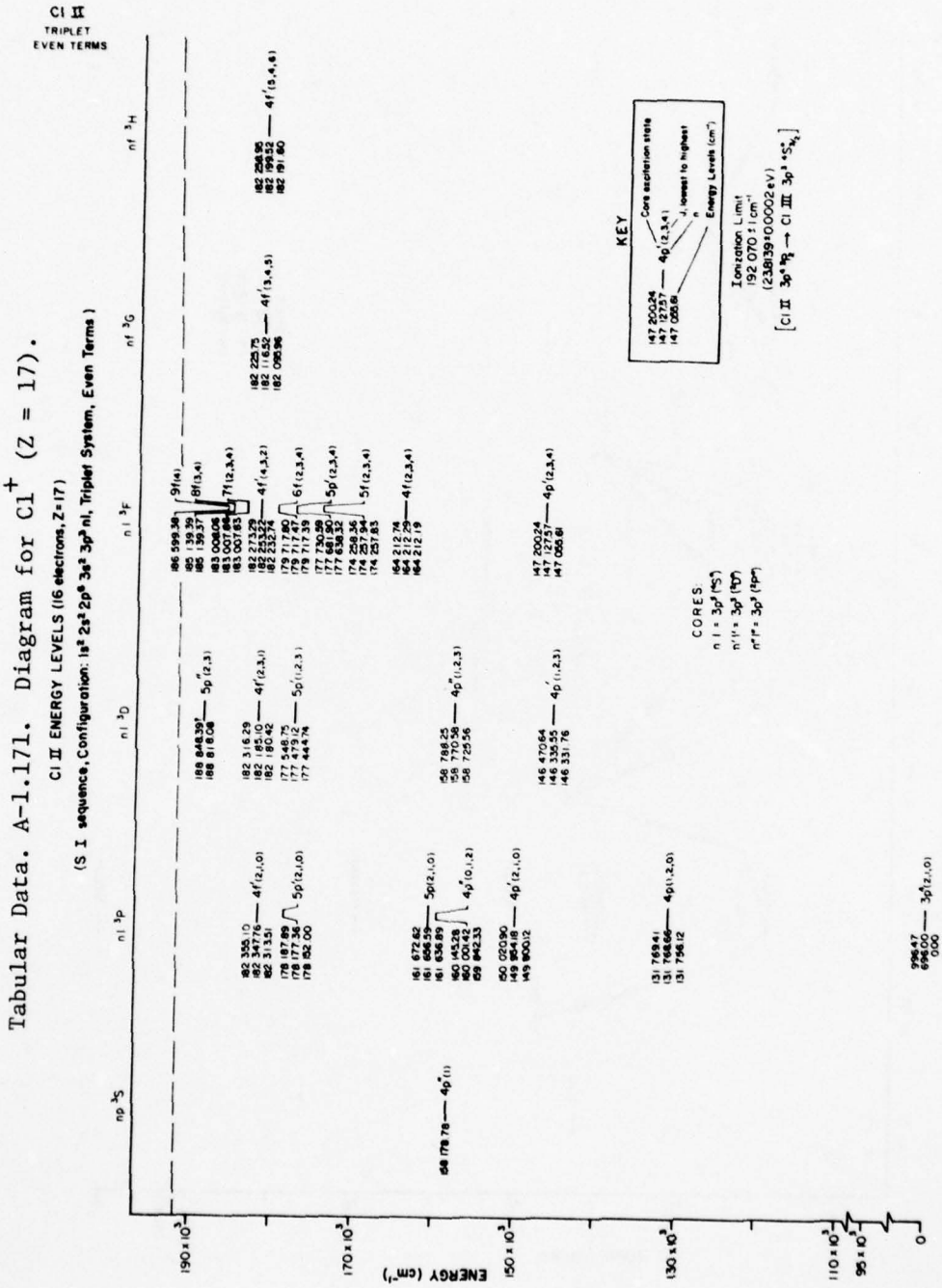

Tabular Data. A-1.172. Diagram for Cl^{+} (Z = 17).

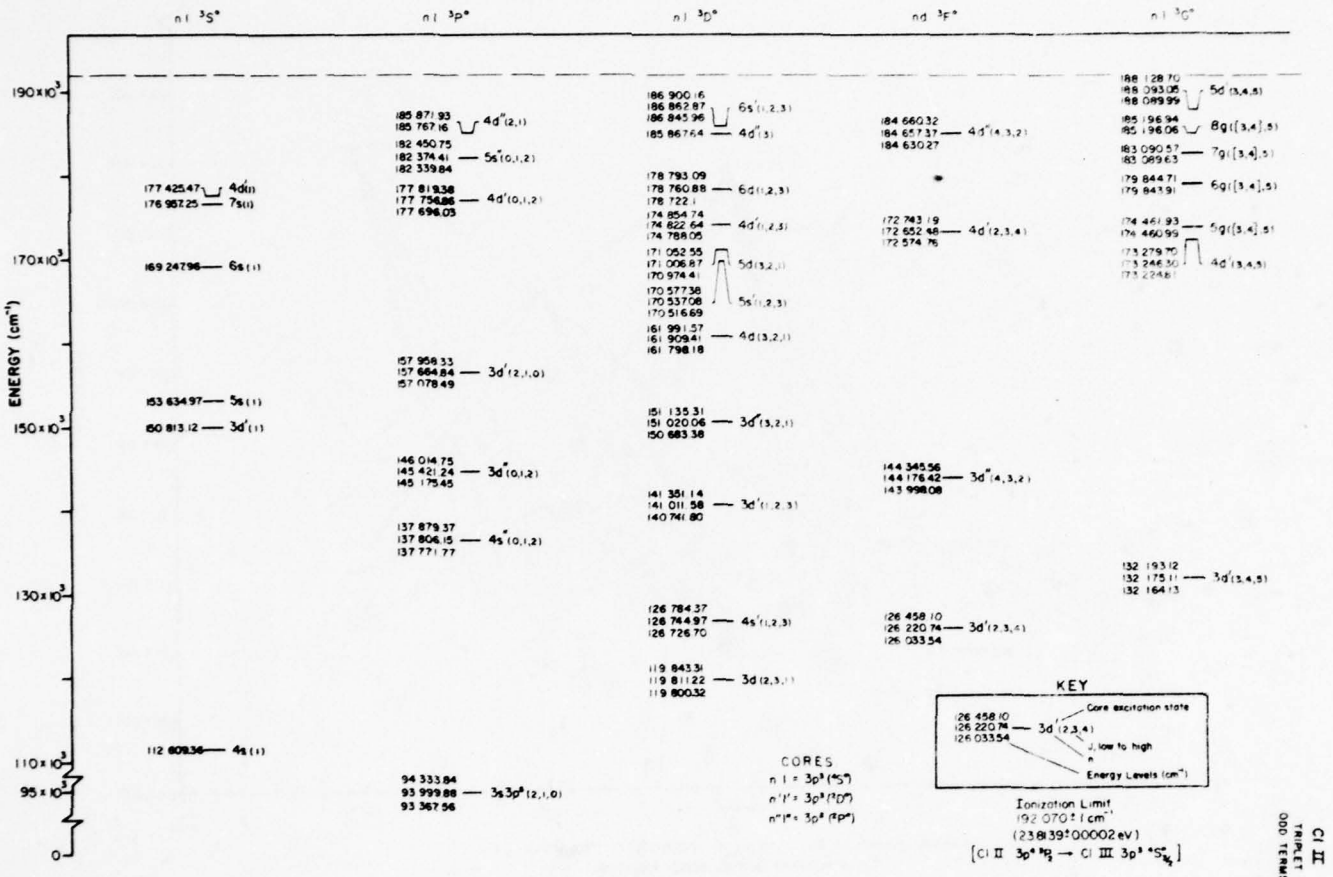

Tabular Data. A-1.173. Diagram for Cl^{+} (Z = 17).

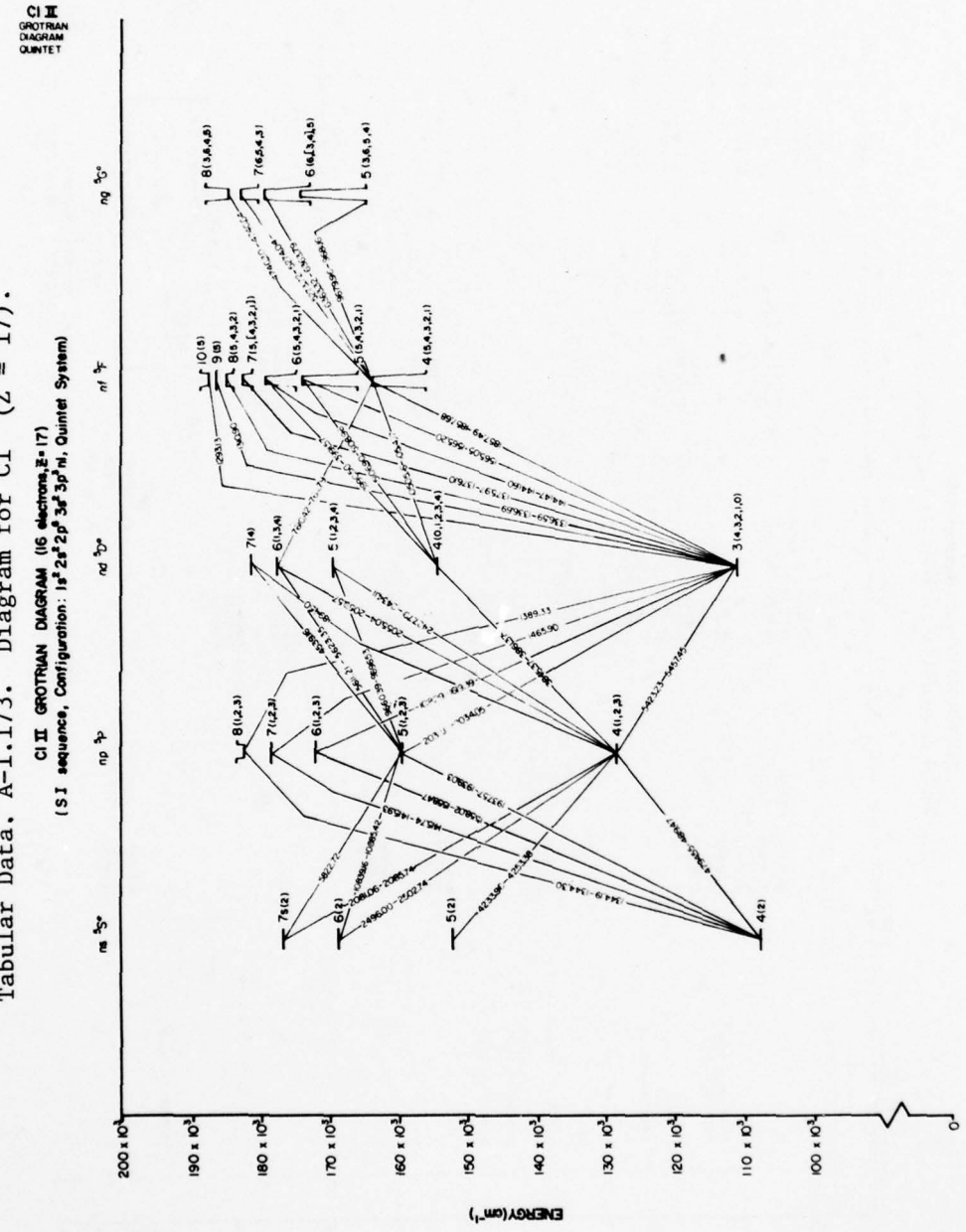

Tabular Data. A-1.174. Diagram for Cl^{+} (Z = 17).

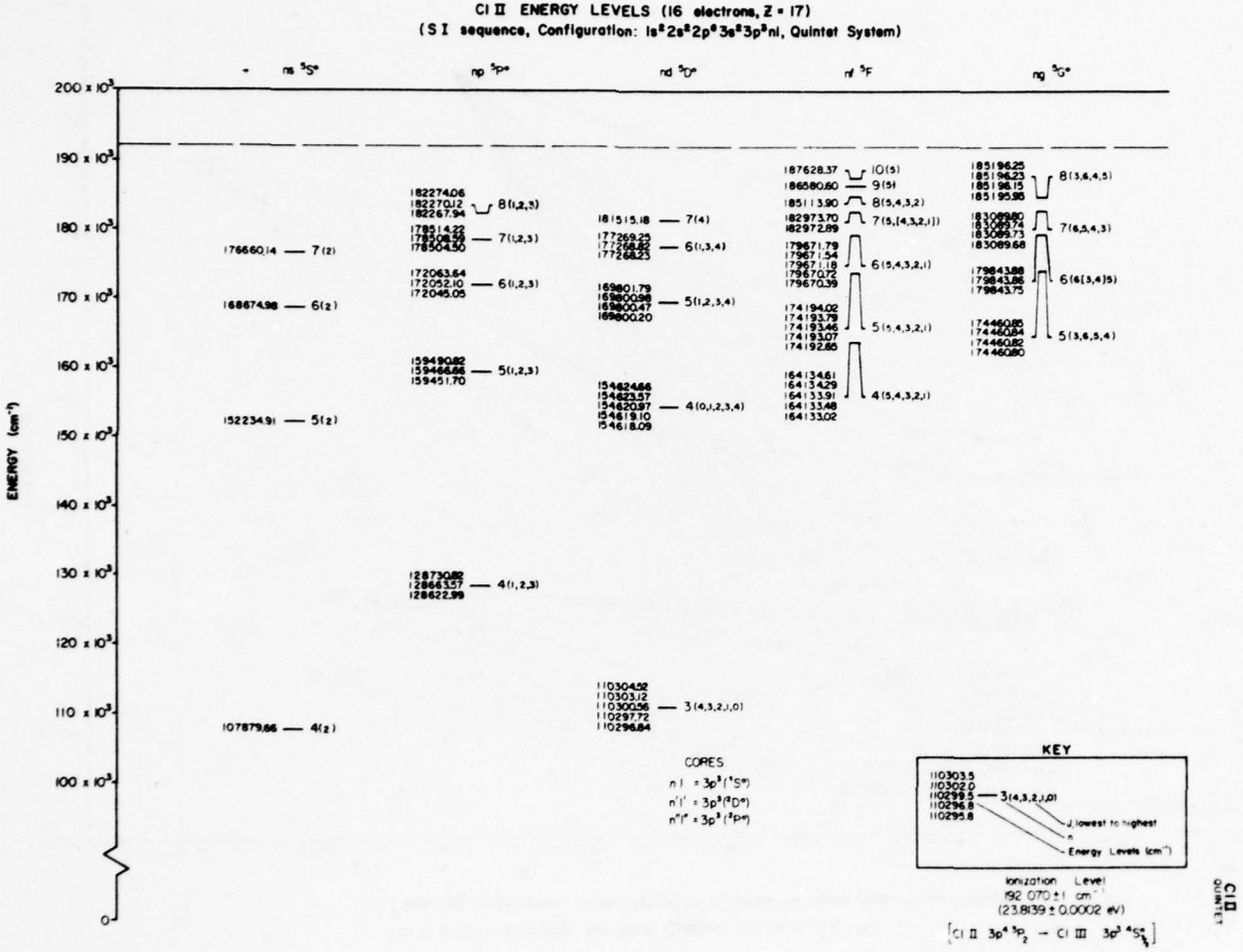

Tabular Data. A-1.175. Diagram for Cl^{+} ($Z = 17$).

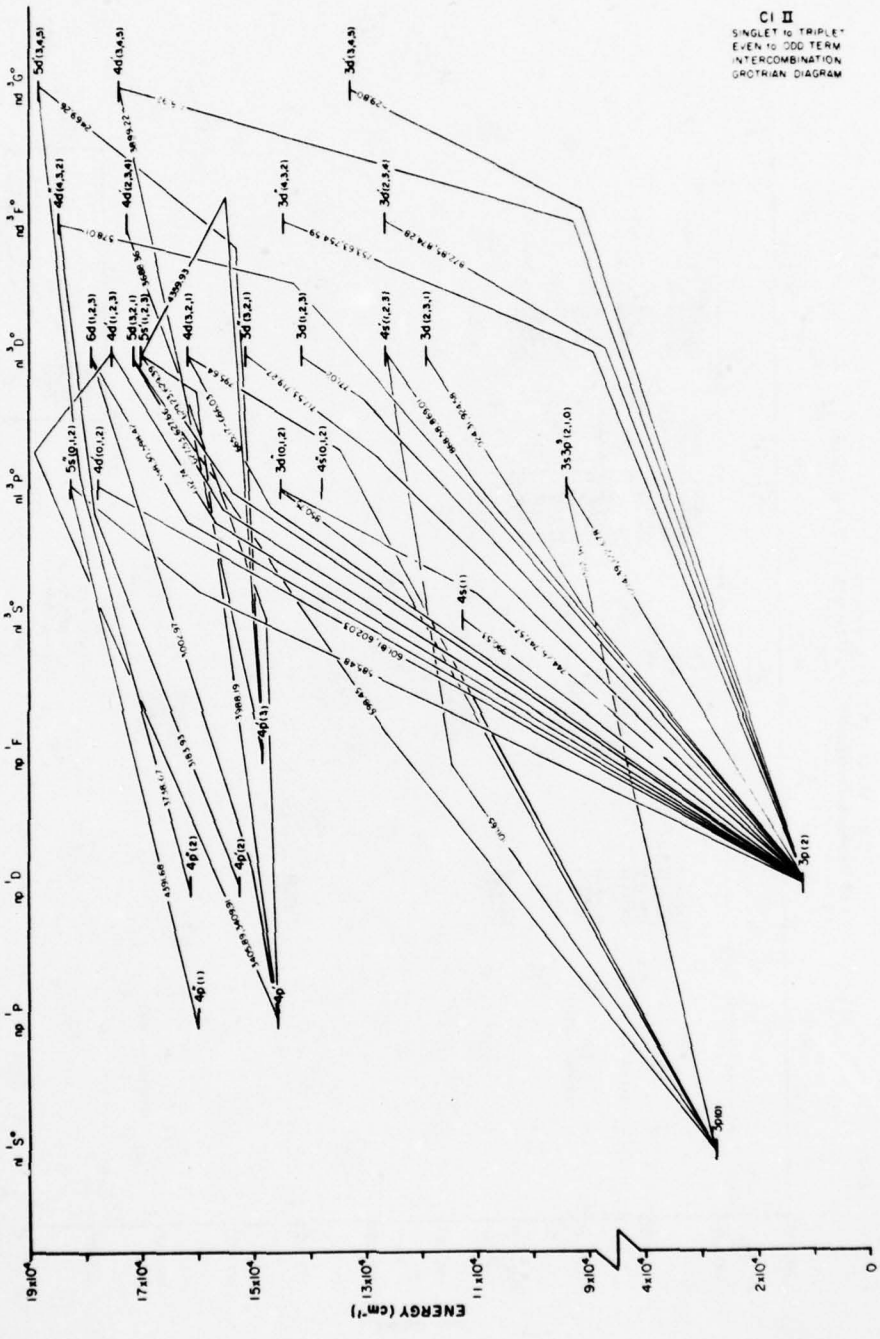

Tabular Data. A-1.176. Diagram for Cl^{+} (Z = 17).

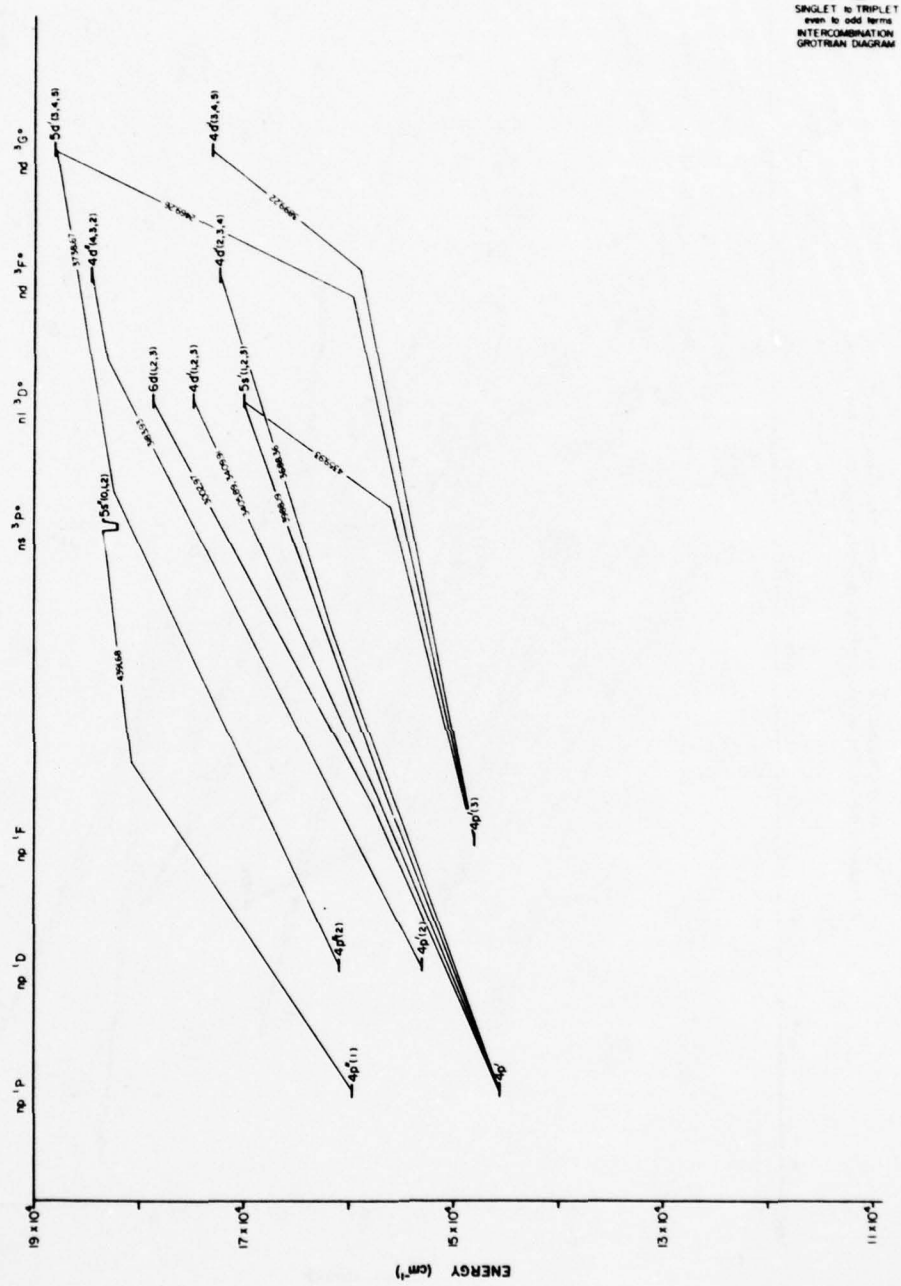

Tabular Data. A-1.177. Diagram for Cl^{+} (Z = 17).

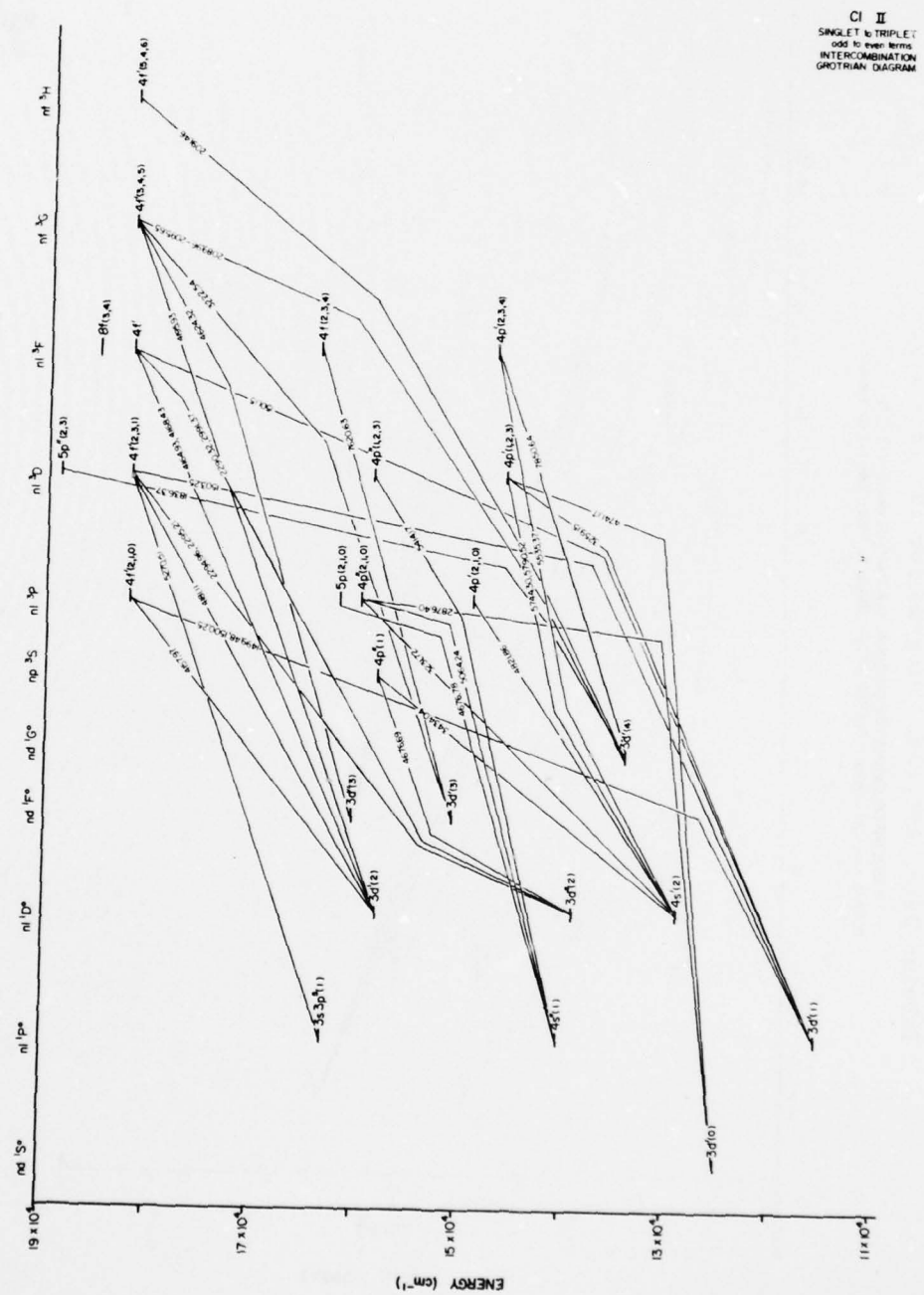

AD-A068 679 ARMY MISSILE RESEARCH AND DEVELOPMENT COMMAND REDSTO--ETC F/G 20/5
COMPILATION OF DATA RELEVANT TO NUCLEAR PUMPED LASERS. VOLUME I--ETC(U)
DEC 78 E W MCDANIEL, M R FLANNERY, E W THOMAS

UNCLASSIFIED DRDMI-H-78-1-VOL-3 NL

3 OF 5

AD A068679

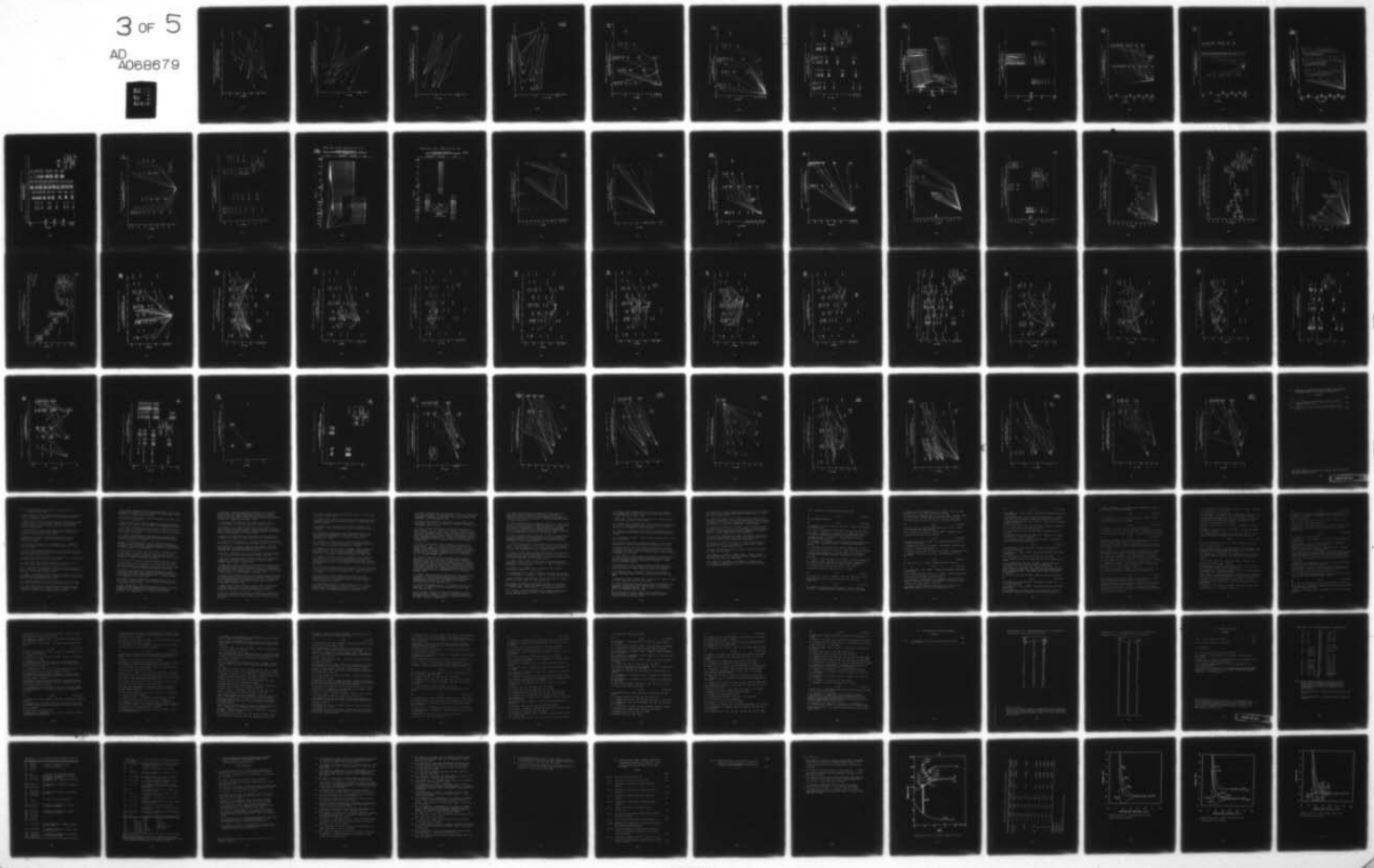

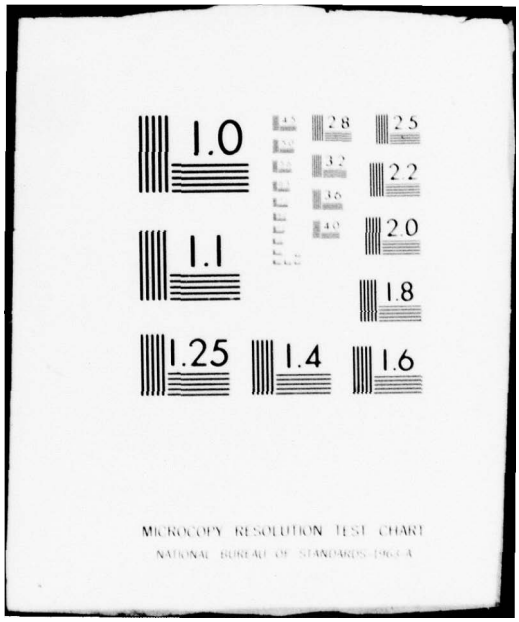
1.0
1.1
1.25
1.4
1.6
2.8
3.2
3.6
4.0
2.5
2.2
2.0
1.8
MICROCOPY RESOLUTION TEST CHART
NATIONAL BUREAU OF STANDARDS-1963-A

Tabular Data. A-1.178. Diagram for Cl^{+} (Z = 17).

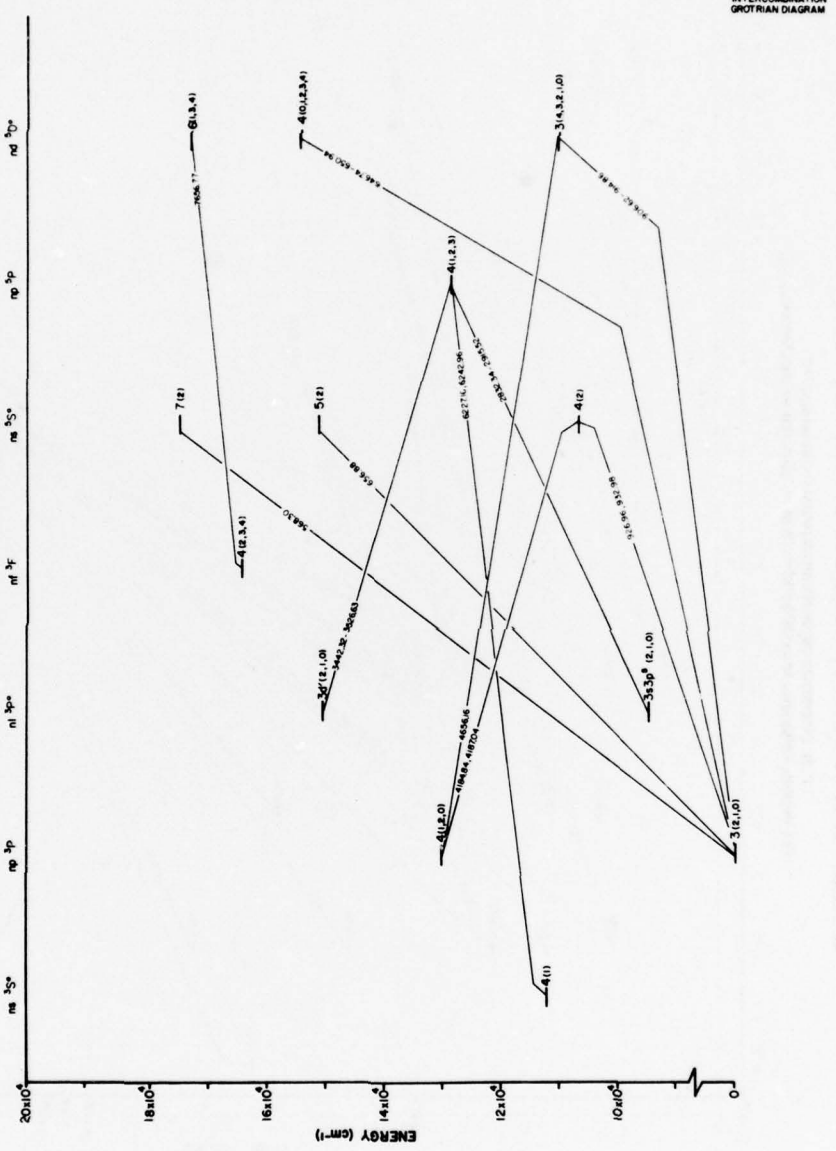

Tabular Data. A-1.179. Diagram for Cl^+ (Z = 17).

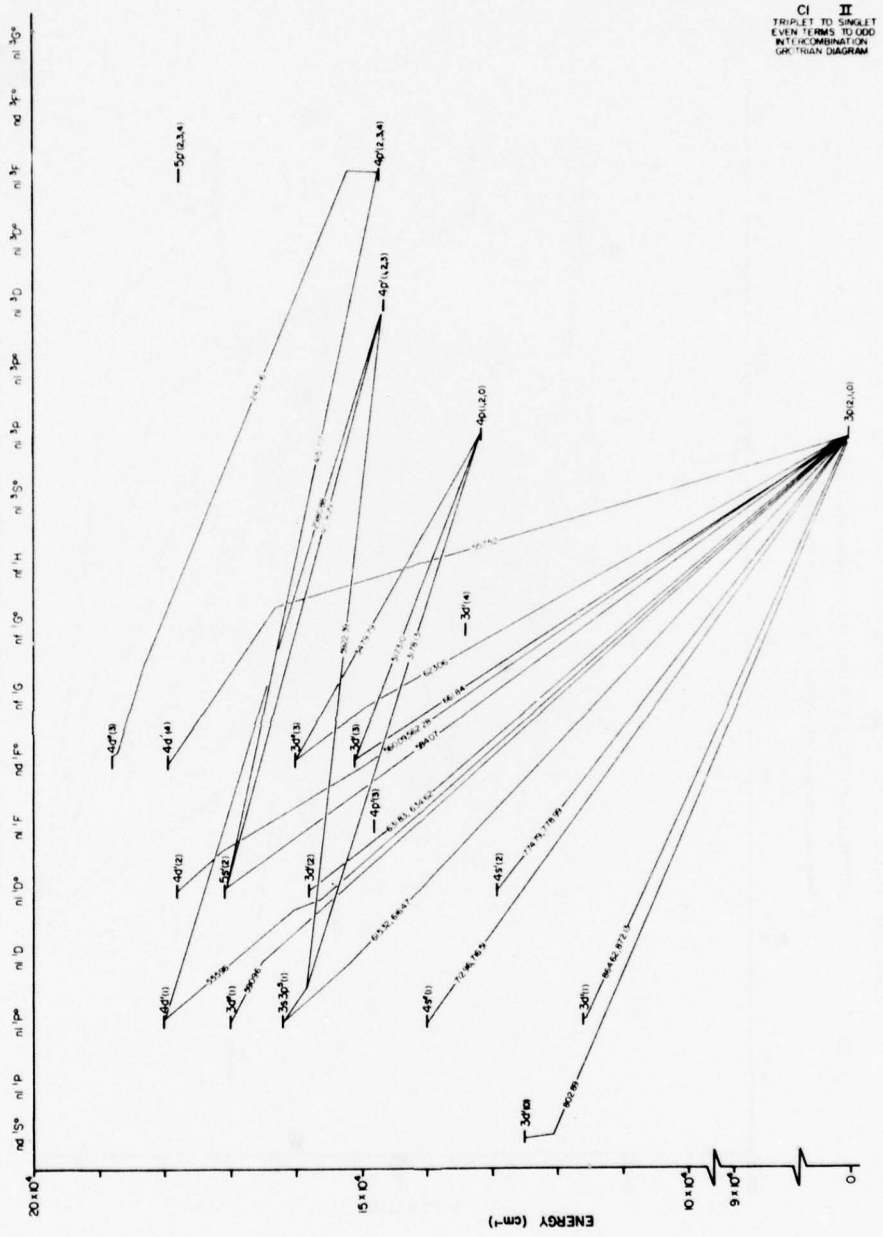

Tabular Data. A-1.180. Diagram for Cl^{+} (Z = 17).

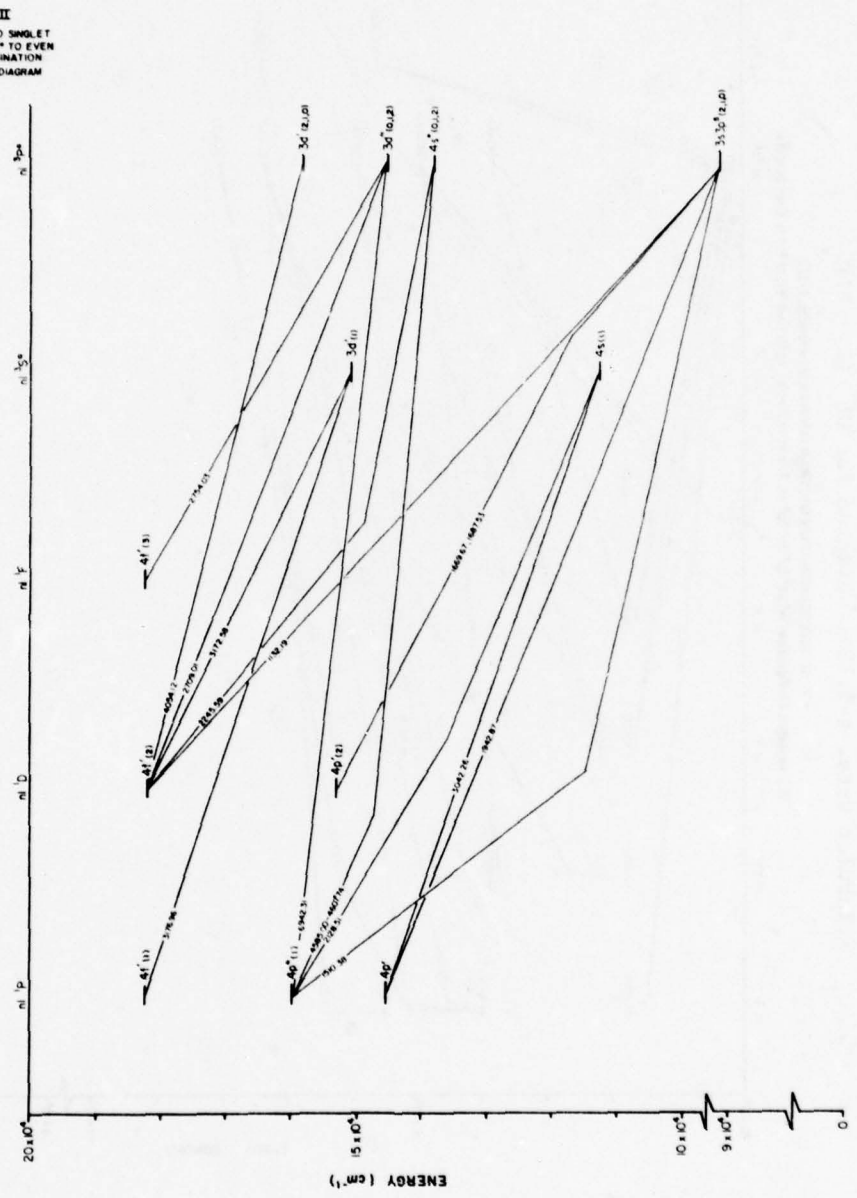

Tabular Data. A-1.181. Diagram for Cl^{+} (Z = 17).

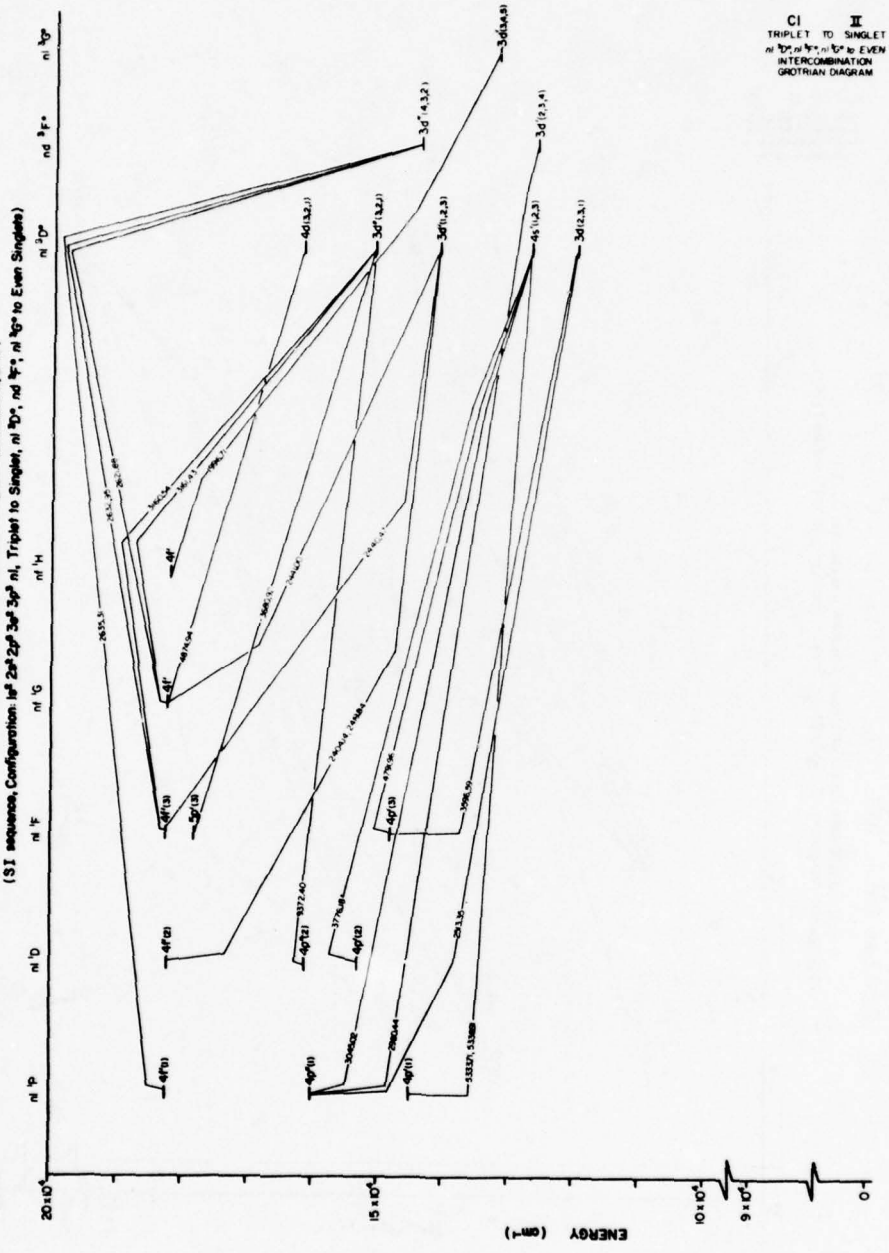

Tabular Data. A-1.182. Diagram for Ar (Z = 18).

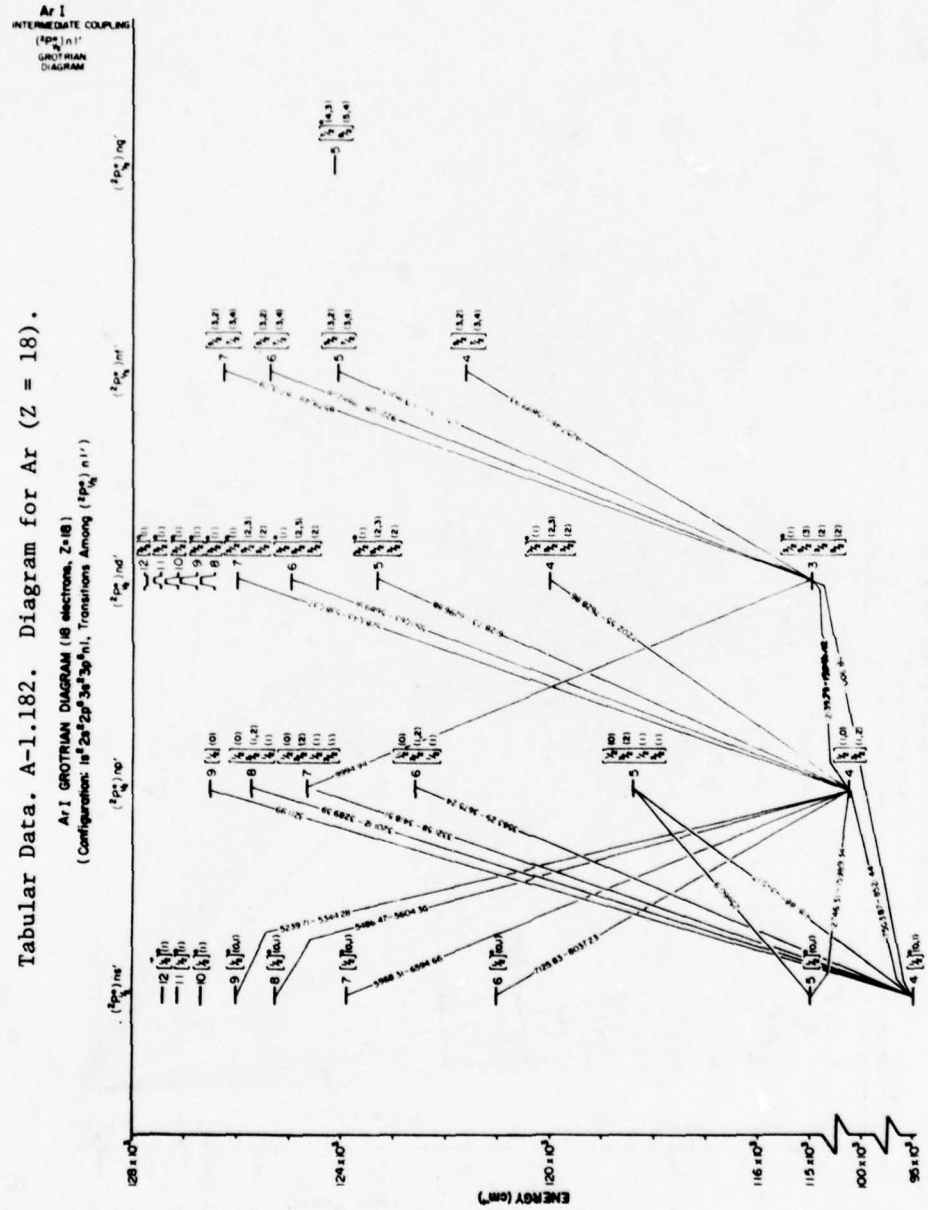

Tabular Data. A-1.183. Diagram for Ar (Z = 18).

Tabular Data. A-1.184. Diagram for Ar (Z = 18).

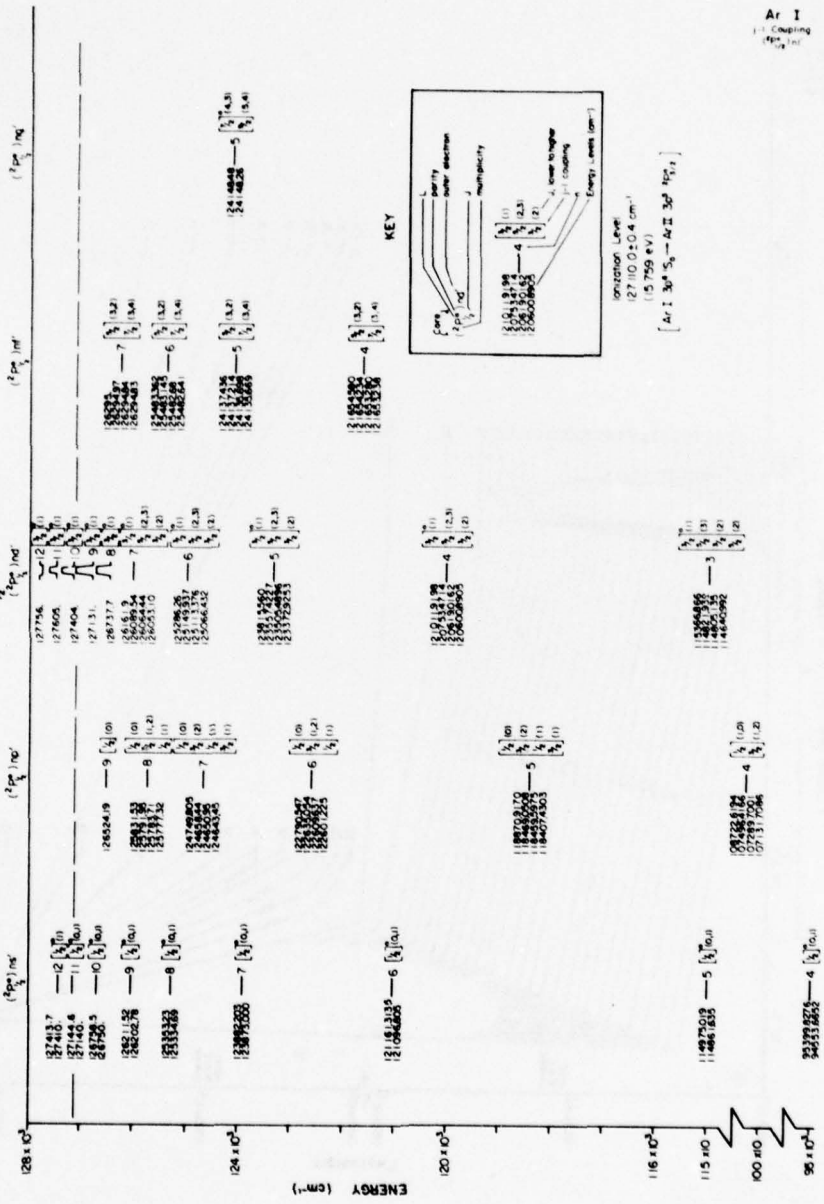

Tabular Data. A-1.185. Diagram for Ar (Z = 18).

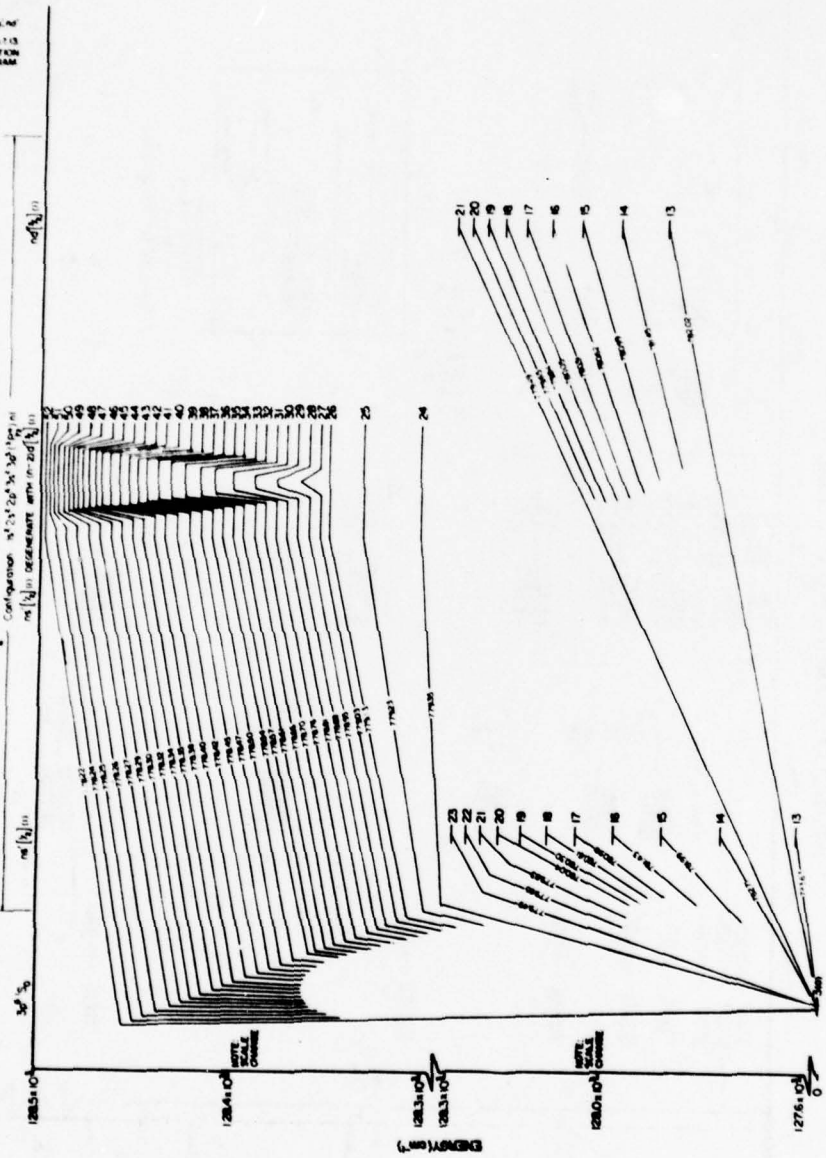

Tabular Data. A-1.186. Diagram for Ar (Z = 18).

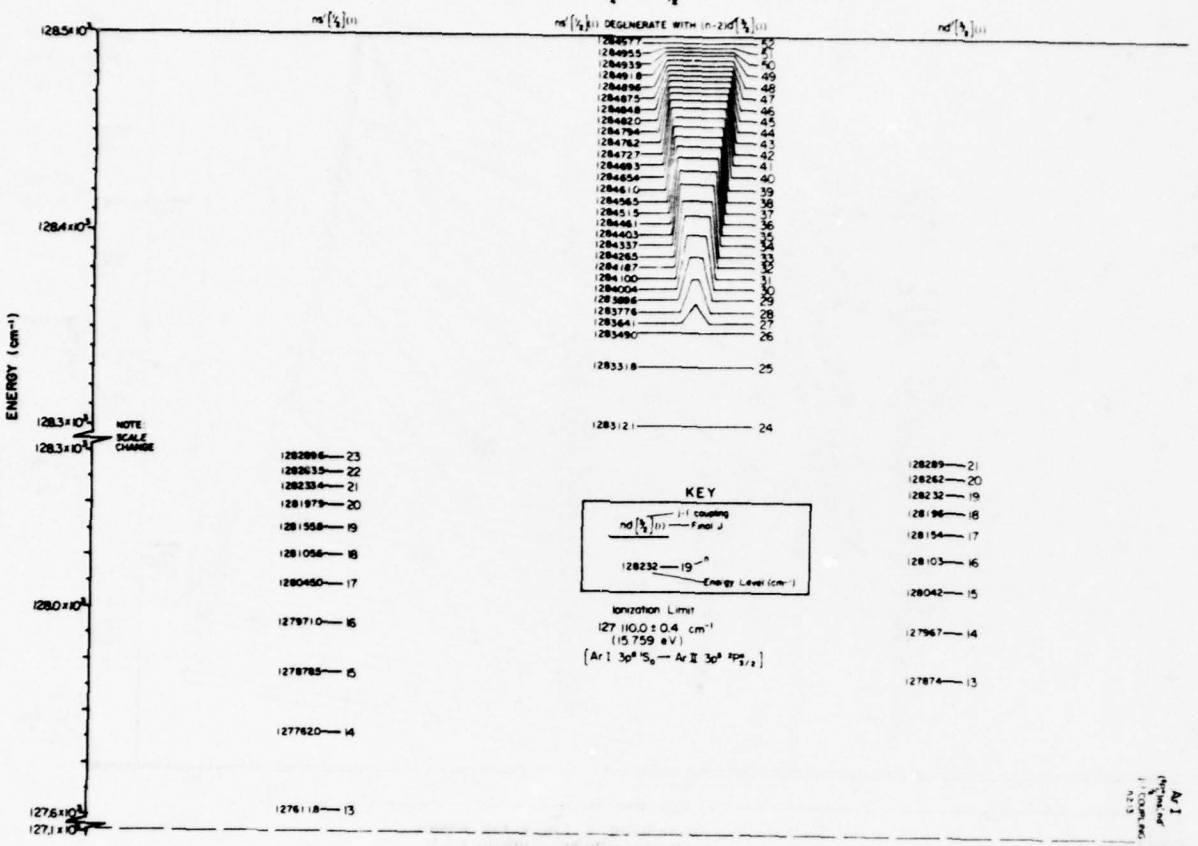

Tabular Data. A-1.187. Diagram for Ar (Z = 18).

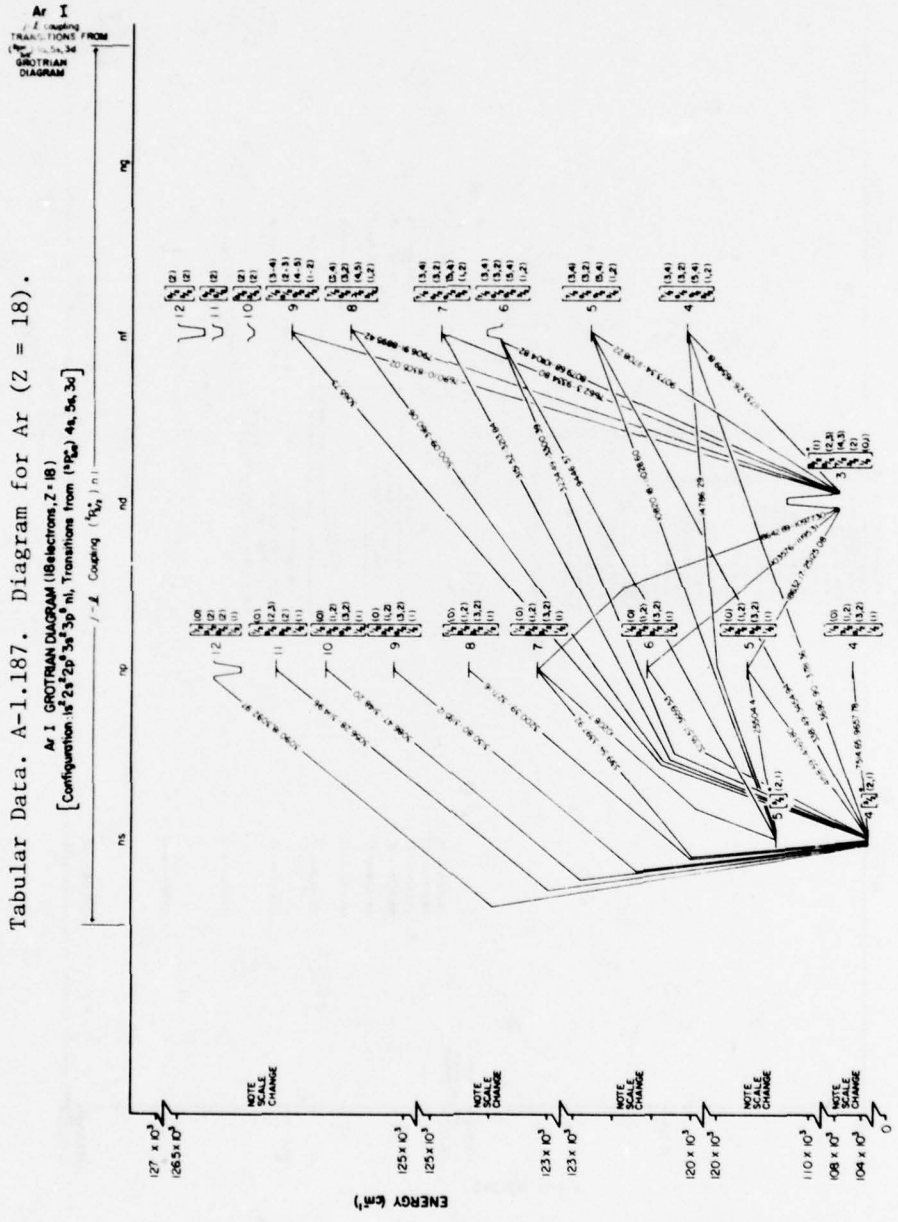

Tabular Data. A-1.188. Diagram for Ar (Z = 18).

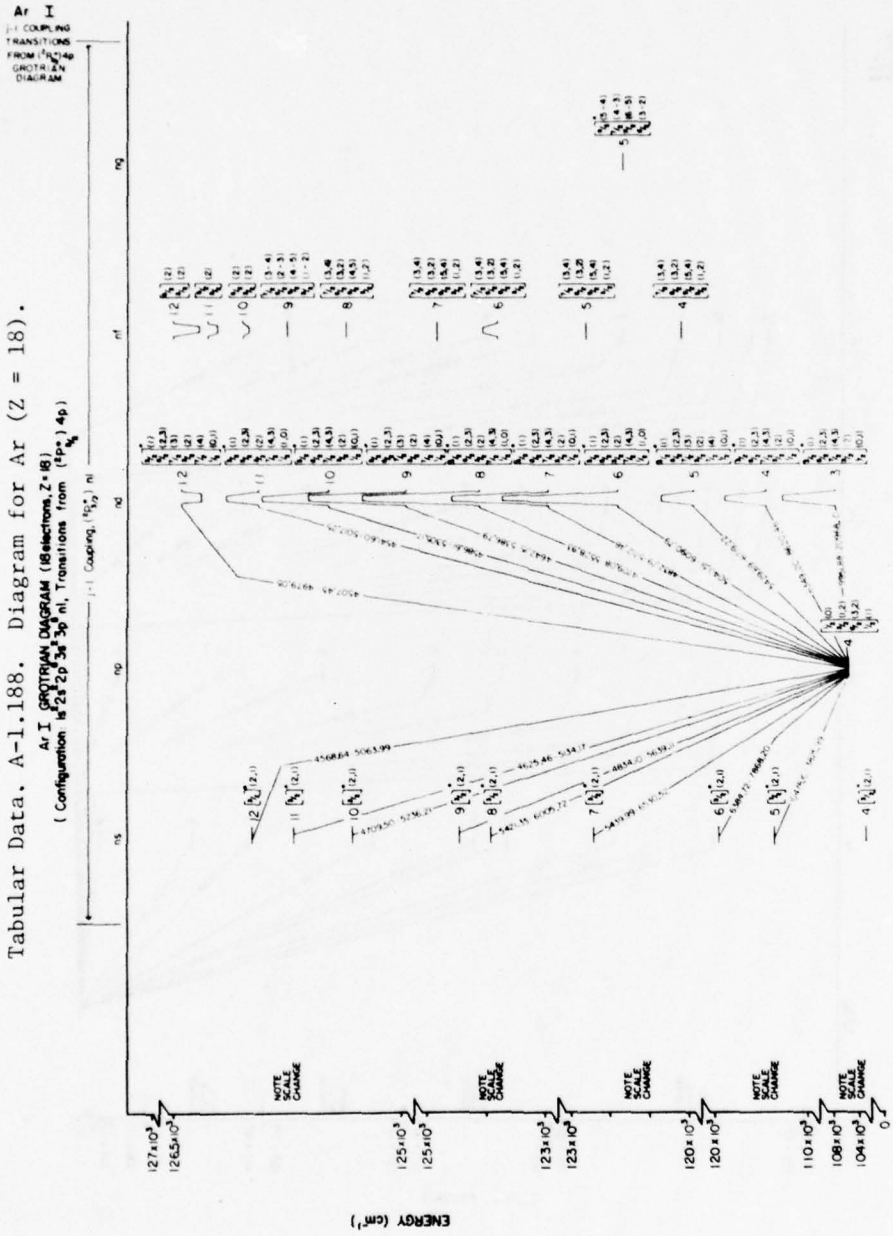

Tabular Data. A-1.189. Diagram for Ar (Z = 18).

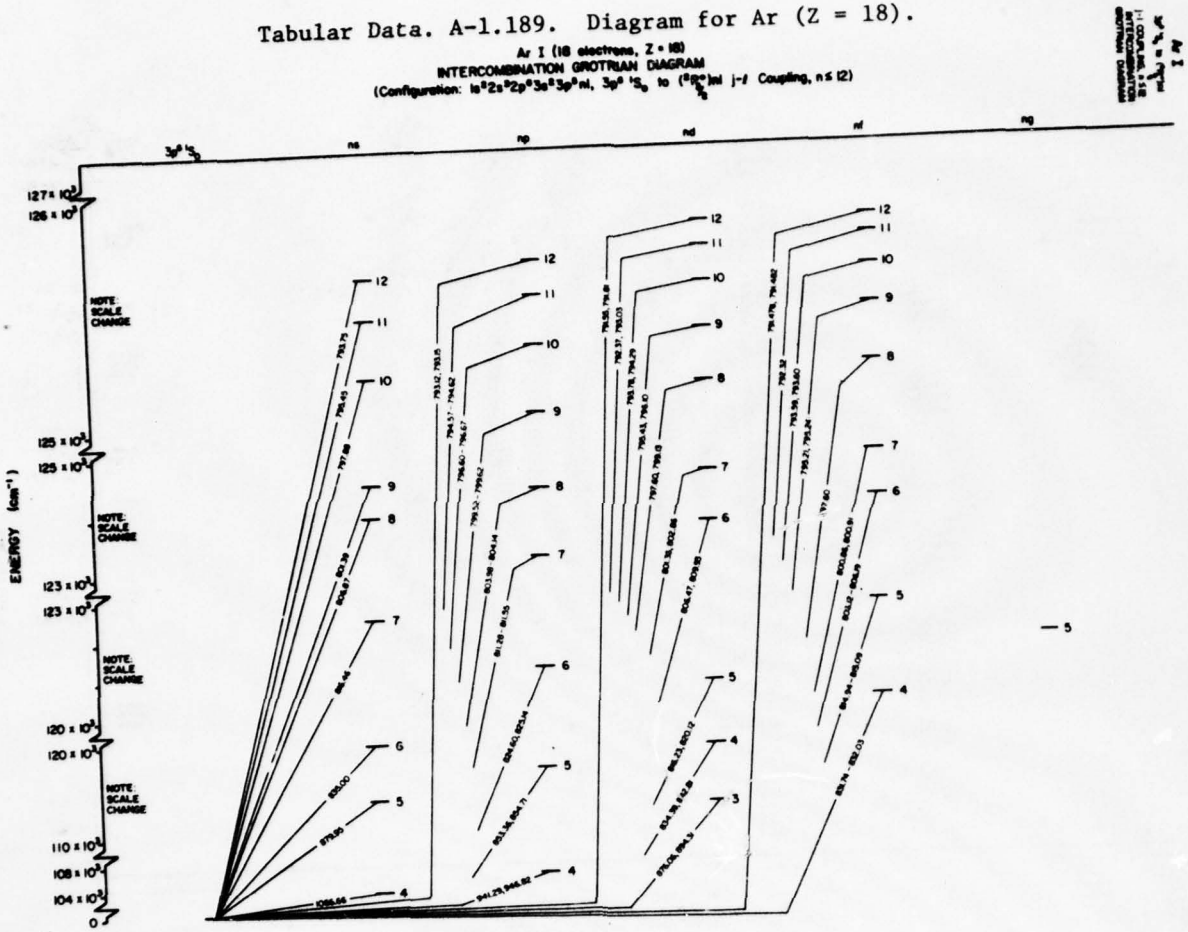

Tabular Data. A-1.190. Diagram for Ar (Z = 18).

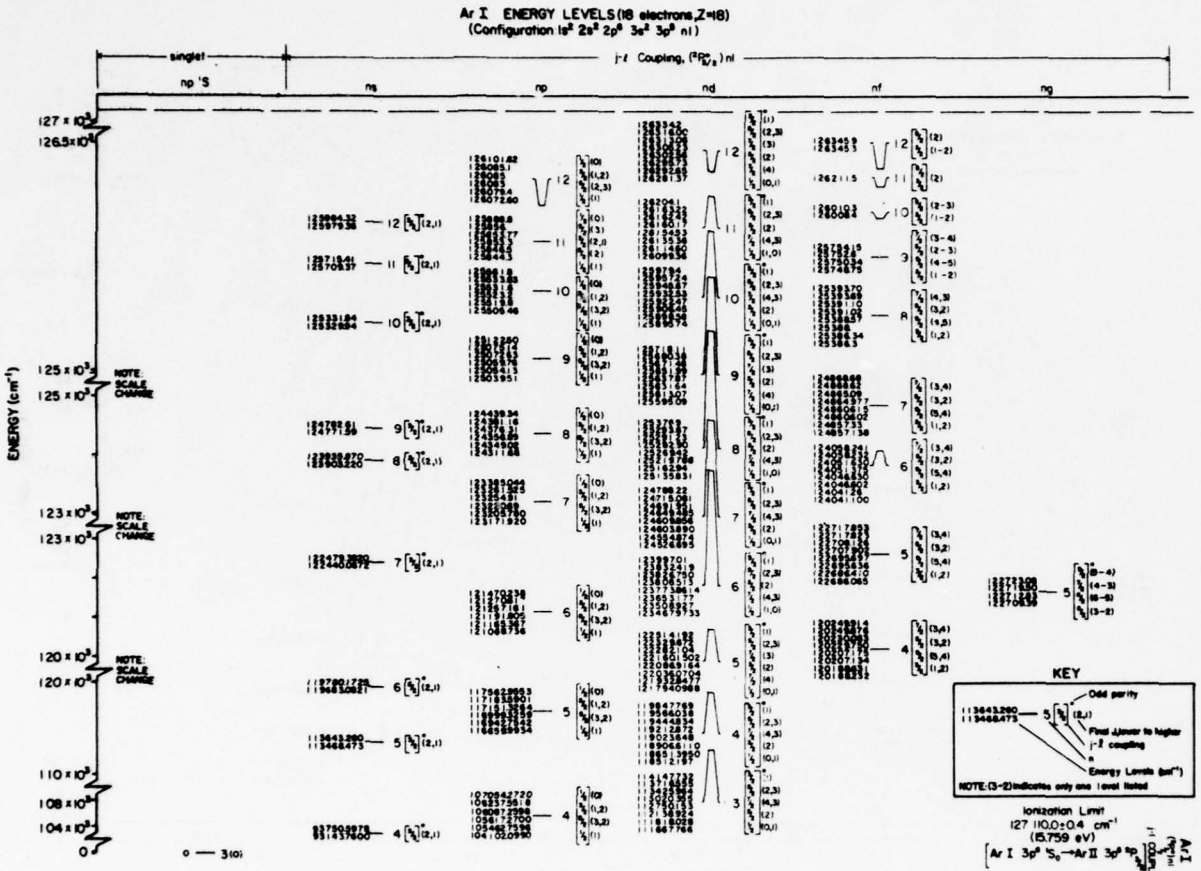

Tabular Data. A-1.191. Diagram for Ar (Z = 18).

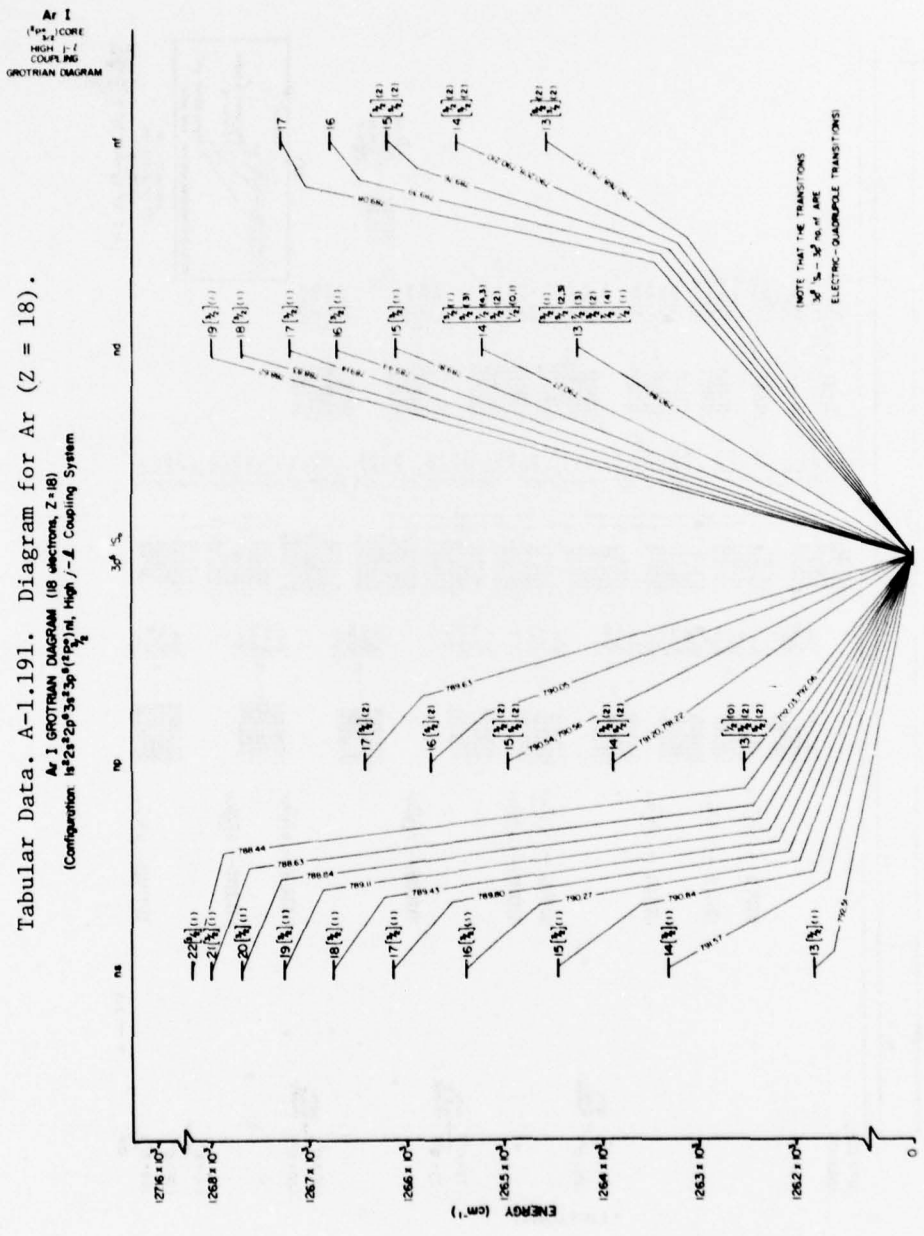

Tabular Data. A-1.192. Diagram for Ar (Z = 18).

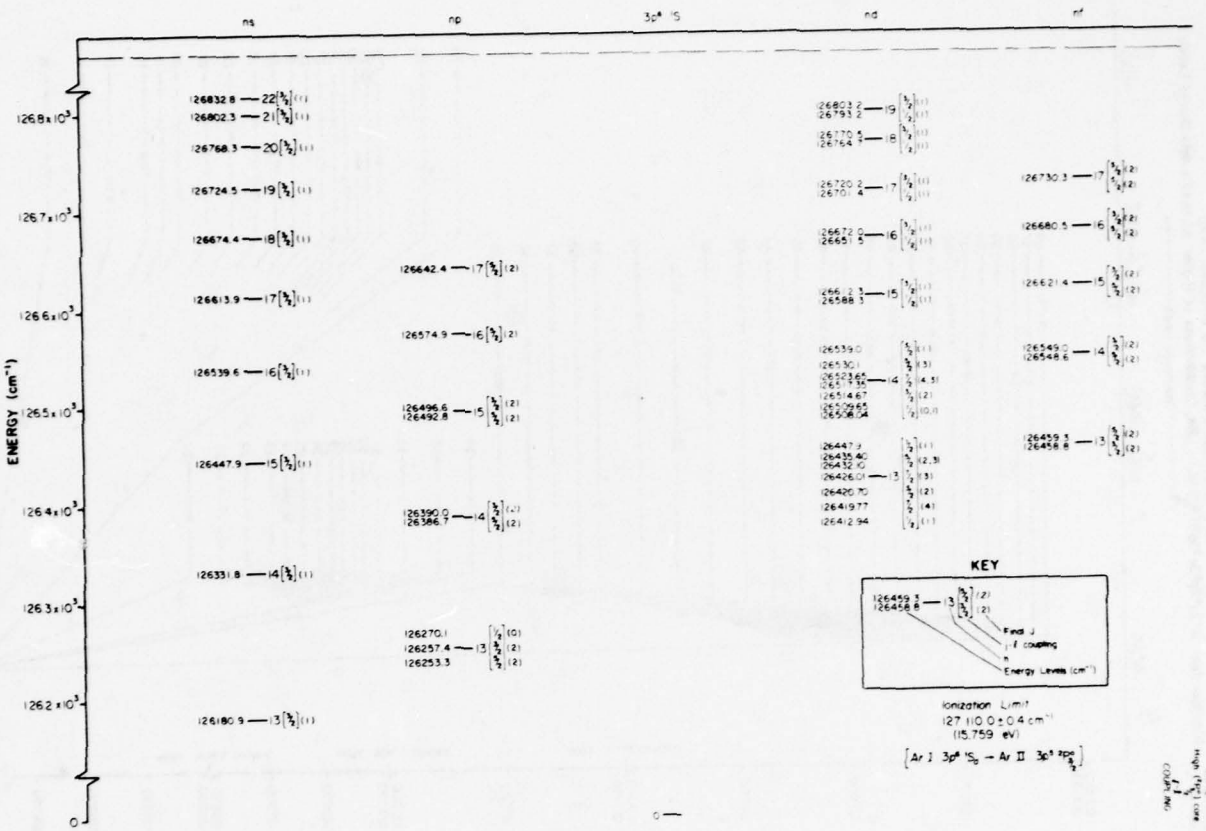

Tabular Data. A-1.193. Diagram for Ar (Z = 18).

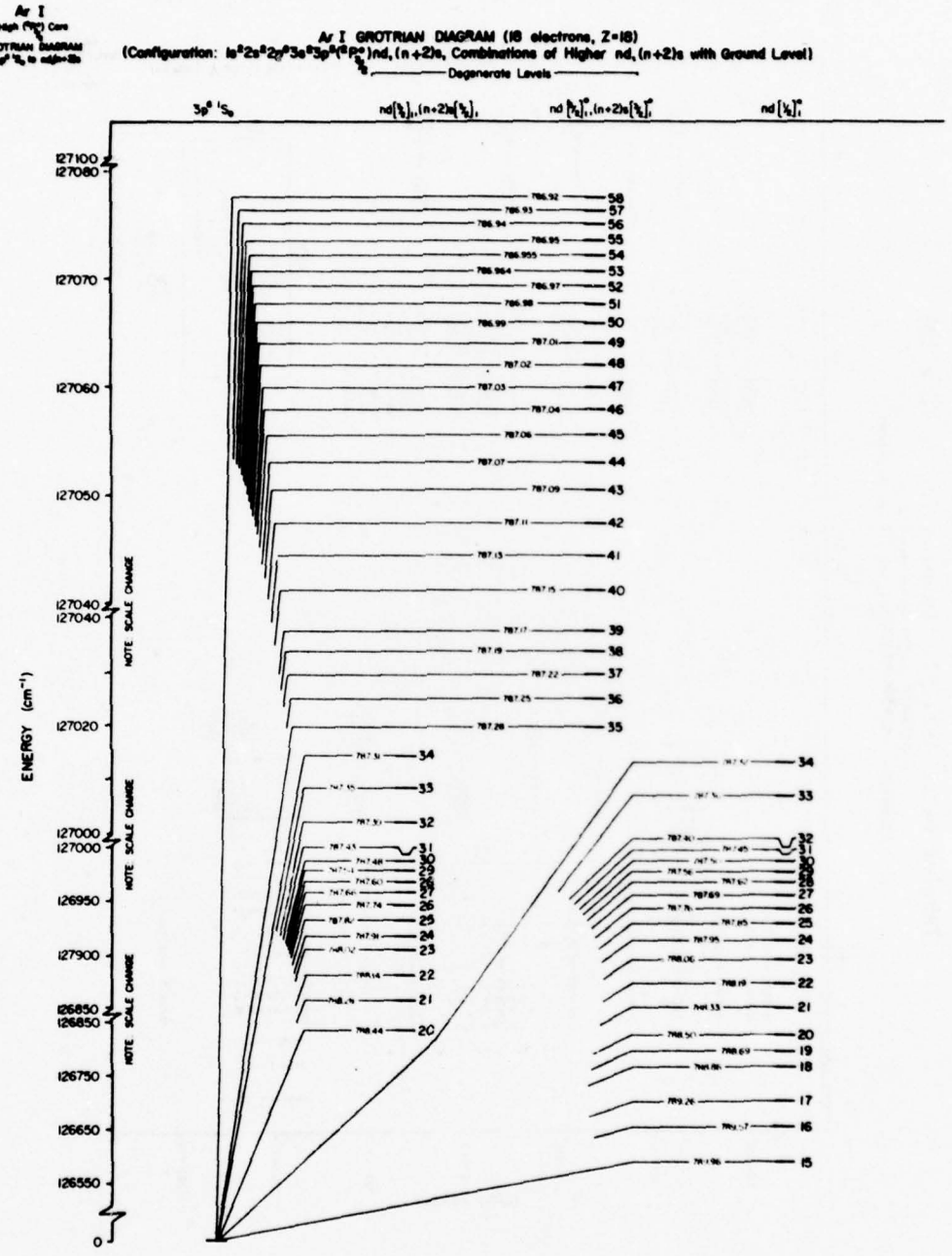

Tabular Data. A-1.194. Diagram for Ar (Z = 18).

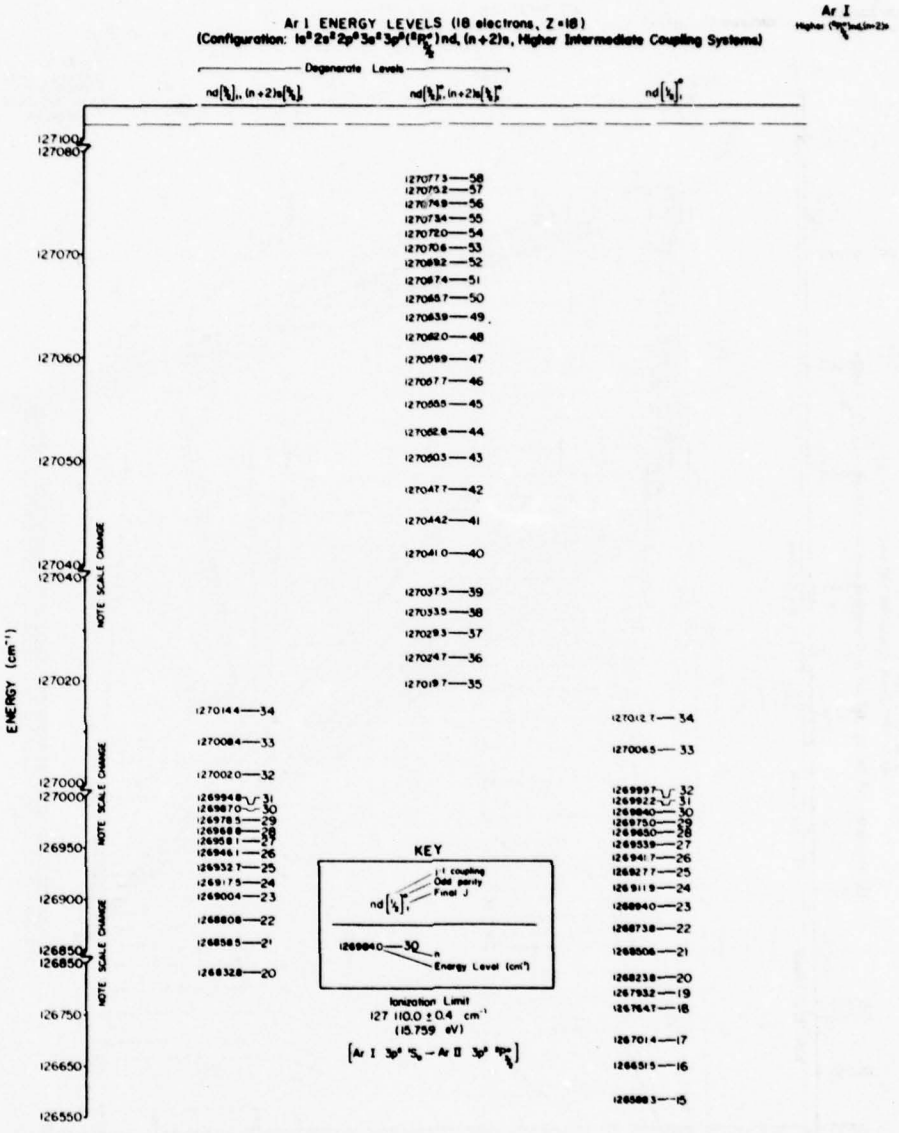

Tabular Data. A-I.195. Diagram for Ar (Z = 18).

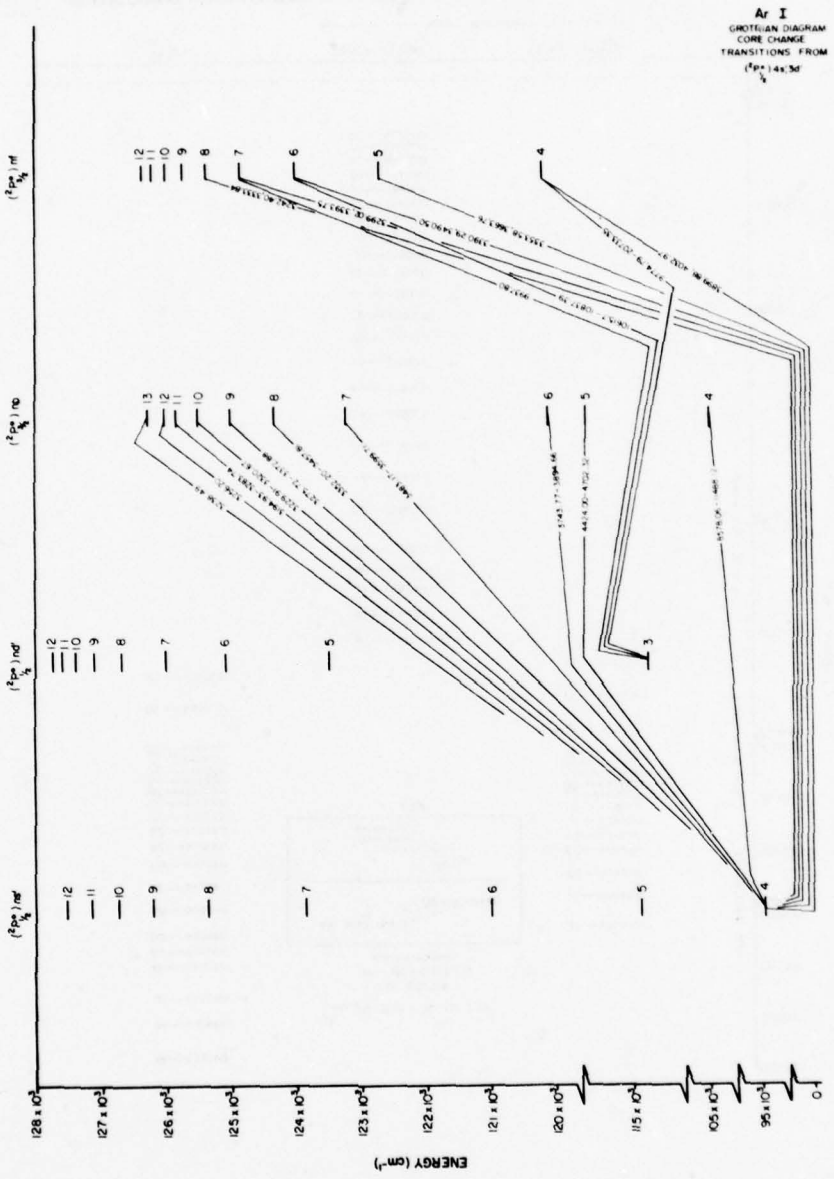

Tabular Data. A-1.196. Diagram for Ar (Z = 18).

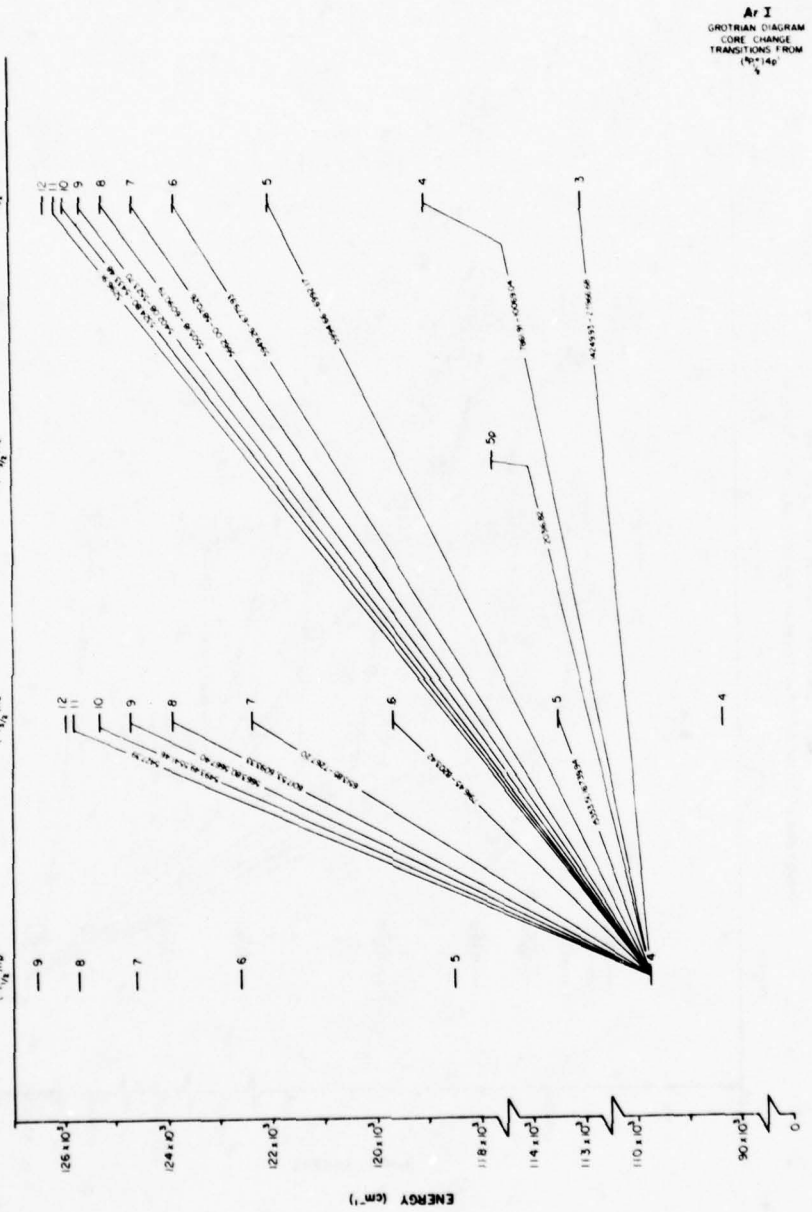

Tabular Data. A-1.197. Diagram for Ar (Z = 18).

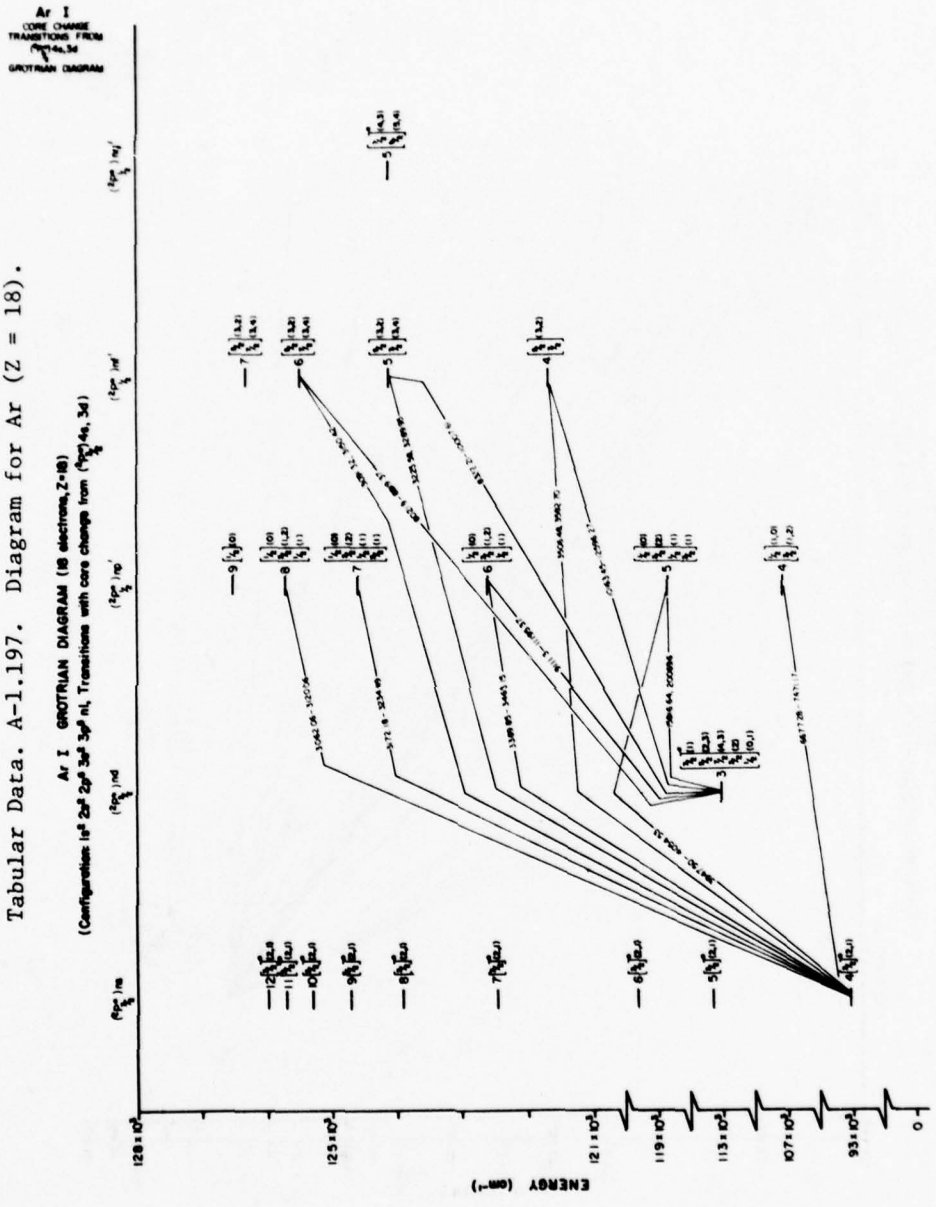

Tabular Data. A-1.198. Diagram for Ar (Z = 18).

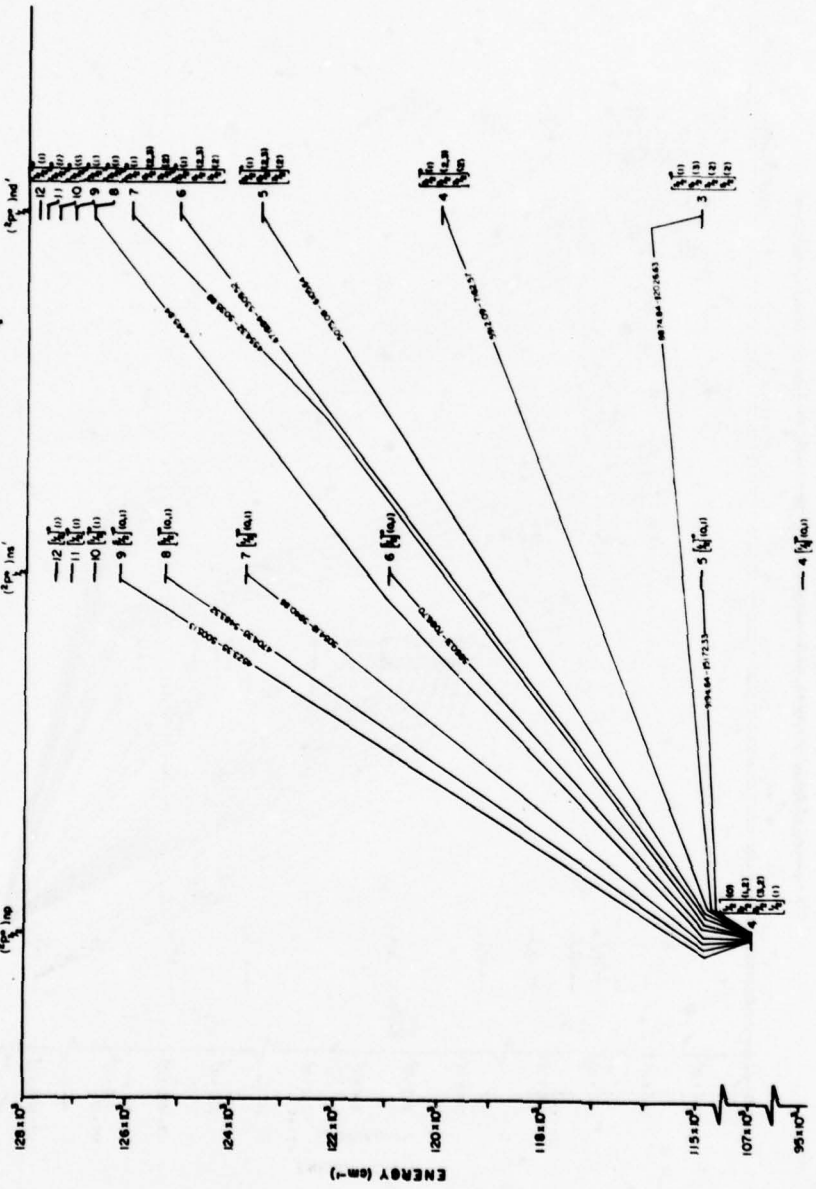

Tabular Data. A-1.199. Diagram for Ar (Z = 18).

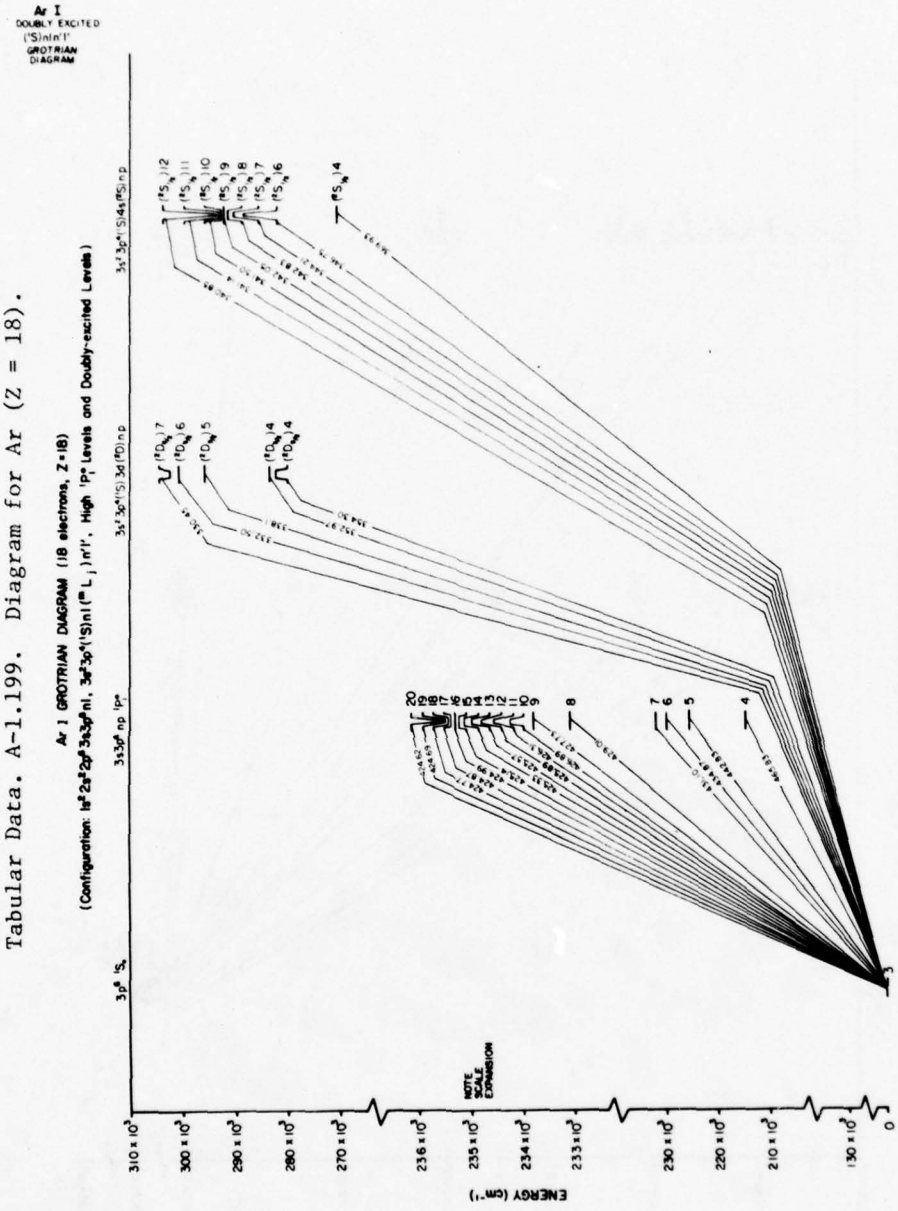

Tabular Data. A-1.200. Diagram for Ar (Z = 18).

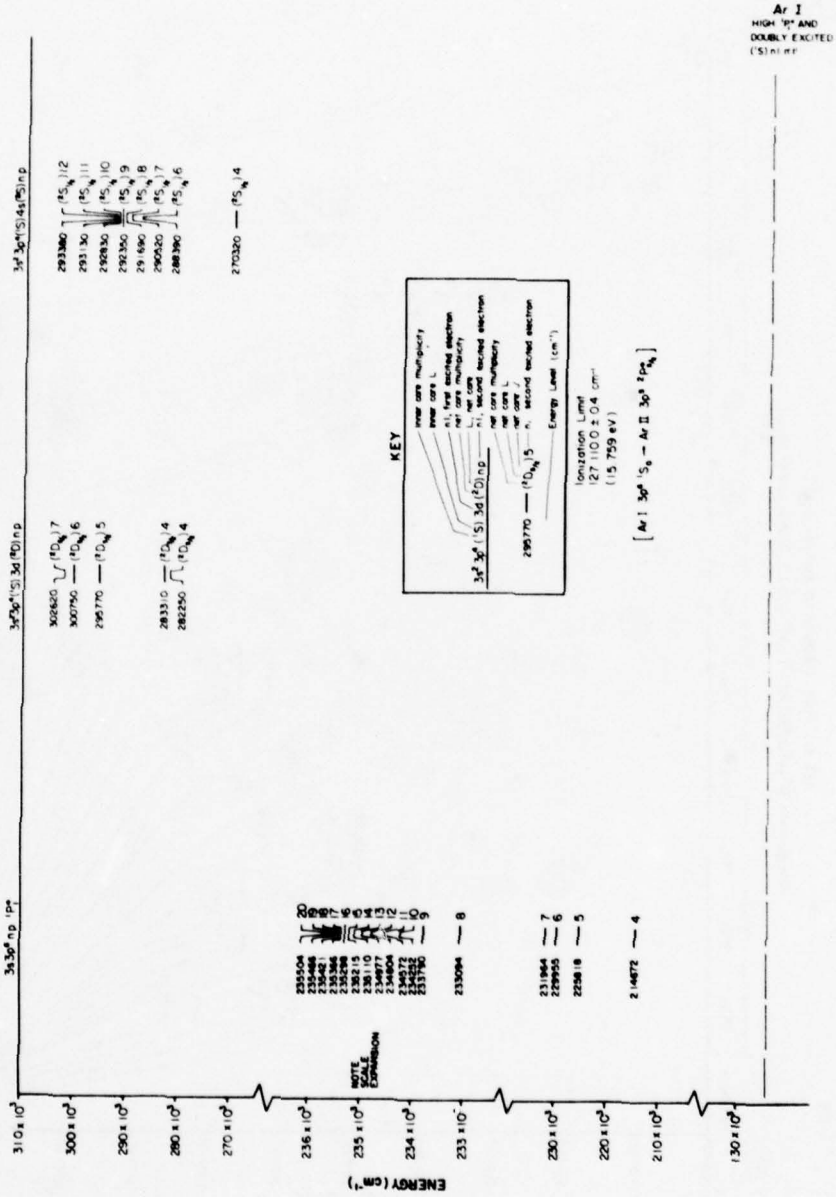

Tabular Data. A-1.201. Diagram for Ar (Z = 18).

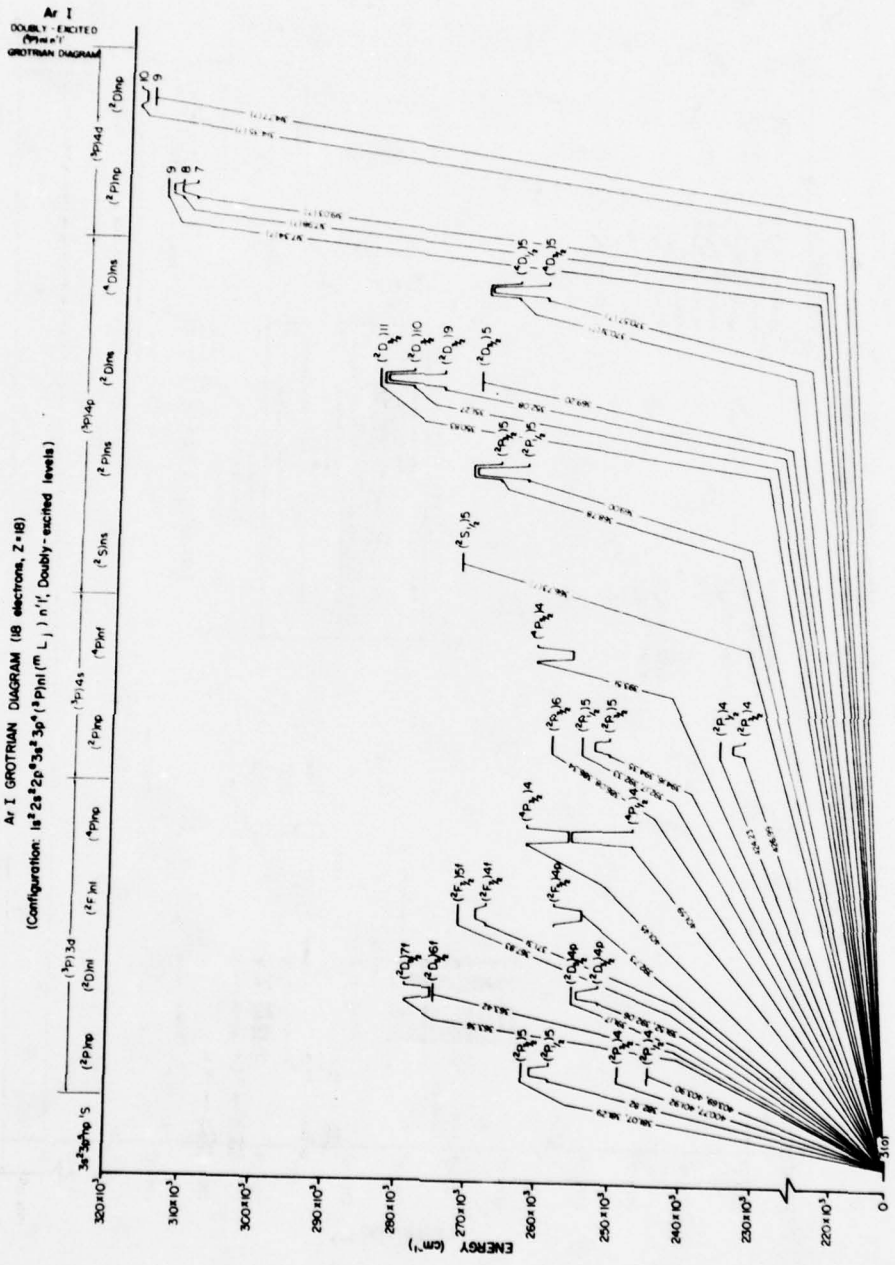

Tabular Data. A-1.202. Diagram for Ar (Z = 18).

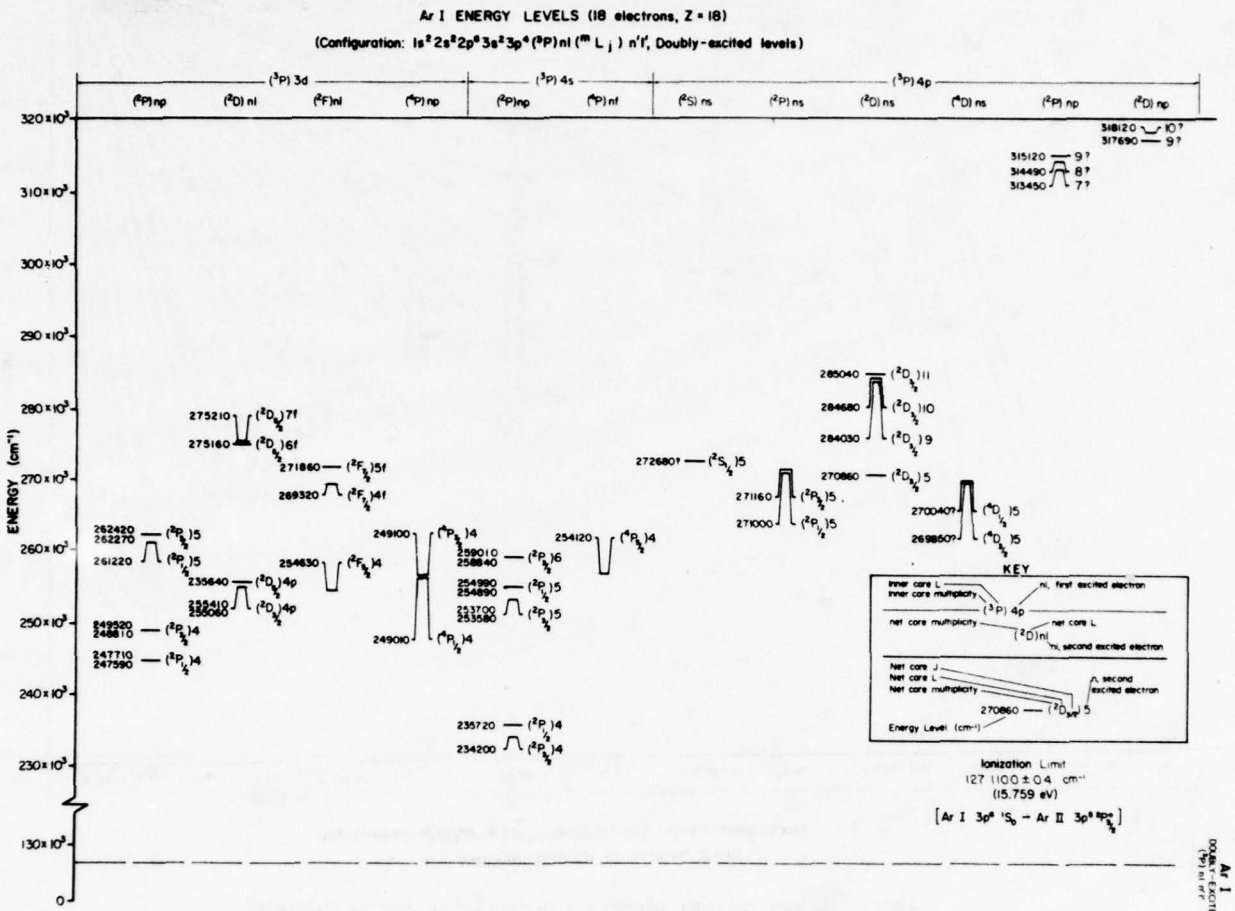

Tabular Data. A-1.203. Diagram for Ar (Z = 18).

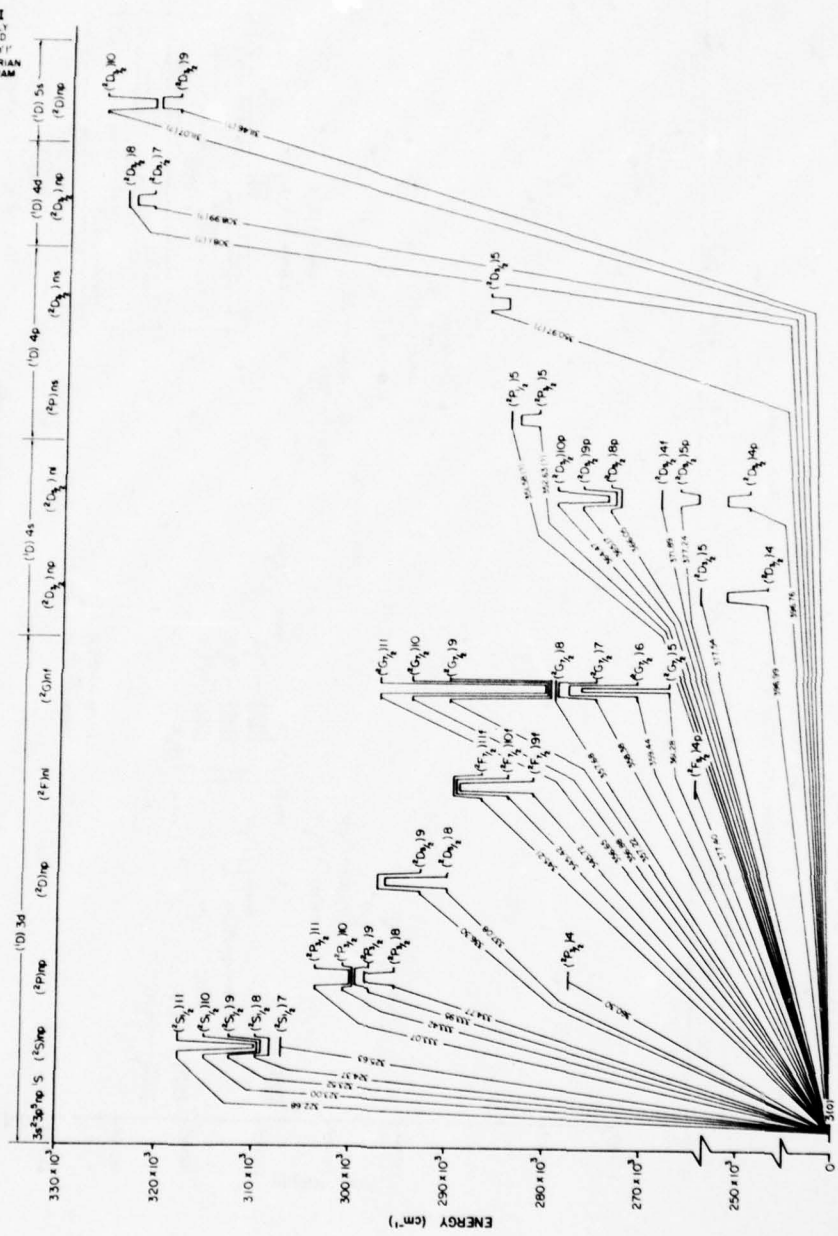

Tabular Data. A-1.204. Diagram for Ar (Z = 18).

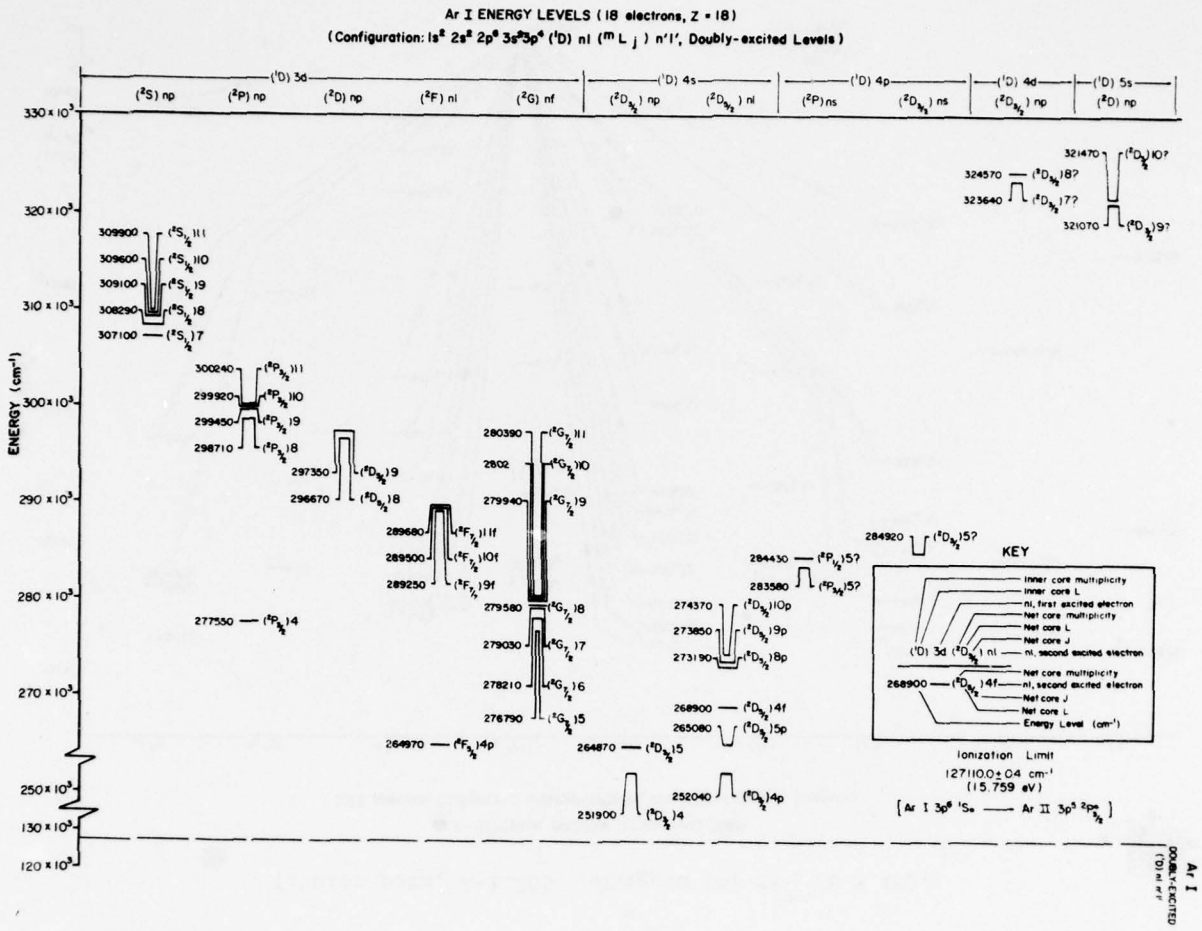

Tabular Data. A-1.205. Diagram for Ar^{+} (Z = 18).

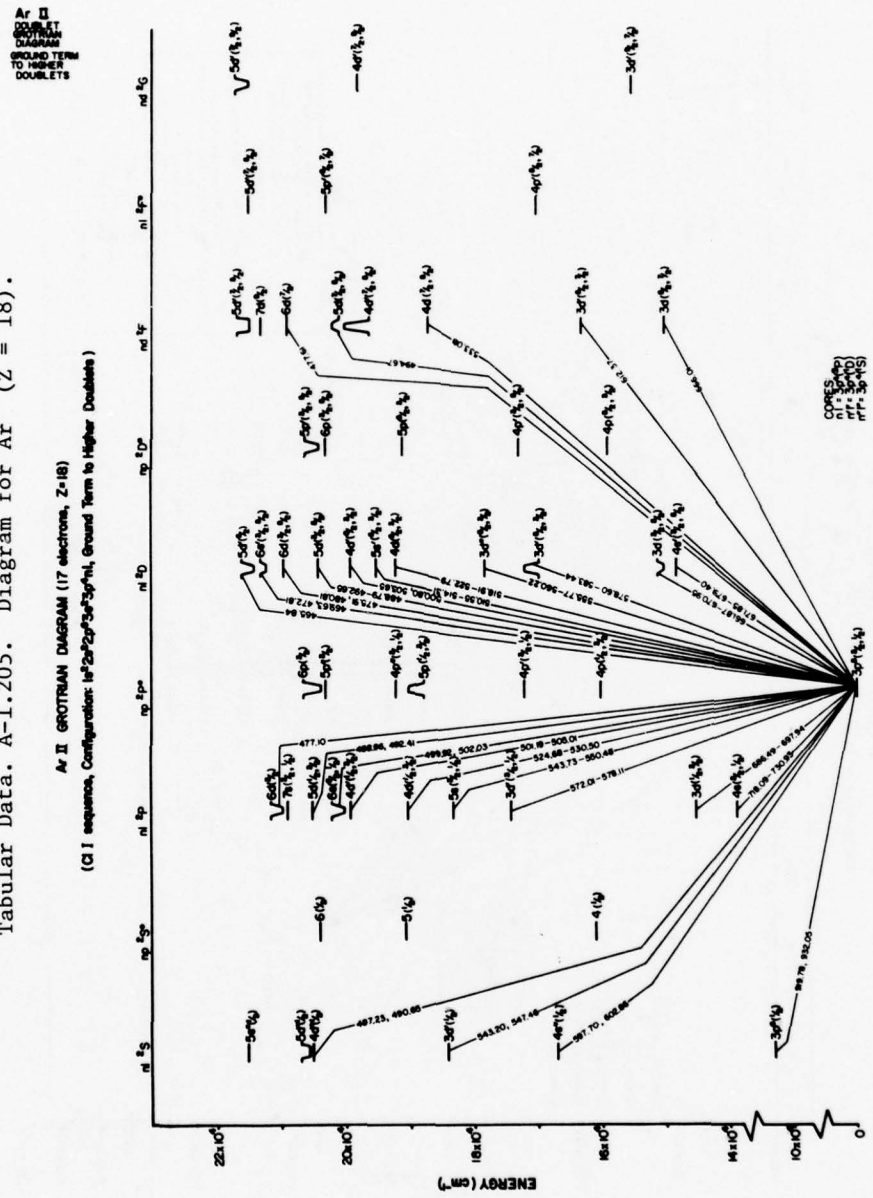

Tabular Data. A-1.206. Diagram for Ar^{+} (Z = 18).

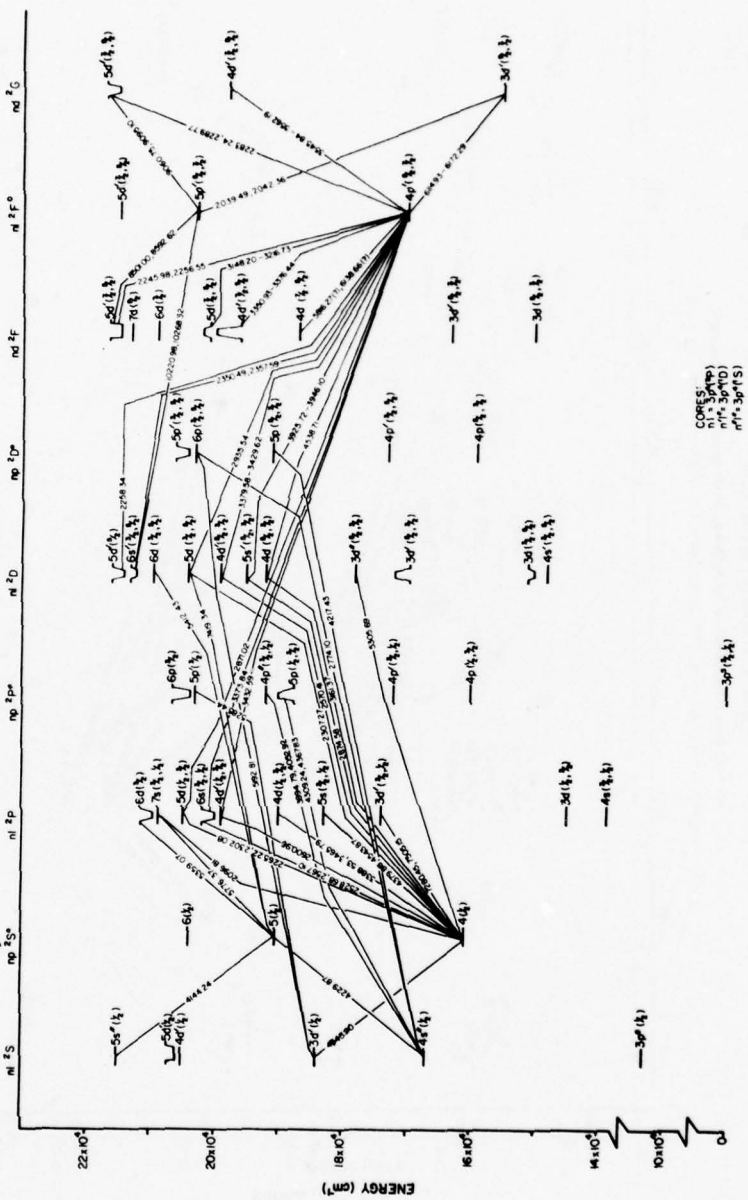

Tabular Data. A-1.207. Diagram for Ar^{+} (Z = 18).

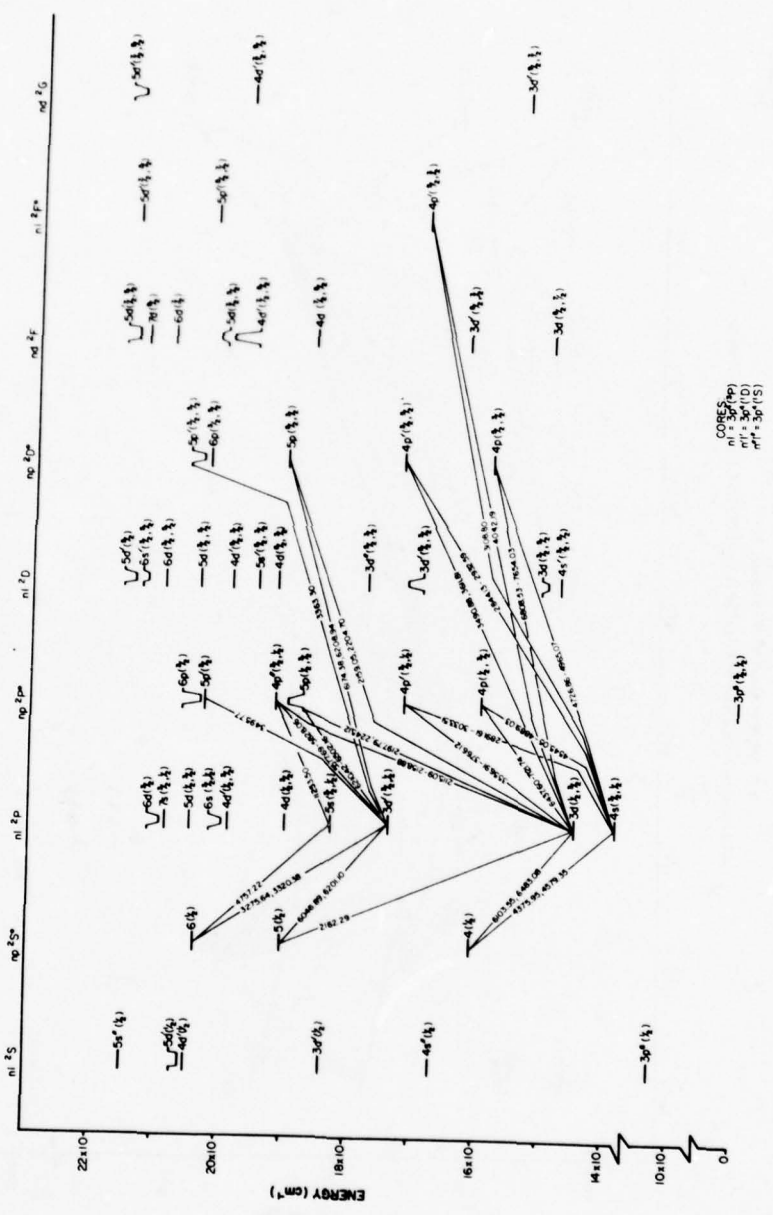

Tabular Data. A-1.208. Diagram for Ar^{+} ($Z = 18$).

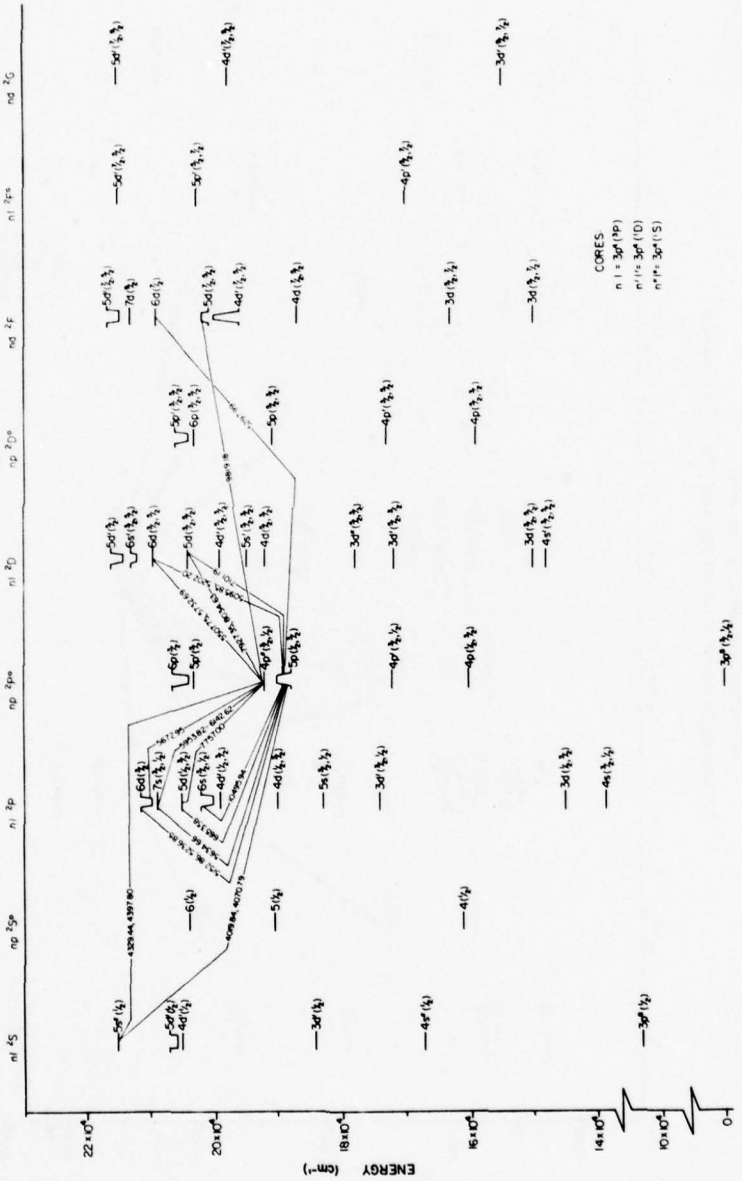

Tabular Data. A-1.209. Diagram for Ar^{+} (Z = 18).

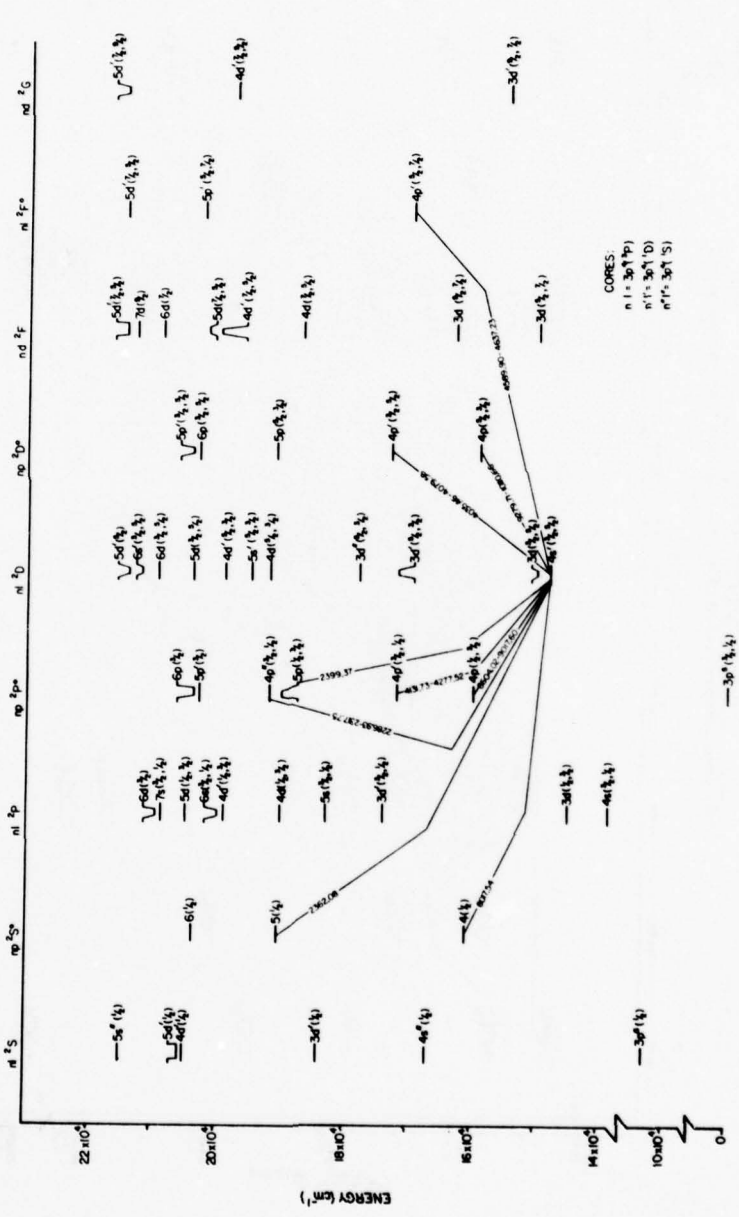

Tabular Data. A-1.210. Diagram for Ar^{+} (Z = 18).

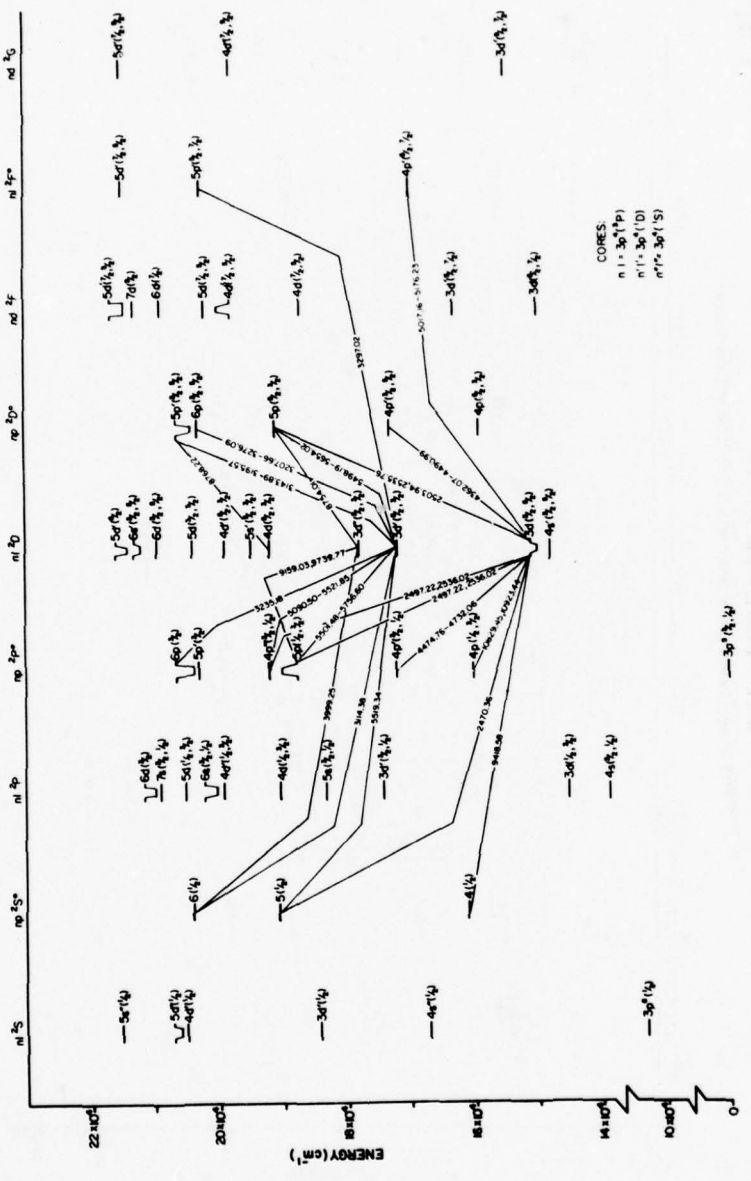

Tabular Data. A-1.211. Diagram for Ar^{+} (Z = 18).

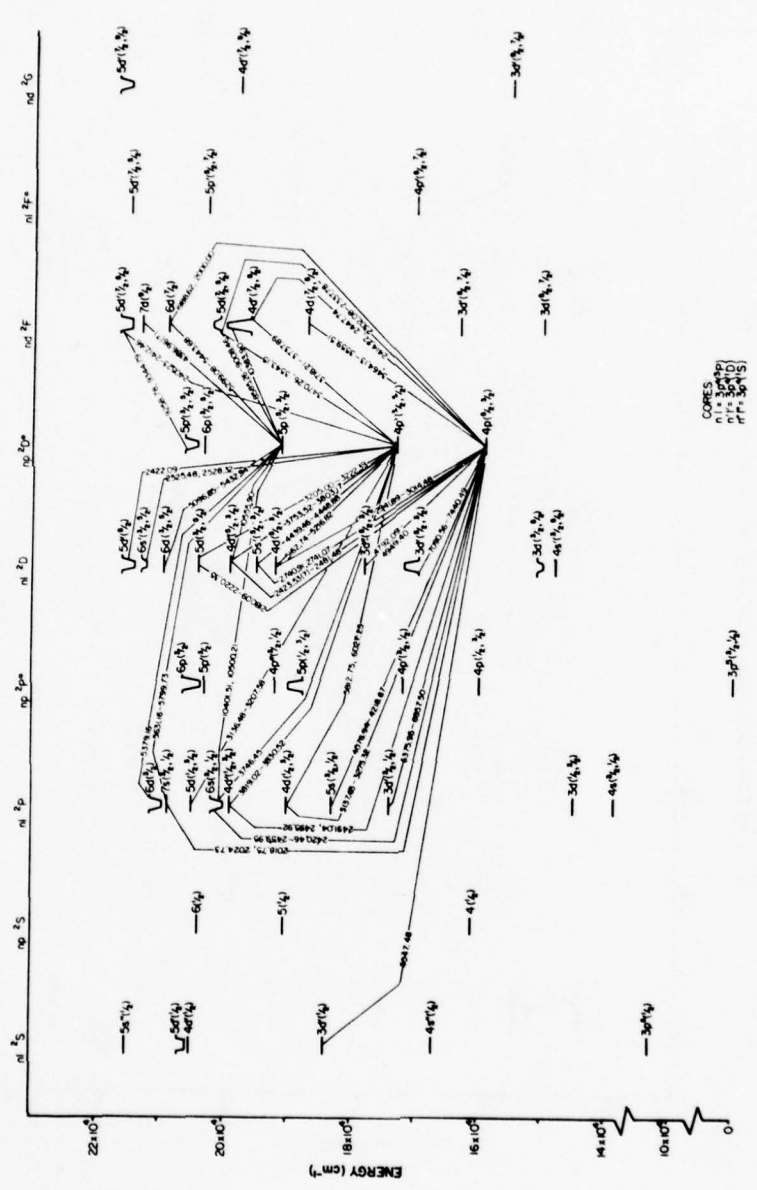

Tabular Data. A-1.212. Diagram for Ar^{+} (Z = 18).

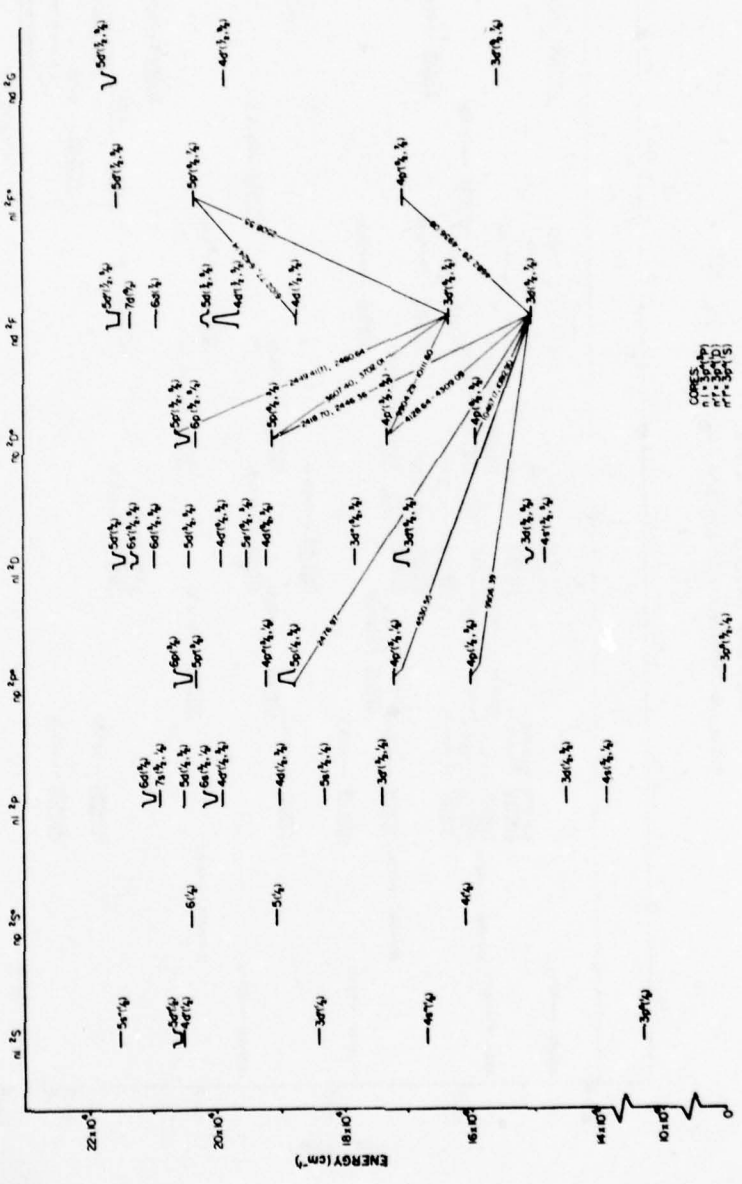

Tabular Data. A-1.213. Diagram for Ar^{+} (Z = 18).

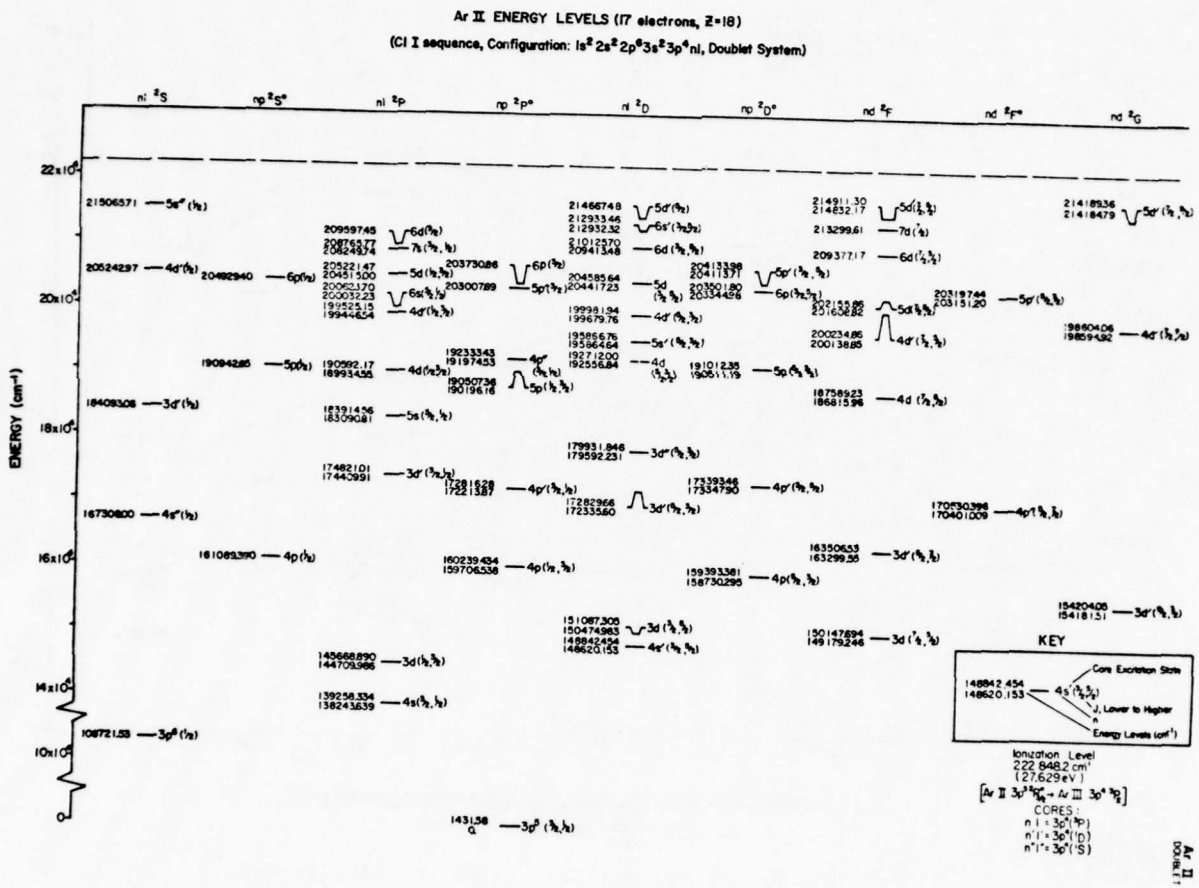

Tabular Data. A-1.214. Diagram for Ar^{+} (Z = 18).

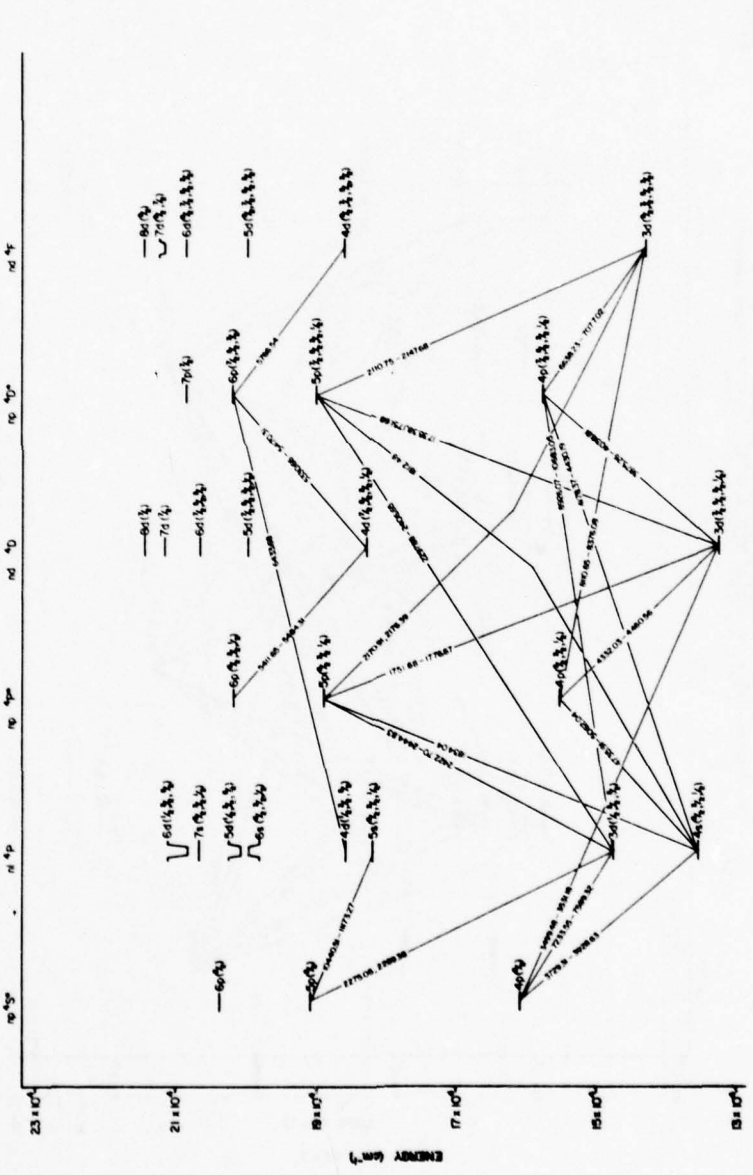

Tabular Data. A-1.215. Diagram for Ar^{+} (Z = 18).

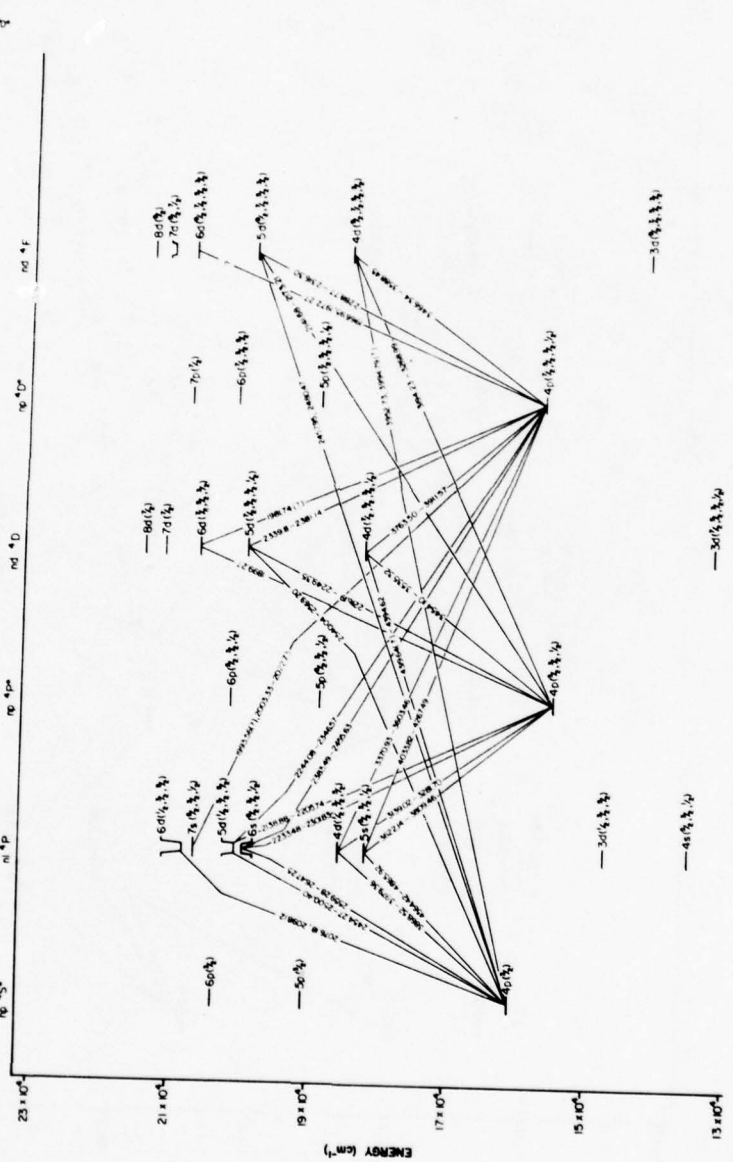

Tabular Data. A-1.216. Diagram for Ar^{+} (Z = 18).

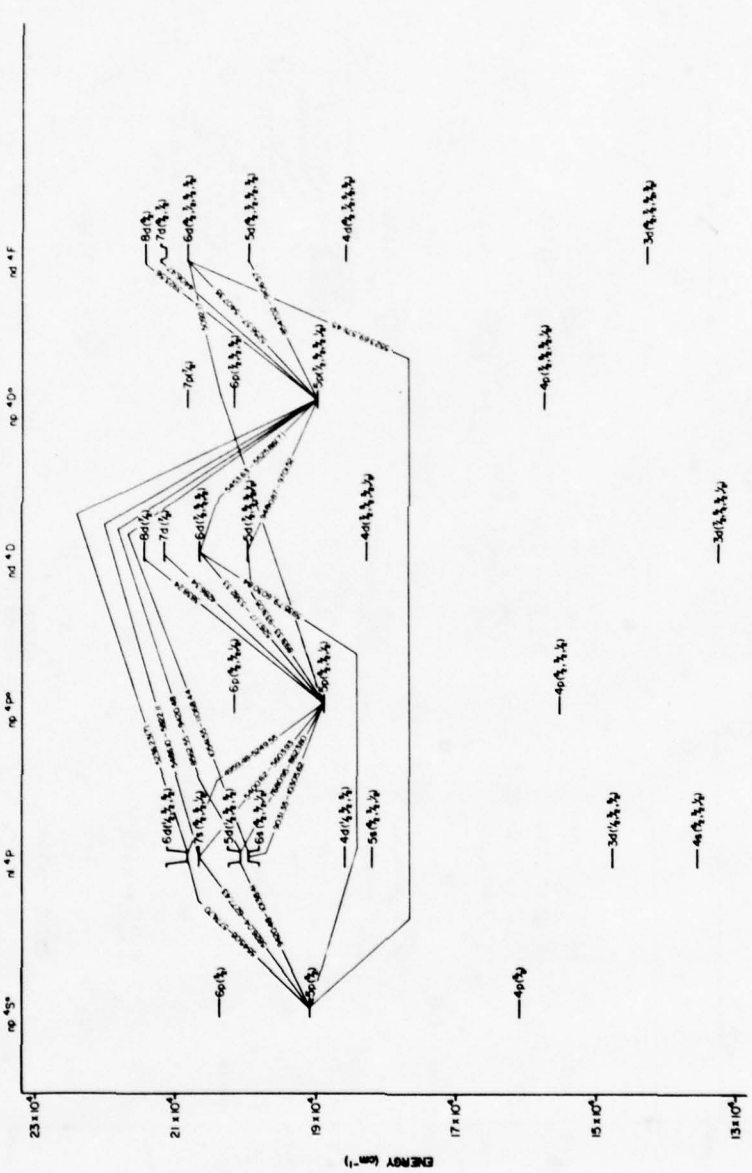

Tabular Data. A-1.217. Diagram for Ar^{+} (Z = 18).

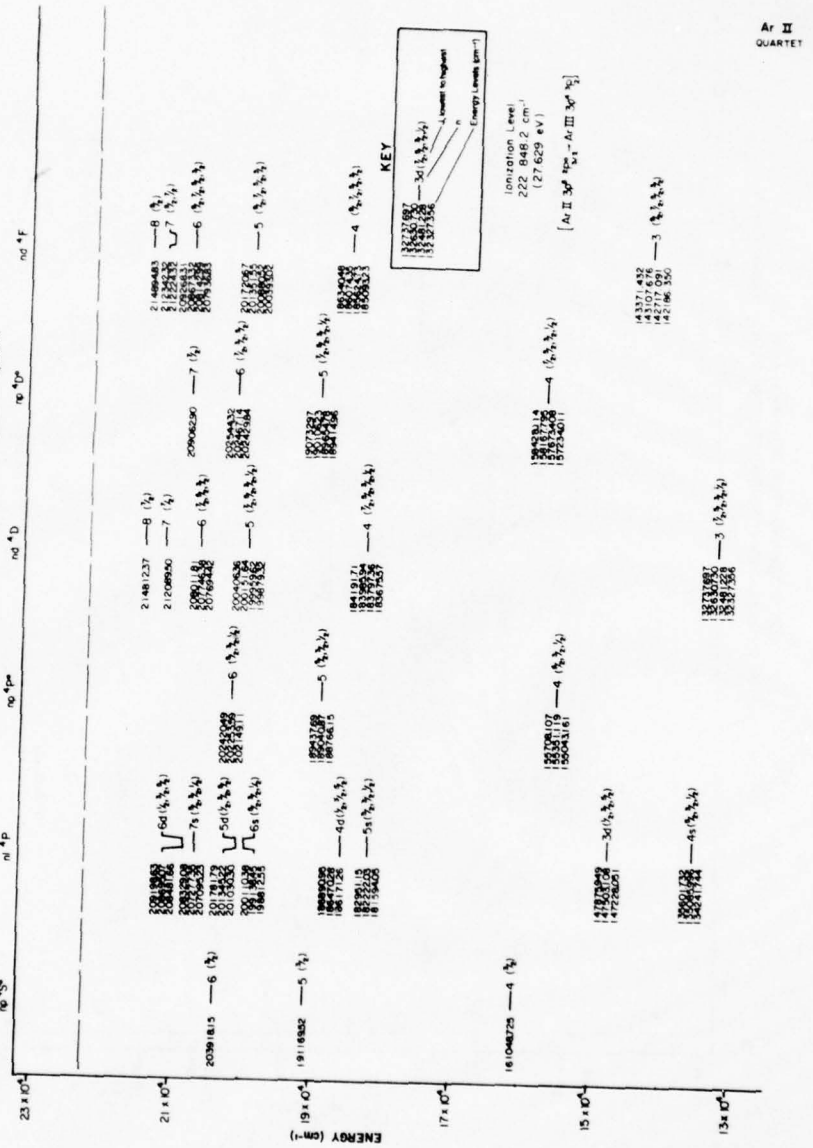

Tabular Data. A-1.218. Diagram for Ar^{+} (Z = 18).

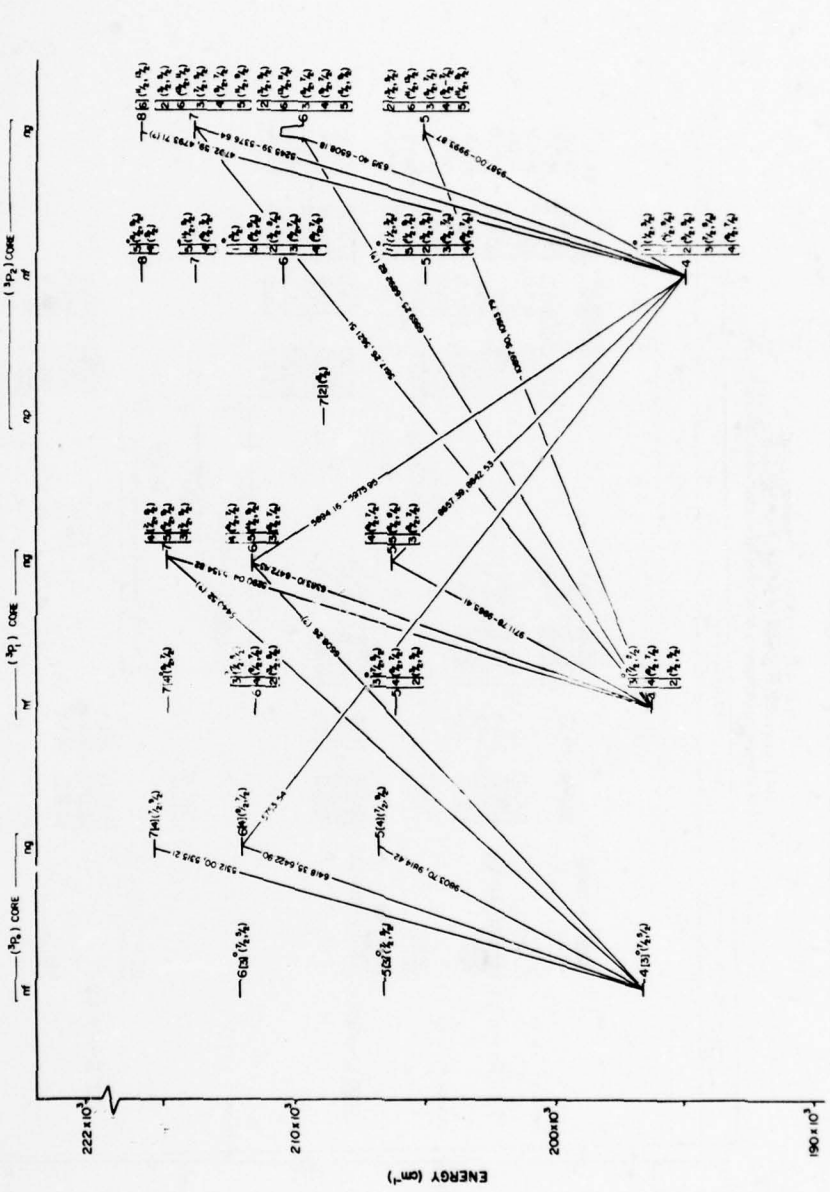

Tabular Data. A-1.219. Diagram for Ar^{+} (Z = 18).

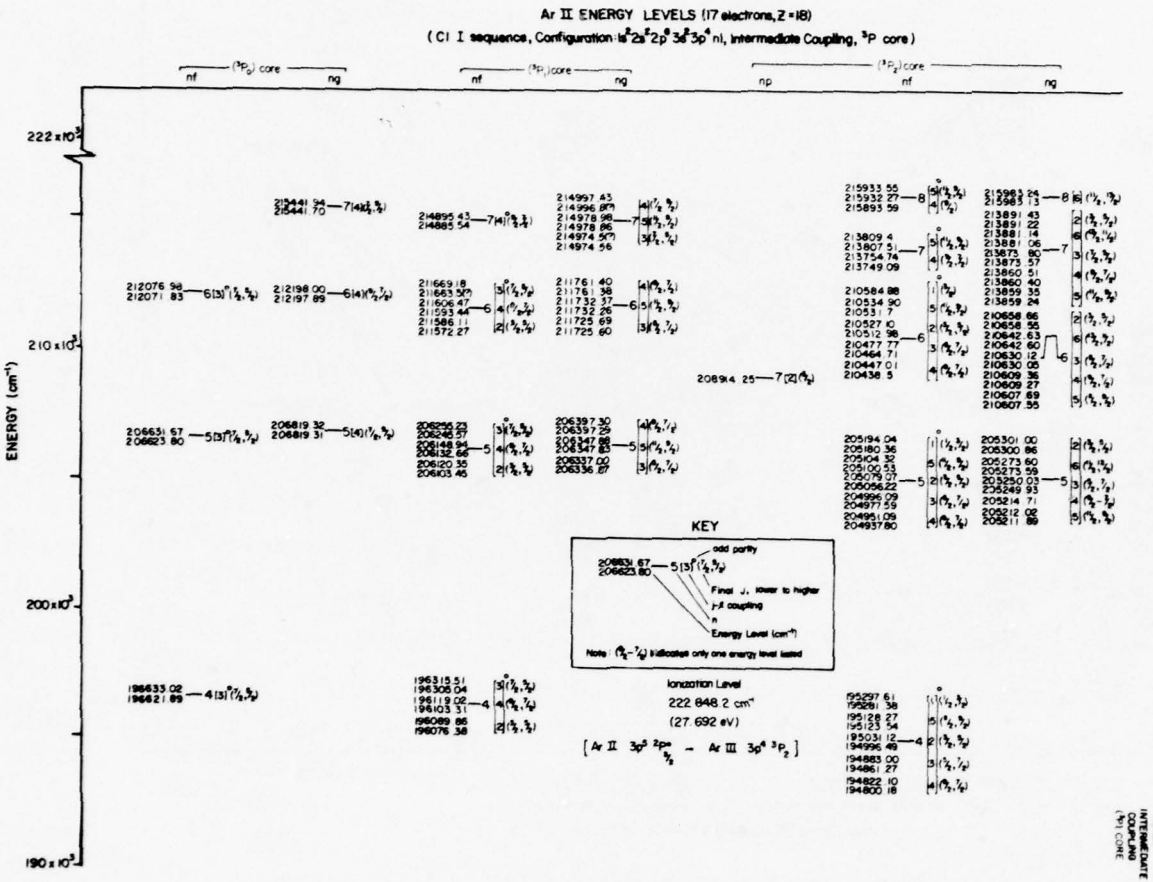

Tabular Data. A-1.220. Diagram for Ar^{+} (Z = 18).

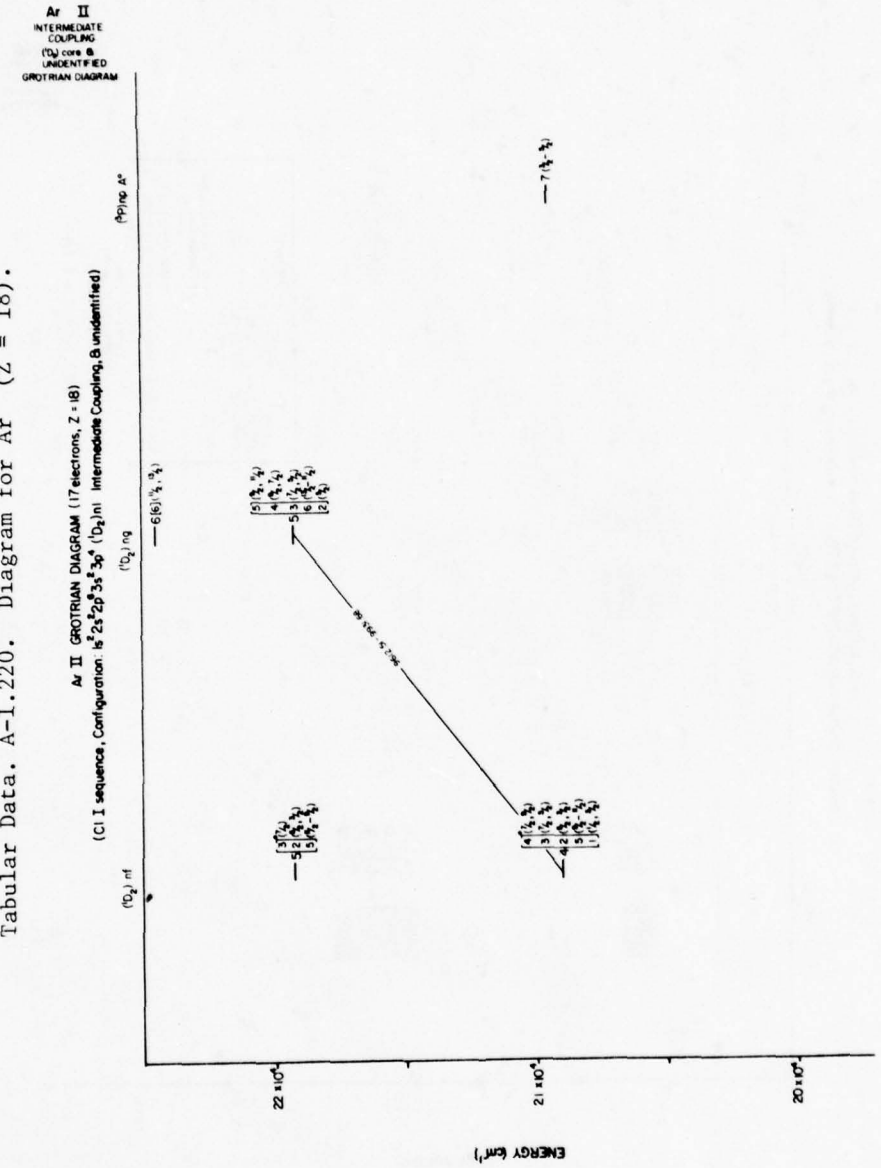

Tabular Data. A-1.221. Diagram for Ar^{+} (Z = 18).

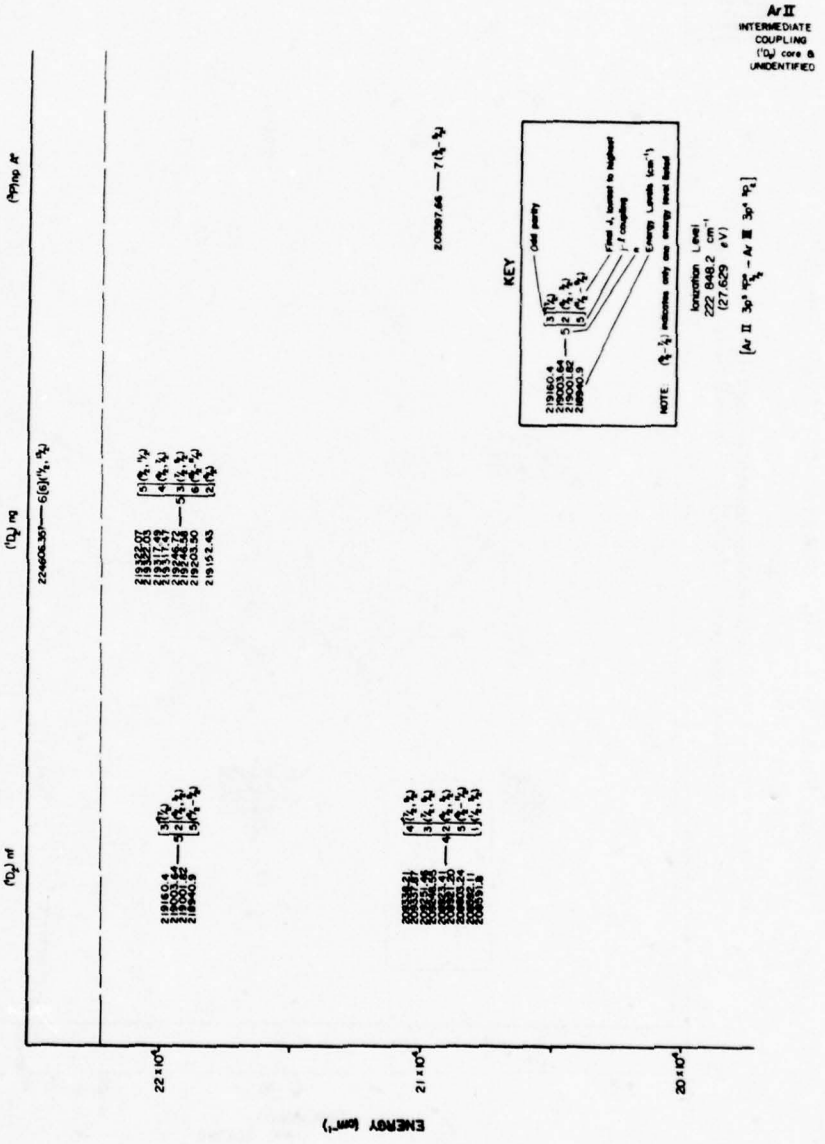

Tabular Data. A-1.222. Diagram for Ar^{+} (Z = 18).

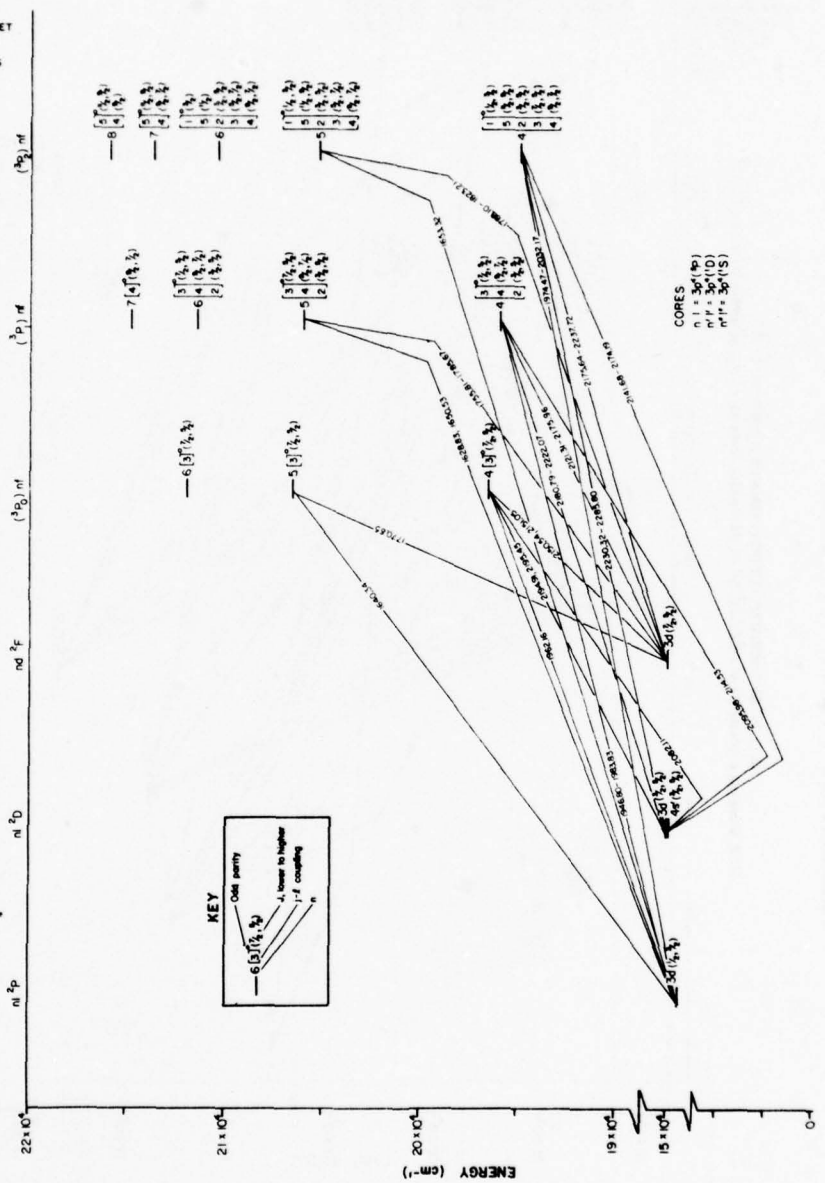

Tabular Data. A-1.223. Diagram for Ar^{+} (Z = 18).

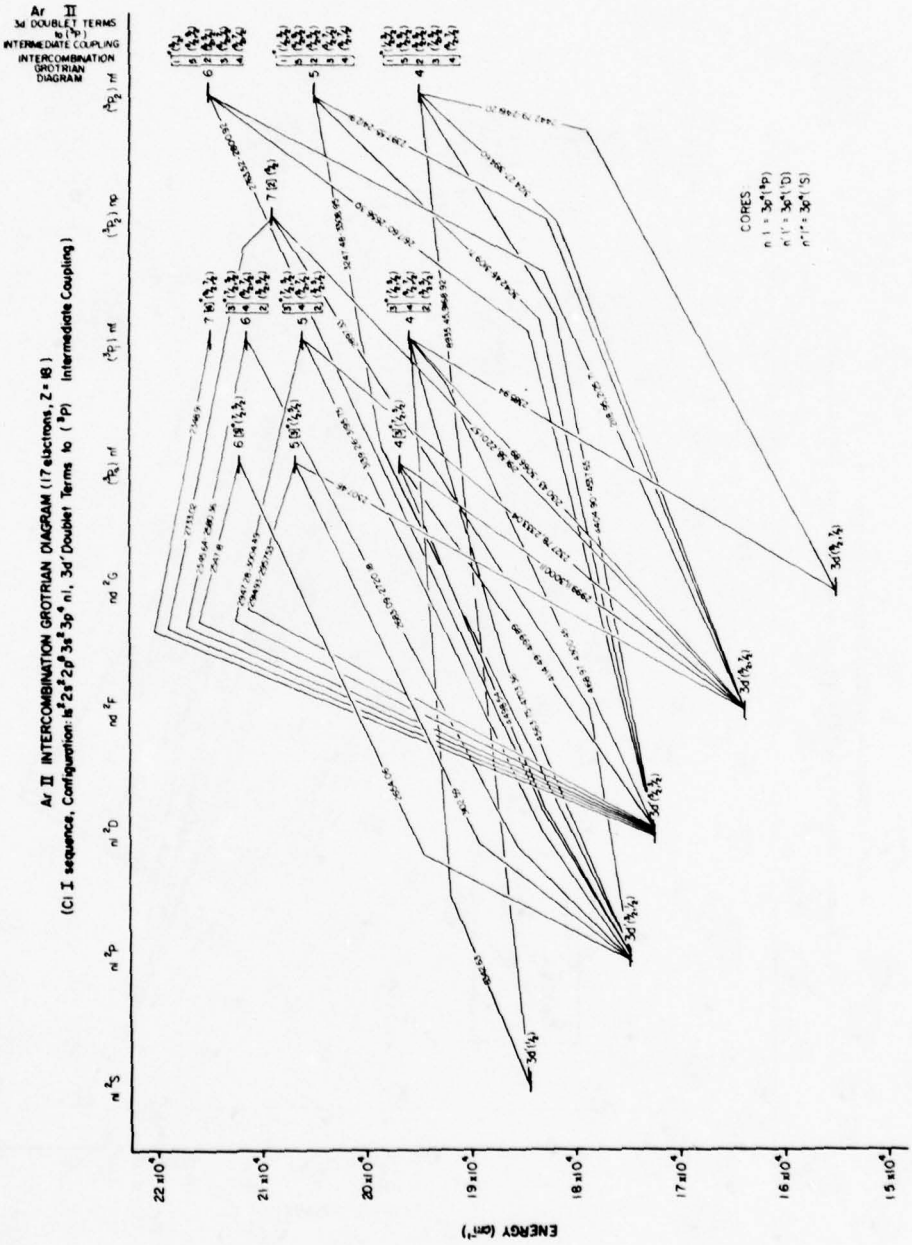

...ular Data. A-1.224. Diagram for Ar^{+} (Z = 18).

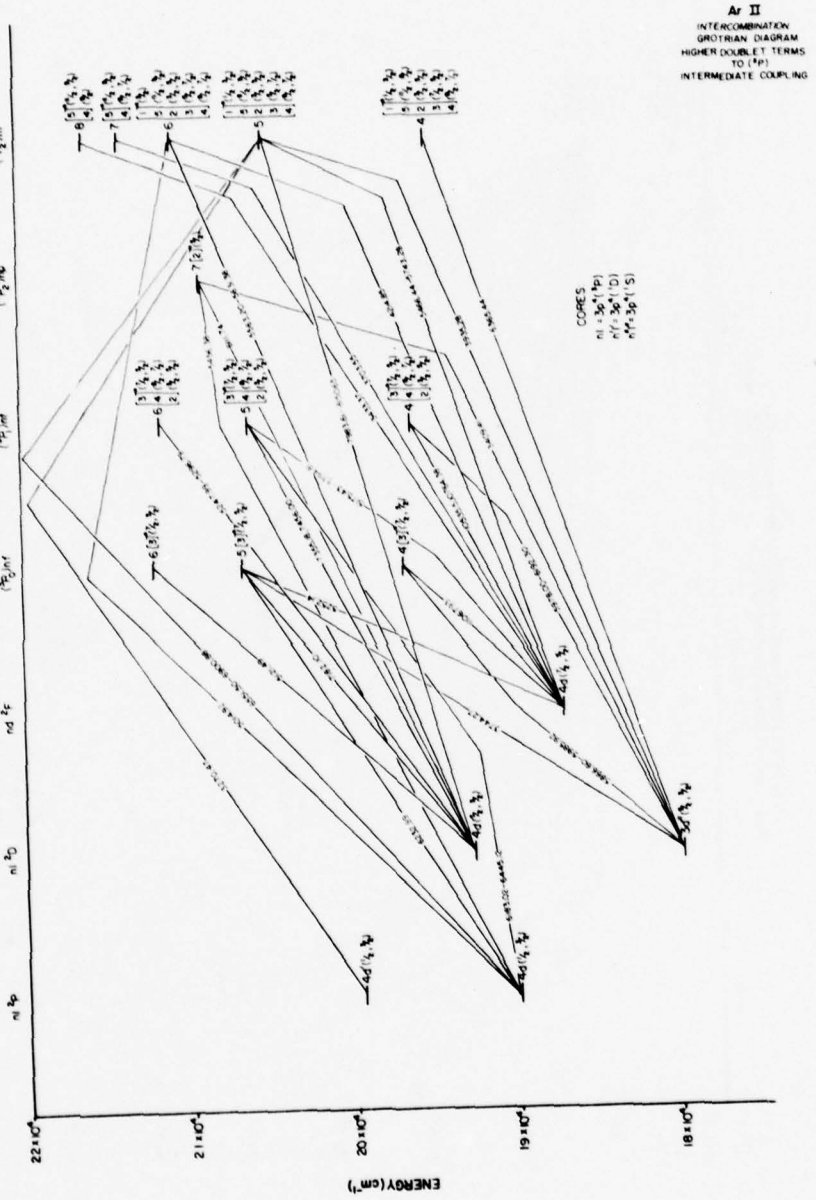

Tabular Data. A-1.225. Diagram for Ar^{+} (Z = 18).

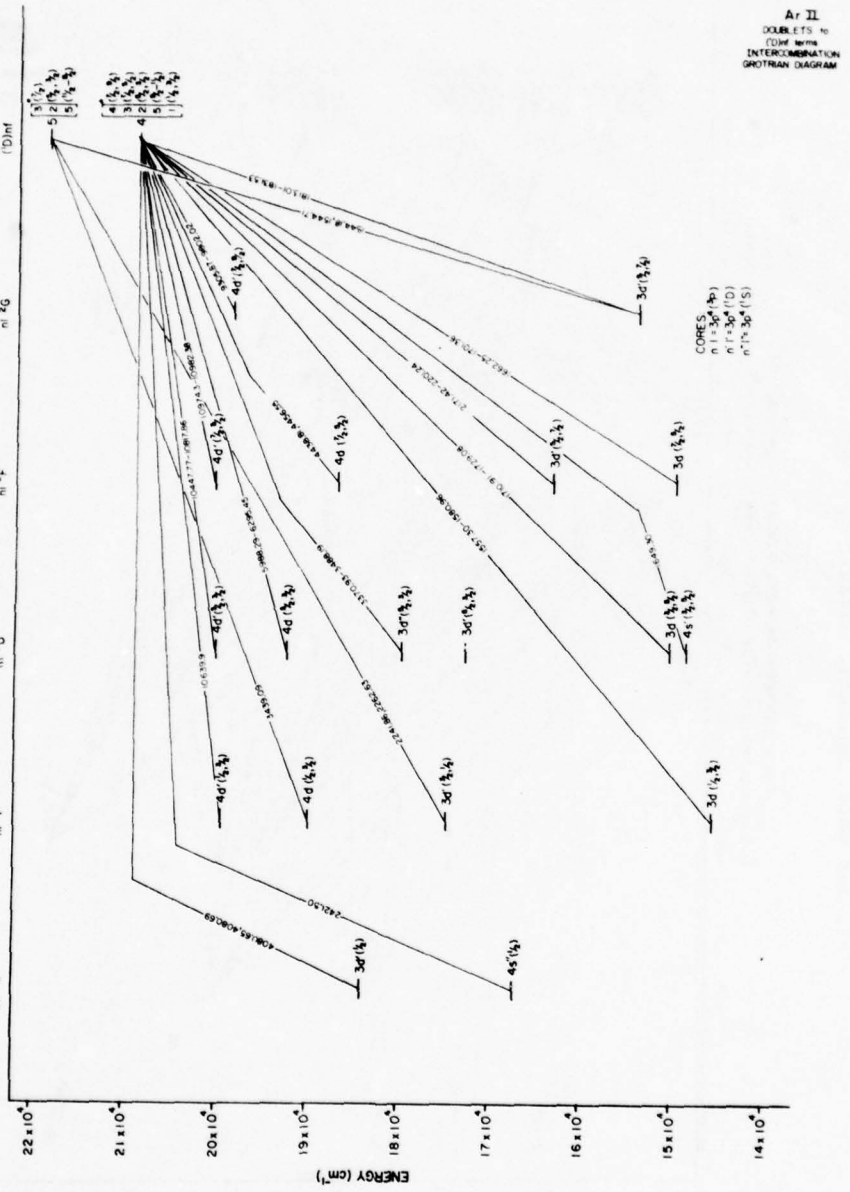

Tabular Data. A-1.226. Diagram for Ar^{+} (Z = 18).

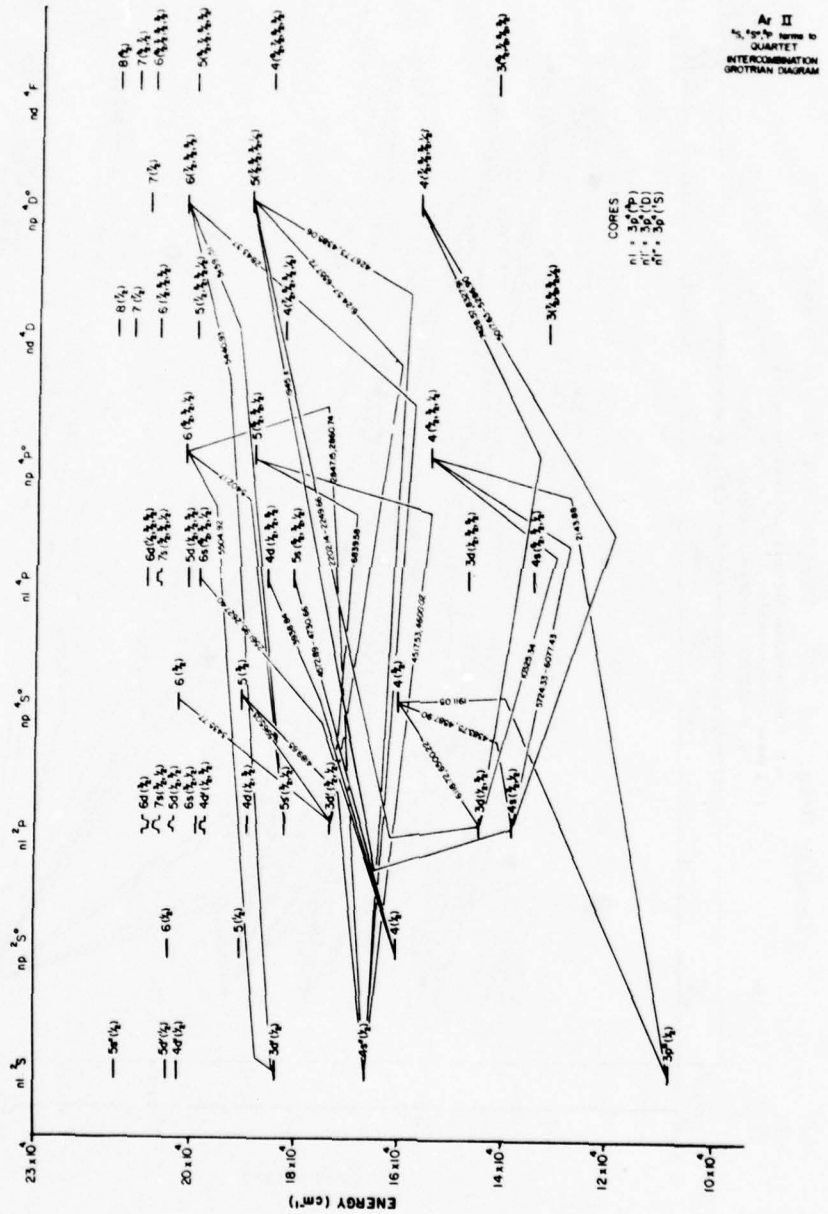

Tabular Data. A-1.227. Diagram for Ar^{+} (Z = 18).

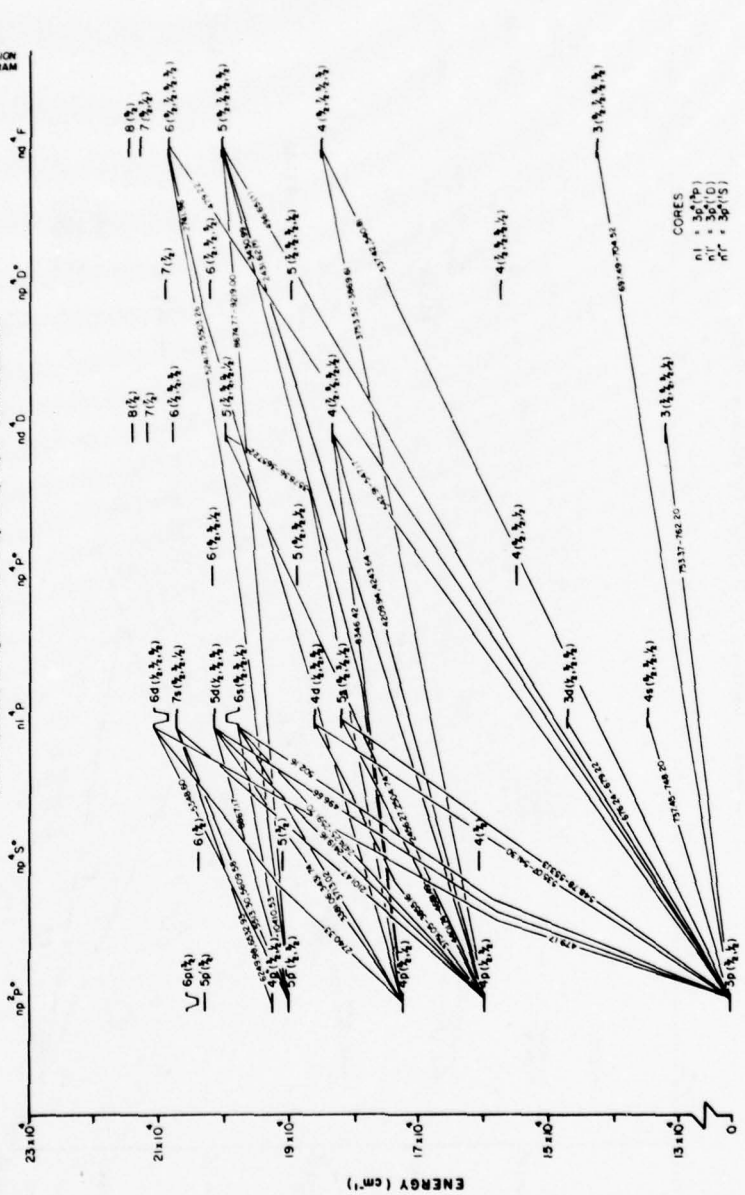

Tabular Data. A-1.228. Diagram for Ar^{+} (Z = 18).

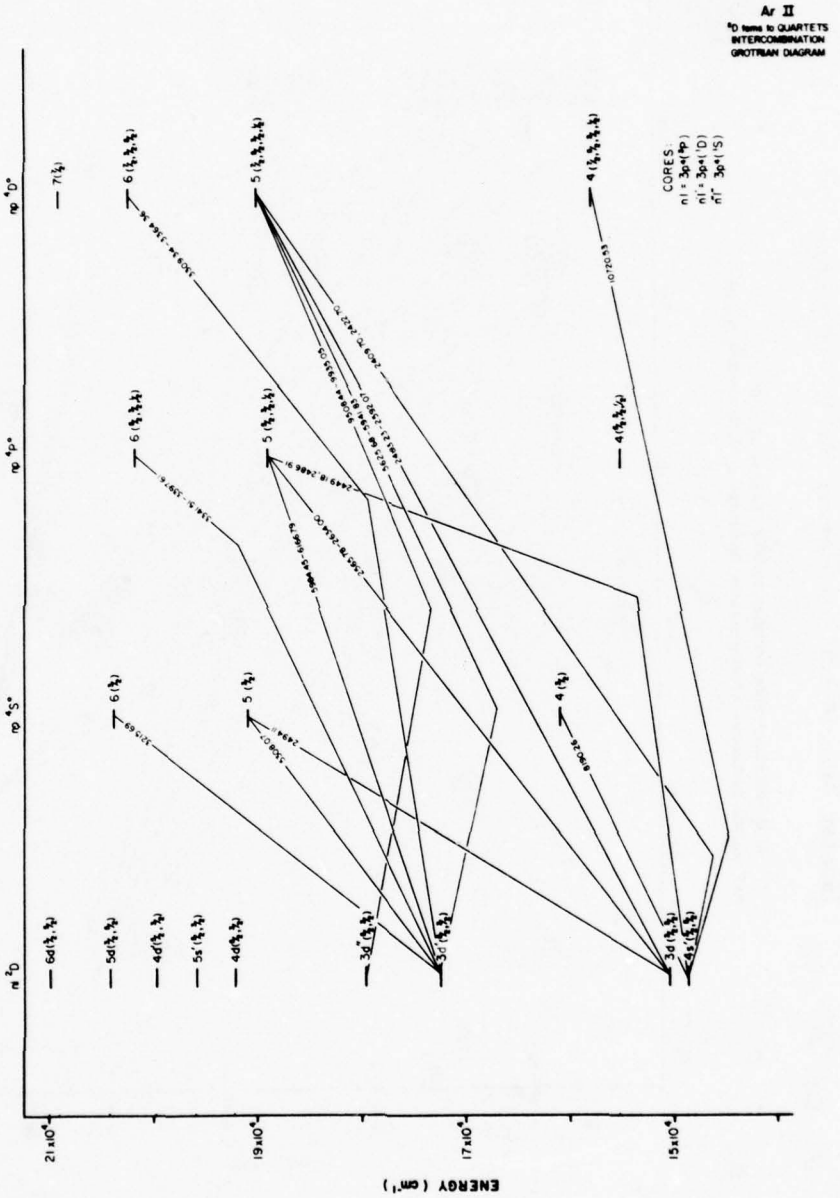

Tabular Data. A-1.229. Diagram for Ar^{+} (Z = 18).

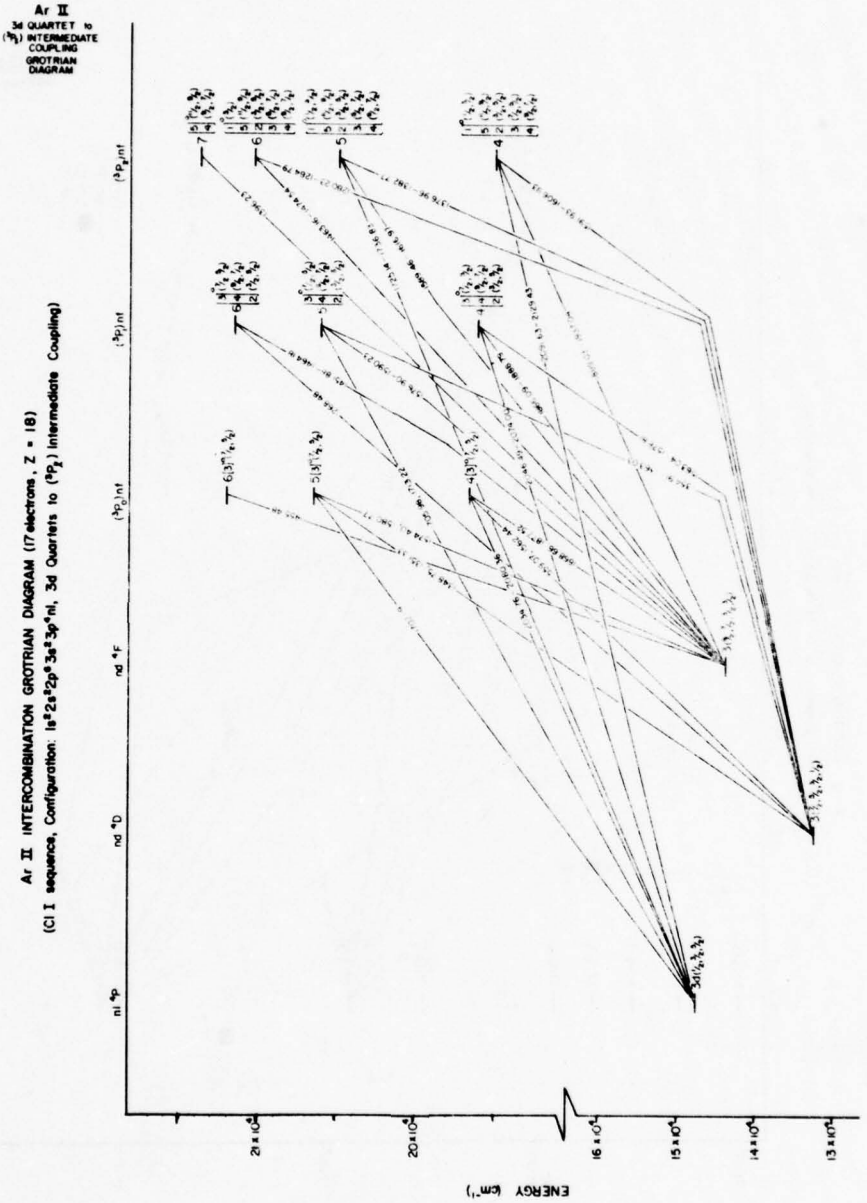

Tabular Data. A-1.230. Diagram for Ar^{+} (Z = 18).

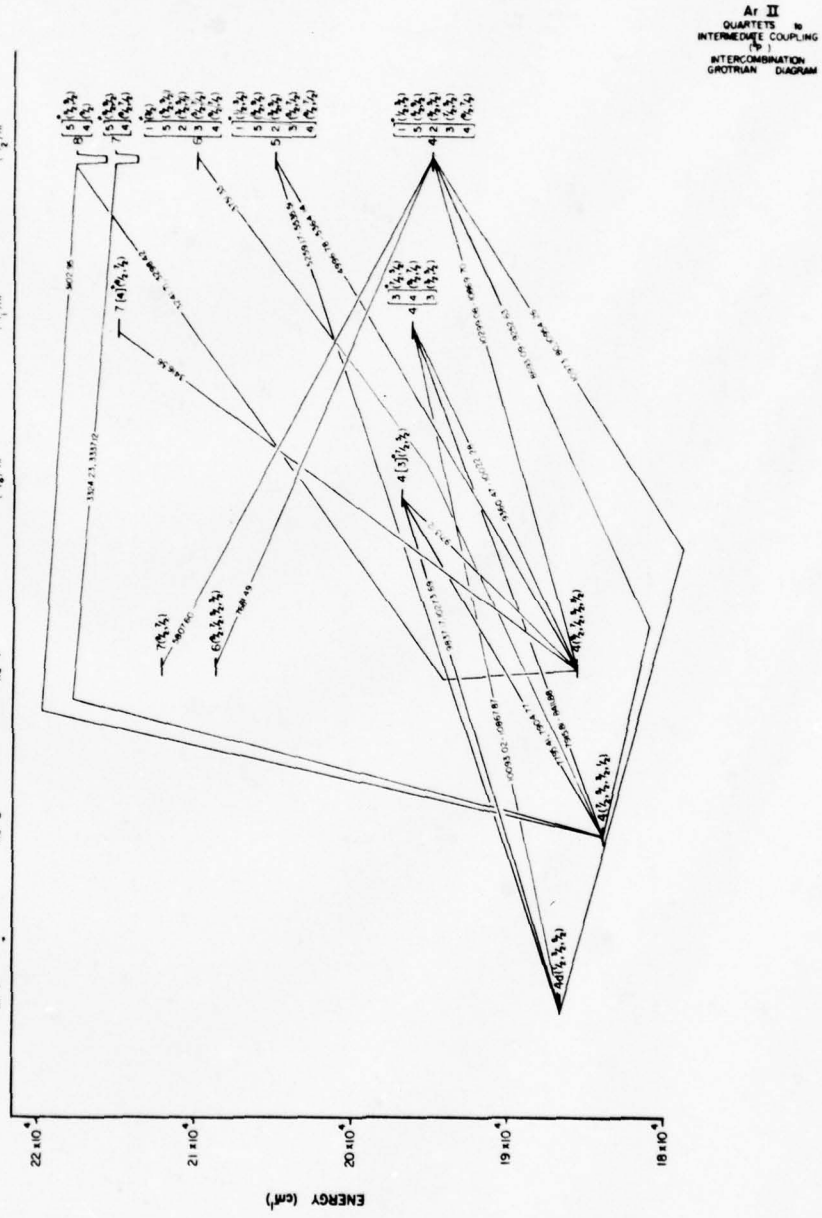

A-2. REFERENCES ON ATOMIC ENERGY LEVELS, SPECTRAL LINES, LIFTIMES, OSCILLATOR STRENGTHS, AND TRANSITION PROBABILITIES*

CONTENTS

		Page
A-2.1.	General References and References to Specific Atoms of Secondary Interest Here	1132
A-2.2.	References on Specific Atoms and Singly-Charged Positive Ions.	1140

*For data on radiative lifetimes of the rare gas atoms and molecules, see pages 194-212 of Vol. I.

PRECEDING PAGE BLANK

A-2.1. General References and References to Specific Atoms of Secondary Interest Here

S. Bashkin and J. O. Stoner, "Atomic Energy Levels and Grotrian Diagrams — Vol. I: Hydrogen I — Phosphorus XV," (North-Holland, Amsterdam 1975). Also "Addenda" (1978).

S. Bashkin and J. O. Stoner, "Atomic Energy Levels and Grotrian Diagrams — Vol. II: Sulfur I — Titanium XXII," (Elsevier - North-Holland, Amsterdam, 1978). Additional volumes dealing with other atoms and ions are in preparation.

J. A. Bearden and A. F. Burr, "Atomic Energy Levels," USAEC Division of Technical Information, Final Report, Washington, D.C. (NYO-2543-1), 244 (1965). Rev. Mod. Phys. 39, 125 (1967).

E. Biemont and N. Grevesse, Infrared Wavelengths and Transition Probabilities for Atoms, $3<Z<20$," Atomic Data and Nuclear Data Tables 12, 217 (1973).

T. A. Carlson, C. W. Nestor, Jr., N. Wasserman, and J. D. McDowell, "Calculated Ionization Potentials for Multiply Charged Ions," Atomic Data 2, 63 (1970).

A. Corney, "The Measurement of Lifetimes of Free Atoms, Molecules, and Ions," in L. Marton (Ed.), "Advances in Electronics and Electron Physics" 29, 116 (Academic, New York, 1970).

C. Corliss and J. Sugar, "Energy Levels of Manganese, Mn I through Mn XXV," Jour. Phys. Chem. Ref. Data 6, (4), 1253 (1977).

M. Crance, "Theoretical Transition Probabilities and Energy Levels in Ne I Isoelectronic Sequence," Atomic Data 5, 185 (1973).

R. J. S. Crossley, "The Calculation of Atomic Transition Probabilities," in D. R. Bates and I. Estermann (Eds.), "Advances in Atomic and Molecular Physics" 5, 237 (Academic, New York, 1969).

A. Dalgarno. "Spontaneous Two-Photon Transitions in Hydrogen and Helium," in F. Bopp and H. Kleinpoppen (Eds.), "Physics of the One- and Two-Electron Atoms," 261 (North-Holland, Amsterdam, 1970).

J. P. Desclaux, "Relativistic Dirac-Fock Expectation Values for Atoms with $Z=1$ to $Z=120$," Atomic Data and Nuclear Data Tables 12, 311 (1973).

H. T. Doyle, "Relativistic Z Dependent Corrections to Atomic Energy Levels," in D. R. Bates and I. Estermann (Eds.), "Advances in Atomic and Molecular Physics" 5, 337 (Academic, New York, 1969).

G. W. F. Drake, "Radiative Decay of the Metastable States of the H and He Sequences - Theory," in S. J. Smith and G. K. Walters (Eds.), "Atomic Physics 3," 269 (Plenum, New York, 1973).

G. W. Erickson, "Energy Levels of One-Electron Atoms," Jour. Phys. Chem. Ref. Data 6, (3), 831 (1977).

U. Fano and J. W. Cooper, "Spectral Distribution of Atomic Oscillator Strengths," Rev. Mod. Phys. 40, 441 (1968). See Addendum 41, 724 (1969).

B. C. Fawcett, "Wavelengths and Classifications of Emission Lines Due to $2s^2 2p^n - 2s2p^{n+1}$ and $2s2p^n - 2p^{n+1}$ Transitions, $Z \leq 28$," Atomic Data and Nuclear Data Tables 16, 135 (1975).

C. F. Fischer, "Average-Energy-of-Configuration Hartree-Fock Results for the Atoms Helium to Radon," Atomic Data and Nuclear Data Tables 4, 301 (1972), Erratum 12, 87 (1973).

S. Fraga, K. M. S. Saxena, and B. W. N. Lo, "Hartree-Fock Values of Energies, Interaction Constants, and Atomic Properties for Groundstates of Negative Ions, Neutral Atoms, and First Four Positive Ions from Helium to Krypton," Atomic Data 3, 323 (1971).

S. Fraga and K. M. S. Saxena, "Hartree-Fock Values of Energies, Interaction Constants, and Atomic Properties for Excited States with p^N Configurations of Negative Ions, Neutral Atoms, and First Positive Ions from Boron to Bromine," Atomic Data 4, 255 (1972).

S. Fraga and K. M. S. Saxena, "Hartree-Fock Values of Energies, Interaction Constants, and Atomic Properties for Excited States with $3d^N 4s^0$ and $3d^N 4s^2$ Configuration of Negative Ions, Neutral Atoms, and First Four Positive Ions of Transition Elements," Atomic Data 4, 269 (1972).

J. B. Fuhr, B. J. Miller, and G. A. Martin, "Bibliography on Atomic Transition Probabilities," (1914 through October 1977), National Bureau of Standards (U.S.) Special Publication 505, U.S. Government Printing Office, Washington, D.C. (April, 1978).

A. H. Gabriel, "Spectral Intensities from Helium-Like Ions," in T. R. Carson and M. J. Roberts (Eds.), "Atoms and Molecules in Astrophysics," 311 (Academic, New York, 1972).

L. Hagan, "Bibliography on Atomic Energy Levels and Spectra," (July 1971 through June 1975), National Bureau of Standards (U.S.) Special Publication 363, Supplement 1, U.S. Government Printing Office, Washington, D.C. (January 1977).

G. R. Harrison, "Wavelength Tables with Intensities in Arc, Spark, or Discharge Tube of More than 100,000 Spectrum Lines, Most Strongly Emitted by the Atomic Elements Under Normal Conditions of Excitation Between 10,000 A and 2,000 A Arranged in Order of Decreasing Wavelengths," 463 (MIT Press, Cambridge, Massachusetts, 1969).

C. J. Humphreys, "First Spectra of Neon, Argon, and Xenon 136 in the 1.2-4.0 μm Region," J. Phys. Chem. Ref. Data 2, 519-530 (1973).

J. Karwowski, K. M. S. Saxena, B. Bray, and S. Fraga, "Atomic Energy Levels: Isoelectronic Series 2psup(N), 3psup(N), 4psup(N), and 3dsup(N)," Alberta University, Edmonton (Canada), Division of Theoretical Chemistry, Technical Report (TC-AEL-1-75), 59 pages (1975).

V. Kaufman and B. Edlen, "Reference Wavelengths from Atomic Spectra in the Range 15 A to 25000 A," J. Phys. Chem. Ref. Data 3, 825-895 (1974).

R. L. Kelly and D. E. Harrison, Jr., "Ionization Potentials, Experimental and Theoretical, of Elements Hydrogen to Krypton," Atomic Data 3, 177 (1971).

R. L. Kelly and L. J. Palumbo, "Atomic and Ionic Emission Lines Below 2,000 Angstroms, Hydrogen through Krypton," Naval Research Laboratory, Washington, D.C. (NRL-7599) 1003 pages (June 1973).

L. Lang (Ed.), "Absorption Spectra in the Ultraviolet and Visible Region" 1, 20, 438 pages (Akademiai Kiado, Budapest, Hungary, 1966-1975).

L. Lang (Ed.), "Absorption Spectra in the Ultraviolet and Visible Region, A Theoretical and Technical Introduction, Third Edition, 80 pages (Akademiai Kiado, Budapest, Hungary (1963).

I. Lindgren and A. Rosén, "Relativistic Self-Consistent-Field Calculations with Application to Atomic Hyperfine Interaction. Part I: Relativistic Self-Consistent Fields, Part II: Relativistic Theory of Atomic Hyperfine Interaction," in E. W. McDaniel and M. R. C. McDowell (Eds.), "Case Studies in Atomic Physics" 4, 97 (North-Holland, Amsterdam, 1975).

I. Lindgren and A. Rosén, "Relativistic Self-Consistent-Field Calculations with Atomic Hyperfine Interaction. Part III: Comparison Between Theoretical and Experimental Hyperfine-Structure Results," in E. W. McDaniel and M. R. C. McDowell (Eds.), "Case Studies in Atomic Physics" 4, 199 (North-Holland, Amsterdam, 1975).

L. Lipsky, "Energy Levels and Classifications of Doubly Excited States in Two-Electron Systems (Z = 1,2,3,4,5) Below the N = 2 and N = 3 Thresholds," Atomic Data and Nuclear Data Tables 20, 127 (1977).

C. C. Lu, T. A. Carlson, F. B. Malik, T. C. Tucker, and C. W. Nestor, Jr., "Relativistic Hartree-Fock-Slater Eigenvalues, Radial Expectation Values, and Potentials for Atoms, 2<Z<126," Atomic Data 3, 1 (1971) Erratum 14, 89 (1974).

W. C. Martin, "Energy Levels of Neutral Helium (^{4}He I)," J. Phys. Chem. Ref. Data 2, 257-266 (1973).

G. A. Martin and W. L. Wiese, "Tables of Critically Evaluated Oscillator Strengths for the Lithium Isoelectronic Sequence," J. Phys. Chem. Ref. Data 5, 537 (1976).

W. C. Martin, et al., "Ground Levels and Ionization Potentials for Lanthanide and Actinide Atoms and Ions," Jour. Phys. Chem. Ref. Data 3, 771 (1974).

W. C. Martin, R. Zalubas, and L. Hagan, "Atomic Energy Levels - The Rare-Earth Elements," NSRDS-NBS 60, 422 pages (1978). For sale by Superintendent of Documents, U.S. Government Printing Office, Washington, D.C. 20402.

D. L. Mathews, B. M. Johnson, and C. F. Moore, "Calculated K Auger-Electron and K X-Ray Transition Energies for the Multiply Ionized Neon Atom," Atomic Data and Nuclear Data Tables 15, 41 (1975).

W. F. Meggers, C. H. Corliss, and B. F. Scribner, "Tables of Spectral-Line Intensitities, Part 1," Arranged by Elements, Supersedes NBS-Monograph-32 (Vols. 1 and 2) and Its Supplement NBS Monograph 145, 387 pages, U.S. Department of Commerce, Washington, D.C. (May 1975).

W. F. Meggers, C. H. Corliss, and B. F. Scribner, "Tables of Spectral-Line Intensities, Part 2," Arranged by Wavelengths, Supersedes NBS-Monograph-32, Part 1 and 2 and its supplements, Second Edition, 228 pages [NBS-Monograph-145 (pt. 2)], U.S. Department of Commerce, Washington, D.C. (May 1975)

B. M. Miles and W. L. Wiese, "Critically Evaluated Transition Probabilities for Ba I and II," National Bureau of Standards (U.S.), Technical Note 474, U.S. Government Printing Office, Washington, D.C. (1969); At. Data 1, 1-17 (1969).

B. M. Miles and W. L. Wiese, "Bibliography on Atomic Transition Probabilities (January 1916 through June 1969)," National Bureau of Standards (U.S.), Special Publication 320. U.S. Government Printing Office, Washington, D.C. (1970).

C. E. Moore, "Selected Tables of Atomic Spectra, Part A, B. Atomic Energy Levels (Second Edition). Multiplet Tables, N I, N II, N III," National Bureau of Standards, Washington, D.C., National Standard Reference Data System (NSRDS-NBS-3, Section 5)(May 1975).

C. E. Moore, "Selected Tables of Atomic Spectra, Part A, B. Atomic Energy Levels (Second Edition). Multiplet Tables, H I, D, T." National Bureau of Standards, Washington, D.C., National Standard Reference Data System (NSRDS-NBS-3, Section 6)(September 1972).

C. E. Moore, "Selected Tables of Atomic Spectra, Atomic Energy Levels and Multiplet Tables of O," U.S. Department of Commerce, Washington, D.C. (NSRDS-NBS-3, Section 7)(1976).

C. E. Moore, "Atomic Energy Levels, As Derived from the Analysis of Optical Spectra. Vol. 1 - The Spectra of Hydrogen, Deuterium, Tritium, Helium, Lithium, Beryllium, Boron, Carbon, Nitrogen, Oxygen, Fluorine, Neon, Sodium, Magnesium, Aluminum, Silicon, Phosphorus, Sulfur, Chlorine, Argon, Potassium, Calcium, Scandium, Titanium, and Vanadium," National Bureau of Standards, Washington, D.C., National Standard Reference Data System (NSRDS-NBS-35, Vol. 1). Reprint of NBS-Circ-467 1, 359 pages (December 1971).

C. E. Moore, "Atomic Energy Levels. As Derived from the Analysis of Optical Spectra. Vol. 2 - The Spectra of Chromium, Magnesium, Iron, Cobalt, Nickel, Copper, Zinc, Gallium, Germanium, Arsenic, Selenium Bromine, Krypton, Rubidium, Strontium, Yttrium, Zicronium, and Niobium," National Bureau of Standards, Washington, D.C., National Standard Reference Data System, Reprint of NBS-Circ-467, Vol. 2 (NSRDS-NBS-35, Vol. 2), 227 pages (December 1971).

C. E. Moore, "Atomic Energy Levels. As Derived from the Analyses of Optical Spectra. Vol. 3 - The Spectra of Molybdenum, Technetium, Ruthenium, Rhodium, Palladium, Silver, Cadmium, Indium, Tin, Antimony, Tellurium, Iodine, Xenon, Cesium, Barium, Lanthanum-Hafnium, Tantalum, Tungsten, Rhenium, Osmium, Iridum, Platinum, Gold, Mercury, Thallium, Lead, Bismuth, Polonium, Radon, Radium, and Actinium," National Bureau of Standards, Washington, D.C., National Standard Reference Data System. Reprint of NBS-Circ-467 (Vol. 3)(NSRDS-NBS-35, Vol. 3), 245 pages (December 1971).

C. E. Moore, "Ionization Potentials and Ionization Limits Derived from the Analyses of Optical Spectra," National Bureau of Standards, Washington, D.C., National Standard Reference Data System, National Standard Reference Data Service, National Bureau of Standards (NSRDS-NBS-34), 34 8 pages (September 1970).

C. E. Moore, "Atomic Energy Levels," U.S. Government Printing Office, Washington, D.C., National Bureau of Standards Circular 467 I-III (1949, 1952, and 1958).

C. E. Moore and P. W. Merrill, "Partial Grotrian Diagrams of Astrophysical Interest," Appendix A of Lines of the Chemical Elements in Astronomical Spectra, Carnegie Institution of Washington Publication 610 (1958). Reprinted as NSRDS-NBS-23.

C. E. Moore, "Multiplet Table of Astrophysical Interest, Part 1, 2, Table of Multiplets. Finding List of All Lines in the Table of Multiplets," National Bureau of Standards, Washington, D.C., National Standard Reference Data System, Reprint of NBS-TN-36 (NSRDS-NBS-40, Rev.), 253 pages (February 1972).

C. E. Moore, "Selected Tables of Atomic Spectra, Part A.: Atomic Energy Levels — Second Edition, Part B: Multiplet Tables, Si II, Si III, Si IV, Data Derived from the Analyses of Optical Spectra," U.S. Government Printing Office, Washington, D.C., National Standard Reference Data Service, National Bureau of Standards, Category 3 — Atomic and Molecular Properties (NSRDS-NBS-3, Section 1) 3, (1), 40 pages (1965).

C. E. Moore, Selected Tables of Atomic Spectra, Part A, B, Atomic Energy Levels (Second Edition), Multiplet Tables, Si I," National Bureau of Standards, Washington, D.C., National Standard Reference Data System (NSRDS-NBS-3, Section 2)(November 1967).

C. E. Moore, "Selected Tables of Atomic Spectra, Part A, B, Atomic Energy Levels. Multiplet Tables C I, C II, C III, C IV, C V, C VI," National Bureau of Standards, Washington, D. C., National Standard Reference Data System A32 0647 (NSRDS-NBS-3, Section 3) (November 1970).

C. E. Moore, "Selected Tables of Atomic Spectra, Part A, B, Atomic Energy Levels (Second Edition), Multiplet Tables, N IV, N V, N VI, N VII," National Bureau of Standards, Washington, D.C., National Standard Reference Data System (NSRDS-NBS-3, Section 4)(August 1971).

C. E. Moore, "Selected Tables of Atomic Spectra, Atomic Energy Levels and Multiplet Tables for O," U.S. Department of Commerce, Washington, D.C. (NSRDS-NBS-3, Section 7)(1976).

C. C. Nelson, B. C. Saunders, and S. I. Salem, "K X-Ray Transition Probabilities," Atomic Data 1, 377 (1970).

P. D. Noerdlinger and S. E. Dynan, "Ultraviolet Absorption Lines Arising on Metastable States," Astrophys. J. Suppl. Ser. 29 (283), 185-191 (1975).

M. Outred, "Tables of Atomic Spectral Lines for the 10,000 Å to 40,000 Å Region," Jour, Phys. Chem. Ref. Data 7, (1)(1978).

D. J. Pegg, P. M. Griffin, I. A. Sellin, W. W. Smith, and B. Donnally, "Metastable States of Highly Excited Heavy Ions," in S. J. Smith and G. K. Walters (Eds.), "Atomic Physics 3" 327 (Plenum, New York, 1973).

R. T. Poe and T. N. Chang, "Theoretical Study of Atomic Rydberg States," in S. J. Smith and G. K. Walters (Eds.), "Atomic Physics 3," 143 (Plenum, New York, 1973).

N. F. Ramsey, "Atomic Hydrogen Hyperfine Structure," in F. Bogg and H. Kleinpoppen (Eds.), "Physics of the One- and Two-Electron Atoms," 218 (North-Holland, Amsterdam, 1970).

J. Reader and J. Sugar, "Energy Levels of Iron, Fe I through Fe XXVI," J. Phys. Chem. Ref. Data 4, 353-439 (1975).

A. L. Risinger and A. D. Medven (Eds.), "TRC Selcted Ultraviolet Spectral Data," Vol. 1, Thermodynamics Research Center Data Project, College Station, Texas A&M University, Texas (June 1973).

S. I. Salem, S. L. Panossiam, and R. A. Krause, "Experimental K and L Relative X-Ray Emission Rates," Atomic Data and Nuclear Data Tables 14, 91 (1974).

S. I. Salem and C. W. Schultz, "L X-Ray Transition Probabilities," Atomic Data 3, 215 (1971).

J. H. Scofield, "Relativistic Hartree-Slater Values for K and L X-Ray Emission Rates," Atomic Data and Nuclear Data Tables 14, 121 (1974).

O. Sinanoglu, "Atomic Structure, Transition Probabilities, and Theory of Electron Correlation in Ground and Excited States," in V. W. Hughes, B. Bederson, V. W. Cohen, and F. M. J. Pichanick (Eds.), "Atomic Physics 1," 131 (Plenum, New York, 1969).

M. W. Smith and W. L. Wiese, "Graphical Presenations of Systematic Trends of Atomic Oscillator Strengths along Isoelectronic Sequences and New Oscillator Strengths Derived by Interpolation" Astrophys. J. Suppl. Ser. 23, (196) 103-192 (1971).

M. W. Smith and W. L. Wiese, "Atomic Transition Probabilities for Forbidden Lines of the Iron Group Elements (A Critical Data Compilation for Selected Lines)," J. Phys. & Chem. Ref. Data 2, 85-120 (1973).

A. R. Striganov and N. S. Sventitskii, "Tables of Spectral Lines of Neutral and Ionized Atoms," Translated from Russian (Plenum, New York, 1968).

J. Sugar and C. Corliss, "Energy Levels of Chromium, Cr I through Cr XXIV," Jour. Phys. Chem. Ref. Data 6, (2), 317 (1977).

W. L. Wiese, "Transition Probabilities for Allowed and Forbidden Lines; Lifetimes of Excited States," in B. Bederson and W. L. Fite (Eds.), "Methods of Experimental Physics - Vol. 7, Atomic and Electron Physics, Part A," 117 (Academic, New York, 1968).

W. L. Wiese and B. M. Glennon, "Atomic Transition Probabilities," American Institute of Physics Handbook," Third Edition, Chapter 7, 200-263 (McGraw-Hill, New York, 1971).

W. L. Wiese and J. R. Fuhr, "Atomic Transition Probabilities for Scandium and Titanium (A Critical Data Compilation of Allowed Lines)," J. Chem. Ref. Data 4, 263-352 (1975).

W. L. Wiese, M. W. Smith, and B. M. Glennon, "Atomic Transition Probabilities (H through Ne - A Critical Data Compilation)," National Bureau of Standards, U.S. Government Printing Office, Washington, D.C., National Standard Reference Data Service (NSRDS-NBS-I, Section 4)(1966).

W. L. Wiese, M. W. Smith, and B. M. Miles, "Atomic Transition Probabilities (Na through Ca - A Critical Data Compilation)," National Bureau of Standards, U.S. Government Printing Office, Washington, D.C., National Bureau of Standards (NSRDS-NBS-II, Section 22)(1969).

C. E. Tull, R. P. McEachran, and M. Cohen, "Relativistic Corrections to Ionization Energies and Theoretical Dipole Oscillator Strengths for Fe XVI, Co XVII, and Ni XVIII," Atomic Data 3, 169 (1971).

W. H. Wing, K. R. Lea, and W. E. Lamb, Jr., "Highly Excited States of Helium and Neon," in S. J. Smith and G. K. Walters (Eds.), "Atomic Physics 3," 119, (Plenum, New York, 1973).

E. Worden, "The Emission Spectrum of Curium," Atomic Data and Nuclear Data Tables 18, 459 (1976).

S. M. Younger, J. R. Fuhr, G. A. Martin, and W. L. Wiese, "Atomic Transition Probabilities for Vanadium, Chronium, and Manganese," Jour. Phys. Chem. Ref. Data 7, (2), 495 (1978).

A. N. Zaidel, V. K. Prokofev, S. M. Raiskii, A. V. Slavnyi, and E. Ya. Shreider, "Tables of Spectral Lines," Translated from Russian, 782 (Plenum, New York, 1970).

A-2.2. References on Specific Atoms of Relevance Here

H Z = 1 1 electron

See the general references.

He Z = 2 2 electrons

R. Arrathoon, J. Opt. Soc. Amer. 61, 332 (1971). (Transition wavelengths and probabilities).

H. G. Berry, J. Desesquelles, and M. Dufay, Phys. Rev. A6, 600 (1972).

H. G. Berry, I. Martinson, L. J. Curtis, and L. Lundin, Phys. Rev. A3, 1934 (1971). (Energies and transitions for doubly-excited states).

J. Humphreys and H. J. Kostkowski, J. Research NBS 49, 73 (1952). (Observed infrared spectra).

A. N. Ivanova, U. I. Safronova, and V. N. Kharitonova, Opt. and Spectros. 24, 55 (1968). (Energy level table of calculated and experimental values).

E. J. Knystautus and R. Drovin, Nucl. Instrum. Methods 110, 95 (1973).

U. Litzen, Physica Scripta 2, 103 (1970). (Improved infrared wavelengths).

R. Madden and K. Codling, Ap. J. 141, 364 (1965). (Line and energy level tables for resonant absorption lines observed in the region 165-200 Å).

W. C. Martin, J. Opt. Soc. Amer. 50, 174 (1960). (Observed wavelengths).

W. C. Martin, J. Phys. Chem. Ref. Data 2, 257 (1973). (Compilation of all levels observed to date with one and two electrons excited).

J. R. Woodworth and H. W. Moos, Phys. Rev. 12, 2455 (1975). (Single-photon rates for transitions 1s $^1S_0$ - 2s $^3S_1$).

He^+ Z = 2 1 electron

E. G. Kessler, Jr., and F. L. Roesler, J. Opt. Soc. Amer. 62, 440 (1972). (Fine structure of n=4-5, and n=4-6 transitions in He^+ at low temperature).

B Z = 5 5 electrons

C. M. Brown, S. G. Tilford, and M. L. Guiter, J. Opt. Soc. Amer. 64, 877 (1974). (Transitions from the ground term to high D and S terms).

B. Edlén, A. Olme, G. Herzberg, and J. W. C. Johns, J. Opt. Soc. Amer. 60, 889 (1970). (Line tables from observed spectra).

P. Gunnvald and L. Minnhagen, Ark. Fys. 22, 327 (1962). (Line and energy level tables and a Grotrian diagram for the transitions observed).

U. Litzen, Physica Scripta 1, 251 (1970). (Infrared observations).

B^+ Z = 5 4 electrons

H. G. Berry and J. L. Subtil, Physcia Scripta 9, 217 (1973). (These authors classify some displaced terms).

E. W. H. Selwyn, Proc. Phys. Soc. 41, 392 (1929). (Observed lines of wavelengths in the region 1600 to 2000 Å).

C Z = 6 6 electrons

I. S. Bowen, Ap. J. 132, 1 (1960). (Line table from empirical data of forbidden transitions).

L. Johansson, Ark. Fys. 25, 425 (1963). (Line tables for spectral lines observed in the range 3420 to 9659 Å).

L. Johansson and U. Litzén, Ark. Fys. 29, 175 (1965). (Infrared spectrum).

L. Johansson, Ark. Fys. 31, 201 (1966). (Detailed analysis of the spectrum).

C^+ Z = 6 5 electrons

S. Glad, Ark. Fys. 7, 7 (1952). (Extended analysis of spectrum).

N Z = 7 7 electrons

I. S. Bowen, Ap. J. 132, 1 (1960). (Transition wavelengths from nebular observations).

K. B. S. Eriksson, Physica Scripta 9, 151 (1974). (Line and energy-level tables based on wavelengths from 860 to 9100 Å).

J. W. McConkey, D. J. Burns, and J. A. Kernahan, J. Quant. Spectrosc. Radiat. Transfer 8, 823 (1968). (Spectrogram and line table for lines observed in the region 10,105 to 10,775 Å).

C. E. Moore, Selected Tables of Atomic Spectra, N I, N II, N III, NSRDS-NBS-3, Section 5 (U.S. Govt. Printing Office, 1975).

N^+ Z = 7 6 electrons

I. S. Bowen, Ap. J. 132, 1 (1960). (Transition wavelengths from nebular observations).

W. B. Bridges and A. N. Chester, IEEE J. Qu. Electronics 1, 66 (1965). (Line table for transitions calculated and observed in ion lasers).

B. Edlén, Handbuch der Phys. 27, 172 (1964). (Corrections to Eriksson's energy level values).

K. B. S. Eriksson, Phys. Rev. 102, 102 (1956). (Theory of coupling of ^2P core with f and g electrons, applied to N^+).

K. B. S. Eriksson, Ark. Fys. 13, 303 (1958). (Extended analysis of spectrum).

T. Sasaki, N. Kaifu, N. Itoh, K. Sakai, and I. Shimada, Sci. of Light 14, 142 (1965). (Grotrian diagrams).

J. B. Tatus, Mon. Not. R. Astr. Soc. 140, 87 (1968). (Line table of calculated and observed wavelengths).

O Z = 8 8 electrons

I. S. Bowen, Ap. J. 121, 306 (1955). (Transition wavelengths from nebular observations).

I. S. Bowen, Ap. J. 132, 1 (1960). (Transition wavelengths from nebular observations).

P. M. Dehmer and W. A. Chupka, J. Chem. Phys. 62, 584 (1975).

K. B. S. Eriksson and H. B. S. Isberg, Ark. Fys. 24, 549 (1963); 37, 221 (1968).

K. B. S. Eriksson, Ark. Fys. 30, 199 (1965). (Observed transition wavelengths and energy levels of the ground configuration).

R. E. Huffman, J. C. Larrabee, and Y. Tanaka, J. Chem. Phys. 46, 2213 (1967). (Line and energy level tables from observed absorption spectra in the vacuum ultraviolet. Spectrograms and an energy level diagram are included).

B. Isberg, Ark, Fys. 35, 495 (1967). (Detailed analysis of spectrum).

O^+ Z = 8 7 electrons

I. S. Bowen, Ap. J. 121, 306 (1955). (Transition wavlengths from nebular observations).

I. S. Bowen, Ap. J. 132, 1 (1960). (Transition wavelengths from nebular observations).

W. B. Bridges and A. N. Chester, IEEE J. Qu. Electronics 1, 66 (1965). (Calculated and observed wavelengths of lines in ion gas lasers).

T. Sasaki, N. Kaifu, N. Itoh, K. Sakai, and I. Shimada, Sci. of Light 14, 142 (1965). (Grotrian diagrams).

F Z = 9 9 electrons

J. E. Hansen and W. Persson, Physica Scripta 8, 197 (1973). ($2p^4ns$ and $2p^4nd$ configurations in F and Ne^+).

F^+ Z = 9 8 electrons

I. S. Bowen, Ap. J. 132, 1 (1960). (Observed wavelengths).

H. Palenius, J. Opt. Soc. Amer. 56, 828 (1966). (Transition wavelengths).

H. P. Palenius, Ark. Fys. 39, 15 (1968). (Extends analysis of spectrum).

Ne Z = 10 10 electrons

O. Andrade, M. Gallardo, and K. Bockasten, Appl. Phys. Letters 11, 99 (1967). (Table of lines observed in noble-gas lasers.)

K. Codling, R. P. Madden, and D. L. Ederer, Phys. Rev. 155, 26 (1967). (Line table of resonance lines in the absorption spectrum in the range 80 to 570 Å).

K. G. Ericsson and L. R. Lidholt, IEEE J. Qu. Electronics 3, 94 (1967). (Wavelengths of superrandiant transitions, observed and calculated).

W. L. Faust, R. A. McFarlane, C. K. N. Patel, and C. G. B. Garrett, Phys. Rev. 133A, 1476 (1964). (Line table, term table, and partial Grotrian diagram based on observations in the region 20,000 to 350,000 Å.)

C. J. Humphreys, E. Paul, Jr., R. D. Cowan, and K. L. Andrew, J. Opt. Soc. Amer. 57, 855 (1967). (Line table and energy level array from observations in the region 39,000 to 40,160 Å).

U. Litzén, Ark. Fys. 38, 317 (1968). (Line table based on observation and an energy level table of values observed and calculated).

Ne^+ Z = 10 9 electrons

W. B. Bridges and A. N. Chester, IEEE J. Qu. Electronics 1, 66 (1965). (Table of lines observed and calculated in ion gas lasers.)

K. G. Ericsson and L. R. Lidholt, IEEE J. Qu. Electronics 3, 94 (1967). (Wavelengths of superradiant transitions, observed and calculated).

U. Fink, S. Bashkin, and W. S. Bickel, J. Quant. Spectrosc. Radiat. Transfer 10, 1241 (1970). (Line table of calculated and observed values in the region 3195 to 4515 Å).

J. E. Hansen and W. Persson, Physica Scripta 8, 197 (1973). ($2p^4ns$ and $2p^4nd$ configurations in F and Ne^+).

K. W. Meissner, R. D. Van Veld, and P. G. Wilkinson, J. Opt. Soc. Amer. 48, 1001 (1958). (Line tables in the vacuum ultraviolet region).

W. Persson and L. Minnhagen, Ark. Fys. 37, 273 (1967). (Line tables, energy level tables, and a partial energy level diagram for lines observed in the region 10,200 to 2500 Å.)

W. Persson, Physica Scripta, 3, 133 (1971). (Intermediate coupling terms).

W. Persson, J. Opt. Soc. Amer. 59, 285 (1969). (Revised and extended analysis of spectrum).

P. G. Wilkinson and K. L. Andrew, J. Opt. Soc. Amer. 53, 710 (1963). (Improved wavelength determinations for some lines in Ne II).

Al $Z = 13$ 13 electrons

K. B. S. Eriksson, Ark. Fys. 39, 421 (1969). (Identifies the term $3s3p^2\ ^2D$ at 48,654 cm^{-1}).

K. B. S. Eriksson and H. B. S. Isberg, Ark. Fys. 33, 593 (1967). {Line and energy level tables in comparison of their results with Penkin and Shabanova [Opt. and Spectros. 18, 425 (1925)]}.

N. P. Penkin and L. N. Shabanova, Opt. and Spectros. 18, 425 (1925). (Line and energy level tables for lines observed in the region 2000 to 2300 Å.)

E. W. H. Selwyn, Proc. Phys. Soc. 41, 392 (1929). (Table of lines observed in the region 1600 to 2100 Å).

M. Shimauchi, Sci. of Light 7, 101 (1958). (Tables of lines observed in air, nitrogen, oxygen, and argon atmospheres.)

M. Shimauchi, Sci. of Light 12, 31 (1962). (Line table and spectrograms of observed lines in a helium atmosphere).

P. S. P. Wei, K. T. Tang, and R. B. Hall, J. Chem. Phys. 61, 3593 (1974). (These authors classify some forbidden transitions in this spectrum).

S. Weniger, Ann. d'Astrophysics Suppl. 28, 117 (1965). (Tables of lines observed in the region 4000 to 2100 Å studied under variations of temperature).

T. Yamashita, Sci. of Light 14, 28 (1965). (Line and term tables from lines observed in the region 2120 to 2080 Å).

Al^+ Z = 13 12 electrons

S. Bashkin, W. S. Bickel, H. D. Dieselman, and J. B. Schroeder, J. Opt. Soc. Amer. 57, 1395 (1967). (Wavelengths of lines observed in the region 4140 to 4670 Å).

E. W. H. Selwyn, Proc. Phys. Soc. 41, 392 (1929). (Table of lines observed in the region 1600 to 2100 Å).

S. Weniger, Ann. d'Astrophysics Suppl. 28, 117 (1965). (Tables of lines observed in the region 4000 to 2100 Å studied under variations of temperature).

S Z = 16 16 electrons

I. S. Bowen, Ap. J. 121, 306 (1955).

I. S. Bowen, Ap. J. 132, 1 (1960). (Line table of observed forbidden transitions).

K. B. S. Eriksson, J. Opt. Soc. Am. 63, 632 (1973). (Remeasured wavelengths of two forbidden spectral lines).

G. Hubner and C. Wittig, J. Opt. Soc. Am. 61, 415 (1971). (Two laser lines are identified with transitions in SI.)

L. R. Jakobsson, Ark. Fys. 34, 19 (1966). (Author gives the line tables, energy level tables, a transition array chart, and a partial energy level diagram based on observations in the extra-photographic infrared region, in the region around 9700 to 10,000 Å, and in the region 9212 to 34,270 Å.)

V. Kaufman and L. J. Radziemski, Jr., J. Opt. Soc. Am. 59, 227 (1969). (Energy level table based on observations).

J. W. McConkey, D. J. Burns, K. A. Moran, and J. A. Kernahan, Nature 217, 538 (1968). (Term table based on observations. The values for the $3p^4$ levels do not fully agree with Kelly's tables.)

Y. G. Toresson, Ark. Fys. 18, 417 (1960). (Line and term tables from lines observed in the vacuum ultraviolet region).

S^+ Z = 16 15 electrons

NOTE: The levels designated "N" are taken from Moore's AEL tables.

H. G. Berry, R. M. Schectman, I. Martinson, W. S. Bickel, and S. Bashkin, J. Opt. Soc. Am. 60, 335 (1970).

L. M. Beyer, W. E. Maddox, and L. B. Bridwell, J. Opt. Soc. Am. 63 365 (1973).

L. Block and E. Block, J. Phys. Rad. 6, 30 (1935). (Line tables from observations in the region 320 to 1260 Å).

I. S. Bowen, Ap. J. 121, 306 (1955). (Wavelengths of forbidden transitions observed in nebulae).

I. S. Bowen, Ap. J. 132, 1 (1960). (Line tables from nebular observations).

Cl $Z = 17$ 17 electrons

B. Edlén, Z. Physik, 104, 407 (1937). (Line table from observations in the region 6610 to 7660 Å).

J. E. Hansen, J. Opt. Soc. Am. 67, 754 (1977). (Position and wavefunction for the $sp^6\ ^2S$ term).

C. J. Humphreys and E. Paul, Jr., J. Opt. Soc. Am. 49, 1180 (1959). (Line and energy tables based on observations in the regions 10,221 to 25,323 Å and 6920 to 10,002 Å).

C. J. Humphreys and E. Paul, Jr., J. Opt. Soc. Am. 62, 432 (1972). (Line table for observations in the region 19,800 to 28,570 Å).

C. J. Humphreys, E. Paul, Jr. and L. Minnhagen, J. Opt. Soc. Am. 61, 110 (1971). (Line and energy level tables based on observations in the region 39,600 to 40,530 Å).

L. Minnhagen, J. Opt. Soc. Am. 51, 298 (1961). (Line and energy level tables based on calculations and observations; wavelengths listed are in the region 10,280 to 16,290 Å.)

L. J. Radziemski, Jr. and V. Kaufman, J. Opt. Soc. Am. 59, 424 (1969). (Line and energy level tables from lines observed in the region 960 to 40,535 Å).

Cl^+ $Z = 17$ 16 electrons

I. S. Bowen, Ap. J. 132, 1 (1960). (Line table of observed and predicted values).

W. B. Bridges and A. N. Chester, IEEE J. Qu. Electronics 1, 66 (1965). (Line table of lines observed and calculated in the region 4780 to 6100 Å in ion lasers).

B. Edlén, Phys. Rev. 61, 434 (1942).

V. Kaufman and L. J. Radziemski, Jr., J. Opt. Soc. Am. 59, 227 (1969). (Term table from observations).

C. C. Kiess and T. L. de Bruin, J. Research NBS 23, 443 (1939). (Term diagram, a term array, and tables of lines observed in the regions 2100 to 9485 Å and 555 to 1925 Å).

K. Marakawa, Z. Physik 109, 162 (1939). (Line and term tables for lines observed in the region 3095 to 6720 Å).

L. J. Radziemski, Jr., and V. Kaufman, J. Opt. Soc. Am. 64, 366 (1974). (Observed lines of Cl 11 from 500 to 11,000 Å).

Ar Z = 18 18 electrons

O. Andrade, M. Gallardo, and K. Bockasten, Appl. Phys. Letters 11, 99 (1967). (Transition wavelengths of observed superradiant lines in lasers).

K. Bockasten and O. Andrade, Nature 215, 382 (1967).

K. Bockasten, T. Lundholn, and O. Andrade, Phys. Letters 22, 145 (1966). (Three observed transitions wavelengths in the near infrared).

J. C. Boyce, Phys. Rev. 48, 396 (1935). (Table of observed and calculated lines in the region 800 to 1070 Å).

K. Burns and K. B. Adams, J. Opt. Soc. Am. 43, 1020 (1953). (Line and energy level tables for lines observed in the region 5450 to 9657 Å).

R. D. Cowan, J. Opt. Soc. Am. 58, 924 (1968). (Line table and an energy level table of experimental and calculated values.)

K. G. Ericsson and L. R. Lidholt, IEEE J. Qu. Electronics 3, 94 (1967). (Authors observe and identify a line at 7067.2 Å).

W. L. Faust, R. A. McFarlane, C. K. N. Patel, and C. G. B. Garrett, Phys. Rev. 133A, 1476 (1964). (Line table of observed stimulated emission spectral lines).

G. Hepner, Compt. Rend. 248, 1142 (1959). (Line table of observations in the region 18,420 to 25,660 Å).

C. J. Humphreys and H. J. Kostkowski, J. Research NBS 49, 73 (1952). (Line table of observations in the region 12,110 to 16,940 Å.)

C. J. Humphreys, E. Paul, Jr. R. D. Cowan, and K. L. Andrew, J. Opt. Soc. Am. 57, 855 (1967). (Line table and a supermultiplet array based on observations in the region 39,650 to 40,480 Å).

P. G. Kruger and S. G. Weissberg, Phys. Rev. 48, 659 (1935). (Term table from observations).

P. G. Kruger, S. G. Weissberg, and L. W. Phillips, Phys. Rev. 51, 1090 (1937). (Term table from observations).

H. H. Li and C. J. Humphreys, J. Opt. Soc. Am. 64, 1072 (1974). (These authors observe this spectrum interferometrically in the range 3173 to 11,672 Å.)

S. Liberman, Compt. Rend. 261, 2601 (1965). (Table of lines observed in the region 20,620 to 72,170 Å).

T. A. Littlefield and W. R. C. Rowley, Proc. Roy. Soc. 276 A, 502 (1963). (Line and energy level tables from lines observed in the region 12,405 to 16,950 Å and calculated for 2p-3d and 2p-3s transitions in the region 9195 to 32,310 Å).

T. A. Littlefield and D. T. Turnball, Proc. Roy. Soc. 281A, 577 (1954). (Line and energy level tables of lines observed in the region 3550 to 6540 Å).

R. P. Madden, D. L. Ederer, and K. Codling, Phys. Rev. 177, 136 (1969). (Tables of lines observed in the regions 290 to 430 Å and 210 to 280 Å).

L. Minnhagen, J. Opt. Soc. Am. 63, 1185 (1973). (Author reobserves and reanalyzes this spectrum over the range 3000 to 12,356 Å).

G. Norlén, Ark. Fys. 35, 119 (1967). (Line and energy level tables from lines observed in the region 5150 to 6960 Å.)

G. Norlén, Physica Scripta 8, 249 (1973). (This author reobserves and reanalyzes this spectrum in the range 3400 to 9800 Å.)

E. Paul, Jr. and C. J. Humphreys, J. Opt. Soc. Am. 49, 1186 (1959). (Table of lines observed in the region 13,860 to 25,125 Å).

E. R. Peck, B. N. Khanna, and N. C. Anderholm, J. Opt. Soc. Am. 52, 536 (1962). (Wavelengths in the near infrared as secondary standards).

B. Petersson, Ark. Fys. 27, 317 (1964). (Two transition wavelengths in the vacuum ultraviolet and a table of Ritz standards in the vacuum ultraviolet region).

E. K. Plyler, L. R. Blaine, and E. D. Tidwell, J. Research NBS 55, 279 (1955). (Wavelengths for standards in the infrared region).

T. Sasaki, N. Kaifu, N. Ito, K. Shimada, and I Sakai, Sci. of Light 13, 115 (1964). (Grotrian diagram).

W. R. Sittner and E. R. Peck, J. Opt. Soc. Am. 39, 474 (1949). (Table of wave numbers from lines observed in the region 1200 to 22,000 Å).

K. Yoshino, J. Opt. Soc. Am. 60, 1220 (1970). (Detailed study of the absorption spectrum in the vacuum ultraviolet).

Ar^+ Z = 18 17 electrons

J. C. Boyce, Phys. Rev. 48, 396 (1935). (Line and term tables for lines observed in the region 1980 to 480 Å).

W. G. Bridges and A. N. Chester, IEEE J. Qu. Electronics 1, 66 (1965). (Line table of lines observed and calculated in ion lasers).

G. Convert, M. Armand, and P. Martinot-Lagarde, Compt. Rend. 258, 4467 (1961). (Line table and a partial Grotrian diagram for lines observed in region 4765 to 4545 Å).

B. Edlén, Z Physik 104, 407 (1937). (Line table for lines observed in the region near 2530 Å).

K. G. Ericsson and L. R. Lidholt, IEEE J. Qu. Electronics 3, 94 (1967). (Two wavelengths from superradiant transitions observed in lasers).

U. Fink, S. Bashkin, and W. S. Bickel, J. Quant, Spectrosc. Radiat. Transfer 10, 1241 (1970). (Line table of calculated and observed values in the region 3375 to 4965 Å).

J. E. Hansen, J. Opt. Soc. Am. 67, 754 (1977). (Position and wavefunction for the $sp^6\ ^2S$ term).

G. Herzberg, Proc. Phys. Soc. 248A, 309 (1958). (Energy level diagram and line tables for lines observed in the near vacuum ultraviolet regions, and for lines calculated in the far ultraviolet region).

B. Kjöllerstrom, N. H. Möller, and H. Svensson, Ark. Fys. 29, 167 (1965).

H. H. Li and C. J. Humphreys, J. Opt. Soc. Am. 64, 1072 (1974). (Spectrum of Ar II in the photographic infrared).

L. Maissel, J. Opt. Soc. Am. 48, 853 (1958). (Table of lines observed in the region 3460 to 3660 Å in a study of the Stark shift).

L. Minnhagen, Ark. Fys. 14, 483 (1958). (Transition and energy level arrays and line tables for lines observed in the regions 2000 to 1260 Å and 1000 to 480 Å).

L. Minnhagen, Ark. Fys. 14, 123 (1958). (Partial energy level diagram and an energy level table).

L. Minnhagen, Ark. Fys. 18, 97 (1960). (Energy level tables and arrays, and a partial energy level diagram from empirical data and from calculations for the nf and ng levels).

L. Minnhagen, Ark. Fys. 25, 203 (1963). (Line tables for lines observed in the region 12,500 to 2000 Å and 2000 to 1400 Å, and energy level tables, term tables, and a partial energy level diagram from observations and calculations).

L. Minnhagen, J. Opt. Soc. Am. 61 1257 (1971), and 63, 1185 (1973). (Line and energy level tables and a partial energy level diagram from observations and calculations).

G. Norlén, Ark. Fys. 35, 119 (1967). (Line table for lines observed in the region 6870 to 4880 Å).

G. Norlén, Physica Scripta 8, 249 (1973). (Interferometrically-determined wavelengths and levels).

E. H. Pinnington, B. Curnette, and M. Dufay, J. Opt. Soc. Am. 61, 978 (1971). (Table of lines observed in the region 520 to 1000 Å).

T. Sasaki, N. Kaifu, N. Ito, K. Shimada, and I. Sakai, Sci. of light 13, 115 (1964). (Table of unidentified lines and a Grotrian diagram).

Br $Z = 35$ 35 electrons

M. A. Catalan and F. R. Rico, "Anales de la Real Sociedad Espanola de Fisica y Quimical, 54A, 301 (1958).

J. E. Hansen, Jour. Opt. Soc. Amer. 67, (6), 754 (1977).

C. J. Humphreys and E. Paul, Jour. Opt. Soc. Amer. 62, (3), 432 (1972).

C. J. Humphreys, E. Paul, and L. Minnehagen, Jour. Opt. Soc. Amer. 61, 110 (1971).

J. L. Tech, Journal of Research, NBS 67A, 505 (1963).

J. L. Tech and C. H. Corliss, Journal of Research, NBS 65A, (3), 159 (1961).

Br^+ $Z = 35$ 34 electrons

R. D. Bengtson and M. H. Miller, Physical Review A 14, (5), 1915 (1976).

M. A. Catalan and F. R. Rico, Anales de la Real Sociedad 54A, 301 (1958).

V. Henc-Bartolic, D. Soldo, and A. Persin, Jour. Opt. Soc. Amer. 68, (2), 259 (1978).

E. Moore, Bulletin of the American Astronomical Society 2, (1), (1970).

K. Rahimullah and M. S. Z Chaghtai, J. Quant. Spectrosc. Rad. Trans. 16, (2), 105 (1976).

R. Ramanadham, and K. R. Rao, Ind. J. Phys. 18, 317 (1944).

Y. B. Rao, Ind. J. Phys. 32, 497 (1957).

T. Anderson, O. H. Madsen, and G. Sorensen, Phys. Scripta 6, 125 (1972).

O. Andrade, M. Gallardo, and K. Bockasten, App. Phys. Letters 11, (3), 99 (1967).

M. A. Catalan and F. R. Rico, Annales de la Real 54A, 301 (1958).

K. Codling and R. P. Madden, Phys. Rev. A 4, (6), 2261 (1971).

R. Damachini, L. Cahen, J. Brochard, and R. Vetler, J. Phys. B. 9, (9), L211 (1976).

K. B. S. Ericksson and G. Norlén, Phys. Scripta 1, 247 (1970).

W. L. Faust, R. A. McFarlane, C. K. N. Patel, and C. G. B. Garret, Phys. Rev. 133, (6A), A1476 (1964).

M. Aymar and M. Coulombe, Atomic Data and Nuclear Data Tables 21, 537 (1978).

C. J. Humphreys and H. J. Kostkowski, Journal of Research, NBS 49, (2), 73 (1952).

C. J. Humphreys, E. Paul, R. D. Cowan, and K. L. Andrew, Jour. Opt. Soc. Amer. 57, (7), 855 (1967).

C. J. Humphreys and E. Paul, Jour. Opt. Soc. Amer. 60, (2), 200 (1970).

D. J. Irwin, J. A. Kernahan, E. H. Pinnington, and A. E. Livingston, Jr., Jour. Opt. Soc. Amer. 66, (12), 1397 (1976).

V. Kaufman and C. J. Humpreys, Jour. Opt. Soc. Amer. 59, (12), 1614 (1969).

S. Liberman, Acad. Sci. Paris 261, (14), 2601 (1965).

R. A. Lilly, Jour. Opt. Soc. Amer. 66, (3), 245 (1976).

R. P. Madden and K. Codling, Jour. Opt. Soc. Amer. 54, 268 (1964).

Yu I. Malakhov and V. A. Fabrikant, Opt. Spectrosk. 34, 645 (1973).

W. F. Meggers, T. L. de Bruin, and C. J. Humphreys, Journal of Research, NBS 7, 643 (1931).

W. F. Meggers and C. J. Humphreys, Journal of Research, NBS 10, 427 (1932).

P. W. Murphy, Jour. Opt. Soc. Amer. 58, (9), 1200 (1968).

E. Paul and C. J. Humphreys, Jour Opt. Soc. Amer. 49, (12), 1186 (1959).

B. Peterson, Ark. Fysik 27, (23), 317 (1964).

E. K. Plyler, L. R. Blaine, and E. D. Tidwell, Journal of Research, NBS 55, (5) 279 (1955).

W. R. Sittner and E. R. Peck, Jour. Opt. Soc. Amer. 39, (6) 474 (1949).

J. C. Boyce, Phys. Rev. 47, 718 (1935).

Kr^{+} Z = 36 35 electrons

O. P. Bochkova, I. A. Zubkova, and S. E. Frish, Opt. Specktrosk 36, 29-35 (1974).

W. B. Bridges and A. W. Chester, IEEE J. of Qu. Electronics, 60 (1965).

M. A. Catalan and P. R. Rico, Anales de la Real 54A, 301 (1958).

T. L. de Bruin, C. J. Humphreys, and W. F. Meggers, Journal of Research, NBS 11, 409 (1933).

K. E. Donnelly, P. J. Kindlmann, and W. R. Bennett, Jr., Jour. Opt. Soc. Amer. 65, (11), 1359 (1975).

U. Fink, S. Bashkin, and W. S. Bickel, J. Quant. Spec. Rad. Trans. 10, 1241 (1970).

J. E. Hansen, Jour. Opt. Soc. Amer. 67, (6), 754 (1977).

D. J. Irwin, J. A. Kernahan, E. H. Pinnington, and A. E. Livingston, Jr., Jour. Opt. Soc. Amer. 66, (12), 1396 (1976).

L. Minnhagen, H. Strihed, and B. Petersson, Ark. Fysik 39, (34), 471 (1968).

V. P. Podbiralina, Yu. M. Smirnov, and N. V. Stegnova, Opt. Specktrosk. 34, 467 (1973).

G. S. Rostovikova, V. P. Samoilov, and Yu. M. Smirnov, Opt. Specktrosk. 35, 600 (1973).

N. Spector and S. Garpman, Jour. Opt. Soc. Amer. 67, (2), 155 (1977).

J. C. Boyce, Phys. Rev. 47, 718 (1935).

I Z = 53 53 electrons

F. E. Eshback and R. A. Fisher, Jour. Opt. Soc. Amer. 44, (11), 868 (1954).

J. E. Hansen, Jour. Opt. Soc. Amer. 67, (6), 754 (1977).

C. J. Humphreys and E. Paul, Jour. Opt. Soc. Amer. 62, (3), 432 (1972).

C. J. Humphreys, E. Paul, and L. Minnehagen, Jour. Opt. Soc. Amer. 61, (1) 110 (1971).

C. C. Kiess and C. H. Corliss, Journal of Research, NBS 63A, 1 (1959).

E. Luc-Koenig and J. Verges, Phys. Scripta 12, 199 (1975).

L. Minnhagen, Ark. Fysik 21, (26), 415 (1961).

K. Murakawa, Ziet. Phys. 109, (1939).

I^+ Z = 53 52 electrons

W. B. Bridges and A. W. Chester, IEEE J. Qu. Electronics, 1, 66 (1965).

P. Lacroute, Am d' Astroph. 2, (1939).

W. C. Martin and C. H. Corliss, Journal of Research, NBS 64A (6) (1960).

K. Murakawa, Zeit. Phys. 109, (1939).

W. C. Martin and C. H. Corliss, J. Res. Nat. Bur. Stand. 64A 443 (1960).

Xe Z = 54 54 electrons

T. Andersen, O. H. Madsen, and G. Sorensen, Phys. Scripta 6, 125 (1972).

O. Andrade, M. Gallardo, and K. Bockasten, Appl. Phys. L 11, (3), 99 (1967).

K. Codling and R. P. Madden, Phys. Rev. A 4, (6), 2261 (1971).

M. F. Coulombe and J. Sinzelle, J. de Physique 36, 773 (1975).

M. Dakhil and J. F. Kielkopf, Jour. Opt. Soc. Amer. 67, (6), 844 (1977).

C. C. Davis and T. A. King, J. Quan. Sp. Rad. Trans. 13, 825 (1973).

W. L. Faust, R. A. McFarlane, C. K. N. Patel, and C. G. B. Garrett, Phys. Rev. 133, (6A) A1476 (1964).

L. Herman and K. C. Clark, J. Quant. Spec. Rad. Trans. 5, 765 (1965).

C. J. Humphreys and H. J. Kostkowski, Journal of Research, NBS, 49, (2) 73 (1952).

C. J. Humphreys and E. Paul, Jour. Opt. Soc. Amer. 60, (10), 1302 (1970).

C. J. Humphreys, E. Paul, R. D. Cowan, and K. L. Andrew, Jour. Opt. Soc. Amer. 57, (7), 855 (1967).

A. Lesage and J. Richou, J. Quant. Spec. Rad. Trans. 12, 1313 (1972).

S. Liberman, Acad. Sci. Paris 261, (14), 2601 (1965).

S. Liberman, J. de Physique 30, 53 (1969).

T. A. Littlefield and M. Rafi, J. Phys. B 7, (5), 612 (1974).

K. T. Lu, Phys. Rev. A 4, (2), 579 (1971).

B. Petersson, Ark. Fysik 27, (23), 317 (1964).

E. K. Plyler, L. R. Blaine, and E. D. Tidwell, NBS 2630 55, (5) 279 (1955).

G. S. Rostovikova, V. P. Samoilov, and Yu. M. Smirnov, Opt. Spect. 34, (1), 3 (1973).

W. R. Sittner and E. R. Peck, Jour. Opt. Soc. Amer. 39, (6), 474 (1949).

Xe^{+} Z = 54 53 electrons

M. Aymar and M. Coulombe, Atomic Data and Nuclear Data Tables 21, 537 (1978).

T. Andersen, O. H. Madsen, and G. Sorensen, Phys. Scripta 6, 125 (1972).

W. B. Bridges and A. W. Chester, IEEE J. Qu. Electronics, 1, 66 (1965).

B. Edlen, Phys. Rev. 65, 798 (1944).

U. Fink, S. Bashkin, and W. S. Bickel, J. Quant. Spec. Rad. Trans. 10, 1241 (1970).

S. Garpman, Jour. Opt. Soc. Amer. 66, (9) 904 (1976).

J. E. Hansen, Jour. Opt. Soc. Amer. 67, (6), 754 (1977).

C. J. Humphreys and E. Paul, Jour. Opt. Soc. Amer. 60, (11), 1302 (1970).

C. J. Humphreys and E. Paul, Jour. Opt. Soc. Amer. 60, (11), 1454 (1970).

G. W. Hoffman and P. E. Toschek, Jour. Opt. Soc. Amer. 66, (2), 152 (1976).

E. G. Lluesma, A. A. Tagliaferri, C. A. Massone, M. Garavaglia, and M. Gallardo, Jour. Opt. Soc. Amer. 63, (3), 362 (1973).

C. J. Humphreys, W. F. Meggers, T. L. de Bruin, NBS 23, 683 (1939).

V. P. Podbiralina, Yu. M. Smirnov, and N. U. Stegnova, Opt. Spect. 34, (4), 467 (1973).

G. S. Rostovikova, U. P. Samoilov, and Yu. M. Smirnov, Opt. Spect. 34, (1), 3 (1973).

T. M. El Sherbini, J. Phys. B 9, (10), 1665 (1976).

C. J. Humphreys, J. Res. Nat. Bur. Stand. 22, 19 (1939).

U Z = 92 92 electrons

J. Blaise and L. J. Radziemski, "Energy Levels of Neutral Atomic Uranium", J. Opt. Soc. Am. 66, 644 (1976).

D. W. Steinhaus, L. J. Radziemski, Jr., R. D. Cowan, J. Blaise, F. Guelachvili, Z. B. Osman, and J. Verges, "Present Status of the Analyses of the First and Second Spectra of Uranium (U I and U II) as Derived from Measurements of Optical Spectra," Los Angeles Scientific Laboratory Report LA-4501 (October 1971).

D. W. Steinhaus, M. V. Phillips, J. B. Moody, L. J. Radziemski, Jr., K. J. Fisher, and D. R. Hahn, "The Emission Spectrum of Uranium Between 19,080 and 30,261 cm^{-1}", Los Alamos Scientific Laboratory Report LA-4944 (August 1972).

A-3. POLARIZABILITIES AND MULTIPOLE MOMENTS

CONTENTS

Page

A-3.1. Recommended Values for the Polarizabilities of Ground State Atoms. 1156

Tabulated Data. A-3.1. Recommended values for the polarizabilities of ground state atoms in units of 10^{-24} cm^3.*

Estimated accuracy (%)	Atom	Average polarizability
"Exact"	H	0.666793
"Exact"	He	0.204956
0.5	Li	24.3
2	Be	5.60
2	B	3.03
2	C	1.76
2	N	1.10
2	O	0.802
2	F	0.557
2	Ne	0.395
2	Na	23.6
2	Mg	10.6
2	Al	8.34
2	Si	5.38
2	P	3.63
2	S	2.90
2	Cl	2.18
0.5	Ar	1.64
2	K	43.4
8	Ca	25.0
50	Sc	16.9
50	Ti	13.6
50	V	11.4
50	Cr	6.8
50	Mn	8.6
50	Fe	7.5
50	Co	6.8
50	Ni	6.5
50	Cu	6.1
2	Zn	7.08
2	Ga	8.12
2	Ge	6.07
2	As	4.31
2	Se	3.77
2	Br	3.05
0.5	Kr	2.48
2	Rb	47.3
8	Sr	27.6
50	Y	22
50	Zr	18

*From T. M. Miller and B. Bederson, "Atomic and Molecular Polarizabilities-A Review of Recent Advances," in "Advances in Atomic and Molecular Physics" (D. R. Bates and B. Bederson, Eds.), Vol. 13, Academic Press, New York (1977).

Tabulated Data A-3.1. Recommended values for the polarizabilities of ground states atoms in units of 10^{-24} cm^3 (Continued).

Estimated accuracy (%)	Atom	Average polarizability
50	Nb	14
50	Mo	13
50	Tc	10.0
50	Ru	8.6
50	Rh	7.6
50	Pd	6.9
50	Ag	6.3
50	Cd	6.0
50	In	4.5
50	Sn	4.4
50	Sb	4.0
50	Te	3.9
50	I	3.9
0.5	Xe	4.04
2	Cs	59.6
8	Ba	39.7
50	La	37
50	Ce	36
50	Pr	34
50	Nd	32
50	Pm	30
50	Sm	29
50	Eu	27
50	Gd	26
50	Tb	25
50	Dy	25
50	Ho	23
50	Er	23
50	Tm	22
50	Yb	22
50	Lu	20
50	Hf	15
50	Ta	13
50	W	10
50	Re	9
50	Os	8
50	Ir	7
50	Pt	6.3
50	Au	5.7
50	Hg	5.1
50	Tl	3.5
50	Pb	3.7
50	Bi	4.0
50	Po	4.6
50	At	5.1
50	Rn	6.3
50	Fr	67
50	Ra	46
50	Ac	53
50	Th	50
50	Pa	48
50	U	46
50	Np	45
50	Pu	43
50	Am	41
50	Cm	40
50	Bk	39
50	Cf	38
50	Es	36
50	Fm	35
50	Md	34
50	No	33
50	Lw	32

A-4. ELECTRON AFFINITIES*

CONTENTS

	Page
A-4.1. Electron Affinities of Atoms.	1161
A-4.2. Electron Affinities of Molecules.	1162

A-4. References:

A. P. M. Baede, Adv. Chem. Phys. 30, 463 (1975).

R. N. Compton, P. W. Reinhardt, and C. D. Cooper, J. Chem. Phys. 68, 2023 (1978).

H. Hotop and W. C. Lineberger, "Binding Energies in Atomic Negative Ions", J. Phys. Chem. Ref. Data 4, 539-576 (1975).

H. S. W. Massey, Negative Ions (Third Edition) (Cambridge University Press, Cambridge 1976).

B. L. Moiseiwitsch, "Negative Ions", in Atomic Processes and Applications (edited by P. G. Burke and B. L. Moiseiwitsch), 291-319 (North-Holland Publishing Co., Amsterdam, 1976).

*For discussions of the difference between electron affinities and vertical detachment energies for molecules, see H.S.W. Massey, "Negative Ions," (Third Edition) Cambridge University Press, Cambridge (1976), pg. 166 and E. W. McDaniel, "Collision Phenomena in Ionized Gases," Wiley, New York (1964), pg. 379.

PRECEDING PAGE BLANK

Tabular Data. A-4.1. Electron Affinities of Atoms (in eV).

He	< 0	Ag	1.303 (7)
Ne	< 0	Al	0.46 (3)
Ar	< 0	B	0.28 (1)
Kr	< 0	C	1.268 (5)
Xe	< 0	Cd	< 0
		Cu	1.226 (10)
F	3.399 (3)	D*	0.757 ± 0.005
Cl	3.615 (4)	H	0.7542 (3)
Br	3.364 (4)	Hg	< 0
I	3.061 (4)	In	0.30 (15)
		N	- 0.07 (8)
Li	0.620 (7)	O	1.462 (3)
Na	0.546 (5)	P	0.743 (10)
K	0.5012(5)	S	2.0772 (5)
Rb	0.4860(5)	Se	2.0206 (3)
Cs	0.4715 ($^{5}_{20}$)	Te	1.9708 (3)
Fe†	0.164 ± 0.035	U	unmeasured at this date

Note: Unless otherwise indicated, the data here are recommended values from Table 10 in the critical review: H. Hotop and W. C. Lineberger, "Binding Energies in Atomic Negative Ions," Jour. Phys. Chem. Ref. Data 4, 539-576 (1975).

*K. E. McCulloh and J. A. Walker, Chem. Phys. Lett. 25, 439 (1974).

†P. C. Engelking and W. C. Lineberger, Phys. Rev. A 19, 149 (1979).

Tabular Data. A-4.2. Electron Affinities of Molecules (in eV).

F_2	3.08 ± 0.1	
Cl_2	2.38 ± 0.1	W. A. Chupka, J. Berkowitz, and D. Gutman.
Br_2	2.51 ± 0.1	J. Chem. Phys. 55, 2724 (1971).
I_2	2.58 ± 0.1	
IBr	2.7 ± 0.2	
ICl	1.43	J. Jortner and U. Sokolov, Nature 190, 1003 (1961).
LiCl	0.61 ± 0.02	J. L. Carlsten, J. R. Peterson, and W. C. Lineberger, Chem. Phys. Lett. 37, 5 (1976).
FeO	1.492 ± 0.020	P. C. Engelking and W. C. Lineberger, J. Chem. Phys. 66, 5054 (1977).
$NH(X^3\Sigma)$	0.381 ± 0.014	P. C. Engelking and W. C. Lineberger, J. Chem. Phys. 65, 4323 (1976).
$NH(a^1\Delta)$	1.960 ± 0.010	
PO	1.092 ± 0.010	P. F. Zittel and W. C. Lineberger, J. Chem. Phys. 65, 1236 (1976).
PH	1.028 ± 0.010	
PH_2	1.271 ± 0.010	
UF_6	≥ 5.1	R. N. Compton, J. Chem. Phys. 66, 4478 (1977).
UF_5	4.0 ± 0.4	
CF_3Br	0.91 ± 0.2	R. N. Compton, P. W. Reinhardt, and C. D. Cooper, J. Chem. Phys. 68, 4360 (1978).
CF_3I	1.57 ± 0.2	
SF_6	0.46 ± 0.2	R. N. Compton, P. W. Reinhardt, and C. D. Cooper, J. Chem. Phys. 68, 2023 (1978).
SeF_6	2.9 ± 0.2	
TeF_6	3.3 ± 0.2	
SF_5	2.71 ± 0.2	
SF_4	0.78 ± 0.2	
SF_3	3.07 ± 0.2	
CH	1.238 ± 0.008	A. Kasdan, E. Herbst and W. C. Lineberger, Chem. Phys. Lett. 31, 78 (1975).
NH_2	0.779 ± 0.037	R. J. Celotta, R. A. Bennett and J. L. Hall, J. Chem. Phys. 60, 1740 (1974).
CH_3O	1.570 ± 0.022	P. C. Engelking, G. B. Ellison, and W. C. Lineberger, J. Chem. Phys. 69, 1826 (1978).
CD_3O	1.552 ± 0.022	
CH_3S	1.882 ± 0.024	

Tabular Data. A-4.2. Electron Affinities of Molecules (in eV) (Continued).

CN	3.82 ± 0.02	J. Berkowitz, W. A. Chupka and T. A. Walter, J. Chem. Phys. 50, 1497 (1969).
C_2H	3.73	D. Feldmann, Z. Naturforsch. Teil A 25, 621 (1970).
C_2	3.54	
OH	1.8255 ± 0.002	H. Hotop, R. A. Bennett and W. C. Lineberger, J. Chem. Phys. 58, 2373 (1973).
NO	0.024 $^{+0.010}_{-0.005}$	M. W. Siegel, R. J. Celotta, J. L. Hall, J. Levine and R. A. Bennett, Phys.Rev. A 6, 607 (1972).
O_2	0.440 ± 0.008	R. J. Cellotta, R. A. Bennett, J. L. Hall, M. W. Siegel and J. Levine, Phys. Rev. A 6, 631 (1972).
CH_2	0.21 ± 0.03	P. F. Zittell, G. B. Ellison, S. V. O'Neil, E. Herbst, W. C. Lineberger and W. P. Reinhardt, J. Am. Chem. Soc. 98, 3731 (1976).
CO_2	-0.6	R. N. Compton, P. W. Reinhardt, and C. D. Cooper, J. Chem. Phys. 63, 3821 (1975).
N_2O	0.22 ± 0.1	D. G. Hopper, A. C. Wahl, R. L. C. Wu and T. O. Tiernan, J. Chem. Phys. 65, 5474 (1976).
O_3	2.14 ± 0.15	E. W. Rothe, S. Y. Tang, and G. Reck, J. Chem. Phys. 62, 3829 (1975).
NO_2	2.36 ± 0.1	E. Herbst, T. A. Patterson, and W. C. Lineberger, J. Chem. Phys. 61, 1300 (1974).
BO_2	4.07 ± 0.2	D. E. Jensen, Trans. Faraday Soc. 65, 2123 (1969).
CO_3	2.9 ± 0.3	J. T. Moseley, P. C. Cosby and J. R. Peterson, J. Chem.Phys. 65, 2512 (1976).
HNO_3	0.57 ± 0.15	B. P. Mathur, E. W. Rothe, S. Y. Tang, and Kanwai Mahajan, J. Chem. Phys. 64, 1247 (1976).
NO_3	3.68 ± 0.2	
CO_4	1.22	J. L. Pack and A. V. Phelps, J. Chem. Phys. 45, 4316 (1966).

H_2	-1.7	NCO	≥2.6 ± 0.4
CH_3	1.08	CS	≤1.2
OD	1.823 ± 0.002	SO	1.09 ± 0.05
C_2	3.54 ± 0.05	S_2	1.663 ± 0.040
C_2H	3.73 ± 0.05	O_4	negative ion detected
SiH	1.277 ± 0.009	SO_2	1.097 ± 0.036
SiH_2	1.124 ± 0.020	$CO_3(H_2O)$	2.1
SH	2.319 ± 0.010		

*From the chapter "Negative Ions" by B. L. Moiseiwitsch in "Atomic Processes and Applications", P. G. Burke and B. L. Moiseiwitsch, (Eds). 314-315 (North-Holland Publishing Co., Amsterdam, 1976).

A-5. GENERAL REFERENCES ON POTENTIAL ENERGY CURVES, ELECTRONIC ENERGIES, SPECTROSCOPIC CONSTANTS AND ABSORPTION AND EMISSION SPECTRA OF EXCIMER SYSTEMS *

General References

1. W. C. Ermler, Yoon S. Lee, K. S. Pitzer, and N. W. Winter, "Ab initio Effective Core Potentials Including Relativistic Effects. II. Potential Energy Curves for Xe_2, Xe_2^+ and Xe_2^*," J. Chem. Phys. 69, 976 (1978).

2. W. R. Wadt, "The Electronic States of Ar_2^+, Kr_2^+ and Xe_2^+. I. Potential Curves With and Without Spin-Orbit Coupling," J. Chem. Phys. 68. 402 (1978).

3. W. R. Wadt, R. J. Hay, and L. R. Kahn, "Relativistic and Nonrelativistic Effective Core Potentials for Xenon. Applications to XeF, Xe_2 and Xe_2^+," J. Chem. Phys. 68, 1752 (1978).

4. H. H. Michels, R. H. Hobbs, L. A. Wright, and J. W. D. Connolly, "Electronic Structure of Excimer Molecular Lasers," Int. Jour. Quant. Chem. 13, 167 (1978).

5. G. Brual and S. M. Rothstein, "Rare Gas Interactions Using an Improved Statistical Method," J. Chem. Phys. 69, 1177 (1978).

6. J. S. Cohen and R. T. Pack, "Modified Statistical Method for Intermolecular Potentials. Combining Rules for Higher Van der Waals Coefficients," J. Chem. Phys. 61, 2372 (1974).

7. Y. S. Lee, W. C. Ermler, and K. S. Pitzer, "Ab initio Effective Core Potentials Including Relativistic Effects. I. Formalism and Applications to the Xe and Au Atoms," J. Chem. Phys. 67, 5861 (1977).

8. J. M. Farrar and Y. T. Lee, "Intermolecular Potentials from Crossed Beam Differential Elastic Scattering Measurements. V. The Attractive Well of He_2," J. Chem. Phys. 56, 5801 (1972).

9. J. M. Farrar, Y. T. Lee, V. V. Goldman, and M. L. Klein, "Neon Interatomic Potentials from Scattering Data and Crystalline Properties," Chem. Phys. Letts. 19, 359 (1973).

---

*These references are in addition to those previously given in Vol. I, Section A, pages 8-14.

10. J. M. Parson, P. E. Siska, and Y. T. Lee, "Intermolecular Potentials from Crossed-Beam Differential Elastic Scattering Measurements. IV. Ar + Ar," J. Chem. Phys. 56, 1151 (1972).

11. J. A. Barker, R. O. Watts, J. K. Lee, T. P. Schafer, and Y. T. Lee, "Interatomic Potentials for Krypton and Xenon," J. Chem. Phys. 61, 3081 (1974).

12. C. H. Chen, P. E. Siska, and Y. T. Lee, "Intermolecular Potentials from Crossed-Beam Differential Elastic Scattering Measurements. VIII. He + Ne, He + Ar, He + Kr and He + Xe," J. Chem. Phys. 59, 601 (1973).

13. C. Y. Ng, Y. T. Lee, and J. A. Barker, "Improved Potentials for Ne + Ar, Ne + Kr and Ne + Xe," J. Chem. Phys. 61, 1996 (1974).

14. J. M. Parson, T. P. Schafer, P. E. Siska, F. P. Tully, Y. C. Wong, and Y. T. Lee, "Intermolecular Potentials from Crossed Beam Differential Elastic Scattering Measurements. II. Ar + Kr and Ar + Xe," J. Chem. Phys. 53, 3755 (1970).

15. R. G. Gordon and Y. S. Kim, "Theory for the Forces Between Closed-Shell Atoms and Molecules," J. Chem. Phys. 56, 3122 (1972).

16. A. I. M. Rae, "A Theory for the Interactions Between Closed-Shell Systems," Chem. Phys. Letts. 18, 574 (1973).

17. A. I. M. Rae, "A Calculation of the Interaction Between Pairs of Rare-Gas Atoms," Mol. Phys. 29, 467 (1975).

18. U. Buck, F. Huisken, H. Pauly, and J. Schleusener, "Intermolecular Potentials by the Inversion of Differential Cross Sections. V. ArKr," J. Chem. Phys. 68, 3334 (1978).

19. R. Luckx, Ph. Coulon, and H. N. W. Lekkerker, "Dispersion Forces Between Noble Gas Atoms," J. Chem. Phys. 69, 2424 (1978).

20. H. H. Michels, R. H. Hobbs, and L. A. Wright, "Electronic Structure of the Noble Gas Dimer Ions. I. Potential Energy Curves and Spectroscopic Constants" (in press).

21. W. R. Wadt, D. C. Cartwright, and J. S. Cohen, "Theoretical Absorption Spectra for Ne_2^+, Ar_2^+, Kr_2^+ and Xe_2^+ in the Near Ultraviolet," Appl. Phys. Letts. 31, 672 (1977).

22. C. F. Bender and N. W. Winter, "Theoretical Absorption Spectra of $ArKr^+$," Appl. Phys. Letts. 33, 29 (1978).

23. W. J. Stevens, M. Gardner, A. Karo, and P. Julienne, "Theoretical Determination of Bound-Free Absorption Cross Sections in Ar_2^+," J. Chem. Phys. 67, 2860 (1977).

24. N. W. Winter, C. F. Bender, and T. N. Rescigno, "Potential Energy Curves and Predicted Fluorescence for Neon Fluoride," J. Chem. Phys. 67, 3122 (1977).

25. N. W. Winter and T. N. Rescigno, "Theoretical Calculation of the Bound-Free Emission Spectra of KrF," J. Chem. Phys. (in press).

26. T. H. Dunning and P. J. Hay, "Electronic States of KrF," Appl. Phys. Letts. 28, 649 (1976).

27. P. J. Hay and T. H. Dunning, "The Electronic States of KrF," J. Chem. Phys. 66, 1306 (1977).

28. P. J. Hay and T. H. Dunning, "The Covalent and Ionic States of the Xenon Halides," J. Chem. Phys. 69, 2209 (1978).

29. T. H. Dunning and P. J. Hay, "The Low Lying States of the Rare-Gas Fluorides," J. Chem. Phys. 69 134 (1978).

30. J. Tellinghuisen, A. K. Hays, J. M. Hoffman, and G. C. Tisone, "Spectroscopic Studies of Diatomic Noble Gas Halides. II. Analysis of Bound-Free Emission from XeBr, XeI and KrF," J. Chem. Phys. 65, 4473 (1976).

31. J. Tellinghuisen, G. C. Tisone, J. M. Hoffman, and A. K. Hays, "Analysis of Spontaneous and Laser Emission from XeF," J. Chem. Phys. 64, 4796 (1976).

32. J. Tellinghuisen, P. C. Tellinghuisen, G. C. Tisone, J. M. Hoffman, and A. K. Hays, "Spectroscopic Studies of Diatomic Noble Gas Halides. III. Analysis of XeF 3500 Å Band System," J. Chem. Phys. 68, 5177 (1978).

33. P. C. Tellinghuisen, J. Tellinghuisen, J. A. Coxon, J. E. Velazco, and D. W. Setser, "Spectroscopic Studies of Diatomic Noble Gas Halides. IV. Vibrational and Rotational Constants for the X, B and D States of XeF," J. Chem. Phys. 68, 5187 (1978).

34. W. R. Wadt and P. J. Hay, "The Low Lying Electronic States of Ar_2F," Appl. Phys. Letts. 30, 573 (1977).

35. W. R. Wadt and P. J. Hay, "Electronic States of Ar_2F and Kr_2F," J. Chem. Phys. 68, 3859 (1978).

36. D. L. Huestis and N. E. Schlotter, "Diatomics-in-Molecules Potential Surfaces for the Triatomic Rare Gas Halides: Rg_2X," J. Chem. Phys. 69, 3100 (1978).

37. T. H. Dunning and P. J. Hay, "Low-Lying Electronic States of the Rare-Gas Oxides," J. Chem. Phys. 66, 3767 (1977).

38. W. R. Wadt, "The Electronic Structure of HgCℓ and HgBr," Appl. Phys. Letts. (in press).

39. T. H. Dunning, M. Valley, and H. S. Taylor, "Theoretical Studies of the Low-Lying Electronic States of GaKr, Including Extrapolation to InKr and TℓKr," J. Chem. Phys. 69, 2672 (1978).

40. P. J. Hay, W. R. Wadt, L. R. Kahn, and F. W. Bobrowitz," Ab initio Studies of AuH, AuCℓ, HgH and $HgCℓ_2$ Using Relativistic Core Potentials," J. Chem. Phys. 69, 984 (1978).

A-6. POTENTIAL ENERGY CURVES, ELECTRONIC ENERGIES AND SPECTROSCOPIC CONSTANTS FOR Xe_2^+ AND Xe_2^*. INTERACTIONS BETWEEN LIKE AND UNLIKE PAIRS OF RARE-GAS ATOMS

CONTENTS

		Page
A-6.1.	Electronic transition laser - Xe_2	1170
A-6.2.	Spectroscopic constants for Xe_2^+ and Xe_2^*	1171
A-6.3.	Xe_2^+ potential energy curves without spin-orbit coupling	1172
A-6.4.	Xe_2^+ potential energy curves including spin-orbit coupling	1173
A-6.5.	Xe_2^* potential energy curves without spin-orbit coupling	1174
A-6.6.	Xe_2^* potential energy curves including spin-orbit coupling	1175
A-6.7.	Valence SCF energies of electronic states of diatomic Xe	1176
A-6.8.	Xe_2, Xe_2^*, and Xe_2^+ potential energy curves including spin-orbit coupling.	1177
A-6.9.	Selected Xe_2^+ and Xe_2^* vertical transition energies	1178
A-6.10.	Variation of the magnitude of the transition moment for Xe_2^* with internuclear distance	
A-6.11.	Interaction energies for $^1\Sigma_g^+$ states of He_2, Ne_2, Ar_2, and Kr_2 as determined by experiment and by various theoretical models	1180
A-6.12.	Interaction energies of He-Ne ($^1\Sigma^+$), He-Ar ($^1\Sigma^+$) and He-Kr ($^1\Sigma^+$) as determined by experiment and by various theoretical models	1181

Page

A-6.13. Interaction energies of Ne-Ar ($^1\Sigma^+$), Ne-Kr ($^1\Sigma^+$), and Ar-Kr ($^1\Sigma^+$) as determined by experiment and by various theoretical models 1182

A-6. References:

1. W. C. Ermler, Y. S. Lee, K. S. Pitzer, and N. W. Winter, "Ab initio Effective Core Potentials Including Relativistic Effects. II. Potential Energy Curves for Xe_2, Xe_2^+ and Xe_2^*," J. Chem. Phys. 69, 976 (1978).

2. W. R. Wadt, "The Electronic States of Ar_2^+, Kr_2^+ and Xe_2^+. I. Potential Energy Curves With and Without Spin-Orbit Coupling," J. Chem. Phys. 68, 402 (1978).

3. W. R. Wadt, P. J. Hay, and L. R. Kahn, "Relativistic and Nonrelativistic Effective Core Potentials for Xenon. Applications to XeF, Xe_2, and Xe_2^+," J. Chem. Phys. 68, 1752 (1978).

4. G. Brual and S. M. Rothstein, "Rare Gas Interactions Using an Improved Statistical Method," J. Chem. Phys. 69, 1177 (1978).

5. H. H. Michels, R. H. Hobbs, L. A. Wright, and J. W. D. Connolly, "Electronic Structure of Excimer Molecule Lasers," Int. Jour. Quant. Chem. 13, 167 (1978).

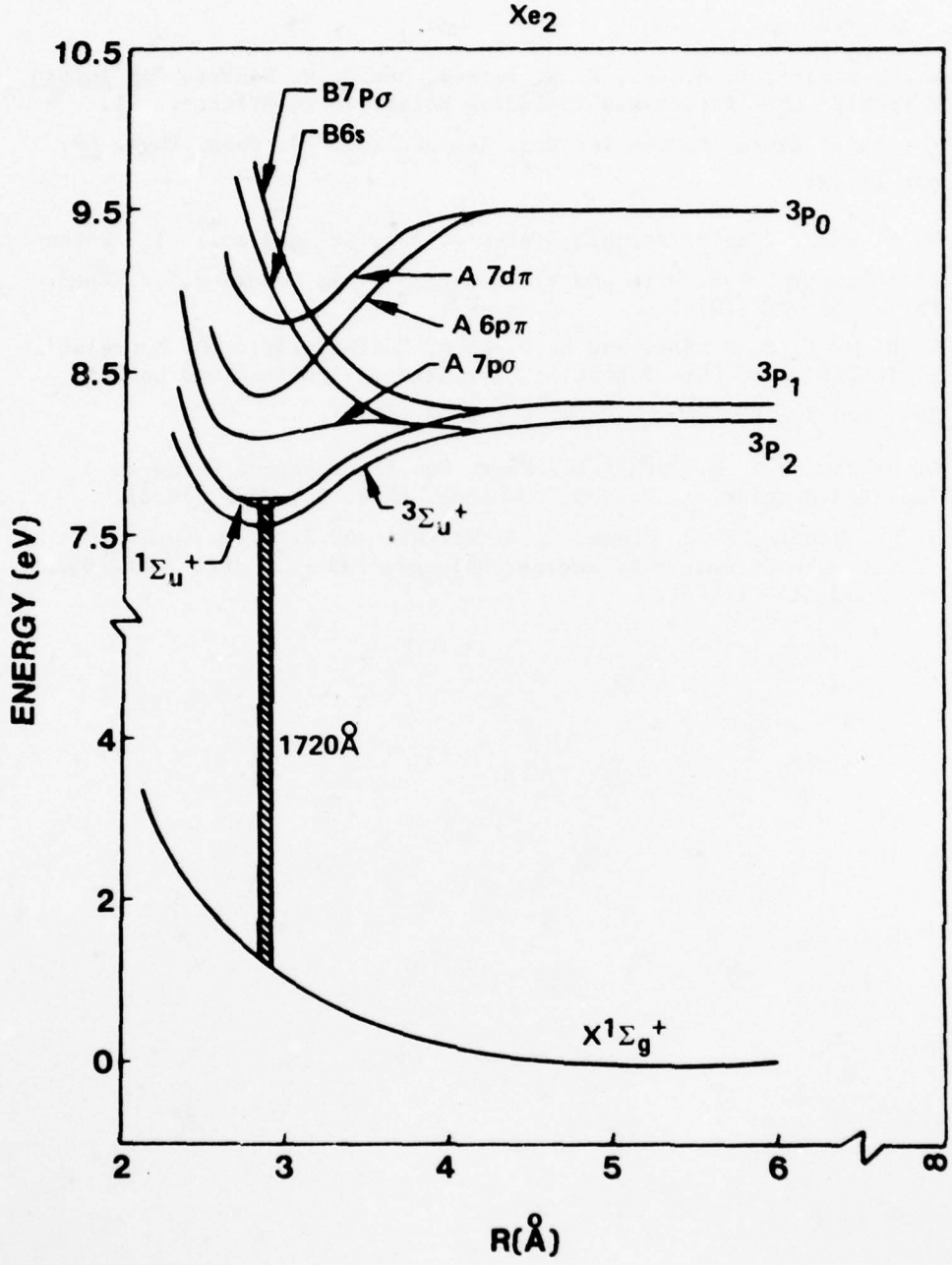

Graphical Data. A-6.1. Electronic transition laser—Xe_2.

Tabular Data A-6.2. Spectroscopic constants for Xe_2^+ and Xe_2^* [a].

		$R_e(a_o)$	D_e(eV)	$\omega_e(cm^{-1})$	$\omega_e X_e(cm^{-1})$	$B_e(cm^{-1})$	$\alpha_e(cm^{-1})$
$Xe_2^+ \ ^2\Sigma_u^+$	a	5.74	0.99	122.5	0.45	0.02786	0.00011
	b	6.08	1.08	124			
	c	5.84	1.04	125			
$(1/2)_u$ [d]	a	5.82	0.70	110.4	0.53	0.02704	0.00013
	b	6.18	0.79	112			
	c	5.91	0.76	112			
$Xe_2^* \ ^3\Sigma_u^+$	a	5.67	1.00	128.3	0.62	0.02856	0.00012
$^1\Sigma_u^+$	a	5.65	1.03	129.2	0.45	0.02868	0.00011
0_u^+	a	5.72	0.77	118.5	0.53	0.02800	0.00013
0_u^-	a	5.73	0.78	117.3	0.59	0.02793	0.00014
1_u	a	5.73	0.79	118.0	0.59	0.02796	0.00014

[a] Reference 1.

[b] Reference 2.

[c] Reference 3.

[d] Empirical estimate of D_o = 1.03 eV, R_e = 6.14 a_o.

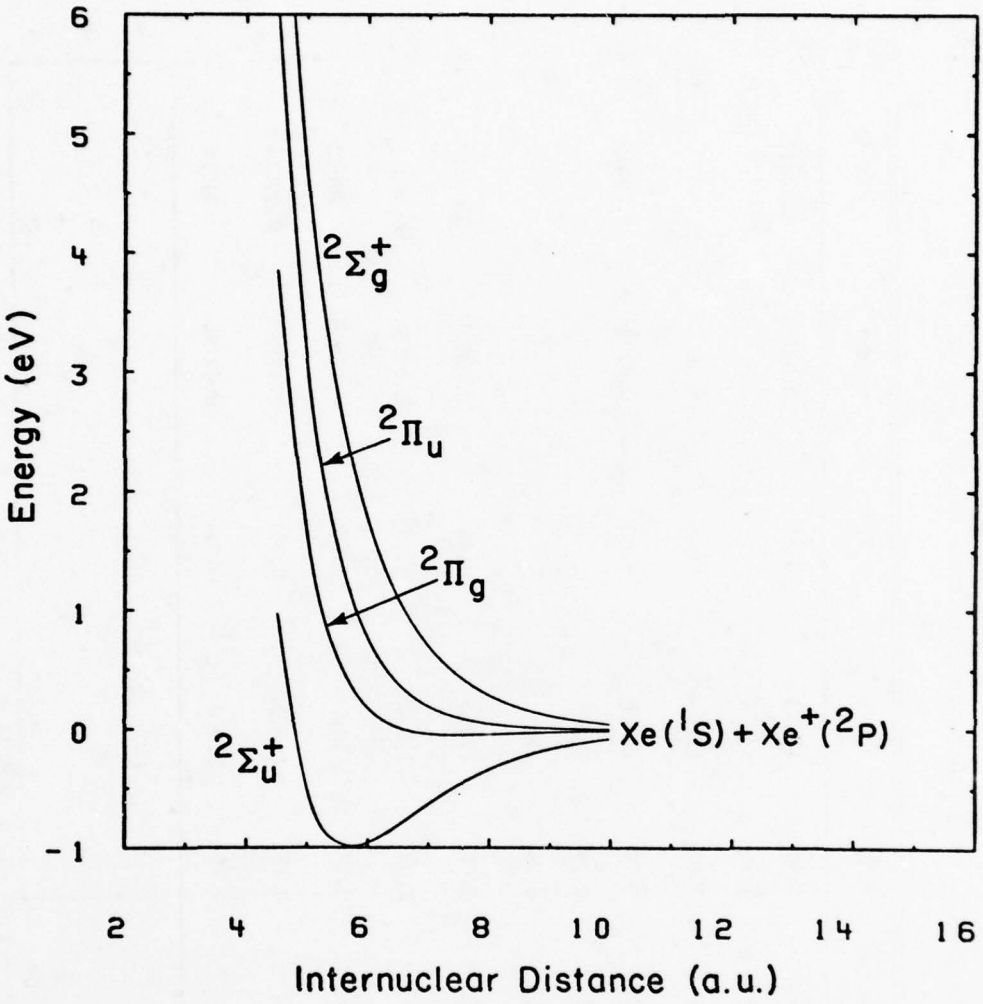

Graphical Data. A-6.3. Xe_2^+ potential energy curves without spin-orbit coupling.

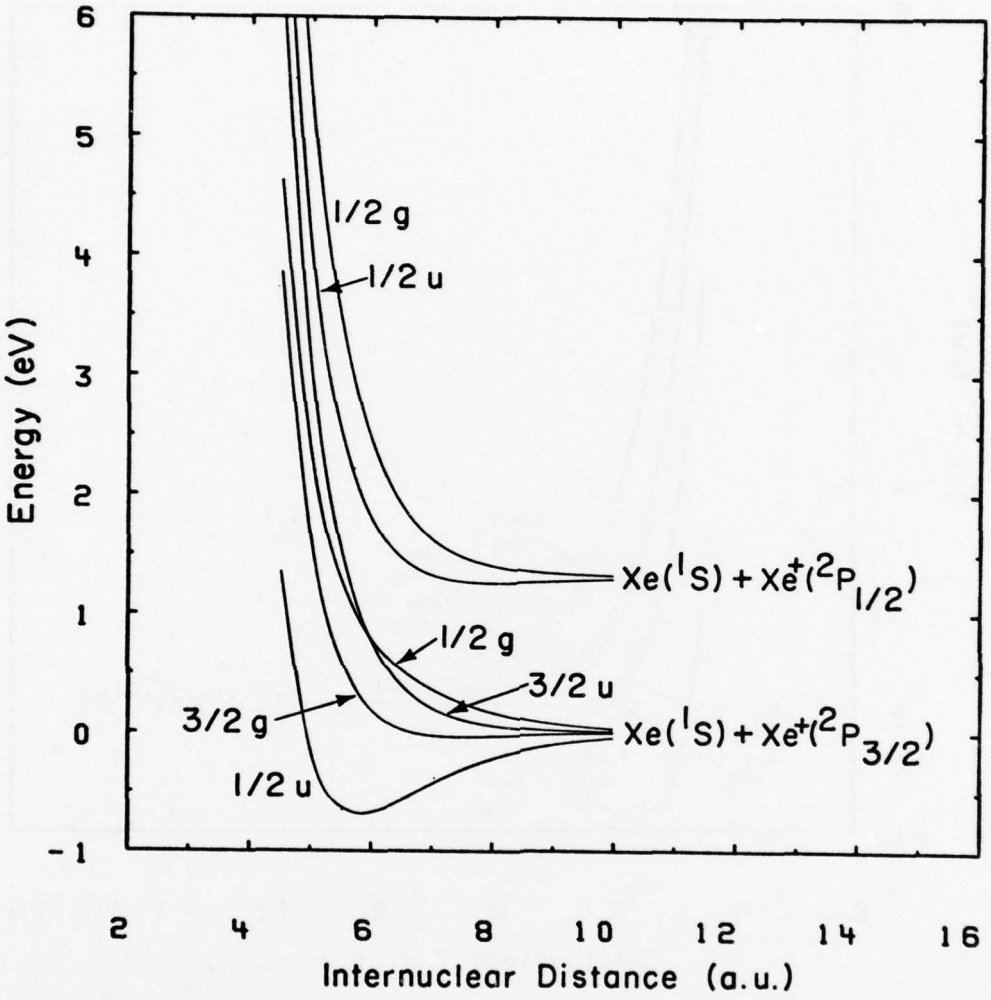

Graphical Data. A-6.4. Xe_2^+ potential energy curves including spin-orbit coupling.

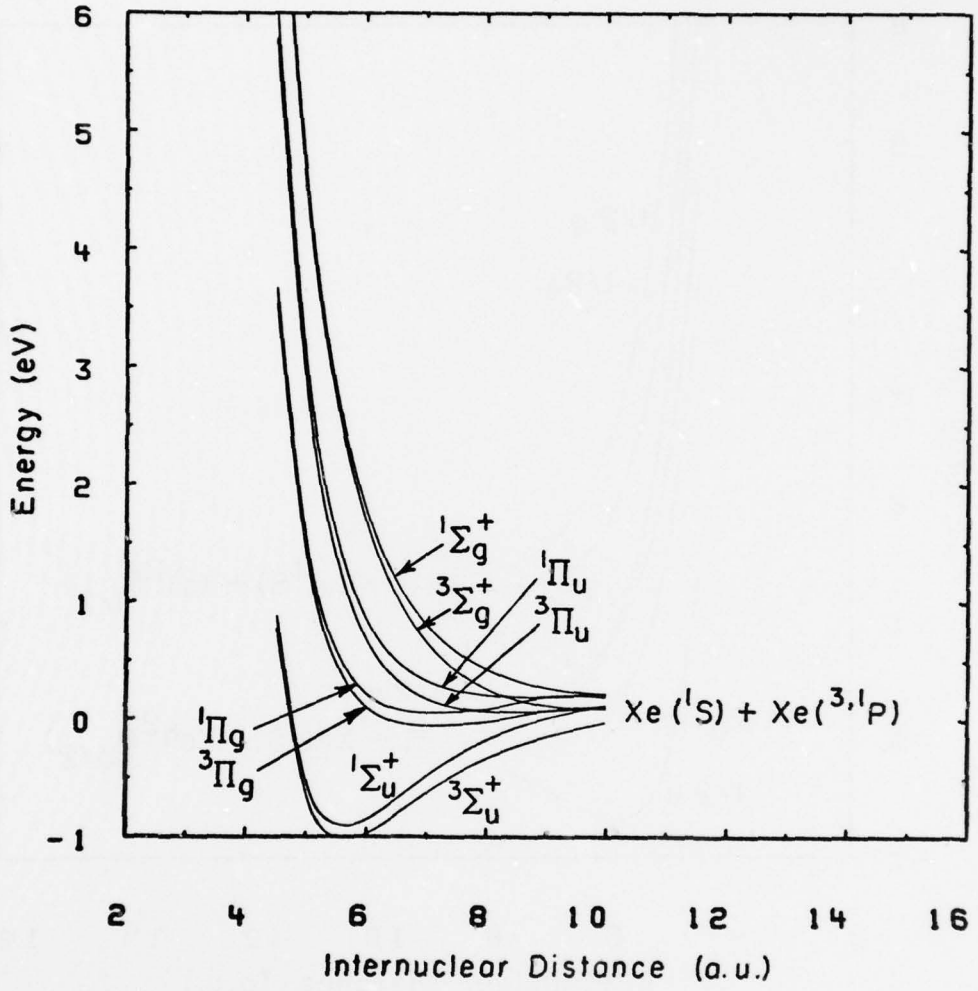

Graphical Data. A-6.5. Xe_2^* potential energy curves without spin-orbit coupling.

AD-A068 679 ARMY MISSILE RESEARCH AND DEVELOPMENT COMMAND REDSTO--ETC F/G 20/5
COMPILATION OF DATA RELEVANT TO NUCLEAR PUMPED LASERS. VOLUME I--ETC(U)
DEC 78 E W MCDANIEL, M R FLANNERY, E W THOMAS

UNCLASSIFIED DRDMI-H-78-1-VOL-3 NL

4 OF 5
AD A068679

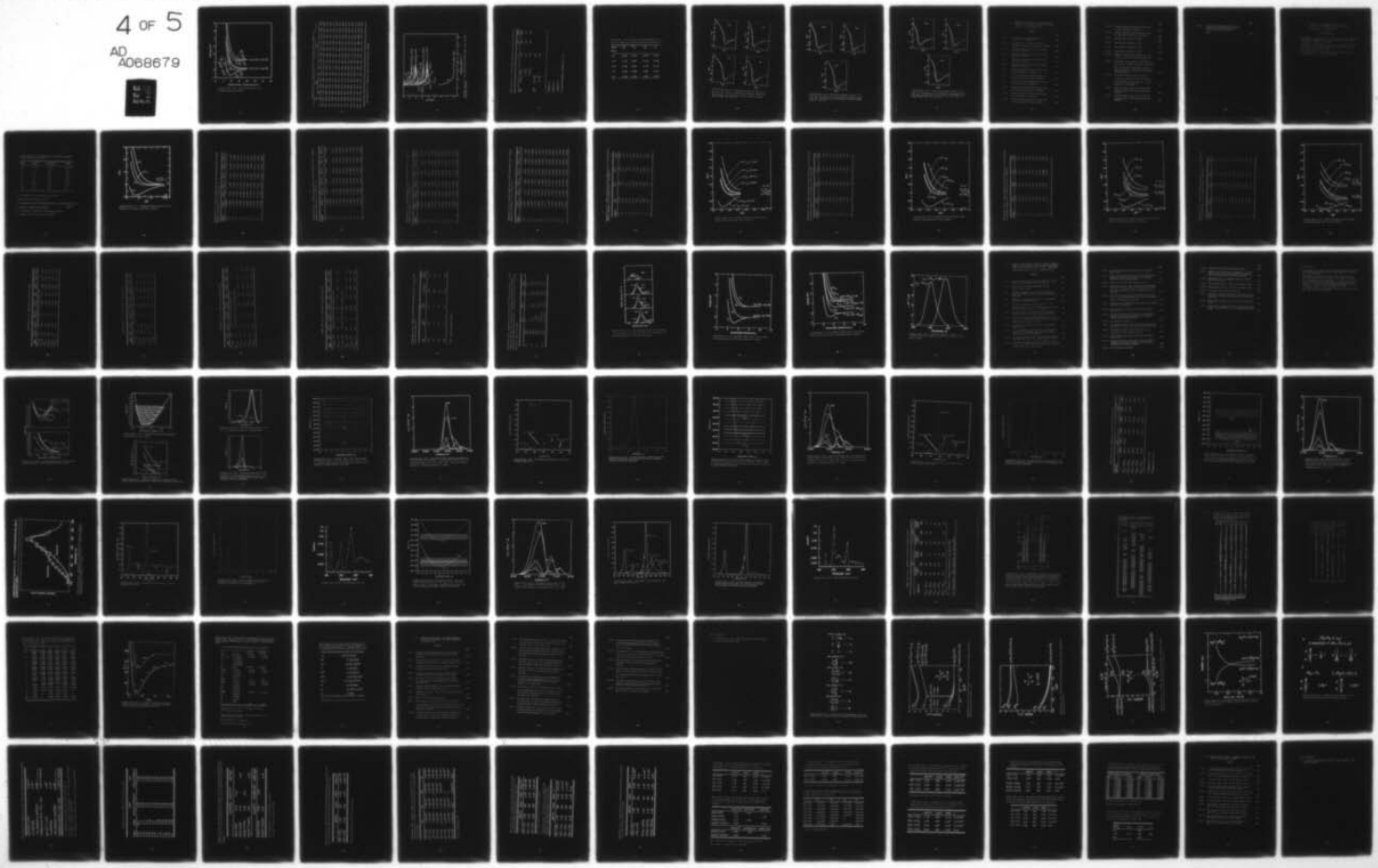

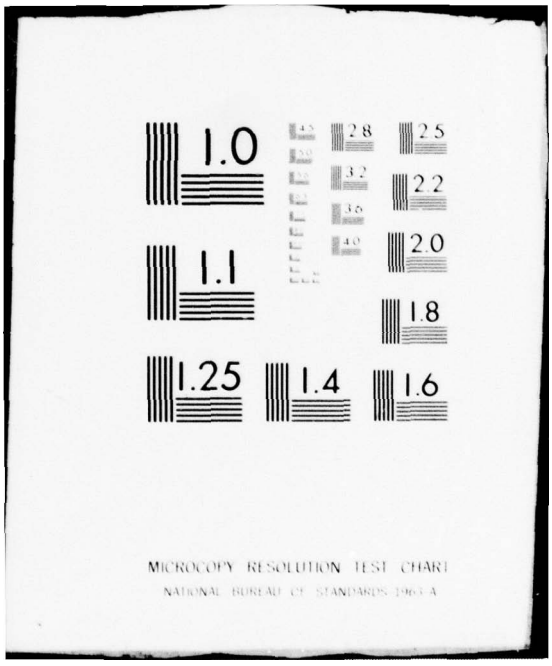
1.0
1.1
1.25
1.4
1.6
1.8
2.0
2.2
2.5
2.8
3.2
3.6
4.0
MICROCOPY RESOLUTION TEST CHART
NATIONAL BUREAU OF STANDARDS 1963 A

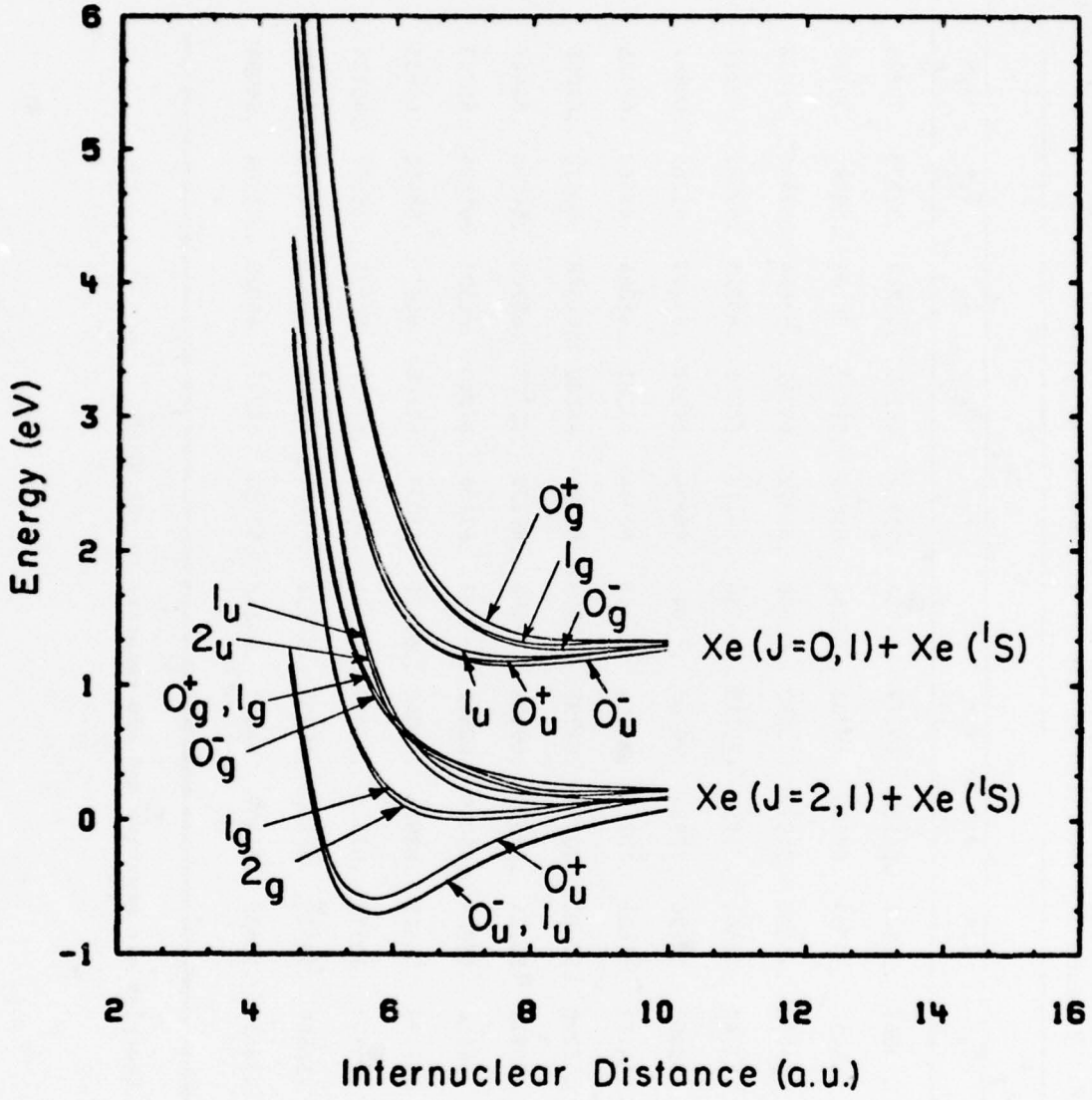

Graphical Data. A-6.6. Xe_2^* potential energy curves including spin-orbit coupling.

Tabular Data. A-6.7. Valence SCF energies of electronic states of diatomic Xe[a].

R	Xe_2	Xe_2^+				Xe_2^*							
	$^1\Sigma_g^+$	$^2\Sigma_u^+$	$^2\Pi_g$	$^2\Pi_u$	$^2\Sigma_g^+$	$^3\Sigma_u^+$	$^1\Sigma_u^+$	$^3\Pi_g$	$^1\Pi_g$	$^3\Pi_u$	$^1\Pi_u$	$^3\Sigma_g^+$	$^1\Sigma_g^+$
4.50	.81444	.53110	.42507	.34045	.27521	.64589	.64179	.54394	.53932	.46150	.45212	.32973	.38823
5.00	.90935	.58558	.50808	.45424	.39509	.69706	.69303	.62280	.61849	.57027	.56233	.50881	.50497
5.50	.95534	.60159	.54494	.51093	.46317	.71099	.70680	.65688	.65272	.62362	.61664	.57446	.57078
5.75	.96839	.60283	.55440	.52742	.48561	.71151	.70718	.66530	.66118	.63888	.63223	.59607	.59227
6.00	.97740	.60176	.56040	.53902	.50286	.70983	.70540	.67044	.66634	.64948	.64309	.61269	.60867
6.25	.98361	.59936	.56409	.54717	.51621	.70712	.70244	.67343	.66934	.65681	.65064	.62560	.62125
6.50	.98789	.59630	.56629	.55290	.52662	.70381	.69893	.67504	.67096	.66189	.65588	.63570	.63098
7.00	.99288	.58972	.56814	.55979	.54124	.69699	.69173	.67598	.67192	.66773	.66206	.64996	.64447
7.50	.99527	.58377	.56844	.56324	.55043	.69099	.68542	.67557	.67155	.67040	.66503	.65894	.65290
8.00	.99643	.57898	.56821	.56499	.55629	.68618	.68040	.67471	.67077	.67148	.66641	.66456	.65835
9.00	.99730	.57271	.56755	.56633	.56252	.67945	.67369	.67264	.66897	.67137	.66694	.66977	.66426
10.00	.99755	.56952	.56711	.56666	.56515	.67486	.66954	.67032	.66701	.66981	.66600	.67056	.66618
20.00	.99703	.56655	.56653	.56653	.56655	.64309	.64067	.64242	.64024	.64241	.64020	.64304	.64098

[a] All quantities in a.u. Energies are negative and are relative to -32.00000.

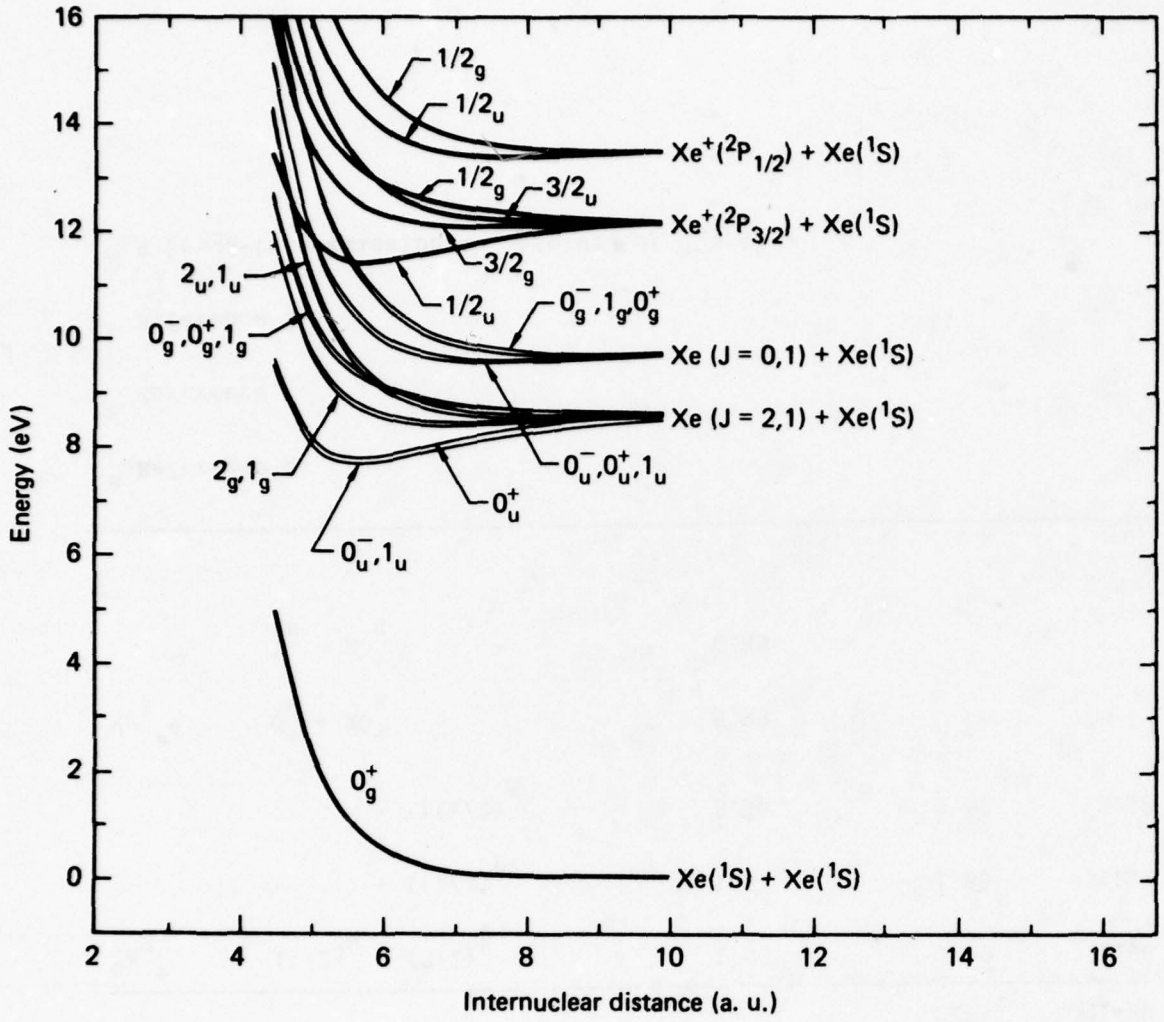

Graphical Data. A-6.8. Xe_2, Xe_2^*, and Xe_2^+ potential energy curves including spin-orbit coupling.

Tabular Data. A-6.9. Selected Xe_2^+ and Xe_2^* vertical transition energies (eV).

		a	CI[b]	CI-EP[c]
Xe_2^+	$(1/2)_u \rightarrow (3/2)_g$	1.03	0.99	0.96
	$\rightarrow I(1/2)_g$	1.67	1.60	1.57
	$\rightarrow II(1/2)_g$	3.56	3.31	3.32
Xe_2^*[d]	$0_u^+ \rightarrow XO_g^+$	6.99		
	$1_u \rightarrow XO_g^+$	6.88		

[a] Reference 1.

[b] Reference 2.

[c] Reference 3.

[d] A bound-free emission is observed at 7.3 eV.

Tabular Data. A-6.10. Variation of the magnitude of the transition moment for Xe_2^* with internuclear distance (a.u.).

State R(a_o)	$^1\Sigma_u^+$	$^1\Pi_u$	0_u^+	1_u
5.5	0.691	0.953	0.678	0.115
5.75	0.723	0.944	0.705	0.130
6.25	0.785	0.922	0.752	0.159
7.5	0.901	0.866	0.804	0.207
8.0	0.926	0.841	0.803	0.209

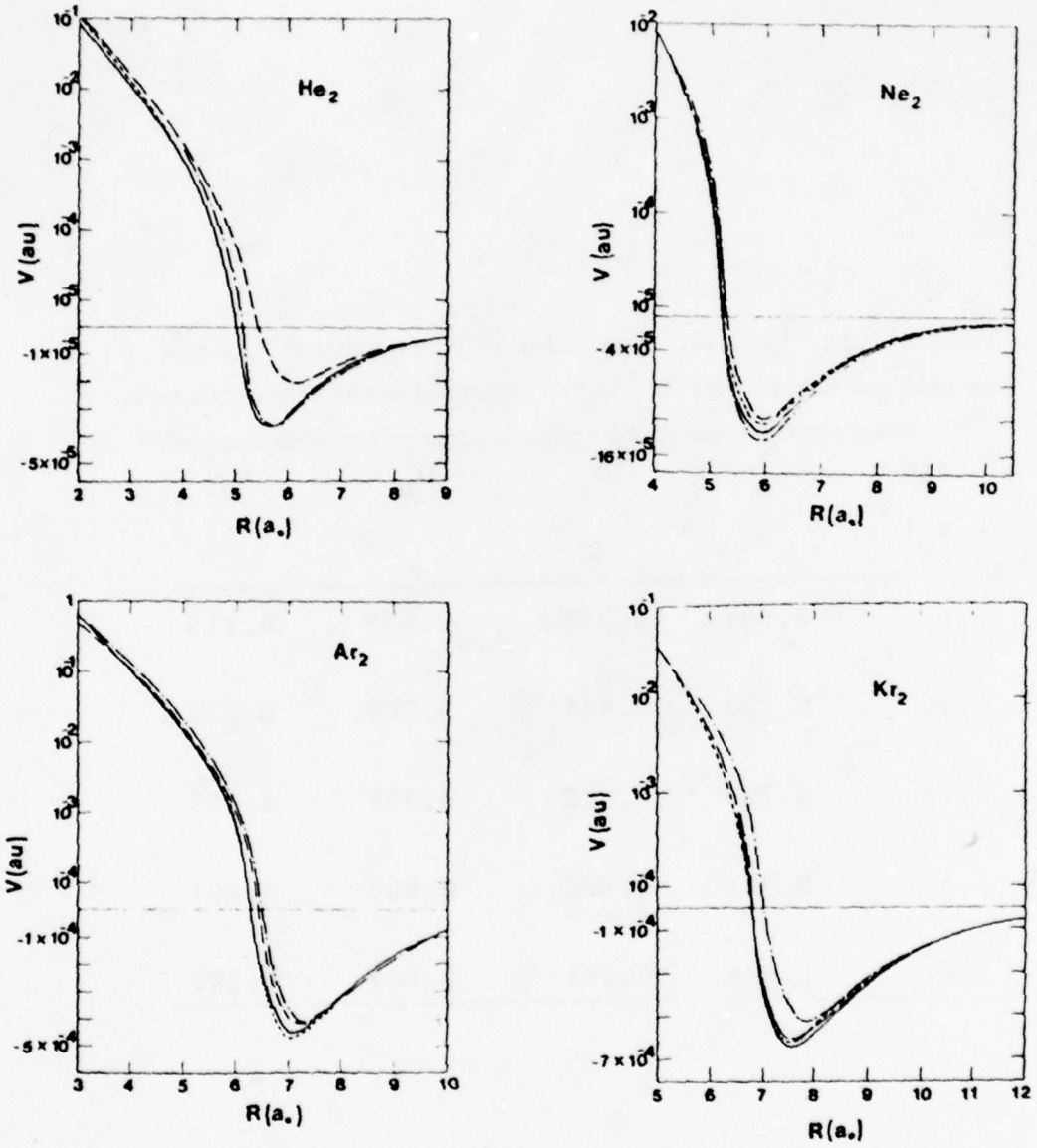

Graphical Data. A-6.11. Interaction energies for $^1\Sigma_g^+$ states of He_2, Ne_2, Ar_2, and Kr_2 as determined by experiment [solid line, Refs. (A-5.8) - (A-5.11)] and by various theoretical models [broken lines, Ref. (A-5.5)].

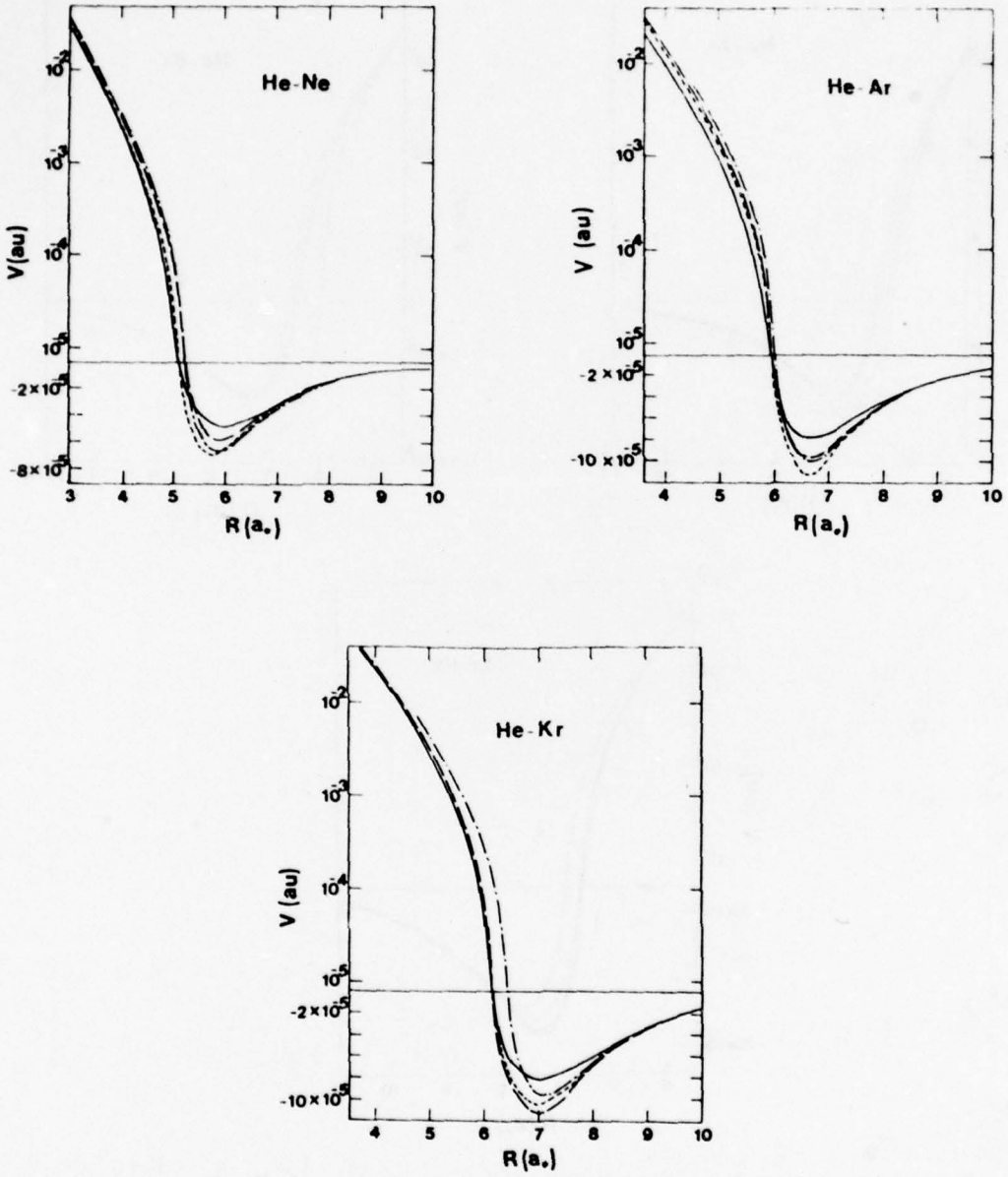

Graphical Data. A-6.12. Interaction energies of He-Ne ($^1\Sigma^+$), He-Ar ($^1\Sigma^+$) and He-Kr ($^1\Sigma^+$) as determined by experiment [solid line, Ref. (A-5.12)] and by various theoretical models [broken line, Ref. (A-5.5)].

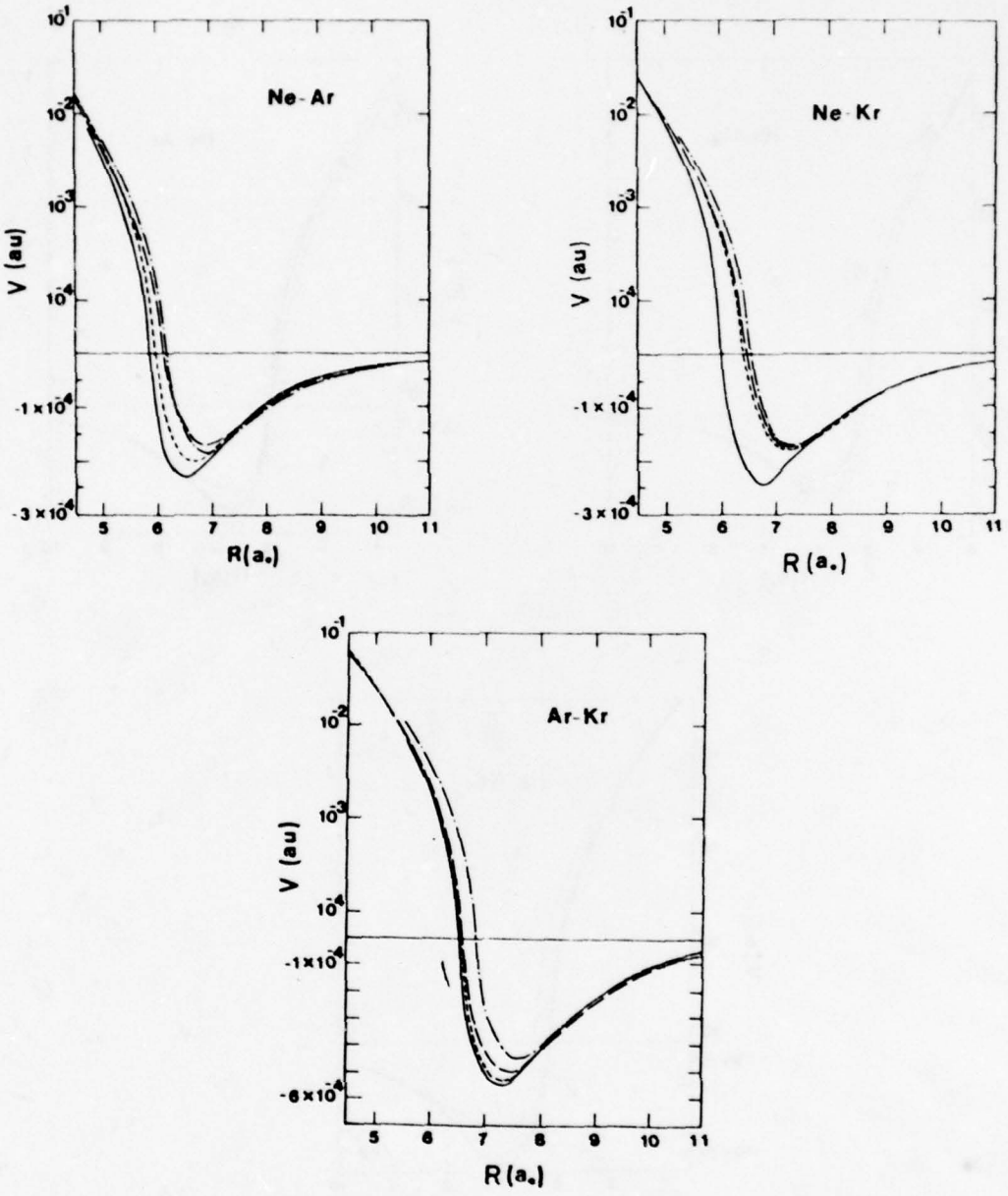

Graphical Data. A-6.13. Interaction energies of Ne-Ar ($^1\Sigma^+$), Ne-Kr ($^1\Sigma^+$), and Ar-Kr ($^1\Sigma^+$) as determined by experiment [solid line, Refs. (A-5.13) and (A-5.14)] and by various theoretical models [broken lines, ref. (A-5.5)].

A-7. POTENTIAL ENERGY CURVES, ELECTRONIC ENERGIES, SPECTROSCOPIC CONSTANTS, AND ABSORPTION SPECTRA FOR Ne_2^+, Ar_2^+, Kr_2^+, Xe_2^+, AND $ArKr^+$

CONTENTS

		Page
A-7.1.	Long-range-force interaction parameters for the noble gas dimer ions	1187
A-7.2.	Ab initio potential energy curves for Ar_2^+ without inclusion of spin-orbit coupling . .	1188
A-7.3.	Potential energy curves for Ne_2^+ including spin-orbit coupling	1189
A-7.4.	Potential energy curves for Ar_2^+ including spin-orbit coupling	1190
A-7.5.	Potential energy curves for Kr_2^+ including spin-orbit coupling	1191
A-7.6.	Potential energy curves for Xe_2^+ including spin-orbit coupling	1192
A-7.7.	Density functional potential energy curves for Ne_2^+ assuming Λ-S coupling	1193
A-7.8.	Density functional potential energy curves for Ne_2^+ (spin-orbit effects included).	1194
A-7.9.	Density functional potential energy curves for Ar_2^+ assuming Λ-S coupling	1195
A-7.10.	Density functional potential energy curves for Ar_2^+ (spin-orbit effects included)	1196
A-7.11.	Density functional potential energy curves for Kr_2^+ assuming Λ-S coupling	1197
A-7.12.	Density functional potential energy curves for Kr_2^+ (spin-orbit effects included)	1198

Page

A-7.13. Density functional potential energy curves for Xe_2^+ assuming A-S coupling 1199

A-7.14. Density functional potential energy curves for Xe_2^+ (spin-orbit effects included) 1200

A-7.15. Spectroscopic constants for Ne_2^+ 1201

A-7.16. Spectroscopic constants for Ar_2^+ 1202

A-7.17. Spectroscopic constants for Kr_2^+ 1203

A-7.18. Spectroscopic constants for Xe_2^+ 1204

A-7.19. Summary of spectroscopic constants for the $A\ ^2\Sigma^+_{1/2u}$ state of the noble gas dimer ions . . 1205

A-7.20. Absorption cross sections (in 10^{-18} cm^2) for the $I(1/2)_u \rightarrow II(1/2)_g$ transition in Ne_2^+, Ar_2^+, Kr_2^+, and Xe_2^+ based on ab initio calculated spectra shifted to coincide with experimental absorption maxima 1206

A-7.21. The absorption spectra for the $I(1/2)_u \rightarrow II(1/2)_g$ transition in Ne_2^+, Ar_2^+, Kr_2^+ and Xe_2^+ determined from ab initio configuration interaction calculations 1207

A-7.22. Potential energy curves for the ground and excited states of $ArKr^+$ without spin-orbit coupling 1208

A-7.23. Potential energy curves for the ground and excited states of $ArKr^+$ including spin-orbit coupling 1209

Page

A-7.24. Theoretical absorption curves for the transitions from the ground state to the $III_{1/2}$ and $IV_{1/2}$ excited states of $ArKr^+$ 1210

A-7. POTENTIAL ENERGY CURVES, ELECTRONIC ENERGIES, SPECTROSCOPIC CONSTANTS AND ABSORPTION SPECTRA FOR Ne_2^+, Ar_2^+, Kr_2^+, Xe_2^+ AND $ArKr^+$.

General References

1. H. H. Michels, R. H. Hobbs, and L. A. Wright, "Electronic Structure of the Noble Gas Dimer Ions. I. Potential Energy Curves and Spectroscopic Constants" (in press).
2. W. R. Wadt, D. C. Cartwright, and J. S. Cohen, "Theoretical Absorption Spectra for Ne_2^+, Ar_2^+, Kr_2^+ and Xe_2^+ in the Near Ultraviolet," Appl. Phys. Letts. 31, 672 (1977).
3. C. F. Bender and N. W. Winter, "Theoretical Absorption Spectra of $ArKr^+$," Appl. Phys. Letts. 33, 29 (1978).

Tabular Data. A-7.1. Long-range-force interaction parameters for the noble gas dimer ions.

Species	α_o (bohr^3)	$\sum_i \langle r_i^2 \rangle$ (bohr^2)	I (eV)
Ne	2.66 [a,b]	9.699 [d]	21.564 [e,f]
Ne^+	(1.32) [c]	6.842	40.962
Ar	11.08	26.145	15.759
Ar^+	(6.52)	20.054	27.629
Kr	16.74	39.674	13.999
Kr^+	(10.78)	31.847	24.359
Xe	27.29	62.511	12.127
Xe^+	(18.90)	52.022	21.2

[a] R. R. Teachout and R. T. Pack, Atomic Data 3, 195 (1971).

[b] A. Dalgarno, Adv. Physics 11, 281 (1962).

[c] The ion polarizabilities are scaled from the atomic α_o using the hydrogenic form, $\alpha_o \sim \sum_i \langle r_i^2 \rangle^2$

[d] Non-relativistic Hartree-Fock calculation.

[e] R. L. Kelly and D. E. Harrison, Jr., Atomic Data 3, 177 (1971).

[f] C. E. Moore, Nat. Bur. Std. (U.S.) Circ. 467 (1958).

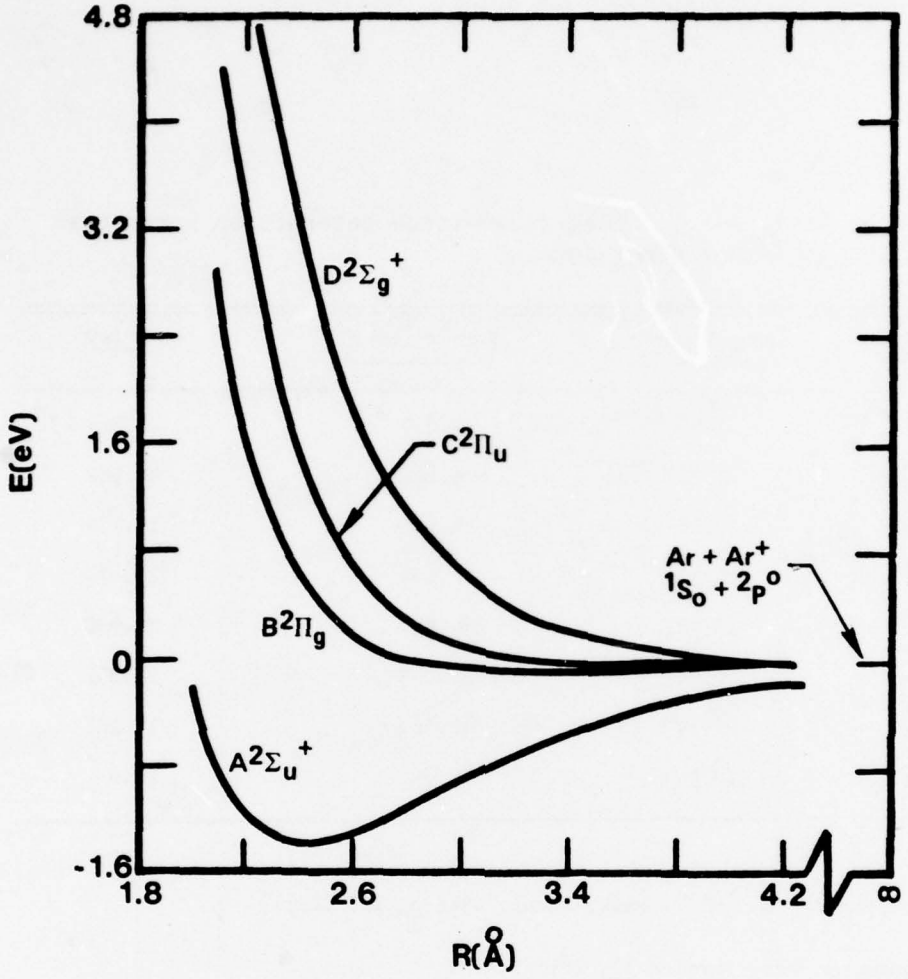

Graphical Data. A-7.2. Ab initio potential energy curves for Ar_2^+ without inclusion of spin-orbit coupling.

Tabular Data. A-7.3. Potential energy curves for Ne_2^+ including spin-orbit coupling. Energies in eV relative to c.g. of Ne_2^+ at R = ∞.

R (a.u.)	$A\,^2\Sigma^+_{1/2u}$	$B\,^2\Pi_{3/2g}$	$B\,^2\Pi_{1/2g}$	$C\,^2\Pi_{3/2u}$	$C\,^2\Pi_{1/2u}$	$D\,^2\Sigma^+_{1/2u}$
2.8	-0.89497	-	-	-	-	-
3.0	-1.28953	1.26194	1.32586	2.57256	2.63768	4.50598
3.2	-1.37990	0.48908	0.55283	1.43735	1.50265	3.06507
3.4	-1.31808	0.07755	0.14109	0.76574	0.83129	2.11391
3.6	-1.18232	-0.12882	-0.06558	0.37242	0.43830	1.47550
3.8	-1.01630	-0.21895	-0.15609	0.14705	0.21334	1.04125
4.0	-0.84617	-0.24597	-0.18362	0.02207	0.08890	0.74236
4.2	-0.68726	-0.24091	-0.17924	-0.04416	0.02338	0.53395
4.4	-0.54766	-0.22074	-0.15998	-0.07598	-0.00748	0.38739
4.6	-0.43046	-0.19535	-0.13579	-0.08868	-0.01897	0.28363
∞	-0.03230	-0.03230	-0.03230	-0.03230	0.06460	0.06460

Tabular Data. A-7.4. Potential energy curves for Ar_2^+ including spin-orbit coupling. Energies in eV relative to c.g. of Ar_2^+ at R = ∞.

R (a.u.)	$A\ ^2\Sigma^+_{1/2}$	$B\ ^2\Pi_{3/2g}$	$B\ ^2\Pi_{1/2g}$	$C\ ^2\Pi_{3/2u}$	$C\ ^2\Pi_{1/2u}$	$D\ ^2\Sigma^+_{1/2u}$
4.2	-1.18618	1.65365	1.76982	2.77055	2.89064	4.95560
4.4	-1.34226	-	-	-	-	-
4.6	-1.38227	0.44736	0.56260	1.14139	1.26240	2.81570
4.8	-1.34896	0.14654	0.26118	0.69322	0.81483	2.14999
5.0	-1.27160	-0.03714	0.07676	0.39334	0.51563	1.65681
5.2	-1.16918	-0.14504	-0.03200	0.19416	0.31726	1.28605
5.4	-1.05453	-0.19620	-0.08425	0.07089	0.19489	1.01491
5.8	-0.82182	-0.22463	-0.11562	-0.05891	0.06740	0.64328
6.0	-0.71382	-0.21307	-0.10599	-0.08259	0.04512	0.52554
6.2	-0.61523	-0.19933	-0.09464	-0.09647	0.03290	0.43043
∞	-0.05919	-0.05919	-0.05919	-0.05919	0.11837	0.11837

Tabular Data. A-7.5. Potential energy curves for Kr_2^+ including spin-orbit coupling. Energies in eV relative to c.g. of Kr_2^+ at R = ∞.

R (a.u.)	$A\ ^2\Sigma^+_{1/2u}$	$B\ ^2\Pi_{3/2g}$	$B\ ^2\Pi_{1/2g}$	$C\ ^2\Pi_{3/2u}$	$C\ ^2\Pi_{1/2u}$	$D\ ^2\Sigma^+_{1/2u}$
4.8	-1.28087	-	-	-	-	-
5.0	-1.38709	0.69575	1.09151	1.43876	1.91284	3.18488
5.2	-1.41503	0.27628	0.66358	0.87603	1.35598	2.46023
5.4	-1.38910	0.00729	0.38423	0.48908	0.97546	1.92201
5.6	-1.32866	-0.16482	0.19960	0.22295	0.71627	1.51846
5.8	-1.24730	-0.28795	0.06150	0.02825	0.52948	1.19889
6.0	-1.15345	-0.33612	-0.00457	-0.08468	0.42439	0.98465
6.4	-0.95763	-0.39054	-0.10324	-0.22768	0.30020	0.68250
6.8	-0.77681	-0.38945	-0.15500	-0.28414	0.26501	0.52489
7.0	-0.69752	-0.37898	-0.17192	-0.27435	0.26591	0.48097
7.2	-0.62696	-0.36673	-0.18626	-0.29870	0.27285	0.45125
∞	-0.22197	-0.22197	-0.22197	-0.22197	0.44393	0.44393

Tabular Data. A-7.6. Potential energy curves for Xe_2^+ including spin-orbit coupling. Energies in eV relative to c.g. of Xe_2^2 at R = ∞.

R (a.u.)	$A\,^2\Sigma^+_{1/2u}$	$B\,^2\Pi_{3/2g}$	$B\,^2\Pi_{1/2g}$	$C\,^2\Pi_{3/2u}$	$C\,^2\Pi_{1/2u}$	$D\,^2\Sigma^+_{1/2u}$
5.6	-1.40193	-	-	-	-	-
5.8	-1.48344	0.33100	0.95693	0.93646	1.92269	2.74968
6.0	-1.50867	0.02237	0.61482	0.52197	1.52369	2.25511
6.2	-1.49362	-0.16564	0.38771	0.24616	1.26243	1.89954
6.4	-1.45490	-0.33783	0.17473	0.00150	1.03543	1.59142
6.6	-1.39811	-0.44565	0.02261	-0.16640	0.88498	1.36717
6.8	-1.33076	-0.52015	-0.09755	-0.29043	0.77902	1.19677
7.0	-1.25[illegible]1	-0.55939	-0.18338	-0.37035	0.71648	1.07791
7.4	-1.10398	-0.58459	-0.29772	-0.45724	0.66367	0.93575
7.6	-1.03040	-0.58149	-0.33514	-0.47699	0.66026	0.89673
7.8	-0.95973	-0.57425	-0.36461	-0.48069	0.67123	0.87026
8.0	-0.89665	-0.56304	-0.38755	-0.49278	0.67575	0.85330
8.2	-0.83747	-0.54924	-0.40162	-0.49133	0.69129	0.84609
∞	-0.43549	-0.43549	-0.43549	-0.43549	0.87098	0.87098

Tabular Data. A-7.7. Density functional potential energy curves for Ne_2^+ assuming Λ-S coupling. Energies in a.u. relative to E(∞) = -256.3646 a.u.

R (a.u.)	$A\,^2\Sigma_u^+$	$B\,^2\Pi_g$	$C\,^2\Pi_u$	$D\,^2\Sigma_g^+$
3.0	-.04737	.04756	.09573	.16557
3.2	-.05068	.01916	.05401	.11261
3.4	-.04840	.00404	.02933	.07765
3.6	-.04340	-.00355	.01487	.05417
3.8	-.03729	-.00686	.00659	.03820
4.0	-.03101	-.00785	.00200	.02720
4.2	-.02515	-.00767	-.00044	.01951
4.4	-.01998	-.00693	-.00161	.01410
4.6	-.01563	-.00599	-.00207	.01024
∞	0.	0.	0.	0.

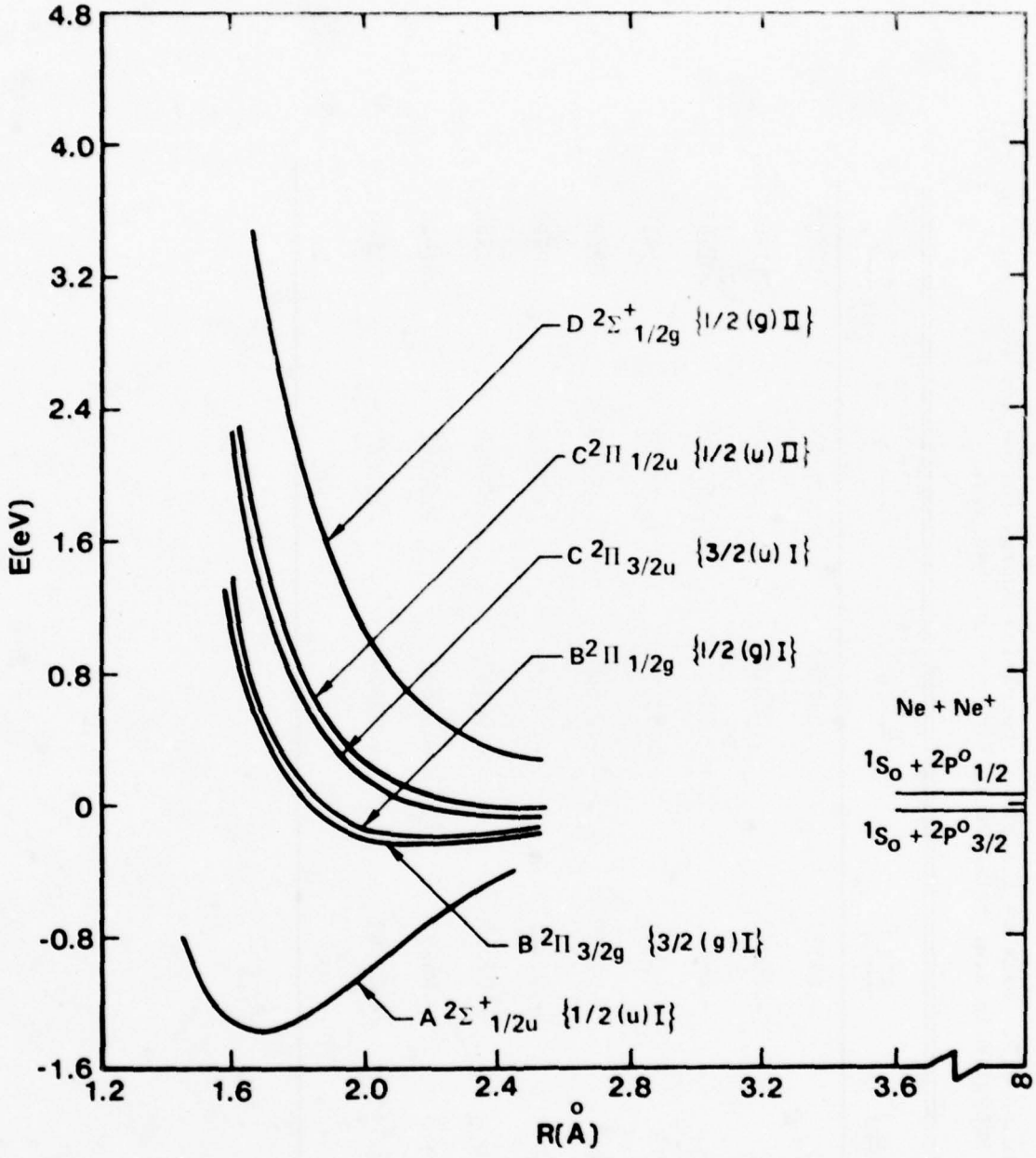

Graphical Data. A-7.8. Density functional potential energy curves for Ne_2^+ (spin-orbit effects included).

Tabular Data. A-7.9. Density functional potential energy curves for Ar_2^+ assuming Λ-S coupling. Energies in a.u. relative to $E(\infty)^2 = -1053.0921$.

R (a.u.)	$A\,^2\Sigma^+_u$	$B\,^2\Pi_g$	$C\,^2\Pi_u$	$D\,^2\Sigma^+_g$
4.2	-.04353	.06295	.10399	.18203
4.6	-.05070	.01862	.04412	.10336
4.8	-.04945	.00756	.02765	.07887
5.0	-.04659	.00081	.01663	.06072
5.2	-.04279	-.00316	.00931	.04707
5.4	-.03855	-.00504	.00478	.03706
5.8	-.02991	-.00608	.00001	.02330
6.0	-.02589	-.00566	-.00086	.01890
6.2	-.02221	-.00515	-.00137	.01532
∞	0.	0.	0.	0.

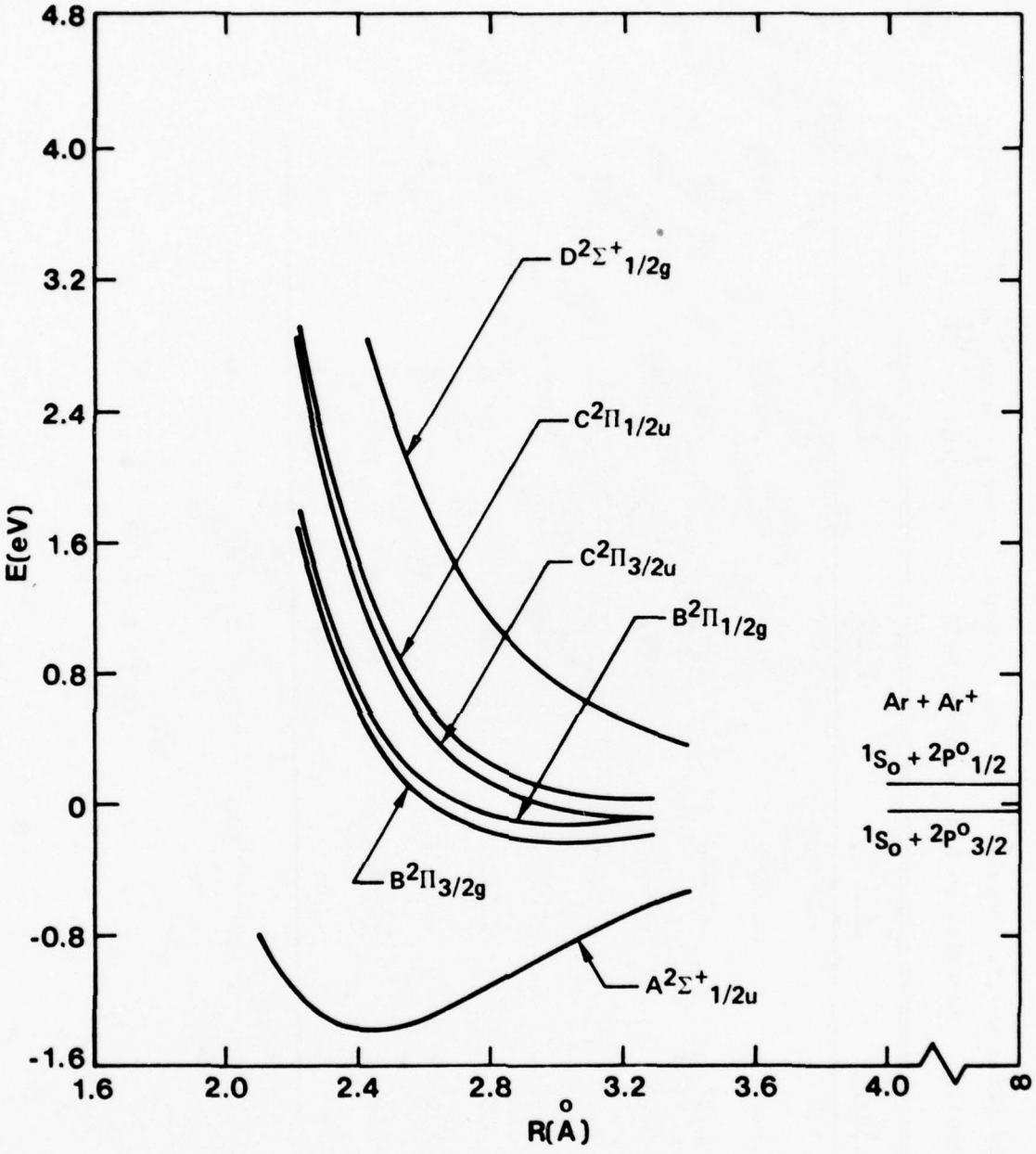

Graphical Data. A-7.10. Density functional potential energy curves for Ar_2^+ (spin-orbit effects included).

Tabular Data. A-7-11. Density functional potential energy curves for Kr_2^+ assuming Λ-S coupling. Energies in a.u. relative to E(∞) = -5503.6239.

R (a.u.)	$A\,^2\Sigma_u^+$	$B\,^2\Pi_g$	$C\,^2\Pi_u$	$D\,^2\Sigma_g^+$
5.0	-.04987	.03373	.06103	.11527
5.2	-.05068	.01831	.04035	.08833
5.4	-.04949	.00843	.02613	.06817
5.6	-.04701	.00210	.01635	.05288
5.8	-.04373	-.00243	.00920	.04059
6.0	-.03999	-.00420	.00505	.03206
6.4	-.03211	-.00620	-.00021	.01933
6.8	-.02468	-.00616	-.00229	.01159
7.0	-.02136	-.00577	-.00266	.00897
7.2	-.01835	-.00532	-.00282	.00690
∞	0.	0.	0.	0.

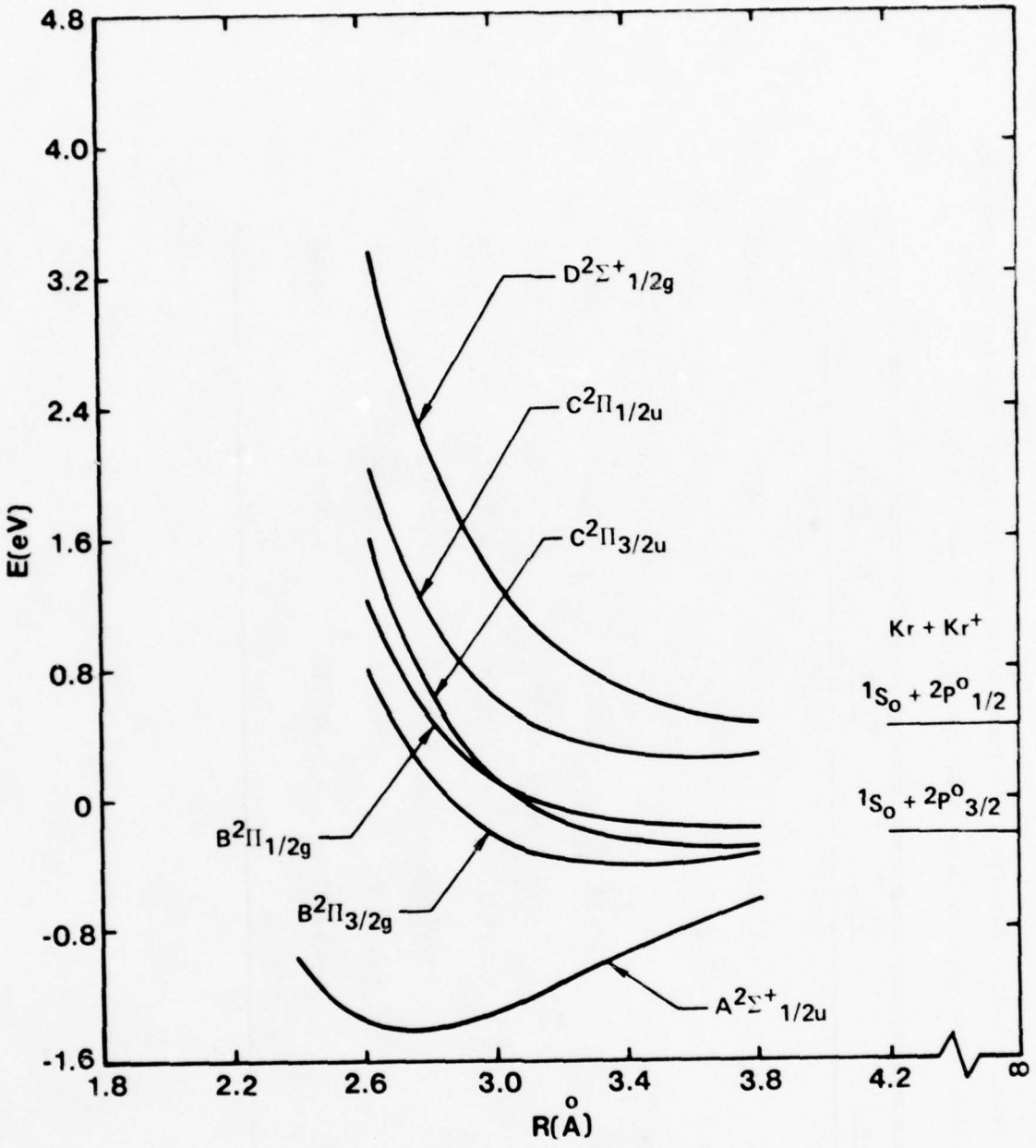

Graphical Data. A-7.12. Density functional potential energy curves for Kr_2^+ (spin-orbit effects included).

Tabular Data. A-7.13. Density functional potential energy curves for Xe_2^+ assuming Λ-S coupling. Energies in a.u. relative to E(∞) = -14463.8615.

R(a.u.)	$A\,^2\Sigma_u^+$	$B\,^2\Pi_g$	$C\,^2\Pi_u$	$D\,^2\Sigma_g^+$
5.8	-.05028	.02817	.05042	.09204
6.0	-.05064	.01683	.03519	.07264
6.2	-.04955	.00992	.02505	.05813
6.4	-.04748	.00359	.01606	.04531
6.6	-.04475	-.00037	.00989	.03544
6.8	-.04161	-.00311	.00533	.02750
7.0	-.03825	-.00455	.00239	.02142
7.4	-.03139	-.00548	-.00080	.01292
7.6	-.02808	-.00537	-.00153	.01000
7.8	-.02494	-.00510	-.00166	.00768
8.0	-.02202	-.00469	-.00211	.00580
8.2	-.01932	-.00418	-.00205	.00451
∞	0.	0.	0.	0.

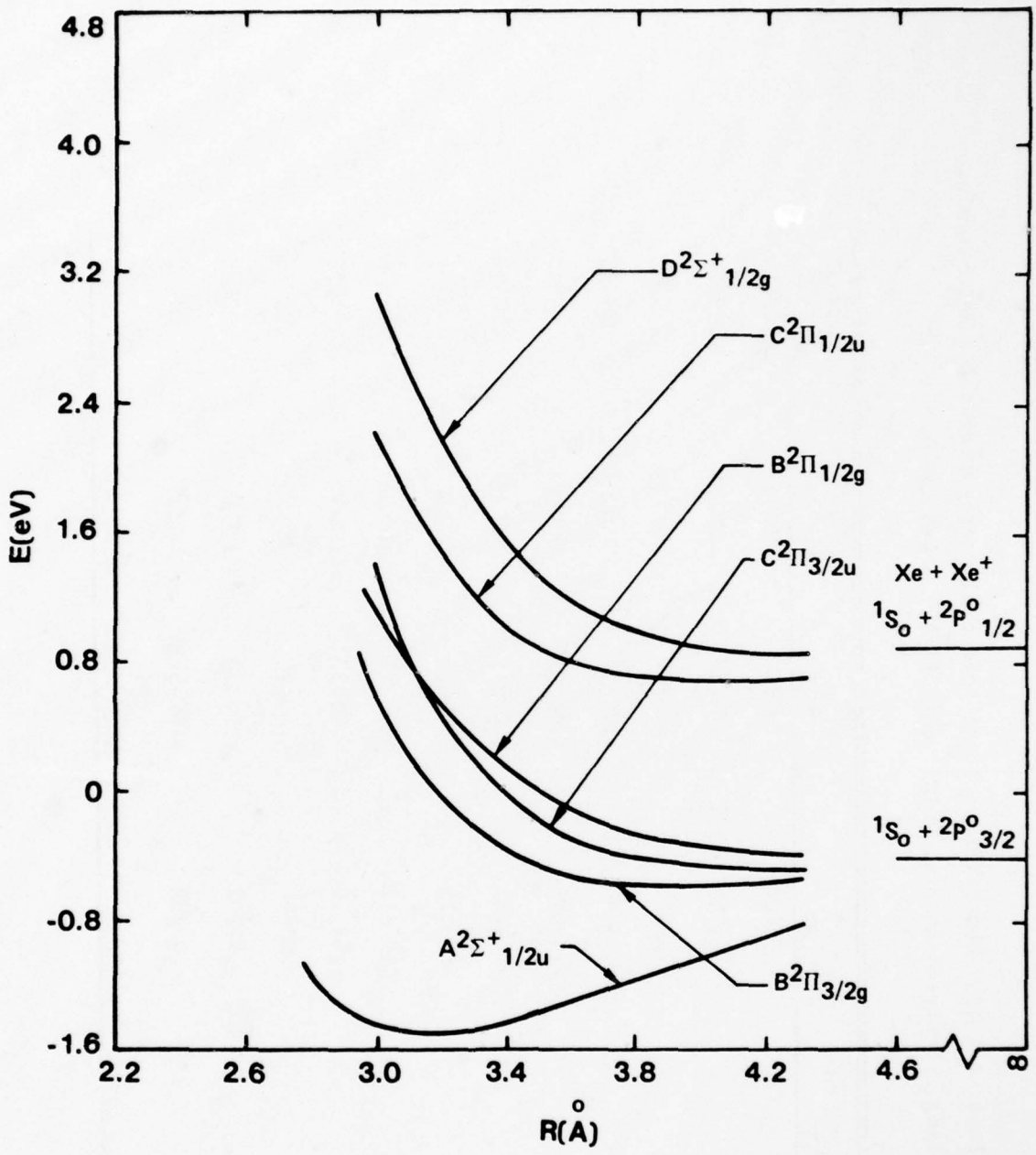

Graphical Data. A-7.14. Density functional potential energy curves for Xe_2^+ (spin-orbit effects included).

Tabular Data. A-7.15. Spectroscopic constants for Ne_2^+.

State	T_e (eV)	$\omega_e(cm^{-1})$	$\omega_e X_e(cm^{-1})$	$\alpha_e(cm^{-1})$	$r_e(\mathring{A})$	$B_e(cm^{-1})$	D_e(eV)	D_o(eV)
D $^2\Sigma^+_{1/2g}$	4.445	(vertical excitation energy, repulsive curve)						
C $^2\Pi_{1/2u}$	1.359	122.5	8.4	0.0166	2.50	0.2665	0.085	0.078
C $^2\Pi_{3/2u}$	1.287	103.9	8.7	0.0194	2.54	0.2579	0.060	0.054
B $^2\Pi_{1/2g}$	1.195	246.5	9.0	0.0125	2.15	0.3626	0.152	0.137
B $^2\Pi_{3/2g}$	1.132	250.8	9.8	0.0122	2.14	0.3634	0.215	0.199
A $^2\Sigma^+_{1/2u}$	0.0	597.0	6.1	0.0090	1.69	0.5840	1.347	1.310

Tabular Data. A-7.16. Spectroscopic constants for Ar_2^+.

State	T_e(eV)	ω_e(cm^{-1})	$\omega_e x_e$(cm^{-1})	α_e(cm^{-1})	r_e(Å)	B_e(cm^{-1})	D_e(eV)	D_o(eV)
$D\ ^2\Sigma^+_{1/2g}$	4.198	(vertical excitation energy, repulsive curve)						
$C\ ^2\Pi_{1/2u}$	1.413	62.4	9.3	0.0047	3.40	0.0732	0.087	0.084
$C\ ^2\Pi_{3/2u}$	1.285	53.7	3.7	0.0043	3.40	0.0732	0.037	0.034
$B\ ^2\Pi_{1/2g}$	1.264	146.9	12.0	0.0030	3.02	0.0924	0.058	0.049
$B\ ^2\Pi_{3/2g}$	1.155	153.7	10.1	0.0024	3.02	0.0927	0.167	0.158
$A\ ^2\Sigma^+_{1/2u}$	0.0	297.9	1.7	0.0011	2.43	0.1428	1.322	1.304

Tabular Data. A-7.17. Spectroscopic constants for Kr_2^+.

State	T_e(eV)	ω_e(cm^{-1})	$\omega_e x_e$(cm^{-1})	α_e(cm^{-1})	r_e(Å)	B_e(cm^{-1})	D_e(eV)	D_o(eV)
$D\ ^2\Sigma^+_{1/2g}$	3.875	(vertical excitation energy, repulsive curve)						
$E\ ^2\Pi_{1/2g}$	2.079	(vertical excitation energy, repulsive curve)						
$C\ ^2\Pi_{1/2u}$	1.679	70.2	1.3	0.0004	3.64	0.0304	0.179	0.175
$C\ ^2\Pi_{3/2u}$	1.115	51.7	0.4	0.0001	3.85	0.0271	0.077	0.074
$B\ ^2\Pi_{3/2g}$	1.019	78.0	1.9	0.0004	3.48	0.0333	0.173	0.168
$A\ ^2\Sigma^+_{1/2u}$	0.0	176.7	0.7	0.0002	2.75	0.0533	1.192	1.181

Tabular Data. A-7.18. Spectroscopic constants for Xe_2^+.

State	T_e(eV)	ω_e(cm^{-1})	$\omega_e X_e$(cm^{-1})	α_e(cm^{-1})	r_e(Å)	B_e(cm^{-1})	D_e(eV)	D_o(eV)
D $^2\Sigma^+_{1/2g}$	3.764	(vertical excitation energy, repulsive curve)						
C $^2\Pi_{1/2u}$	2.169	54.5	0.3	0.0002	3.97	0.0163	0.209	0.206
B $^2\Pi_{1/2g}$	2.123	(vertical excitation energy, repulsive curve)						
C $^2\Pi_{3/2u}$	1.034	58.5	0.3	0.0009	4.00	0.0160	0.042	0.038
B $^2\Pi_{3/2g}$	0.923	49.7	0.3	0.0003	3.91	0.0168	0.149	0.146
A $^2\Sigma^+_{1/2u}$	0.0	117.2	0.4	0.0001	3.18	0.0253	1.072	1.065

Tabular Data. A-7.19. Summary of spectroscopic constants for the A $^2\Sigma^+_{1/2u}$ state of the noble gas dimer ions.

Ion	D_e(eV)	{-SO} D_e(eV)	$\langle \bar{r} \rangle$(a.u.)	{-SO}* R_e(a.u.)
Ne_2^+	1.35	1.37	0.965	3.19
Ar_2^+	1.32	1.40	1.663	4.59
Kr_2^+	1.19	1.39	1.952	5.17
Xe_2^+	1.07	1.38	2.338	5.94

*{-SO}: Without spin-orbit effects.

Tabular Data. A-7.20. Absorption cross sections (in 10^{-18} cm^2) for the $I(1/2)_u \rightarrow II(1/2)_g$ transition in Ne_2^+, Ar_2^+, Kr_2^+, and Xe_2^+ based on ab initio calculated spectra shifted to coincide with experimental absorption maxima. The unshifted cross sections for Ar_2^+, Kr_2^+, and Xe_2^+ are shown in parentheses.

		KrF 248 nm	XeBr 282 nm	XeCl 308 nm	XeF 352 nm
Ne_2^*	(300°K)	23	17	7.4	0.96
	(600°K)	21	15	8.6	2.5
Ar_2^*	(300°K)	10 (1.2)	44 (18)	39 (38)	8.7 (31)
	(600°K)	14 (3.4)	34 (19)	32 (30)	15 (27)
Kr_2^*	(300°K)	0.31 (0.061)	14 (5.1)	40 (24)	36 (42)
	(600°K)	1.7 (0.45)	19 (9.4)	32 (23)	31 (31)
Xe_2^*	(300°K)	0.0031 (7.4×10^{-8})	1.7 (0.041)	16 (2.9)	48 (31)
	(600°K)	0.041 (1.8×10^{-7})	5.9 (0.14)	18 (7.0)	34 (27)

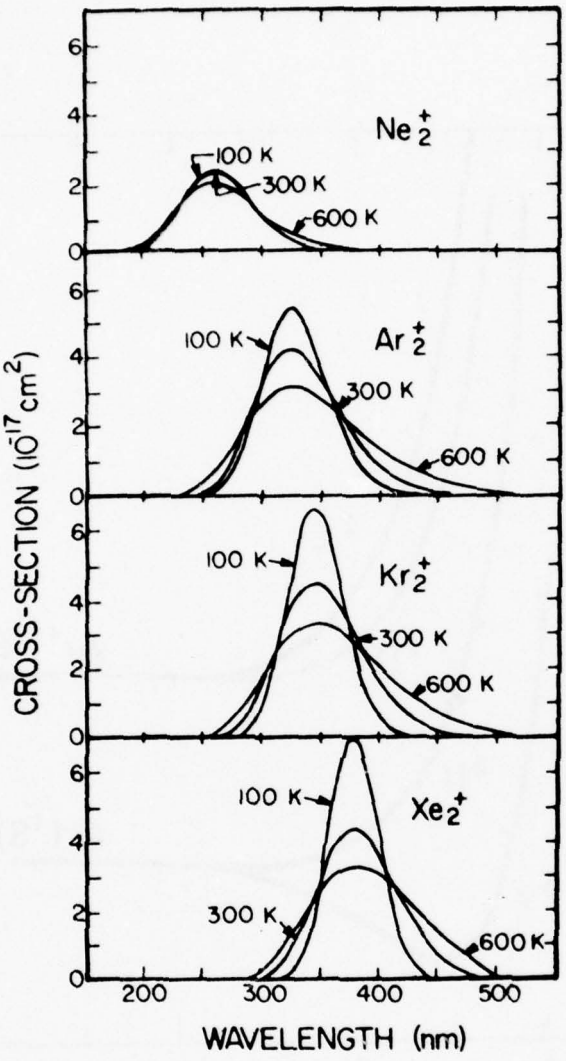

Graphical Data. A-7.21. The absorption spectra for the $I(1/2)_u \rightarrow II(1/2)_g$ transition in Ne_2^+, Ar_2^+, Kr_2^+, and Xe_2^+ determined from ab initio configuration interaction calculations.

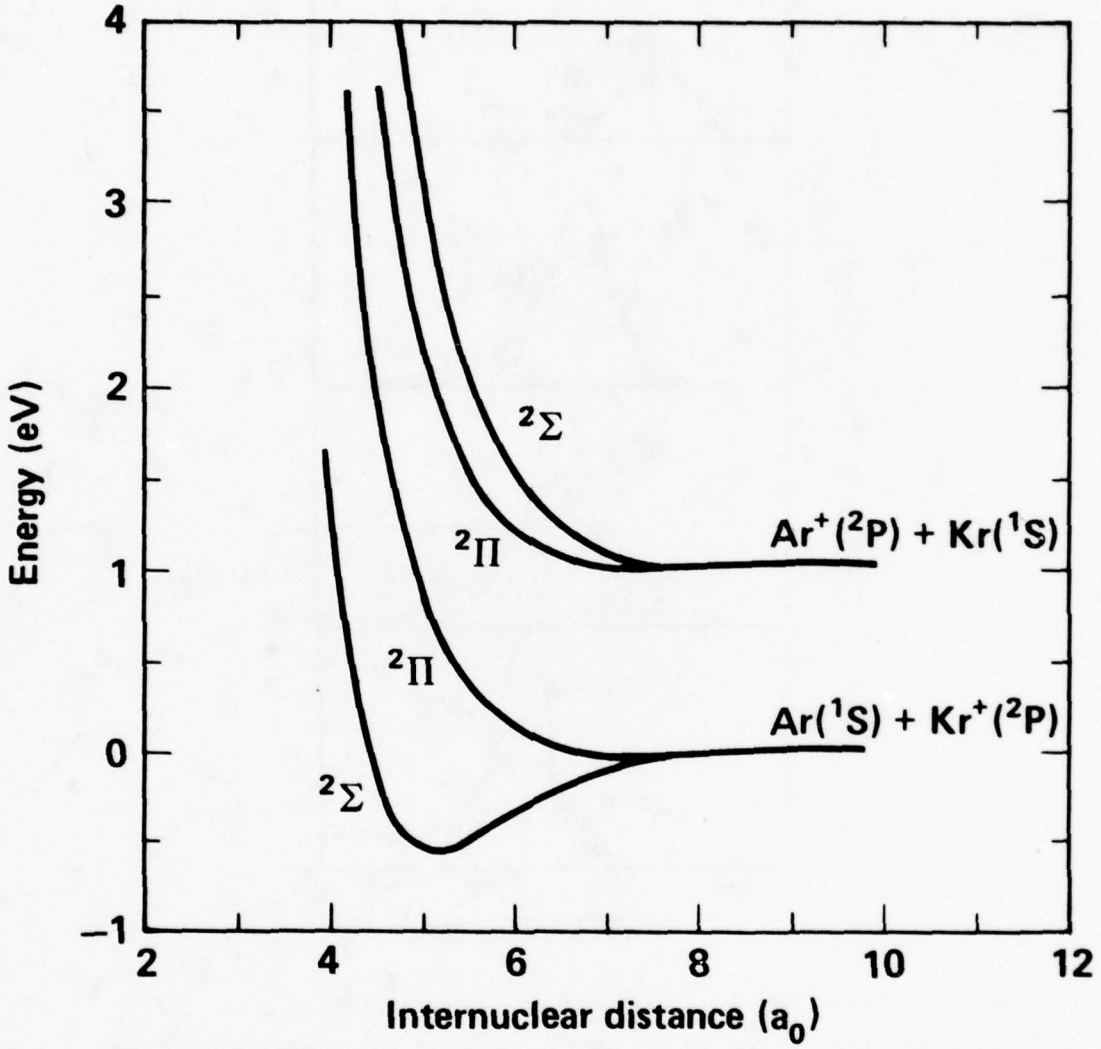

Graphical Data. A-7.22. Potential energy curves for the ground and excited states of $ArKr^+$ without spin-orbit coupling.

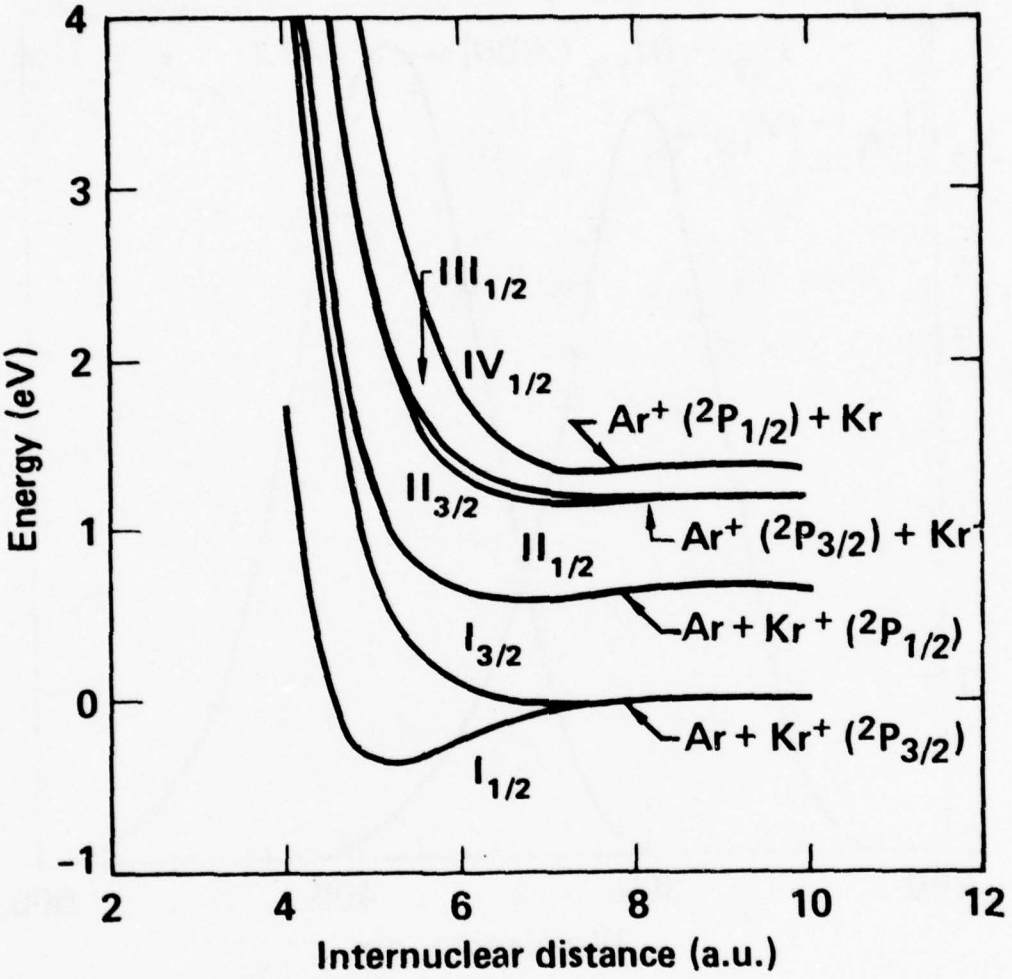

Graphical Data. A-7.23. Potential energy curves for the ground and excited states of $ArKr^+$ including spin-orbit coupling.

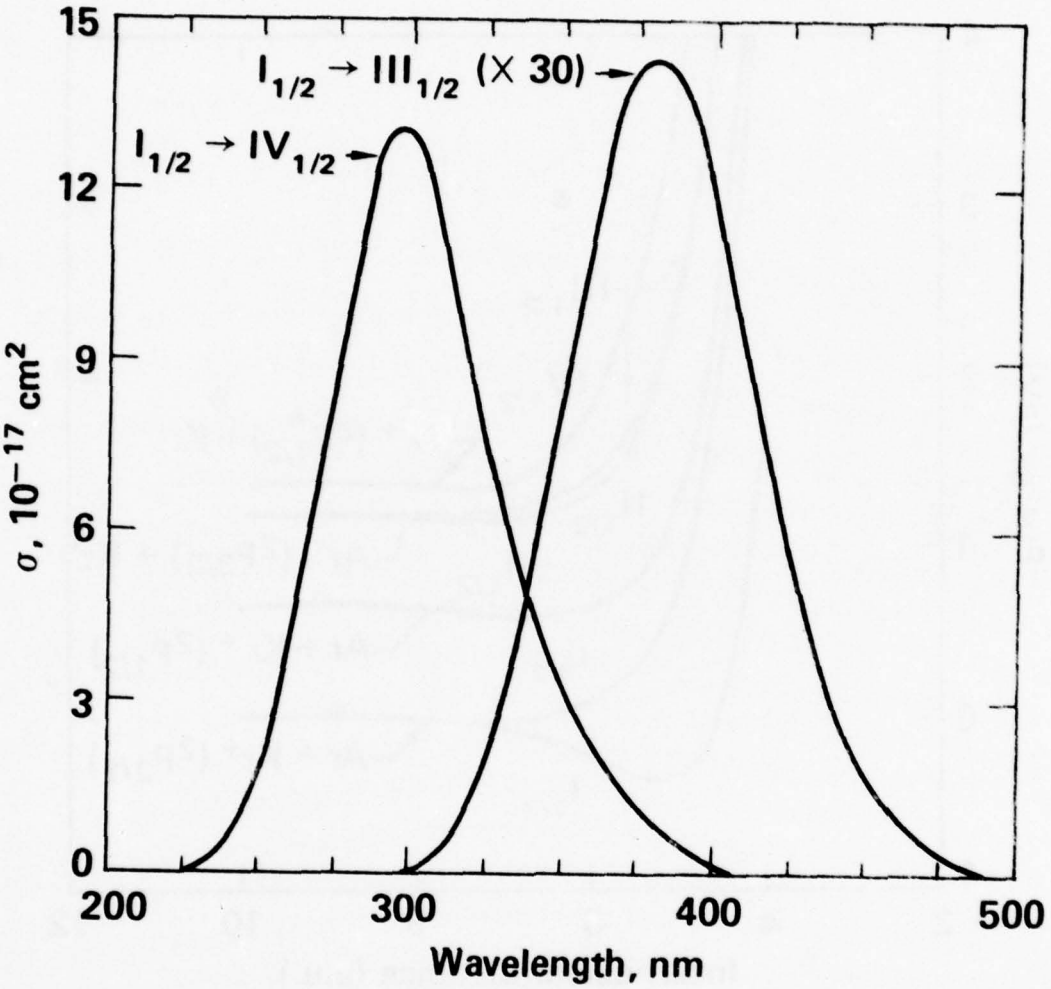

Graphical Data. A-7.24. Theoretical absorption curves for the transitions from the ground state to the $III_{1/2}$ and $IV_{1/2}$ excited states of $ArKr^{+}$.

A-8. POTENTIAL ENERGY CURVES, VIBRATIONAL LEVELS, TRANSITION MOMENTS, FLUORESCENCE AND EINSTEIN TRANSITION PROBABILITIES FOR NeF, ArF, ArCℓ, KrF, and KrCℓ. WAVENUMBERS, FRANCK-CONDON FACTORS, AND R^n - CENTROIDS FOR XeF

CONTENTS

		Page
A-8.1.	Potential energy curves for the covalent and ion-pair states of NeF including spin-orbit coupling	1215
A-8.2.	Vibrational levels and wavefunctions for the $B(^2\Sigma_{1/2})$ state of NeF	1216
A-8.3	Transition moments for the states of NeF without spin-orbit interaction as a function of internuclear separation	1216
A-8.4.	Calculated fluorescence for the $2^2\Sigma \rightarrow 1^2\Sigma$ transition of NeF at T = 450 and 2000°K	1217
A-8.5.	Calculated fluorescense of NeF for the $2^2\Sigma \rightarrow 1^2\Sigma$ transition, the $2^2\Pi \rightarrow 1^2\Pi$ transition, and the sum of the two rescaled to unity at its maximum	1217
A-8.6.	Potential energy curves and six lowest vibrational levels for the $II_{3/2}$, $III_{1/2}$, $IV_{1/2}$ states of ArF . . .	1218
A-8.7.	Calculated Einstein transition probabilities for the $III_{1/2} - I_{1/2}$ transition from the first four vibrational levels of the $III_{1/2}$ state of ArF	1219
A-8.8.	The Einstein A-coefficients for the five strongest bands of ArF	1220
A-8.9.	The total Einstein A-coefficient for ArF obtained by summing the contributions from the five strongest transitions with equal weightings.	1221
A-8.10.	The potential energy curves and six lowest vibrational levels for the $II_{3/2}$, $III_{1/2}$, and $IV_{1/2}$ states ArCl . .	1222
A-8.11.	Calculated Einstein transition probabilities for the $III_{1/2} - I_{1/2}$ transition from the first four vibrational levels of the $III_{1/2}$ state of ArCl	1223

Page

A-8.12. The Einstein A-coefficients for the five strongest bands of ArCl 1224

A-8.13. The total Einstein A-coefficients for ArCl obtained by summing the contributions from the five strongest transitions with equal weightings 1225

A-8.14. Comparison of ArF and ArCl emission features 1226

A-8.15. The potential energy curves and six lowest vibrational levels for the $II_{3/2}$, $III_{1/2}$, and $IV_{1/2}$ states of KrF including the positions of the vibrational levels for each state 1227

A-8.16. Calculated Einstein transition probabilities for the $III_{1/2} - I_{1/2}$ transition from the first four vibrational levels of the $III_{1/2}$ state of KrF 1228

A-8.17. Comparison of the experimental KrF fluorescence using Ne and Ar as diluent gases 1229

A-8.18. The Einstein A-coefficients for the five strongest bands of KrF 1230

A-8.19. The total Einstein A-coefficient for KrF obtained by summing the contributions from the five strongest transitions with equal weighting 1231

A-8.20. KrF fluorescence spectrum 1232

A-8.21. The potential energy curves and six lowest vibrational levels for the $II_{3/2}$, $III_{1/2}$, and $IV_{1/2}$ states of KrCl . 1233

A-8.22. The Einstein A-coefficient for the $III_{1/2} - I_{1/2}$ transition for KrCl in absolute units 1234

A-8.23. The Einstein A-coefficients for the five strongest bands of KrCl 1235

A-8.24. The total Einstein A-coefficient for KrCl obtained by summing the contributions from the five strongest transitions with equal weightings 1236

A-8.25. KrCl fluorescence spectrum 1237

Page

A-8.26. Comparison of KrF and KrCl emission features 1238

A-8.27. Abbreviated rotational level diagram for X, B, and D states of XeF, illustrating theoretically predicted branch structures for B-X and D-X transitions 1239

A-8.28. Wavenumbers (cm^{-1}) of assigned lines in 1-2 band of XeF B → X transition 1240

A-8.29. Franck-Condon factors ($\times 10^3$) for B-X system of XeF . . 1241

A-8.30. Franck-Condon factors ($\times 10^3$) for D-X system of XeF . . 1242

A-8.31. R centroids (Å) for B-X system of XeF 1243

A-8.32. Potential curves and energy levels for X state of XeF: rotationless potential (solid) and effective potential for N = 70 1244

A-8.33. Spectroscopic parameters (cm^{-1}) for X, B, and D states of XeF 1245

A-8.34. Spectroscopic constants (cm^{-1}) for 1-2 band of XeF B-X system, from least-squares fit of assigned lines having $N \leq 40$ 1246

A-8. References:

1. N. W. Winter, C. F. Bender, and T. N. Rescigno, "Potential Energy Curves and Predicted Fluorescence for Neon Fluoride," J. Chem. Phys. 67, 3122 (1977).

2. N. W. Winter, T. N. Rescigno, "Theoretical Calculation of the Bound-Free Emission Spectra of KrF," J. Chem. Phys. (in press).

3. P. C. Tellinghuisen, J. Tellinghuisen, J. A. Coxon, J. E. Velazco, and D. W. Setser, "Spectroscopic Studies of Diatomic Noble Gas Halides. IV. Vibrational and Rotational Constants for the X, B and D States of XeF," J. Chem. Phys. 68, 5187 (1978).

4. J. R. Murray and H. T. Powell, "KrCℓ Laser Oscillation at 222 nm," Appl. Phys. Letts. 27, 252 (1976).

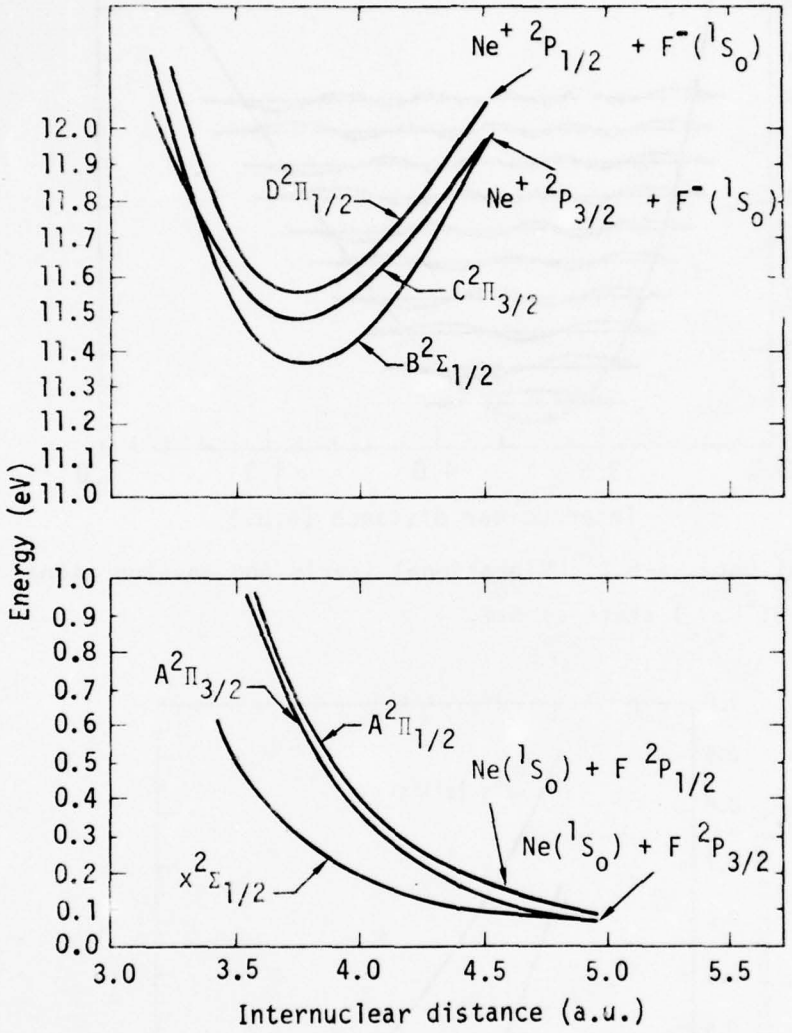

Graphical Data. A-8.1. Potential energy curves for the covalent and ion-pair states of NeF including spin-orbit coupling.

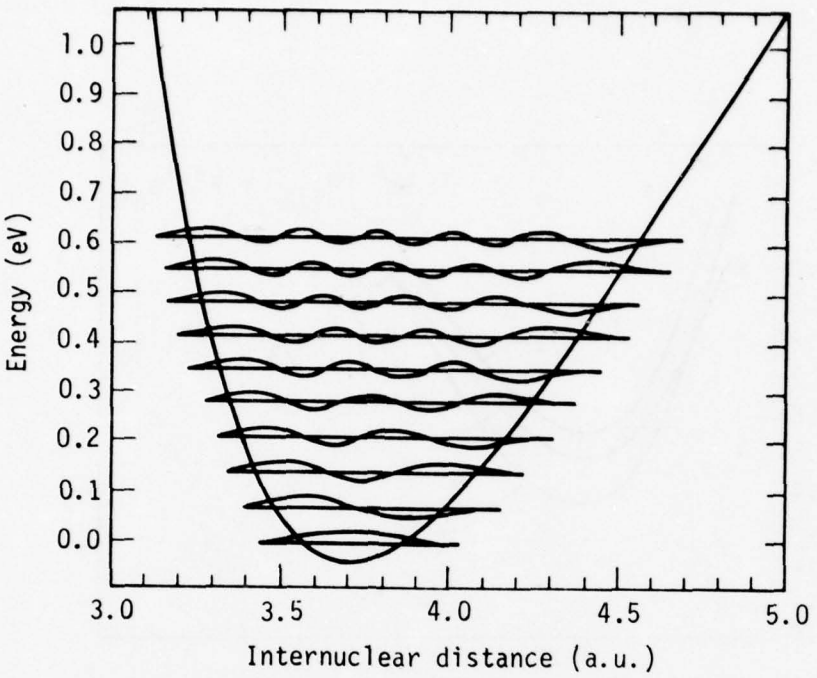

Graphical Data. A-8.2. Vibrational levels and wavefunctions for the B($^2\Sigma_{1/2}$) state of NeF.

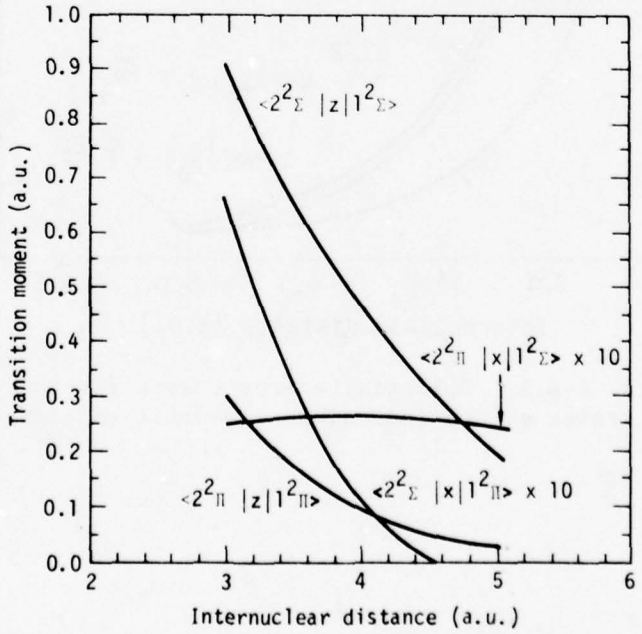

Graphical Data. A-8.3. Transition moments for the states of NeF without spin-orbit interaction as a function of internuclear separation.

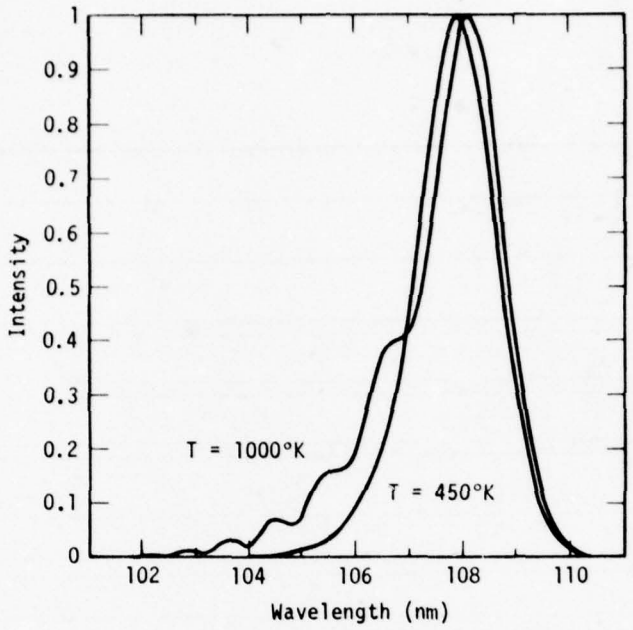

Graphical Data. A-8.4. Calculated fluorescence for the $2^2\Sigma \rightarrow 1^2\Sigma$ transition of NeF at T = 450 and 1000°K.

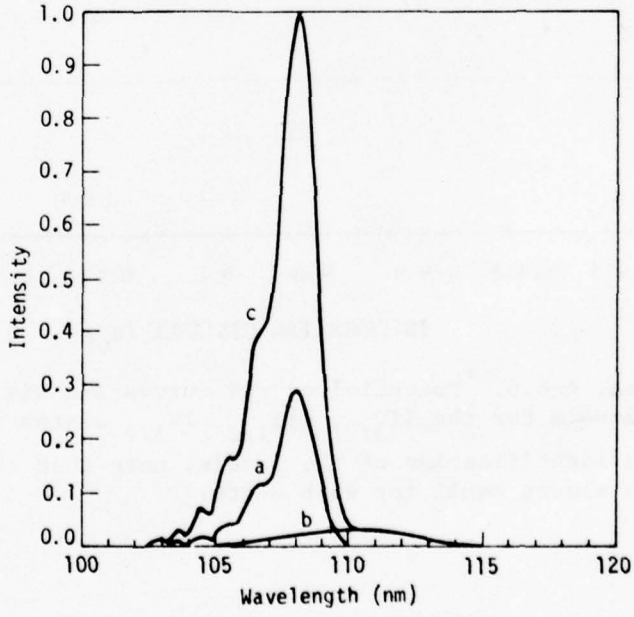

Graphical Data. A-8.5. Calculated fluorescence of NeF for the $2^2\Sigma \rightarrow 1^2\Sigma$ transition (curve a), the $2^2\Pi \rightarrow 1^2\Pi$ transition (curve b), and the sum of the two (curve c) rescaled to unity at its maxium.

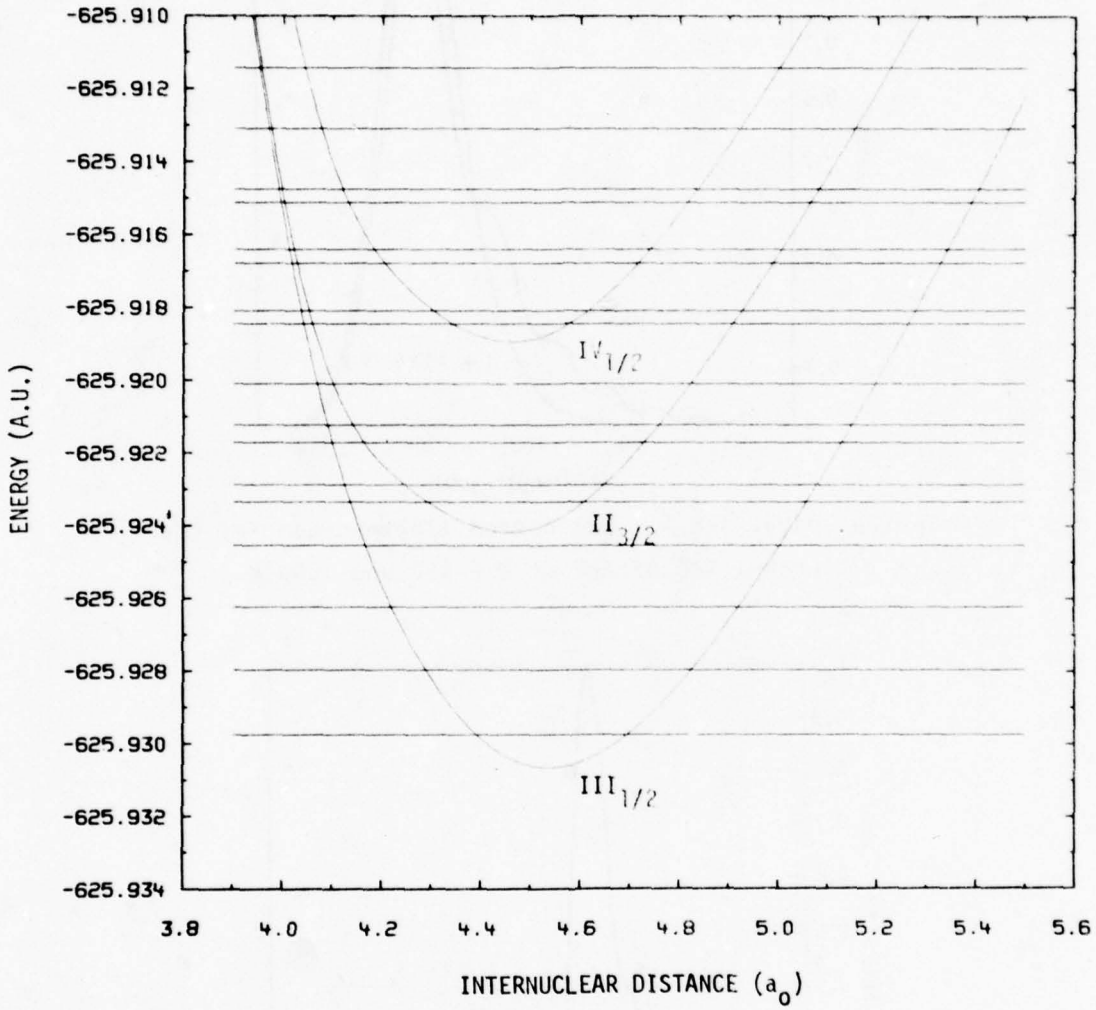

Graphical Data. A-8.6. Potential energy curves and six lowest vibrational levels for the $II_{3/2}$, $III_{1/2}$, $IV_{1/2}$ states of ArF.

To facilitate identification of the levels, note that the level separation is almost equal for each state.

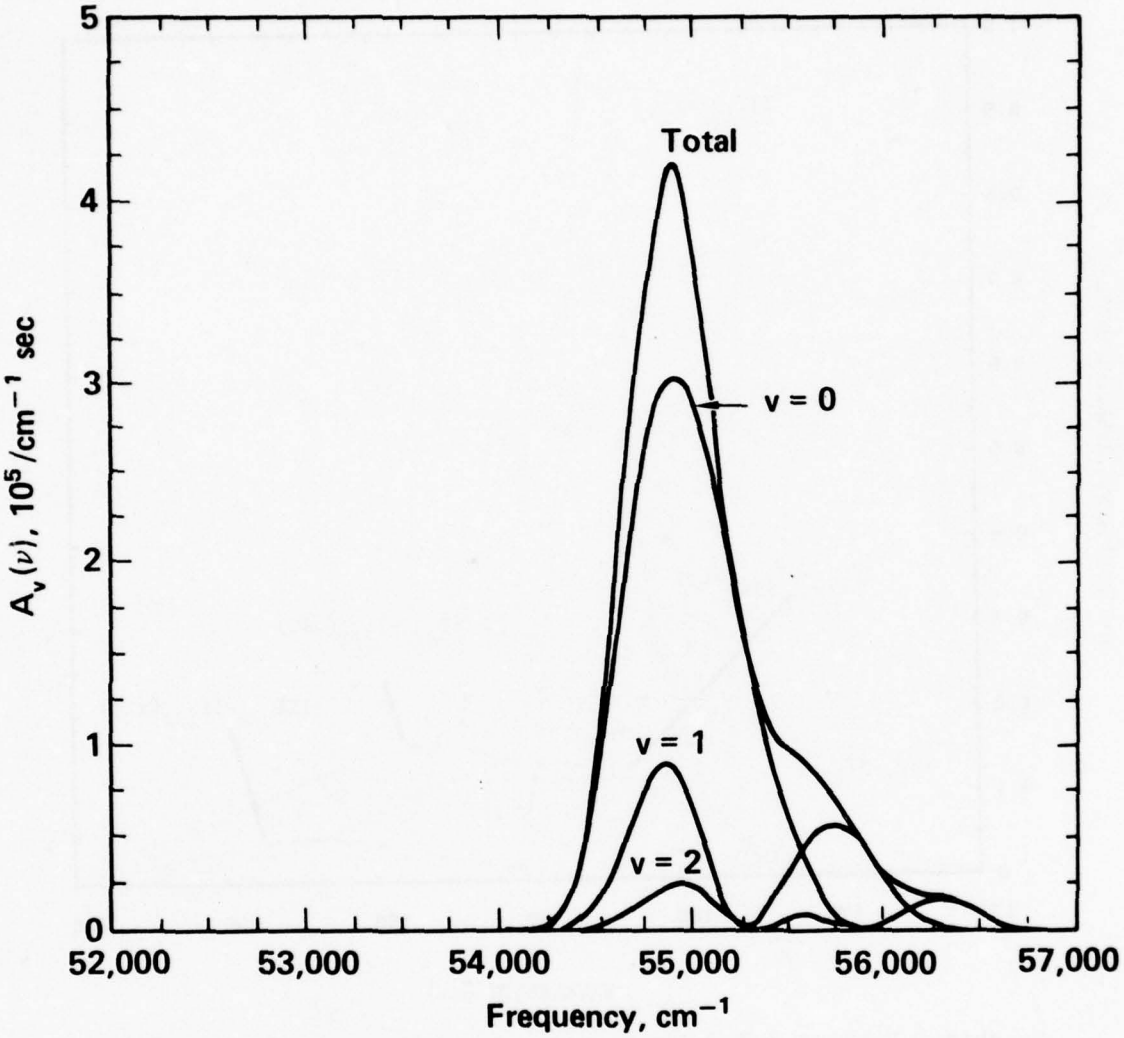

Graphical Data. A-8.7. Calculated Einstein transition probabilities (A-coefficients) for the $III_{1/2} - I_{1/2}$ transition from the first four vibrational levels of the $III_{1/2}$ state of ArF. Each curve has been weighted by a Boltzmann factor for T = 450°K.

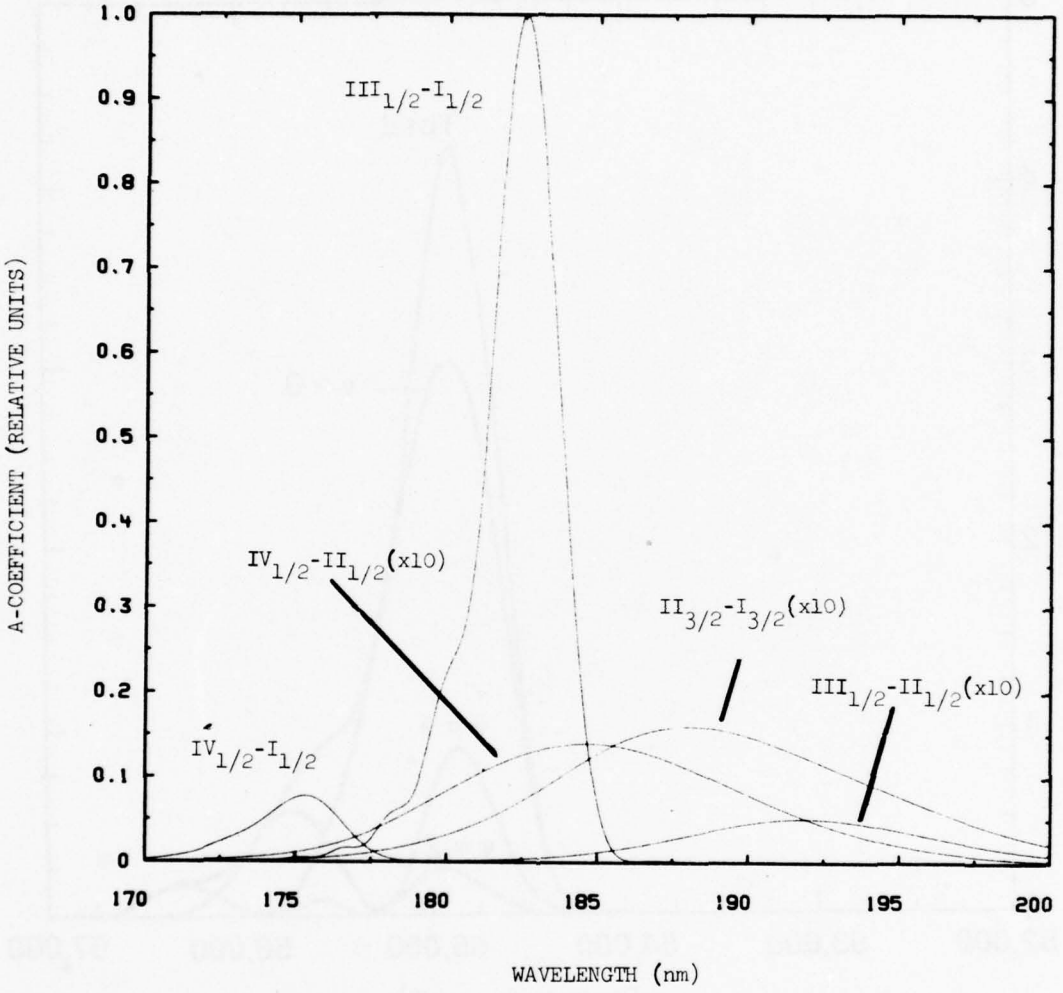

Graphical Data. A-8.8. The Einstein A-coefficients for the five strongest bands of ArF.

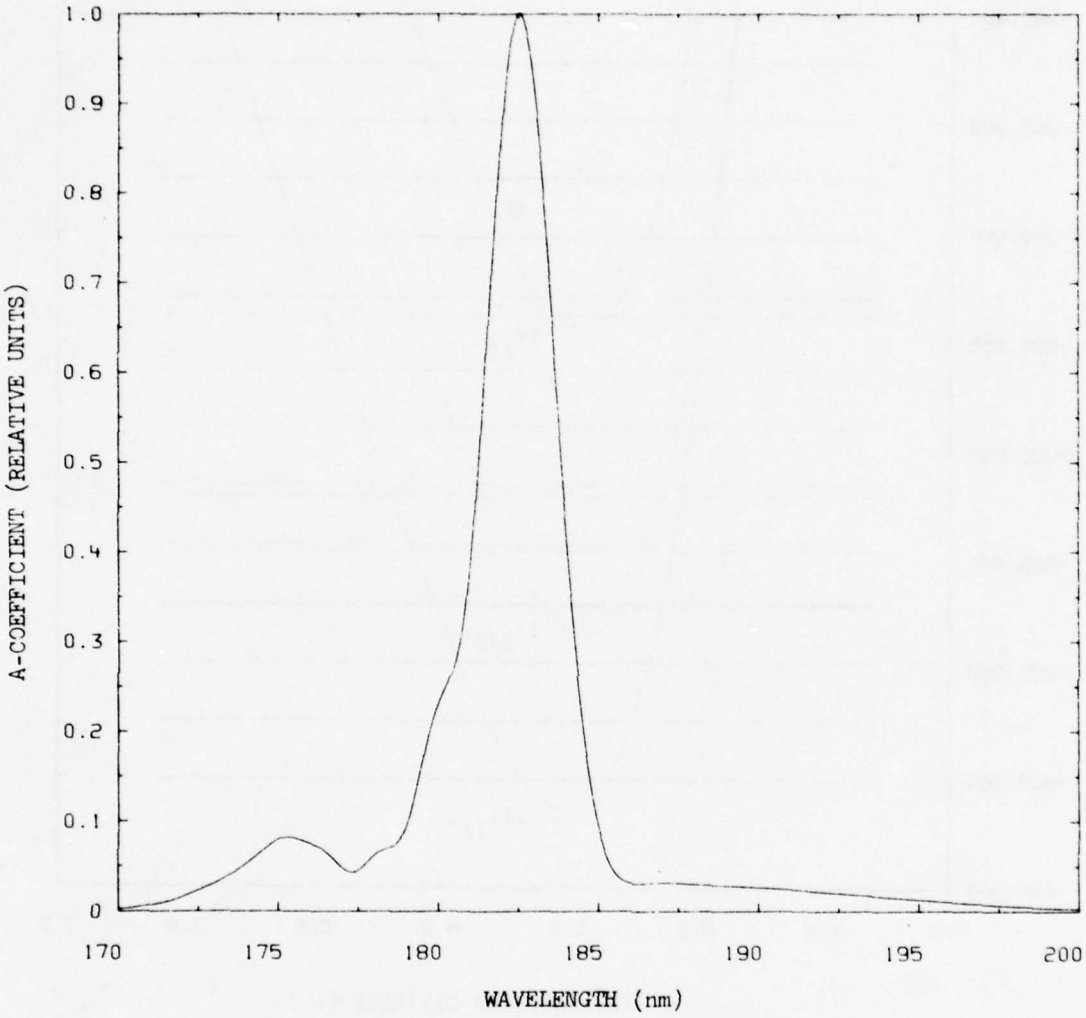

Graphical Data. A-8.9. The total Einstein A-coefficient for ArF obtained by summing the contributions from the five strongest transitions with equal weightings.

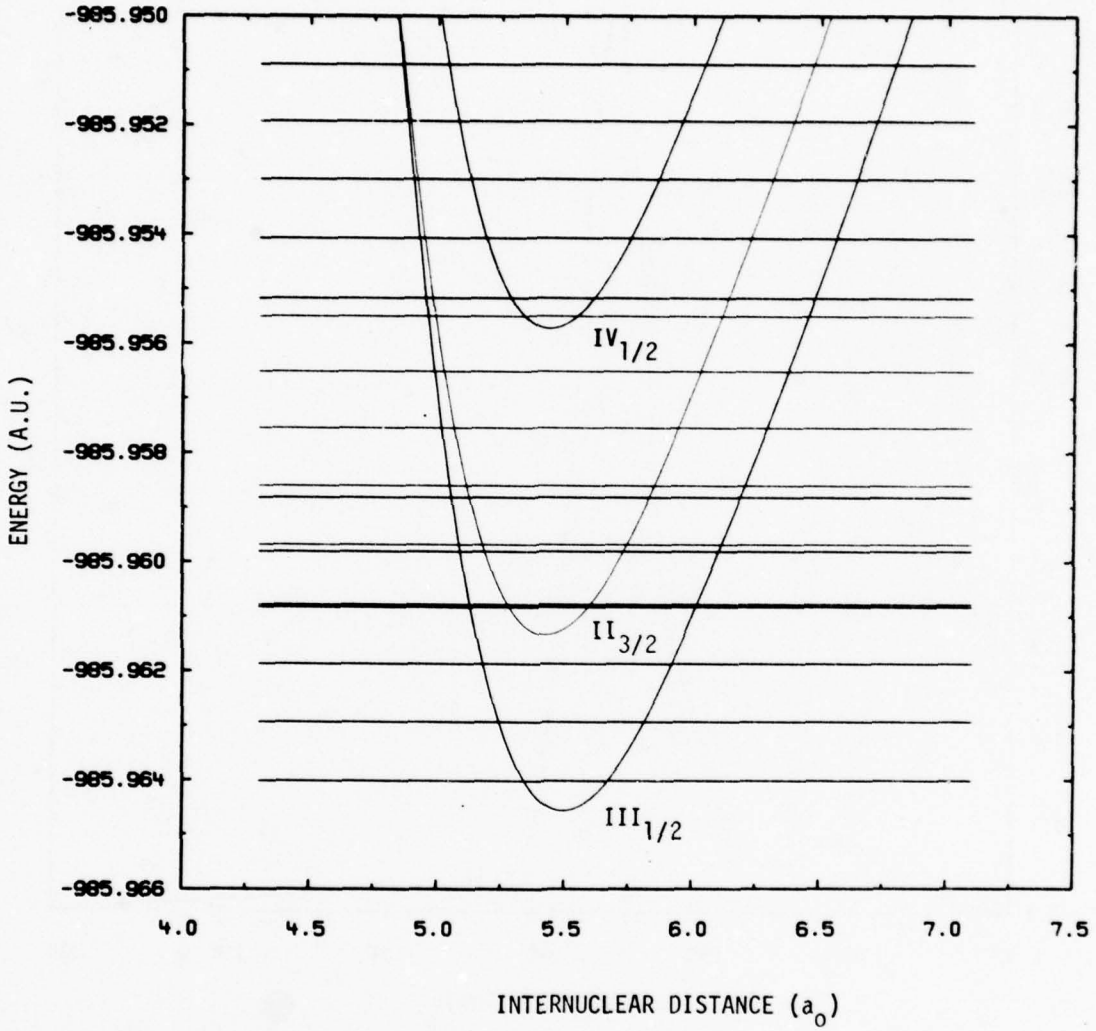

Graphical Data. A-8.10. The potential energy curves and six lowest vibrational levels for the $II_{3/2}$, $III_{1/2}$, and $IV_{1/2}$ states of ArCl. To facilitate identification of the levels note that level separation is almost equal for each state.

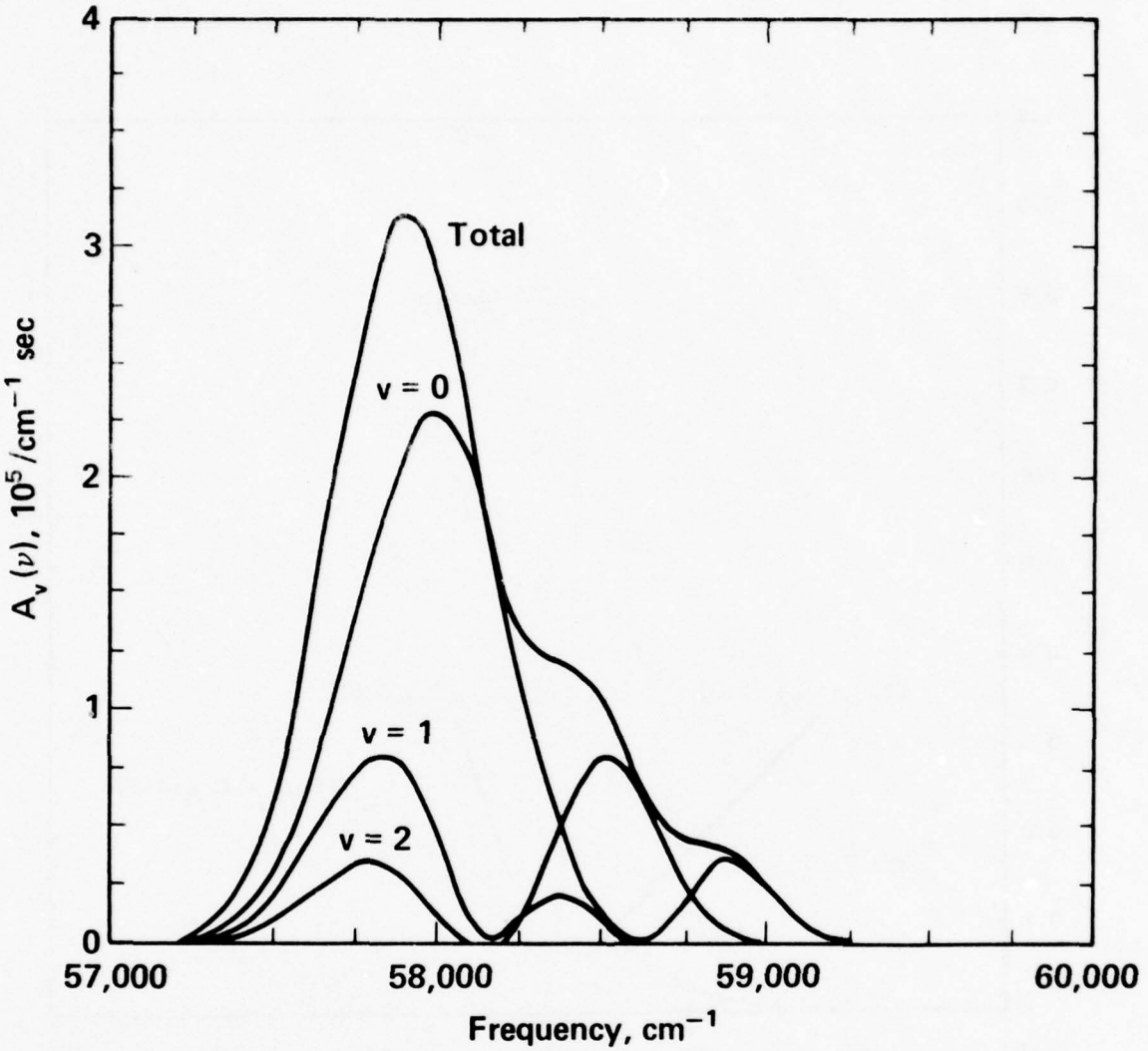

Graphical Data. A-8.11. Calculated Einstein transition probabilities (A-coefficients) for the $III_{1/2} - I_{1/2}$ transition from the first four vibrational levels of the $III_{1/2}$ state of ArCl. Each curve has been weighted by a Boltzmann factor for T = 450°K.

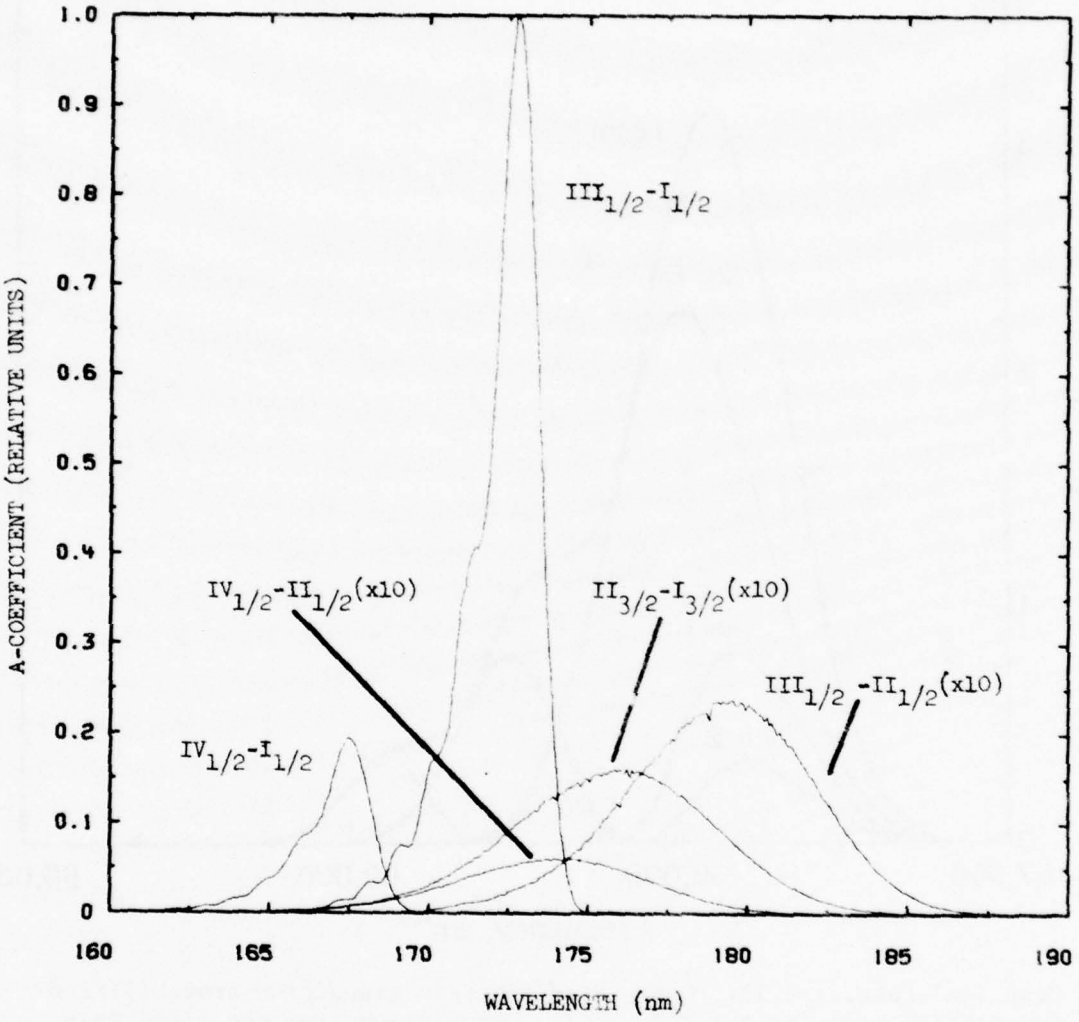

Graphical Data. A-8.12. The Einstein A-coefficients for the five strongest bands of ArCl.

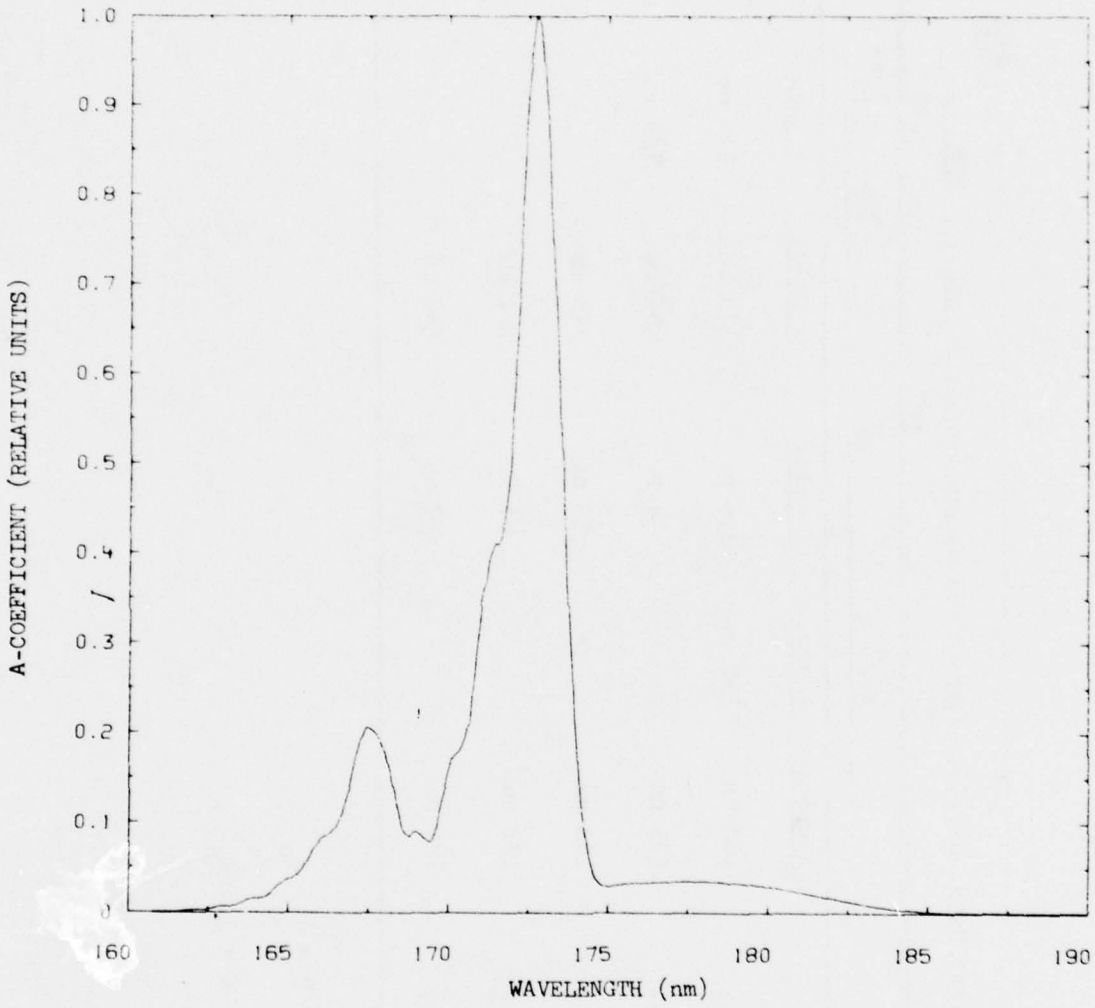

Graphical Data. A-8.13. The total Einstein A-coefficient for ArCl obtained by summing the contributions from the five strongest transitions with equal weightings.

Tabular Data. A-8.14. Comparison of ArF and ArCl emission features.

Transition	ArF*			ArCl**		
	λ calc.	λ exp.	τ calc.	λ calc.	λ exp.	τ calc.
$B^2\Sigma_{1/2} \rightarrow X^2\Sigma_{1/2}$	183 nm	190 nm	3.6 ns	173 nm	174 nm	4.4 ns
$D^2\Pi_{1/2} \rightarrow X^2\Sigma_{1/2}$	175 nm		34 ns	167 nm	169 nm	19 ns
$C^2\Pi_{3/2} \rightarrow A^2\Pi_{3/2}$	188 nm		53 ns	175 nm		79 ns
$D^2\Pi_{1/2} \rightarrow A^2\Pi_{1/2}$	185 nm		64 ns	174 nm		223 ns
$B^2\Sigma_{1/2} \rightarrow A^2\Pi_{1/2}$	194 nm		227 ns	180 nm		62 ns

* Evaluated at R = 4.5 a_o

** Evaluated at R = 5.5 a_o

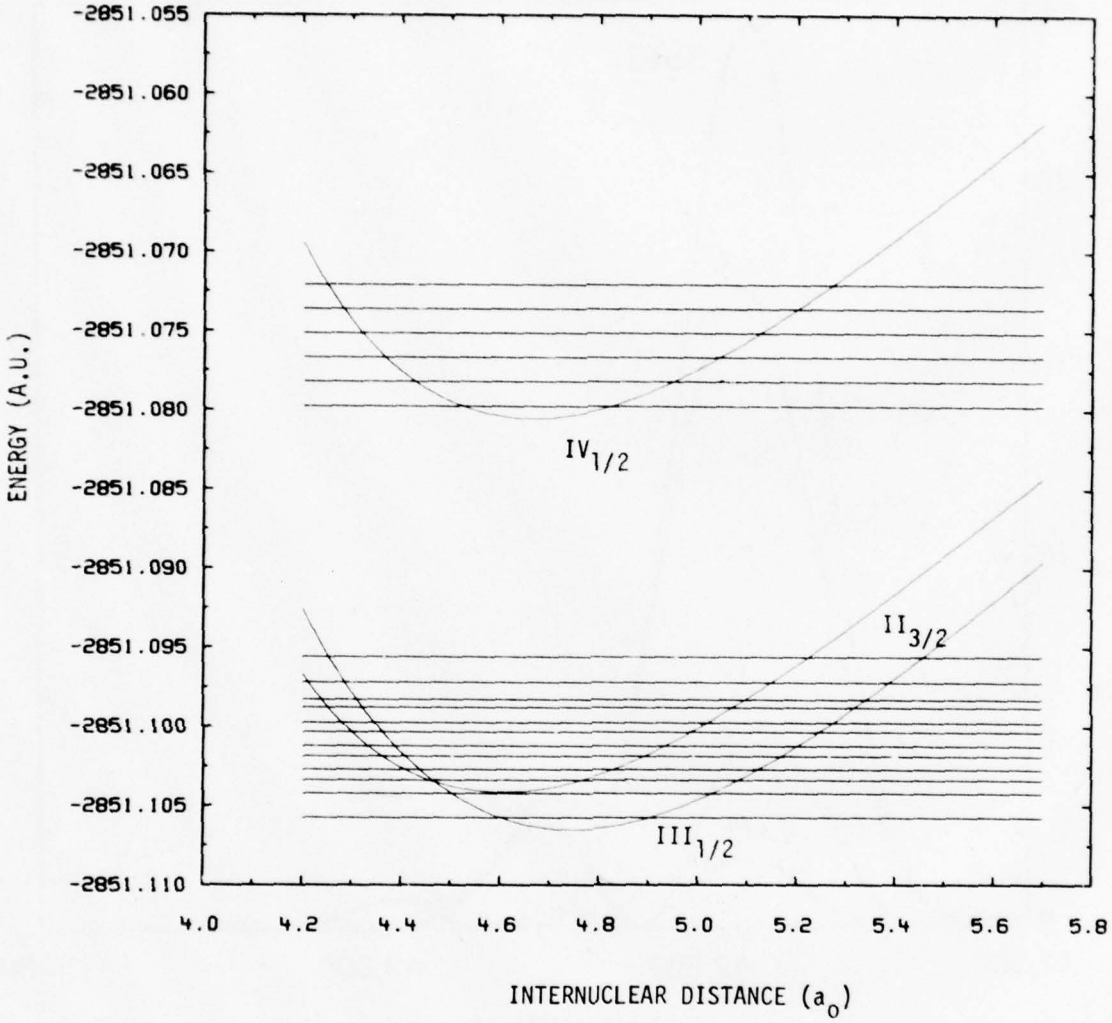

Graphical Data. A-8.15. The potential energy curves and six lowest vibrational levels for the $II_{3/2}$, $III_{1/2}$, and $IV_{1/2}$ states of KrF including the positions of the vibrational levels for each state. To facilitate identification of the levels, note that level separation is almost constant for each state.

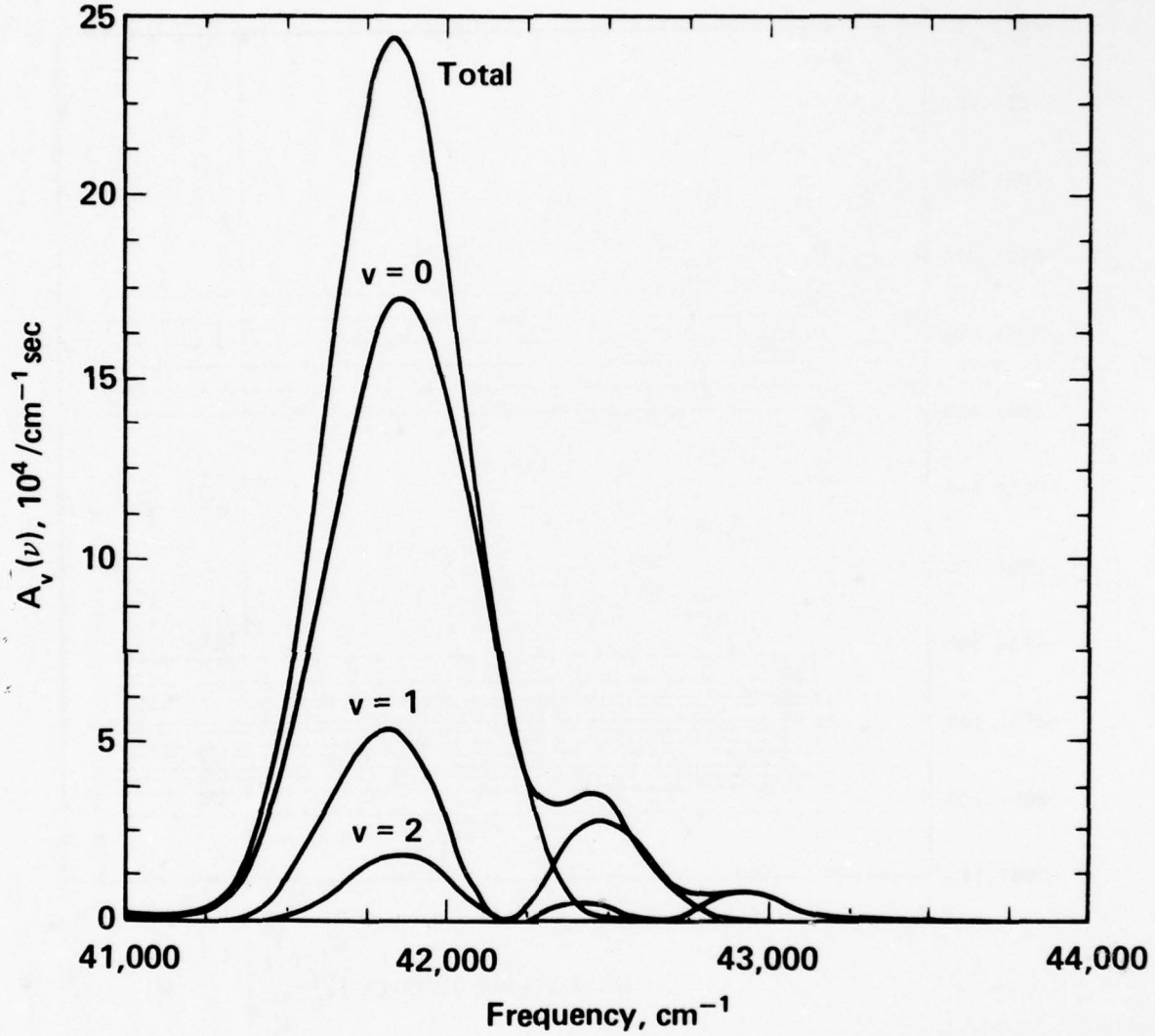

Graphical Data. A-8.16. Calculated Einstein transition probabilities (A-coefficients) for the $III_{1/2} - I_{1/2}$ transition from the first four vibrational levels of the $III_{1/2}$ state of KrF. Each curve has been weighted by a Boltzmann factor for T = 450°K.

COMPARISON OF THE KrF III 1/2 → I 1/2 TRANSITION WITH Ne AND Ar AS BUFFER GASES

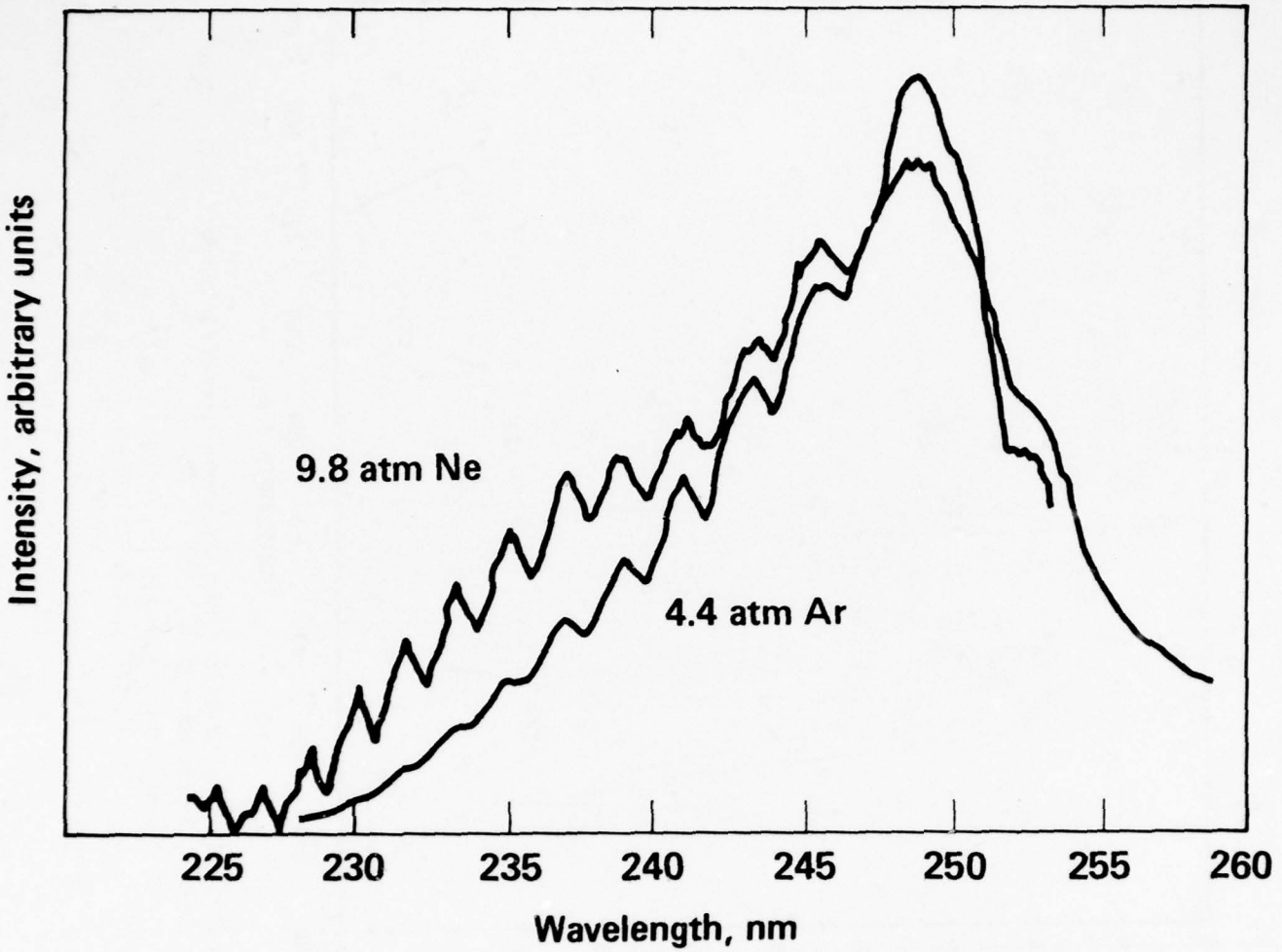

Graphical Data. A-8.17. Comparison of the experimental KrF fluorescence using Ne and Ar as diluent gases as measured by J. R. Murray and H. T. Powell (in Electronic Transition Lasers II, edited by L. E. Wilson).

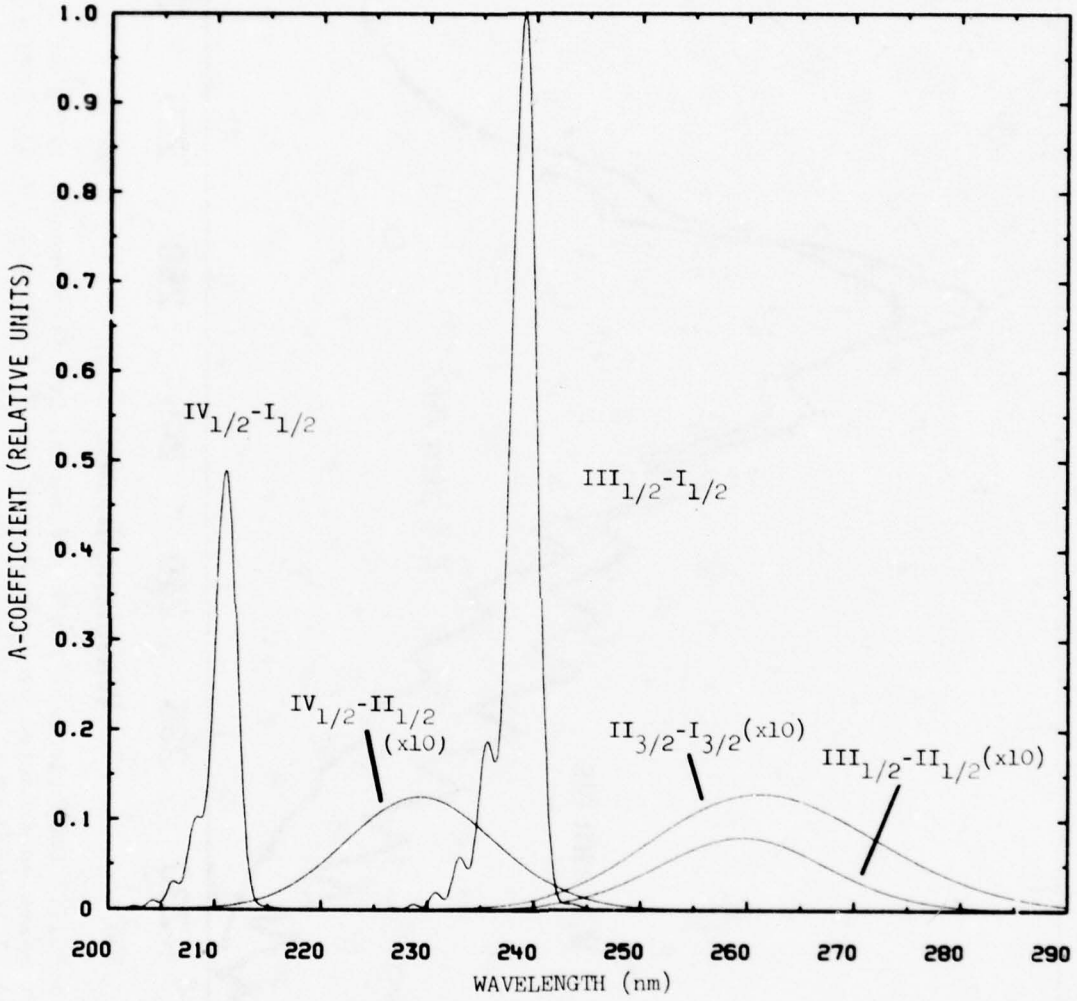

Graphical Data. A-8.18. The Einstein A-coefficients for the five strongest bands of KrF.

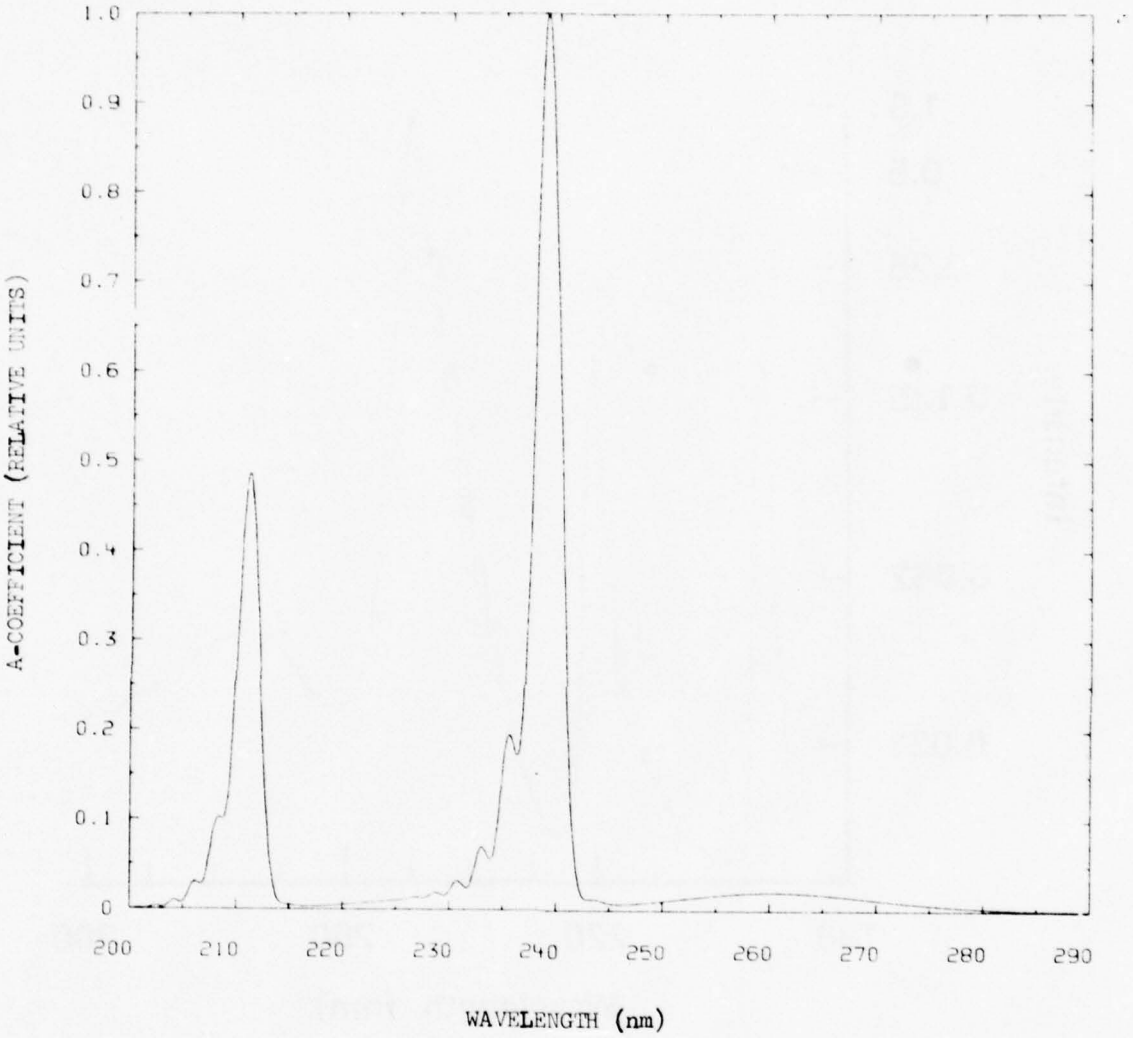

Graphical Data. A-8.19. The total Einstein A-coefficient for KrF obtained by summing the contributions from the five strongest transitions with equal weighting.

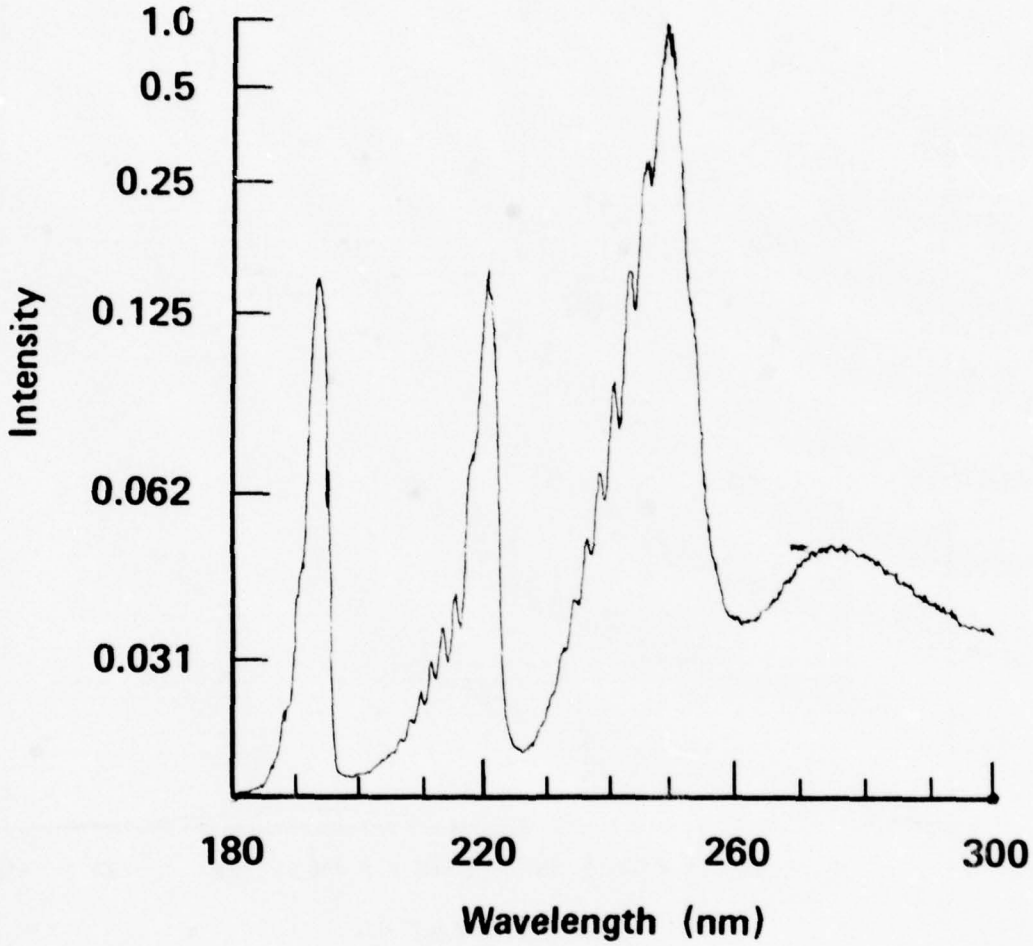

Graphical Data. A-8.20. KrF fluorescence spectrum.

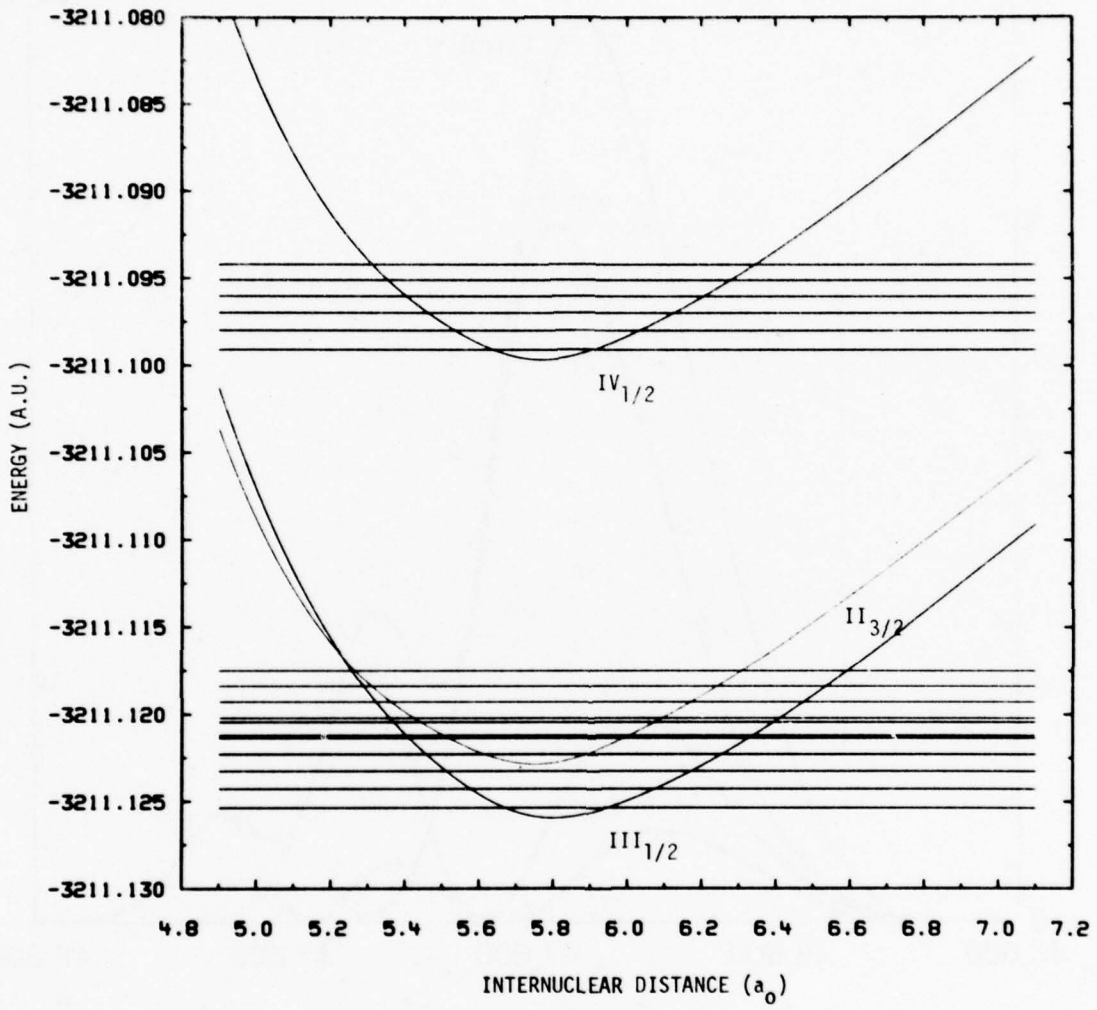

Graphical Data. A-8.21. The potential energy curves and six lowest vibrational levels for the $II_{3/2}$, $III_{1/2}$, and $IV_{1/2}$ states of KrCl. To facilitate identification of levels, note the level separation is almost constant for each state.

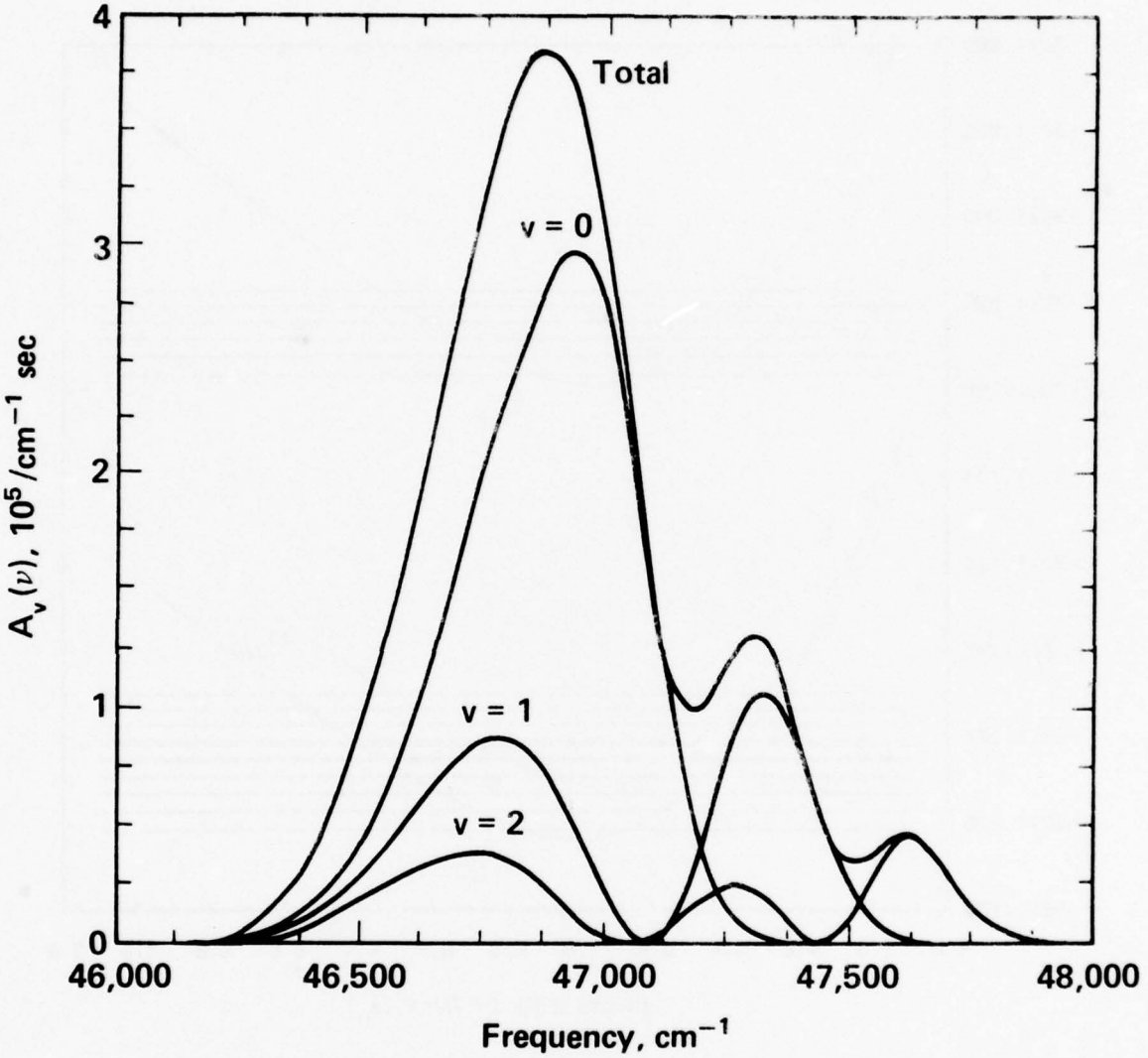

Graphical Data. A-8.22. The Einstein A-coefficient for the $III_{1/2}$ - $I_{1/2}$ transition for KrCl in absolute units. Each curve has been weighted by a Boltzmann factor for T = 450°K.

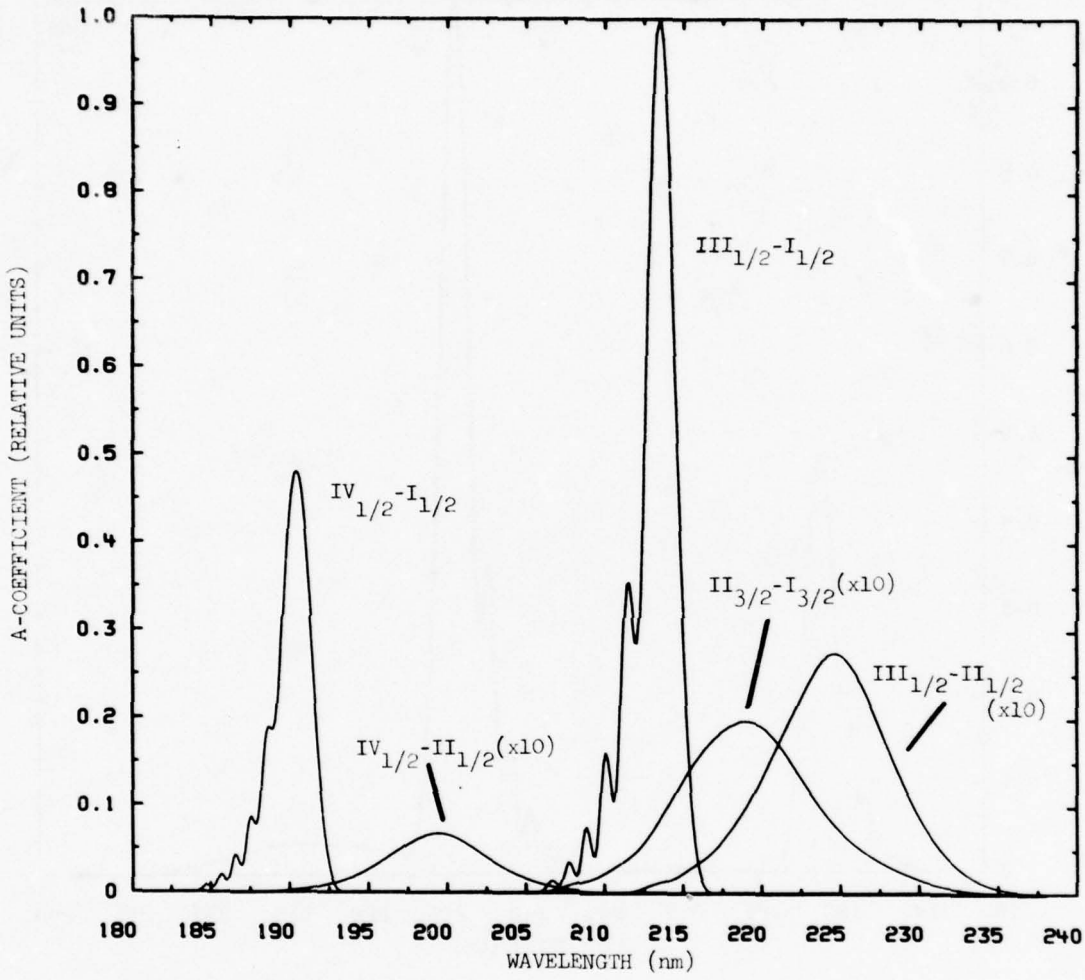

Graphical Data. A-8.23. The Einstein A-coefficients for the five strongest bands of KrCl.

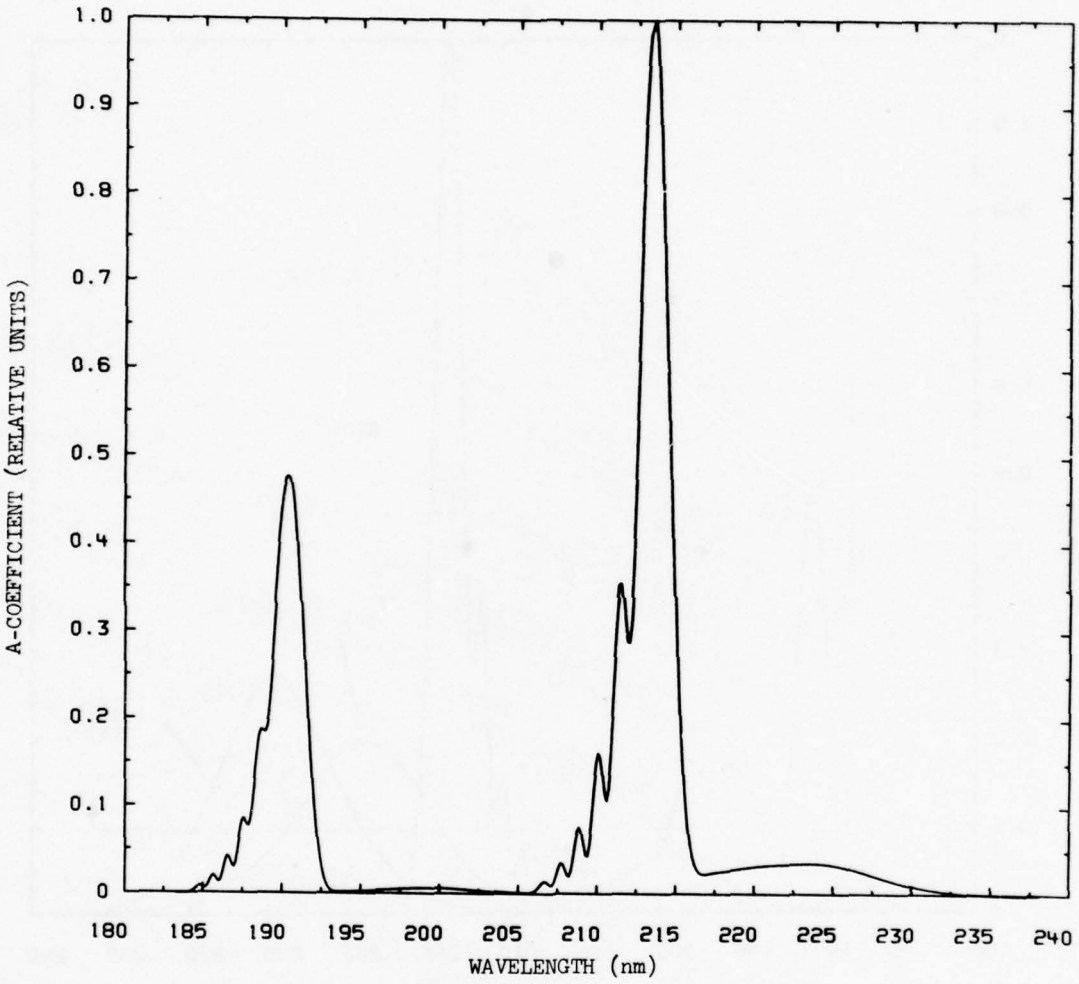

Graphical Data. A-8.24. The total Einstein A-coefficient for KrCl obtained by summing the contributions from the five strongest transitions with equal weightings.

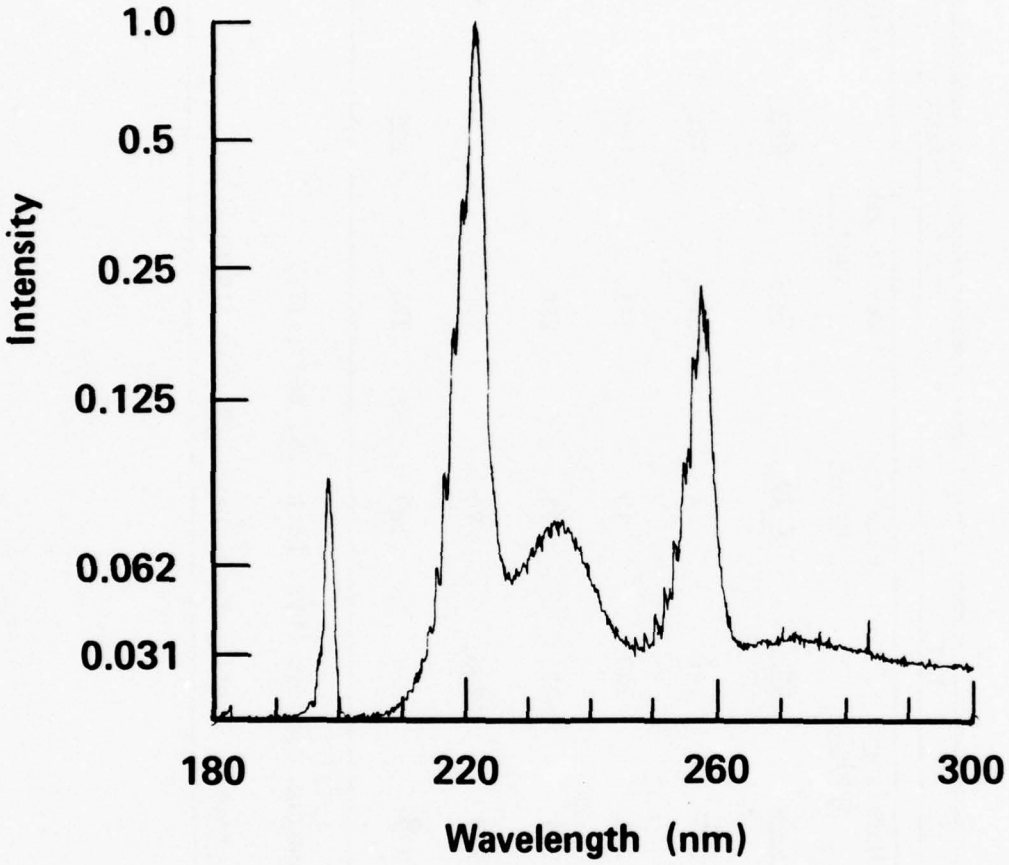

Graphical Data. A-8.25. KrCl fluorescence spectrum.

Tabular Data. A-8.26. Comparison of KrF and KrCl emission features.

Transition	KrF			KrCl		
	Wavelength (nm)		Lifetime (nsec)	Wavelength (nm)		Lifetime (nsec)
	Calc[a]	Exp[b]	Calc[a]	Calc	Exp[b]	Calc
$B^2\Sigma_{1/2} \rightarrow X^2\Sigma_{1/2}$	239	248	7	214	222	6.4
$D^2\Pi_{1/2} \rightarrow X^2\Sigma_{1/2}$	211	220	13	191	199	11
$C^2\Pi_{3/2} \rightarrow A^2\Pi_{3/2}$	264	~275	75	220		87
$D^2\Pi_{1/2} \rightarrow A^2\Pi_{1/2}$	228	~236	96	200		278
$B^2\Sigma_{1/2} \rightarrow A^2\Pi_{1/2}$	259		180	226	235	77

[a] P. J. Hay and T. H. Dunning, Applied Phys. Lett. 28, 649 (1976).

[b] J. R. Murray and H. T. Powell, Applied Phys. Lett. 29, 252 (1976).

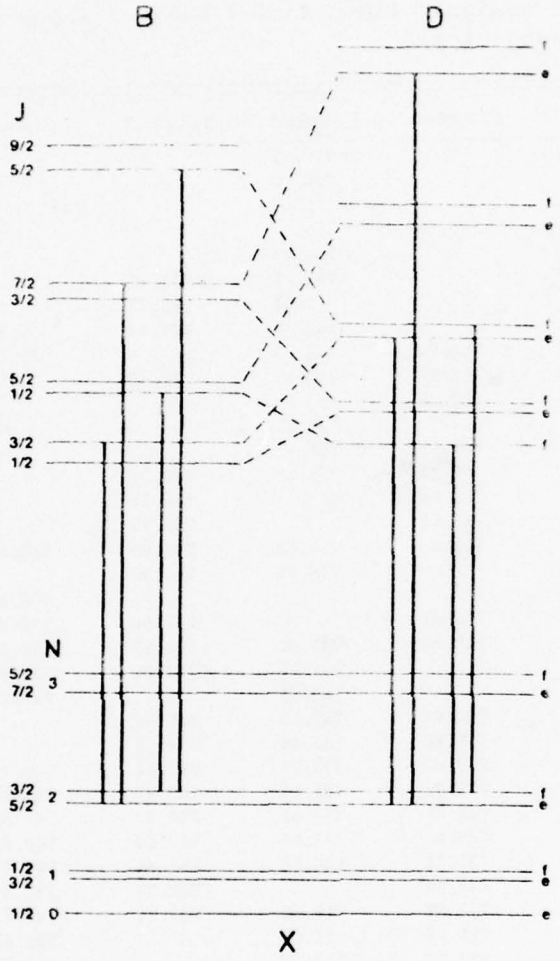

Graphical Data. A-8.27. Abbreviated rotational level diagram for X, B, and D states of XeF, illustrating theoretically predicted branch structures for B-X and D-X transitions. The energies are arbitrary, with X levels taken as $K''_{e,f}$ with $\alpha = -0.135$, and B and D levels taken as $K'_{e,f}$ with $\delta_B = 1.87$ and $\delta_D = -0.87$. In our notation the illustrated transitions for each system are, from left to right, $P_e(2)$, $R_e(2)$, $P_f(2)$, and $R_f(2)$.

Tabular Data. A-8.28. Wavenumbers (cm^{-1}) of assigned lines in 1-2 band of XeF B → X transition.

N'	P_f branch	P_e branch	R_f branch	R_e branch
4		28770.77		
5		770.02		
6				28772.78
7	28769.85			
9		766.63		
10		765.61	28774.05	
11		764.54	773.73	
12		763.41	773.44	770.43
13	765.00	762.23		769.85
14	763.97	760.99	772.59	
15	762.87	759.68		
16		758.31		
17	760.56	756.88		
18	759.32	755.38	770.31	
19	758.01		769.55	
20	756.65		768.75	
21	755.25	750.62	767.89	762.87
22		748.93	766.96	
23				760.56
24	750.62		765.00	759.32
25	748.93	743.52	763.97	758.01
26		741.57	762.87	756.65
27		739.61		755.25
28	743.64	737.55	760.43	
29	741.80	735.46	759.16	
30	739.89	733.34	757.81	750.75
31	737.95	731.14	756.43	749.18
32	735.92	728.91	754.99	747.52
33	733.86	726.66	753.49	745.81
34	731.74	724.28	751.96	744.06
35	729.57		750.38	742.27
36	727.37	719.50	748.74	740.43
37	725.12	717.05		738.55
38	722.80	714.50		736.62
39	720.44	711.95	743.64	734.65
40	718.05	709.34	741.80	732.64
41	715.65	706.71	739.89	730.58
42	713.13	704.07		728.50
43	710.64	701.31	736.06	726.36
44	708.09	698.58	734.09	724.28
45	705.51	695.80	732.09	
46	702.84	693.02	730.03	719.86
47		690.23	727.99	717.63
48	697.48	687.33	725.83	715.41
49	694.75		723.69	713.13
50	692.02		721.51	710.91
51			719.32	
52			717.05	
53			714.81	

Tabular Data. A-8.29. Franck-Condon factors ($\times 10^3$) for B-X system of XeF. Successive entries for each band are values for N' = N'' = 0, 20, 30, 40, 50, 60, 70.

v''	$v'=0$	1	2	3	4	5
0	3	8	15	24	32	40
	4	9	17	25	34	42
	4	10	19	28	36	44
	5	12	21	31	40	48
	7	15	25	35	45	52
	10	20	32	42	51	58
	16	27	40	51	59	64
1	60	85	101	99	86	68
	66	90	104	99	85	66
	75	96	108	100	83	63
	90	105	113	100	80	57
	114	116	118	97	74	50
	151	127	121	91	64	39
	211	133	121	78	50	25
2	323	129	68	16	1	3
	345	122	62	12	0	5
	372	110	53	7	0	8
	412	91	42	2	1	13
	463	63	28	0	5	20
	521	27	14	4	12	30
	567	0	5	24	20	42
3	489	20	12	68	40	32
	480	37	14	74	37	29
	463	65	15	81	31	25
	427	119	15	89	22	19
	360	214	10	97	9	12
	249	354	1	104	0	7
	98	479	1	109	22	6
4	77	518	11	24	43	9
	53	526	25	22	59	8
	29	517	50	20	80	5
	6	468	103	20	116	2
	1	343	184	23	165	1
	30	129	256	29	206	21
5	34	31	401	39	123	70
	39	8	373	52	117	97
	42	0	312	68	105	131
	38	29	193	80	80	173
	19	101	41	64	34	176
6	0	116	26	103	15	128
	1	97	66	59	8	88
	4	62	120	18	2	41
	10	13	154	1	2	1
7	4	37	30	124	4	38
	1	47	4	112	8	50
	0	45	4	73	10	47
8	3	5	57	41	4	1
	2	14	22	57	0	8
9	2	0	44	8	12	1
10	1	0	29	1	13	2

[a] (v'', N'') levels (7,30), (6,40), (5,50), (4,50), (4,60), (3,60), (3,70), (2,70), and (1,70) lie above the dissociation limit; hence they can rotationally predissociate.

Tabular Data. A-8.30. Franck-Condon factors ($\times 10^3$) for D-X system of XeF. Multiple entries, where they occur, are for N' = N'' = 0, 20, and 30, successively.

v''	v' = 0	1	2	3	4	5
0	75	96	111	111	104	93
	81	100	114	112	105	92
	89	105	117	114	105	91
1	425	114	54	8	0	6
	443	106	49	6	0	7
	464	94	43	3	1	9
2	441	105	27	88	35	25
	425	130	26	91	31	22
	401	165	25	93	26	19
3	16	535	68	7	85	14
	9	516	92	7	98	11
	2	482	126	7	114	8
4	34	0	401	85	81	122
	34	5	356	101	78	144
	32	20	291	118	73	171
5	2	76	89	100	33	100
	4	59	125	61	27	76
	6	37	166	25	18	46
6	1	42	8	182	4	18
	0	44	0	167	11	26
	0	41	8	126	20	34
7	2	9	46	66	17	2
	1	14	22	86	3	0
	0	18	4	86	0	2
8	1	1	40	11	36	5
	1	4	24	28	13	2
9	1	0	26	1	33	3
10	0	0	16	0	24	1

Tabular Data. A-8.31. R centroids (Å) for B-X system of XeF. The first entry is for N' = N" = 0, and the second (where given) is for N' = N" = 40. Omitted values are ill defined owing to weak Franck-Condon overlap.

v''	$v'=0$	1	2	3	4	5
0	2.536	2.494	2.466	2.443	2.423	2.406
	2.546	2.500	2.472	2.448	2.428	2.410
1	2.565	2.508	2.479	2.453	2.432	2.413
	2.576	2.511	2.485	2.456	2.436	2.416
2	2.600	2.499	2.496	2.435	2.404	2.458
	2.613	2.476	2.515	2.344	2.443	2.450
3	2.650	2.858	2.326	2.536	2.412	2.458
	2.673	2.730	2.198	2.572	2.329	2.514
4	2.785	2.683	3.352	2.884	2.702	2.091
	3.131	2.698	2.877	3.162	2.712	•••
5	2.592	2.877	2.714	3.182	2.839	2.899
	2.698	2.518	2.698	2.941	2.985	2.828
6	•••	2.695	2.640	2.665	3.361	2.856
	2.588	2.880	2.699	•••	2.657	3.444
7	2.830	2.604	2.775	2.742	3.779	2.708
8	2.724	2.445	2.725	2.758	2.257	•••
9	2.674	•••	2.704	2.771	2.622	•••
10	2.641	•••	2.689	2.811	2.700	3.617

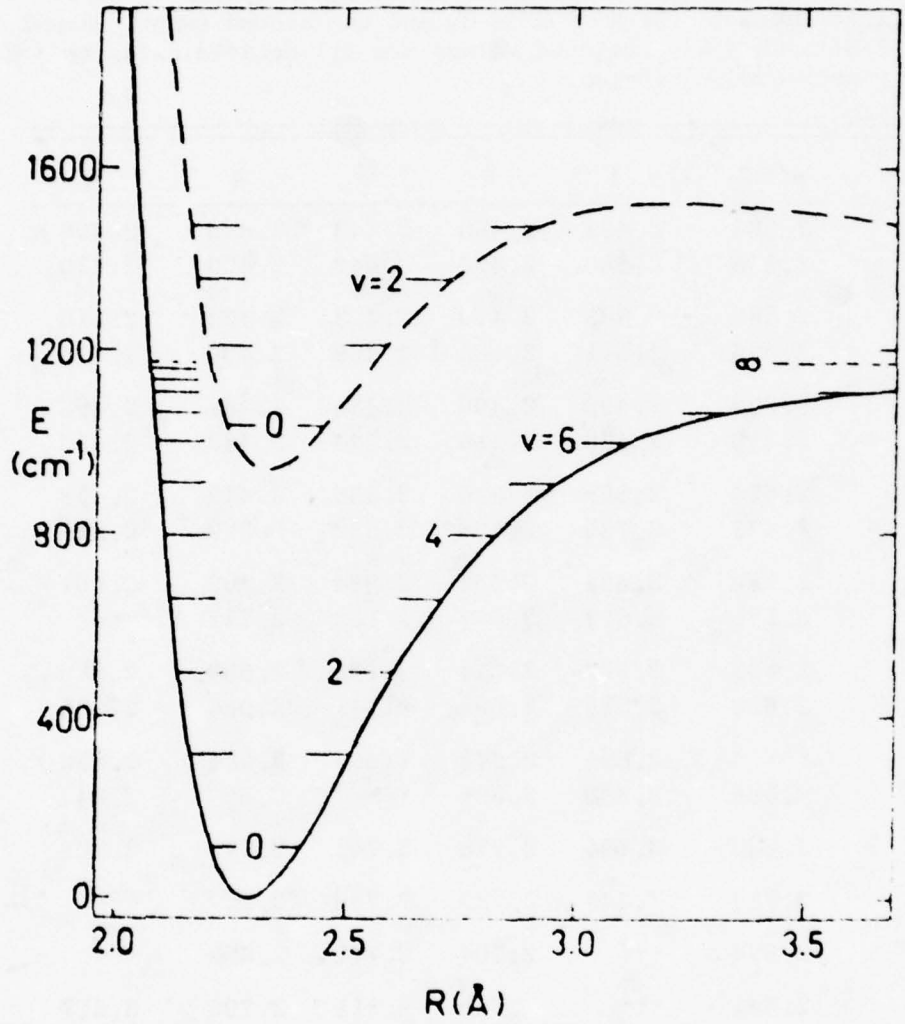

Graphical Data. A-8.32. Potential curves and vibrational energy levels for X state of XeF: rotationless potential (solid) and effective potential for N = 70.

Tabular Data. A-8.33. Spectroscopic parameters (cm^{-1}) for X, B, and D states of XeF. Standard errors (1σ, in parentheses) from the vibrational parameter determination are given in terms of last significant digits.

	X	B	D
T_e	0	28 811.0(7)	38 051.4(7)
$c_{v1}(\omega_e)$	225.40(150)	309.02(11)	350.14(19)
$c_{v2}(-\omega_e x_e)$	−10.874(1000)	−1.505(9)	−1.899(18)
c_{v3}	0.2981(2700)		
c_{v4}	−0.08125(3100)		
c_{v5}	0.004963(1330)		
D_e	1175(20)	42 783(20)[a]	44 080(20)[a]
$c_{r1}(B_e)$	0.19326[b]	0.14670	0.1608
$c_{r2}(-\alpha_e)$	-6.985×10^{-3}	-9.9×10^{-4}	-1.20×10^{-3}
c_{r3}	1.596×10^{-4}		
c_{r4}	-7.167×10^{-5}		
R_e(Å)	2.293	2.631	2.513
$c_{d1}(D_e)$	5.36×10^{-7}	1.32×10^{-7}	1.36×10^{-7}
c_{d2}	1.53×10^{-7}	1.6×10^{-10}	1.4×10^{-10}
c_{d3}	-3.45×10^{-8}		
c_{d4}	1.08×10^{-8}		
$c_{h1}(H_e)$	-5.6×10^{-12}	-4.4×10^{-14}	-8.1×10^{-14}
c_{h2}	-1.48×10^{-11}		
c_{h3}	6.6×10^{-12}		
c_{h4}	-1.9×10^{-12}		
a	−0.04[c]		
δ		1.82[c]	−0.82[d]

[a] Dissociation to F^- (^1S) + Xe^+ ($^2P_{3/2}$) for B state, Xe^+ ($^2P_{1/2}$) for D state.

[b] Rotational and centrifugal distortion parameters for X state valid for v'' = 0-6.

[c] From analysis of 1-2 band only.

[d] Calculated from δ_B, using $\delta_B + \delta_D = 1$.

Tabular Data. A-8.34. Spectroscopic constants (cm^{-1}) for 1-2 band of XeF B-X system, from least-squares fit of assigned lines having $N \leq 40$. Standard errors (1σ, in parentheses) are in terms of last significant digits.

ν'_0	28 773.070(7)
B'	0.14521(4)
D'	$(1.35\times10^{-7})^a$
δ	1.820(17)
B''	0.17568(5)
D''	$9.67(12)\times10^{-7}$
H''	$(-3.0\times10^{-11})^a$
a	−0.041(14)
b	$-4.3(11)\times10^{-10}$
σ	0.023

[a]Calculated at the outset and held fixed in the fit.

A-9. POTENTIAL ENERGY CURVES, ELECTRONIC ENERGIES, SPECTROSCOPIC CONSTANTS, AND TRANSITION MOMENTS FOR Ar_2F and Kr_2F

CONTENTS

		Page
A-9.1.	Schematic orbit representation of the nine lowest electronic states of Ar_2F for isosceles triangle geometries	1251
A-9.2.	Potential curves for Ar_2F in an isosceles triangle configuration with the Ar-Ar distance fixed at 2.51 Å	1252
A-9.3.	Potential curves for Ar_2F in an isosceles triangle configuration with R_2 fixed at 2.25 Å	1253
A-9.4.	Potential curves for Ar_2F in a collinear configuration varying both the Ar-Ar and adjacent Ar-F distances	1254
A-9.5.	Potential curves for the lowest two ionic states of Ar_2F in a right triangle configuration as a function of the Ar-Ar distance	1255
A-9.6.	Schematic orbital diagram of the two dipole-allowed emissions from the 2^2B_2 state in Ar_2F	1256
A-9.7.	Estimate of the $2^2B_2 \rightarrow 1^2B_2$ (1^2A_1) transition energy in Ar_2F and Kr_2F	1257
A-9.8.	Effect of F^- on the states of Ar_2^+	1258
A-9.9.	Spectroscopic data for the 2^2B_2 ($4^2\Gamma$) state of Ar_2F with analogous data for the $2^2\Sigma^+$ [III(1/2)] state of ArF and the $1^2\Sigma^+$ [I(1/2)u] state of Ar_2^+ without and with spin-orbit coupling	1259
A-9.10.	Calculated data for the dipole-allowed emissions from the 2^2B_2 state of Ar_2F in its equilibrium isosceles triangle geometry neglecting spin-orbit effects	1260

Page

A-9.11. Transition moment from the $4^2\Gamma$ state of Ar_2F (including the spin-orbit coupling) for the equilibrium isosceles triangle geometry of the 2^2B_2 state 1261

A-9.12. Calculated data including spin-orbit coupling for the dipole-allowed emissions from the $4^2\Gamma$ state of Ar_2F at the equilibrium isosceles triangle geometry of the 2^2B_2 state 1262

A-9.13. Calculated data for the dipole-allowed absorptions from 2^2B_2 state of Ar_2F in its equilibrium isosceles triangle geometry neglecting spin-orbit effects. . . . 1262

A-9.14. Calculated data for the dipole-allowed absorptions in Ar_2^+ without $(^2\Sigma_u^+)$ and with $[1(1/2)_u]$ spin-orbit coupling 1263

A-9.15. Calculated data including spin-orbit coupling for the dipole-allowed absorptions from the $4^2\Gamma$ state of Ar_2F at the equilibrium isosceles triangle geometry of the 2^2B_2 state 1264

A-9.16. Spectroscopic data for the 2^2B_2 $(4^2\Gamma)$ state of Kr_2F with analogous data for the $2^2\Sigma^+$ [III(1/2)] state of KrF and the $1^2\Sigma_u^+[(1/2)_u]$ state of Kr_2^+ without and with spin-orbit coupling 1264

A-9.17. Calculated data for the dipole-allowed emissions from 2^2B_2 state of Kr_2F in its equilibrium isosceles triangle geometry neglecting spin-orbit effects. . . . 1265

A-9.18. Transition moments (in a.u.) from $4^2\Gamma$ state of Kr_2F (including spin-orbit coupling) for the equilibrium isosceles triangle geometry of the 2^2B_2 state. 1265

Page

A-9.19. Calculated data including spin-orbit coupling for the dipole-allowed emissions from the $4^2\Gamma$ state of Kr_2F at the equilibrium isosceles triangle geometry of the 2^2B_2 state. 1266

A-9.20. Calculated data for the dipole-allowed absorptions from 2^2B_2 state of Kr_2F in its equilibrium isosceles triangle geometry neglecting the spin-orbit effects 1266

A-9.21. Calculated data for the dipole-allowed absorptions in Kr_2^+ without ($^2\Sigma_u^+$) and with [I(1/2$_u$)] spin-orbit coupling 1267

A-9.22. Calculated data including spin-orbit coupling for the dipole-allowed absorptions from the $4^2\Gamma$ state of Kr_2F at the equilibrium isosceles triangle geometry of the 2^2B_2 state 1267

A-9.23. Electronic state energies for Ar_2F and Kr_2F at their respective equilibrium isosceles triangle geometries without and with spin-orbit coupling 1268

A-9.24. The overall radiative life-time (in nsec) of the 2^2B_2 state in Ar_2F as a function of geometry. 1268

A-9. References:

1. W. R. Wadt and P. J. Hay, "Electronic States of Ar_2F and Kr_2F," J. Chem. Phys. 68, 3850 (1978).

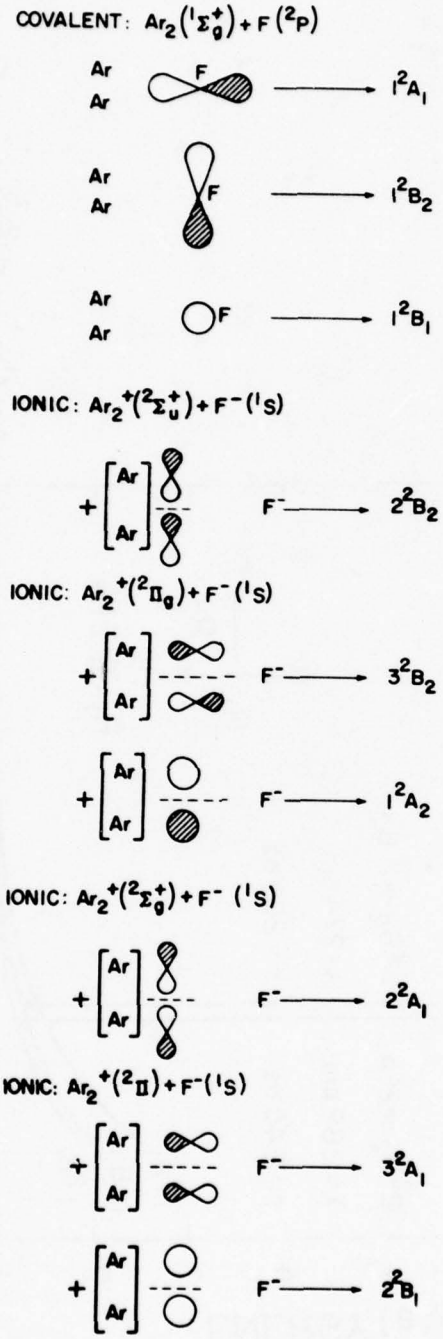

Graphical Data. A-9.1. Schematic orbit representation of the nine lowest electronic states of Ar_2F for isosceles triangle geometries.

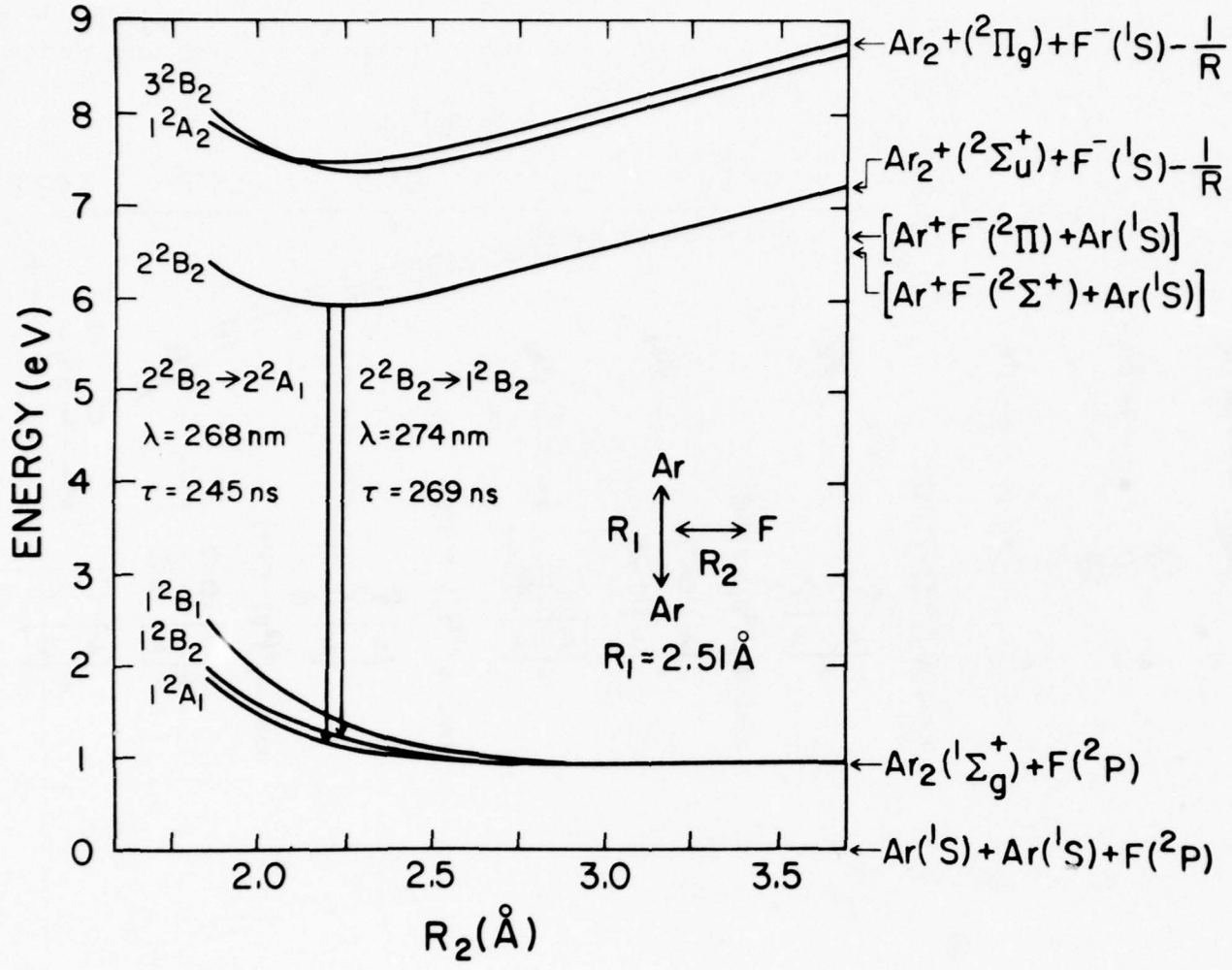

Graphical Data. A-9.2. Potential curves for Ar_2F in an isosceles triangle configuration with the Ar-Ar distance fixed at 2.51 Å.

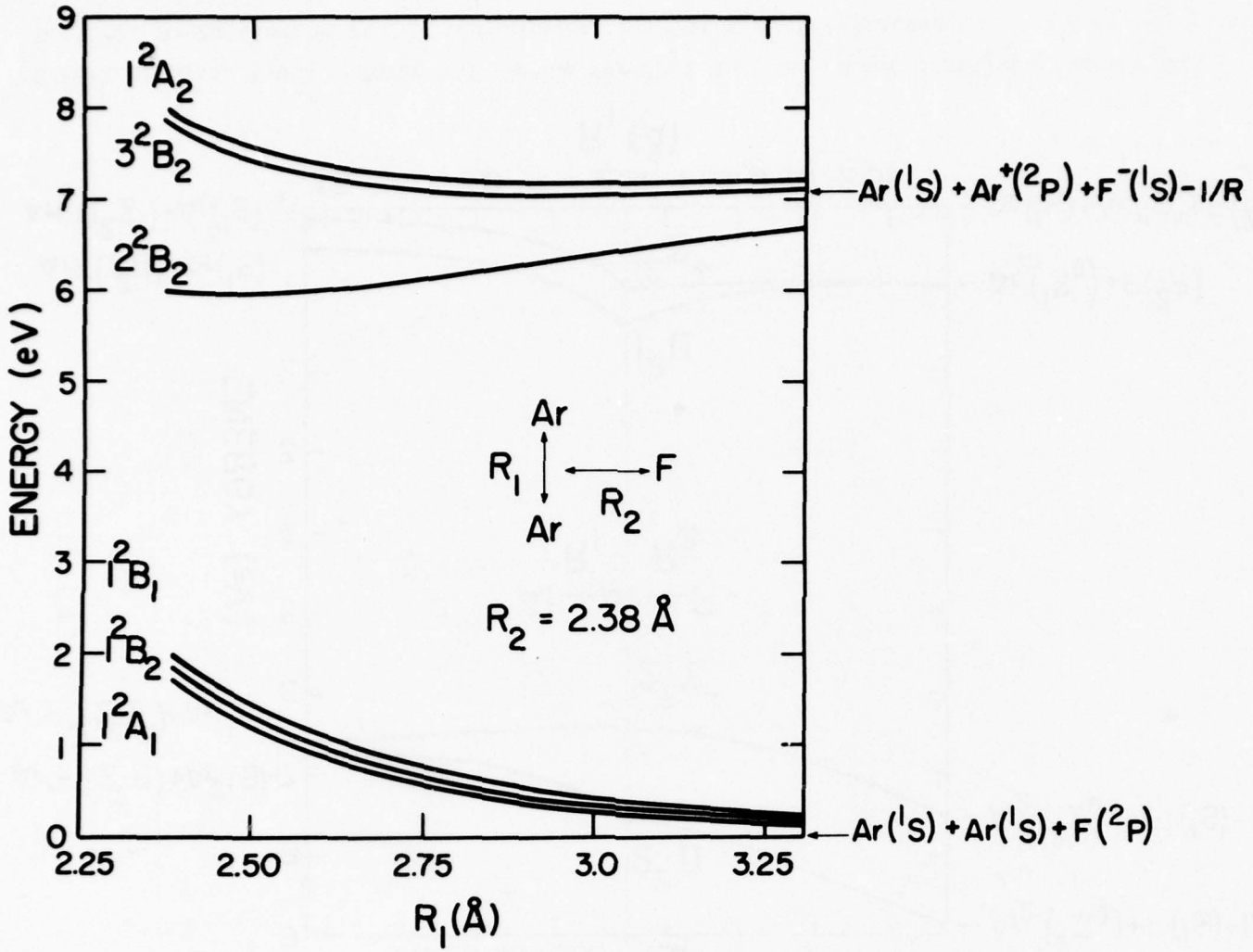

Graphical Data. A-9.3. Potential curves for Ar_2F in an isosceles triangle configuration with R_2 fixed at 2.25 Å.

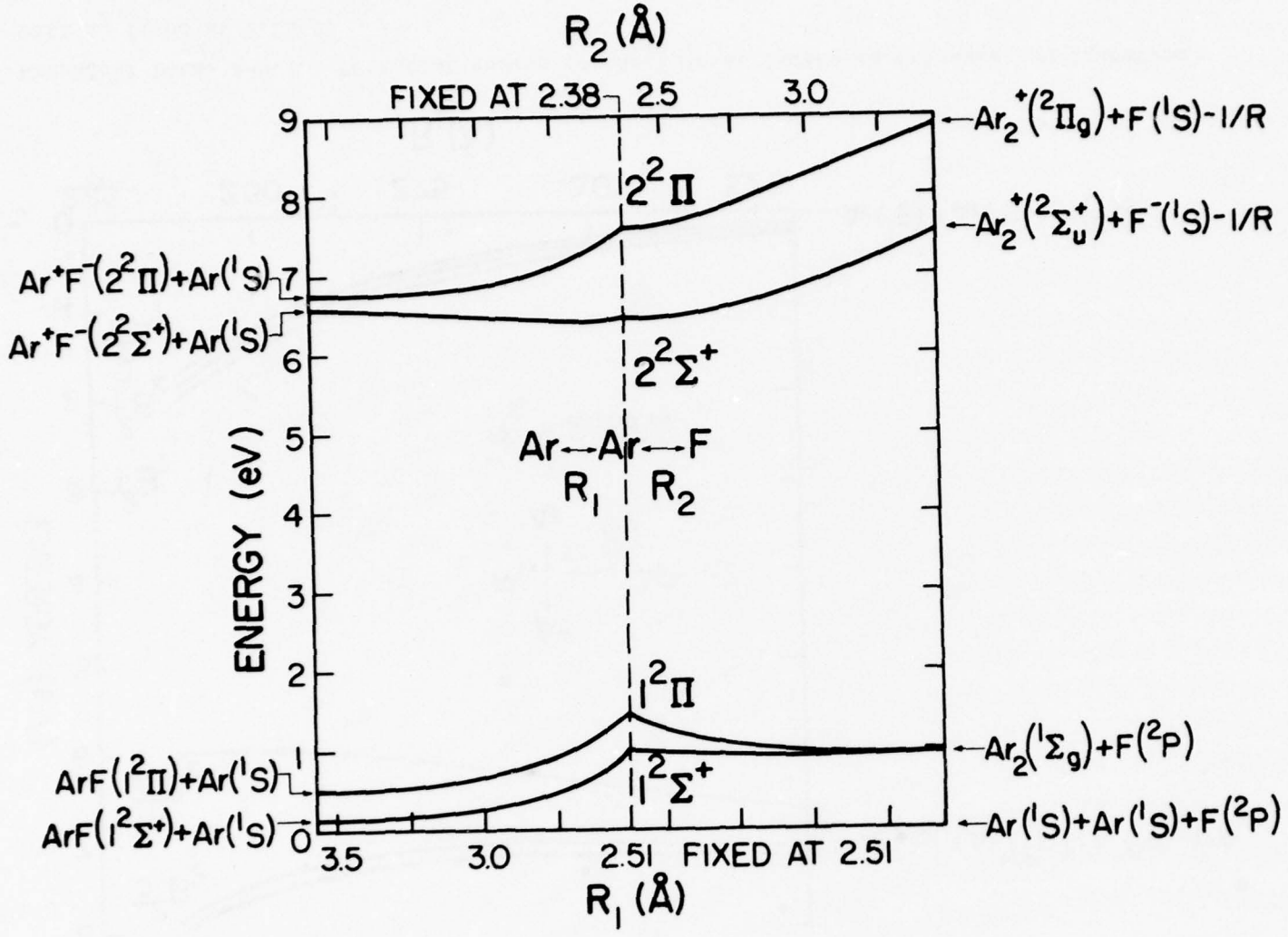

Graphical Data. A-9.4. Potential curves for Ar_2F in a collinear configuration varying both the Ar-Ar (bottom scale) and adjacent Ar-F (top scale) distances.

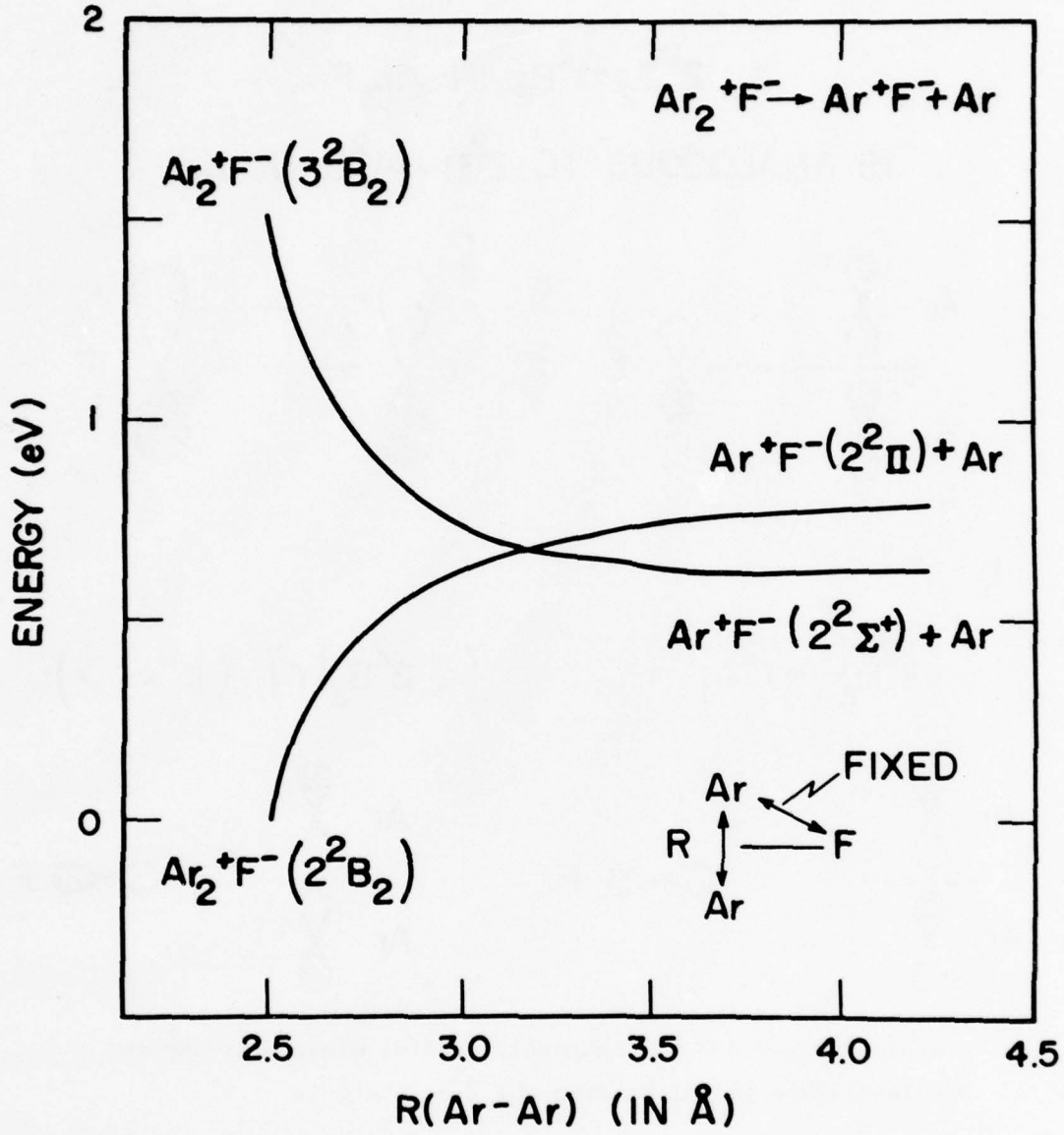

Graphical Data. A-9.5. Potential curves for the lowest two ionic states of Ar_2F in a right triangle configuration as a function of the Ar-Ar distance.

a. $2^2B_2 \rightarrow 1^2B_2$ IN Ar_2F

IS ANALOGOUS TO $2^2\Pi \rightarrow 1^2\Pi$ IN ArF

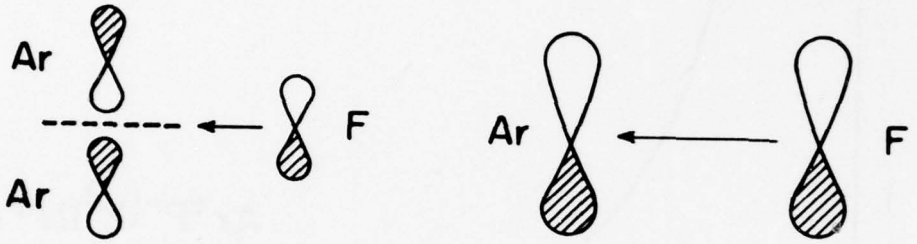

b.

$2^2B_2 \rightarrow 1^2A_1$ $\quad (<2^2B_2|Y)\ (|1^2A_1>)$

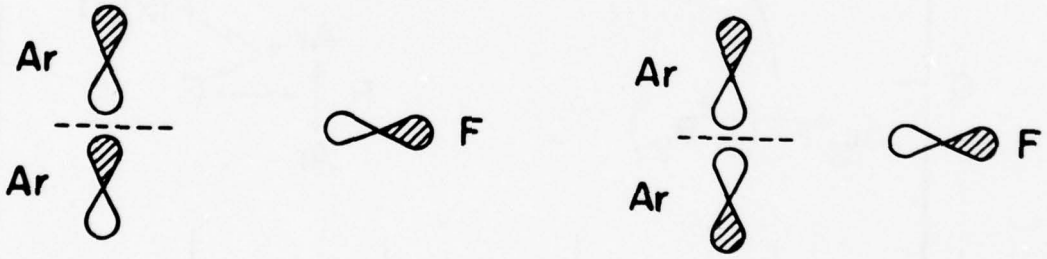

Graphical Data. A-9.6. Schematic orbital diagram of the two dipole-allowed emissions from the 2^2B_2 state in Ar_2F.

Tabular Data. A-9.7. Estimate of the $2^2B_2 \rightarrow 1^2B_2$ (1^2A_1) transition energy in Ar_2F and Kr_2F.

ArF ($2^2\Sigma^+ \rightarrow 1^2\Sigma^+$)	6.42 eV[a]
$-D_e$ [$Ar_2^+(^2\Sigma_u^+)$]	−1.23[b]
− Ar_2 repulsion at $Ar_2^+(^2\Sigma_u^+)$ R_e	−0.86[c]
Predicted Ar_2F ($2\,^2B_2 \rightarrow 1\,^2B_2$, $1\,^2A_1$)	4.33 eV or 286 nm
KrF ($2^2\Sigma^+ \rightarrow 1^2\Sigma^+$)	5.00[d]
$-D_e$ [$Kr_2^+(^2\Sigma_u^+)$]	−1.15[b]
− Kr_2 repulsion at $Kr_2^+(^2\Sigma_u^+)R_e$	−0.86[c]
Predicted Kr_2F($2\,^2B_2 \rightarrow 1\,^2B_2$, $1\,^2A_1$)	2.99 eV or 415 nm

[a] J. J. Ewing and C. A. Brau, Appl. Phys. Letts. 27, 350 (1975)

[b] C. Y. Ng., D. J. Trevor, B. H. Mahan, and Y. T. Lee, J. Chem. Phys. 66, 446 (1977).

[c] W. R. Wadt, J. Chem. Phys. 68, 402 (1978).

[d] J. M. Hoffman, A. K. Hays, and G. C. Tisone, Appl. Phys. Letts. 28, 538 (1976).

Tabular Data. A-9.8. Effect of F^- on the states of Ar_2^+.

		$Ar_2^+F^-$	Ar_2^+
$R_1(a_0)$	$R_2(a_0)$	$E(1\,^2A_2)-E(2\,^2B_2)$(eV)	$E(^2\Pi_g)-E(^2\Sigma_u^+)$(eV)
4.75	20.0	1.56	1.59
4.75	7.0	1.56	1.59
4.75	5.0	1.57	1.59
4.75	4.5	1.57	1.59
4.75	4.25	1.58	1.59
4.75	4.0	1.57	1.59
4.75	3.5	1.53	1.59
4.5	4.25	1.94	1.96
4.75	4.25	1.58	1.59
5.0	4.25	1.29	1.29
5.25	4.25	1.05	1.05
5.75	4.25	0.72	0.69
6.0	4.25	0.60	0.56

Tabular Data. A-9.9. Spectroscopic data for the 2^2B_2 ($4^2\Gamma$) state of Ar_2F with analogous data for the $2^2\Sigma^+$ [III(1/2)] state of ArF and the $1^2\Sigma^+$ [$I(1/2)_u$] state of Ar_2^+ without and with spin-orbit coupling.

	$Ar_2F(2\,^2B_2)$	$ArF(2\,^2\Sigma^+)$[a]	$Ar_2^+(1\,^2\Sigma_u^+)$[b]
R_e(Ar–F)(Å)	2.54	2.40	
R_e(Ar–Ar)(Å)	2.48		2.50
$D_e(Ar_2^+ + F^-)$(eV)	5.00	5.52	
$D_e(Ar^+F^- + Ar)$(eV)	0.60		1.24
	$Ar_2F(4\,^2\Gamma)$	ArF[III(1/2)][a]	$Ar_2^+[I(1/2)_u]$[b]
$D_e(Ar_2^+ + F^-)$(eV)	5.00	5.49	
$D_e(Ar^+F^- + Ar)$(eV)	0.57		1.19

[a] T. H. Dunning and P. J. Hay, Chem. Phys. (in press).

[b] W. R. Wadt. J. Chem. Phys. 68, 402 (1978).

Tabular Data. A-9.10. Calculated data for the dipole-allowed emissions from the 2^2B_2 state of Ar_2F in its equilibrium isosceles triangle geometry neglecting spin-orbit effects.

	ΔE(eV)	λ(nm)	M(D)	A(sec^{-1})[a]
$2\,^2B_2 \rightarrow 1\,^2A_1$	4.64	267	0.49	3.95×10^6
$2\,^2B_2 \rightarrow 1\,^2B_2$	4.53	274	0.49	3.60×10^6

[a] The overall lifetime of the 2^2B_2 state is 132 nsec.

Tabular Data. A-9.11. Transition moment (in a.u.)[a] from the $4^2\Gamma$ state of Ar_2F (including spin-orbit coupling) for the equilibrium isosceles triangle geometry of the 2^2B_2 state.

	M_x	M_y	M_z	M
$4^2\Gamma \rightarrow 1^2\Gamma$	5.09×10^{-4}	1.92×10^{-1}	-4.12×10^{-2}	1.96×10^{-1}
$4^2\Gamma \rightarrow 2^2\Gamma$	1.43×10^{-4}	1.66×10^{-2}	1.85×10^{-1}	1.86×10^{-1}
$4^2\Gamma \rightarrow 3^2\Gamma$	5.98×10^{-4}	-1.29×10^{-2}	-2.75×10^{-2}	3.04×10^{-2}
$4^2\Gamma \rightarrow 5^2\Gamma$	-6.04×10^{-3}	5.61×10^{-2}	2.13×10^{-2}	6.03×10^{-2}
$4^2\Gamma \rightarrow 6^2\Gamma$	-1.48×10^{-2}	-1.36×10^{-1}	8.94×10^{-3}	1.37×10^{-1}
$4^2\Gamma \rightarrow 7^2\Gamma$	-5.14×10^{-5}	1.65×10^{-1}	0	1.65×10^{-1}
$4^2\Gamma \rightarrow 8^2\Gamma$	9.72×10^{-5}	-4.12×10^{-2}	0	4.25×10^{-2}
$4^2\Gamma \rightarrow 9^2\Gamma$	-4.60×10^{-3}	2.08	1.25×10^{-4}	2.08

[a] $1\ ea_0 = 2.541765$ debye (D).

Tabular Data. A-9.12. Calculated data including spin-orbit coupling for the dipole-allowed emissions from the $4^2\Gamma$ state of Ar_2F at the equilibrium isosceles triangle geometry of the 2^2B_2 state.

	ΔE(eV)	λ(nm)	M(D)	$A(sec^{-1})$[a]
$4^2\Gamma \rightarrow 1^2\Gamma$	4.64	267	0.50	4.08×10^6
$4^2\Gamma \rightarrow 2^2\Gamma$	4.52	274	0.47	3.40×10^6
$4^2\Gamma \rightarrow 3^2\Gamma$	4.38	283	0.08	8.27×10^4

[a]The overall lifetime of the $4^2\Gamma$ state is 132 nsec.

Tabular Data. A-9.13. Calculated data for the dipole-allowed absorptions from 2^2B_2 state of Ar_2F in its equilibrium isosceles triangle geometry neglecting spin-orbit effects.

	ΔE(eV)	λ(nm)	M(D)	f
$2^2B_2 \rightarrow 3^2B_2$	1.54	805	0.06	2.0×10^{-5}
$2^2B_2 \rightarrow 1^2A_2$	1.66	749	0.04	1.0×10^{-5}
$2^2B_2 \rightarrow 2^2A_1$	2.34	529	0.43	1.7×10^{-3}
$2^2B_2 \rightarrow 3^2A_1$	3.88	320	5.29	0.41

Tabular Data. A-9.14. Calculated data for the dipole-allowed absorptions in Ar_2^+ without ($^2\Sigma_u^+$) and with [$I(1/2)_u$] spin-orbit coupling.

	ΔE(eV)	λ(nm)	M(D)	f
$1\,^2\Sigma_u^+ \rightarrow 1\,^2\Pi_g$	1.66	745	0.09	5.0×10^{-5}
$1\,^2\Sigma_u^+ \rightarrow 1\,^2\Sigma_g^+$	3.89	319	5.26	0.41
$I(1/2)_u \rightarrow I(3/2)_g$	1.61	772	0.06	2.4×10^{-5}
$I(1/2)_u \rightarrow I(1/2)_g$	1.72	720	0.38	9.2×10^{-4}
$I(1/2)_u \rightarrow II(1/2)_g$	3.89	318	5.22	0.40

Tabular Data. A-9.15. Calculated data including spin-orbit coupling for the dipole-allowed absorptions from the $4^2\Gamma$ state of Ar_2F at the equilibrium isosceles triangle geometry of the 2^2B_2 state.

	ΔE (eV)	λ(nm)	M(D)	f
$4^2\Gamma \rightarrow 5^2\Gamma$	1.52	818	0.15	1.4×10^{-4}
$4^2\Gamma \rightarrow 6^2\Gamma$	1.68	737	0.35	7.7×10^{-4}
$4^2\Gamma \rightarrow 7^2\Gamma$	2.33	531	0.42	1.6×10^{-3}
$4^2\Gamma \rightarrow 8^2\Gamma$	2.58	481	0.11	1.1×10^{-4}
$4^2\Gamma \rightarrow 9^2\Gamma$	3.88	319	5.29	0.41

Tabular Data. A-9.16. Spectroscopic data for the 2^2B_2 ($4^2\Gamma$) state of Kr_2F with analogous data for the $2^2\Sigma^+$ [III(1/2)] state of KrF and the $1^2\Sigma_u^+$ [$(1/2)_u$] state of Kr_2^+ without and with spin-orbit coupling.

	$Kr_2F(2^2B_2)$	$KrF(2^2\Sigma^+)$[a]	$Kr_2^+(1^2\Sigma_u^+)$[b]
R_e(Kr–F)(Å)	2.67	2.53	
R_e(Kr–Kr)(Å)	2.77		2.79
$D_e(Kr_2^+ + F^-)$(eV)	4.95	5.36	
$D_e(Kr^+F^- + Kr)$(eV)	0.63		1.23
	$Kr_2F(4^2\Gamma)$	KrF[III(1/2)][a]	$Kr_2^+[I(1/2)_u]$[b]
$D_e(Kr_2^+ + F^-)$(eV)	4.95	5.31	
$D_e(Kr^+F^- + Kr)$(eV)	0.49		1.05

[a] P. J. Hay and T. H. Dunning, J. Chem. Phys. 66, 1306 (1977).

[b] W. R. Wadt. J. Chem. Phys. 68, 402 (1978).

Tabular Data. A-9.17. Calculated data for the dipole-allowed emissions from 2^2B_2 state of Kr_2F in its equilibrium isosceles triangle geometry neglecting spin-orbit effects.

	ΔE(eV)	λ(nm)	M(D)	$A(sec^{-1})^a$
$2\,^2B_2 \rightarrow 1\,^2A_1$	3.47	357	0.66	2.97×10^6
$2\,^2B_2 \leftarrow 1\,^2B_2$	3.38	368	0.85	4.61×10^6

[a]The overall lifetime of the 2^2B_2 state is 132 nsec.

Tabular Data. A-9.18. Transition moments (in a.u.)[a] from $4^2\Gamma$ state of Kr_2F (including spin-orbit coupling) for the equilibrium isosceles triangle geometry of the 2^2B_2 state.

	M_x	M_y	M_z	M
$4\,^2\Gamma \rightarrow 1\,^2\Gamma$	1.2×10^{-3}	2.59×10^{-1}	-1.24×10^{-1}	2.87×10^{-1}
$4\,^2\Gamma \rightarrow 2\,^2\Gamma$	5.22×10^{-4}	3.52×10^{-3}	3.13×10^{-1}	3.13×10^{-1}
$4\,^2\Gamma \rightarrow 3\,^2\Gamma$	3.51×10^{-3}	-1.26×10^{-2}	-4.81×10^{-2}	4.98×10^{-2}
$4\,^2\Gamma \rightarrow 5\,^2\Gamma$	-1.63×10^{-2}	7.94×10^{-2}	4.20×10^{-2}	9.13×10^{-2}
$4\,^2\Gamma \rightarrow 6\,^2\Gamma$	-2.11×10^{-2}	-6.18×10^{-1}	-3.29×10^{-2}	6.19×10^{-1}
$4\,^2\Gamma \rightarrow 7\,^2\Gamma$	-1.73×10^{-5}	1.53×10^{-1}	0	1.53×10^{-1}
$4\,^2\Gamma \rightarrow 8\,^2\Gamma$	1.01×10^{-4}	-9.30×10^{-2}	0	9.30×10^{-2}
$4\,^2\Gamma \rightarrow 9\,^2\Gamma$	-8.91×10^{-4}	2.12	-1.53×10^{-3}	2.12

[a]1 ea_0 = 2.541765 debye (D).

Tabular Data. A-9.19. Calculated data including spin-orbit coupling for the dipole-allowed emissions from the $4^2\Gamma$ state of Kr_2F at the equilibrium isosceles triangle geometry of the 2^2B_2 state.

	ΔE(eV)	λ(nm)	M(D)	A(sec^{-1})[a]
$4^2\Gamma \rightarrow 1^2\Gamma$	3.44	361	0.73	3.55×10^6
$4^2\Gamma \rightarrow 2^2\Gamma$	3.34	371	0.80	3.88×10^6
$4^2\Gamma \rightarrow 3^2\Gamma$	3.14	395	0.13	8.18×10^4

[a]The overall lifetime of the $4^2\Gamma$ state is 133 nsec.

Tabular Data. A-9.20. Calculated data for the dipole-allowed absorptions from 2^2B_2 state of Kr_2F in its equilibrium isosceles triangle geometry neglecting the spin-orbit effects.

	ΔE(eV)	λ(nm)	M(D)	f
$2^2B_2 \rightarrow 3^2B_2$	1.46	849	0.14	1.0×10^{-4}
$2^2B_2 \rightarrow 1^2A_2$	1.56	794	0.07	2.8×10^{-5}
$2^2B_2 \rightarrow 2^2B_1$	2.15	577	0.46	1.8×10^{-3}
$2^2B_2 \rightarrow 3^2A_1$	3.60	344	5.62	0.43

Tabular Data. A-9.21. Calculated data for the dipole-allowed absorptions in Kr_2^+ without ($^2\Sigma_u^+$) and with [$I(1/2)_u$] spin-orbit coupling.

	ΔE(eV)	λ(nm)	M(D)	f
$1\,^2\Sigma_u^+ \rightarrow 1\,^2\Pi_g$	1.57	790	0.15	1.3×10^{-4}
$1\,^2\Sigma_u^+ \rightarrow 1\,^2\Sigma_g^+$	3.59	346	5.39	0.40
$I(1/2)_u \rightarrow I(3/2)_g$	1.36	911	0.10	5.6×10^{-5}
$I(1/2)_u \rightarrow I(1/2)_g$	1.75	708	1.55	1.6×10^{-2}
$I(1/2)_u \rightarrow II(1/2)_g$	3.66	339	5.20	0.38

Tabular Data. A-9.22. Calculated data including spin-orbit coupling for the dipole-allowed absorptions from the $4^2\Gamma$ state of Kr_2F at the equilibrium isosceles triangle geometry of the 2^2B_2 state.

	ΔE(eV)	λ(nm)	M(D)	f
$4\,^2\Gamma \rightarrow 5\,^2\Gamma$	1.32	938	0.23	2.7×10^{-4}
$4\,^2\Gamma \rightarrow 6\,^2\Gamma$	1.73	718	1.57	1.6×10^{-2}
$4\,^2\Gamma \rightarrow 7\,^2\Gamma$	2.06	603	0.39	1.2×10^{-3}
$4\,^2\Gamma \rightarrow 8\,^2\Gamma$	2.59	478	0.24	5.2×10^{-4}
$4\,^2\Gamma \rightarrow 9\,^2\Gamma$	3.69	336	5.39	0.41

Tabular Data. A-9.23. Electronic state energies for Ar_2F and Kr_2F at their respective equilibrium isosceles triangle geometries without and with spin-orbit coupling. (Energies are in hartrees).

Without spin–orbit coupling			With spin–orbit coupling		
State	Ar_2F[a]	Kr_2F[b]	State	Ar_2F[a]	Kr_2F
$1\,^2A_1$	−0.89765	−0.13053	$1\,^2\Gamma$	−0.89777	−0.13066
$1\,^2B_2$	−0.89336	−0.12717	$2\,^2\Gamma$	−0.89337	−0.12713
$1\,^2B_1$	−0.88822	−0.11997	$3\,^2\Gamma$	−0.88810	−0.11988
$2\,^2B_2$	−0.72706	−0.00295	$4\,^2\Gamma$	−0.72716	−0.00439
$3\,^2B_2$	−0.67043	0.05070	$5\,^2\Gamma$	−0.67137	0.04418
$1\,^2A_2$	−0.66624	0.05443	$6\,^2\Gamma$	−0.66542	0.05907
$2\,^2A_1$	−0.64096	0.07596	$7\,^2\Gamma$	−0.64148	0.07117
$2\,^2B_1$	−0.63293	0.08467	$8\,^2\Gamma$	−0.63230	0.09090
$3\,^2A_1$	−0.58464	0.12934	$9\,^2\Gamma$	−0.58452	0.13123

[a]Energies are relative to −1152 hartree.

[b]Energies are relative to −5603 hartree.

Tabular Data. A-9.24. The overall radiative life-time (in nsec) of the $2\,^2B_2$ state in Ar_2F as a function of geometry. Ar_2F has a C_{2v} isosceles triangle geometry with base = R_1 and height = R_2. R_1 and R_2 are in bohr ($1a_0$ = 0.529177 Å).

R_1 \ R_2	4.0	4.25	4.5
4.5		222	
4.75	87.1	126	206
5.0		85.8	

A-10. POTENTIAL ENERGY CURVES, SPECTROSCOPIC CONSTANTS, AND EMISSION DATA, FOR HgCℓ and HgBr

CONTENTS

		Page
A-10.1.	Potential energy curves for the $X^2\Sigma^+$, $A^2\Pi$, and $B^2\Sigma^+$ states of HgCℓ without spin-orbit coupling.	1271
A-10.2.	Potential energy curves for the $X^2\Sigma^+$, $A^2\Pi$, $B^2\Sigma^+$, and $C,D^2\Pi$ states of HgCℓ without spin-orbit coupling . . .	1272
A-10.3.	Potential energy curves for HgCℓ doublet states. . . .	1273
A-10.4.	Potential energy curves for HgCℓ quartet states. . . .	1274
A-10.5.	Potential energy curves for the $X^2\Sigma^+$, $A^2\Pi$, and $B^2\Sigma^+$ states of HgBr without spin-orbit coupling	1275
A-10.6.	Potential energy curves for the $X^2\Sigma^+$, $A^2\Pi$, $B^2\Sigma^+$, and $C,D^2\Pi$ states of HgBr without spin-orbit coupling . . .	1276
A-10.7.	Potential energy curves for the HgBr doublet states. .	1277
A-10.8.	Potential energy curves for the HgBr quartet states. .	1278
A-10.9.	Spectroscopic constants for the X and B states of Hg^{202} Cl^{35} with and without spin-orbit coupling. . . .	1279
A-10.10.	Spectroscopic constants for the X and B states of Hg^{202} Br^{79} with and without spin-orbit coupling. . . .	1280
A-10.11.	Emission data for the B → X lasing transition in HgCl with and without spin-orbit coupling.	1281
A-10.12.	Emission data for the B → X lasing transition in HgBr with and without spin-orbit coupling	1281

A-10. References:

1. W. R. Wadt, "The Electronic Structure of HgCℓ and HgBr," Appl. Letts. (in press).

AD-A068 679 ARMY MISSILE RESEARCH AND DEVELOPMENT COMMAND REDSTO--ETC F/G 20/5
COMPILATION OF DATA RELEVANT TO NUCLEAR PUMPED LASERS. VOLUME I--ETC(U)
DEC 78 E W MCDANIEL, M R FLANNERY, E W THOMAS

UNCLASSIFIED DRDMI-H-78-1-VOL-3 NL

5 OF 5
AD A068679

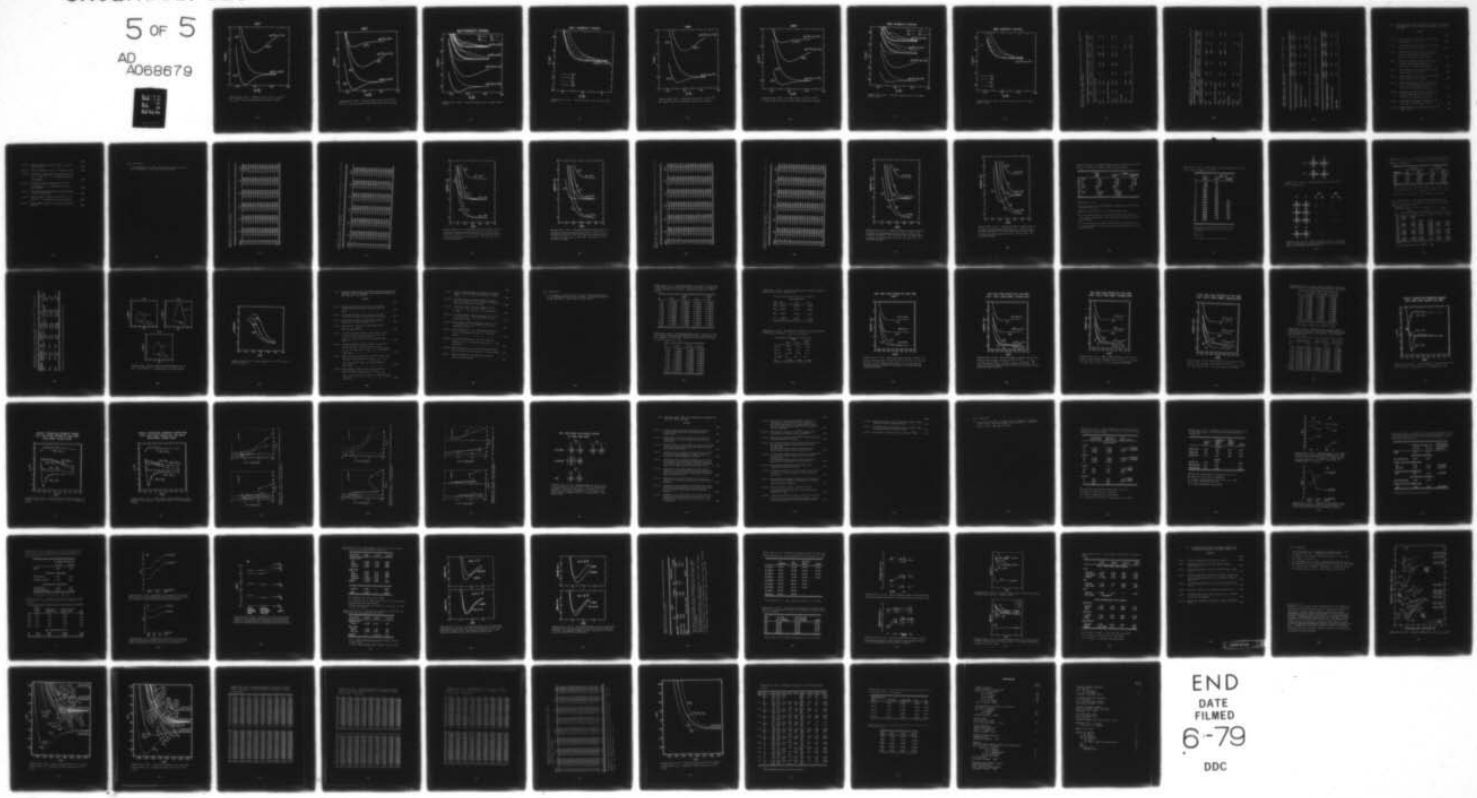

END
DATE FILMED
6-79
DDC

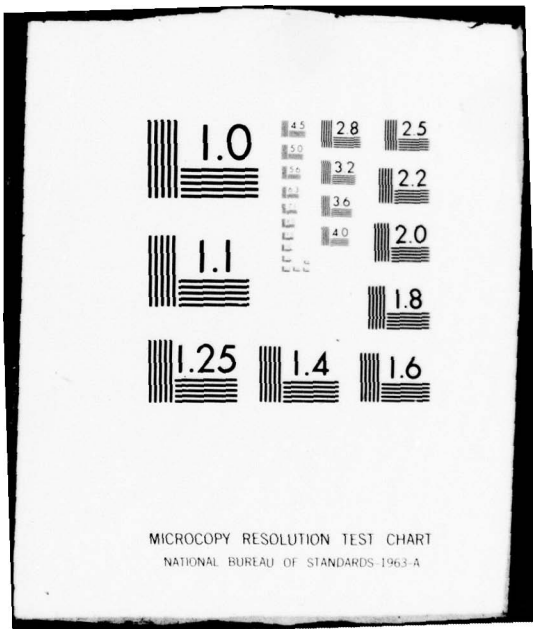
1.0
1.1
1.25
1.4
1.6
1.8
2.0
2.2
2.5
2.8
3.2
3.6
4.0
4.5
5.0
MICROCOPY RESOLUTION TEST CHART
NATIONAL BUREAU OF STANDARDS-1963-A

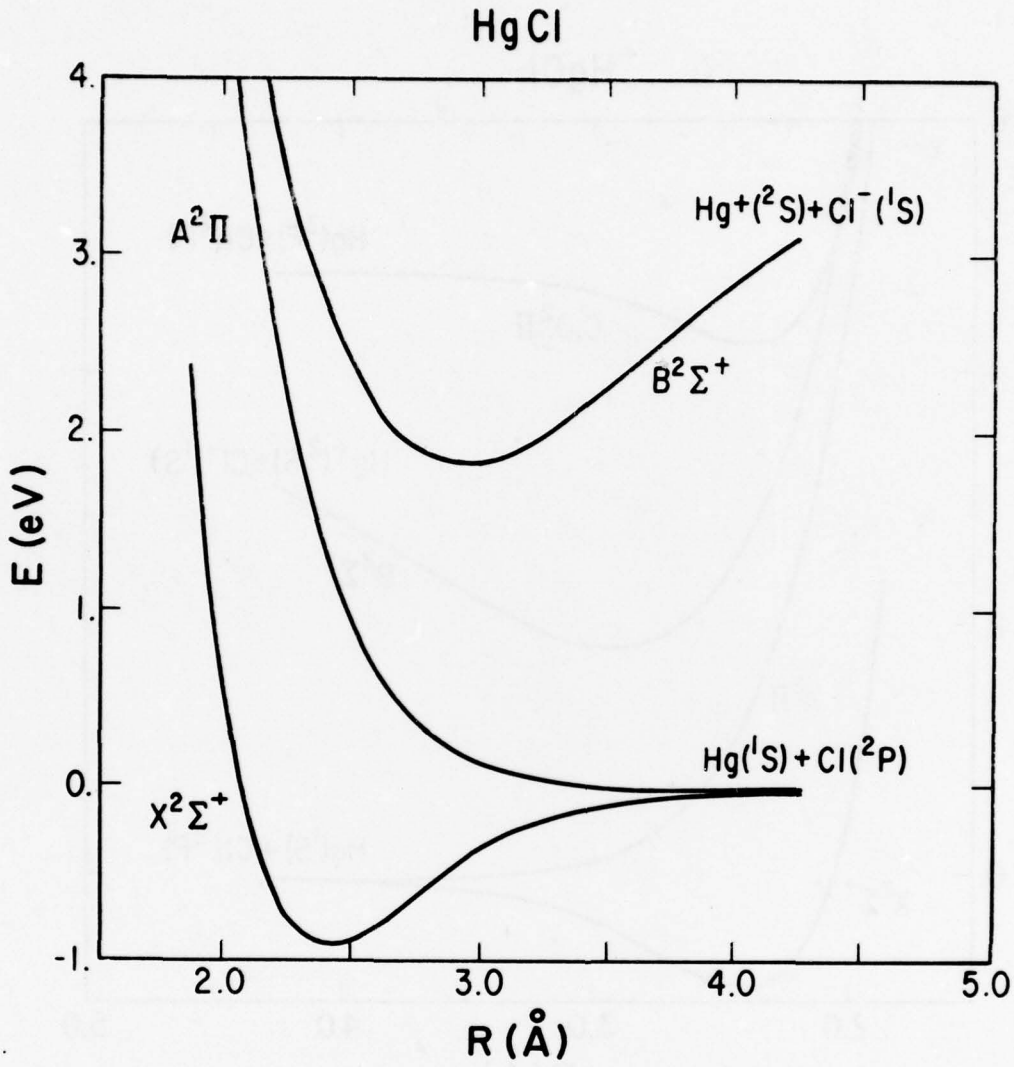

Graphical Data. A-10.1. Potential energy curves for the $X^2\Sigma^+$, $A^2\Pi$, and $B^2\Sigma^+$ states of HgCℓ without spin-orbit coupling.

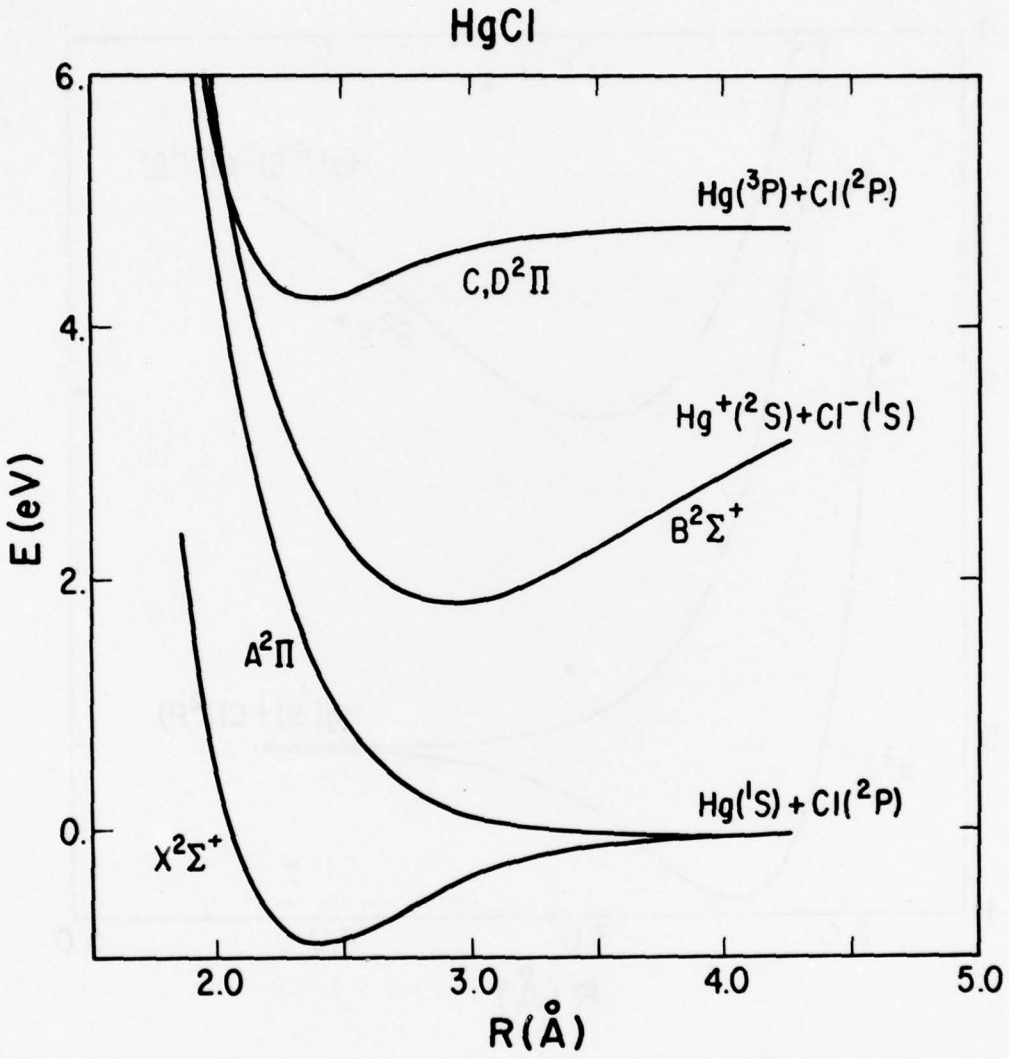

Graphical Data. A-10.2. Potential energy curves for the $X^2\Sigma^+$, $A^2\Pi$, $B^2\Sigma^+$, and $C,D^2\Pi$ states of HgCℓ without spin-orbit coupling.

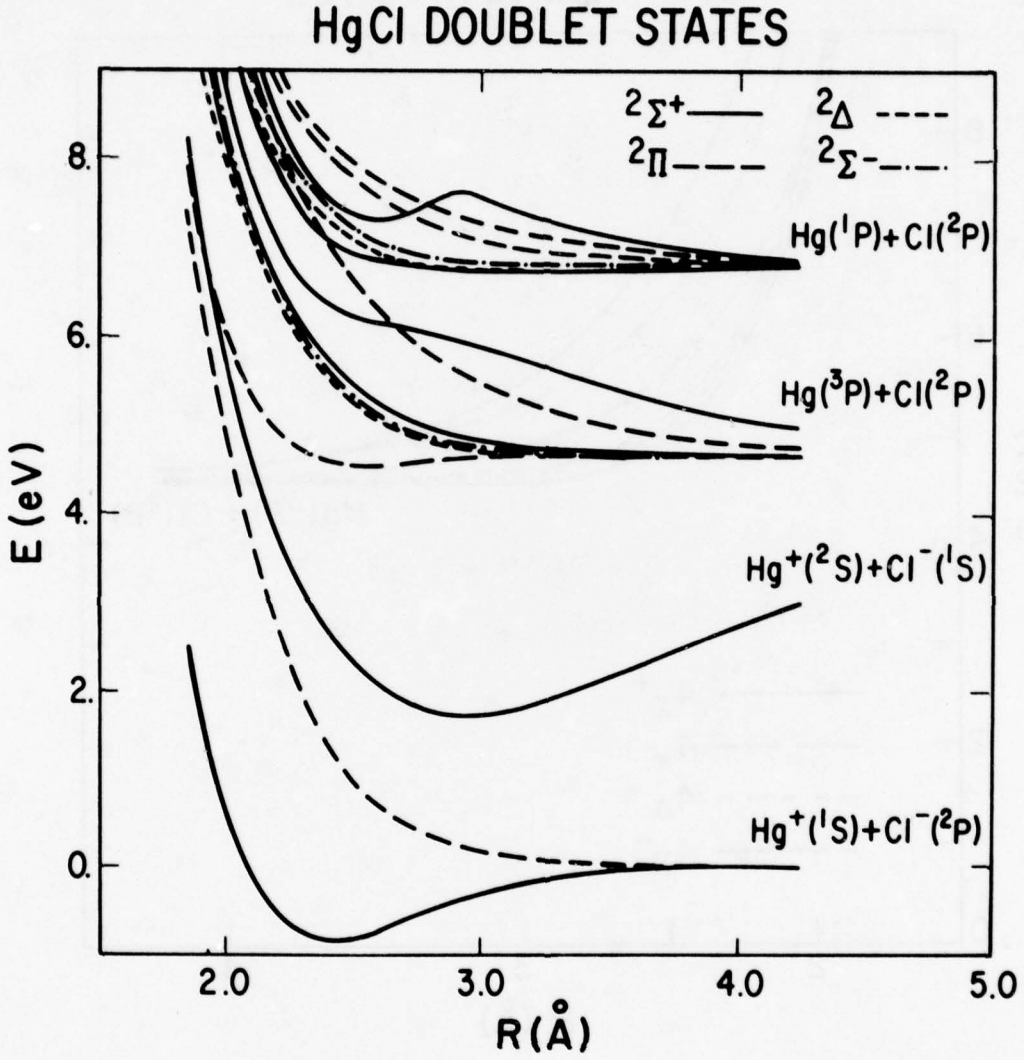

Graphical Data. A-10.3. Potential energy curves for HgCℓ doublet states.

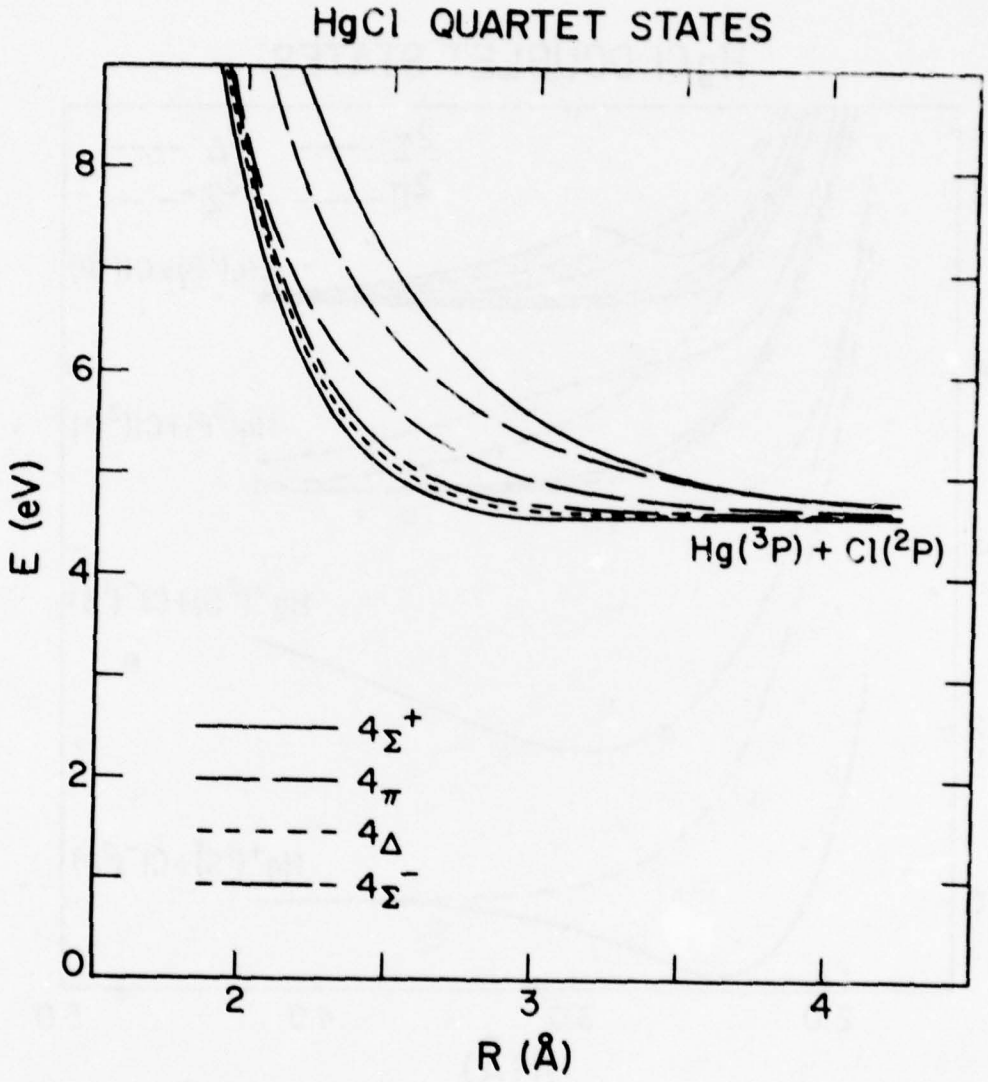

Graphical Data. A-10.4. Potential energy curves for HgCℓ quartet states.

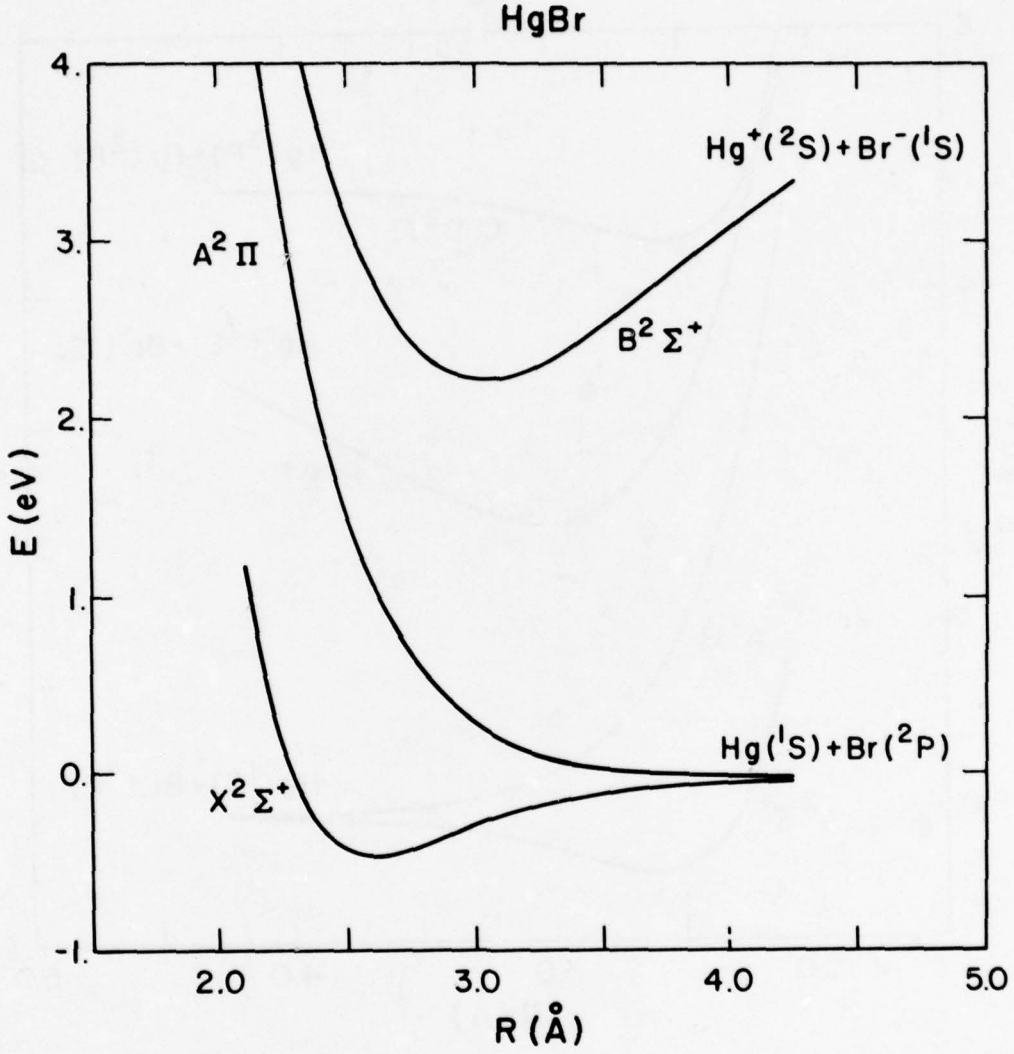

Graphical Data. A-10.5. Potential energy curves for the $X^2\Sigma^+$, $A^2\Pi$, and $B^2\Sigma^+$ states of HgBr without spin-orbit coupling.

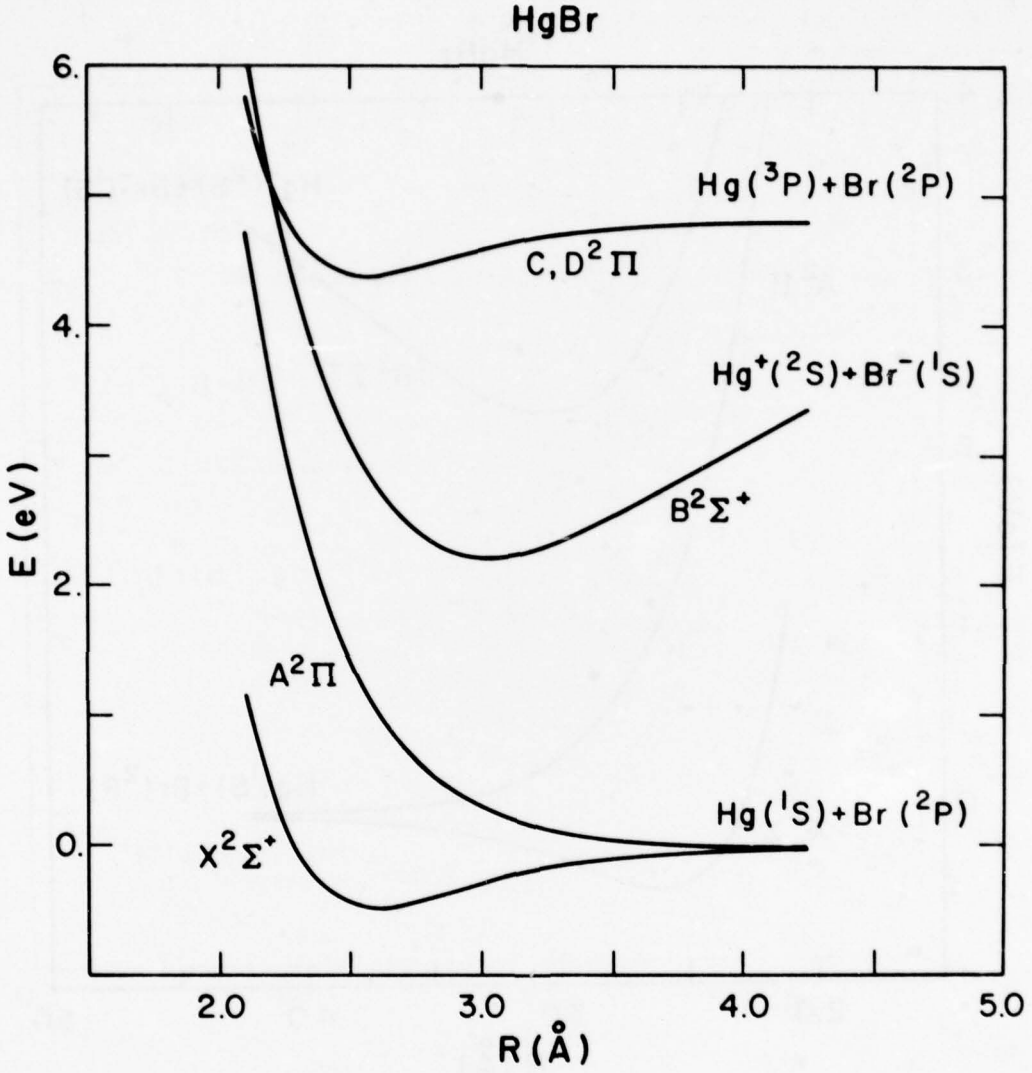

Graphical Data. A-10.6. Potential energy curves for the $X^2\Sigma^+$, $A^2\Pi$, $B^2\Sigma^+$, and $C,D^2\Pi$ states of HgBr without spin-orbit coupling.

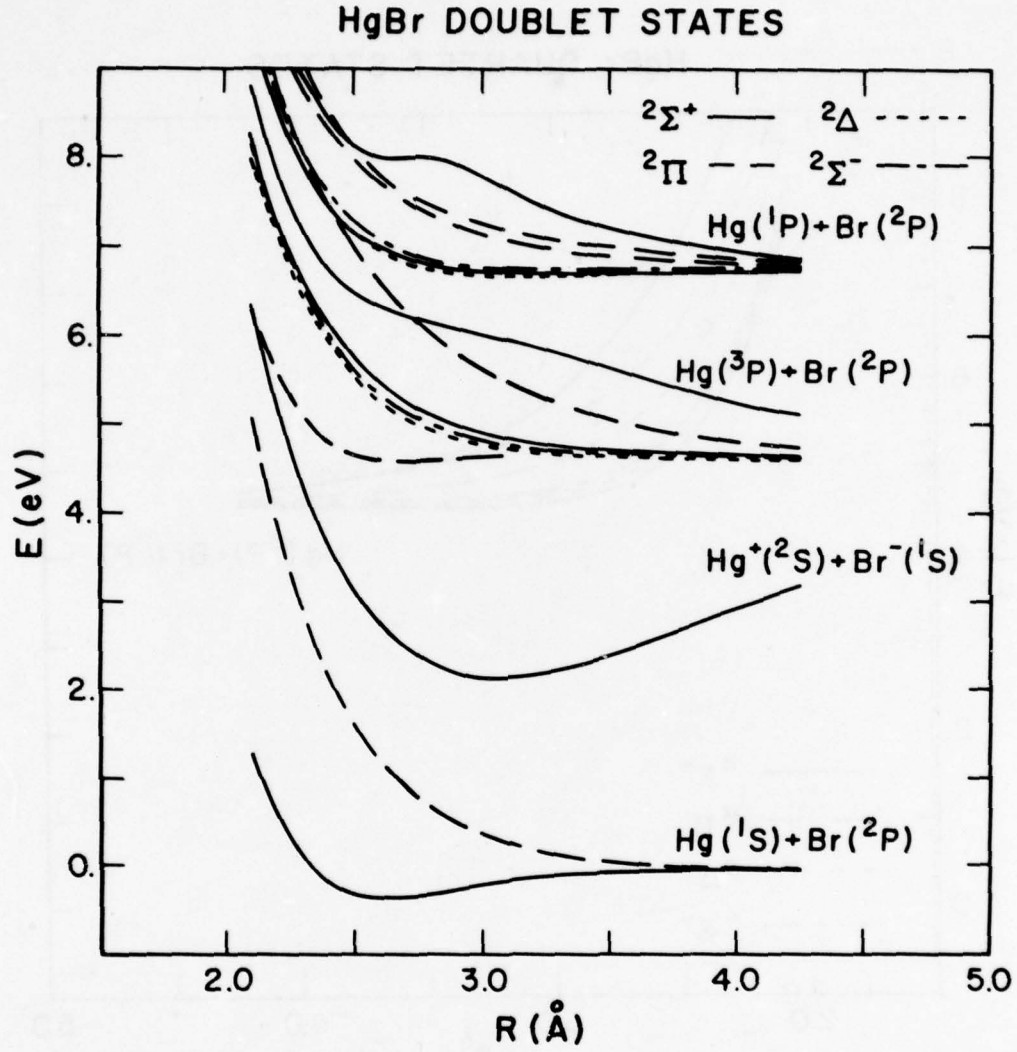

Graphical Data. A-10.7. Potential energy curves for the HgBr doublet states.

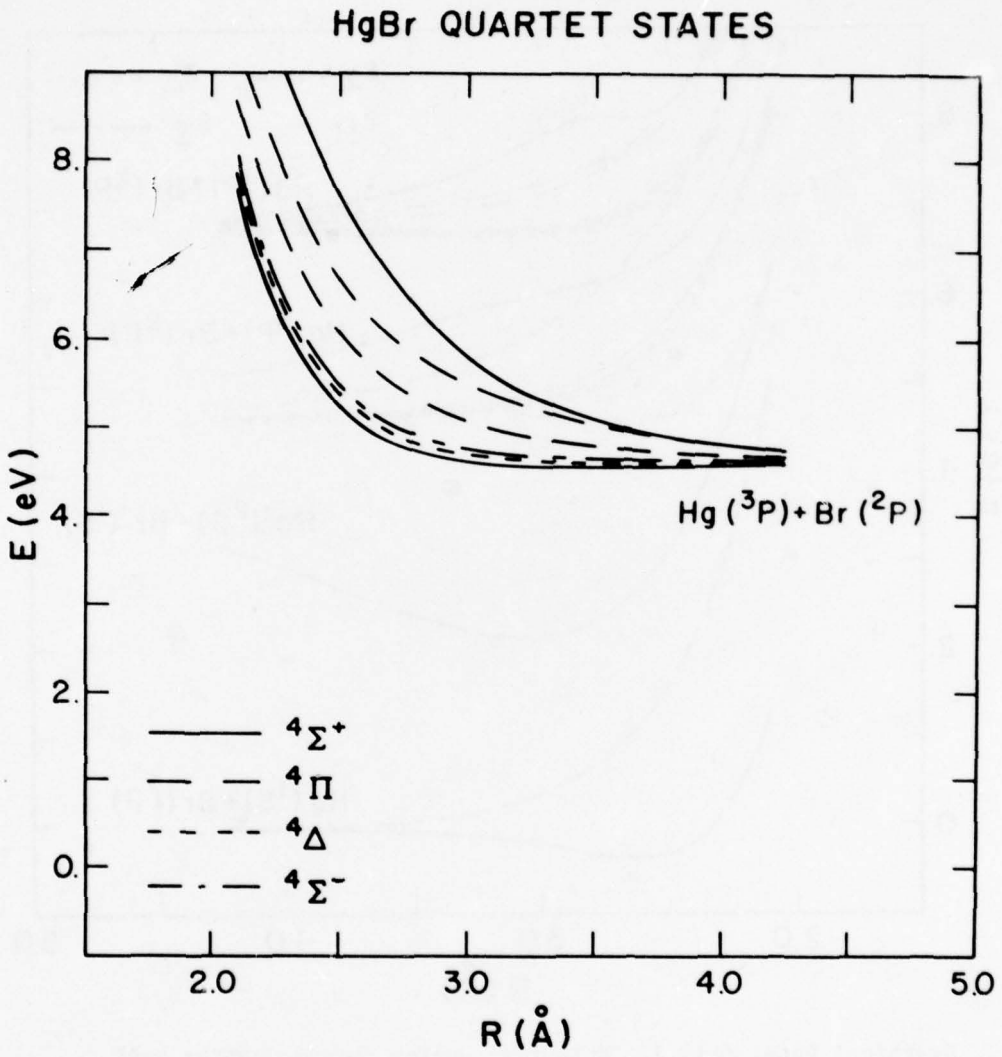

Graphical Data. A-10.8. Potential energy curves for the HgBr quartet states.

Tabular Data. A-10.9. Spectroscopic constants for the X and B states of Hg^{202} Cl^{35} with and without spin-orbit coupling.

	R_e(Å)	$\omega_e(cm^{-1})$	$x_e\omega_e(cm^{-1})$	$B_e(cm^{-1})$	$\alpha_e(cm^{-1})$	D_e(eV)	μ(D)
Without Spin-Orbit Coupling							
$X^2\Sigma^+$	2.41	285.3	2.25	.098	.00076	.91	3.28
$B^2\Sigma^+$	2.93	198.8	.51	.066	.00015	4.77	5.41
With Spin-Orbit Coupling							
$X^2\Sigma^+_{1/2}$	2.42	285.6	2.29	.098	.00077	.87	3.28
$B^2\Sigma^+_{1/2}$	2.93	198.0	.56	.066	.00015	4.77	5.41
Experiment							
$X^2\Sigma^+_{1/2}$	—	292.6	1.60	—	—	1.08	—
$B^2\Sigma$	—	192.0	.50	—	—	4.99	—

Tabular Data. A-10.10. Spectroscopic constants for the X and B states of Hg^{202} Br^{79} with and without spin-orbit coupling.

	R_e(Å)	$\omega_e(cm^{-1})$	$x_e\omega_e(cm^{-1})$	$B_e(cm^{-1})$	$\alpha_e(cm^{-1})$	$D_e(eV)$	$\mu(D)$
Without Spin-Orbit Coupling							
$X^2\Sigma^+$	2.61	159.4	1.64	0.044	.00040	.48	2.62
$B^2\Sigma^+$	3.04	141.8	.29	.032	.00006	4.77	5.51
With Spin-Orbit Coupling							
$X^2\Sigma^+_{1/2}$	2.62	159.4	1.64	.044	.00044	.33	2.62
$B^2\Sigma^+_{1/2}$	3.05	141.8	.29	.032	.00006	4.77	5.51
Experiment							
$X^2\Sigma^+_{1/2}$	—	186.5	.97	—	—	.71	—
$B^2\Sigma^+_{1/2}$	—	135.1	.28	—	—	4.87	—

Tabular Data. A-10.11. Emission data for the B → X lasing transition in HgCl with and without spin-orbit coupling.

	T_e(eV)	ΔE(eV)	λ(nm)	M(D)	τ(ns)
Without Spin-Orbit Coupling	2.73	2.25	552	4.37	27.4
With Spin-Orbit Coupling	2.73	2.25	552	4.36	27.5
Experiment	2.90	2.22	558	3.52	44.6
				4.99	22.2

Tabular Data. A-10.12. Emission data for the B → X lasing transition in HgBr with and without spin-orbit coupling.

	T_e(eV)	ΔE(eV)	λ(nm)	M(D)	τ(ns)
Without Spin-Orbit Coupling	2.70	2.50	497	3.88	26.0
With Spin-Orbit Coupling	2.70	2.50	497	3.77	27.6
Experiment	2.91	2.47	502	4.12	23.7

A-11. POTENTIAL ENERGY CURVES, ELECTRONIC ENERGIES, SPECTROSCOPIC CONSTANTS, AND DIPOLE AND TRANSITION MOMENTS FOR THE RARE GAS OXIDES

CONTENTS

		Page
A-11.1.	Total energies of the states of NeO arising from Ne (^1S) + O (^3P, ^1D, ^1S)	1285
A-11.2.	Total energies of the states of ArO arising from Ar (^1S) + O (^3P, ^1D, ^1S)	1286
A-11.3.	Calculated potential energy curves for the states of NeO arising from the Ne (^1S) + O (^3P, ^1D, ^1S) separated atom limits	1287
A-11.4.	Calculated potential energy curves for the states of ArO arising from the Ar (^1S) + O (^3P, ^1D, ^1S) separated atom limits	1288
A-11.5.	Total energies of the states of KrO arising from Kr (^1S) + O (^3P, ^1D, ^1S)	1289
A-11.6.	Total energies of the states of XeO arising from Xe (^1S) + O (^3P, ^1D, ^1S)	1290
A-11.7.	Calculated potential energy curves for the states of KrO arising from the Kr (^1S) + O (^3P, ^1D, ^1S) separated atom limits	1291
A-11.8.	Calculated potential energy curves for the states of XeO arising from the Xe (^1S) + O (^3P, ^1D, ^1S) separated atom limits	1292
A-11.9.	Calculated spectroscopic constants for the $1\,^1\Sigma^+$ states of $^{84}Kr^{16}O$ and $^{132}Xe^{16}O$	1293
A-11.10.	Vibrational levels and spacings for the $1\,^1\Sigma^+$ state of XeO	1294

Page

A-11.11. Orbital diagrams for the $^{3,1}\Pi$ and $^{3}\Sigma^{-}$, and $^{1}\Delta$ states of ArO 1295

A-11.12. Orbital diagrams for the 1,2 $^{1}\Sigma^{+}$ states of ArO . . . 1295

A-11.13. Calculated crossing points and energies for the $1^{1}\Sigma^{+}$ - $^{3}\Pi$ and $1^{1}\Sigma^{+}$ - $^{3}\Sigma^{-}$ crossings in the rare gas monoxides 1296

A-11.14. Calculated transition moments for the $2^{1}\Sigma^{+}$ - $1^{1}\Sigma^{+}$ and $2^{1}\Sigma^{+}$ - $^{1}\Pi$ transitions in the rare gas monoxides 1296

A-11.15. Calculated pseudo-lifetimes for the $2^{1}\Sigma^{+}$ states of the rare gas oxides 1297

A-11.16. Dipole transition moments for the $2^{1}\Sigma^{+}$ - $1^{1}\Sigma^{+}$ and $2^{1}\Sigma^{+}$ - $^{1}\Pi$ transitions in ArO, KrO and XeO 1298

A-11.17. Dipole moments for the $1^{1}\Sigma^{+}$ states of ArO, KrO, and XeO 1299

A-11. References:

1. T. H. Dunning and P. J. Hay, "Low-Lying Electronic Data of the Rare-Gas Oxides," J. Chem. Phys. 66, 3767 (1977).

Tabular Data. A-11.1 Total energies of the states of NeO arising from Ne (^1S) + O (^3P, ^1D, ^1S). Energies are relative to -203 hartree.

$R(a_0)$	$^3\Pi$	$^3\Sigma^-$	$1\,^1\Sigma^+$	$^1\Pi$	$^1\Delta$	$2\,^1\Sigma^+$
2.50	−0.10974	0.07731	−0.19091	−0.03497	0.15266	0.20825
2.75	−0.22077	−0.10267	−0.23476	−0.14415	−0.02472	0.03748
3.00	−0.28369	−0.20963	−0.25589	−0.20469	−0.12986	−0.06148
3.25	−0.31950	−0.27310	−0.26673	−0.23847	−0.19217	−0.11767
3.50	−0.33990	−0.31077	−0.27304	−0.25750	−0.22909	−0.14886
3.75	−0.35145	−0.33308	−0.27701	−0.26827	−0.25091	−0.16589
4.00	−0.35792	−0.34626	−0.27946	−0.27438	−0.26377	−0.17516
4.25	−0.36151	−0.35402	−0.28088	−0.27782	−0.27133	−0.18026
4.50	−0.36347	−0.35859	−0.28165	−0.27976	−0.27577	−0.18309
5.00	−0.36508	−0.36283	−0.28219	−0.28141	−0.27987	−0.18556
5.50	−0.36546	−0.36424	−0.28223	−0.28185	−0.28123	−0.18631
6.00	−0.36550	−0.36467	−0.28215	−0.28191	−0.28164	−0.18649
7.00	−0.36542	−0.36475	−0.28203	−0.28184	−0.28172	−0.18647
8.50	−0.36539	−0.36473	−0.28199	−0.28181	−0.28169	−0.18644
12.00	−0.36539	−0.36472	−0.28198	−0.28180	−0.28169	−0.18644

Tabular Data. A-11.2. Total energies of the states of ArO arising from Ar (^1S) + O ($^3P, ^1D, ^1S$). Energies are relative to -601 hartree.

$R(a_0)$	$^3\Pi$	$^3\Sigma^-$	$1\,^1\Sigma^+$	$^1\Pi$	$^1\Delta$	$2\,^1\Sigma^+$
2.75	−0.29182	−0.06217	−0.44208	−0.24285	−0.00417	0.03161
2.875	−0.35262	−0.15344	−0.46954	−0.30044	−0.09150	−0.05269
3.00	−0.40244	−0.23193	−0.48830	−0.34717	−0.16622	−0.12417
3.25	−0.47548	−0.35453	−0.50857	−0.41414	−0.28227	−0.23285
3.50	−0.52268	−0.43958	−0.51604	−0.45558	−0.36285	−0.30585
3.75	−0.55285	−0.49694	−0.51786	−0.48064	−0.41755	−0.35331
4.00	−0.57201	−0.53483	−0.51800	−0.49573	−0.45394	−0.38287
4.25	−0.58409	−0.55947	−0.51812	−0.50489	−0.47773	−0.40042
4.50	−0.59159	−0.57528	−0.51848	−0.51050	−0.49304	−0.41045
5.00	−0.59896	−0.59165	−0.51924	−0.51607	−0.50894	−0.41932
5.50	−0.60156	−0.59812	−0.51953	−0.51815	−0.51521	−0.42227
6.00	−0.60241	−0.60062	−0.51952	−0.51886	−0.51763	−0.42328
6.50	−0.60261	−0.60152	−0.51940	−0.51904	−0.51850	−0.42359
7.00	−0.60260	−0.60178	−0.51927	−0.51902	−0.51875	−0.42362
8.50	−0.60247	−0.60180	−0.51907	−0.51889	−0.51876	−0.42352
12.00	−0.60245	−0.60178	−0.51905	−0.51887	−0.51875	−0.42350

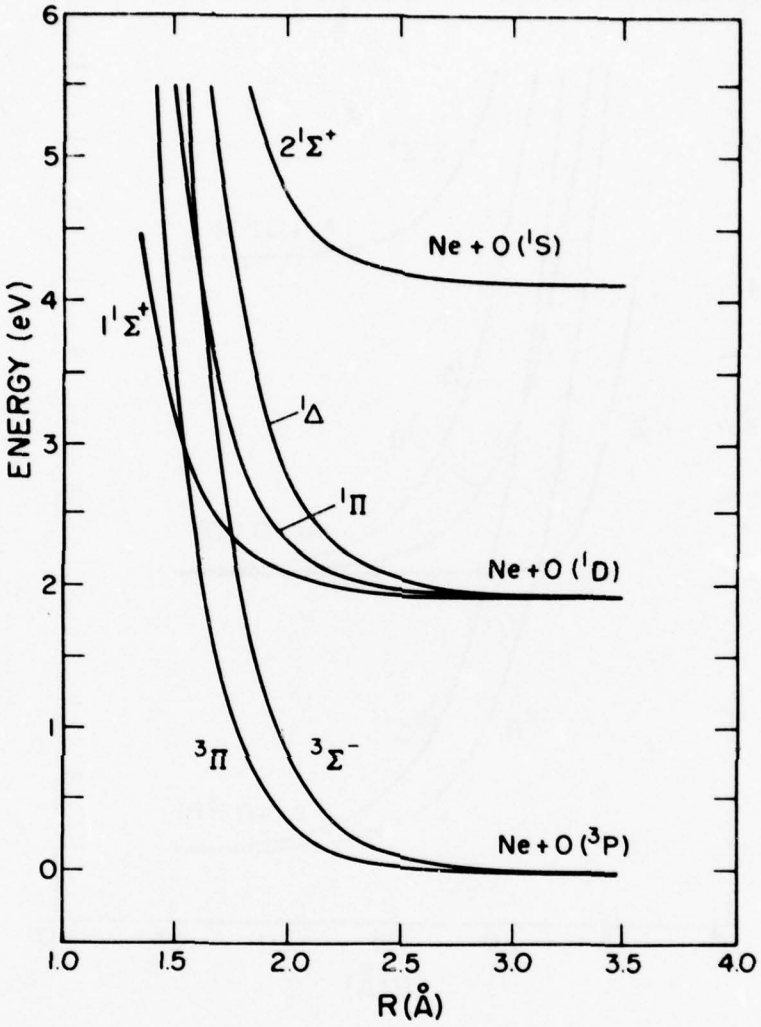

Graphical Data. A-11.3. Calculated potential energy curves for the states of NeO arising from the Ne (^{1}S) + O (^{3}P, ^{1}D, ^{1}S) separated atom limits. The curves have been uniformly shifted to correct for the errors in the O (^{1}D - ^{3}P) and O (^{1}S - ^{3}P) excitation energies.

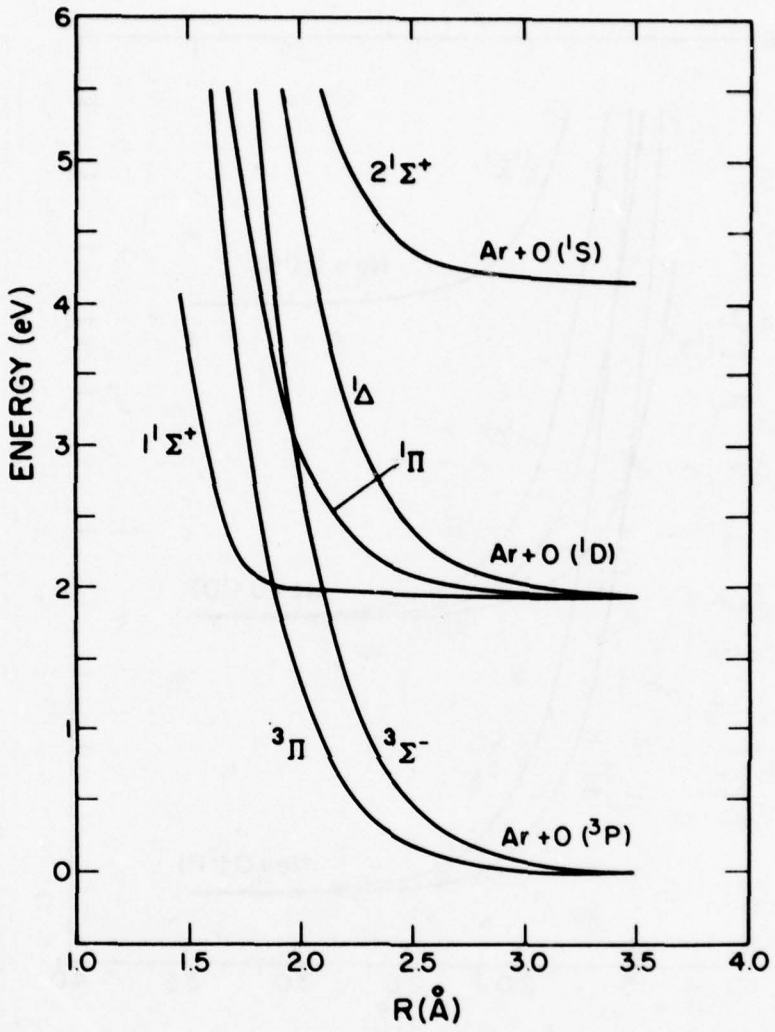

Graphical Data. A-11.4. Calculated potential energy curves for the states of ArO arising from the Ar (^{1}S) + O (^{3}P, ^{1}D, ^{1}S) separated atom limits. The curves have been uniformly shifted to correct for the errors in the O (^{1}D - ^{3}P) and O (^{1}S - ^{3}P) excitation energies.

Tabular Data. A-11.5. Total energies of the states of KrO arising from Kr (^1S) + O (^3P, ^1D, ^1S). Energies are relative to -2826 hartree.

$R(a_0)$	$^3\Pi$	$^3\Sigma^-$	$1\,^1\Sigma^+$	$^1\Pi$	$^1\Delta$	$2\,^1\Sigma^+$
2.875	−0.40859	−0.19828	−0.55182	−0.36789	−0.14745	−0.11674
3.00	−0.46706	−0.27803	−0.58546	−0.42315	−0.22337	−0.19086
3.125	−0.51513	−0.34767	−0.60858	−0.46801	−0.28906	−0.25437
3.25	−0.55449	−0.40802	−0.62400	−0.50422	−0.34548	−0.30813
3.375	−0.58656	−0.45990	−0.63382	−0.53318	−0.39359	−0.35311
3.50	−0.61252	−0.50418	−0.63955	−0.55604	−0.43439	−0.39033
3.75	−0.65040	−0.57327	−0.64338	−0.58776	−0.49801	−0.44611
4.00	−0.67496	−0.62156	−0.64207	−0.60655	−0.54289	−0.48311
4.25	−0.69085	−0.65452	−0.63947	−0.61754	−0.57393	−0.50673
4.50	−0.70106	−0.67656	−0.63736	−0.62403	−0.59493	−0.52092
4.75	−0.70756	−0.69107	−0.63612	−0.62794	−0.60886	−0.52892
5.00	−0.71164	−0.70050	−0.63552	−0.63036	−0.61796	−0.53329
5.50	−0.71572	−0.71049	−0.63508	−0.63284	−0.62764	−0.53701
6.00	−0.71719	−0.71457	−0.63487	−0.63381	−0.63160	−0.53825
6.50	−0.71765	−0.71619	−0.63467	−0.63413	−0.63317	−0.53867
7.00	−0.71773	−0.71676	−0.63449	−0.63417	−0.63372	−0.53876
8.50	−0.71757	−0.71689	−0.63418	−0.63399	−0.63386	−0.53862
12.00	−0.71753	−0.71686	−0.63413	−0.63394	−0.63383	−0.53858

Tabular Data. A-11.6. Total energies of the states of XeO arising from Xe (^1S) + O (^3P, ^1D, ^1S). Energies are relative to -7306 hartree.

$R(a_0)$	$^3\Pi$	$^3\Sigma^-$	$1\,^1\Sigma^+$	$^1\Pi$	$^1\Delta$	$2\,^1\Sigma^+$
3.00	−0.31839	−0.14551	−0.44467	−0.28890	−0.10619	−0.08134
3.125	−0.37811	−0.21500	−0.49122	−0.34653	−0.17279	−0.14771
3.25	−0.42548	−0.27347	−0.52356	−0.39120	−0.22770	−0.20198
3.375	−0.46388	−0.32392	−0.54568	−0.42648	−0.27416	−0.24731
3.50	−0.49542	−0.36797	−0.56045	−0.45476	−0.31415	−0.28579
3.625	−0.52136	−0.40656	−0.56975	−0.47748	−0.34875	−0.31852
3.75	−0.54255	−0.44043	−0.57481	−0.49545	−0.37858	−0.34592
4.00	−0.57376	−0.49605	−0.57659	−0.52010	−0.42645	−0.38701
4.25	−0.59438	−0.53783	−0.57246	−0.53405	−0.46238	−0.41435
4.50	−0.60812	−0.56823	−0.56659	−0.54156	−0.48927	−0.43243
4.75	−0.61736	−0.58972	−0.56128	−0.54550	−0.50888	−0.44388
5.00	−0.62355	−0.60457	−0.55744	−0.54762	−0.52275	−0.45039
5.25	−0.62767	−0.61467	−0.55506	−0.54887	−0.53231	−0.45362
5.50	−0.63037	−0.62143	−0.55370	−0.54969	−0.53878	−0.45500
6.00	−0.63323	−0.62888	−0.55250	−0.55065	−0.54596	−0.45576
6.50	−0.63434	−0.63208	−0.55203	−0.55110	−0.54907	−0.45591
7.00	−0.63474	−0.63340	−0.55179	−0.55128	−0.55037	−0.45596
8.50	−0.63481	−0.63411	−0.55144	−0.55124	−0.55107	−0.45587
12.00	−0.63474	−0.63407	−0.55134	−0.55116	−0.55104	−0.45579

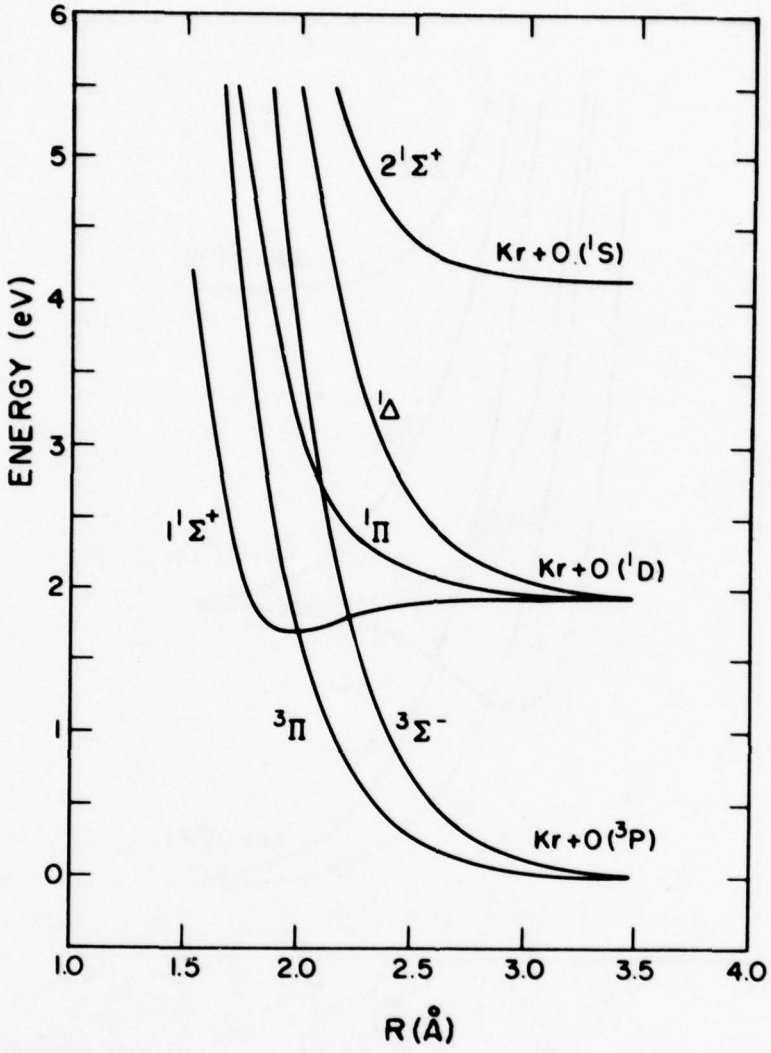

Graphical Data. A-11.7. Calculated potential energy curves for the states of KrO arising from the Kr (^{1}S) + O (^{3}P, ^{1}D, ^{1}S) separated atom limits. The curves have been uniformly shifted to correct for the errors in the O (^{1}D - ^{3}P) and O (^{1}S - ^{3}P) excitation energies.

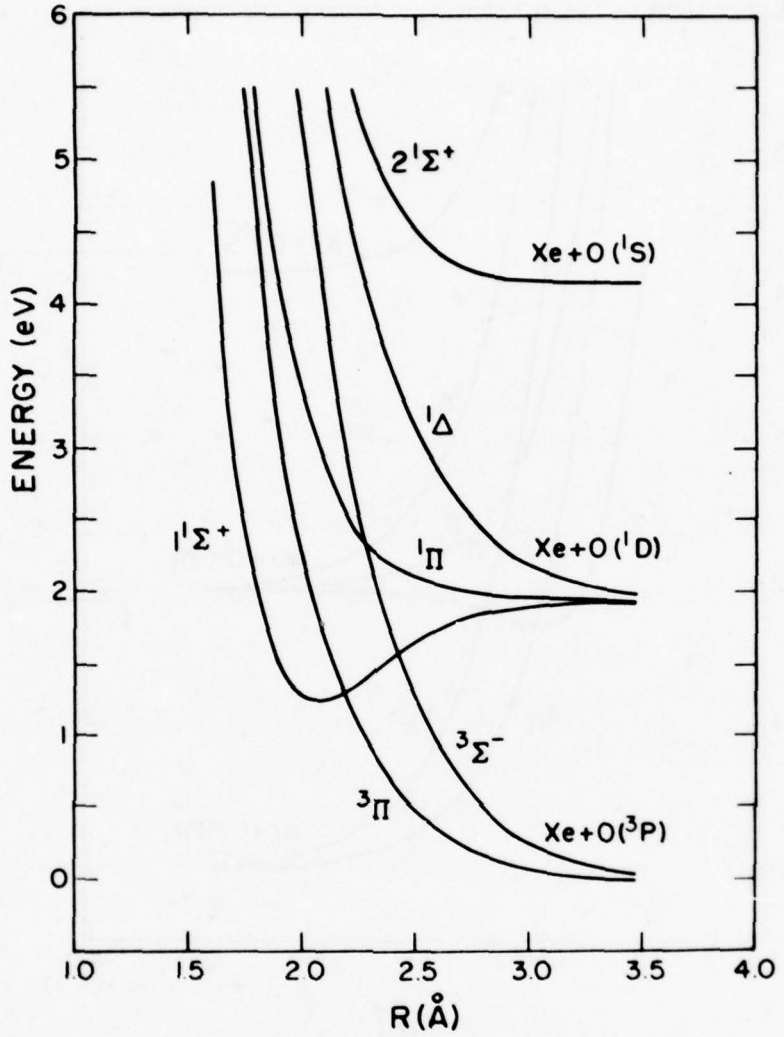

Graphical Data. A-11.8. Calculated potential energy curves for the states of XeO arising from the Xe (^1S) + O (^3P, ^1D, ^1S) separated atom limits. The curves have been uniformly shifted to correct for the errors in the O (^1D - ^3P) and O (^1S - ^3P) excitation energies.

Tabular Data. A-11.9. Calculated spectroscopic constants for the $1^1\Sigma^+$ states of $^{84}Kr^{16}O$ and $^{132}Xe^{16}O$. Units are as indicated.

	KrO	XeO	
	Calc	Calc	Exptl [a,b]
T_e, eV[c]	1.71	1.26	1.60
R_e, Å	2.00	2.08	2.65
D_e, eV	0.25	0.70	0.36
ω_e, cm^{-1}	375[d]	470[d]	372
$\omega_e x_e$	12	6.6	12
B_e, cm^{-1}	0.317[e]	0.275[e]	
α_e	0.011	0.0045	

[a] References 1, A-11.

[b] For a discussion of the "experimental" constants of the $1^1\Sigma^+$ state of XeO, see A-11 Ref. 1.

[c] Relative to the Rg (^1S) + O (^3P) separated atom limit.

[d] The calculated ω_e and $\omega_e x_e$ were obtained from a least-squares fit of the lowest 8 (KrO) or 16 (XeO) vibrational energies with a four term expansion.

[e] The calculated B_e and α_e were obtained from a least-squares fit of the lowest 8 (KrO) or 16 (XeO) rotation constants (B_v) with a four term expansion.

Tabular Data. A-11.10. Vibrational levels and spacings for the $1^1\Sigma^+$ state of XeO. Energies are in cm^{-1}.

v	$G(v)$ Calc[a]	$\Delta G(v+\frac{1}{2})$ Calc	$\Delta G(v+\frac{1}{2})$ Exptl[b]
0	232	457	
1	690	44	
2	1134	431	
3	1565	416	
4	1981	401	
5	2382	385	
6	2767	367	
7	3134	349	347
8	3483	328	328
9	3811	306	302
10	4118	282	272
11	4400	256	252
12	4656	226	224
13	4882	193	201
14	5075	158	186
15	5233		
[c]			

[a] Obtained by solving the vibrational (J = 0) Schroedinger equation with the calculated potential.

[b] Reference 1.

[c] Seven higher levels are omitted here.

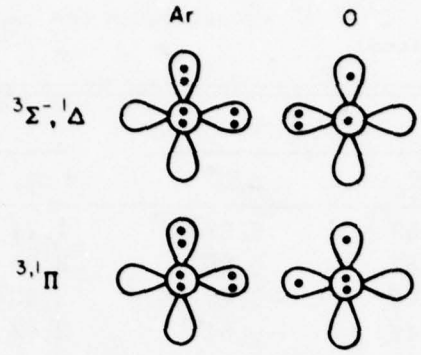

Graphical Data. A-11.11. Orbital diagrams for the $^{3,1}\Pi$ and $^3\Sigma^-$, and $^1\Delta$ states of ArO.

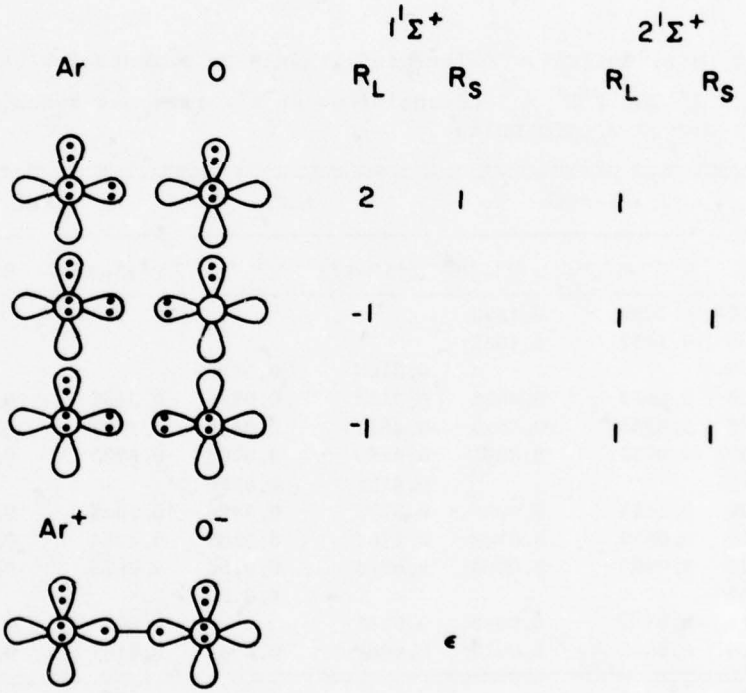

Graphical Data. A-11.12. Orbital diagrams for the 1,2 $^1\Sigma^+$ states of ArO. Configuration coefficients (unnormalized) for both large $R(R_L)$ and short $R(R_S)$ have been listed.

Tabular Data. A-11.13. Calculated crossing points and energies for the $1\,^1\Sigma^+ - {}^3\Pi$ and $1\,^1\Sigma^+ - {}^3\Sigma^-$ crossings in the rare gas monoxides.[a] Units are as indicated.

	$1\,^1\Sigma^+ - {}^3\Pi$		$1\,^1\Sigma^+ - {}^3\Sigma^-$	
Molecule	R_c	ΔE_c[b]	R_c	ΔE_c[b]
NeO	1.53 Å	0.92 eV	1.74 Å	0.39 eV
ArO	1.87	0.068	2.09	0.028
KrO	2.00	−0.25	2.23	−0.16
XeO	2.19	−0.64	2.42	−0.37

[a] The curves have been shifted to correct for the error in the calculated O (^{1}D) - O (^{3}P) excitation energy; see A-II Ref. 1.

[b] Relative to the Rg (^{1}S) + O (^{1}D) separated atom energy.

Tabular Data. A-11.14. Calculated transition moments for the $2\,^1\Sigma^+ - 1\,^1\Sigma^+$ and $2\,^1\Sigma^+ - {}^1\Pi$ transitions in the rare gas monoxides. Moments are in atomic units.

	ArO		KrO		XeO	
R (a_0)	$2\,^1\Sigma^+ - 1\,^1\Sigma^+$	$2\,^1\Sigma^+ - {}^1\Pi$[a]	$2\,^1\Sigma^+ - 1\,^1\Sigma^+$	$2\,^1\Sigma^+ - {}^1\Pi$[a]	$2\,^1\Sigma^+ - 1\,^1\Sigma^+$	$2\,^1\Sigma^+ - {}^1\Pi$[a]
2.75	0.0099	0.1273				
3.00	0.1847	0.1062				
3.25			0.2165	0.0835		
3.50	0.3512	0.0819	0.3123	0.0894	0.2165	0.0584
4.00	0.3862	0.0598	0.4951	0.0880	0.4093	0.1211
4.50	0.2703	0.3091	0.4890	0.0704	0.6723	0.0822
4.75			0.4132	0.0590		
5.00	0.1464	0.0236	0.3233	0.0480	0.7033	0.0468
5.50	0.0690	0.0142	0.1762	0.0305	0.4784	0.0253
6.00	0.0403	0.0089	0.0886	0.0196	0.2628	0.0146
6.50				0.0132		
7.00	0.0403	0.0089	0.0287		0.0728	0.0063
8.50	0.0043	0.0019	0.0085	0.0041	0.0167	0.0027

[a] The matrix element given is $\left\langle 2\,^1\Sigma^+ \middle| \chi \middle| {}^1\Pi_\chi \right\rangle$.

Tabular Data. A-11.15. Calculated pseudo-lifetimes for the $2\,^1\Sigma^+$ states of the rare gas oxides. Units are as indicated.

Molecule	Transition	R^*	$\Delta E(R^*)$[a]	$\mu_{ij}(R^*)$	A_p	τ_p
ArO	$2\,^1\Sigma^+ - 1\,^1\Sigma^+$	2.97 Å	2.26 eV	0.0598 ea_0	4.4×10^4 sec^{-1}	23 μsec
	$-\,^1\Pi$		2.22	0.0128	4.4×10^3	230
KrO	$2\,^1\Sigma^+ - 1\,^1\Sigma^+$	3.02	2.27	0.134	2.2×10^5	4.5
	$-\,^1\Pi$		2.22	0.0254	1.7×10^4	60
XeO	$2\,^1\Sigma^+ - 1\,^1\Sigma^+$	2.89	2.32	0.496	3.3×10^6	0.31
	$-\,^1\Pi$		2.21	0.0264	1.6×10^4	62

[a] Corrected for the error in the calculated $O(^1S)$-$O(^1D)$ excitation energy.

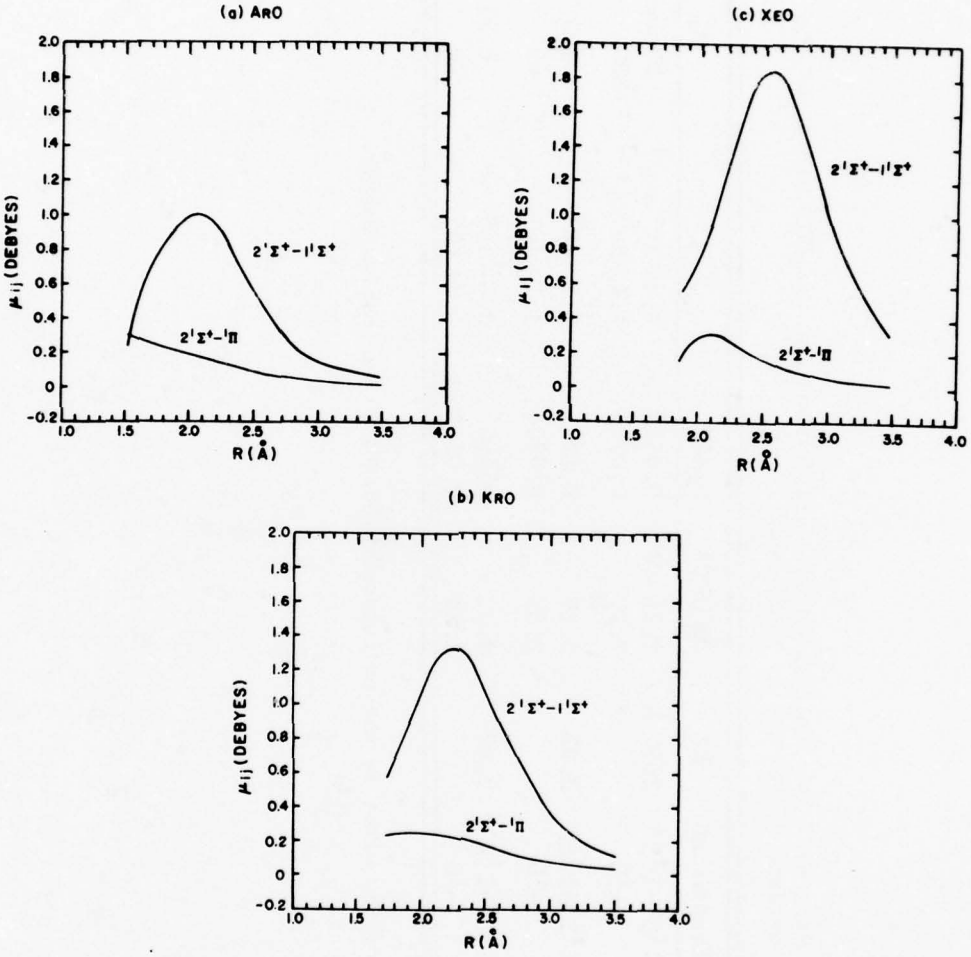

Graphical Data. A-11.16. Dipole transition moments for the $2^1\Sigma^+ - 1^1\Sigma^+$ and $2^1\Sigma^+ - {}^1\Pi$ transitions in ArO, KrO and XeO.

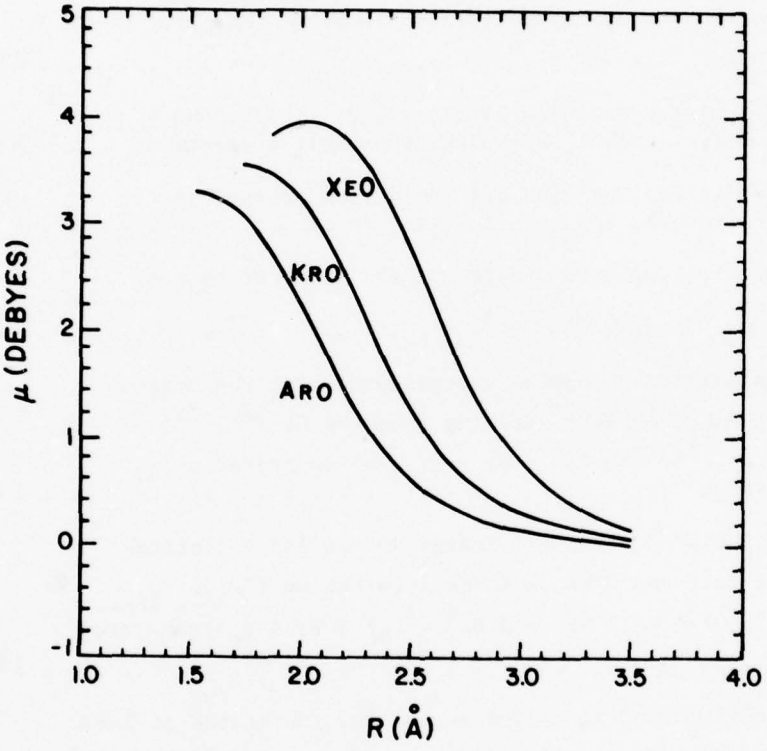

Graphical Data. A-11.17. Dipole moments for the $1^1\Sigma^+$ states of ArO, KrO, and XeO.

A-12. POTENTIAL ENERGY CURVES, ELECTRONIC ENERGIES, SPECTROSCOPIC CONSTANTS, TRANSITION MOMENTS AND EMISSION AND ABSORPTION DATA FOR GaKr, InKr, AND TlKr

CONTENTS

Page

A-12.1. Energies obtained from the POL-CI calculations on the low-lying electronic states of GaKr and $GaKr^+$ 1303

A-12.2. Calculated energies of the I 1/2, II 1/2, and I 3/2 states of GaKr with spin-orbit corrections . . . 1303

A-12.3. Excitation energies and ionization potentials for the Ga, In, and Tl atoms, in eV 1304

A-12.4. Spectroscopic constants for the bound states of $^{69}Ga^{84}Kr$ and $^{69}Ga^{84}Kr^+$ 1304

A-12.5. Calculated potential energy curves for the states of GaKr and $GaKr^+$ arising from the Ga (^2P, ^2S) + Kr (^1S) and Ga^+ (^1S) + Kr (^1S) separated atom limits 1305

A-12.6. Calculated potential energy curves for the states of GaKr and $GaKr^+$ arising from the Ga ($^2P_{1/2, 3/2}$, $^2S_{1/2}$) + Kr ($^1S_0$) and Ga^+ ($^1S_0$) + Kr ($^1S_0$) separated atom limits 1306

A-12.7. Model potential energy curves for the states of InKr and $InKr^+$ arising from the In ($^2P_{1/2, 3/2}$, $^2S_{1/2}$) + Kr ($^1S_0$) and In^+ ($^1S_0$) + Kr ($^1S_0$) separated atom limits 1307

A-12.8. Model potential energy curves for the states of TlKr and $TlKr^+$ arising from the Tl ($^2P_{1/2, 3/2}$, $^2S_{1/2}$) + Kr ($^1S_0$) and In^+ ($^1S_0$) + Kr ($^1S_0$) separated atom limits 1308

Page

A-12.9. Dipole transition moments coupling the low-lying states of GaKr obtained from the POL-CI calculations 1309

A-12.10. Calculated dipole transition moments coupling the III 1/2 and I 1/2, II 1/2 and I 3/2 states of GaKr with spin-orbit corrections 1309

A-12.11. Calculated dipole transition moments for $1^2\Sigma^+ - 1^2\Pi$, $2^2\Sigma^+ - 1^2\Pi$, and $2^2\Sigma^+ - 1^2\Sigma^+$ transitions in GaKr 1310

A-12.12. Calculated dipole transition moments for III 1/2 - I 1/2, III 1/2 - I 3/2, and III 1/2 - II 1/2 transitions in GaKr 1311

A-12.13. Model dipole transition moments for the III 1/2 - I 1/2, III 1/2 - I 3/2, and III 1/2 - II 1/2 transitions in TlKr 1312

A-12.14. Model absorption, K_v (T), and simulated emission, g_v (T), coefficients for InKr at T = 3000 and 1200°K 1313

A-12.15. Calculated absorption, K_v (T), and stimulated emission, g_v (T), coefficients for GaKr at T = 300 and 1500°K 1314

A-12.16. Model absorption, K_v (T), and stimulated emission, g_v (T), coefficients for TlKr at T = 300 and 1090°K . 1315

A-12.17. Orbital diagrams for the low-lying electronic states of GaKr and $GaKr^+$ 1316

A-12. References:

1. T. H. Dunning, M. Valley, and H. S. Taylor, "Theoretical Studies of the Low-Lying Electronic States of GaKr, Including Extrapolation to InKr and TlKr," J. Chem. Phys. 69, 2672 (1978).

Tabular Data. A-12.1. Energies obtained from the POL-CI calculations on the low-lying electronic states of GaKr and $GaKr^+$. Distances are in bohr; energies are in hartree. Energies are relative to -4674 hartree.

	GaKr			$GaKr^+$
R	$1\,^2\Pi$	$1\,^2\Sigma^+$	$2\,^2\Sigma^+$	$1\,^1\Sigma^+$
3.75	−1.02539	−0.96866	−0.93379	−0.85625
4.00	−1.07933	−1.01870	−0.99238	−0.90683
4.50	−1.14810	−1.08688	−1.06440	−0.96758
5.00	−1.17924	−1.13516	−1.08855	−0.99287
5.50	−1.19225	−1.16324	−1.09545	−1.00070
6.00	−1.19772	−1.17938	−1.09677	−1.00202
6.50	−1.19984	−1.18865	−1.09631	−1.00107
7.00	−1.20045	−1.19396	−1.09545	−0.99950
8.00	−1.20020	−1.19865	−1.09420	−0.99670
10.00	−1.19933	−1.20029	−1.09406	−0.99402
15.00	−1.19878	−1.20012	−1.09502	−0.99304

Tabular Data. A-12.2. Calculated energies of the I 1/2, II 1/2, and I 3/2 states of GaKr with spin-orbit corrections. Distances are in bohr; energies are in hartree. Energies are relative to the energy of the $1^2\Sigma^+$ state at R = 15 a_0.

R	*I* 1/2	*I* 3/2	*II* 1/2
3.75	0.17228	0.17484	0.23152
4.00	0.11835	0.12091	0.18147
4.50	0.04957	0.05213	0.11329
5.00	0.01841	0.02099	0.06502
5.50	0.00538	0.00799	0.03698
6.00	−0.00015	0.00252	0.02089
6.50	−0.00234	0.00040	0.01170
7.00	−0.00307	−0.00022	0.00650
8.00	−0.00316	0.00003	0.00215
10.00	−0.00280	0.00090	0.00103
15.00	−0.00251	0.00126	0.00126

Tabular Data. A-12.3. Excitation energies and ionization potentials for the Ga, In, and Tl atoms, in eV.

	Group IIIA atoms		
State	Ga	In	Tl
$^2P_{1/2}$	0.000	0.000	0.000
$^2P_{3/2}$	0.102	0.274	0.966
$^2S_{1/2}$	3.073	3.022	3.282
$^1S_0$	5.998	5.786	6.108

Tabular Data. A-12.4. Spectroscopic constants for the bound states of $^{69}Ga^{84}Kr$ and $^{69}Ga^{84}Kr^+$. Units are as indicated.

	GaKr		GaKr$^+$
	$1\,^2\Pi$	$2\,^2\Sigma^+$	$1\,^2\Sigma^+$
T_e, eV	0.00	2.82	5.40
R_e, Å	3.78	3.17	3.14
D_e, eV	0.041	0.047	0.24
ω_e, cm^{-1}	36	66	83
B_e	0.0312	0.0442	0.0452

THE LOW-LYING STATES OF GaKr AND $GaKr^+$

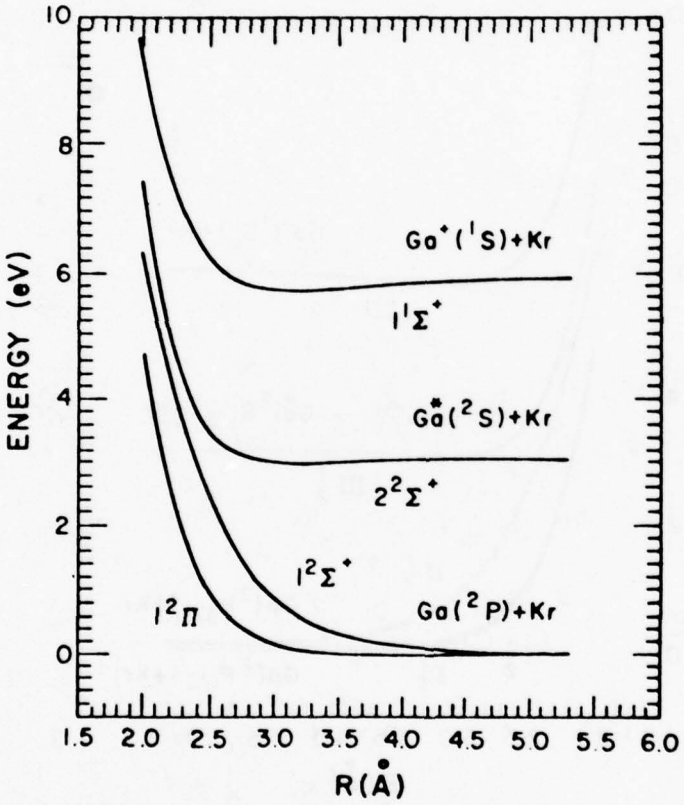

Graphical Data. A-12.5. Calculated potential energy curves for the states of GaKr and $GaKr^+$ arising from the Ga (^2P, ^2S) + Kr (^1S) and Ga^+ (^1S) + Kr (^1S) separated atom limits. The curves have been uniformly shifted to correct for the errors in the gallium atom excitation energies.

THE LOW-LYING STATES OF GaKr AND $GaKr^+$ WITH SPIN-ORBIT CORRECTIONS

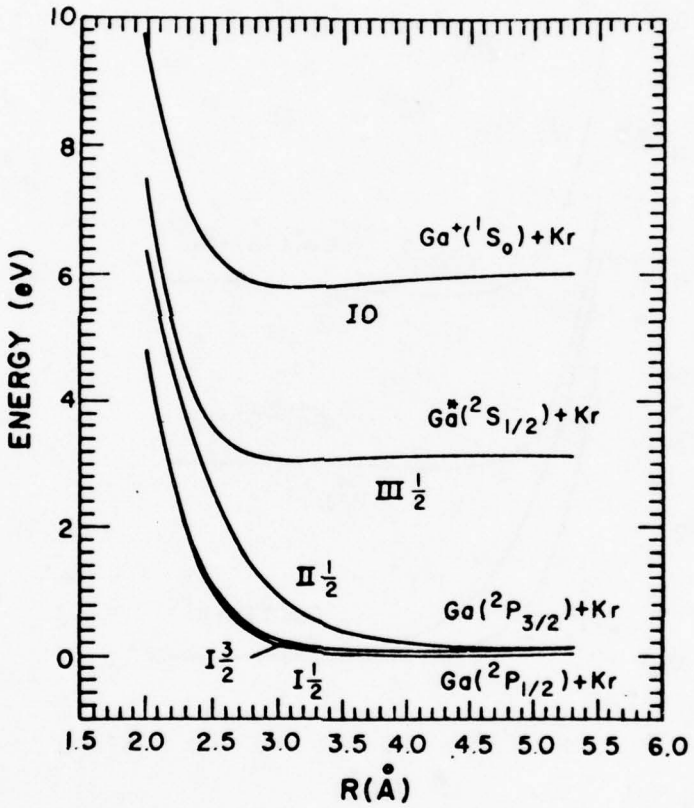

Graphical Data. A-12.6. Calculated potential energy curves for the states of GaKr and $GaKr^+$ arising from the Ga ($^2P_{1/2,\ 3/2}$, $^2S_{1/2}$) + Kr ($^1S_0$) and Ga^+ ($^1S_0$) + Kr ($^1S_0$) separated atom limits. The curves have been uniformly shifted to correct for the errors in the gallium excitation energies.

THE LOW-LYING STATES OF InKr AND $InKr^+$ WITH SPIN-ORBIT CORRECTIONS

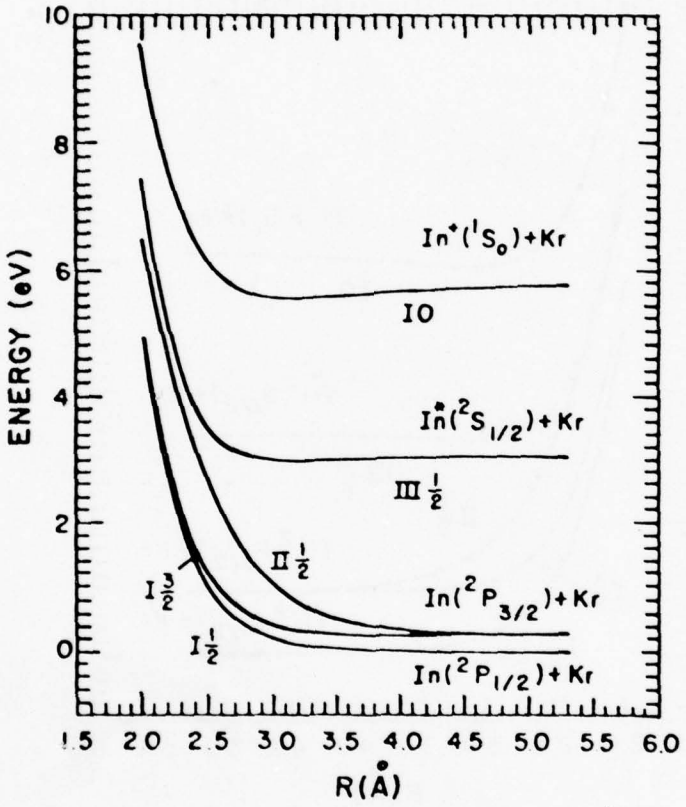

Graphical Data. A-12.7. Model potential energy curves for the states of InKr and $InKr^+$ arising from the In ($^2P_{1/2,\ 3/2}$, $^2S_{1/2}$) + Kr ($^1S_0$) and In^+ ($^1S_0$) + Kr ($^1S_0$) separated atom limits.

THE LOW-LYING STATES OF TlKr AND $TlKr^+$ WITH SPIN-ORBIT CORRECTIONS

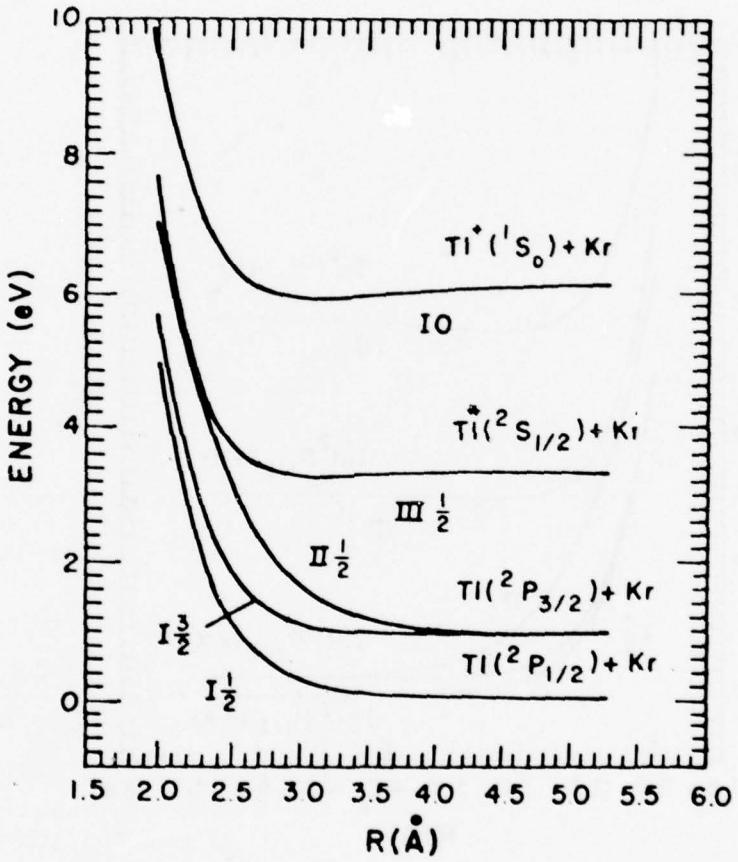

Graphical Data. A-12.8. Model potential energy curves for the states of TlKr and $TlKr^+$ arising from the Tl ($^2P_{1/2,\ 3/2}$, $^2S_{1/2}$) + Kr ($^1S_0$) and In^+ ($^1S_0$) + Kr ($^1S_0$) separated atom limits.

Tabular Data. A-12.9. Dipole transition moments coupling the low-lying states of GaKr obtained from the POL-Cl calculations.

R	$1\,^2\Sigma^+-1\,^2\Pi$[a]	$2\,^2\Sigma^+-1\,^2\Pi$[a]	$2\,^2\Sigma^+-1\,^2\Sigma^+$
3.75	−0.9037	−0.7877	0.4095
4.00	−0.8462	−0.8680	−0.3055
4.50	−0.1365	−1.2090	−2.0676
5.00	0.0992	−1.2349	−1.4402
5.50	0.1257	−1.2469	−1.2456
6.00	0.1166	−1.2554	−1.1893
6.50	0.0984	−1.2619	−1.1800
7.00	0.0789	−1.2677	−1.1902
8.00	0.0476	−1.2777	−1.2310
10.00	0.0163	−1.2898	−1.2976
15.00	0.0018	−1.2917	−1.3101

[a]The matrix element given is $\langle n^2\Sigma^+|\chi|1^2\Pi_\chi\rangle$.

Tabular Data. A-12.10. Calculated dipole transition moments coupling the III 1/2 and I 1/2, II 1/2 and I 3/2 states of GaKr with spin-orbit corrections. Distances are in bohr; moments are in atomic units.

	III 1/2–*I* 1/2		*III* 1/2–*II* 1/2		*III* 1/2–*I* 3/2
R	z	(x,y)	z	(x,y)	(x,y)
4.00	−0.0086	0.6135	−0.3054	−0.0173	−0.6138
4.50	−0.0576	0.8545	−2.0667	−0.0238	−0.8549
5.00	−0.0549	0.8726	−1.4392	−0.0333	−0.8732
5.50	−0.0701	0.8803	−1.2437	−0.0496	−0.8817
6.00	−0.1007	0.8845	−1.1850	−0.0752	−0.8877
6.50	−0.1504	0.8850	−1.1704	−0.1138	−0.8923
7.00	−0.2249	0.8803	−1.1688	−0.1694	−0.8964
8.00	−0.4405	0.8436	−1.1495	−0.3233	−0.9035
10.00	−0.7254	0.7562	−1.0759	−0.5098	−0.9120
15.00	−0.7564	0.7457	−1.0697	−0.5273	−0.9134

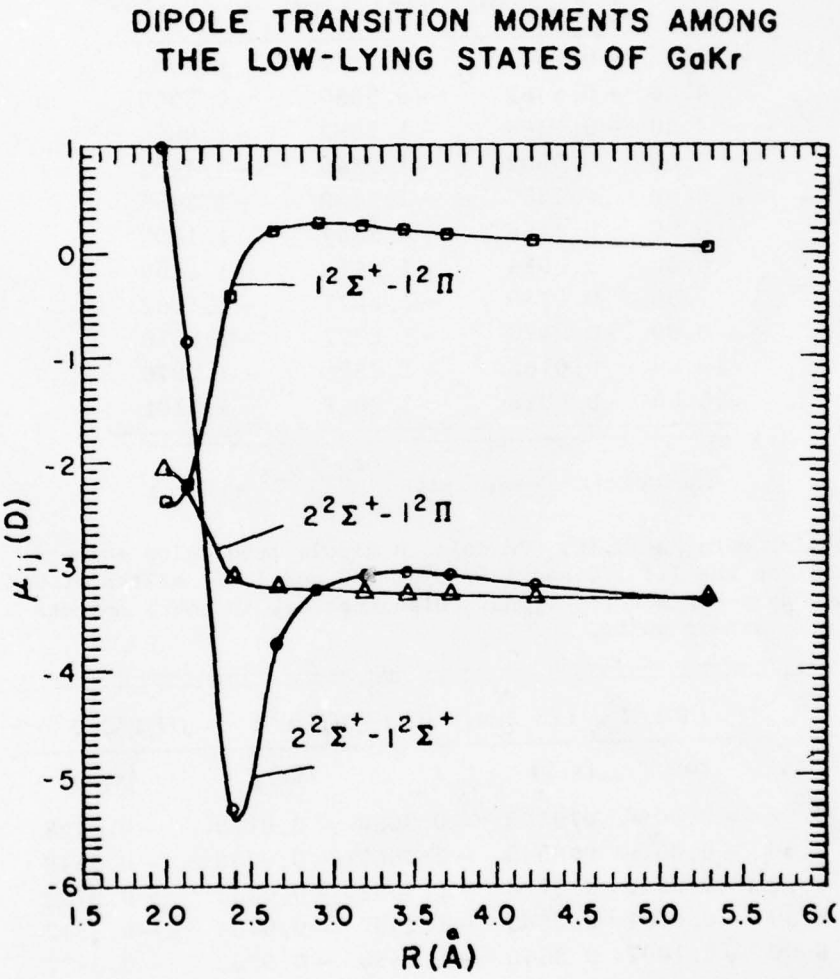

Graphical Data. A-12.11. Calculated dipole transition moments for $1^2\Sigma^+ - 1^2\Pi$, $2^2\Sigma^+ - 1^2\Pi$, and $2^2\Sigma^+ - 1^2\Sigma^+$ transitions in GaKr.

DIPOLE TRANSITION MOMENTS AMONG THE LOW-LYING STATES OF GaKr WITH SPIN-ORBIT CORRECTIONS

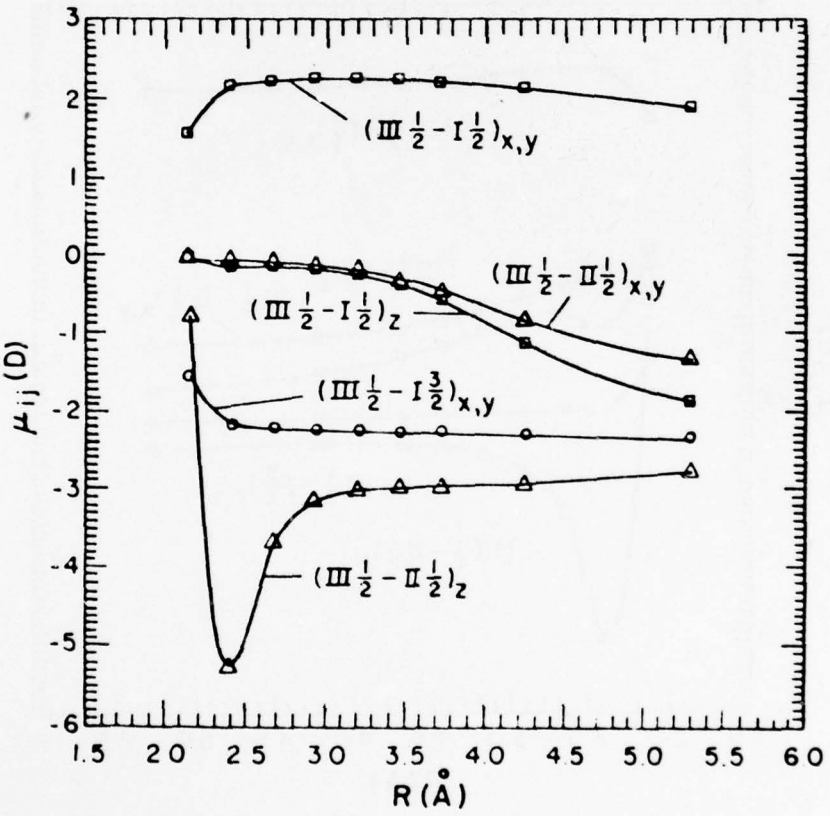

Graphical Data. A-12.12. Calculated dipole transition moments for III 1/2 - I 1/2, III 1/2 - I 3/2, and III 1/2 - II 1/2 transitions in GaKr.

DIPOLE TRANSITION MOMENTS CONNECTING THE LOW-LYING STATES OF TlKr WITH SPIN-ORBIT CORRECTIONS

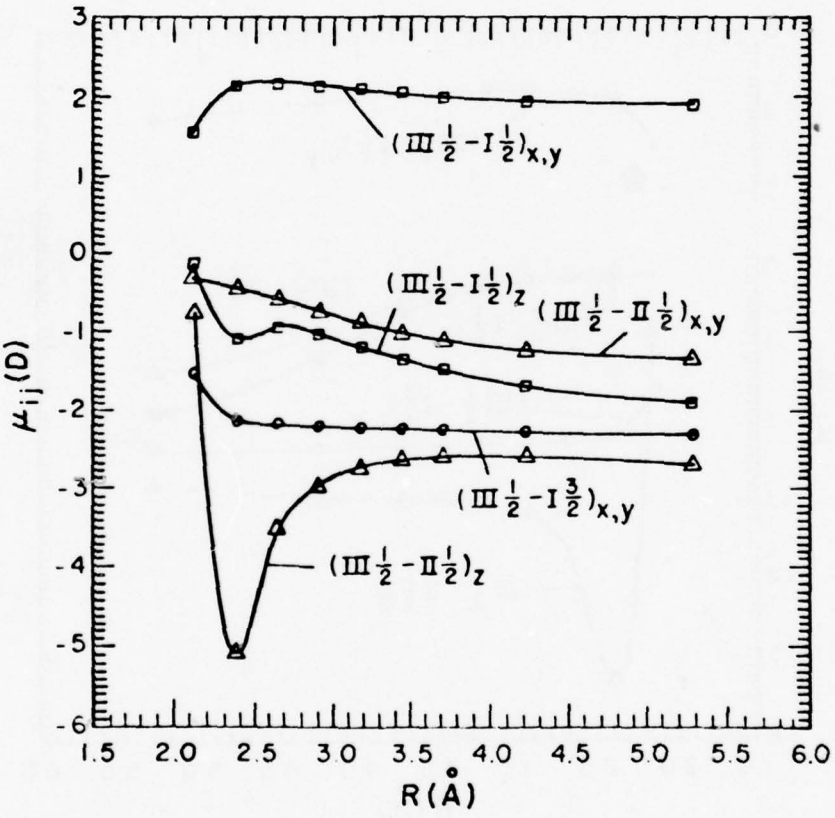

Graphical Data. A-12.13. Model dipole transition moments for the III 1/2 - I 1/2, III 1/2 - I 3/2, and III 1/2 - II 1/2 transitions in TlKr.

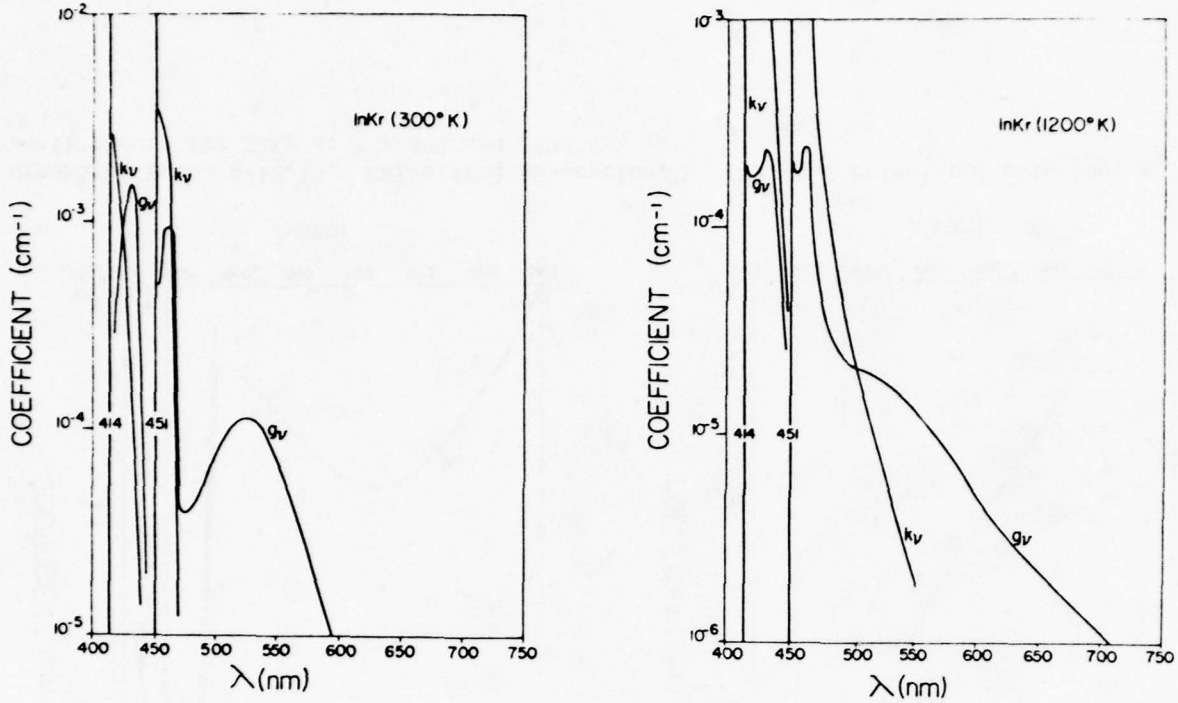

Graphical Data. A-12.14. Model absorption, K_v (T), and simulated emission, g_v (T), coefficients for InKr at T = 3000 and 1200°K.

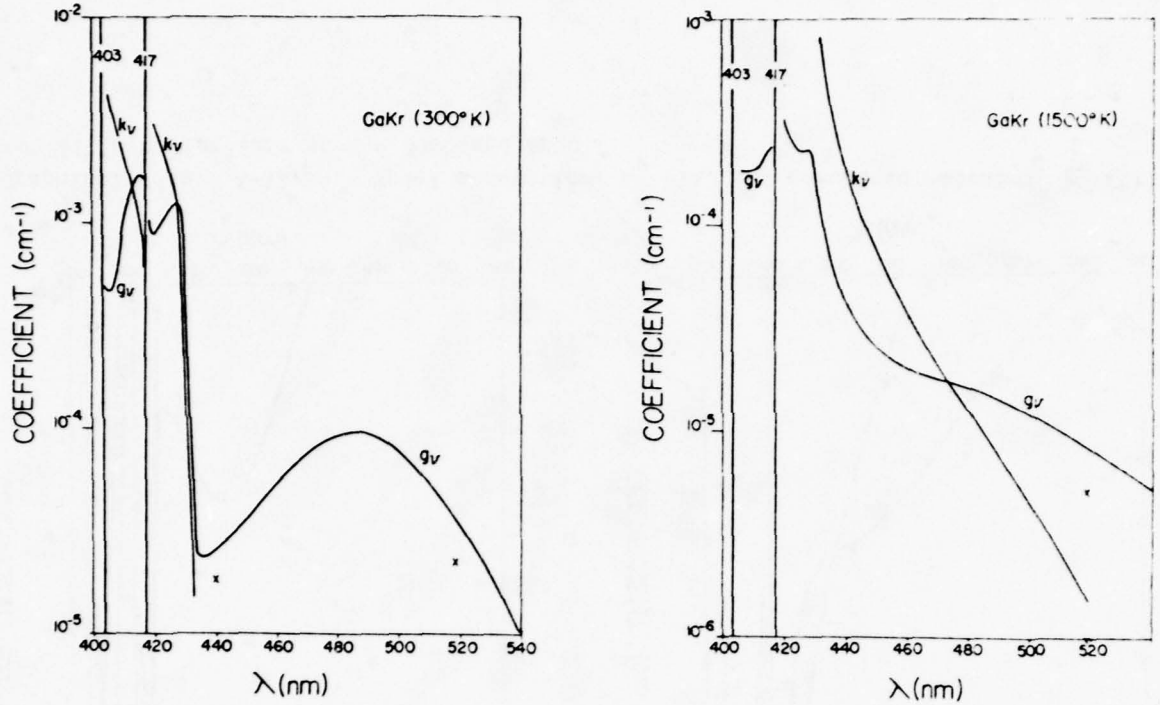

Graphical Data. A-12.15. Calculated absorption, K_ν (T), and stimulated emission, g_ν (T), coefficients for GaKr at T = 300 and 1500°K.

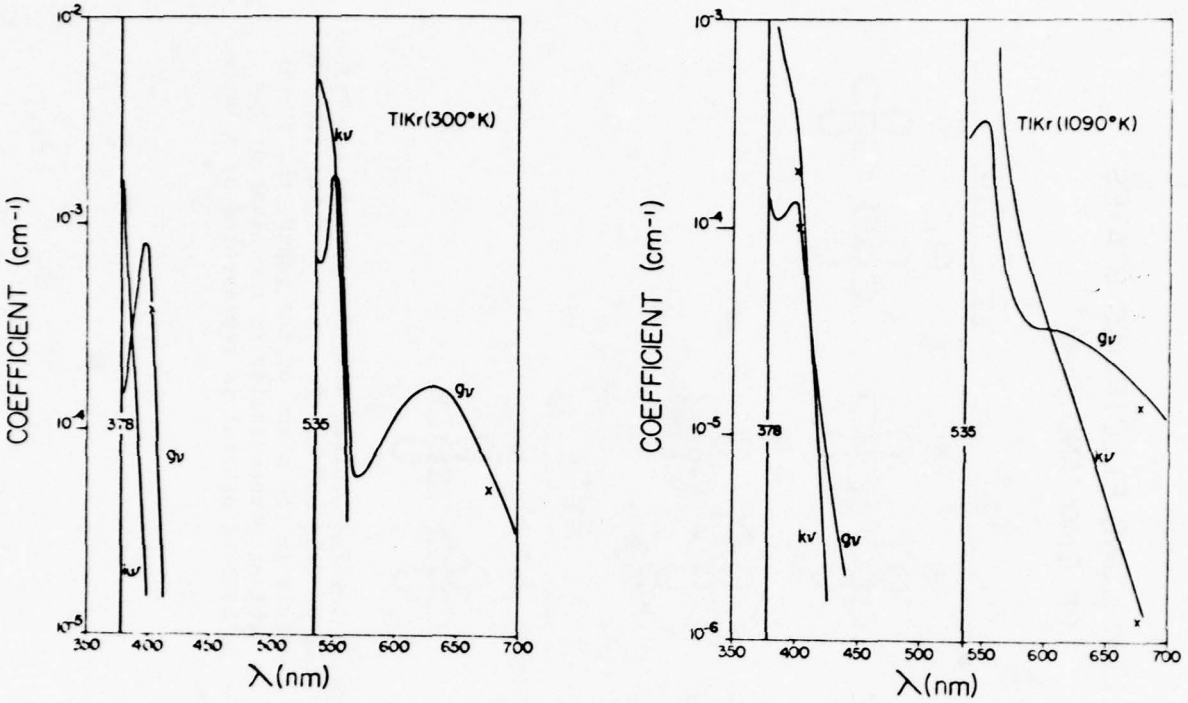

Graphical Data. A-12.16. Model absorption, K_ν (T), and stimulated emission, g_ν (T), coefficients for TlKr at T = 300 and 1090°K.

THE LOW-LYING ELECTRONIC STATES OF GaKr AND $GaKr^+$

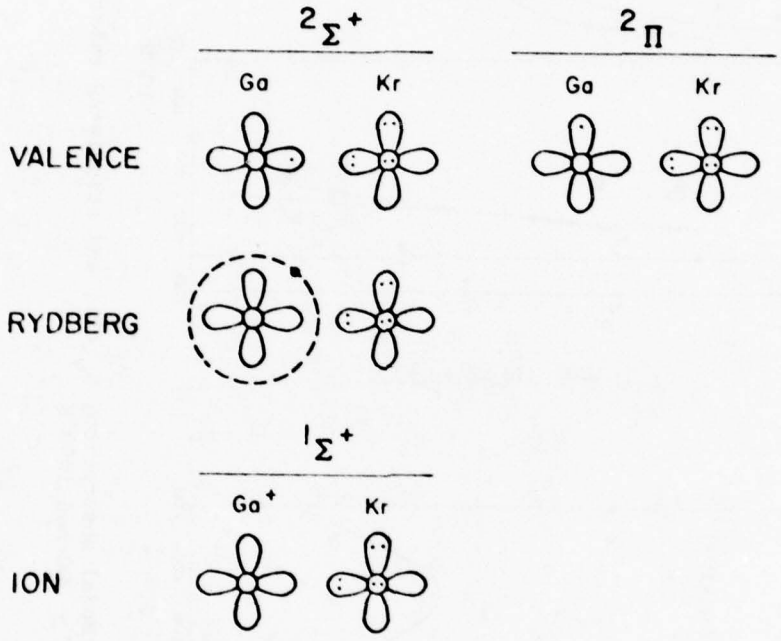

Graphical Data. A-12.17. Orbital diagrams for the low-lying electronic states of GaKr and $GaKr^+$. The two lobed figures represent 4p orbitals in the plane of the paper; the circle represents a 4p orbital perpendicular to the plane of the paper; and the 5s Rydberg orbital is represented by a large dashed circle.

A-13. POTENTIAL ENERGY CURVES AND SPECTROSCOPIC CONSTANTS FOR AuH, AuCℓ, $HgCℓ_2$, AND HgH

CONTENTS

		Page
A-13.1.	Orbital energies and radial expectation values for Au and Hg from relativistic and nonrelativistic wavefunctions.	1321
A-13.2	Comparison of excitation energies in (eV) for the lowest states of Au and Hg atoms from all-electron calculations	1322
A-13.3.	Orbital energies of the valence electrons in Au and Hg atoms from nonrelativistic (NR) and relativistic (R) all-electron calculation	1323
A-13.4.	Comparison of the energies of the lowest three states of Au atom from nonrelativistic (NR) all-electron calculations with experimental energies.	1323
A-13.5.	Comparison of the excitation energies (in eV) for Hg atom computed from all-electron and valence-electron calculations, where the valence electron calculations explicitly treated the outer 12 electrons of Hg . . .	1324
A-13.6.	Comparison of excitation energies for Au from all-electron and valence-electron calculations, where the valence-electron calculations explicitly treated the outer 11 electrons of Au	1325
A-13.7.	Comparison of excitation energies (in eV) for the states of the Au atom with spin-orbit coupling effects included	1325
A-13.8.	Comparison of the energies of the lowest three states of Hg atom from nonrelativistic (NR) and relativistic (R) all electron calculations with experimental energies	1326
A-13.9.	Comparison of the relativistic all-electron (AE) and valence-electron (VE) results for the states of Hg atom where the relativistic ECP was used for the VE calculations	1326

Page

A-13.10. Comparison of valence-electron (VE) results for Au atom using the relativistic ECP and including spin-orbit coupling effects by perturbation theory with the results of Dirac-Hartree-Fock calculations and with experiment. 1327

A-13.11. Spectroscopic constants for $Au^{197}H$ computed from relativistic and nonrelativistic potentials. 1328

A-13.12. Spectroscopic constants for $Au^{197}Cl^{37}$ from relativistic and nonrelativistic potentials 1328

A-13.13. (a) Potential energy curves for AuH using relativistic (R) and nonrelativistic (NR) potentials for GVB wavefunctions.
(b) Potentials energy curves for AuH using the R potentials with GVB and POL-CI wavefunctions 1329

A-13.14. (a) Potential energy curves for AuCl using relativistic (R) and nonrelativistic (NR) potentials for GVB wavefunctions.
(b) Potential energy curves for AuCl using the R potential with GVB and POL-CI wavefunctions. 1330

A-13.15. Calculated and experimental bond lengths and dissociation energies for $HgCl_2$. 1331

A-13.16. Ionization potentials (in eV) for $HgCl_2$ from orbital energies ($-\varepsilon_i$) and from separate SCF calculations (ΔE - SCF) 1332

A-13.17. Calculated and experimental ionization potentials for the 5d orbitals of $HgCl_2$, where spin-orbit coupling effects have been included 1332

A-13.18. Orbital energies of $HgC\ell_2$, from Hartree-Fock calculations using relativistic and nonrelativistic potentials for Hg. 1333

A-13.19. Ionization potentials for $HgC\ell_2$ using the relativistic potential for Hg as predicted from Koopmans' theorem ($-\varepsilon_i$) and from separate SCF calculations (ΔE-SCF). . . . 1333

Page

A-13.20. Potential energy curves for the lowest states of HgH without spin-orbit coupling effects 1334

A-13.21. Potential energy curves for the lowest states of HgH including spin-orbit coupling effects 1334

A-13.22. Spectroscopic constants for the states of ^{202}HgH . . . 1335

A-13. References:

1. P. J. Hay, W. R. Wadt, L. R. Kahn, and F. W. Bobrowicz, "Ab Initio Studies of AuH, AuCℓ, HgH and $HgCℓ_2$ Using Relativistic Core Potentials," J. Chem. Phys. 69, 984 (1978).

Tabular Data. A-13.1. Orbital energies (in hartree) and radial expectation values (in bohr) for Au and Hg from relativistic and nonrelativistic wavefunctions.

	Nonrelativistic Hartree–Fock	Relativistic Hartree–Fock[a]	Dirac–Hartree–Fock[b–d]
		Orbital energies	
Au atom			
$5d$	−0.5210	−0.6047	−0.4547 {−0.4287($5d_+$) −0.4935($5d_-$)}
$6s$	−0.2208	−0.2902	−0.2917
$6p$	−0.1182	−0.1264	•••
Hg atom			
$5d$	−0.7141	−0.6047	−0.6048 {−0.5746($5d_+$) −0.6501($5d_-$)}
$6s$	−0.2620	−0.3267	−0.3280
$6p$	−0.1716	−0.1778	•••
Au atom		$\langle r \rangle$	
$5d$	1.54	1.58	1.59 {1.62($5d_+$) 1.54($5d_-$)}
$6s$	3.70	3.07	3.06
$6p$	5.54	5.14	5.12
Hg atom			
$5d$	1.43	1.47	1.47 {1.50($5d_+$) 1.43($5d_-$)}
$6s$	3.33	2.84	2.84
$6p$	4.26	4.07	•••

[a] Present work using Cowan-Griffin method, A-13 Ref. 1.

[b] Averaged over fine-structure components.

[c] J. B. Mann (unpublished and calculations).

[d] J. P. Desclaux, At. Data Nucl. Data Tables 12, 311 (1973).

Tabular Data. A-13.2. Comparison of excitation energies in (eV) for the lowest states of Au and Hg atoms from all-electron calculations.

	Hartree–Fock	Relativistic Hartree–Fock[a]	Dirac–Hartree–Fock[b,d]	Exptl[b,c]
		Au atom		
$5d^{10}\,6s^{1}\,(^{2}S)$	0.00	0.00	0.00	0.00
$5d^{9}\,6s^{2}\,(^{2}D)$	5.13	1.86	1.86	1.74
$5d^{10}\,6p^{1}\,(^{2}P)$	2.71	4.24	4.24	4.95
		Hg atom		
$5d^{10}\,6s^{2}\,(^{1}S)$	0.00	0.00		0.00
$5d^{10}\,6s\,6p\,(^{3}P)$	2.15	3.81		5.18
$5d^{10}\,6s\,6p\,(^{1}P)$	4.14	5.66		6.70

[a]Present work using Cowan-Griffin method, A-13 Ref. 1.

[b]Averaged over fine-structure components.

[c]C. E. Moore, "Atomic Energy Levels," Natl. Bur. Stand. (U.S.) Circ. 476 (1958), Vol. III.

[d]J. B. Mann (unpublished calculations).

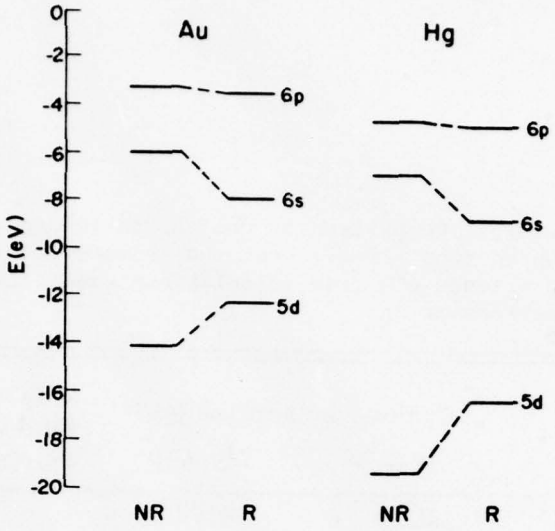

Graphical Data. A-13.3. Orbital energies of the valence electrons in Au and Hg atoms from nonrelativistic (NR) and relativistic (R) all-electron calculation. The $6p$ energies correspond to the $5d^{10}6p^1$ and $5d^{10}6p^1(^3P)$ configurations, respectively.

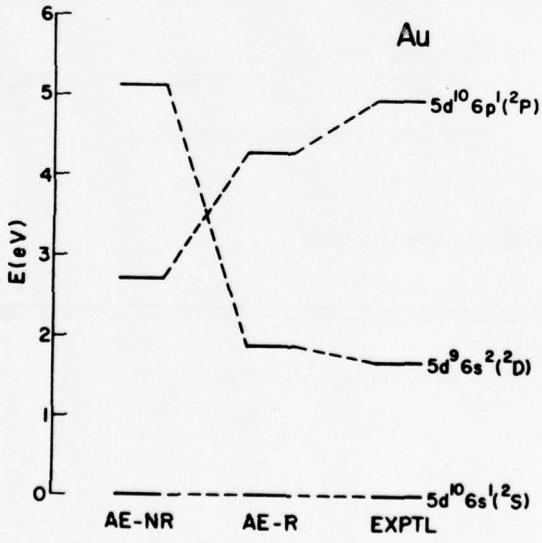

Graphical Data. A-13.4. Comparison of the energies of the lowest three states of Au atom from nonrelativistic (NR) all-electron calculations with experimental energies.

Tabular Data. A-13.5. Comparison of the excitation energies (in eV) for Hg atom computed from all-electron and valence-electron calculations, where the valence electron calculations explicitly treated the outer 12 electrons of Hg.

	Excitation energies (eV)		Ground state total energies (hartree)
	$^1S \rightarrow {}^3P$	$^1S \rightarrow {}^1P$	
Expt[a]	5.18	6.70	
Relativistic calculations			
All-electron HF	3.81	5.66	
Valence-electron ($3s3p3d$) basis			
HF	3.81	5.88	−43.47818
MC-SCF	4.58	6.65	−43.50711
Valence-electron ($3s4p4d$) basis			
HF	3.78	5.64	−43.55284
Nonrelativistic calculations			
All-electron HF	2.15	4.14	
Valence-electron ($3s3p4d$) basis			
HF	2.04	4.21	−44.14543

[2]Averaged over fine-structure components.

Tabular Data. A-13.6. Comparison of excitation energies for Au from all-electron and valence-electron calculations, where the valence-electron calculations explicitly treated the outer 11 electrons of Au.

	Excitation energy (eV)	
	$^2S \leftarrow {}^2D$	$^2S \leftarrow {}^2P$
Expt[a]	1.74	4.95
Relativistic calculations		
All-electron	1.86	4.24
Valence-electron	1.67	4.22
Nonrelativistic calculations		
All-electron	5.13	2.71
Valence-electron	4.87	2.70

[a]Averaged over fine-structure components.

Tabular Data. A-13.7. Comparison of excitation energies (in eV) for the states of the Au atom with spin-orbit coupling effects included.

	Dirac–Hartree–Fock	Relativistic Hartree–Fock	Valence-electron Hartree–Fock	Expt
$^1S_{1/2}$	0.00	0.00	0.00	0.00
$^2D_{5/2}$	1.27	1.23	1.04	1.14
$^2D_{3/2}$	2.74	2.80	2.62	2.66
$^2P_{1/2}$	4.01	4.01	3.99	4.63
$^2P_{3/2}$	4.36	4.36	4.34	5.10
	Spin–orbit parameters (cm^{-1})			
5*d*	−4734	−5105	(−5105)	−4910
6*p*	1879	1834	(1843)	2543

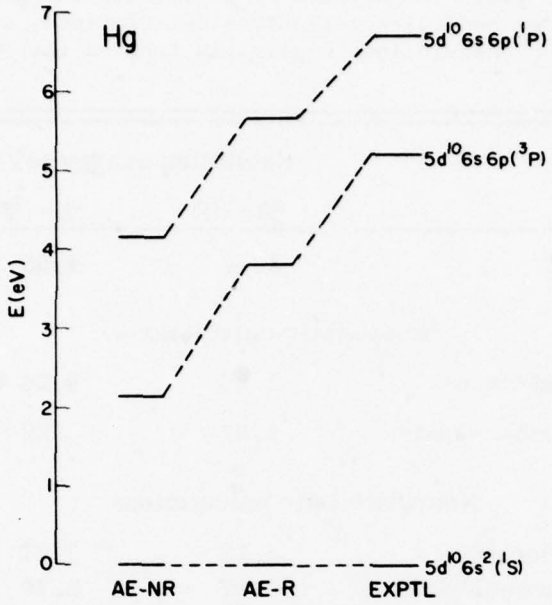

Graphical Data. A-13.8. Comparison of the energies of the lowest three states of Hg atom from nonrelativistic (NR) and relativistic (R) all-electron calculations with experimental energies.

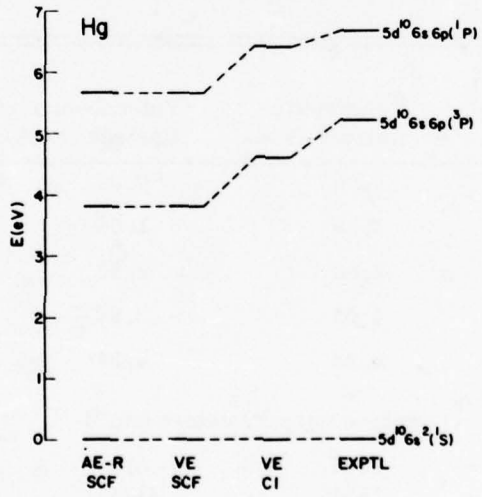

Graphical Data. A-13.9 Comparison of relativistic all-electron (AE) and valence-electron (VE) results for the states of Hg atom where the relativistic ECP was used for the VE calculations.

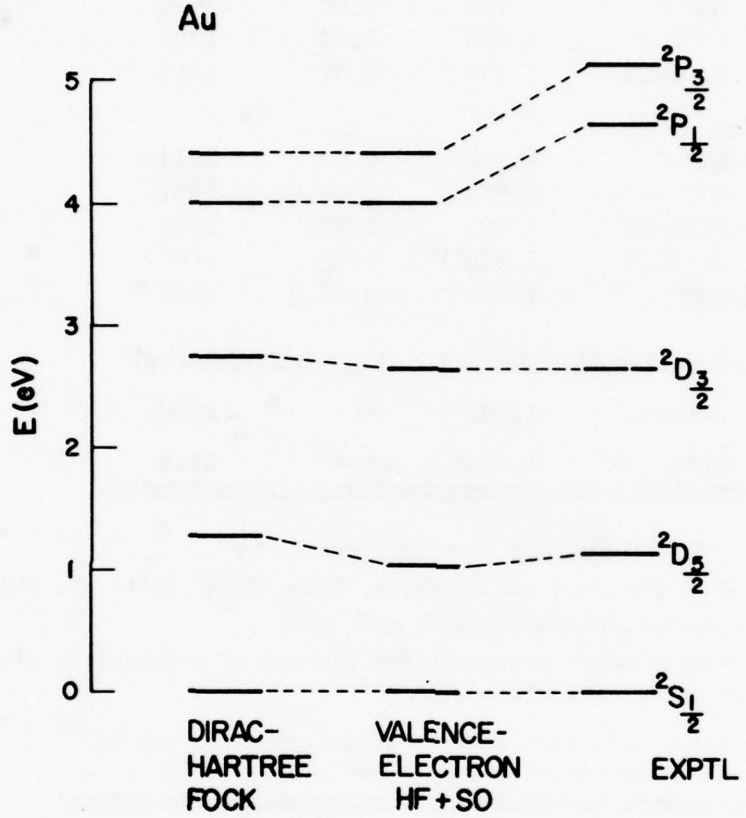

Graphical Data. A-13.10. Comparison of valence-electron (VE) results for Au atom using the relativistic ECP and including spin-orbit coupling effects by perturbation theory with the results of Dirac-Hartree-Fock calculations and with experiment.

Tabular Data. A-13.11 Spectroscopic constants for $Au^{197}H$ computed from relativistic and nonrelativistic potentials.

AuH—$X\,^1\Sigma^+$	R_e(Å)	D_e(eV)	ω_e(cm^{-1})
Nonrel. ECP			
HF	1.763	0.99	1387
GVB–1	1.820	1.52	1203
POL-CI	1.807	1.57	1217
Rel. ECP			
HF	1.508	1.55	2014
GVB–1	1.514	2.14	1891
POL-CI	1.522	2.23	1871
(1+2)CI	(1.5237)[c]	2.66	•••
Exptl[a]	1.5237	3.37	2305
1-Center numerical Dirac–Fock (all-electron)[b]			
Nonrel.	1.745	•••	2296
Rel.	1.659[d]	•••	2178

[a] U. Ringström, Ark. Fys. 27, 227 (1964).

[b] J. P. Desclaux and P. Pyykö, Chem. Phys. Lett. 39, 300 (1976).

[c] Experimental bond length assumed.

[d] Using a Morse potential fit instead of a quadratic fit leads to an R_e of 1.622 Å.

Tabular Data. A-13.12. Spectroscopic constants for $Au^{197}Cl^{37}$ from relativistic and nonrelativistic potentials.

AuCl—$X\,^1\Sigma^+$	R_e(Å)	D_e(eV)	ω_e(cm^{-1})
Nonrel. ECP			
GVB–1	2.447	2.58	277
Rel. ECP			
GVB–1	2.283	1.96	298
POL–CI	2.291	2.39	306
Exptl[a,b]	•••	3.5 ± 0.1	382

[a] A. G. Gaydon, Dissociation Energies (Chapman and Hall, London, 1968).

[b] B. Rosen, Spectroscopic Data (Pergamon, Oxford, 1970).

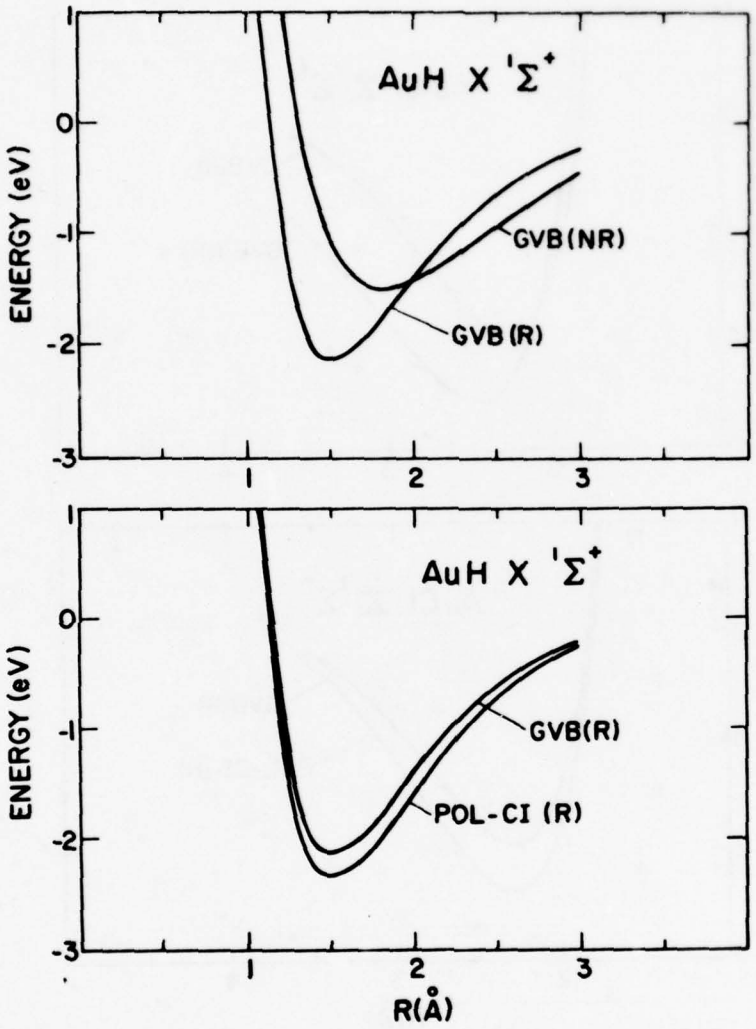

Graphical Data. A-13.13. (a) Potential energy curves for AuH using relativistic (R) and nonrelativistic (NR) potentials for GVB (2-configuration) wavefunctions. (b) Potentials energy curves for AuH using the R potentials with GVB and POL-CI wavefunctions.

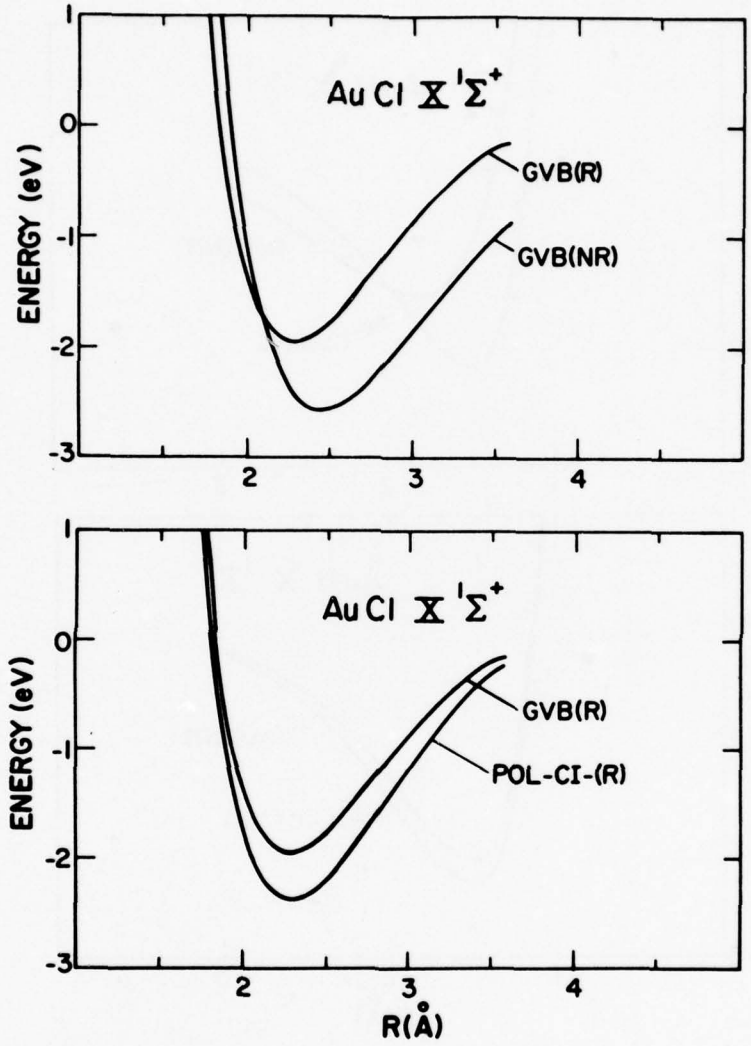

Graphical Data. A-13.14. (a) Potential energy curves for AuCl using relativistic (R) and nonrelativistic (NR) potentials for GVB wavefunctions. (b) Potential energy curves for AuCl using the R potential with GVB and POL-CI wavefunctions.

Tabular Data. A-13.15. Calculated and experimental bond lengths and dissociation energies (into Hg + 2Cl) for $HgCl_2$.

	R_e(Å)		D_e(kcal/mole)	
	HF	2-config.	HF	2-config.
Rel. ECP	2.290	2.301	57.5	59.6
Nonrel. ECP	2.409	2.412	97.6	100.0
Nonrel. ECP[c]	2.313	2.315	•••	115.7
Expt.	2.29 ± 0.02[a], 2.252[d]		106.4[b]	

[a] P.A. Akisin, V.P. Spiridonov, and A.N. Khodchenkov, Zh. Fiz. Khim. 33, 20 (1959); earlier determinations were discussed by L. R. Maxwell and V. M. Mosley, Phys. Rev. 57, 21 (1940).

[b] JANAF Thermochemical Tables" Natl. Stand. Ref. Data Ser. Natl. Bur. Stand. 37 (1971) where zero-point corrections have not been applied.

[c] H. Basch, M.D. Newton, J. Jafri, J.W. Moskowitz and S. Topiol, J. Chem. Phys. (in press).

[d] K. Kashiwabara, S. Konaka, and M. Kimura, Bull. Chem. Soc. Jpn 46, 410 (1973).

Tabular Data. A-13.16. Ionization potentials (in eV) for $HgCl_2$ from orbital energies ($-\epsilon_i$) and from separate SCF calculations (ΔE - SCF).

	$-\epsilon_i$ (Nonrel.)	$-\epsilon_i$ (Rel.)	ΔE-SCF (Rel.)	Exptl[a]
$2\pi_g$ ($3p_{Cl}$)	12.21	12.56	11.98	11.43
$1\pi_u$ ($3p_{Cl}$)	12.64	13.06	12.48	12.13
$2\sigma_u$ ($3p_{Cl}$)	12.86	13.01	12.43	12.74
$3\sigma_g$ ($3p_{Cl}$)	13.08	14.09	13.60	13.74
$1\delta_g$ ($5d_{Hg}$)	22.66	20.14	17.15	
$1\pi_g$ ($5d_{Hg}$)	22.99	20.81	17.98	
$2\sigma_g$ ($5d_{Hg}$)	22.67	20.70	18.63	
$1\sigma_u$ ($3s_{Cl}$)	28.58	29.00		
$1\sigma_g$ ($3s_{Cl}$)	29.35	29.62		

[a]J.H.D. Elana, Int. J. Mass. Spectrom. Ion Phys. 4, 37 (1970).

Tabular Data. A-13.17. Calculated and experimental ionization potentials for the 5d orbitals of $HgCl_2$, where spin-orbit coupling effects have been included.

State (Ω)	$-\epsilon_i$ with *S–O* coupling	ΔE-SCF with *S–O* coupling	Exptl[a]
5/2	19.39	16.40	16.71
3/2	19.88	16.99	17.05
1/2	20.00	17.51	17.27
3/2	21.44	18.51	18.65
1/2	21.89	19.42	•••

[a]J.H.D. Elana, Int. J. Mass. Spectrom. Ion Phys. 4, 37 (1970).

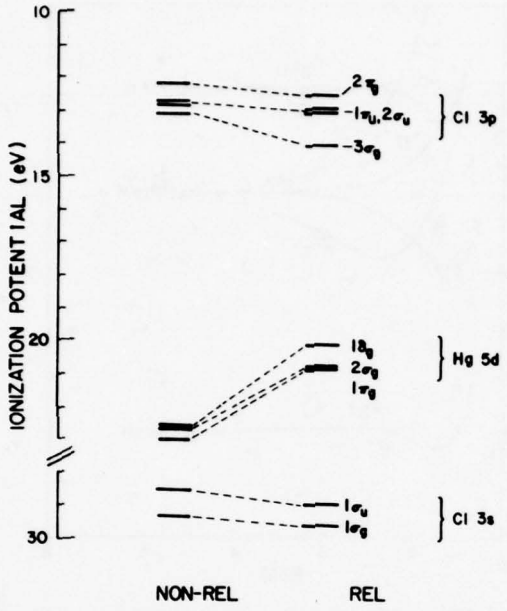

Graphical Data. A-13.18. Orbital energies of $HgC\ell_2$ from Hartree-Fock calculations using relativistic and nonrelativistic potentials for Hg.

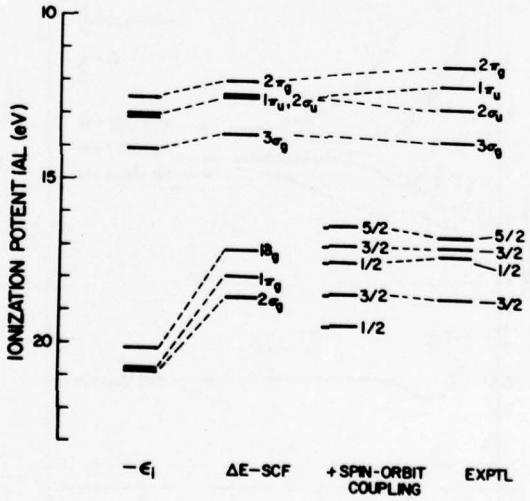

Graphical Data. A-13.19. Ionization potentials for $HgC\ell_2$ using the relativistic potential for Hg as predicted from Koopmans' theorem ($-\varepsilon_i$) and from separate SCF calculations (ΔE-SCF).

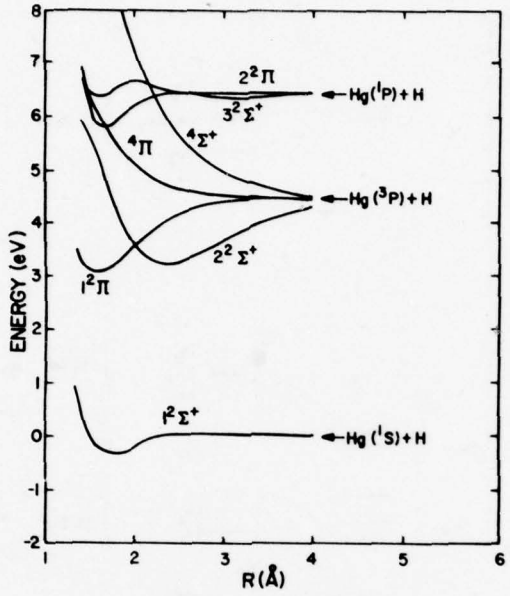

Graphical Data. A-13.20. Potential energy curves for the lowest states of HgH without spin-orbit coupling effects.

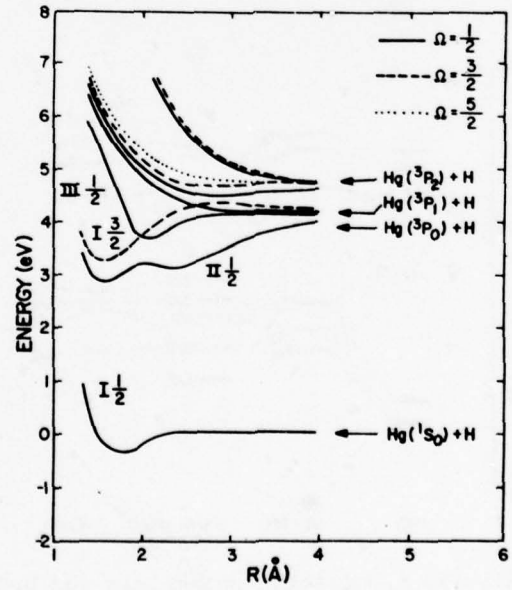

Graphical Data. A-13.21. Potential energy curves for the lowest states of HgH including spin-orbit coupling effects. The states dissociating to Hg(^{1}P) + H are not shown.

Tabular Data. A-13.22. Spectroscopic constants for the states of ^{202}HgH.

	R_e(Å)	D_e(eV)	ω_e(cm^{-1})	T_e(eV)
States without spin–orbit coupling				
$X\,^2\Sigma^+$				
Present	1.763	0.33	1227	0.00
Das, Wahl[a]	1.783	0.37	1123	0.00
Exptl[b,c]	1.7404	0.46	1387	0.00
$1\,^2\Pi$				
Present	1.574	1.41	1693	3.32
Das, Wahl	1.593	•••	2032	3.80
$2\,^2\Sigma^+$				
Present	2.390	1.25	•••	3.46
Das, Wahl	(repulsive)			
States including spin–orbit coupling				
II $\frac{1}{2}$ ($^2\Pi_{1/2}$)				
Present	1.579	1.09	1629	3.11
Exptl	1.586	2.08	2066	3.05
I $\frac{3}{2}$ ($^2\Pi_{3/2}$)				
Present	1.575	0.98	1686	3.48
Exptl	1.580	1.85	2067	3.50
III $\frac{1}{2}$ ($2\,^2\Sigma^+_{1/2}$)				
Present	2.078	0.53	1604	3.94
Exptl	(r_0=2.03)	1.15	•••	4.20

[a] G. Das and A. C. Wahl, J. Chem. Phys. 64, 4672 (1974).

[b] T. L. Porter, J. Opt. Soc. Am. 52, 1201 (1962).

[c] W. C. Stwalley, J. Chem Phys. 63, 3062 (1975).

A-14. POTENTIAL ENERGY CURVES, ELECTRONIC ENERGIES, AND SPECTROSCOPIC CONSTANTS FOR VALENCE STATES OF O_2

CONTENTS

		Page
A-14.1.	Potential energy curves for O_2^-, O_2, and O_2^+	1339
A-14.2.	Calculated potential curves for singlet valence states of O_2	1340
A-14.3.	Calculated potential curves for triplet valence states of O_2	1341
A-14.4.	Calculated potential curves for 62 valence states of O_2 given in hartrees relative to the asymptotic energy of each state	1342
A-14.5.	Calculated potential curves for quintet valence states of O_2	1346
A-14.6.	Molecular constants for 12 electronic states of O_2	1347
A-14.7.	*Separated-atom energy levels of* O_2 given in eV relative to the $^3P + {}^3P$ asymptote	1348
A-14.8.	Equilibrium constants for five new, weakly bound states of O_2	1348

PRECEDING PAGE BLANK

A-14. References:

1. R. P. Saxon and B. Liu, "Ab initio Configuration Study of the Valence States of O_2," J. Chem. Phys. 67, 5432 (1977).
2. P. Krupenie, "The Spectrum of Molecular Oxygen," J. Phys. Chem. Ref. Data. 1, 423 (1977)*.
3. H. F. Schaefer and F. E. Harris, "Ab initio Calculations on 62 Low-Lying States of the O_2 Molecule," J. Chem. Phys. 48, 4946 (1968).
4. B. J. Moss and W. A. Goddard, "Configuration Interaction Studies on Low-Lying States of O_2^*," J. Chem. Phys. 63, 3523 (1975).

*Reference 2 is a critical review and compilation of the observed and predicted spectroscopic data on O_2 and its ions O_2^-, O_2^+, and O_2^{2+}. The ultraviolet, visible, infrared, Raman, microwave, and electron para-magnetic resonance spectra are included. Each electronic band system is discussed in detail, and tables of band origins and heads are given. The microwave and EPR data are also tabulated. Special subjects such as the dissociation energy of O_2, perturbations, and predissociations are discussed. Potential energy curves are given, as well as f-values, Franck-Condon integrals, and other intensity factors. A summary table lists the molecular constants for all known electronic states of O_2 and O_2^+. Electronic structure and theoretical calculations are also discussed.

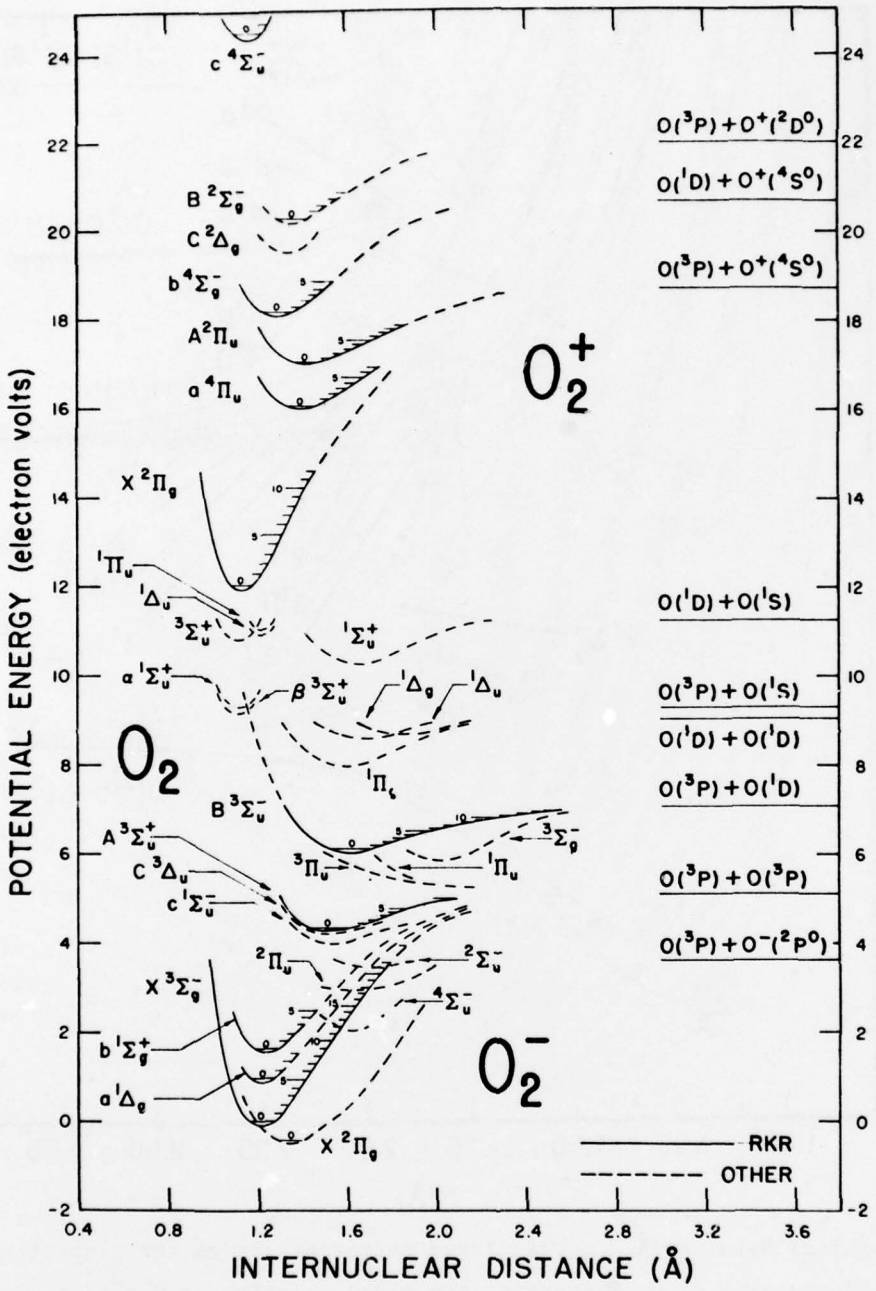

Graphical Data. A-14.1. Potential energy curves for O_2^-, O_2, and O_2^+.

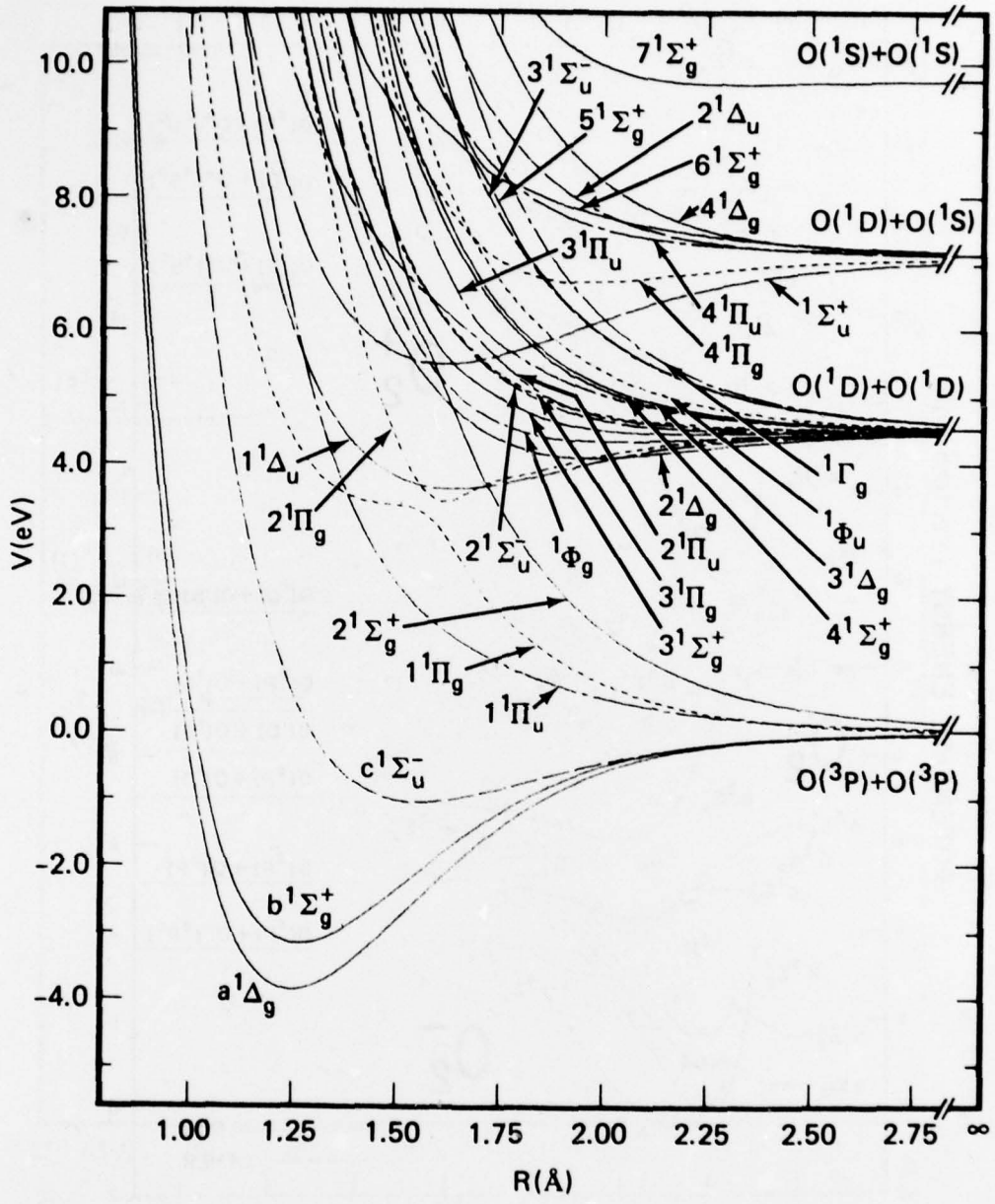

Graphical Data. A-14.2. Calculated potential curves for singlet valence states of 0_2. Energies are given relative to 0 (^{3}P) + 0 (^{3}P).

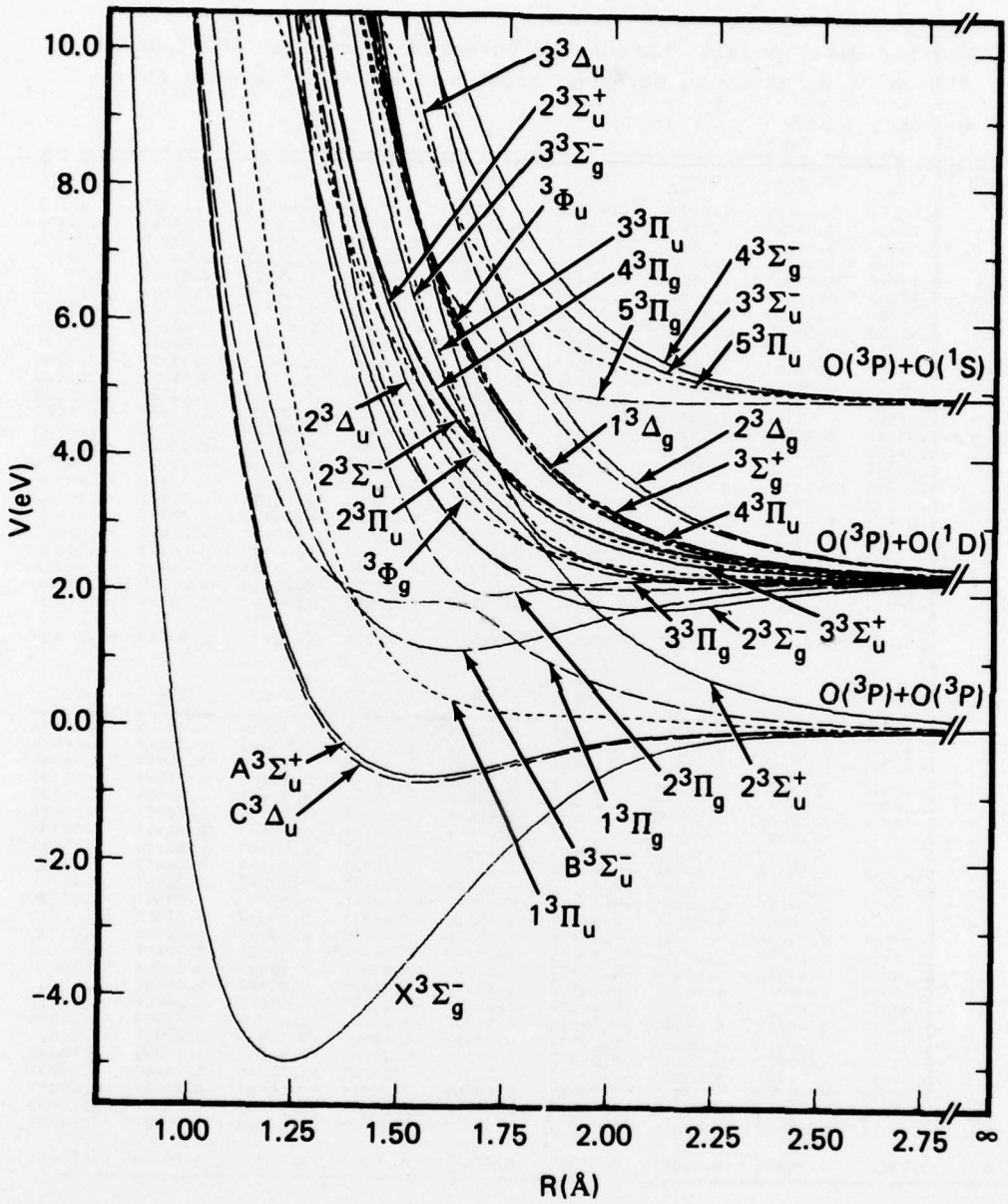

Graphical Data. A-14.3. Calculated potential curves for triplet valence states of O_2. Energies are given relative to O (^3P) + O (^3P).

Tabular Data. A-14.4 Calculated potential curves for 62 valence states of O_2 given in hartrees relative to the asymptotic energy of each state.

R(a_0)	$b^1\Sigma_g^+$	$2^1\Sigma_g^+$	$3^1\Sigma_g^+$	$4^1\Sigma_g^+$	$5^1\Sigma_g^+$	$6^1\Sigma_g^+$	$7^1\Sigma_g^+$	$1^1\Sigma_u^+$	$C^1\Sigma_u^-$
1.8	0.10650	0.62422	0.81921	0.83779	0.87063	0.91214	0.87560	0.48987	0.48807
2.0	-0.04505	0.51873	0.54599	0.63957	0.65576	0.59581	0.64727	0.24190	0.22479
2.2	-0.10362	0.49603	0.37025	0.41849	0.57767	0.51852	0.43434	0.09649	0.08365
2.3	-0.11384	0.46416	0.33526	0.35037	0.49961	0.46287	0.39552	0.04919	0.04091
2.4	-0.11643	0.40322	0.30070	0.34183	0.39506	0.38980	0.35502	0.01368	0.01068
2.6	-0.10791	0.31138	0.22689	0.23073	0.32221	0.27880	0.29188	-0.03164	-0.02397
2.8	-0.09069	0.25123	0.11568	0.17928	0.21730	0.22615	0.21178	-0.05347	-0.03717
3.0	-0.07133	0.20055	0.04904	0.12488	0.16833	0.11892	0.15911	-0.06056	-0.03879
3.2	-0.05327	0.14393	0.02474	0.08006	0.14368	0.05140	0.08909	-0.05882	-0.03472
3.4	-0.03817	0.10261	0.01038	0.05043	0.09958	0.03626	0.04508	-0.05231	-0.02850
3.5	-0.03190	0.08646	0.00581	0.03997	0.08297	0.03116	0.03040	-0.04816	-0.02524
3.6	-0.02649	0.07276	0.00256	0.03170	0.06931	0.02688	0.01949	-0.04375	-0.02209
3.8	-0.01801	0.05138	-0.00105	0.01998	0.04864	0.02006	0.00607	-0.03493	-0.01649
4.0	-0.01214	0.03619	-0.00220	0.01264	0.03427	0.01493	-0.00009	-0.02694	-0.01203
4.5	-0.00463	0.01499	-0.00148	0.00400	0.01436	0.00702	-0.00272	-0.01303	-0.00534
5.0	-0.00189	0.00624	-0.00050	0.00115	0.00612	0.00333	-0.00151	-0.00623	-0.00244
5.5	-0.00083	0.00265	-0.00009	0.00020	0.00272	0.00166	-0.00068	-0.00316	-0.00119
6.0	-0.00039	0.00117	0.00004	-0.00011	0.00129	0.00089	-0.00033	-0.00175	-0.00062
6.5	-0.00019	0.00054	0.00005	-0.00016	0.00067	0.00051	-0.00018	-0.00105	-0.00036
7.0	-0.00010	0.00027	0.00003	-0.00012	0.00037	0.00032	-0.00011	-0.00067	-0.00021
7.5	-0.00005	0.00015	0.00002	-0.00008	0.00022	0.00022	-0.00007	-0.00045	-0.00013
8.0	-0.00002	0.00009	0.00002	-0.00005	0.00014	0.00016	-0.00005	-0.00031	-0.00008
9.0	0.00000	0.00004	0.00002	-0.00002	0.00007	0.00009	-0.00002	-0.00016	-0.00004
10.0	0.00001	0.00003	0.00002	-0.00001	0.00004	0.00006	-0.00001	-0.00009	-0.00001
20.0	0.00000	0.00125	0.16571	0.16600	0.16625	0.26219	0.35923	0.26219	-0.00000

R(a_0)	$2^1\Sigma_u^-$	$3^1\Sigma_u^-$	$1^1\Pi_g$	$2^1\Pi_g$	$3^1\Pi_g$	$4^1\Pi_g$	$1^1\Pi_u$	$2^1\Pi_u$	$3^1\Pi_u$
1.8	0.59036	0.72444	0.50684	0.38172	0.39743	0.76760	0.70054	0.57396	0.59596
2.0	0.48587	0.65267	0.32532	0.24879	0.29786	0.57251	0.50662	0.38767	0.48550
2.2	0.45371	0.49053	0.20859	0.23629	0.28489	0.30248	0.33331	0.26014	0.46368
2.3	0.38626	0.45984	0.17509	0.24471	0.29205	0.19934	0.26410	0.21669	0.43307
2.4	0.30725	0.46294	0.15253	0.20847	0.25949	0.20914	0.20858	0.18150	0.39737
2.6	0.19072	0.42491	0.12935	0.08402	0.18976	0.18861	0.13135	0.12955	0.28989
2.8	0.11579	0.29095	0.12353	0.00285	0.11464	0.09548	0.08581	0.09470	0.17539
3.0	0.06423	0.20045	0.11408	-0.03843	0.06808	0.03756	0.05909	0.06970	0.10133
3.2	0.03845	0.13924	0.07824	-0.03235	0.03941	0.00523	0.04264	0.04853	0.05753
3.4	0.02329	0.09742	0.05342	-0.02529	0.02215	-0.01011	0.03145	0.02660	0.03780
3.5	0.01425	0.08166	0.04401	-0.02194	0.01646	-0.01364	0.02703	0.01865	0.03128
3.6	0.00871	0.06852	0.03616	-0.01885	0.01220	-0.01533	0.02317	0.01287	0.02581
3.8	0.00394	0.04834	0.02416	-0.01355	0.00674	-0.01526	0.01684	0.00598	0.01735
4.0	0.00104	0.03414	0.01590	-0.00949	0.00380	-0.01298	0.01203	0.00281	0.01148
4.5	-0.00089	0.01431	0.00495	-0.00378	0.00091	-0.00668	0.00475	0.00054	0.00381
5.0	-0.00084	0.00607	0.00100	-0.00165	0.00010	-0.00325	0.00162	0.00008	0.00107
5.5	-0.00064	0.00267	-0.00024	-0.00086	-0.00011	-0.00173	0.00042	-0.00007	0.00015
6.0	-0.00046	0.00125	-0.00052	-0.00052	-0.00015	-0.00102	0.00000	-0.00008	-0.00013
6.5	-0.00033	0.00064	-0.00049	-0.00032	-0.00014	-0.00065	-0.00011	-0.00005	-0.00021
7.0	-0.00023	0.00035	-0.00040	-0.00020	-0.00013	-0.00043	-0.00012	-0.00002	-0.00019
7.5	-0.00016	0.00021	-0.00030	-0.00012	-0.00011	-0.00030	-0.00010	-0.00002	-0.00015
8.0	-0.00011	0.00014	-0.00022	-0.00007	-0.00009	-0.00021	-0.00007	-0.00001	-0.00011
9.0	-0.00005	0.00007	-0.00012	-0.00003	-0.00006	-0.00011	-0.00004	0.00000	-0.00006
10.0	-0.00003	0.00004	-0.00006	-0.00001	-0.00003	-0.00006	-0.00002	0.00001	-0.00003
20.0	0.16600	0.16625	0.00061	0.16585	0.16612	0.26233	0.00062	0.16585	0.16612

Tabular Data. A-14.4 Calculated potential curves for 62 valence states of O_2 given in hartrees relative to the asymptotic energy of each state. (Continued).

R(a_0)	$4^1\Pi_u$	$a^1\Delta_g$	$2^1\Delta_g$	$3^1\Delta_g$	$4^1\Delta_g$	$1^1\Delta_u$	$2^1\Delta_u$	$^1\Phi_g$	$^1\Phi_u$
1.8	0.54772	0.07303	0.44183	0.81141	0.78295	0.52510	0.53453	0.39220	0.64196
2.0	0.44275	-0.07635	0.33837	0.59776	0.53975	0.26985	0.42168	0.29999	0.53868
2.2	0.38046	-0.13196	0.31716	0.36249	0.46403	0.12428	0.38110	0.28713	0.51136
2.3	0.35327	-0.14051	0.27976	0.32183	0.44640	0.07721	0.35421	0.29497	0.49255
2.4	0.33574	-0.14133	0.21382	0.33185	0.38321	0.04198	0.31217	0.26490	0.47536
2.6	0.23706	-0.12912	0.11913	0.31593	0.26386	-0.00292	0.23946	0.14653	0.34171
2.8	0.15818	-0.10807	0.05918	0.20517	0.29479	-0.02485	0.19071	0.07417	0.22628
3.0	0.09671	-0.08492	0.02210	0.13171	0.22231	-0.03269	0.14287	0.03210	0.14980
3.2	0.05738	-0.06333	0.00030	0.08396	0.14570	-0.03239	0.09062	0.00923	0.09934
3.4	0.03406	-0.04520	-0.01113	0.05345	0.09402	-0.02799	0.05623	-0.00193	0.06610
3.5	0.02641	-0.03767	-0.01406	0.04271	0.07511	-0.02512	0.04402	-0.00474	0.05401
3.6	0.02061	-0.03118	-0.01560	0.03418	0.05978	-0.02214	0.03432	-0.00633	0.04419
3.8	0.01286	-0.02106	-0.01576	0.02202	0.03750	-0.01647	0.02062	-0.00719	0.02967
4.0	0.00835	-0.01412	-0.01371	0.01428	0.02328	-0.01182	0.01223	-0.00651	0.02000
4.5	0.00337	-0.00538	-0.00730	0.00488	0.00707	-0.00516	0.00326	-0.00387	0.00750
5.0	0.00161	-0.00222	-0.00354	0.00163	0.00232	-0.00263	0.00085	-0.00230	0.00280
5.5	0.00083	-0.00099	-0.00184	0.00051	0.00082	-0.00153	0.00013	-0.00147	0.00103
6.0	0.00046	-0.00048	-0.00105	0.00014	0.00030	-0.00097	-0.00008	-0.00099	0.00038
6.5	0.00029	-0.00026	-0.00066	0.00002	0.00011	-0.00065	-0.00013	-0.00068	0.00014
7.0	0.00018	-0.00014	-0.00043	-0.00001	0.00004	-0.00044	-0.00012	-0.00048	0.00005
7.5	0.00013	-0.00008	-0.00029	-0.00002	0.00001	-0.00031	-0.00010	-0.00034	0.00002
8.0	0.00009	-0.00005	-0.00020	-0.00001	0.00000	-0.00022	-0.00007	-0.00024	0.00001
9.0	0.00005	-0.00002	-0.00010	-0.00001	0.00000	-0.00011	-0.00004	-0.00013	0.00001
10.0	0.00003	-0.00000	-0.00005	-0.00000	0.00000	-0.00006	-0.00002	-0.00007	0.00001
20.0	0.26233	0.00000	0.16597	0.16600	0.26239	0.16597	0.26239	0.16612	0.16612

R(a_0)	$^1\Gamma_g$	$^3\Sigma_g^+$	$X^3\Sigma_g^-$	$2^3\Sigma_g^-$	$3^3\Sigma_g^-$	$4^3\Sigma_g^-$	$A^3\Sigma_u^+$	$2^3\Sigma_u^+$	$3^3\Sigma_u^+$
1.8	0.85720	0.48328	0.02825	0.50430	0.81931	0.80922	0.50973	0.77601	0.83606
2.0	0.68388	0.38790	-0.12072	0.40243	0.61562	0.55214	0.24318	0.67036	0.69923
2.2	0.60857	0.37171	-0.17448	0.38002	0.38406	0.48151	0.09950	0.59077	0.56181
2.3	0.59068	0.37819	-0.18168	0.30006	0.38657	0.45847	0.05574	0.49613	0.56036
2.4	0.58057	0.38975	-0.18093	0.23430	0.39656	0.35303	0.02465	0.41659	0.54220
2.6	0.54370	0.35125	-0.16494	0.13940	0.28595	0.32792	-0.01125	0.29756	0.38770
2.8	0.37589	0.23825	-0.13934	0.07840	0.18311	0.27285	-0.02517	0.21796	0.24472
3.0	0.25742	0.16139	-0.11061	0.03906	0.11287	0.20421	-0.02711	0.16473	0.14581
3.2	0.17646	0.10925	-0.08304	0.01339	0.06801	0.13845	-0.02319	0.12943	0.07716
3.4	0.12114	0.07392	-0.05825	-0.00343	0.04048	0.08888	-0.01724	0.10663	0.02935
3.5	0.10043	0.06080	-0.04743	-0.00930	0.03122	0.07045	-0.01425	0.09283	0.01709
3.6	0.08330	0.05000	-0.03787	-0.01366	0.02413	0.05548	-0.01151	0.07763	0.01107
3.8	0.05738	0.03378	-0.02278	-0.01829	0.01447	0.03371	-0.00709	0.05427	0.00339
4.0	0.03957	0.02278	-0.01300	-0.01848	0.00866	0.01994	-0.00417	0.03794	-0.00029
4.5	0.01571	0.00841	-0.00354	-0.01110	0.00210	0.00493	-0.00123	0.01554	-0.00189
5.0	0.00633	0.00304	-0.00145	-0.00515	0.00010	0.00118	-0.00056	0.00642	-0.00110
5.5	0.00262	0.00106	-0.00078	-0.00235	-0.00043	0.00024	-0.00033	0.00272	-0.00052
6.0	0.00114	0.00035	-0.00047	-0.00111	-0.00051	-0.00002	-0.00021	0.00119	-0.00024
6.5	0.00053	0.00010	-0.00030	-0.00055	-0.00047	-0.00009	-0.00013	0.00055	-0.00012
7.0	0.00028	0.00002	-0.00019	-0.00028	-0.00039	-0.00009	-0.00007	0.00027	-0.00006
7.5	0.00016	-0.00000	-0.00013	-0.00015	-0.00030	-0.00008	-0.00004	0.00015	-0.00003
8.0	0.00010	-0.00000	-0.00008	-0.00009	-0.00022	-0.00006	-0.00002	0.00009	-0.00001
9.0	0.00005	0.00000	-0.00003	-0.00004	-0.00011	-0.00003	0.00000	0.00004	-0.00000
10.0	0.00003	0.00000	-0.00001	-0.00002	-0.00006	-0.00001	0.00001	0.00003	0.00000
20.0	0.16625	0.08300	-0.00000	0.04300	0.08345	0.17974	0.00000	0.00125	0.08300

Tabular Data. A-14.4 Calculated potential curves for 62 valence states of O_2 given in hartrees relative to the asymptotic energy of each state. (Continued).

R(a_0)	$B^3\Sigma_u^-$	$2^3\Sigma_u^-$	$3^3\Sigma_u^-$	$1^3\Pi_g$	$2^3\Pi_g$	$3^3\Pi_g$	$4^3\Pi_g$	$5^3\Pi_g$	$1^3\Pi_u$
1.8	0.51595	0.69461	0.74252	0.43650	0.42217	0.46823	0.89067	0.85222	0.63719
2.0	0.25852	0.58419	0.59300	0.26433	0.32904	0.37538	0.69775	0.61916	0.44513
2.2	0.11369	0.50650	0.48563	0.15112	0.31672	0.36241	0.42547	0.38047	0.27091
2.3	0.06710	0.41117	0.40759	0.11872	0.32361	0.32540	0.36610	0.28031	0.20252
2.4	0.03230	0.33260	0.36182	0.09685	0.24153	0.28681	0.33320	0.24330	0.14870
2.6	-0.01199	0.21813	0.29060	0.07389	0.12419	0.16387	0.21717	0.22581	0.07620
2.8	-0.03361	0.14454	0.24239	0.06692	0.05160	0.08651	0.14436	0.12997	0.03660
3.0	-0.04126	0.09709	0.16851	0.06717	0.00710	0.03962	0.09844	0.06733	0.01705
3.2	-0.04065	0.06605	0.10917	0.06018	-0.01129	0.01297	0.06790	0.03005	0.00887
3.4	-0.03566	0.04532	0.06914	0.04210	-0.00850	-0.00054	0.04633	0.01074	0.00631
3.5	-0.03237	0.03761	0.05445	0.03513	-0.00726	-0.00397	0.03804	0.00549	0.00592
3.6	-0.02888	0.03122	0.04254	0.02930	-0.00680	-0.00513	0.03113	0.00213	0.00571
3.8	-0.02202	0.02147	0.02529	0.02026	-0.00758	-0.00401	0.02074	-0.00108	0.00516
4.0	-0.01608	0.01465	0.01452	0.01391	-0.00692	-0.00276	0.01375	-0.00190	0.00412
4.5	-0.00687	0.00525	0.00330	0.00510	-0.00384	-0.00121	0.00474	-0.00137	0.00114
5.0	-0.00311	0.00152	0.00075	0.00164	-0.00194	-0.00070	0.00144	-0.00077	-0.00036
5.5	-0.00153	0.00014	0.00012	0.00038	-0.00101	-0.00052	0.00028	-0.00047	-0.00075
6.0	-0.00078	-0.00032	-0.00005	-0.00002	-0.00051	-0.00044	-0.00009	-0.00031	-0.00071
6.5	-0.00039	-0.00043	-0.00010	-0.00013	-0.00023	-0.00039	-0.00019	-0.00021	-0.00057
7.0	-0.00020	-0.00039	-0.00009	-0.00013	-0.00009	-0.00031	-0.00018	-0.00014	-0.00042
7.5	-0.00012	-0.00030	-0.00008	-0.00010	-0.00005	-0.00021	-0.00015	-0.00010	-0.00031
8.0	-0.00008	-0.00022	-0.00006	-0.00008	-0.00003	-0.00014	-0.00012	-0.00006	-0.00022
9.0	-0.00004	-0.00011	-0.00003	-0.00004	-0.00000	-0.00007	-0.00007	-0.00003	-0.00012
10.0	-0.00002	-0.00006	-0.00001	-0.00002	0.00001	-0.00003	-0.00004	-0.00001	-0.00006
20.0	0.08300	0.08345	0.17974	0.00062	0.08285	0.08312	0.08360	0.17924	0.00061

R(a_0)	$2^3\Pi_u$	$3^3\Pi_u$	$4^3\Pi_u$	$5^3\Pi_u$	$1^3\Delta_g$	$2^3\Delta_g$	$C^3\Delta_u$	$2^3\Delta_u$	$3^3\Delta_u$
1.8	0.53440	0.65994	0.71111	0.75065	0.47807	0.87063	0.50075	0.68513	0.82344
2.0	0.40706	0.55385	0.60059	0.51157	0.38295	0.70058	0.23574	0.58003	0.69787
2.2	0.31432	0.41100	0.52034	0.43980	0.36679	0.62815	0.09337	0.48618	0.55229
2.3	0.28349	0.35716	0.49528	0.42641	0.37333	0.60569	0.05019	0.38976	0.55091
2.4	0.24738	0.33122	0.47765	0.39673	0.38494	0.50823	0.01962	0.31071	0.54006
2.6	0.17747	0.30900	0.32361	0.25337	0.34655	0.41475	-0.01537	0.19487	0.44992
2.8	0.12552	0.19872	0.23133	0.17971	0.23456	0.37807	-0.02855	0.11941	0.31130
3.0	0.08777	0.12014	0.15366	0.11638	0.15840	0.25955	-0.02989	0.07025	0.21627
3.2	0.05878	0.06959	0.10220	0.07269	0.10681	0.17837	-0.02550	0.03843	0.15086
3.4	0.03208	0.04325	0.06804	0.04503	0.07191	0.12276	-0.01916	0.01839	0.10555
3.5	0.02136	0.03505	0.05553	0.03539	0.05896	0.10190	-0.01601	0.01161	0.08835
3.6	0.01314	0.02844	0.04532	0.02779	0.04832	0.08462	-0.01311	0.00652	0.07397
3.8	0.00293	0.01859	0.03016	0.01707	0.03239	0.05842	-0.00841	0.00025	0.05187
4.0	-0.00155	0.01200	0.02003	0.01042	0.02162	0.04040	-0.00525	-0.00250	0.03639
4.5	-0.00288	0.00372	0.00703	0.00290	0.00764	0.01619	-0.00180	-0.00292	0.01499
5.0	-0.00174	0.00091	0.00229	0.00067	0.00252	0.00662	-0.00084	-0.00167	0.00623
5.5	-0.00096	0.00000	0.00060	0.00001	0.00071	0.00279	-0.00048	-0.00087	0.00266
6.0	-0.00051	-0.00027	0.00003	-0.00015	0.00012	0.00123	-0.00029	-0.00047	0.00119
6.5	-0.00023	-0.00032	-0.00014	-0.00015	-0.00005	0.00058	-0.00019	-0.00027	0.00056
7.0	-0.00008	-0.00030	-0.00017	-0.00012	-0.00008	0.00029	-0.00012	-0.00016	0.00029
7.5	-0.00005	-0.00021	-0.00015	-0.00009	-0.00007	0.00016	-0.00007	-0.00010	0.00016
8.0	-0.00003	-0.00014	-0.00012	-0.00006	-0.00005	0.00010	-0.00005	-0.00006	0.00010
9.0	-0.00000	-0.00007	-0.00007	-0.00003	-0.00002	0.00005	-0.00001	-0.00002	0.00005
10.0	0.00001	-0.00003	-0.00004	-0.00001	-0.00001	0.00003	-0.00000	-0.00001	0.00003
20.0	0.08295	0.08312	0.08360	0.17924	0.08300	0.08374	0.00000	0.08300	0.08374

Tabular Data. A-14.4 Calculated potential curves for 62 valence states of O_2 given in hartrees relative to the asymptotic energy of each state. (Continued).

R(a_0)	$^3\Phi_g$	$^3\Phi_u$	$1^5\Sigma_g^+$	$2^5\Sigma_g^+$	$^5\Sigma_u^-$	$^5\Pi_g$	$^5\Pi_u$	$^5\Delta_g$
1.8	0.46347	0.70406	1.18893	1.32424	0.95557	0.94008	0.91197	0.94106
2.0	0.37205	0.60298	0.95967	1.07451	0.71817	0.71078	0.69442	0.77333
2.2	0.35965	0.56491	0.73495	0.84102	0.46895	0.43643	0.59166	0.70400
2.3	0.36758	0.53812	0.60427	0.80470	0.37435	0.33463	0.56513	0.59879
2.4	0.28329	0.52080	0.49597	0.77697	0.29813	0.25320	0.50356	0.49100
2.6	0.17215	0.35281	0.33339	0.55335	0.18901	0.13835	0.33477	0.32933
2.8	0.10003	0.23510	0.22374	0.38083	0.12065	0.06909	0.22230	0.22045
3.0	0.05677	0.15615	0.14995	0.26218	0.07802	0.02909	0.14742	0.14731
3.2	0.03153	0.10333	0.10034	0.18071	0.05125	0.00739	0.09759	0.09824
3.4	0.01720	0.06809	0.06705	0.12472	0.03415	-0.00325	0.06442	0.06538
3.5	0.01264	0.05518	0.05477	0.10366	0.02799	-0.00596	0.05228	0.05329
3.6	0.00928	0.04465	0.04472	0.08618	0.02238	-0.00751	0.04238	0.04341
3.8	0.00497	0.02910	0.02976	0.05963	0.01550	-0.00838	0.02774	0.02874
4.0	0.00260	0.01880	0.01974	0.04131	0.01040	-0.00772	0.01804	0.01894
4.5	0.00017	0.00591	0.00691	0.01663	0.00354	-0.00486	0.00588	0.00649
5.0	-0.00047	0.00152	0.00231	0.00680	0.00097	-0.00287	0.00169	0.00209
5.5	-0.00055	0.00014	0.00070	0.00285	0.00010	-0.00174	0.00032	0.00058
6.0	-0.00047	-0.00023	0.00017	0.00124	-0.00014	-0.00110	-0.00007	0.00009
6.5	-0.00035	-0.00027	0.00001	0.00057	-0.00018	-0.00071	-0.00015	-0.00005
7.0	-0.00025	-0.00023	-0.00002	0.00028	-0.00015	-0.00048	-0.00014	-0.00007
7.5	-0.00018	-0.00017	-0.00002	0.00015	-0.00011	-0.00033	-0.00011	-0.00006
8.0	-0.00013	-0.00012	-0.00001	0.00009	-0.00008	-0.00023	-0.00008	-0.00004
9.0	-0.00006	-0.00006	0.00000	0.00004	-0.00003	-0.00012	-0.00004	-0.00001
10.0	-0.00003	-0.00003	0.00001	0.00003	-0.00001	-0.00006	-0.00002	-0.00000
20.0	0.08312	0.08312	0.00000	0.00125	-0.00000	0.00061	0.00062	0.00000

[a]The asymptotic energy for each state is taken to be the calculated energy at R = $20a_0$. The energies for R = $20a_0$ are given relative to the calculated $^3P + {}^3P$ asymptote of -149.695177 hartrees. $1a_0$ = 0.52918 Å; 1 hartree = 27.2116 eV.

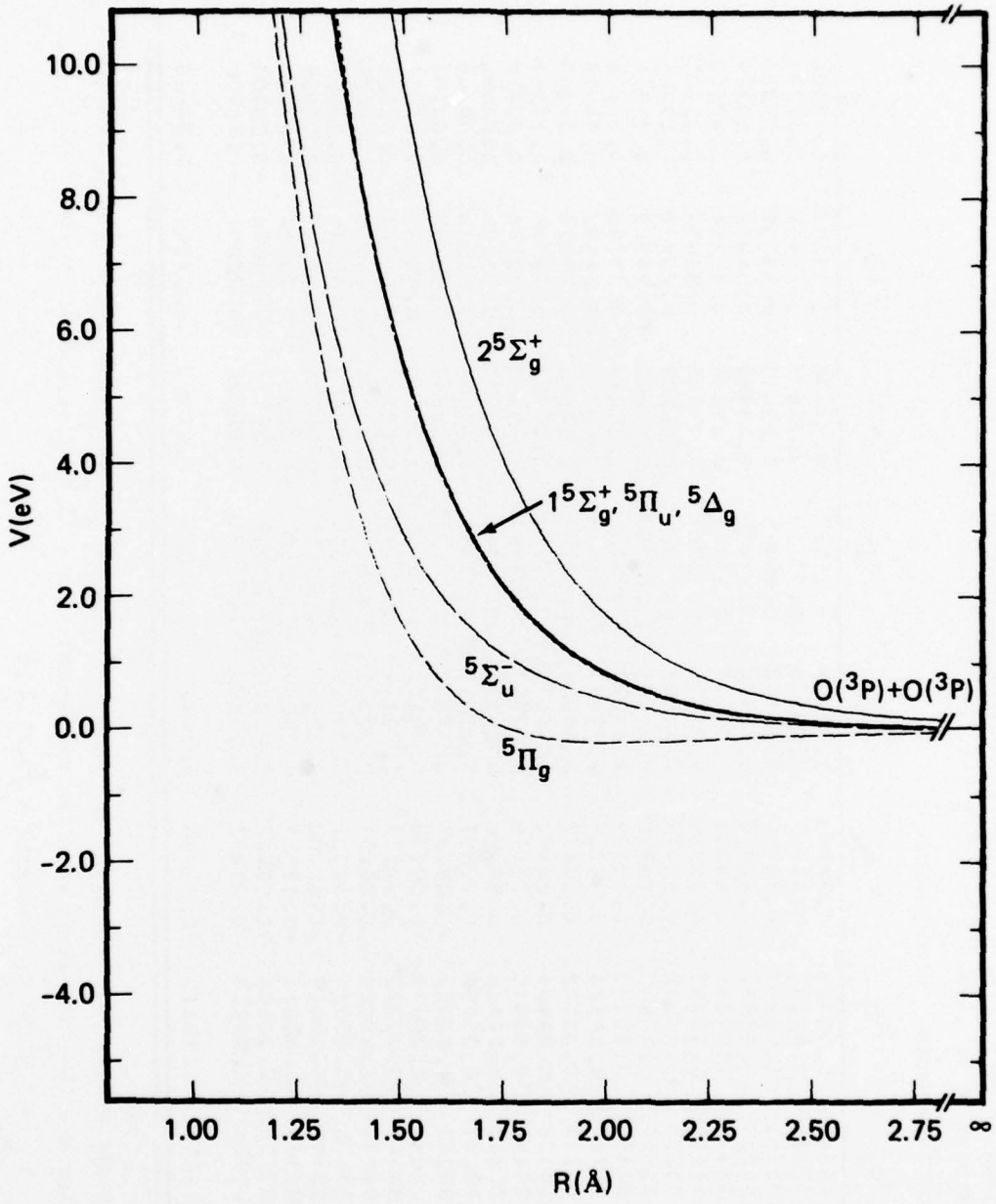

Graphical Data. A-14.5. Calculated potential curves for quintet valence states of O_2. Energies are given relative to O (^3P) + O (^3P).

Tabular Data. A-14.6. Molecular constants for 12 electronic states of O_2.[a]

State	Ref.	R_e(Å)	D_e(eV)	D_0(eV)	T_e(eV)	T_0(eV)	ω_e(cm^{-1})	$\omega_e x_e$(cm^{-1})	B_e(cm^{-1})	α_e(cm^{-1})
$X^3\Sigma_g^-$	1	1.236	4.957	4.864			1498.8	9.87	1.38	0.0141
	Exptl. 2	1.208	5.213	5.115			1580.2	11.98	1.45	0.0159
	3	1.30	3.81	3.72			1582.	14.	1.25	0.0127
	4	1.238	4.876				1692.7			
$a^1\Delta_g$	1	1.250	3.857	3.771	1.098	1.091	1403.4	8.74	1.35	0.0158
	Exptl. 2	1.216	4.231	4.138	0.982	0.977	1509.3	12.9	1.43	0.0171
	3	1.33	2.81	2.72		1.00	1406.	16.	1.19	0.0134
	4	1.249	3.787		1.089		1595.0			
$b^1\Sigma_g^+$	1	1.267	3.168	3.087	1.776	1.764	1310.8	10.44	1.31	0.0172
	Exptl. 2	1.227	3.577	3.489	1.636	1.627	1432.7	13.93	1.40	0.0182
	3	1.34	2.44	2.36		1.36	1318.	18.	1.17	0.017
	4	1.260	3.185		1.691		1505.1			
$c^1\Sigma_u^-$	1	1.555	1.062	1.016	3.888	3.842	759.8	12.25	0.872	0.0146
	Exptl. 2	1.517	1.114	1.066	4.098	4.050	794.3	12.74	0.916	0.0139
	3	1.56	0.90	0.85		2.87	920.	27.	0.87	0.017
	4	1.525	0.939		3.937		832.6			
$C^3\Delta_u$	1	1.550	0.825	0.778	4.130	4.085	780.1	13.18	0.877	0.0146
	Exptl. 2	~1.5	0.907	0.861	4.306	4.255	750.	27.		
	3	1.55	0.67	0.61		3.11	958.		0.88	0.016
	4	1.522	0.703		4.173		858.6			
$A^3\Sigma_u^+$	1	1.558	0.745	0.698	4.206	4.160	764.6	13.94	0.868	0.0151
	Exptl. 2	1.522	0.824	0.775	4.389	4.340	799.1	12.16	0.911	0.0142
	3	1.56	0.61	0.55		3.16	943.	29.	0.87	0.017
	4	1.528	0.626		4.249		836.6			
$B^3\Sigma_u^-$	1	1.627	1.136	1.091	6.079	6.032	724.9	7.04	0.791	0.0077
	Exptl. 2	1.604	1.007	0.963	6.173	6.119	709.1	10.61	0.819	0.0119
	3	1.68	0.30	0.26		6.01	593.	27.	0.74	0.012
	4	1.625	0.805		6.308		667.8			
$2^3\Sigma_g^-$	1	2.069	0.511	0.479	6.699	6.638	537.0	13.73	0.490	0.0045
	3	2.00	0.38	0.33		5.94	872.	18.	0.53	−0.009
	4	2.101	0.314		6.798		482.6			
$2^1\Pi_g$	1	1.620	1.111	1.005	8.411	8.423	1626.4	163.67	0.819	0.0388
	3	1.57	0.84	0.69		8.13	2559.	65.	0.84	0.005
$1^1\Delta_u$	1	1.631	0.905	0.862	8.570	8.521	705.6	9.59	0.788	0.0101
	3	1.70	0.20	0.17		8.64	549.	35.	0.73	0.027
	4	1.648	0.556		8.794		627.2			
$2^1\Delta_g$	1	1.961	0.437	0.406	9.031	8.968	499.5	13.51	0.547	0.0102
	3	1.88	0.14	0.10		8.71	597.	26.	0.60	0.015
$^1\Sigma_u^+$	1	1.611	1.653	1.555	10.430	10.386	792.4	7.71	0.811	0.0092
	3	1.66	0.74	0.70		10.28	625.	−1.	0.76	0.022
	4	1.655	0.920		10.187		652.8			

[a]All experimental values are taken from Ref. 2.

Tabular Data. A-14.7. Separated-atom energy levels of O_2 given in eV relative to the $^3P + {}^3P$ asymptote.

Separated-atom limit	This work	Experiment	SH	MG
$^1S + {}^1S$	9.79	8.380	9.46	8.05
$^1D + {}^1S$	7.14	6.157	7.28	6.36
$^3P + {}^1S$	4.88	4.190	4.73	4.02
$^1D + {}^1D$	4.51	3.935	5.10	4.67
$^3P + {}^1D$	2.25	1.967	2.55	2.34

Tabular Data. A-14.8. Equilibrium constants for five new, weakly bound states of O_2.

State	R_e(Å)	D_e(eV)	T_e(eV)
$1\,^5\Pi_g$	1.996	0.228	4.746
$2\,^3\Pi_g$	1.721	0.327	6.884
$3\,^3\Pi_g$	1.922	0.147	7.072
$1\,^1\Phi_g$	2.002	0.196	9.282
$4\,^1\Pi_g$	1.952	0.428	11.667

DISTRIBUTION

	No. of Copies
School of Physics	
Georgia Institute of Technology	
Attn: Dr. E. W. McDaniel	50
K. J. McCann	10
Dr. F. L. Eisele	10
E. W. Thomas	10
Dr. W. M. Pope	10
Dr. M. R. Flannery	10
Atlanta, Georgia 30332	
Joint Institute for Laboratory Astrophysics	
University of Colorado	
Attn: J. W. Gallagher	10
J. R. Rumble	10
E. C. Beaty	10
Boulder, Colorado 80302	
Eckerd College	
Attn: Dr. H. W. Ellis	10
St. Petersburg, Florida 33733	
Physics Department	
Georgia State University	
Attn: S. T. Manson	10
Atlanta, Georgia 30303	
Defense Documentation Center	
Cameron Station	
Alexandria, Virginia 22314	2
Director	
Ballistic Missile Defense Advanced Technology Center	
Attn: ATC, Mr. J. D. Carlson	1
ATC-O, Mr. W. Davies	1
Mr. G. Sanmann	1
Mr. J. Hagefstration	1
-T, Dr. E. Wilkinson	1
-R, Mr. Don Schenk	1
P. O. Box 1500	
Huntsville, Alabama 35807	
Defense Advanced Research Project	
1400 Wilson Boulevard	
Attn: Director, Laser Division	1
Arlington, Virginia 22209	

	No. of Copies
Lawrence Livermore Laboratory P. O. Box 808 Attn: Dr. Joe Fleck Dr. John Emmet Livermore, California 94550	 1 1
Los Alamos Scientific Laboratory P. O. Box 1663 Attn: Dr. Keith Boyer (MS 550) Los Alamos, New Mexico 87544	 1
Central Intelligence Agency Attn: Mr. Julian C. Nall (OSI/PSTD) Washington, D.C. 20505	 1
US Army Research Office Attn: Dr. Robert Lontz P. O. Box 12211 Research Triangle Park, North Carolina 27709	 2
DRCPM-HEL, COL D. H. Lueders HEL-T, Dr. C. J. Albers	1 1
DRSMI-LP, Mr. Voigt	1
DRDMI-X, Mr. McKinley -T, Dr. Kobler -H, Dr. Hallowes -HS, Dr. Honeycutt Mr. Cason Dr. Roberts (Additional Distribution) -NS -TBD -TI (Record Set) (Reference Copy)	1 1 1 1 1 485 1 3 1 1